CHAPTER ONE

INTRODUCTION

1.1 Background of the study

Over the last few decades, adsorption has gained importance as a purification, separation and recovery process on an industrial scale. Activated carbon (AC) is perhaps one of the most widely used adsorbents in industry for environmental applications. Activated carbons are carbons of highly microporous structure with both high internal surface area and porosity, and commercially the most common adsorbents used for the removal of organic and inorganic pollutants from air and water streams (Gottipati, 2012). Any cheap material with a high carbon content, low inorganics can be used as a raw material for the production of activated carbon (Bansal et. al., 1988). The high adsorption capacities of activated carbons are related to the properties such as surface area, pore volume and pore size distribution (PSD). These unique characteristics depend on the type of raw materials employed for preparation of AC and the method of activation. Due to the increasing demand of AC, there is a strong need for the sorting out new precursors for the preparation of AC which should be cost effective compared with the commercially available AC. Although a variety of raw materials were explored for the preparation of AC in earlier studies, scientists are still trying to explore new materials depending on their availability and suitability for AC production.

Basically, there are two different processes for the preparation of AC: physical activation and chemical activation. Physical activation involves carbonization of carbonaceous material followed by the activation of the resulting char at high temperatures (800 – 1100°C) in presence of oxidizing agents such as CO_2 and steam (Gottipati, 2012). In chemical activation the precursor is mixed with a chemical agent and then pyrolyzed at low temperatures in absence of air. The pyrolysis can be done using conventional or microwave techniques. Chemical activation offers several advantages over physical activation as it is carried out in a single step combining carbonization and activation, performed at lower temperatures and therefore resulting in the development of a better porous structure. Moreover, the added chemicals for activation can be easily recovered (Ahmadpour & Do, 1996). Activated carbon has been widely used as an adsorbent due to its great adsorption capacity towards a variety

of solutes (Zhang et. al., 2008). After reaching its uptake capacity, activated carbon must either be disposed of as solid waste and replaced with fresh carbon or be regenerated (Nahm et. al., 2012). The relative high initial cost of activated carbon and the fact that disposal of spent adsorbents via landfills or incineration adds pollutants to the environment, mandates serious consideration of carbon regeneration. The objectives during regeneration are the selective removal of the adsorbates that have accumulated during the adsorption operation, and the restoration of the original porous structure and activity of the carbon with as little damage as possible to the carbon itself (Vliet, 1991). Regeneration of activated carbon cannot only economize the natural resources, reduce the secondary pollution, but also bring along considerable economic profit (Oin et. al., 2001). In recent years, many scientists have focused on the research of the mechanism and technology of activated carbon regeneration (Liu, et. al., 2001). The methods of regenerating spent activated carbons can be categorized as (1) thermal and gas treatments, (2) chemical and extraction treatment, (3) Biological treatment, (4) Vacuum treatment, (5) Electric and electrochemical treatment, (6) Supercritical fluid and electrochemical treatment, (7) Wet oxidation treatment, (8) Other methods including microwave, ultrasounds, X-ray irradiation, photo chemical treatment and superficial water oxidation.

Selection of an appropriate regeneration process greatly depends on several factors such as type of adsorbate (that is, toxicity, ignitable, corrosive and radioactive), types of adsorption (that is, physical adsorption or chemisorption), the cost of regeneration and the conditions of processing (Mckay, 1996a; Huling, et. al., 2011; Jeon, et. al., 2011). Each method has its own advantages as well as disadvantages.

Thermal regeneration involves oxidizing the organic substances adsorbed onto the activated carbon by heating spent carbon to a temperature between 500 – 1000°C in a furnace. Drawbacks associated with thermal regeneration includes a 5 – 10% loss of carbon due to oxidation and attrition, a decrease in adsorption capacity, and high energy costs associated with the required high temperature (Magne & Walker, 1986). Chemical regeneration involves the elution of adsorbed compounds using specific extracting agents or by decomposition of adsorbed species using oxidizing chemical agents under subcritical/supercritical conditions (Menard et. al., 2007). However, this technique is usually only adopted if there is a risk of ignition or decomposition of the adsorbate. The efficiency of this process depends primarily on the solubility of the

adsorbed substance and an extra step for recovery of extraction agent is usually involved after the desorption process (Foo & Hameed, 2012a).

Microwave regeneration occurs through the interaction of the electric field component of the microwave with (a) the dipoles (permanent or induced) or (b) the charged particles present in some materials (Caliskan et. al., 2012).

In this regard, carbon materials are good microwave adsorbers as a consequence of the interaction of the delocalized π electrons with the microwaves, thus converting microwave energy into heat. Microwave assisted regeneration offers many advantages over conventional regeneration including rapid and precise temperature control, small space requirements, fast heating, economic savings due to shorter exposure times, superior regeneration efficiency over a larger number of cycles, energy savings and greater efficiency during intermittent use (Salema & Ani, 2011). Although microwave heating is considered to be a beneficial alternative for conventional heating techniques in waste management and conversion processes, it is also worth mentioning that there are some limitations concerning microwave heating processes. These include; the absence of sufficient knowledge on the dielectric properties of materials such as biomass and the need of more complicated design and implementation of the technology, as well as uncertainty about the actual cost of these technologies (Fernandez et. al., 2011)

In the present study, microwave irradiation and conventional treatments were used in preparation of activated carbons. Comparative studies were done on regeneration of activated carbons using microwave, conventional and chemical methods.

1.2. Statement of problem

The economic feasibility of processes using activated carbon for treatment of water and waste water is contingent upon re-use of the carbon in multiple adsorption-regeneration cycle. Activated carbon has been used in treating waste water due to its known high adsorptive capacity over various solutes, but after activated carbon has reached its uptake capacity, it must either be disposed off and replaced with fresh carbon or be regenerated. The relative high cost of activated carbon, and the fact that disposal of spent activated via landfills or incineration adds pollutants to the environment, mandates serious consideration of carbon regeneration. Carbon regeneration saves cost and helps to solve the associated environmental problem.

Some researchers have studied regeneration of spent carbon using microwave, conventional and chemical methos, it is still not clear which method offers clear advantages over another. Therefore, this work compared the three methods of regeneration in terms of regeneration efficiency, carbon loss and carbon yield.

1.3.Aim and objectives

The aim of this work is to undertake the regeneration and reuse studies of spent activated carbons. The specific objectives are as follows:

i. To prepare adsorbents from different precursors (Brewer's spent grain and hamburger seed shell) using microwave and conventional methods;
ii. To compare the effect of microwave activation and conventional activation on the Swiss blue dye removal efficiency;
iii. To evaluate the kinetics, isotherm and thermodynamics of the adsorption process;
iv. To evaluate the kinetics, isotherm and thermodynamics of the desorption process;
v. To assess the reuse of the regenerated activated carbons;
vi. To compare chemical, microwave and conventional regeneration methods on the spent activated carbons.

1.4. Scope of the work

This work is limited to preparation of activated carbons from hamburger seed shell and brewers' spent grain using microwave and conventional techniques. Effect of process factors on the activation of the samples was considered. Swiss blue dye was used as the adsorbate. Adsorption process was limited to batch process and the conditions were constant for all activated carbon. Activated carbons were considered spent by saturating it with Swiss blue dye. Conventional, Microwave and Chemical processes were used for the regeneration process. Desorption data were fitted to kinetics and equilibrium models. Regeneration methods were compared in terms of regeneration efficiency, carbon loss and carbon yield. Regeneration study was limited to six cycles of aadsorption-regeneration process.

Changes on the activated carbon after regeneration were studied with scanning electrom microscope, Fourier transform infra red spectroscopy and methylene blue adsorption process for surface area determination.

1.5.Significance of the work

This work has added to the existing literature more information on regeneration of spent carbon. Other benefits include; that the cost of replacing spent carbon with the fresh one can be saved through regeneration, environmental pollution as a result of disposing spent carbon through land fill can be mininized through regeneration, activated carbons can be prepared from hamburger seed shell and brewers'spent grain using microwave irradiation, the work compared microwave, conventional and chemical regeneration processes, large data bank will be generated for desorption kinetics and isotherm studies, and it will generate thermodynamic parameters for the desorption process.

CHAPTER TWO
LITERATURE REVIEW

2.1 Methods of removing dyes form waste water

Most of dyes are known to be non-biodegradable. Thus the conventional primary and secondary systems are not suitable to treat these effluents (Gürses et. al., 2004). Some investigations have focused on the development of a treatment process for dye wastewater, such as biological and advanced oxidation processes. For the former, it has been found that it may be efficient in the removal of suspended solids and reduction of chemical oxygen demand but is largely ineffective in removing colour from wastewater. For the latter, because of the higher organic concentration and complex composition of dye wastewater, the dye wastewater cannot be efficiently purified and treated. Many physical and chemical processes for colour removal have been applied including coagulation and flocculation, biosorption, photo-decomposotion and ultrafiltration, oxidizing agents, membrane and electrochemical. Due to relatively high operating costs and low removal efficiencies using the above-mentioned processes, textile, tannery, pulp and paper industries seldom apply these to treat their effluents. Adsorption process has been found to be an efficient and economic process to remove dyes, pigments and other colorants (Wang et. al., 2003). It is also has been found to be superior to other technique for wastewater treatment in terms of initial costs, simplicity of design, ease of operation and insensitivity to toxic substances. Adsorption using activated carbon is rapidly becoming a prominent method of treating aqueous effluents and has been used in industrial processes for variety of separation and purification process.

2.2. Adsorption

Adsorption involves the interphase accumulation or concentration of substances at a surface or interface. The process can occur at an interface between any two phases, such as, liquid-liquid, gas-solid, gas-liquid, or liquid-solid interfaces. The material being concentrated or adsorbed is the adsorbate, and the adsorbing phase is termed the adsorbent (Weber, 1972).

Absorption, conversely, is a process in which the molecules or atoms of one phase Inter penetrate nearly uniformly among those of another phase to form a “solution” with the second phase. The term sorption, which includes both adsorption and absorption, is a general expression for a process in which a component moves from one phase to be accumulated in another, particularly for cases in which the second phase is solid (Weber, 1972).

2.2.1. Causes and Types of Adsorption

Adsorption is a spontaneous process accompanied by the release of energy (the stronger the adsorption, the more exothermic the process will be) (Bansal & Goyal, 2005). If the attraction between the adsorbate and the adsorbent is due to van der Waals forces, the adsorption is said to be physical, however if there are exchange or sharing of electrons between the compound and the solid surface, then the adsorption process is called chemisorption. This is accompanied by a higher release of energy than the former case because of the chemical bonding. Another dissimilarity between both adsorption scenarios is the possibility of forming layers of adsorbed compounds on the surface of the solid if the adsorption is purely physical, while in the case of chemisorption the adsorption is limited to a monolayer. If both chemisorption and physisorption happens at the same time, then the process is better defined as sorption. The type of adsorption, if physical, chemical or electrostatic, is determined by many variables: the properties of the contaminant, its concentration, the structure and nature of the carbon surface, the experimental conditions such as the flow rate, the temperature, pH, the ionic strength of the solution and the time exposure of water to activated carbon (Bansal & Goyal, 2005; Wang et. al., 2005). Figure 2.1 illustrates how the surface coverage of the adsorbent changes with the size of the molecule being adsorbed, and points out the difference between a monolayer and a multilayer system, where N represents the number of layers.

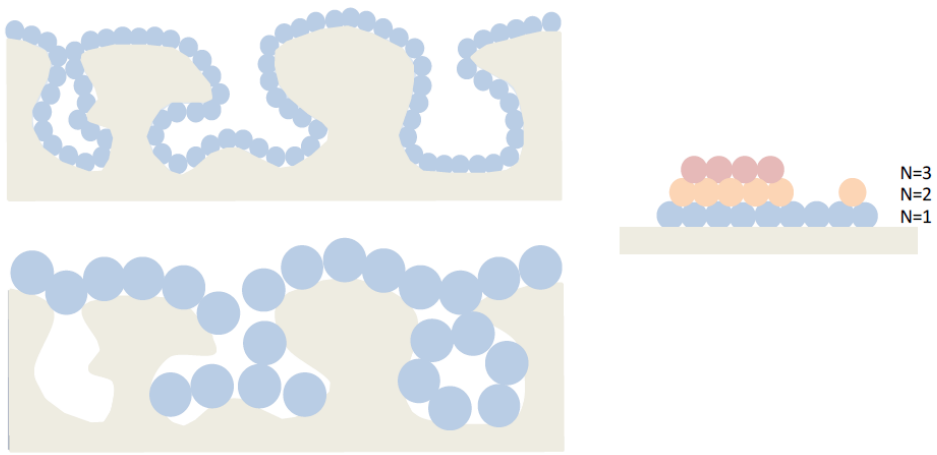

Figure 2.1: Diagram of molecules of different sizes adsorbed onto the pore system of the carbon material (left), and a three layer molecules (N=3) on the carbon surface (right), adapted from Bandosz (2006)

Adsorption of ionic dyes by carbons relies upon the chemistry of the adsorbent surface primarily and secondarily on the porous structure of the carbon (Bansal & Goyal, 2005). Methylene blue adsorption onto activated carbon was described to be profoundly affected by the carbon surface chemistry and solution pH (Bottani & Tascón, 2008). It has been reported that molecular dyes will adsorb only in pores where the average micropore diameter increased to about 1.7 times the molecule's second widest dimension (>1.43 nm in the case of methylene blue) (Pelekani & Snoeyink, 1999), although Pelekani & Snoeyink (2000) pointed out that this might not be universally valid because those authors used shorter contact times than required for a molecule to access pores similar in size. The shorter contact time and very high concentration used by those researchers would focus the adsorption in the larger pores rather than occurring in small micropores.

2.3: Agricultural By-product Based Granular Activated Carbon

In addition to being an adsorbent used for many different purposes, activated carbon can be produced from a wealth of different raw materials, making it an incredibly versatile product that can be produced in many different areas depending on what raw material is available. Some of these materials include shells of plants, the stones of fruits, woody materials, asphalt, metal carbides, carbon blacks, scrap waste deposits from sewage, and polymer scraps. Different types of coal, which already exist in a

carbonaceous form with a developed pore structure, can be further processed to create activated carbon.

Although activated carbon can be produced from almost any raw material, it is most cost effective and environmentally conscious to produce activated carbon from waste materials. Activated carbons produced from coconut shells have been shown to have high volumes of micropores, making them the most commonly used raw material for applications where high adsorption capacity is needed. Sawdust and other woody scrap materials also contain strongly developed microporous structures which are good for adsorption from the gas phase. Producing activated carbon from olive, plum, apricot, and peach stones yields highly homogenous adsorbents with significant hardness, resistance to abrasion and high micropore volume. PVC scrap can be activated if HCl is removed beforehand, and results in an activated carbon which is a good adsorbent for methylene blue. Activated carbons have even been produced from tire scrap.

In order to distinguish between the wide range of possible precursors, it becomes necessary to evaluate the resulting physical properties after activation. When choosing a precursor the following properties are of importance: specific surface area of the pores, pore volume and pore volume distribution, composition and size of granules, and chemical structure/character of the carbon surface (Jankowska, et. al., 1991).

Choosing the correct precursor for the right application is very important because variation of precursor materials allows for controlling the carbons pore structure. Different precursors contain varying amounts of macropores (> 50 nm,) which determine their reactivity. These macropores are not effective for adsorption, but their presence allows more channels for creation of micropores during activation. Additionally, the macropores provide more paths for adsorbate molecules to reach the micropores during adsorption. Precursors which contain a greater amount of volatile substances yield a proportional increase in the reactivity of the activated substance (Beguin & Frackowiak 2010). If the reactivity is too high, the degree of activation can be lowered. Achieving the correct of amount of reactivity is of the utmost importance, since the extent of reaction occurring determines the carbons internal structure (Jankowska et. al., 1991).

2.3.1: Brewer's spent grain (BSG)

Brewers' grains often referred to as spent grains are major co-products of the brewing process, generated at a rate of up to 30% of the weight of the initial malt grist (Brewers' guardian 2011). Worldwide generation of BSG has been estimated at 30 billion kilograms per annum. Traditionally this material has either been discarded or sold as animal feed, but increasingly industry is seeking to find added value applications which change traditional views of waste streams and reclassify them as co-products. It contains about 17% cellulose, 28% non cellulosic polysaccharides, mostly arabinoxylans and 28% lignin, and they have very little or no economically interesting further uses (Mussatto et. al., 2006). Their water content is approximately 80% when produced, therefore, they cannot be stored for a long period (Andrej Gregon et. al., 2008). Drying large amount of BSG requires considerable energy and represents a great financial burden to the brewing industry. Owing to their high protein and fiber content (approximately 20 and 70% dry basis respectively) they can also represent an attractive adjunct in the human diet and biotechnological processes such as cultivation of mushrooms and action bacteria (Mussatto, et. al., 2006). It has been proposed that BSG favors the growth of mushrooms not only due to their high moisture content and physical properties such as particle size, volume weight, specific density, porosity and water holding capacity (Wang, 2001). Table 2.1 shows the chemical composition of brewers' spent grain.

Table 2.1: Chemical composition of brewer's spent grain (BSG) and germinated barley foodstuff (GBE).

Component (% dry wt)	BSG[a]	BSG[b]	GBF[a]	GBF[c]
Cellulose	25.4	16.8	8.9	9.1
Arabinoxylan	21.8	28.4	17.0	19.2
Lignin	11.9	27.8	8.2	6.7
Protein	24.0	15.2	46.0	48.0
Lipid	10.6	Nd	10.2	9.2
Ash	2.4	4.6	2.0	2.0

[a]Fom kanauchi et. al. (2001)

[b]From Mussatto and Roberto (2006)

[c]From Fukuda et. al. (2002)

Protein bound amino acids include leucine, valine, alamine, serine, glycine, glutamic acid and aspartic acid in the largest amounts and tyrosine, proline, threonine, arginine, and lysine in smaller amounts.

2.3.2. Hamburgar seed (Mucuna Slonei)

The enormous Legume Family (Fabaceae) contains many species of tropical vines, but some of the most interesting belong to the genus Mucuna. There are many species of Mucuna throughout tropical regions of the world, including *M. urens*, *M. pruriens* and *M. sloanei.* Most species of Mucuna are climbing woody vines called lianas that twine through the rain forest trees like "botanical boa constrictors." Their bat-pollinated flowers and pods are produced on long, rope-like stems that hang from the forest canopy. The seed pods are covered with microscopic velvety hairs (called trichomes) that can be extremely painful if they get into your eyes. At maturity, each pod produces several hard, marble-like seeds. The seed is called "ojo de buey" because of its striking resemblance to the eye of a bull. The seeds are also known as "sea beans," because they are commonly carried by rivers into the ocean. The seeds of both genera are commonly polished and made into seed necklaces.

(*Mucuna slonei*) is among one of the legumes found in the tropical and sub-tropical regions of the world. The inner part is a food thickener known to originate from Asia and was introduced into the western hemisphere via *Mauritus* (Nkpa, 2004). It is known as “horse eye bean”; and with other local names in respect to different tribes and ethnic groups. It is called ‘ukpo’ by Ibos; ‘karasuu’ by Hausas and ‘Yerepe’ by Yorubas (Adewale & Mozie, 2010). They belong to the legume family fabaceae. There are other species of *Mucuna* throughout tropical regions of the world including *Mucuna urensi*, *M. pruriens* and *M. veracrua* (Nkpa, 2004). Nutritionally, the importance of *Mucuna sloanei* (Ukpo) lies in high content of protein and lysine. They are usually limited in the sulfur containing amino-acids particularly methionine.

‘Ukpo’ (*Mucuna sloanei*) is used in preparing various soups as soup thickeners (Ezueh, 1997). In addition to their thickening property, Ukpo has gelation properties and imparts a gummy texture when used in soups. This is a desirable attribute for the eating of ‘gari’, ‘fufu’, pounded yam etc. As a result of increasing interest in the use of soup

thickners for food preparation and industrial purposes, especially in new product development, the issue of disposal of its husk became one of the optimum concerns. The seed shell constitutes environmental hazard as it litters the whole environment.

2.4. Manufacturing of activated Carbon

Activated carbon is produced from any carbonaceous organic material which contains elemental carbon.

Activation carbon can be produced by two main methods: physical activation and chemical activation.

2.4.1: Physical activation

The production of activated carbon by physical activation can be done using two methods. These methods are called one-step activation and two-step activation depending on whether the carbonization and activation processes occur simultaneous or in the separate steps.

2.4.1.1 Two-step activation method

This method involves two main steps: 1- carbonization of carbonaceous raw material or pyrolysis, 2- activation or gasification of char or carbonized raw material. In two-steps method carbonization and activation are not carried out simultaneously, but in distinct steps.

1). Pyrolysis or carbonization

In this step the carbonaceous raw material is heated up in the absence of oxygen. Almost all of the volatile fractions of the raw material leave the material in the form of permanent gases and tar. The residue that contains mostly carbon is called carbonized material or char. Three products are obtained from the decomposition of raw material namely: char, tar and product gas. To maximize the char fraction in this step, the raw material has to be heated with a slow heating rate and the temperature is usually between 400-850°C (El-Hendawy et. al., 2001; Girgis, 2002). Parameters that determine the characteristic of the pores in this step are heating rate, temperature, properties of the raw material and the type of activating agent. Pores characteristic include the total pore volume, pore diameter and pore size distribution.

The carbonized material needs further treatment because its adsorption capacity is too low for commercial application. Thus the char needs to be treated to increase the porosity and widened the existing micropores and some mesopores. This further treatment process is called activation. Table 2.2 shows various physical activating agents and precursors used for activated carbon production.

2). Activation

This is the second step in the production of activated carbon by two steps method. In the physical activation process, oxidizing gases such as steam, carbon dioxide or a mixture of both is used for gasification of the carbonized material or char. Physical activation involves the contact between the char and activating agent followed by reaction between the surface carbons on the pores and the activating agent. These agents extract carbon atoms from the structure of the porous carbon. Steam and CO_2 react with surface carbons according to reactions 2.1 and 2.2 below.

$$C + CO_2 \rightarrow 2CO(+163.18\ kJ/mole) \quad (2.1)$$

$$C + H_2O \rightarrow CO + H_2(+121.33\ kJ/mole) \quad (2.2)$$

The result is that the pores are formed. The most important effects of the activation step are: the formation of micropores and mesopores and the increase of the volume and the diameter of existing pores. The residence time can be controlled to have a larger internal surface area as this is an important indication that determines the quality of the activated carbon. Besides the appropriate oxidizing agent, a suitable temperature, usually between 800 to 1100°C (Bansal et. al., 1988), has to be applied.

Table 2.2: Various physical activating agents and precursors used for AC production (Ramakrishna Gottipati 2012)

Activating agent	Material
Steam	Rice husk, corn cob, olive residues, sunflower shells, pinecone, rapeseed, cotton residues, olive-waste cakes, coal, rubberwood sawdust, fly ash, coffee endocarp
CO_2	Oak, corn hulls, coconut shells, corn stover, rice straw, rice hulls, pecan

	shells, pistachio nutshells, coffee endocarp, sugarcane bagasse, corn cob, waste tyres, textile fibers, anthracite
Air	Peanut hulls, almond shells, olivetree wood, almond tree pruning, coal

This temperature is usually higher than the pyrolysis temperature. This process requires heat, because the reaction of carbon and these oxidizing gases is endothermic. The high temperature of activation causes a water gas shift reaction that is catalyst by the surface of the carbon according to reaction 2.3 below (Marsh, & Rodríguez-Reinoso, 2006). It increases the hydrogen content of the gasification product at the expense of carbon monoxide.

$$CO + H_2O \leftrightarrow CO_2 + H_2 \text{ (- 41KJ/mole)} \quad (2.3)$$

This is a pre-step in syngas production in the downstream of a gasifier, where the ratio of hydrogen and carbon monoxide in the product gas is critical. This shift reaction is sensitive to temperature, with the tendency to shift towards reactants as temperature increases based on Le Chatelier's principle.

2.4.1.2 One-Step activation

Many studies show that it is possible to produce the activated carbon with physical activation method in one step without pre-carbonization of the raw material (El-Hendawy et. al., 2001; Girgis, et. al., 2002; Marsh, and Rodríguez-Reinoso 2006; Fan, et. al., 2004; Minkova, et. al., 2001). One-step activation means that the carbonaceous raw material from the beginning comes in contact with the activation agent, which in most cases is steam or carbon dioxide, so that both carbonization and activation occur simultaneously at the same temperature. Marsh and Rodríguez-Reinoso (2002) used CO_2 for the activation of almond shells and olive stones by the one-step or direct activation method from the room temperature to 825-850°C. The results were compared with the activated carbon produced by the two-steps method, pre-carbonization followed by activation with CO_2 at 825°C. The result showed that both methods have the same yield and almost similar surface area and volume of micropores. Other studies (El-Hendawy et. al., 2001; Girgis, et. al., 2002; Marsh, & Rodríguez-Reinoso 2002; Fan, et. al., 2004; Minkova, et. al., 2001) used steam as

oxidizing agent for the production of activated carbon in one step. In these studies, the carbonaceous raw material was pyrolyzed at temperatures 500-700°C and 700-800°C under the flow of steam. The results shows that the direct contact and reaction of the raw material with steam or CO_2 does not make any considerable differences in the quality of the produced AC as compared to the AC produced by the two-steps method.

2.4.2 Chemical activation

Chemical activation involves the impregnation of the carbonized material by mixing it with an excess amount of a given chemical, usually in the form of concentrated solution. The commonly used activating agents are: H_2SO_4, $ZnCl_2$, H_3PO_4, KOH and NaOH. Other chemicals that can also be used include ferric iron carbonates of alkali metals and potassium sulphide. Impregnation has to be carried out with special care to ensure an intimate contact between the reagent and the precursor. Impregnation results in the dehydration of the carbon skeleton and swelling of the interior canals of the botanic structure followed by the formation of a porous structure. The residence time and the temperature of the operation for this step are important parameters that have to be considered. The chemically impregnated raw material is then pyrolyzed and carbonized in an inert atmosphere. Then the pyrolyzed product is cooled and washed with distilled water or by mild acid to extrude the rest of the activating agent and the agent is recycled. Impregnation (dehydration) is done at a temperature lower than the boiling temperature for the mixture or water. The temperature range for the activation and carbonization step can be up to 1000°C, but is usually between 450 to 600°C, which is much lower than those for physical activation (Bansal et. al., 1988; Marsh, & Rodríguez-Reinoso, 2002). Chemical activation results in a better development of the porous structure and carbon with higher density. The impregnation process takes up to 24 hours depending on the activating agent, the precursors and the subsequent processes (Paraskeva, et. al., 2008).

The most important function of the activating agents in a chemical activation process is the dehydrating of the carbon skeleton that subsequently influences the pyrolytic decomposition of the raw material. The degree of impregnation (ratio of the activating agent to carbonized raw material) is an important factor that determines the quality and the size distribution of the pores. Larger degree of impregnation yields larger pore diameter and larger active surface area in the product. Table 2.3 shows various chemical activating agents and precursors used for activated carbon production

Table 2.3: Various chemical activating agents and precursors used for AC production (Gottipati 2012)

Activating agent	Materials
$ZnCl_2$	Corn cob, coconut shells, macadamia nutshells, peanut hulls, almond shells, hazelnut shells, apricot stones, rice husk, tamarind wood, cattle-manure, pistachio-nut shells, bagasse, sunflower seed hulls.
KOH	Rice straw, corn cob, macadamia nutshells, peanut hulls, olive seed, rice straw, cassava peel, petroleum coke, coal, cotton stalk, pine apple peel.
H_3PO_4	Hemp, Peanut hulls, almond shells, pecan shells, corn cob, bagasse, sunflower seed hulls, lignin, grain sorghum, rice straw, oak, birch, sewage sludge, chestnut wood, eucalyptus bark, rice hull, cotton stalk, jackfruit peel.
K_2CO_3	Pine apple peel, corn cob, cotton stalk, almond shell, coconut shell, oil palm shell, pistachio shell, walnut shell, bamboo.

2.5. Classification of Activated Carbon

Activated carbons are complex products and the classification is difficult based on their preparation methods, physical properties, and surface characteristics. However, the general classification of activated carbons based on particle size divides them into Powered Activated Carbon (PAC), Granular Activated Carbon (GAC), and Activated Carbon Fibres (ACF) (Babel & Kurniawan, 2004).

2.5.1. Powered Activated Carbon

Powered Activated Carbon (PAC), has a typical particle size of less than 0.1 mm and the common size of the particle ranges from 0.015 to 0.025 mm. Typical applications

of PAC are industrial and municipal waste water treatments, sugar decolorization, in food industry, pharmaceutical, and mercury and dioxin removal from a flue gas stream (Cook et. al., 2001; Foo & Hameed, 2009).

2.5.2. Granular Activated Carbon

Granular Activated Carbon (GAC), has mean particle size between 0.6 to 4 mm. It is usually used in continuous processes of both liquid and gas phase applications. GAC has an advantage over PAC, of offering a lower pressure drop along with the fact that it can be regenerated and therefore reused more than once. In addition to the proper micropore size distribution, its high apparent density, high hardness, and a low abrasion index made GAC more suitable over PAC for various applications (Zhang et. al., 2008).

2.5.3. Activated Carbon Fibers

Activated carbon Fibers (ACFs) are carbonized carbons which are subsequently heat treated in an oxidizing atmosphere. ACF began to be developed in 1970 using the precursor viscose rayon which mainly consists of cellulose (Doying, 1966). Later thermoset polymer materials like saran and phenolic resins were used as precursors to produce ACF (Menendez- Diaz & Martin-Gullon, 2006). A good ACF precursor must be non-graphitic and nongraphitizable carbon fibre which was isotropic in nature. From the end of 1980s, interest is still centered on the production of ACFs from various inexpensive precursors (Derbyshire et. al. 2001; Ko et. al. 2002; Nahil & Williams, 2011; Oh & Jang, 2003; Oya et. al., 1993).

2.6. Conventional heating process

Conventional heating technologies are a wide classification of techniques that rely on basic heat transfer concepts; conduction, convection and radiation. Owing to the wide range of technologies it uses, conventional heating is highly adaptable to a variety of applications. This method is well established and by far the most common heating method in society and industry and thus benefits from thorough understanding of the science behind the method.

Conventionally heated electrical furnaces use heating elements which generally are made from resistance wires. The basis of heat production by these elements is the resistance of the element material against the flow of the electric current. The generated heat is then transferred to the surface of the material by means of conduction, convection or radiation through intermediate media. Once heat is received by the material, it is transferred from its surface towards the body centre, mainly by conduction. During the course of conventional heating, a large heat gradient is formed from the surface to the core of material. Due to the thermal inertia of the system, the temperature of material is always lower than the furnace, to the point that in many cases deep inside the workload cannot reach the desired temperature (Fernandez et. al., 2011). Conventional heating methods, despite having been used for many years, are still problematic to control due to the slow and imprecise heating of the workspace surface. Moreover, assuming that the surface temperature is controlled precisely, the heat transfer rate from the surface into the body is highly limited by the physical properties of the material such as specific heat, thermal conductivity and density, or in general the thermal diffusivity of the workspace.

Furthermore, larger workspace implies longer time to heat the workspace by conventional methods and is also much more difficult, as well as non-uniform, when the material is thick (Meredith, 1998).

2.7. Introduction of Microwave heating process

In order to overcome the apparent limitations of conventional heating methods, alternative heating methods have been developed and applied in science and technology. In this category, electro-heat technologies have emerged to include induction, radio-frequency, infrared and microwave heating, all utilising specific parts of the electro-magnetic wave spectrum (Appleton et. al., 2005).

Microwave heating is a potentially attractive method as it allows for improved heating efficiencies compared to conventional methods. Magnetrons (microwave sources) were invented in 1940, initially for military purposes. After the war microwaves were increasingly used in other applications. The first commercial microwave oven (Radarange®) was developed and manufactured in early 1950. However, they were not used in industry until 1962 (Clark & Sutton, 1996). Since then, microwave heating has been successfully used in various industrial and domestic applications such as food industry, vacuum drying, pasteurisation and sterilization, ceramic, rubber and plastic

industries, crude oil exploration and processing, forestry and agriculture, as well as many other applications in chemical industry and civil engineering (Meredith, 1998, Udo & Christof, 2010). The mechanism of microwave heating is different from conventional heating in terms of its "volumetric heating" effects and the "selective heating" which results in a more efficient heating of material. Unlike conventional heating methods, where material is heated through heat flux, microwave heating is achieved throughout the volume of material by direct conversion of electro-magnetic waves energy to heat as waves penetrate the substance (volumetric heating). As a result, the rate of heating is not limited by the thermal diffusivity of material and therefore more uniform heating is assumed to be achieved (Meredith, 1998). Also, microwave heating is referred to as selective heating, as electromagnetic wave energy is only dissipated as heat in materials with suitable dielectric properties and not necessarily everything in contact with them. By enabling high heating rates, utilising microwave energy may lead to significant savings in total energy consumption and process time. In the recent years, microwave heating has been used in thermal processing of municipal waste, sewage sludge, contaminated soil, plastic and rubber waste and many other dielectric materials.

Complete reviews on the application of microwaves in industry, environmental engineering and more specifically in pyrolysis of biomass have been gathered by Clark and Sutton, 1996, and Fernandez et. al. 2011, respectively.

Although microwave heating is considered to be a beneficial alternative for conventional heating techniques in waste management and conversion processes, it is also worth mentioning that there are some limitations concerning microwave heating processes. These include; the absence of sufficient knowledge on the dielectric properties of materials such as biomass and the need of more complicated design and implementation of the technology, as well as uncertainty about the actual cost of these technologies (Fernandez et. al., 2011).

2.7.1. Mechanism of microwave heating of carbons

Microwaves lie between infrared radiation and radiowaves in the region of the electromagnetic spectrum. More specifically, they are defined as those waves with wavelengths between 0.001 and 1 m, which correspond to frequencies between 300 and 0.3 GHz. The microwave band is widely used in telecommunications. In order to avoid interference with these uses, the wavelengths of industrial, research, medical and

domestic equipment are regulated both at national and international levels. Thus, the main operating frequency in the majority of countries is 2.450 (+/- 0.050) GHz (Meredith 1998; Zlotorzynski 1995). Dielectric heating refers to heating by high-frequency electromagnetic radiation, i.e., radio and microwave frequency waves. The interaction of charged particles in some materials with the electric field component of electromagnetic radiation causes these materials to heat up. The heat resulting from this interaction is mainly due to two different effects. In the case of polar molecules, the electric field component of the microwaves causes both permanent and induced dipoles to rotate as they try to align themselves with the alternating field (2450 million times per second). This molecular movement generates friction among the rotating molecules and, subsequently, the energy is dissipated as heat (Dipolar Polarization). This is the case of water and other polar fluids. In the case of dielectric solid materials with charged particles which are free to move in a delimited region of the material, such as π–electrons in carbon materials, a current traveling in phase with the electromagnetic field is induced. As the electrons cannot couple to the changes of phase of the electric field, energy is dissipated in the form of heat due to the so called Maxwell-Wagner effect (Interfacial or Maxwell- Wagner Polarization) (Meredith 1998; Zlotorzynski 1995). The materials which interact with microwaves to produce heat are called microwave absorbers. The ability of a material to be heated in the presence of a microwave field is defined by its dielectric loss tangent: $\tan\delta = \varepsilon''/\varepsilon'$. The dielectric loss tangent is composed of two parameters, the dielectric constant (or real permittivity), ε', and the dielectric loss factor (or imaginary permittivity), ε''; i.e., $\varepsilon = \varepsilon' - i\,\varepsilon''$, where ε is the complex permittivity. The dielectric constant (ε') determines how much of the incident energy is reflected and how much is absorbed, while the dielectric loss factor (ε'') measures the dissipation of electric energy in form of heat within the material (Meredith 1998; Zlotorzynski 1995). For optimum microwave energy coupling, a moderate value of ε' should be combined with high values of ε'' (and so high values of $\tan\delta$), to convert microwave energy into thermal energy. Thus, while some materials do not possess a sufficiently high loss factor to allow dielectric heating (transparent to microwaves), other materials, e.g. some inorganic oxides and most carbon materials, are excellent microwave absorbers. On the other hand, electrical conductor materials reflect microwaves. For example, graphite and highly graphitized carbons may reflect a considerable fraction of microwave radiation. In the case of carbons, where delocalized π-electrons are free to move in relatively broad

regions, an additional and very interesting phenomenon may take place. The kinetic energy of some electrons may increase enabling them to jump out of the material, resulting in the ionization of the surrounding atmosphere. At a macroscopic level, this phenomenon is perceived as sparks or electric arcs formation. But, at a microscopic level, these hot spots are actually plasmas. Most of the time these plasmas can be regarded as microplasmas both from the point of view of space and time, since they are confined to a tiny region of the space and last for just a fraction of a second. An intensive generation of such microplasmas may have important implications for the processes involved. The microwave heating of a dielectric material, which occurs through the conversion of electromagnetic energy into heat within the irradiated material, offers a number of advantages over conventional heating such as: (i) non-contact heating; (ii) energy transfer instead of heat transfer; (iii) rapid heating; (iv) selective material heating; (v) volumetric heating; (vi) quick start-up and stopping; (vii) heating from the interior of the material body; and, (viii) higher level of safety and automation (Haque,1999). Due to these advantages, microwaves are used in various technological and scientific fields in order to heat different kinds of materials [Zlotorzynski 1995; Haque, 1999). Most of the industrial applications of microwave heating are based on heating substances that contain polar molecules, for example: food processing, sterilization and pasteurization, different drying processes, rubber vulcanization, polymerization or curing of resins and polymers by elimination of polar solvents, etc. In addition, solid materials with a high dielectric loss factor, i.e., microwave absorbers, can be subjected to different processes based on microwave heating. Among these materials, carbons are, in general, very good microwave absorbers, so they can be easily produced or transformed by microwave heating. Moreover, carbon materials can be used as microwave receptors to indirectly heat materials which are transparent to microwaves. Thus, carbon materials have been used as microwave receptors in soil remediation processes, the pyrolysis of biomass and organic wastes, catalytic heterogeneous reactions, etc. The high capacity of carbon materials to absorb microwave energy and convert it into heat is illustrated in table 2.4, where the dielectric loss tangents of different carbons are listed.

Table 2.4: Dielectric loss tangents for different carbon materials at a frequency of 2.45 GHz and room temperature, 298 K

Carbon material	tanδ = ε”/ ε’	Reference
Coal	0.02-0.08	Yang and Wu 1987; Marland et. al., 2001.
Carbon foam	0.05-0.2	Fang et. al., 2007
Charcoal	0.11-0.29	Wu et al., 2008; Challa et al., 1994
Carbon black	0.35-0.83	Atwater and Wheeler 2004; Ma et. al., 1997.
Activated carbon	0.57-0.80	Challa et. al., 1994.
Carbon nanotube	0.25-1.14	Zhang and Zhu 2009.
CSi nanofibres	0.58-1.00	Yao et. al., 2008.

As can be seen, the loss tangents of most of the carbons, except for coal, are higher than the loss tangent of distilled water (tanδ of distilled water = 0.118 at 2.45 GHz and 298 K). The search and compilation of these data is not a straightforward matter. Although this parameter is helpful for the study of microwave heating, few research groups have determined the dielectric loss tangents of carbons and the data that can be found are scattered throughout bibliography. The first commercial microwave oven was developed in 1952, although it was during 1970s and 1980s when the widespread domestic use of microwave ovens occurred, as a result of Japanese technology transfer and global marketing (Stuerga & Delmotte 2002). Curiously, the industrial applications of microwaves were initiated by the domestic ovens. However, in recent years, the number of processes that combine the use of carbons and microwave heating to obtain benefits with respect to other traditional methods based on conventional heating has increased enormously.

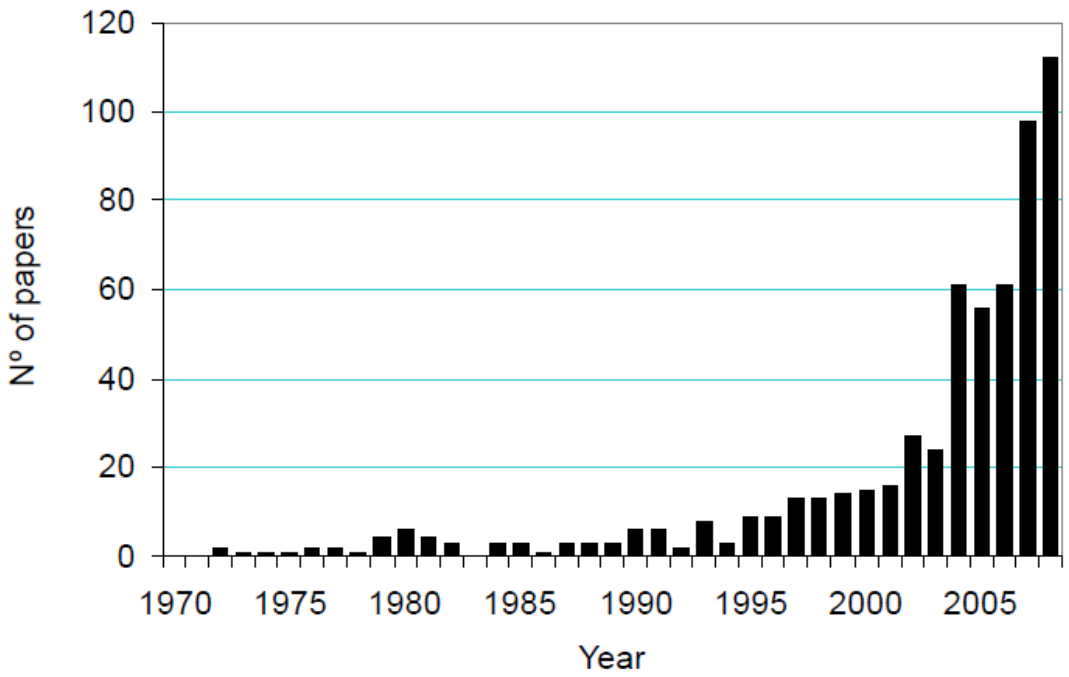

Fig. 2.2: Evolution of the number of research papers published on microwave-assisted processes involving carbon materials (Menéndez et. al., 2010).

Thus, as can be seen from Figure 2.2, the number of scientific publications related to these topics was very low until the late 1990s, but interest has risen drastically in the last decade and especially so in the last five years.

2.7.2. Microwave Heating Efficiency

Microwave heating efficiency could be named as one of the most important features of this method in comparison with the conventional heating techniques. Higher energy efficiency has been reported by researchers in various fields such as organic and inorganic chemistry (Moseley & Woodman, 2009; Pinchukova et. al., 2011), food industry (Berteli & Marsaioli, 2005), and extraction techniques (Pérez-Cid et. al., 1999). Nevertheless, it should be noted that microwave heating efficiency depends on the type of application and material being heated; as a result, some researchers have been sceptical about the higher efficiency of microwave heating techniques. These researchers argue that the typical efficiency of conversion of electrical to microwave energy being 50-65% (assuming that all the microwave energy is absorbed by the material) will not result in dramatically increased overall efficiency comparing with conventional techniques (Moseley & Woodman, 2009).

As stated earlier, the type of material being heated has a profound influence on the efficiency of microwave heating process; in other words, according to their microwave responsivity some materials cannot be efficiently heated by microwaves. In general, it can be concluded that the benefit of using microwave heating can be substantial only when applied to suitable material; this is of more significance when heating time is a crucial factor, as the slow heating rates achievable by conventional methods results in considerably high energy consumption.

2.8. Desorption and Regeneration of spent activated carbon

Desorption studies help to elucidate the nature of adsorption and recycling of the spent adsorbent and the dye. Activated carbon can be desorbed by a variety of methods. In most processes, desorption is achieved by subjecting the exhausted carbon to conditions that shift the adsorption equilibrium in favour of desorption. The most common method used for desorption is thermal process, other methods include chemical, wet air oxidation, solvent, etc. An adsorbed species present on a surface at low temperatures may remain almost indefinitely in that state. As the temperature of the substrate is increased, however, there will come a point at which the thermal energy of the adsorbed species is such that one of several things may occur:

1. Molecular species may decompose to yield either gas phase products or other surface species.
2. An atomic adsorbate may react with the substrate to yield a specific surface compound, or diffuse into the bulk of the underlying solid.
3. The species may desorb from the surface and return into the gas phase.

The last of these options is the desorption process. In the absence of decomposition the desorbing species will generally be the same as that originally adsorbed but this is not necessarily always the case.

The objective of the regeneration of spent activated carbon is to desorb accumulated adsorbates and restore the original porous structure with little or no damage to the carbon itself. Spent activated carbon can be regenerated by a variety of methods, but the process fundamentals are essentially the same. In most processes, regeneration is accomplished by subjecting the exhausted carbons to conditions that shift the adsorption equilibrium in favour of desorption. The relative ease of regeneration is dependent upon the type of adsorption (physical or chemical).

For physiosorption, this shift can usually be accomplished by heating, lowering the pressure or washing with solvent. In the case of chemisorptions, a supply of energy greater than the sorptive force is required to break the strong ionic or covalent bonds.

The most common method used for the regeneration of SAC is the thermal process. In addition to thermal regeneration, other methods discussed in the following sections include wet air oxidation, chemical, and solvent regeneration. No matter which method is used, it is important to note that the regeneration of SAC is dependent upon the characteristics of the base material, the activation process, and the type or types of adsorbate.

2.8.1. Methods and types of regeneration

Regeneration have been also referred as reactivation (Cabal et. al., 2009), Literature survey suggests that regeneration is better term for reuse of adsorbents as it includes both desorption and activation and also carves difference between desorption and regeneration. In better case the agent of desorption is also candidate for activation and hence activation step is skipped and hence regeneration can be explained as combination of desorption and activation. In the regeneration process the following factors influence on the effectiveness of the installation performance: the degree of solution purification, the separation of a mixture into the components, adsorbent stability, the degree of recovery of adsorbed components and energy consumption (Irfan et. al., 2013). The chosen regeneration method should ensure (Pelech et. al., 2005).

• The highest possible degree of desorption of the adsorbed compound
• The least possible erosion and the mechanical destruction of used adsorbent
• Easy access and the ecological safety of used regeneration agent
• Ease of separation of recovered or removed compounds from desorbate
• Invariable qualitative composition of desorbed components

Regeneration process can be either carried out on the site or can be carried offsite. Off site regeneration is generally carried out when the spent adsorption generation is very high. In this case spent adsorbent must be removed from the site and transported to regeneration site as hazardous material. Thermal offsite regeneration using kilns and furnaces have been reported. Off site regeneration facility should be designed to regenerate huge amount of adsorbents at a time to harvest more economical benefits.

However this situation becomes complicated when adsorbents laden with different target compounds from different sources arrive at regeneration facility and need to be commingled before regeneration. Onsite regeneration is considered to be expensive and thus rendering it impractical for smaller installations (Brady, 2005). On site regeneration is carried out for small adsorption facilities where the adsorbate concentration is high. On site regeneration is also recommended if spent adsorbent is considered as hazardous waste11. On-site regeneration is generally not cost-effective unless the carbon exhaustion rate is over 910 kg per day. Carbon reactivation unit cost rises rapidly if carbon usage is less than 2272 kg/day (Irfan et. al., 2013). .

In case of thermal regeneration which is most common the temperature of regeneration decides the site for regeneration, offsite regeneration in such case is only preferred when regeneration temperature is between 700^0C-1000^0C, moreover because of liability and economic concerns, many design manuals recommend that regeneration should be done offsite whenever possible, regardless of whether land and utilities are available on-site (Irfan et. al., 2013). The adsorbent losses due to attrition have been estimated as 5-10% for *in situ* regeneration and 10-15% for offsite regeneration (McKay 1996b).

However in actual practice the method adopted depends upon the cost of adsorbent and the nature of adsorbate. Amount of adsorbate adsorbed on virgin activated carbon can be determined from isotherm data however same adsorption capacity cannot be met after regeneration. This fraction of undesorbed adsorbate has been referred as heel (Alley 2007). As adsorption capacity is an experimentally determined parameter and on which many design and operation condition depends. In case of in situ regeneration it becomes consistently difficult to determine the adsorption capacity of regenerated adsorbent. Parmele et. al. (1979), expressed the most common rule which assumes half of the solvent adsorbed during the first full loading of the adsorber remains as a residual heel after regeneration, regardless of the properties of the adsorbate and the regeneration conditions but in case of offsite regeneration it can be recalculated before redeployment of adsorbent. In certain cases where adsorbate is a potential pollutant and its concentration is low and bed life is very long non regenerative systems may have a preference. However in such cases disposal after use is a potential hazard and thus regeneration with adsorbate destruction is important from environmental perspective

2.8.2. Steam regeneration

Discovery of steam power has been turning point of human history. Steam has been used in industry since long time now. This industrial familiarity of steam thus is not new. Most industrial setups are well acknowledged with steam operation and maintenance units and hence prefer steam regeneration. Steam regeneration is widely popular and cheap (Alley 2007; Gu & Bart, 2005). Even though steam is readily available in industry it can also be generated by skid mounted boiler units which are available at relatively low cost. Steam works especially well with hydrophobic organics, such as chlorinated solvents (Irfan et. al., 2013). Hydrophobic adsorbates have an added advantage in that they can be separated from the condensed water by gravity. Steam is less useful for hydrophilic contaminants such as alcohols, aldehydes, or ketones. If steam is used for these types of contaminants, the contaminants can be separated from the condensate by distillation. However, distillation raises the Operation and Maintenance costs of the system. Hydrophobic adsorbate desorbs at temperature approaching steam distillation temperature and hydrophilic adsorbate desorbs at temperature approaching their boiling points (Schweiger 1989). After regeneration of adsorbent bed, the condensed adsorbate can be recovered by separation techniques, multiplying benefits of steam regeneration.

Heating and purging properties of steam are important for regeneration and contribute equally to the regeneration of adsorbents (Irfan et. al., 2013). The source of energy for regeneration is heat of steam and heat of adsorption of water. The heat generated by adsorption of water cannot be neglected as a driving force for regeneration of adsorbents. During steam regeneration unlike purge gas regeneration the temperature don't drop significantly along the length of bed as the heat released due to adsorption is uniform throughout the bed. In Steam regeneration, the high heat of condensation of steam allows the bed to be heated up rapidly, allowing for a faster desorption from the adsorbent; the desorbate is however only swept out of the bed when the latter is hot enough such that at least some steam remains in gaseous form and can sufficiently purge the adsorbate (Küntzel et. al., 1999). Pelech et. al. (2005) gave following schematics to explain regeneration of activated carbon by steam at temperature T $<140^0$C and T $>140^0$C (Figure 3)

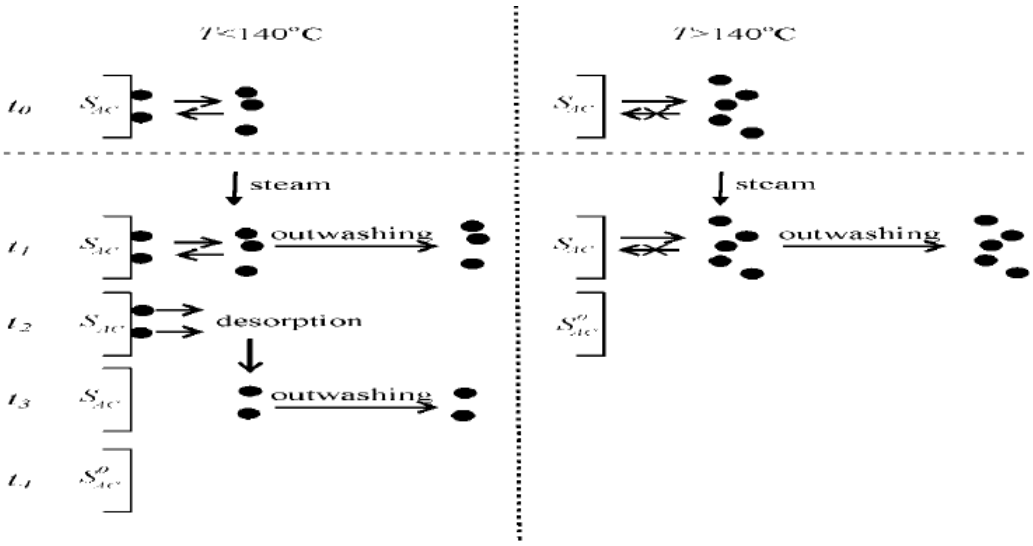

Figure 2.3: Schematics of steam regeneration (Pelech et. al., (2005), Where SAC is the surface of the activated carbon, S0AC is the surface of activated carbon after regeneration, t = time

The above schematics (Fig. 2.3) explain clearly the processes taking place during steam regeneration of adsorbents and also elucidate relation between temperature and steam consumption. The scheme explains more out washing of adsorbate is required at low temperatures. Pelech et. al. (2005) argued that, at temperatures T <140^0C there will be certain equilibrium between adsorbed molecules and that in the vapour phase. The flow of steam causes out washing of non adsorbed molecules. A decrease of the adsorbate is the vapour phase causes a shift of equilibrium in the direction of desorption. The desorption of chloro-organics proceeds to the vapour phase and out washing by the steam jet. The consecutive stages of out washing and desorption proceed up to the moment of the removal of adsorbate from the adsorbent surface. For T >140^0C the equilibrium is completely shifted to desorption and only out washing of adsorbate from the bed occurs. Temperature of adsorbent bed is critical in steam regeneration. Upon contact with a cold bed, the inlet steam immediately condenses and the system pressure drops, however after some time the desired conditions roll back, during this process the heat of condensation leads to rapid but brief heating. Sometimes bed is preheated to avoid condensation. Cabal et. al. (2009) found that time of steam regeneration need to be optimized as prolonged time of regeneration cause over reactivation and leads to gasification of adsorbent and damages porous networks of adsorbents. They also found that the steam doesn't modify the basic nature of

adsorbent and attributed the change in pH PZC of regenerated adsorbent to the non-desorbed adsorbate. Time of regeneration is an important design parameter and also directly linked to energy consumption and thus cost of regeneration. Regeneration is expected to be complete when effluent gas temperature reaches to regeneration temperature (Kumar & Dissinger, 1986), however this is not applicable to adiabatic systems. Irfan et. al. (2013) reported following five elementary processes taking place during steam regeneration of spent granulated activated carbon (GAC) from waste water treatment plant. (i) Thermal decomposition of activated carbon, (ii) oxidizing decomposition of activated carbon with steam, (iii) vaporization or sublimation of adsorbate, (iv) thermal decomposition and carbonization of adsorbate, and (v) oxidizing decomposition of carbonized matter with steam.

Different type of adsorbents responds differently to the steam regeneration depending upon their composition and manufacturing e.g., ACF bed was shown to have faster regeneration with steam then GAC bed (Kim et. al., 2001).

In steam regeneration additional adsorbate is introduced to system as water, which is not desired in both phases and must be removed from adsorber for re-adsorption step. Hence arises need of energy intensive drying step. Despite of this complexity steam is the classical regeneration process in case of activated carbons (Irfan et. al., 2013).

Steam regeneration can be high temperature or low temperature. High temperature steam regeneration is carried in inert environment in order to prevent oxidative reaction of steam with adsorbent and adsorbate which may also cause char formation and result in deterioration of porous network of adsorbent. For the same reason low temperature steam regeneration can be carried in air flow which is cheaper than inert flow. During the heating stage, the carbon passes through the following steps: drying (evaporation of water), thermal desorption (desorption of volatile compounds, 100-260°C), pyrolysis and carbonization (pyrolysis and carbonization of non-volatile compounds, 200-650°C) and gasification of pyrolytic residue at high temperature (650-850°C) in the presence of limited amounts of oxidant such as water vapour, oxygen, (Salvador & Jimenez, 1996). The selection of steam temperature depends upon the heat capacity of the adsorbent and the boiling point of organic adsorbate and solvency of inorganic adsorbate. For organic compounds temperature of steam is generally taken 30-50°C above the boiling point of adsorbate.

2.8.2.1. Reaction of steam with adsorbent

Kuhel and Timken, (2000) found that steaming of zeolite beta at 538°C for 10hours reduced the acid site concentration by 75%. Intense steaming of zeolites cause clefts in its crystalline structure, enhances mesoporosity and increases surface area from 1-3 m^2/g, leaving more freshly created Lewis sites accessible, while at same time leads to small decrease or no change in BET micropores surface area and micropore volume. The process of steam regeneration can be divided into following three steps

1. Desorption
2. Drying
3. Cooling

Desorption is carried by steam at desired temperature depending upon solubility of inorganic adsorbate or boiling point of organic compound. If the boiling point of the compound is less than 200°C effective regeneration can be achieved using steam (McKay 1996). Once temperature for regeneration is fixed, the combination of temperature and pressure is selected using phase diagram of water. Generally consumption of steam would be 3-5 kg of steam per kg of organic compound desorbed. Drying of bed is important as moisture left un-removed in bed can drastically affect the adsorption capacity and other operational performances. Drying ensure that leftover removable moisture as well as adsorbate is removed in order to bring bed back to identical defined starting condition as much as possible. Drying can be fast with heating or slow without heating. Drying is also fast at the beginning, when the bed is still warm, and it is slow after the bed has cooled to ambient temperature. Drying is most time and energy consuming step in steam regeneration. Drying phase should be designed considering time and cost. In fact in the real situations in industry where steam is mostly available drying is only step in steam regeneration where cost implication is very high. Drying gas used is generally air or inert gas like nitrogen (Irfan et. al., 2013).

2.8.3. Thermal Regeneration

The following steps are usual in the thermal regeneration of a spent carbon: drying, thermal desorption (removal of volatile organic compounds at 100-160°C), pyrolysis, carbonization (removal of non-volatile compounds at 200-260°C) and gasification (at 650-850°C) of residue (Salvador & Jimenez, 1996).

The first three steps, viz drying, vaporization, and pyrolysis, normally proceed with few complications. However, pyrolysis should not be conducted at temperatures higher than 500 °C in a non-oxidizing atmosphere, since graphitization of the pyrolysed residue can occur, resulting in a structure similar to that of activated carbon and equally refractive. Hence, during subsequent selective oxidation, it would be difficult to remove the residue without extensively damaging the structure of the activated carbon. Pyrolysed residues obtained at lower temperatures are reported to be more reactive, and therefore more readily oxidizable, than activated carbons. The proper reactivation of carbon does not involve direct oxidation of the pyrolysed residue with oxygen. On the contrary, the atmosphere within that zone of the furnace is deliberately depleted in oxygen so that the following reactions will be minimized:

$C + O_2 - CO2$ (2.4)

$C + 1/2O_2 - CO$ (2.5)

where C denotes the carbonaceous pyrolysed residue or the structure of the activated carbon. Since these reactions are exothermic, and therefore selfpromoting, they would, if allowed to occur, result in aggressive oxidation along the surface of the carbonaceous residue and of the original activated carbon. In practice, this would have the following effects. The pores would widen, the residue would not be removed from deep pores and, in general, the adsorption sites would not be reactivated. The result would be excessive losses of valuable activated carbon (Vliet, 1991).

In an atmosphere consisting of steam or carbon dioxide (besides nitrogen, which may also be present), the following endothermic reactions will predominate:

$C + H_2O - CO + H_2$ (2.6)

$C + CO_2 - 2CO.$ (2.7)

An input of energy is required to sustain these endothermic reactions, which constitute the principal reactions that can be effectively controlled in the oxidation and gasification of pyrolysed adsorbate with minimal damage to the structure of the activated carbon. Reaction (3) and the gas-phase reaction

$CO + H_2O \longrightarrow CO_2 + H_2.$ (2.8)

constitute the overall steam-carbon (water-gas) reaction that will predominate when the partial pressure of carbon dioxide, P_{CO2}, PH_2 is low compared with that of steam. Response of Different Compounds to Thermal Regeneration In thermal regeneration, the adsorbates associated with a spent carbon can be conveniently classified according to their responses, which are of the following types (Vliet, 1991).

Type I

Volatile organic compounds that were initially adsorbed onto the activated carbon but were not irreversibly bound to active surface sites undergo thermal desorption.

Type Il

Organic compounds that are not sufficiently volatile for thermal desorption, and or that are tenaciously bound to surface sites, undergo thermal decomposition (cracking) and form volatile fragments.

Type III

The remaining compounds are pyrolysed, and a carbonaceous residue is deposited concomitantly at about 800°c. Compounds that participate in this type of reaction are most critical in the regeneration process, since the carbonaceous residue has to be removed selectively, through endothermic oxidation with steam or carbon dioxide, at comparatively high temperatures (above 800°C). Within this temperature domain, losses of energy increase significantly, equipment specifications become more stringent and equipment more costly, and losses of the activated carbon backbone invariably occur concomitantly with the oxidation of the pyrolysed adsorbate residues. In reality, many organic adsorbates display different combinations of Types I to III behaviour.

2.8.3.1. Thermal Regeneration Conditions

Operating conditions during regeneration can be controlled to affect the required degree of regeneration of a spent carbon. The following parameters have an important influence on regeneration: furnace atmosphere, presence of inorganic constituents, and temperature and residence time.

a) Furnace Atmosphere

Thermal applications that employ the use of partial or complete steam atmospheres are examined here because this is the approach most commonly applied. The ruleof- thumb guideline of 1 kg of steam per kilogram of activated carbon has often been advanced as the requirement for the complete regeneration of spent carbon. In reality, the quantity of steam required depends on the kinetics of selective oxidation (gasification) of the pyrolysed residue. .

Umehara et. al. (1983) studied the kinetics of the reaction of steam with activated carbon containing a pyrolysed residue of OHS (a synthetic detergent) at 700 to 789°C and atmosphericpressure, and obtained data for different concentrations of steam and hydrogen. The results fitted a Langmuir- Hinshelwood rate equation, which had been developed originally for the oxidation of other types of carbon with steaml5. According to that formulation, equation (2.9) expresses the effect of the concentrations of hydrogen and steam on the gasification rate for a fixed initial loading of adsorbate. (The initial OHS loading on the carbon was 0,522 g/ g, and 45 per cent of this initial loading remained on the carbon as a non-volatile pyrolysed residue, which had to be selectively oxidized.)

$$R = \frac{k_1 P\ H_2O\ ,}{1 + k_2 PH_2 + k_3 PH_2 0} \qquad (2.9)$$

Where *R* is the reaction rate of steam gasification, ie. The kilograms of carbon residue burned per second per kilogram of virgin carbon in existence when the sample reaches the reaction temperature, kg/(kg.2) k_1 is the rate constant for the steam-gasification reaction, kg/(kg.s.Pa) k_2 and k_3 are rate parameters, Pa-^{I}

PH_2O and PH_2 are the partial pressures of steam and hyarogen respectively, pa. Various inorganic constituents can catalyse the steam carbon reaction, and can therefore accelerate the gasification of pyrolysed adsorbate residues, or even of base activated carbon. Such inorganic constituents can be present in the original structure of activated carbon, be adsorbed onto the carbon during usage, or be intrinsic parts of organic adsorbates. In the last-mentioned case, a non-volatile inorganic residue will be deposited, together with the carbonaceous residue, during the pyrolysis step of thermal-regeneration operations. Umehara et. al. (1982) have shown that an inorganic residue (sodium sulphate), which is deposited during the carbonization of a DBS-Ioaded carbon, exerts a substantial catalytic effect on the subsequent steam-motivated gasification of the carbonaceous residue. They obtained their evidence by measuring the rates of gasification for virgin carbon that had adsorbed various amounts of sodium sulphate before being regenerated, and for DBS loaded samples containing different amounts of inorganic residue. In both types of experiment, the rate was found to increase with the amount of inorganic material present. The rate of gasification was approximately the same when the samples contained the same fraction of inorganic material, either as added sodium sulphate (to virgin carbon) or as inorganic residue in the DBS-loaded samples. Furthermore, the reaction rate for thermally regenerated

samples was reduced significantly by washing with water (which dissolves some of the inorganic material), followed by gasification with steam. These findings agree with those of McKee (1981), who demonstrated the catalytic effect of sodium on the gasification rate of carbon. Harriott and Cheng, (1988) showed that the minerals present in activated carbons can change the reactivity of the carbons and of the pyrolysis residues. For example, for spent carbons prepared by the adsorption of sodium benzoate onto the carbon and pyrolysis at 700° C, the reactivity to oxygen increased with the amount of residue produced. Even when the residue represented only 5 per cent by mass of the base carbon, the rate was 3,5 times that for the (base) carbon.

2.8.3.2. Influence of Temperature and Residence Time

The influence of temperature and residence time on the selective oxidation of pyrolysed residues was described earlier. Within strict limits (approximately 650 to 900°C), a trade-off of temperature against residence time can yield optimum thermal reactivation of spent carbon. However, at temperatures above about 950°C, even very short residence times are likely to lead to excessive losses of activated carbon. On the other hand, at temperatures below 650°C, the rate of steam-carbon gasification becomes negligible, and impracticably long residence times may be needed for the proper reactivation of carbon.

2.8.3.3. Structural Changes during Thermal Treatment of New Carbon

In order to understand the various intraparticle structural changes that occur during progressive thermal treatment of an activated carbon, Vliet and Venter, (1985) tested a new activated carbon based on bituminous coal under a range of regeneration conditions. The first 10 minutes of treatment yielded small increases in the volume of the micro pores and. macropores, possibly owing to the removal of small amounts of substances adsorbed during transport and storage, and/or further refinement in the degree of activation of the raw material. During the residence-time interval from 10 to 30 minutes, an almost stoichiometric conversion of the micropores to mesopores took place, but the macropores were largely unaffected. The slight increase in the total pore volume during this period was probably due to erosion of the matrix between the micropores. After 30 minutes, further conversion of the micropores to larger pore types occurred, as well as progressive destruction of the activated-carbon matrix to yield

additional large-pore volume. The net result was an extensive loss of micropore volume, an increase in mesopore and macropore volume, and a concomitant decrease in mechanical strength. Conclusions based on total pore volume alone would therefore be very misleading since the total pore volume reflects only the net effect of substantial intraparticle changes. The micropore volume decreased by 44 per cent during the total 60-minute residence time, and the mesopore and macropore volumes increased by 66 and 50 per cent respectively.

2.8.3.4. Drawbacks of conventional thermal regeneration

Thermal regeneration is the most common type of regeneration for any kind of porous adsorbent. Various studies have discussed the thermal regeneration of saturated adsorbents (Moreno-Castilla et. al., 1995; Sabio et. al., 2004; Suzuki et. al., 1975). Thermal regeneration of activated carbon involves several steps. All the steps require a high temperature (Peng et al., 2006; Su et al., 2009) and therefore consume high energy. Dehydration of the adsorbent by heating becomes successful at around 300°C. (Tamanna, 2012). For activated carbon, another drawback is the loss of carbon due to attrition, burn-off and washout. Adsorbers can be corroded in a steam-generated regeneration unit (Price & Schmidt, 1998). Alvarez et. al. (2004) were able to regenerate spent granular carbon by using a mixture of CO_2 and nitrogen by removing phenol in a fixed bed column. Regeneration started at 127°C and lasted up to 827°C. A 15% weight loss (due to burn off) of the adsorbent was observed (Alvarez et. al., 2004). Baker (2008) developed a thermodynamic model to predict the improvement of the adsorption capacity of an adsorbent under thermal regeneration. The model showed that effective regeneration of zeolite was possible at a temperature greater than 150°C (Baker, 2008). The regeneration of HZSM-5 zeolite by using air (Vitolo et. al., 2001) and fluid catalytic cracking (Schulz & Wei, 1999) has also been reported to be highly energy-consuming. Bagreev et al. (2001) found that the regeneration of spent carbon by thermal regeneration was feasible at 300°C in air (oxidizing atmosphere).

2.8.4. Regeneration of activated carbon by microwave heating

Microwaves were used to regenerate activated carbon by keeping its adsorption capacity intact. This approach was perceived as a novel and economic regeneration method that would solve the problem of long regeneration time and the use of a large volume of purge gas (Mezey & Dinovo, 1982). Previous research highlighted the need

for an easy and convenient design and procedure to enhance regeneration under microwave irradiation (Woodmansee & Carroll, 1993).

The regeneration of activated carbon has been studied extensively by focusing on different methods of adsorbate removal. The success of regenerating granular activated carbon (GAC) by microwave irradiation has been found to be regulated by the adsorbate concentration, number of stages used, applied power, adsorbent dose, and types of bed used (Liu et. al., 2004a; Tai & Jou, 1999). As the concentration of the feed adsorbate increases, the regeneration time also increases. For reactors with initial phenol (adsorbate) concentration of 50 mg/L, complete removal occurred after 240 seconds while for reactors with initial concentrations of 5 mg/L it occurred after 120 seconds. Multistage reactor systems have been more efficient than single-stage reactors for larger surface areas and volumes (which provide more microwave absorption) (Tai & Jou, 1999). Microwave heating sometimes produces high temperature, which is capable of decomposing some of the adsorbates producing non-harmful gases (Liu et. al., 2004a; Tai & Jou, 1999). Typically, a higher microwave power application provides enhanced desorption. However, the applied power has to be greater than a certain minimum value to instigate desorption, and smaller than a certain higher value to prevent hotspots and burning.

Repetitive microwave applications preserve the mesopores of activated carbon but reduce micro porosity. Ania et. al. (2004, 2005) regenerated phenol saturated activated carbon by using microwave heating and compared their results with those from conventional electric furnace heating. It was found that both heating techniques reduced the micropores, but the reduction provided by conventional heating was more significant. The microwave heating was rapid and provided higher regeneration than electric furnace heating. Generally, a minimum sample size is also required for effective heating (Tai & Lee, 2007). Sometimes, microwave heating can produce intermediates depending on the adsorbate compounds. A study found that copper-loaded GAC increased the decomposition rate, but the cost became a concern (Liu et. al., 2004b). The rate of decomposition is regulated by the contact time of the carrier gas and GAC particles. The use of a fluidized bed instead of a fixed bed can compensate for carbon loss and the formation of any toxic intermediates (Jou, 1998).

Microwaves were also found to be successful in regenerating multi-component odorous compound saturated GAC in a relatively brief time (Robers et. al., 2005).

GAC requires a particular amount of energy to initiate the desorption process. The rate of desorption is slower at the beginning, but it gradually increases and then again decreases (when desorption is almost complete). Various studies reported the occurrence of arc formation during the heating period. The arcing of GAC begins during the preliminary state of heating and gradually increases as the temperature increases. The arcing spots illuminate at 5000-10,0000C and can give an audible and visible sense of their existence (Jou & Tai, 1998; Tai & Jou, 1999). Identifying the optimum regeneration condition is always difficult, and a trade-off is essential among the abrasion resistance, activity and adsorption capacity (Bradshaw & Van-Wyk, 1998; Clark & Sutton, 1996).

Activated carbon can be in different physical and chemical forms and shapes which are widely applied in the adsorption-regeneration of VOCs, water, NOx, and many other gasseous compounds. Spent powder-activated carbon (PAC) was successfully regenerated with microwave heating by desorbing ethanol and acetone (Fang & Lai, 1996), but carbon loss was a vital concern in this method.

Palletized activated carbon can also be used to remove VOCs and can be regenerated by microwaves, but its regeneration time is much longer than that of GAC (Cha & Carlisle, 2001, Coss & Cha, 2000).

Activated carbon fiber cloth (ACFC) is another form of activated carbon adsorbent. It can adsorb both polar and non-polar compounds and can be regenerated by microwave irradiation. Microwaves are capable of being selective in heating and therefore can desorb adsorbates, depending on their dielectric properties (Hashisho et. al., 2005). Microwave desorption allows for the sustainability of activated carbon over several cycles. In various studies, the sustainability has been demonstrated for 5 to 25 cycles of adsorption-desorption (Coss & Cha, 2000; Kong & Cha, 1995; Tai & Lee, 2007).

The literature shows that microwave heating enhances NOx adsorption capacity of coke and char, which perform as better adsorbents than activated carbon. Microwave heating increases the char surface area from 82 to 800m^2/g and converts 90% of the NOx gas into CO_2 and nitrogen. Toxic and unwanted pollutants such as CO and HNO_3 are produced as secondary pollutants and require a secondary treatment plant (Cha & Kong, 1995; Kong & Cha, 1995). The microwave desorption of chlorinated compounds provides a high removal rate. Whatever the source of the contaminant is, HCl is always a bi-product of the system. The result is extremely undesirable, so a secondary treatment is needed to remove the HCl (Lee et. al., 2010)**.**

2.8.5. Regeneration using wet air oxidation process

Wet air oxidation (WAO) is an aqueous phase oxidation process that uses molecular oxygen as an oxidant. The process operates at temperature from 125°C to 320°C and pressures from 0.5 – 20.3 MPa (Knopp et. al., 1978). Oxidation conditions vary, depending on whether partial or complete oxidation is desired.

Mundale et. al. (1991) studied the regeneration of activated carbon loaded with phenol. Using a WAO process, experiments were conducted at temperatures 150°C and 185°C and an oxygen partial pressure 0.5 MPa. They reported 5 – 10% and negligible losses, respectively, at temperatures of 185°C and 150°C. The loss of adsorption capacity was attributed to surface oxidation as well as the formation of carbon-oxygen complexes on the surface of carbon.

The rate controlling step was found to be the reaction between the dissolved oxygen and the desorbed phenol. A second set of experiments conducted using non-contaminated carbon showed that surface oxidation occurred even in the absence of the adsorbate.

A study by Gitchel et. al. (1980) reported that an increase in activation was observed after wet oxidation of non-contaminated AC. For temperatures ranging from 200 – 300°C, a pore volume greater than virgin AC was observed for all pore diameters. The largest increase in volume was observed in pore diameters greater than 600 angstroms.

2.8.6. Regeneration using Advanced Oxidation Technologies

Advanced oxidation processes (AOPs) are methods to produce hydroxyl radicals (HO.), highly reactive species that induce non-selective oxidation of a wide range of organic compounds (Augugliaro et. al., 2006), leading in some cases to their complete mineralization. There are different methods to generate hydroxyl radicals based on chemical oxidation (O_3/H_2O_2, Fenton, Permanganate, Persulfate), UV-oxidation (Vacuum UV, Photo-Fenton, H_2O_2/UV, H_2O_2/O_3/UV, TiO_2/UV), non-thermal gas plasmas, electrohydraulic discharge, electrocatalytic and electrochemical oxidation (Maria 2015). The Fenton reaction is a dark process that consists in the combination of Fe (II) with hydrogen peroxide (Fenton's reagent) to produce hydroxyl radicals according to equation (Augugliaro et. al., 2006; Muranaka & Julcour, 2009):

$$Fe^{2+} + H_2O_2 \rightarrow Fe^{3+} + OH- + \cdot OH \qquad (2.10)$$

This process is accelerated by UV irradiation, and is then referred to as the photo-Fenton process. The photo-Fenton reaction is activated up to a light wavelength of 600 nm (Ballari et. al., 2008). Heterogeneous photocatalysis is an AOP based on the generation of hydroxyl radicals (OH.) using UV-Vis radiation (Gogate & Pandit, 2004; Chong et. al., 2010). The free radical mechanism is initiated with catalysts such as TiO_2 (Mozia, 2010). The photocatalyst needs to be activated photonically. The photo-induced reactive species oxidize almost any chemical specie or microorganism yielding carbon dioxide and inorganic ions such as nitrate and sulphate (Gogate & Pandit, 2004). The hydroxyl radical can react in aqueous solution through three possible mechanisms: hydrogen abstraction, electron transfer, and radical addition (Augugliaro et. al., 2006). The overall heterogeneous photocatalytic process can be divided into five steps (Herrmann, 1999): firstly, transfer of reactant in the fluid phase to the photocatalyst surface, secondly, adsorption of reactant on its surface, thirdly reaction in the adsorbed phase, fourthly desorption of the products, and lastly, removal of products from the interface region. Titanium dioxide (TiO_2) belongs to the family of transition metal oxides and titanium is the world's fourth most abundant metal (Carp, 2004). Four natural crystal structures of TiO_2 exist but only anatase and rutile demonstrate photocatalytic properties (Gogate & Pandit, 2004) mainly attributed to its microstructure and physical properties. It is also known that anatase is photocatalytically more active than rutile but a synergistic effect, not well understood yet, has been obtained by combining both crystalline forms (Gogate & Pandit, 2004). Commercially available P25 Degussa, which is a mixture of 75-80 % anatase and 25-20% rutile is generally used in photocatalysis research. TiO_2 semiconductor photocatalysis is explained in terms of a band gap model with five key steps: photoexcitation, diffusion, recombination, hole trapping and oxidation. When a semiconductor of the chalcogenide type (oxides such as TiO_2, ZnO, ZrO_2 and CeO_2, or sulphides such as CdS and ZnS) is irradiated with light (Herrmann, 1999), the photons with an equal or higher energy than its band gap energy can be absorbed and an electron is promoted to the conduction band (CB), leaving a hole in the valence band (VB) and, hence activating the photoinduced reactions (Carp, 2004; Mozia, 2010). One of the drawbacks in that most of the energy is lost because electron-hole recombination occurs faster than the generation of hydroxyl radicals. Highly reactive species pathways occurring in photocatalysis were described by Carp (2004).

The band gap model is comprised by two reactions occurring simultaneously and generated by the UV irradiation (Carp, 2004; Mozia, 2010):

A. Absorption of photons to create electron-hole pairs

$$\boldsymbol{TiO_2} + \boldsymbol{hv} \rightarrow (\boldsymbol{eCB}- + \boldsymbol{hVB}+) \quad (2.11)$$

B. Separation and migration of the photo-generated electrons and holes

C. Oxidation from photo-generated holes

$$\boldsymbol{Organic\ compound} + (\boldsymbol{hVB} +) \rightarrow \boldsymbol{oxidation\ products} \quad (2.12)$$

D. Reduction from photo-generated electrons

$$\boldsymbol{Organic\ compound} + (\boldsymbol{eCB}-) \rightarrow \boldsymbol{reduction\ products} \quad (2.13)$$

E. Oxygen acts as primary electron acceptor and the highly reactive hydroxyl radicals (OH.) are supposed to be the primary oxidizing species in the photocatalytic oxidation processes

$$\boldsymbol{Organic\ compd.} + \boldsymbol{Hydroxyl\ radical} \rightarrow \boldsymbol{degradation\ products} \quad (2.14)$$

compared to water treatment by only photocatalysis. These operations are ultrasonic irradiation, photo-Fenton reaction, ozonation, and electrochemical treatment (Augugliaro et. al., 2006). And also with operations that does not affect the mentioned chemical mechanism but rather improves the overall process through a two-step treatment, such as biological treatment, membrane reactor, and physical adsorption. The photocatalytic process preceding the biological one is intended to modify the structure of pollutants by converting them into biodegradable intermediates, and the coupling of membrane filtration with photocatalysis offers the advantage of easy photocatalyst recovery and continuous regime.

The regeneration of spent adsorbents using UV/TiO_2 heterogeneous photocatalysis has been demonstrated by several researchers. Some researchers have investigated the photocatalytic regeneration of an adsorbent polymer saturated with different cationic dyes using TiO_2 photocatalysis (Dhodapkar et. al., 2007). They concluded that the regeneration of the spent adsorbent was effective through several cycles with only 10% reduction of the adsorption capacity of the original carbon, attributed by the authors to the blocking of active sites by TiO_2. Other researchers studied the regeneration of baker's yeast biosorbent and simultaneous photodegradation of the desorbed dye using acid TiO_2 hydrosol under sunlight (Yu et. al., 2009). Under this particular integrated biosorption and photocatalytic oxidation system, dyes were desorbed and simultaneously degraded at acid conditions. The analysis of the adsorption,

regeneration and reuse of spent modified sugarcane bagasse adsorbent (methylene blue as adsorbate) through TiO_2/UV photocatalysis has been reported (Xing, et. al., 2010). Effective regeneration of the spent adsorbent, but with poorer adsorption (85% of neat adsorption capacity of the adsorbent) was the authors' main conclusion. Other workers have researched the technical feasibility of using heterogeneous advanced oxidation for the regeneration of a spent commercial activated carbon, loaded with chloroform and regenerated in TiO_2 slurry reactor using artificial and solar radiation (Notthakun et. al., 1993). Regeneration times longer than adsorption times were found for capacity recoveries higher than 90% in TiO_2 slurry reactors. Only when TiO_2 was not suspended, but instead impregnated in the carbon, was the regeneration time reduced to one-fifth of the adsorption time, attributed by the authors to the elimination of diffusion step from the exterior surface of the adsorbent to the catalyst where the reaction takes place. But they could not justify the use of the adsorption step, due to the higher amount of oxidant consumed in the hybrid process with respect to conventional AOP. Some researchers (Notthakun et. al., 1993; Mourand et. al., 1995; Muranaka & Julcour, 2009; Yu et. al., 2009) compared the coupled adsorption and AOP system with conventional AOP, whilst other workers (Huling & Arnold, 2000; Dhodapkar et. al., 2007; Xing, et. al., 2010) did not provide a similar comparison, therefore, the full justification of the adsorption and AOP hybrid combination was not fully demonstrated. With the exception of the studies of Notthakun et. al. (1993), all the work undertaken to date with TiO_2 was done at a small scale, using volumes not greater than 500 mL, and regenerated carbon masses of the order of milligrams. Notthakun et al. in a later publication investigated the regeneration of spent adsorbents using homogeneous advanced oxidation (Mourand et. al., 1995), which has led to a greater number of research publication with apparently promising results so far (Huling et. al., 2005, 2012; Huling, et. al., 2009; Muranaka & Julcour, 2009). Whilst most of the adsorbents applied in Fenton experiments were well known commercial types, some of the adsorbents selected to carry out regeneration using TiO_2 photocatalysis were of very low capacity, as low as 22.36 mg/g (Dhodapkar et. al., 2007) or 52.6 mg/g (Yu et. al., 2009). Furthermore, in general the scale of the experiments performed with in TiO_2 investigations as compared with the Fenton approach was lower (Maria, 2015).

2.8.7 Chemical regeneration

Chemical regeneration is a process in which adsorbates are removed from spent carbon by reacting with suitable chemical reagents. In general, two types of reagents are used: those with oxidizing ability and those with solublizing ability. Subsequent washing with water is required to remove the regenerating agent.

Chemical regeneration exhibits several advantages over thermal regeneration. The process can be done in situ which eliminates losses due to pumping, transport and repacking. Additionally, carbon loss due to burn-off is eliminated and the recovery of adsorbates is possible by using subsequent treatment methods such as distillation.

The disadvantages associated with chemical regeneration include the high cost of reagents, danger of pollution from hazardous chemicals, and incomplete regeneration. The amount of regeneration is dependent primarily on the solubility of the adsorbate in the regeneration solution. Additionally, since most industrial wastewater contains a heterogeneous mixture of adsorbates, multiple regenerants are required.

Leng and Pinto, (1996) reported that the solubility of organic adsorbates and surface characteristics of the adsorbent strongly influence regeneration efficiency. By using reactive reagents and controlling surface charge characteristics through pH, they were to enhance the solubility of selected organic adsorbates in aqueous solutions.

2.8.8. Solvent regeneration

Solvent regeneration is an extraction process that involves passing a solvent through a bed of exhausted carbon to dissolve the adsorbed materials. Two types of extraction discussed in literature include water regeneration and supercritical CO_2 regeneration.

Salvador and Jimenez, (1996) studied subcritical water regeneration (300°C and 12.2MPa) of three types of carbon exhausted with phenols, textile dyes and pesticides. They reported that phenol desorbs at low temperature (155°C), dyes (sirrus red) at medium temperature (263°C), and carbofuran, a pesticide, begins to release at 100°C but does not completely desorb until above 325°C. For all cases, even after seven regenerations, complete regeneration of the virgin adsorption capacity was achieved. In some cases, there was an increase in adsorption capacity after the first regeneration. This increase was attributed to a slight increase in carbon activation caused by dissolved gases or a better cleaning of the pores with high temperature water.

Regeneration of spent activated carbon with supercritical CO_2 has been proposed as an alternative to conventional thermal regeneration (Modell et. al., 1980). A significant advantage of supercritical CO_2 is its low critical temperature (31.06^{o}C) and critical pressure (7.38 MPa).studies investigating the use of supercritical CO_2 to regenerate SAC have shown mixed results. It appears the ease of regeneration is dependent upon the strength of adsorption. In most cases, the results indicated that a steady state adsorption capacity was achieved by supercritical CO_2 regeneration. For SAC exhausted with phenol, Model et. al. (1980) reported 20% decline in adsorption capacity after one regeneration stage .This 20% reduction remained constant during successive cycles and was attributed to irreversible binding of phenol to surface oxides during the first adsorption cycle The surface oxides provided high-energy sites capable of chemisorptions. In the same study, they reported complete restoration of activated carbon exhausted with acetic acid after each of eight adsorption and regeneration cycles.

2.9. Review of previous works

Emad et. al. (2006) studied Equilibrium adsorption isotherm for the removal of basic dye (Methylene Blue) from aqueous solution using bituminous coal-based activate carbon. The effect of experimental parameters, namely, pH and adsorbent particle size were studied. The results indicated the potential use of the adsorbent for the removal of Methylene Blue (MB) from aqueous solution. Maximum adsorption capacity of 580 mg/g at equilibrium was achieved. They found that pH played a major role in the adsorption process. The optimum pH for the removal of MB from aqueous solution under the experimental conditions used was 11. The Redlich–Peterson isotherm was found to best fit the experimental data over the whole concentration range as indicating from the high values of the correlation coefficients ($r^2 > 0.99$).

Tan et. al. (2007) studied the Equilibrium and kinetic studies on basic dye adsorption by oil palm fibre activated carbon. Adsorption isotherm of methylene blue onto the prepared activated carbon was determined by batch tests. The adsorption capacity was found to increase with increase in the three parameters (contact time, initial MB concentration, temperature) studied. The equilibrium data were best represented by the Langmuir isotherm, with maximum monolayer adsorption capacity of 277.78 mg/g at 30 ◦C. The adsorption kinetics was found to follow the pseudo-second-order kinetic model.

Tan et. al. (2007) studied Optimization of preparation conditions for activated carbons from coconut husk using response surface methodology Coconut husk was used to prepare activated carbon using physiochemical activation method, consisted of potassium hydroxide (KOH) treatment and carbon dioxide (CO_2) gasification. The effects of the preparation variables which were activation temperature, activation time and chemical impregnation (KOH:char) ratio on the adsorption capacity on methylene blue dye and carbon yield were investigated. Based on the central composite design (CCD), a two factor interaction (2FI) model and a quadratic model were respectively developed to correlate the preparation variables to the adsorption capacity and yield. The optimum conditions for preparing activated carbon from coconut husk were found as follows: activation temperature of 816 ◦C, activation time of 1 h and KOH:char ratio of 3.9.

Emmanuel et. al. (2009) studied Multistage optimization of the adsorption of methylene blue dye onto defatted Carica papaya seeds. The adsorption capacities of the defatted Carica papaya seeds were 1250 and 769.23mgg−1.The presence of carboxylic acid, phenolic and lactone functional groups were confirmed by surface chemistry studies. Adsorption of MB dye onto DPS adsorbent was found to be exothermic and spontaneous.

Yang and Qiu (2010) studied the Preparation of activated carbons from walnut shells via vacuum chemical activation and their application for methylene blue removal. To optimize the preparation method, the effects of the main process parameters (such as system pressure, activation temperature, and impregnation ratio) on the properties (expressed in terms of specific surface area and pore volume) of the obtained activated carbons were studied. It was found that the optimum activated carbon obtained with system pressure of 30 kPa, activation temperature of 450 ◦C, and impregnation ratio of 2.0 has a BET surface area of 1800m^2/g and total pore volume of 1.176cm^3/g. The results showed that the methylene blue adsorption capacity was positively correlated to the BET surface area. The highest methylene blue adsorption capacity was 315 mg/g for the optimum activated carbon.

Mahmoud et. al. (2012) studied on Batch adsorption of basic dye using acid treated kenaf fibre char: Equilibrium, kinetic and thermodynamic studies. An adsorbent (H-KFC) was prepared from kenaf fibre char by acid treatment using HCl (3M). The treatment caused an increase in the BET surface area and as a result there was an

increase in the adsorption of Methylene blue dye (MB) in batch system studies. The adsorption process was investigated by varying the initial dye concentration, adsorbent dose, pH and temperature. The highest percentage removal of Methylene blue dye (MB) was found to be 95 wt% at a concentration of 50 mg/l. At a pH of 8.5, the sorption of dye was favourable. The equilibrium data was analysed using the Langmuir, Freundlich and Temkin isotherm models. It was found that the equilibrium data was best represented by the Langmuir isotherm model. The kinetic data obtained was analysed using a pseudo-first-order and pseudo-second-order equation. The experimental data fitted well the pseudo-second-order kinetic model. The intraparticle diffusion model showed three steps where intraparticle diffusion was not the only rate controlling step of the adsorption process. Thermodynamic studies indicated that the adsorption was endothermic, increasing in randomness of adsorbed species and spontaneous at high temperatures.

Foo and Hameed (2012e) studied effects of activation agents on coconut husk derived carbon via microwave induced activation: Preparation of activated carbon has been attempted from coconut husk (CHAC) via microwave assisted chemical activation. The operational parameters including the effects of activation agents, chemical impregnation ratio (0.25–2.00), microwave power (90–800 W) and irradiation time (4–8 min) on the carbon yield and adsorption capability were investigated. CHAC was examined by pore structural analysis, The best conditions (KOH as activating agent, IR of 1.25, microwave power of 600 W and radiation time of 6 min) resulted in CHAC with a monolayer adsorption capacity of 418.15 mg/g for MB and carbon yield of 80.75%. Equilibrium data were favorably described by the Langmuir isotherm, while the adsorption kinetic was satisfactory fitted to the pseudo-second-order model.

Foo and Hameed (2012b) studied Textural porosity, surface chemistry and adsorptive properties of durian shell derived activated carbon prepared by microwave assisted NaOH activation. This study reports the preparation of activated carbon from durian shell (DSAC) by microwave assisted NaOH activation. The operational parameters including chemical impregnation ratio (0.25–2.00), microwave power (90–800 W) and irradiation time (4–8 min) on the carbon yield and adsorption capability were investigated. The best conditions resulted in DSAC with a monolayer adsorption capacity for MB of 410.85 mg/g, while the BET surface area and total pore volume were identified to be 1475.48 m^2/g and 0.841 m3/g, respectively.

Foo and Hameed (2012f) studied Microwave-assisted preparation of oil palm fiber activated carbon for methylene blue adsorption. Their study explored the viability of microwave irradiation for the preparation of activated carbon (OPAC) from oil palm fiber, abundantly available from the oil palm processing industries. The activation process was performed at the microwave power of 360W and irradiation time of 5 min. The BET surface area, pore volume and average pore size of OPACwere 707.79m2/g, 0.3805m3/g and 22.11A˚ , respectively. The monolayer adsorption capacity of OPAC for methylene blue was 312.5 mg/g. The finding provides a strong evidence to support the potential use of microwave heating as an alternative activation technique.

Ahmad and Alrozi (2010) studied optimization of preparation conditions for mangosteen peel-based activated carbons for the removal of Remazol Brilliant Blue R using response surface methodology. Their study investigates the optimal conditions for preparation of activated carbons from mangosteen peel (MP) for removal of Remazol Brilliant Blue R (RBBR) reactive dye from aqueous solution. The MP activated carbon was prepared using physiochemical activation method which consisted of potassium hydroxide (KOH) treatment and carbon dioxide (CO2) gasification. Central composite design (CCD) was used to determine the effects of the three preparation variables; CO2 activation temperature, CO_2 activation time and KOH impregnation ratio (IR) on RBBR percentage removal and activated carbon yield. Based on the CCD, a quadratic model and a two-factor interaction (2FI) model were respectively developed for RBBR percentage removal and carbon yield. The optimum conditions for MP activated carbon preparation were obtained by using activation temperature of 828°C, activation time of 1 h and IR of 3.0, which resulted in 80.35% of RBBR removal and 20.76% of activated carbon yield.

Auta and Hameed (2011) studied Optimized waste tea activated carbon for adsorption of Methylene Blue and Acid Blue 29 dyes using response surface methodology. Waste tea activated carbon (WTAC) was produced at optimum conditions for adsorption of both anionic and cationic dyes. The WTAC was produced through chemical activation with potassium acetate for adsorption of Methylene Blue (MB) and Acid Blue 29 (AB29) dyes. Response surface methodology statistical technique was used to optimize the preparation conditions which were activation temperature, activation time and chemical impregnation ratio (IR); with percentage yield and removal as the targeted responses. The optimal conditions obtained for good percentage yield and removal of the two dyes were at 800 ^{o}C, IR 1.4 and 120 min. The high surface area of 854.30 m^2/g

and mesoporous adsorbent prepared gave good adsorption capacities of 453.12 and 554.30 mg/g for AB29 and MB, respectively. Adsorption data were modeled using Langmuir, Freundlich and Temkin adsorption isotherms; the adsorption of MB and AB29 on WTAC both obeyed Langmuir model and, pseudo-second-order kinetics was the order that best described the two adsorption processes.

Sener (2008) studied the use of solid wastes of the soda ash plant as an adsorbent for the removal of anionic dyes: Equilibrium and kinetic studies. The results indicated that adsorption was strongly pH dependent. The typical dependence of dye uptake on temperature and the kinetics of adsorption indicated the process to be chemisorption. The results showed that as the pH increased, extent of dye uptake increased and $Ca(OH)_2$ particles precipitated at higher pHs were mainly responsible for the removal of anionic Procion Crimson H-EXL (Reactive Red 231) dye. The necessary time to reach the equilibrium was found to be less than 2 min. Dye uptake process followed the pseudo-second-order rate expression. The Freundlich isotherm best fitted for the adsorption of the dye on SW. The thermodynamics of PC/SW system indicated spontaneous and exothermic nature of the process.

Vliet (1991) reviewed regeneration of activated carbon. He stated that chemical methods of regenerations are effective in restoring the activity of spent activated carbon containing only single or defined adsorbates, while thermal regeneration have to be used when the spent carbon is loaded with a heterogeneous mixture of adsorbates such as those normally present in industrial process stream and effluents.

Sun et. al. (2009) worked on chemical regeneration of exhausted granular activated carbon used in citric acid fermentation solution decolouration. They found out that during chemical regeneration process of granular activated carbon exhausted from citric acid fermentation solution, liquid water washing, oxidant and surfactant working can raise the regeneration efficiency on the base of conventional acid-alkali regeneration. This method got 95% regeneration yield which was much higher than that of steam regeneration (78%).

Nahm et. al. (2012) tested different regeneration methods, thermal air, acid aqueous washing and two-step combined treatment, for regeneration of spent activated carbon and also examined their adsorptive behaviours as alternative adsorbents for removal of toxic compounds. The results of the overall characterization and adsorption breakthrough indicate that the combined treatment of both thermal air (200^oC) and oxalic acid aqueous in series is more efficient in recovering the surface properties of

the spent activated carbon than the individual thermal air and acid aqueous washing treatment.

Guocheng et. al. (2012) worked in regeneration of caramel saturated activated carbon jointly by microwave and extractive method. They found out that microwave assisted activated carbon regeneration could be achieved within 10min with a regeneration efficiency of 85%. Maximum regeneration efficiency and adsorption of MB and iodine were obtained at a microwave radiation power of 680W and an activation value of 9-10.

Foo and Hameed (2012a) worked in microwave assisted regeneration of activated carbon. They found out that microwave irradiation preserved the pore structure, original active sites and adsorption capacity of the regenerated activated carbons. The carbon yield and the monolyger adsorption capacities for MB were maintained at 68.35-82.84% and 154.65-195.22mglg, even after five adsorption-regeneration cycles.

Calisken et al. (2012) worked low temperature regeneration of activated carbon using microwave revising conventional Wisdom. Contrary to expectations, microwave assisted regeneration did not lead to better results than those obtained under conventional electric heating.

Castilla et. al. (1995) worked in thermal regeneration of activated carbon exhausted with different substituted phenols. They found out that during the heat treatment, part of the phenol evolved from the activated carbon and was deposited at the outlet of the reactor and part underwent degradation to light gases and to a residue that remained on the surface of the activated carbon.

Rege et. al. (1998) worked on desorption by ultrasound of phenol on activated carbon and polymeric resin. They found out that both types of sorbents showed an enhancement in desorption rate in the presence of ultrasound at 40kHz that was greater than that observed on the nonsoinic case. However, activated carbon showed a tendency to be pulverized under the action of ultrasound at 40kHz.

Qing-zhu et. al. (2009) studied lead desorption from modified spent grain. They observed that lead desorption was fast, took less than 15mins with 0.1mol/l HCl. The elution efficiency decreased as temperature increased (15-45°C) and also decreased with increasing loads of Pb(ii) at the same temperature.

Dehdashti et. al. (2010) studied regeneration of granular activated carbon saturated with gaseous toluene by microwave irradiation. They noticed that toluene removal increased steeply within a few minutes and reached over 90% under microwave

radiation at higher power level. High recovery efficiency was obtained under microwave treatment. However, they noticed activated carbon loss after ten successive regeneration cycles. They concluded that microwave recovery of saturated activated carbon loaded with toluene maintained the adsorption capacity, surface are and porosity structure of the activated in favourable circumstances.

Mata et. al. (2010) studied the sorption, desorption, regeneration and reuse of sugar-beet pectin gels for heavy metal removal. They found out that the sugar-beet pectin xerogels were stable sorbents able to resist multiple sorption-desorption-regeneration cycles using 0.1M HNO_3 and 1M $CaCl_2$ as desorbing and regenerating agents respectively. Despite an average 20% biomass loss due to biosorbent reuse in successive cycles, regeneration with 1M $CaCl_2$ favoured metal biosorption.

Purkait et. al. (2007) worked on the removal of congo red using activated crbon and its regeneration. The desorption was studied using surfactant enhanced carbon regeneration (SECR) technique. They observed that a highly basic pH lead to better dye desorption (about 32.5% desorption at pH of 11). Use of cationic surfactant resulted in only about 2% desorption (about 40 and 65% respectively) were obtained using anionic surfactants such as SDS and AOT.

Muhammad et. al. (2011) studied the isotherm of desorption of β-carotene from mesoporous carbon coated monolith and its regeneration. The applicability of Langmuir model to desorption data confirms active involvement of homogeneous site in desorption process. The observed increase in desorption rate as temperature was increased from 30-50°C indicated endothermic process. The regeneration study showed loss in RE% by both chemical and thermal process. The RE% after three consecutive cycles was reduced to 60.04% and 81.62% for chemical process and thermal process respectively.

Chern and Wu (2001) studied effect of temperature, pH and alcohol on the desorption of the dye from activated carbon beds. They found out that 25°C water was a poor regenerant for the carbon bed presaturated with the yellow dye compared with 20% alcohol solution.

Hosseini et al., (2011) studied the adsorption and desorption of carbon coated monolith, a mesoporous material for the removal of methyl orange from aqueous phase. They observed that desorption studies showed maximum recovery of methyl orange in alkaline medium. The increase in desorption was observed in MO

concentration. Regeneration studies showed 35-12% drop in adsorption capacity for initial three cycles. The adsorption remains almost constant for the consecutive cycles.

Nwabanne and Igbokwe (2012a) studied the kinetics and thermodynamics of lead (11) uptake from aqueous using palmyra palm nut (PPN) as potential raw material for the preparation of activated carbon. The amount of Pb2+ adsorbed was found to be dependent on adsorbent dosage, pH, and particle size. The equilibrium data conformed to Langmuir and Freundlich models while pseudo second-order best described the kinetics of the adsorption process. The thermodynamics parameters such as enthalpy, entropy and free energy were evaluated using the van't Hoff equations. The determined negative free energy changes (ΔG) and positive entropy changes (ΔS) indicate the feasibility and spontaneous nature of the adsorption process.

Nwabanne et al., (2010) studied the adsorption of methyl orange dye by an agro waste based activated carbon prepared from palmyra nuts. The activated carbon was prepared using chemical activation with phosphoric acid (H3PO4). It was observed that the percentage removal of dye increased with increasing adsorbent dosage and contact time, but decreased with increasing dye concentration and adsorbent particle size. The highest uptake of 97.5% was observed at a pH of 8.0. The adsorption process was well described by Langmuir isotherm and conformed well to pseudo-first-order and pseudo-second-order kinetic models.

Nwabanne and Igbokwe (2011) studied the removal of copper (11) from aqueous solution using palmyra palm nut (PPN) activated carbon. Chemical activation using phosphoric acid (H3PO4) was employed for the preparation of activated carbon. The percentage of Cu2+ adsorbed was found to be dependent on adsorbent dosage, pH and particle size. The equilibrium data was best described by Freundlich model. Pseudo second-order model best described kinetics of the adsorption process.

Nwabanne and Igbokwe (2008) studied kinetics and equilibrium modelling of nickel adsorption by cassava peel. The cassava peel was activated with zinc chloride. It was observed that percentage of nickel removal decreased with increasing adsorbent dosage. The equilibrium data fitted well to Freundlich, Langmuir, and Temkin models. Result indicated that nickel uptake process followed pseudo second order rate expression.

Igwegbe et al., (2015) studied the kinetics, isotherms and thermodynamics of the removal of malachite green on Dacryodes edulis seeds. The adsorbent was prepared by chemical activation methods using phosphoric acid and sodium chloride. The pseudo

second-order kinetic model was found to best correlate the experimental data. The intra-particle diffusion is not the only rate controlling step in the process. The experimental data were found to follow the Langmuir, Freundlich and Tempkin isotherm models. The negative free energy indicated that the adsorption processes were spontaneously feasible. The process of adsorption was found to be endothermic in nature

Nwabanne and Igbokwe (2012b) studied the adsorption of lead(II) from wastewater effluents using indigenous cellulose based waste biomass, such as nipa palm nut (NPN), palmyra palm nut (PPN), oil palm empty fruit bunch (EFB), oil palm fibre (OPF), and oil palm shell (OPS). Chemical activation method was used in preparing the activated carbon. The amount of Pb2+ adsorbed increased with increase in adsorbent dosage, and contact time and decreased with increase in particle size and initial ion concentration. The optimum pH was obtained at pH6 for all the adsorbents. The equilibrium data were best described by Freundlich model.

Elijah and Nwabanne (2014a) studied the adsorption including the kinetics and thermodynamics in the removal of Eriochrome black-T (EBT) dye using local clay. Acid activation was achieved using hydrochloric acid (HCl) and tetraoxosulphate (vi) acid (H_2SO_4). Under the same conditions, the clay activated with HCl was seen to be a better adsorbent than the clay activated with H_2SO_4. In the equilibrium studies, Freundlich isotherm best conformed to the adsorption data. The kinetic study showed that the Pseudo second-order and Battachayra-Venkobachormodels best described the kinetics of the adsorption process. The positive ΔS and negative ΔG values indicated that the adsorption process was feasible and spontaneous.

Elijah, and Nwabanne (2014b) studied the isotherms, kinetics and thermodynamics of the adsorption of malachite green dye from aqueous solution using local clay from Nigeria. The clay was prepared for adsorption by chemical activation with sulphuric acid and hydrochloric acid. It was seen that the adsorption most fitted the Freundlich isotherm. The kinetic study showed that Pseudo second-order model best described the kinetics of the adsorption. A maximum adsorption capacity (qe) of 32.147 mg/g and 32.633 mg/g was obtained for the clay activated with sulphuric acid and hydrochloric acid respectively. The entropy changes (ΔS) and enthalpy change (ΔH) were positive suggesting that the adsorption process increases in entropy and is endothermic in nature respectively. The negative ΔG value confirms the spontaneity of the process.

Ugonabo, et al., (2008) studied the treatment of wastewater from vegetable oil industry using modified laterite adsorbent. Effluent waste water samples were treated in an adsorption column set-up using different dosages of low-cost laterite adsorbent. Results obtained after the treatment process showed that all the parameters tested for conformed to the Federal Ministry of Environment, Housing and Urban Development (FMEHUD) specification guidelines, with exception of the following parameters which the values were astronomically - BOD (179.425mg/l) TSS (111.25 mg/l), oil and grease (4.20 mg/l) and electrical conductivity (1.26 x 103 Ωcm-1). The maximum percentage reduction of the pollutants was achieved at a high dosage of laterite (350g). The adsorption process also obeyed the Freudlich and Langmuir Isotherms.

Ajemba, et al. (2012) studied the kinetics, equilibrium, and thermodynamics studies of colour pigments removal from palm oil using activated ukpor clay.

The data fitted very well to the Pseudo-second order kinetic model with a regression coefficient of 0.995. The equilibrium data conformed to the Freundlich isotherm model with regression coefficient of 0.998. The activation energy was calculated as 18kJ/mol, while the other thermodynamics parameters were determined as $\Delta S = 0.075$J/mol, $\Delta H = 43.565$J/mol, and $\Delta G = -74.347$kJ/mol. These values indicate that the removal of colour pigment from refined palm oil by acid activated Ukpor clay is exothermic and can be attributed to a physico-chemical adsorption process.

Nwabanne and Igbokwe (2012c) studied the mechanism of Copper (II) removal from aqueous solution using activated carbon Prepared from different agricultural materials like; nipa palm nut (NPN), palmyra palm nut (PPN), oil palm empty fruit bunch (EFB), oil palm fiber (OPF), and oil palm shell (OPS). Chemical activation method was adopted in preparing the activated carbon. They found that the amount of Cu2+ adsorbed increased with increase in adsorbent dosage, and contact time and decreased with increase in particle size and initial ion concentration. The optimum pH of 6 was obtained for all the adsorbents. The result of adsorption studies showed that activated carbons produced from NPN and PPN are the most efficient adsorbents for the removal of Cu2+ from aqueous solutions while EFB, OPF and OPS were found to be poor adsorbents for the removal of the adsorbate. The equilibrium data were best described by Freundlich model

2.10. Research gaps

Having gone through series of literatures, these research gaps were found;

i. No thermodynamic studies have been done on desorption studies
ii. Comparative studies have not been done on chemical regeneration, microwave regeneration, and conventional regeneration.
iii. It was observed that the fitting of desorption kinetics data was limited to pseudo second order model only
iv. It was equally observed that the fitting of isotherm data was limited to Langmuir and Freundlich models.
v. Effects of oxidants on the regeneration efficiencies of microwave and conventional methods have not been studied.
vi. Adsorption and regeneration studies have not been done on hamburger seed shell and brewers' spent grain activated carbons.

CHAPTER THREE

MATERIALS AND METHODS

3.1 Materials

3.1.1 Adsorbate

Swiss blue dye commonly known as methylene blue dye is a basic dye with molecular weight of 319.9 and empirical formula of $C_{16}H_{18}N_3SCl$. It is the most commonly used substance for dying cotton, wood, leather and silk (Tan, et. al., 2007). It is a basic dye that is typically cationic or positively charged and reacts well with a material that is anionic or negatively charged. Swiss blue dye was chosen in this study because of its known strong adsorption onto solids. The chemical structure of Swiss blue dye is shows as follows:

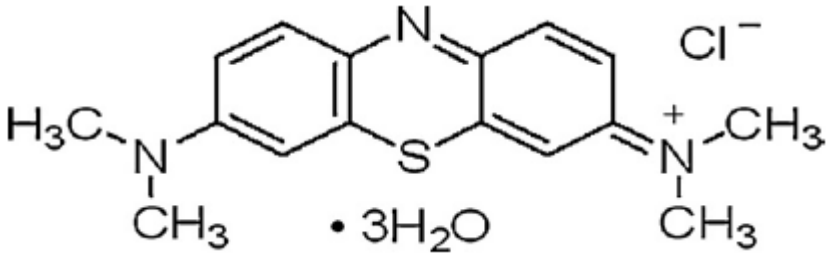

Fig. 3.1: Chemical structure of Swiss blue dye

3.1.2. Activated carbon precursors

The precursors used for the preparation of activated carbons were;

(1) Hamburger bean seed (*Mucuna Sloanei*) shell. The seed belongs to legume family (*fabaceae*). The shells were collected from a local market at Abakpa, Enugu East Local Government Area of Enugu State.

(2) Brewer's spent grain is the main by-product of brewing industry, representing approximately 85% of total by-product generated (Aliyu & Bala 2011). The brewers' spent grain was collected from Nigerian brewery Ninth mile corner Enugu, Enugu State. It was obtained immediately it was generated.

3.2 Experimental methods

The flow chart of the methodology is shown on Figure 3.2.

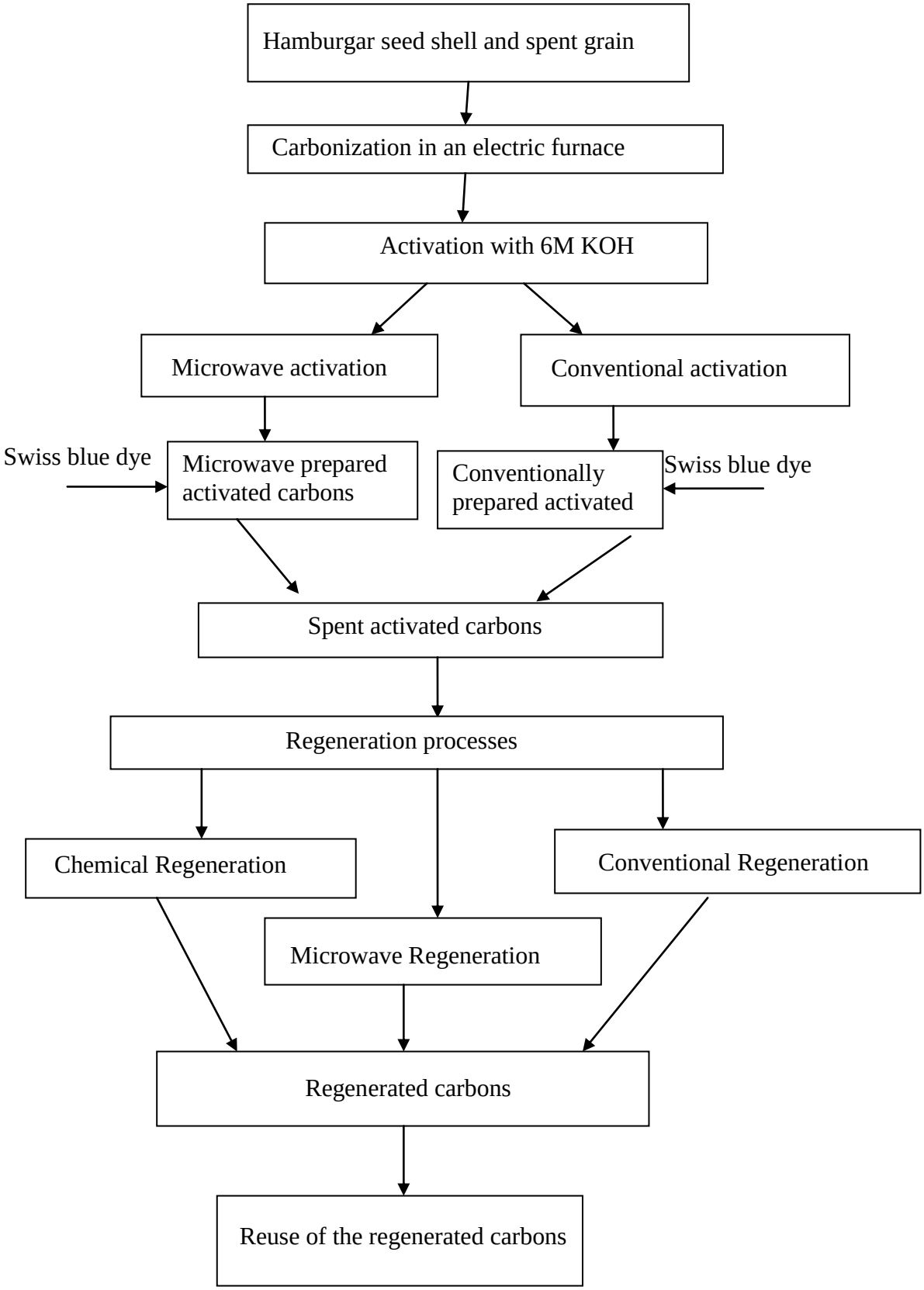

Fig. 3.2. Flow chart for the methodology

3.2.1. Preparation of Swiss Blue Dye solution

Double distilled water supplied by Pymotech Research Center Abakpa Enugu State of Nigeria was used for the preparation of the solutions. A 1000mg/l stock solution was prepared and from there, necessary dilutions were made to obtain the desired concentration.

3.2.2. Modification of Microwave oven

This work utilized a modified Sonik domestic microwave oven model SMW-90023 Japan, with a maximum power output of 900W delivered at a frequency of 2450MHz. As part of the modifications, the microwave casing was penetrated from the top to provide fittings to support the quartz glassware reactor. The reactor was opened from the top end to allow for the escape of the pyrolysis gases. The upper surface of the oven had a removable cover connected to a copper pipe from which the volatiles exited. The volatiles were then transferred to a condensing system made up of large receiving bottle. The quartz glassware which was mounted inside the microwave cavity consisted of 100mls flat bottom flask into which the samples were loaded, and a quartz quick fit connection coller which joined the flask with the outlet connection. Quartz was selected as reactor of choice because is a good material to be used in microwave reactors, it resist temperatures, transparent to microwaves and can resist thermal shock much better than traditional laboratory glass such as pyrex (Bradshaw et. al., 1998). However, the reactor was not completely invulnerable and was found to show signs of devitrification after extended use. Thus, periodic replacement of the reactor was done.

3.2.3 Production of activated carbons

The method was in accordance with the work done by Hammed et. al. (2009). Two step methods of precarbonization followed by chemical activation were involved.

Hamburgar seed shell and spent grain were washed exhaustively with deionized water to remove adhering dirt particles from the surface. They were dried, and ground. The ground samples were screened to the desired mesh size of 1 – 2mm. The carbonization process was performed by loading a known quantity of the ground samples into electrical furnace, and the temperature was ramped from room temperature to the desired temperature of 800°C. The char produced was soaked in 6M KOH solution with 1.5:1 impregnation ratio defined as the volume of activating agent

to weight of char (6MKOH: Char). The mixture was then dehydrated in an oven for one hour to remove moisture. For the conventional activation, the dehydrated samples were charged into an electric furnance to a temperature of 850°C and time of one hour. Microwave heating was conducted in a 2450MHZ domestic microwave oven with modification. The oven has a power controller to select different power levels and a timer for various exposure times at a set microwave power levels. The reaction was performed in a glass reactor fixed in the chamber of microwave oven. The resultant activated carbon was washed repeatedly with 0.1MHCl and distilled water until pH 6-7 was reached in the residual liquid.

The yield of activated carbon was defined as the ratio of final weight of the obtained product after washing and drying to the weight of dried sample initially used. The yield of activated carbon was calculated based on the following equation:

$$\text{Yield (\%)} = \frac{W_f}{W_0} X\ 100 \qquad (3.1)$$

Where W_f and W_0 were the weight of final activated products (g) and the weight of dried precursors (g), respectively

3.3. Characterization of Activated Carbon

3.3.1. Fourier transformed Infrared Spectroscopy (FTIR)

The surface functional groups and structure were studied using Fourier transform infrared spectroscopy [Buck 530 IR] England. The FTIR spectra of the raw materials, activated carbons and the regenerated carbons were scanned at a wavelength of 600–4000nm. This was done at Ahmadu Bello University, Zaria.

3.3.2. Scanning Electron Microscopy (SEM)

The surface morphology of the precursors, activated carbons and regenerated carbons were carried out using Phenom Prox Scanning Element Microscopy by PhenomWorld Eindhoven Netherland. This was done at Chemical Engineering Department, Ahmadu Bello University, Zaria.

3.3.3: Determination of Surface acidity

The surface acidity was done according to the work done by Foo and Hameed (2012a). The surface acidity was estimated by mixing 0.2g of activated carbons with 25mls of 0.05M NaOH in a closed flask, and agitated for 48hrs at room temperature. The

suspension was decanted and the remaining NaOH was titrated with 0.05M HCl. The surface acidity was calculated using equation 3.1 (Nora et. al., 2013).

$$\text{Surface acidity} = \frac{\text{Normality} \times \text{volume consumed}}{\text{molecular weight}} \times \frac{\text{initial volume}}{\text{selected volume for titration}} \quad (3.1)$$

3.3.4: Determination of Surface basicity

The surface basicity was measured according to work done by Foo and Hameed (2012a). This was measured by titrating with 0.05M NaOH, after incubation of 0.2g of activated carbons with 0.05HCl. The surface basicity was calculated with equation 3.1.

3.3.5 Determination of pH of Point of Zero Charge (pHpzc)

The pH of point of zero charge (pHpzc) of the sample was determined by the solid addition method according to Mall et. al. (2006). To a series of five 100ml conical flasks, 45ml of 0.01mol/dm^3 of KNO_3 solution was transferred. The initial solution pH values (pH_i) were roughly adjusted from pH 2 to 10 by adding either 0.01mol/dm^3 HCl or NaOH using a pH meter. The total volume of the solution in each flask was then made up to 50ml by adding KNO_3 solution which was accurately noted, and 0.10g of the sample was added to each of the flask, which was then securely capped immediately. The suspension were then manually shaken and allowed to equilibrate for 48 hours with intermittent manual shaking. The final pH values (pH_f) of the supernant liquid were then noted. The difference between the initial and final pH value was plotted against the pH_i. The point of intersection of the resulting curve at which $\Delta pH = 0$ gives the pHpzc.

3.3.6 Determination of pH

The standard test method for determination of activated carbon pH according to Ekpette and Horsfal (2011) was used. 1g of the activated carbon was weighed and transferred into a beaker. 100ml of distilled water was measured and added and stirred for one hour. The sample was allowed to stabilize before pH was measured using a pH meter.

3.3.7. Determination of moisture content

Thermal drying method was used in the determination of moisture content of the samples according to Rengaraj et. al. (2012). 1.0g of the dried activated carbons were

weighed in triplicates and placed in washed, dried and weighed crucible. The crucibles were placed in an oven and dried at 105°C to constant weight for 4 hours.

The percentage moisture content (%MC) was computed as follows:

$$\text{Moisture \%} = \frac{\text{Loss in weight on drying}}{\text{Initial sample weight}} \text{ x } \frac{100}{1} \quad (3.2)$$

3.3.8. Determination of the amount of iodine adsorbed

This method was according to work done by Gimba and Musa (2007). A stock solution was prepared (0.005mol/L) containing 2.7g of iodine crystal and 4.1g of potassium iodine per litre. Into a 250ml conical flask, 0.5g of the activated carbon and 10ml of 5% V/V hydrochloric acid was introduced.

The flask was swirled until the carbon was wetted. Then 100ml of the stock iodine solution was added and agitated at a fast speed using an electric shaker for a period of 60 minutes. The mixtures were filtered through a sintered glass crucible. An aliquot portion (20ml) was titrated with 0.1M sodium thiosulphate using starch as indicator.

The concentration of iodine adsorbed by the activated carbon at room temperature was calculated as amount of iodine adsorbed in milligrams. A blank was done using the same method without the samples.

$$\frac{\text{Img}}{\text{g}} = \frac{\text{B}-\text{S}}{\text{B}} \frac{\text{V.M}}{\text{W}} \text{ x } 253.81 \quad (3.3)$$

Where B and S are the volume of thiosulphate solution required for blank and sample titration respectively. W is the mass of activated carbon sample. M is the concentration (mol) of the iodine solute. 253.81 is the atomic mass of iodine and V is 20ml aliquot.

3.3.9 Volatile matter (VM)

The procedure was according to Onwu (1999). This is the loss of weight converted for moisture when a sample is heated in a specified apparatus under specified condition. 1g of moisture free sample was put into a furnace at 927°C for a period of 7 minutes. The sample was kept covered and cooled rapidly to prevent oxidation (the aim was to remove only the VM without affecting the fixed carbon).

The loss in weight is measured.

$$\text{\%VM} = \frac{\text{Initial wt} - \text{final wt}}{\text{initia weight}} \text{ x } \frac{100}{1} \quad (3.4)$$

3.3.10. Ash Content

This is the powdered residues left after combustion. The platinum crucible was weighed. 1gm of the sample was taken in the crucible and weighed. The sample was kept in a muffle furnace for 3hours at temperature of 650°C. This was taken out and kept in desiccators to cool down, the weight was taken. It was taken back to furnace for 30 minutes to establish that constant weight was obtained.

$$A(\%) = \frac{F-G}{B-G} \text{ x } 100 \quad (3.5)$$

Where: G = mass of empty platinum crucible

B is the mass of crucible plus sample, F is the mass of crucible + ashed sample

3.3.11 Fixed Carbon Content

Fixed carbon was calculated by difference.

$$\% \text{ carbon} = 100 (\%VM + \%\text{moisture} + \% \text{ Ash}) \quad (3.6)$$

3.3.12. The Bulk Density

For the determination of the bulk densities, a method of Azubike et. al. (2012) was used. 25g of the samples were accurately weighed and poured into a 100ml graduated cylinders each. The cylinder was stopped and the bulk volume (V_o) was recorded.

$$D_{bulk} = W/V_o \quad (3.7)$$

Where W was the weight of the sample, and V_o was the volumes of the bulk samples.

3.3.13 Determination of Specific Surface Area

The solid specific surface area covered by the adsorbate molecule was calculated according to the following expression and using the monolayer capacity from adsorption isotherm experiments and the molecular cross-sectional area (Bansal & Goyal, 2005). This equation was applied in the case where the molecules were adsorbed flat on the entire adsorbent specific surface (Hamdaoui & Naffrechoux, 2007).

$$Ss = \frac{q_{max} \ N_A A_m .10^{-20}}{M} \quad (3.8)$$

where Ss is the specific surface area of the adsorbent (m^2 g-1) (i.e., the surface area covered by the adsorbate molecule), qmax is the monolayer capacity [(gsolute)(gsolid)-1], NA is Avogradro's constant (=6.023·1023 mol-1), Am is the ionic cross-sectional

area of adsorbate (108 $Å^2$), and M is the molecular weight of the solute (284 g mol-1 for methylene blue (Benadjemia et. al., 2011)).

3.4. Batch Adsorption Studies

Batch adsorption process was studied using isothermal shaker in Fig. 3.3. Effect of pH and dosage of activated carbon on the removal efficiency of Swiss blue dye was studied. At the end of the process, the suspension was centrifuged and the residual dye was analysed using Shimadzu UV-Visible (1601) spectrophotometer. All the measurements were made at 661nm, a wavelength corresponding to the maximum adsorbance.

Fig. 3.3: Isothermal shaker

3.4.1 Effect of pH on Swiss blue dye Adsorption

To study effect of pH on adsorption of Swiss blue dye on the activated carbons, the experiments were carried out using 50mg/l, 80mg/l, 110mg/l and 150mg/l initial concentrations of the dye solution, with 0.02g of the adsorbent per 25ml of the adsorbate at room temperature for 4 hours equilibrium time. The initial pH values were adjusted to 2, 4, 6, and 8 with 0.1M Hcl and 0.1M NaOH using pH meter (Jenway Model 3510, England).

3.4.2 Effect of dosage

The effect of adsorbent dosage on equilibrium uptake of Swiss blue dye was studied at initial Swiss blue dye concentration of 50mg/l 80mg/l, 110mg/l and 150mg/l at adsorbent dosage of 0.02g, 0.05g, 0.08g, 0.11g, 0.14g, 0.17g and 2g per 25mls of the solutions. The experiments were performed by shaking the different adsorbate concentration with the above different adsorbent dosage for 3 hours.

3.4.3 Adsorption Kinetic Studies

The kinetic experiments were performed using a procedure similar to the batch adsorption studies. 25ml of different initial concentration of dye (50mg/l, 80mg/l, 110mg/l, and 150mg/l) was mixed with 0.02g of the adsorbent in a flask. Then, the flask was agitated in a shaker incubator for a contact time varied in the range 0- 240mins at a speed of 200rpm under room temperature. The adsorbent was separated from the solution by centrifugation and the filtrate was analyzed. The amount of dye adsorbed at each time interval per unit mass of the adsorbent, q_t (mg/g), was calculated by equation 3.9 while the removal efficiency was be calculated using equation 3.10.

$$qt = \left(\frac{Co - Ct}{W}\right) V \tag{3.9}$$

$$\% \text{ removal} = \frac{C_o - C_t}{C_o} \times \frac{100}{1} \tag{3.10}$$

Where C_o (mg/L) is initial dye concentration, C_t (mg/L) is its concentration at time t, V (L) is the volume of the solution and W (g) is the mass of the adsorbent.

3.4.4 Adsorption equilibrium studies

Batch isotherm studies were carried out in 250ml conical flask at different temperature of 303K, 313K, 323K and 333K on an isothermal shaker for 6 hours to ensure equilibrium. 0.02g of the adsorbent was mixed with 25ml of 50mg/l, 80mg/l, 110mg/l and 150mg/l of the solution at the solution pH. At the end of equilibrium time of 6 hours, the reaction mixture was centrifuged and the residual Swiss blue dye concentration analysed. The amount of Swiss blue dye at equilibrium qe (mg/g) was calculated from the following equation (3.11).

$$qe = \left(\frac{Co - Ce}{W}\right) V \tag{3.11}$$

3.5. Saturation of activated carbons

Prepared initial Swiss blue dye concentrations (100-400mg/l) were used to saturate the activated carbons. The dye loaded activated carbon was immersed in the initial solution of the dye for 24hours to ensure that the active sites were fully saturated. After equilibrium, the saturated adsorbents were washed with distilled water in order to remove un- adsorbed traces of the dye adhering on the surface and dried over night. The initial solid loading concentrations of Swiss blue dye on the saturated activated carbons were calculated using equation 3.12.

$$q_i\left(\frac{mg}{g}\right) = \left(\frac{C_o - C_e}{m}\right)V \qquad (3.12)$$

q_i is the initial solid phase dye concentration (mg/g), C_o is the initial dye concentration used in equilibrating the adsorbent (mg/l), C_e is the equilibrium concentration of the dye solution after equilibrium (mg/l), m is the mass of the adsorbent (g), V is the volume of the eluant (L), q_e is the the solid phase dye concentration after desorption (mg/l).

3.5.1 Desorption studies

Desorption studies were also conducted by batch mode similar to adsorption studies. Firstly effect of eluant types on desorption of dye solution was studied using 0.1M NaOH, 0.1M HCL, n-hexane, Chloroform and ethyl acetate as eluants. 0.02g of the saturated adsorbents was then treated with 25ml of eluant solution to elute the adsorbed dye solution.

At the end of 3hours, the dye remaining on the liquid phase was analyzed using UV-visible spectrophotometer at the maximum adsorbed wavelength of 661nm. The desorption efficiency, and solid phase concentration after equilibrium (desorption capacity) were calculated as (Muhammad et. al., 2011)

$$Desorption\ efficiency\ (\%) = \frac{q_i - q_e}{q_i}\ x\ \frac{100}{1} \qquad (3.13)$$

$$q_e\left(\frac{mg}{g}\right) = q_i - \frac{V\ (C_e - C_i\ )}{m} \qquad (3.14)$$

Where C_i is the initial dye concentration on the eluent before desorption (mg/l), q_i is the initial solid phase dye concentration (mg/g), C_o is the initial dye concentration used in equilibrating the adsorbent (mg/l), C_e is the equilibrium concentration of the dye

solution after equilibrium (mg/l), m is the mass of the adsorbent (g), V is the volume of the eluant (L), q_e is the the solid phase dye concentration after desorption (mg/g).

3.5.2. Effect of initial solid phase dye concentration on the desorptive capacity of the activated carbons

Different initial concentrations of the dye (100mg/l, 200mg/l, 300mg/l, 400mg/l) were used to saturate the adsorbents, after which the initial solid phase dye concentrations were calculated using equation 3.11. 0.02g of different initial solid phase dye concentrations were added to 25mls of the eluent and were agitated for five hours. At the end, they were centrifuged and were analyzed for residual dye concentrations using UV- VIS Spectrophotometer. Desorption capacity qe (mg/g) was calculated using equation 3.14.

3.5.3. Effect of dosage of saturated activated carbons on the desorptive capacity of the activated carbons

Effect of dosage of saturated activated carbon on desorption capacity of the activated carbons was studied at dosage of 0.1, 0.2, 0.3, and 0.4g at different initial solid phase dye concentrations. The known weight was added to 25ml of chloroform and was agitated for five hours. After, it was centrifuged and analysed for the residual dye concentration using aforementioned procedure. The desorption capacity qe (mg/g) was calculated using equation 3.14.

3.5.4. Desorption Kinetics for Swiss blue dye removal from spent activated carbons

For the desorption kinetics, 25ml of chloroform solution was taken in 250ml of stopper corked conical flask. It was then heated in a temperature controlled water bath shaker to certain temperature range (303-323K) and 200rpm. After attaining the required experimental temperature, 0.02g Swiss blue dye saturated activated carbon at different initial loading concentrations was put into the flask and inserted into the isothermal shaker (Figure 3.3). The samples were withdrawn at specified time intervals (20-280mins) and were analysed using Ultra Violet -Visible Spectrophotometer at maximum wavelength of 661nm. The amount of Swiss blue dye remaining on the adsorbent, qt (mg/g) was calculated using a mass balance equation:

$$q_t\left(\frac{mg}{g}\right) = q_i - \frac{V\,(C_t - C_i\,)}{m} \tag{3.15}$$

Where C_t is the Swiss blue dye concentration in solution (mg/l) at any time, C_i is the initial dye concentration on the eluant before desorption (mg/l), q_i can be calculated using equation 3.12. In order to obtain the activation energy and frequency factor for the desorption process, the relationship between the rate constants from kinetic data (Kd) and solution temperature was expressed by Arrhenius equation 3.16 (Kim & Kim, 2004; Scroeder & Gottfried 2002; Do & Wang 1998).

$$Kd = Ad\ \exp\left(\frac{-Edes}{RT}\right) \tag{3.16}$$

Where Ad is the frequency factor or temperature independent factor (min^{-1})

E_{des} is the activation energy (J/mol) for desorption process, R is the gas constant (8.314J/mol.K) and T is the solution temperature (K).

Transformation of equation 3.16 into linear form gave

$$InKd = InAd - \frac{Eds}{RT} \tag{3.17}$$

Plot of InKd Vs 1/T gave slope of $\frac{-Edes}{R}$ and intercept of InAd.

3.5.5. Desorption equilibrium studies for Swiss blue dye removal from spent carbons

For the desorption equilibrium, 25ml of chloroform solution was taken in 250ml of stopper corked conical flask. It was then heated in a temperature controlled water bath shaker (Figure 3.3) to certain temperature range (303-323K) and 200rpm. After attaining the required experimental temperature, 0.02g of Swiss blue dye saturated activated carbon at different initial loading concentrations was put into flask and inserted into the isothermal shaker. The samples were withdrawn at the end of equilibrium time of five hours and were analysed by UV-Vis Spectrophotometer at maximum wavelength of 661nm. The amount of Swiss blue dye remaining on the adsorbent at equilibrium, qe (mg/g) was calculated using a mass balance equation:

$$q_e\left(\frac{mg}{g}\right) = q_i - \frac{V\,(C_e - C_i\,)}{m} \tag{3.18}$$

Where C_e is the swiss blue dye concentration in solution (mg/l) at equilibrium, C_i is the initial dye concentration on the eluant before desorption (mg/l), q_i is the initial solid phase concentration and can be calculated using equation 3.12.

Equally, at equilibrium, the relationship between the concentration of the Swiss blue dye in chloroform (Ce) and the adsorbed amount on the activated (qe) might be expressed like the Freundlich isotherm equation 3.19 (Schroeder & Gottfried 2002).

$$qe = Ke(Ce)^n \tag{3.19}$$

Ke was expressed as an exponential function of temperature as (Kim & Kim, 2003; Madras et. al., 1993; Macnaughton & Foster 1995) as

$$Ke(T) = K_O \exp(\frac{\gamma}{T}) \tag{3.20}$$

Linearization of equation 3.19 gives

$$InKe = InK_O + \gamma\left(\frac{1}{T}\right) \tag{3.21}$$

γ(K) and K_O(mg/g)(mg/l)$^{-n}$ are constants in eqn. (3.21), Ke is Freundlich isotherm constant (mg/g)(mg/l)$^{-n}$ and T is temperature (K).

Plot of InKe against 1/T in equation 3.21 gives InK_O as intercept and γ as slope.

To further understand the nature of the desorption process, Schroeder & Gottfried (2002) stated that differences between activation energy (ΔEdes) and enthalpy change (ΔHdes) were in practice often negligible. Therefore, it was assumed that ΔEdes = ΔHdes. It was equally stated that the frequency factor (Ad) in the Arrhnius equation (3.16) can be equated to the entropy term as follows (Schroeder & Gottfried 2002);

$$Ad = \frac{K_d T}{\gamma} \exp\left(\frac{\Delta \mathrm{Sdes}}{R}\right) \tag{3.22}$$

Entropy of desorption can be extracted from the frequency factor (Ad) above as;

$$\Delta \mathrm{Sdes} = \mathrm{R}.(\frac{InAd.\gamma}{K_d T}) \tag{3.23}$$

Where R is the universal gas constant (J/mol.K), γ is constant from equation (3.21) (K), T is the temperature (K), and K_d is the pseudo second order rate constant (1/min).

Change in the standard free energy (ΔG_{des}) can be calculated from the enthalpy (ΔH_{des}) and entropy (ΔS_{des}) using the following relation (Al-Othman et. al., 2012);

$$\Delta \mathrm{Gdes} = \Delta \mathrm{Hdes} - \mathrm{T}\Delta \mathrm{Sdes} \tag{3.24}$$

3.6. Regeneration studies

Regeneration of spent activated carbons was done using chemical method, microwave method and conventional method for six adsorption-regeneration cycles using 30% H_2O_2 as an oxidant. After regeneration, the sample was immersed in a calculated volume of an oxidant (30% H_2O_2) at a ratio of (0.02g: 25ml) for one hour at room temperature. After which it was washed with distilled water and dried. The

effectiveness of the regeneration was studied by carrying out adsorption study on the regenerated carbons. The adsorptive capacity was calculated with equation 3.11, while the regeneration efficiency (RE %) was calculated as:

$$RE(\%) = \frac{Adsorption\ \ capacity\ \ of\ regenerated\ \ adsorbents}{Adsorption\ \ capacity\ \ of\ fresh\ adsorbents}\ x\ 100 \qquad (3.25)$$

3.6.1. Chemical regeneration of Swiss blue dye loaded activated carbons

Initially, the adsorbents were saturated with 100mg/l, 200mg/l, 300mg/l, and 400mg/l of the Swiss blue dye concentrations for 24hours. The saturated adsorbents were washed with distilled water to remove unadsorbed traces of Swiss blue dye. The chemical regeneration was carried out using chloroform. Into 250ml of chloroform, 0.2g of the saturated adsorbent was added; it was shake in an isothermal shaker (Figure 3.3) for 4hours at room temperature.

3.6.2. Microwave regeneration of Swiss blue dye loaded activated carbons

Microwave regeneration was performed in a modified Sonik domestic microwave oven at a heating efficiency of 2450MHz with a maximum power output of 900W in a Pyrex glass reactor fixed in the chamber of the microwave oven. Initially, the activated carbons were saturated with 100mg/l, 200mg/l, 300mg/l, and 400mg/l of Swiss blue dye for 24 hours. 0.2g of the saturated activated carbon was regenerated at 81% power levels for 10mins.

3.6.3. Conventional regeneration of Swiss blue dye loaded activated carbons

The conventional regeneration was carried out using muffle furnace at $500^{O}C$ for 30mins. Initially, the activated carbons were saturated with 100mg/l, 200mg/l, 300mg/l, and 400mg/l of Swiss blue dye concentrations for 24 hours. 0.2g of the saturated activated carbons was regenerated for 30mins.

3.7. Reuse of the regenerated activated carbon

Effect of microwave and conventional process factors on the adsorptive capacity of the regenerated activated carbons was studied. This involved carrying out the adsorption study on the carbons regenerated at different process conditions. The reuse was equally done with and without an oxidant for one cycle of adsorption-regeneration. For regeneration with an oxidant, at the end of the time intervals, the sample was immersed

in calculated volume of an oxidant (30% H_2O_2) at a ratio of (0.02g: 25ml) for one hour at room temperature. It was washed with distilled water and dried. After regeneration, the regenerated activated carbons were subjected to adsorption process with the same 100mg/l of the Swiss blue dye for 3hours.The adsorptive capacity of the regenerated activated carbon was calculated with equation 3.11.

3.7.1 Effect of Microwave power levels on the Adsorptive Capacity of Regenerated Activated Carbons

Effect of microwave power levels was done at 18%, 36%, 81%, and 100% for 10minues using modified microwave oven. The activated carbons used were saturated with 100mg/l of Swiss blue dye concentration for 24hours. 0.2g of the saturated activated carbons was desorbed at different power levels for 10minutes.

3.7.2 Effect of Microwave irradiation time on the Adsorptive Capacity of Regenerated Activated Carbons

Effect of microwave irradiation time was done at 5mins, 10mins, 15mins and 20mins at 81% power level using modified microwave oven. The activated carbons used were saturated with 100mg/l of Swiss blue dye concentration for 24hours. 0.2g of the saturated activated carbons was desorbed at different stated time intervals.

3.7.3 Effect of Conventional temperatures on the Adsorptive Capacity of Regenerated Activated Carbons

Effect of conventional temperatures was done at $200^{O}C$, $300^{O}C$, $400^{O}C$, $500^{O}C$, and $600^{O}C$ for 30minues using electric furnace. The activated carbons used were saturated with 100mg/l of Swiss blue dye concentration for 24hours. 0.2g of the saturated activated carbons was desorbed at different temperatures for 30minutes.

3.7.4 Effect of Conventional time on the Adsorptive Capacity of Regenerated Activated Carbons

Effect of conventional time was done at 10mins, 20mins, 30mins, 40mins and 50mins at $500^{O}C$. The activated carbons used were saturated with 100mg/l of Swiss blue dye concentration for 24hours. 0.2g of the saturated activated carbons was desorbed at different time intervals.

3.8. Mathematical methods used in analysis of data

The obtained data from kinetics and isotherm studies for both adsorption and desorption processes was analysed using different kinetic and isotherm models. This section listed out different mathematical models and equations used to analyse both the adsorption and desorption processes.

3.8.1. Adsorption and desorption Kinetic models

The kinetic studies for adsorption and desorption processes were done at different time intervals, after which the amount of solute on the adsorbent after adsorption (q_{tads}) and desorption (q_{tdes}) was calculated using equations 3.26 and 3.27 respectively. The same model was used for both adsorption and desorption processes, but the equation for calculating the amount of solute per gram of adsorbent at different time intervals differed as stated in equations 3.26 and 3.27.

$$qtads = \left(\frac{C_O - C_t}{W}\right) V \qquad (3.26)$$

Where C_o (mg/l) is initial dye concentration, C_t (mg/l) is its concentration at time t, V (L) is the volume of the solution and W (g) is the mass of the adsorbent.

$$q_{tdes}\left(\frac{mg}{g}\right) = q_i - \frac{V\,(C_t - C_i)}{m} \qquad (3.27)$$

Where C_t is the Swiss blue dye concentration in solution (mg/l) at any time, C_i is the initial dye concentration on the eluant before desorption (mg/l), q_i is the initial solid phase concentration and can be calculated using equation 3.28.

$$q_i\left(\frac{mg}{g}\right) = \left(\frac{C_o - C_e}{m}\right) V \qquad (3.28)$$

C_o is the initial dye concentration used in equilibrating the adsorbent (mg/l), C_e is the equilibrium concentration of the dye solution after equilibrium (mg/l), m is the mass of the adsorbent (g), V is the volume of the eluant (L),

The calculated data were fitted to six models and the suitability of the adsorption and desorption kinetics models to describe the adsorption or desorption process is judged by the correlation coefficients, R^2 values.

a) First order model

The kinetics may be described by a simple first order equation 3.29;

$$C_t = C_o e^{K1t} \qquad (3.29)$$

Equation (3.29) can be re-arranged to obtain a linear form equation 3.30:

$$\log C_t = \frac{K_1}{2.302}(t) + \log C_O \quad (3.30)$$

Where C_t and C_0 are the concentration of the solute at time t and initial concentration (mg/L) respectively and k_1 is the first order rates constant, (min^{-1}). If the first-order kinetics is applicable to the system, then the plot of $logC_t$ versus t of equation (3.30) will give a linear relationship with $K_1/2.303$ and $logC_0$ as slope and intercept respectively.

b) Pseudo-first-order model

It can be presented as follows, equation 3.31:

$$\frac{dq_t}{q_t} = K_{P1}(q_e - q_t) \quad (3.31)$$

where q_e and q_t (mg/g) are the adsorption capacities at equilibrium and at time t (min), respectively. K_{p1} (min^{-1}) is the pseudo-first-order rate constant for the kinetic model. Integrating Equation (3.31) with the boundary conditions of q_t=0 at t=0 and q_t=q_t, at t=t, yields,

$$\ln q_e - \ln(q_e - q_t) = K_{P1}t \quad (3.32)$$

This can be re-arranged to give;

$$\log(q_e - q_t) = \log q_e - \frac{K_{p1}}{2.303}(t) \quad (3.33)$$

If the Lagergren's first-order kinetics is applicable to the system, then the plot of log (qe-qt) versus t of equation (3.33) will give a linear relationship with $-K_{p1}/2.303$and log q_e as slope and intercept respectively.

c) Second-order model

The typical second-order rate equation in solution systems is as follows (eqn 3.34);

$$\frac{dC_t}{dt} = -K_2C^2t \quad (3.34)$$

Integrating equation above with the boundary conditions of C_t=0 at t=0 and C_t=$C_{t\ at}$ t=t to yield

$$\frac{1}{C_t} = K_2t + \frac{1}{C_0} \quad (3.35)$$

Where C_0 and C_t (mg/L) is the concentration of solute at equilibrium and at time t (min), respectively, and k_2 (L/ (mg. min)) is the rate constant of second order.

If the second-order kinetics is applicable to the system, then the plot of $1/C_t$ versus t of equation (3.35) will give a linear relationship with K_2 and $1/C_0$ as slope and intercept respectively.

d) Pseudo-second-order model

The equation is presented thus; $\frac{dq_t}{dt} = K_{p2}\,(q_e - q_t)^2$ (3.36)

Re-arranging equation (3.36) above as follows:

$$\frac{dq_t}{(q_e - q_t)^2} = K_{p2}\,dt \quad (3.37)$$

Integrating equation (3.37) with the boundary conditions of q_t=0 at t=0 and q_t=q_t at t=t, yields;

$$\frac{1}{(q_e - q_t)} = \frac{1}{q_e} + K_{p2}\,t \quad (3.38)$$

Which can be rearranged as follows to give;

$$\frac{t}{q_t} = \frac{1}{K_{P2}q_e^2} + \frac{1}{q_e}t \quad (3.39)$$

Where $K_{p2}q_e^2$ (mg/ (g. min)) means the initial adsorption rate. If the kinetics is applicable to the system, then the plot of t/qt versus t of equation (3.39) will give a linear relationship with $1/q_e$ and $1/K_2q_e^2$ as slope and intercept respectively.

e) Elovich model

Elovich equation is given as follows (eqn 3.40):

$$\frac{dq_t}{dt} = \alpha e^{-Bqt} \quad (3.40)$$

α and β, known as the Elovich coefficients. Where α is the initial adsorption rate (mg/g.min) and β is the adsorption constant (g/mg) during any experiment. To simplify the Elovich equation, assuming αβ >> t and by applying the boundary conditions at q_t = 0 at t = 0 and q_t = q_t at t = t the equation becomes (eqn 3.41):

$$q_t = {}^{1}/_{\beta}\,\ln(\alpha\beta) + {}^{1}/_{\beta}\,\ln(t) \quad (3.41)$$

If the Elovich's kinetics equation is applicable to the system, then the plot of q_t versus lnt of equation (3.41) will give a linear relationship with 1/β and 1/β ln (αβ) as slope and intercept respectively.

.

f) Intra –particle diffusion model

The intra particle model is given as; $q_t = K_{id}\,t^{1/2}$ (3.42)

The logarithmic form of the above equation (3.42) is;

$$\log q_t = \log K_{id} + 0.5\log t \quad (3.43)$$

where k_{id} is the intra-particle diffusion rate constant. According to Equation (3.43), a plot of $\log q_t$ versus 0.5logt should yield a straight line with a positive intercept for intra particle diffusion controlled adsorption process. For Weber-Morris model, it is

essential for the plot of q_t versus $t^{1/2}$ to go through the origin if the intra-particle diffusion is the sole rate-limiting step. Thus, the slope is not equal to zero.

3.8.2. Adsorption and desorption isotherms models

Adsorption and desorption studies was done to equilibrium and the amount of solute on the activated carbon after adsorption (qeads) and desorption (qedes) was calculated using equation 3.44 and 3.45 respectively. The adsorption and desorption equilibrium data were analyzed by fitting them into different isotherm models. The same model was used for both adsorption and desorption processes but the equation for calculating the amount of solute per adsorbent (qe) differed as stated in equation 3.44 and 3.55 .The suitability of the adsorption and desorption isotherm models to describe the adsorption or desorption process is judged by the correlation coefficients, R^2 values.

$$qeads = \left(\frac{C_0 - C_e}{w}\right) V \tag{3.44}$$

$$q_{edes}\left(\frac{mg}{g}\right) = q_i - \frac{V\,(C_e - C_i)}{m} \tag{3.45}$$

Where C_i is the initial dye concentration on the eluant before desorption (mg/l), q_i is the initial solid phase dye concentration (mg/g) which can be calculated using equation 3.28, C_o is the initial dye concentration used in equilibrating the adsorbent (mg/l), C_e is the equilibrium concentration of the dye solution after equilibrium (mg/l), m is the mass of the adsorbent (g), V is the volume of the eluant (L),

a) Langmuir isotherm model

Langmuir isotherm may be written as;

$$\frac{q_e}{b} = \frac{K_L C_e}{1 + K_L C_e} \tag{3.46}$$

The linear form of Langmuir's isotherm is given by the following equation (3.47):

$$\frac{C_e}{q_e} = \frac{1}{K_L b} + \frac{C_e}{b} \tag{3.47}$$

C_e (mg/L) is the concentration of adsorbate in liquid in equilibrium. The constant b is the monolayer capacity of the adsorbent (mg/g), and K_L relates to the adsorption equilibrium constant and their values were obtained from the slope and intercept of the plot of C_e/q_e versus C_e. The value of K_L is utilized to calculate dimensionless separation parameter R_L. The essential characteristics of the Langmuir isotherm model can be expressed in terms of a dimensionless separation factor (R_L) which is defined by equation 3.48.

$$R_L = \frac{1}{(1+K_L C_0)} \quad (3.48)$$

Where K_L is the Langmuir constant and C_0 is the initial solute concentration (mg/l). The value of R_L indicates the type of the isotherm to be either unfavorable if ($R_L > 1$), linear ($R_L = 1$), favourable ($0 < R_L < 1$) or irreversible ($R_L = 0$).

b) Freundlich isotherm

Freundlich isotherm model can be written as equation 3.49;

$$q_e = K_F C_e^{1/n} \quad (3.49)$$

A linear form of this expression is;

$$\log q_e = \log K_F + {}^{1}/_{n} \log C_e \quad (3.50)$$

Where K_F, is the Freundlich constant and n, the Freundlich exponent. K_F and n can be determined from the linear plot of log q_e versus log C_e.

c) Temkin isotherm

Temkin isotherm model is shown in equation 3.51;

$$q_e = \frac{R_T}{b_T} \ln A_T C_e \quad (3.51)$$

The linear form of it can be written as;

$$q_e = \frac{R_T}{b_T} \ln A_T + \left(\frac{R_T}{b_T}\right) \ln C_e \quad (3.52)$$

A_T is Tempkin constant, T the absolute temperature in ^{o}K and R is the universal gas constant, 8.314 $Jmol^{-1}$ K^{-1}. The constant b is related to the heat of adsorption. The plot of q_e versus ln C_e yields a slope of R_T/b_T and intercept of $\frac{R_T}{b_T} \ln A_T$.

d) Dubinin-Radushkevich isotherm model

The model is represented as equation 3.53;

$$q_e = (q_{max}) \exp(-B_D \varepsilon^2) \quad (3.53)$$

The linear form becomes;

$$\ln(q_e) = \ln(q_{max}) - B_D \varepsilon^2 \quad (3.54)$$

$$\text{Ɛ is Polanyi potential} = R_T \ln(1 + \frac{1}{C_e}) \quad (3.55)$$

Where B_D is the Dubinin-Raduschkevich isotherm constant. The values of q_d and B_D can be calculated from the intercept, and slope of the plot of lnq_e against $Ɛ^2$.

Apparent energy (E) of adsorption from the Dubinin-Radushkevich isotherm is calculated using equation 3.56;

$$E = \frac{1}{\sqrt{2B_D}} \tag{3.56}$$

e) Flory-Huggins Isotherm

It derives the degree of surface coverage and can be calculated using equation 3.57;

$$\frac{\theta}{C_o} = K_{FH}(1-\theta)^{n_{FH}} \tag{3.57}$$

The linear form of it becomes;

$$\log(\frac{\theta}{C_o}) = \log(K_{FH}) + n_{FH}\log(1-\theta) \tag{3.58}$$

A plot of $\log(\frac{\theta}{C_o})$ against $\log(1-\theta)$ gives n_{FH} as slope and log K_{FH} as intercept. K_{FH} is Flory-Huggins equilibrium constant while Θ is the degree of surface coverage. n_{FH} is the number of dye occupying adsorption site.

f) Redlich- Peterson model

It is a hybrid isotherm featuring both Langmuir and freundlich isotherm that incorporate three parameters into an empirical equation. The equation is presented thus (equ 3.59);

$$q_e = \frac{K_R C_e}{1 + a_R C_e^g} \tag{3.59}$$

linearization gives;

$$\ln(K_R \frac{C_e}{q_e} - 1) = g\ln(C_e) + \ln(a_R) \tag{3.60}$$

Plot of $\ln(K_R \frac{C_e}{q_e} - 1)$ verses $\ln(C_e) + \ln(a_R)$ gives Redlich- Peterson constants g and a_R as slope and intercept respectively.

g) Sips Isotherm

This is a combined form of Langmuir and freundlich expression, it can be represented thus;

$$q_e = \frac{K_S C_e^{BS}}{1 + a_S C_e^{BS}} \tag{3.61}$$

Linearisation of the equation gives

$$B_S\ln(C_e) = -\ln(\frac{K_S}{q_e}) + \ln(a_s) \tag{3.62}$$

rearranging the equation (3.62) gives

$$\ln(\frac{K_S}{q_e}) = \ln(a_s) - B_S \ln(C_e) \quad (3.63)$$

Plot of $\ln(\frac{K_S}{q_e})$ against $\ln(C_e)$ gives the sip isotherm constants as slope and intercept.

h) Toth Isotherm

Toth isotherm is another empirical model equation developed to improve Langmuir isotherm fittings. The equation is written as;

$$q_e = \frac{K_T C_e}{(a_T + C_e)^{1/t}} \quad (3.64)$$

Linearisation of the equation 3.64 gives

$$\ln(\frac{q_e}{K_T}) = \ln(C_e) - 1/t \ln(a_T + C_e) \quad (3.65)$$

Rearranging equation 3.65 gives

$$\ln(\frac{q_e}{K_T}) = 1/t \ln(a_T) - \ln C_e(1 - 1/t) \quad (3.66)$$

Plot of $\ln(\frac{q_e}{K_T})$ $verses$ $\ln C_e$ gives Toth isotherm constants (t, a_T and K_T) from slope and intercept.

3.8.3. Adsorption and desorption thermodynamics studies

The Gibb's free energy change of the adsorption process is related to equilibrium constant K_C by equation (3.67) below;

$$\Delta Gads = -RT \ln K_C \quad (3.67)$$

The Gibb's free energy change for adsorption process is related to the enthalpy change (ΔH^o) and entropy change (ΔS^o) for adsorption process as;

$$\ln K_C = \frac{\Delta Sads^{\,O}}{R} - \frac{\Delta Hads^{\,O}}{RT} \quad (3.68)$$

Where R (8.314 J/mol K) is the gas constant, T (K) the absolute temperature, and K_c (L/g) is the standard thermodynamic equilibrium constant defined by equation 3.69;

$$K_C = \frac{q_{eads}}{C_e} \quad (3.69)$$

By plotting a graph of $\ln K_c$ versus 1/T, the values $\Delta Hads^o$ and $\Delta Sads^o$ can be estimated from the slopes and intercepts.

In order to obtain the activation energy and frequency factor for the desorption process, the relationship between the rate constants from kinetic data (Kdes) and solution temperature was expressed by Arrhenius equation 3.70 (Kim & Kim, 2004; Scroeder & Gottfried 2002; Do & Wang 1998).

$$Kd = Ad \exp\left(\frac{-Edes}{RT}\right) \quad (3.70)$$

Transformation of equation 3.70 into linear form gave

$$InKd = InAd - \frac{Eds}{RT} \quad (3.71)$$

Plot of InKd Vs 1/T gave slope of $\frac{-Edes}{R}$ and intercept of InAd.

Schroeder and Gottfried (2002) stated that differences between activation energy (ΔEdes) and enthalpy change (ΔHdes) were in practice often negligible. Therefore, they concluded that activation energy for desorption is equal to enthalpy of desorption (equation 3.72)

$$\Delta E_{des} = \Delta H_{des} \quad (3.72)$$

They equally stated that the frequency factor (Ad) in the Arrhenius equation (3.70) can be equated to the entropy term as follows (Schroeder & Gottfried 2002);

$$Ad = \frac{K_d T}{\gamma} \exp\left(\frac{\Delta \mathrm{Sdes}}{R}\right) \quad (3.73)$$

Entropy of desorption can be extracted from the frequency factor (Ad) above as;

$$\Delta \mathrm{Sdes} = \mathrm{R}.\left(\frac{InAd.\gamma}{K_d T}\right) \quad (3.74)$$

Where R is the universal gas constant (J/mol.K), γ is constant from equation (3.21) (K), T is the temperature (K), and K_d is the pseudo second order rate constant (1/min). Gibbs free energy for both adsorption and desorption process can be estimated from equation 3.75.

$$\Delta G_{ads/des} = \Delta H_{ads/des} - T\Delta S_{ads/des} \quad (3.75)$$

3.9. Experiment design for optimization processes

In the first step of RSM, a suitable approximation is introduced to find true relationship between the dependent variable and the set of independent variables, that is, the single-response modelled using the RSM correspond to independent variables. Then a mathematical model in the form of a second-order polynomial is formed to predict the response as a function of independent variables involving their interactions. Generally the behaviour of the system is explained by the following quadratic equation 3.76;

$$Y = b_0 + \sum_{i=1}^{n} b_i x_i + \sum_{i=1}^{n} biix_{ii}^2 + \sum bijxixj \quad (3.76)$$

where Y is the predicted response, b_0 the offset term, bi the linear effect, bii the squared effect, bij the interaction effect and xi and xj represent the coded independent variables.

Optimization of adsorbents preparation conditions was done using central composite design (CCD) while the optimization of adsorption and desorption conditions were done with Box benhken design (BBD). CCD involves five levels (two factorial points, two axial points and one center point), while BBD has three levels (two factorial points and one center point). BBD is more economical and efficient in terms of number of required runs than CCD. It is useful in avoiding experiments that would be performed under conditions for which unsatisfactory results might occur. These justified its application in optimization of adsorption conditions that has five factors. Optimization of Microwave activation conditions involved three numeric factors which were power levels, KOH concentration and radiation time and one categoric factor which was type of precursor with two levels of hamburger seed shell and spent grain. Optimization of Conventional activation conditions involved three numeric factors which were KOH concentration, activation temperature, and activation time and one categoric factor which was type of precursor with two levels of hamburger seed shell and spent grain. The number of levels of the categoric factor multiplied the number of experiments giving forty experiments for each activation method.

The optimization of adsorption conditions involved four numeric factors of pH, dosage, temperature and initial concentrations and one categoric factor which was the type of adsorbent with four levels namely; conventionally prepared adsorbent from hamburger seed shell (CPAHS), conventionally prepared adsorbent from spent grain (CPASG), microwave prepared adsorbent from hamburger seed shell (MPAHS), and microwave prepared adsorbent from spent grain (MPASG). The number of levels of the categoric factor multiplied the number of experiments (29) giving one hundred and sixteen (116) experiments for the process.

Optimization of desorption process involved three numeric factors of dosage, temperature and initial dye concentration used for saturation and one categoric factor of type of adsorbent with four levels namely; conventionally prepared adsorbent from hamburger seed shell (CPAHS), conventionally prepared adsorbent from spent grain (CPASG), microwave prepared adsorbent from hamburger seed shell (MPAHS), and microwave prepared adsorbent from spent grain (MPASG). The number of levels of the categoric factor multiplied the number of experiments (17) giving sixty eight (68) experiments for the process.

Optimization of microwave and conventional regeneration conditions was done using central composite design (CCD). They involved three numeric factors of power level, radiation time and initial dye concentration used for saturation for microwave regeneration, temperature, time and initial dye concentration used for saturation for conventional regeneration. The categoric factor is the type of activated carbon with four levels of conventionally prepared adsorbent from hamburger seed shell (CPAHS), conventionally prepared adsorbent from spent grain (CPASG), microwave prepared adsorbent from hamburger seed shell (MPAHS), and microwave prepared adsorbent from spent grain (MPASG). The number of levels of the categoric factor multiplied the number of experiments (20) giving eighty (80) experiments for each regeneration process.

The factors and levels and the design matrix for the microwave activation process are showed on tables 3.1 – 3.2. Factors and level for conventional activation, adsorption process, desorption process, microwave regeneration, conventional regeneration and their design matrixes are shown on appendix A to D.

Table 3.1: Factors and levels for Microwave activation using CCD

	Factors	Units	Levels				
			-α	-1	0	+1	+α
1	Power levels	%	13.5	36.0	58.5	81.0	103.5
2	Radiation time	Mins	10.0	15.0	20.0	25.0	30.0
3	KOH Concentration	M	2.0	3.0	4.0	5.0	6.0
4	Type of precursor						
A	Hamb. Seed shell						
b	Brewers' spent grain						

Table 3.2: Design matrix for optimization of microwave activation process using CCD

Std Order	Run order	Power Level(%)	Radiation Time (mins)	KOH Conc.	Type of Precursor	Removal Eff. (%)
1	1	36.00	7.00	3.00	Hamburgar shell	
5	2	36.00	7.00	5.00	Hamburgar shell	
16	3	58.50	10.00	4.00	Hamburgar shell	
17	4	58.50	10.00	4.00	Hamburgar shell	
18	5	58.50	10.00	4.00	Hamburgar shell	
30	6	103.50	10.00	4.00	Spent grain	
15	7	58.50	10.00	4.00	Hamburgar shell	
29	8	13.50	10.00	4.00	Spent grain	

22	9	81.00	7.00	3.00	Spent grain
34	10	58.50	10.00	6.00	Spent grain
9	11	13.50	10.00	4.00	Hamburgar shell
40	12	58.50	10.00	4.00	Spent grain
27	13	36.00	13.00	5.00	Spent grain
6	14	81.00	7.00	5.00	Hamburgar shell
28	15	81.00	13.00	5.00	Spent grain
33	16	58.50	10.00	2.00	Spent grain
4	17	81.00	13.00	3.00	Hamburgar shell
3	18	36.00	13.00	3.00	Hamburgar shell
39	19	58.50	10.00	4.00	Spent grain
31	20	58.50	4.00	4.00	Spent grain
23	21	36.00	13.00	3.00	Spent grain
10	22	103.50	10.00	4.00	Hamburgar shell
11	23	58.50	4.00	4.00	Hamburgar shell
7	24	36.00	13.00	5.00	Hamburgar shell
32	25	58.50	16.00	4.00	Spent grain
20	26	58.50	10.00	4.00	Hamburgar shell
14	27	58.50	10.00	6.00	Hamburgar shell
21	28	36.00	7.00	3.00	Spent grain
35	29	58.50	10.00	4.00	Spent grain
13	30	58.50	10.00	2.00	Hamburgar shell
25	31	36.00	7.00	5.00	Spent grain
24	32	81.00	13.00	3.00	Spent grain
19	33	58.50	10.00	4.00	Hamburgar shell
37	34	58.50	10.00	4.00	Spent grain
8	35	81.00	13.00	5.00	Hamburgar shell
26	36	81.00	7.00	5.00	Spent grain
12	37	58.50	16.00	4.00	Hamburgar shell
2	38	81.00	7.00	3.00	Hamburgar shell
38	39	58.50	10.00	4.00	Spent grain
36	40	58.50	10.00	4.00	Spent grain

CHAPTER FOUR

RESULT AND DISCUSSIONS

4.1. Characterization of activated carbons

The activated carbons used in this study were characterized before adsorption and after regeneration with microwave, chemical and conventional methods. The characterization was done after six cycles of regeneration using 100mg/l initial dye concentration. Results of the characterisation were showed on table 4.1. It was observed that the properties of the activated carbons slightly varied as a result of the precursors used in the production and on the method of activation.

Table 4.1: Properties of Activated carbons used in the Study

S/No	Parameters	Units	Unused activated carbons	Microwave Regenerated activated carbons	Conventionally Regenerated activated carbons	Chemical Regenerated activated carbons
	Microwave prepared activated carbon from Spent Grain (MPASG)					
1	Surface Area	m^2/g	596.3	572.5	456.0	405.2
2	Iodine Number	mgI_2/g	1100.3	1008.9	731.1	663.1
3	Moisture Content	%	4.31	4.4	3.8	3.0
4	Ash	%	2.0	5.1	6.32	3.5
5	Volatile Matter	%	8.9	3.5	2.6	9.1
6	Fixed carbon	%	84.8	84.0	87.3	84.4
7	pH	-	6.8	7.4	7.0	6.9
8	pHpzc	-	6.3	8.5	8.1	8.0
9	Bulk Density	g/ml	0.482	0.47	0.43	0.51
10	Basic Sites	mmol/g	0.98	3.21	2.8	2.5
11	Acidic Sites	mmol/g	3.2	1.3	1.01	1.1
	Microwave prepared activated carbon from Hamburgar seed shell (MPAHS)					
1	Surface Area	m^2/g	621.7	643.0	490.2	420.6
2	Iodine Number	mgI_2/g	1295.2	1220.0	832.1	691.3
3	Moisture Content	%	4.1	4.2	3.6	3.8
4	Ash	%	2.1	4.2	5.8	3.0
5	Volatile Matter	%	6.5	3.8	2.9	8.8

6	Fixed carbon	%	87.3	87.8	87.7	84.4
7	pH	-	6.8	7.3	6.9	7.0
8	pHzpc	-	6.4	8.4	7.9	7.8
9	Bulk Density	g/ml	0.51	0.5	0.48	0.52
10	Basic Sites	mmol/g	0.75	3.5	3.0	2.8
11	Acidic Sites	mmol/g	3.6	0.92	0.97	1.05
	Conventional prepared activated carbon from Spent grain (CPASG)					
1	Surface Area	m^2/g	556.0	532.8	450.2	418.6
2	Iodine Number	mgI_2/g	1068.0	1006.1	708.3	650.7
3	Moisture Content	%	3.5	3.8	3.3	4.2
4	Ash	%	3.4	4.5	6.2	3.8
5	Volatile Matter	%	3.8	3.0	2.6	3.9
6	Fixed carbon	%	89.3	88.7	87.9	88.1
7	pH	-	6.5	6.8	7.0	6.9
8	pHzpc	-	6.2	8.6	8.3	8.0
9	Bulk Density	g/ml	0.49	0.47	0.46	0.51
10	Basic Sites	mmol/g	0.99	3.3	3.1	2.98
11	Acidic Sites	mmol/g	3.5	0.82	0.97	1.00
	Conventional prepared activated carbon from Hamburgar Seed Shell (CPAHS)					
1	Surface Area	m^2/g	548.6	528.7	430.6	400.9
2	Iodine Number	mgI_2/g	1009.3	1001.9	700.3	660.8
3	Moisture Content	%	3.6	3.7	3.2	4.0
4	Ash	%	3.2	3.8	6.0	3.9
5	Volatile Matter	%	3.5	2.8	2.2	3.6
6	Fixed carbon	%	89.7	89.7	88.6	88.5
7	pH	-	6.8	6.8	6.9	7.1
8	PHzpc	-	6.3	8.2	8.1	7.9
9	Bulk Density	g/ml	0.50	0.5	0.48	0.51
10	Basic Sites	mmol/g	0.82	3.5	3.2	3.0
11	Acidic Sites	mmol/g	3.5	0.89	0.91	1.07

4.1.1. Surface sites

It was observed that surface groups dominating all the activated carbon prior to adsorption were acidic groups (carboxylic, phenolic and lactonic). The surface acidity ranged from 3.21 to 3.6 mmol/g and surface basicity ranged from 0.775 to 0.98 mmol/g.

This increased the number of acid site on the activated carbons. The use of chemical reagents (KOH) in the activation process provided an increase in the amount of acid groups present in the activated carbon surface as observed in other studies (El-Sayed & Bandosz, 2004; Vargas, et. al., 2011; Cazetta et. al., 2011). It was observed that after regeneration, the acidic characters changed to basic characters (Table 4.1). According to Cazetta et. al. (2011), basic characters dominate carbon produced from thermal treatment. That is why it was observed that the basic characters of the microwave and conventional regenerations were higher than solvent regeneration. Basic character of microwave regenerated samples were highest because of the dispersive interaction between the adsorbed Swiss blue dye with the π– electron density of the carbon samples by means of microwave induced treatment (Radovic et. al.,1997). Equally, oxidant used in the regeneration has power to remove surface functional groups of activated carbon (Sun et. al., 2009). This is why basic sites equally dominated the chemical regenerated samples.

4.1.2. pHpzc

The pHpzc obtained using pH drift method equally provided important information about the characteristics of acidity and basicity of activated carbon (Cazetta et. al., 2011). According to our results, pHpzc within 6.3 showed that acidic sites dominated the carbon. The pH pzc equally helped in understanding the mechanism of adsorption. pH of sample greater than pHpzc will adsorb on the carbon. This is why Swiss blue dye been a cationic dye adsorbs on the prepared activated carbon. This was in agreement with the work done by other researchers that produced activated carbons from chemical activation (Vargas, et. al., 2011; Hameed et. al., 2008; Foo & Hameed, 2012a). Regardless of the regeneration method used, the regeneration decreased the oxygen surface functional groups with a subsequent increase in pH zpc values of the regenerated sample. As seen, the pHpzc increased to 7.8 – 8.5. This change in pHpzc can still favor the adsorption of cationic dyes (Foo & Hameed 2012a).

4.1.3. Surface area

Another changes observed was on the surface area of the regenerated samples. The extensive network of pores throughout activated carbon particle provides the lager surface area for adsorption to occur. The loss of surface area observed after chemical regeneration can be attributed to pore blockage caused by undesorbed Swiss blue dye.

The loss recorded for conventional regeneration can be attributed to attrition, collapse of carbon matrix and conversion of micropore to larger pore sizes (Vliet, 1991). The high surface area after regeneration with microwave suggested that microwave exposure resulted in an increase in surface activation of the carbon. During microwave regeneration, new pores developed and existing pores were either widened or deepened, the result was an increase in surface area. The increase in surface area also indicated that excessive burn-off or surface oxidation was minimal during microwave regeneration (Sufnarski, 1999). This shows that after successive adsorption – regeneration cycles, the adsorptive capacity of microwave regenerated carbon was preserved (Foo & Hameed, 2012a; Dehdashti et. al., 2010).

4.1.4. Iodine number

Another changes observed was on the iodine number of the regenerated carbons. According to Rouquerol et. al. (1994), micropore capacity can be expressed as the iodine number. It is assumed that iodine can penetrate into micropore while Swiss blue dye cannot (Rouquerol et. al., 1994). This was the reason why conventional regenerated samples recorded low iodine number because the micropore volume has been decreased.

4.1.5. Scanning Electron Microscopy (SEM)

Fig.4.1 (a-e) show surface morphology of non activated samples, activated carbon and activated carbons regenerated with the three methods for MPAHS. SEM of activated carbons showed the presence of pores on the surface compared to the non activated one (Fig. 4.1b). The pores of microwave regenerated sample (Fig. 4.1c) were more distinct and sharp compared to conventional and chemical regenerated ones. This is attributed to the fact that microwave regeneration preserved the porous structure and partially increased it. The surface of conventional regenerated samples showed larger pores (Fig.4.1d). This is probably due to the conversion of micropores to mesopores as a result of thermal treatment (Vliet, 1991). There were small grains internally and on the surface of the chemical regenerated sample (Fig. 4.1e). This can be as a result of undesorbed Swiss blue dye blocking the pores as a result of inadequate desorption.

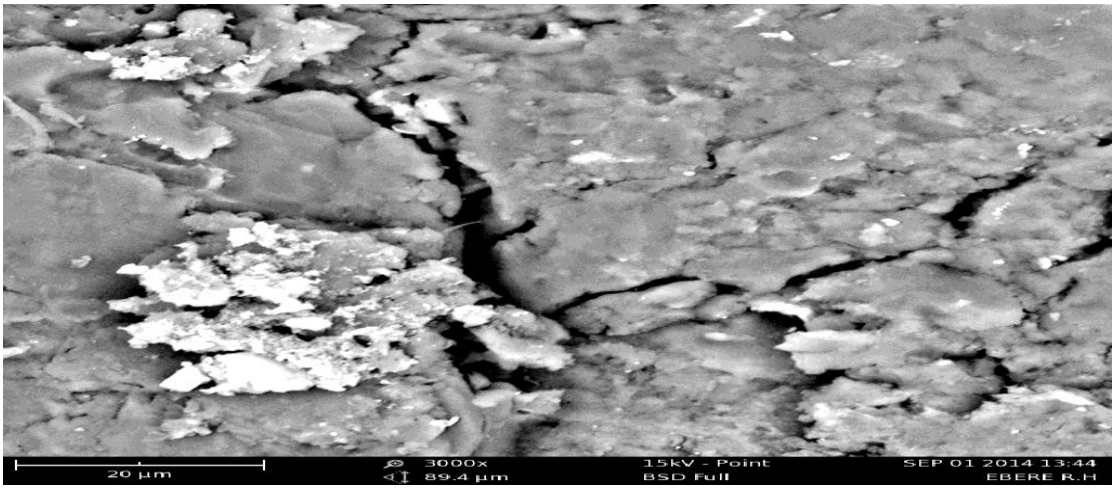
20 µm
3000x
89.4 µm
15kV - Point
BSD Full
SEP 01 2014 13:44
EBERE R.H

(a)

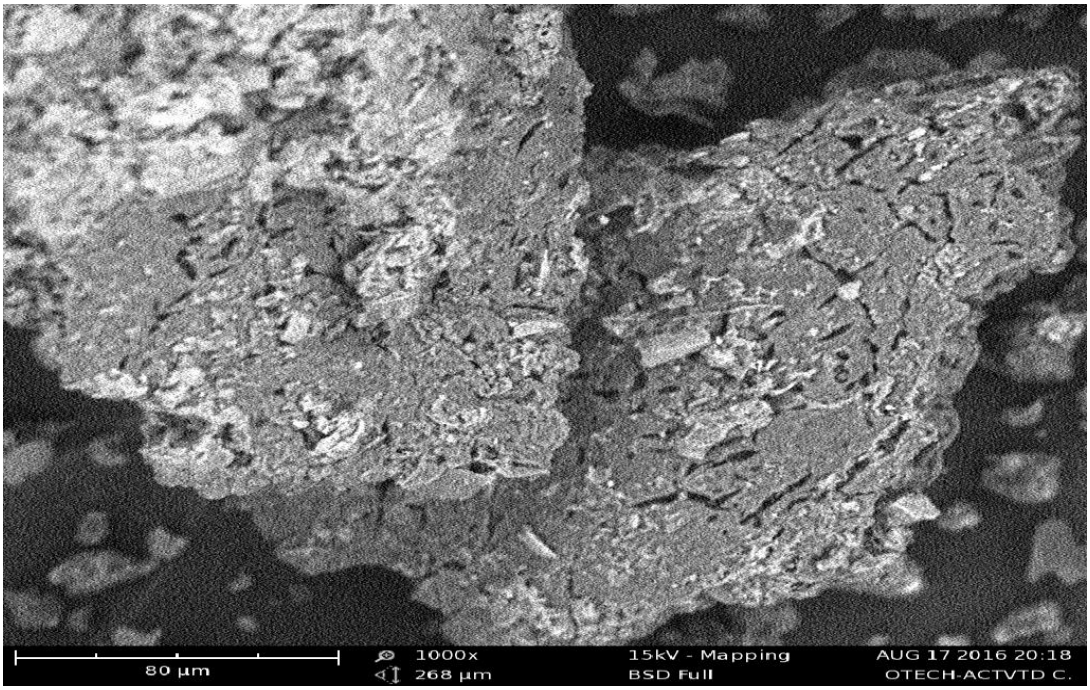
80 µm
1000x
268 µm
15kV - Mapping
BSD Full
AUG 17 2016 20:18
OTECH-ACTVTD C.

(b)

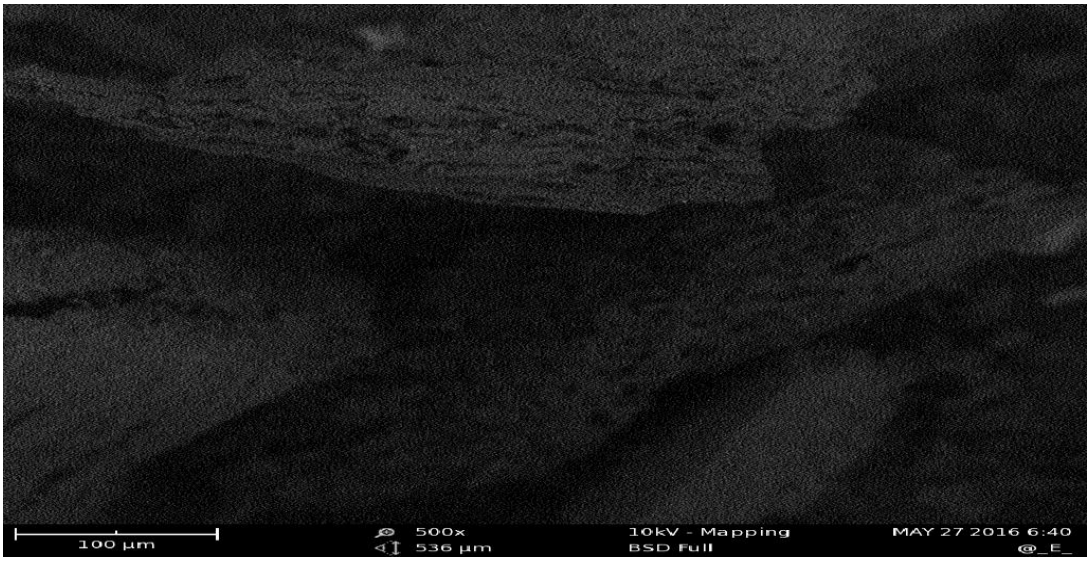

(c)

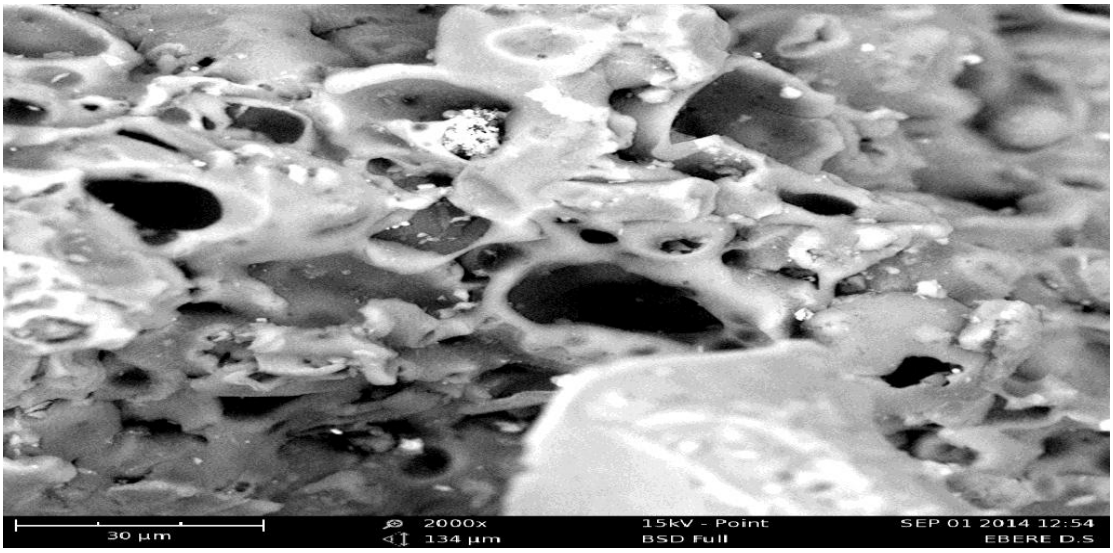

(d)

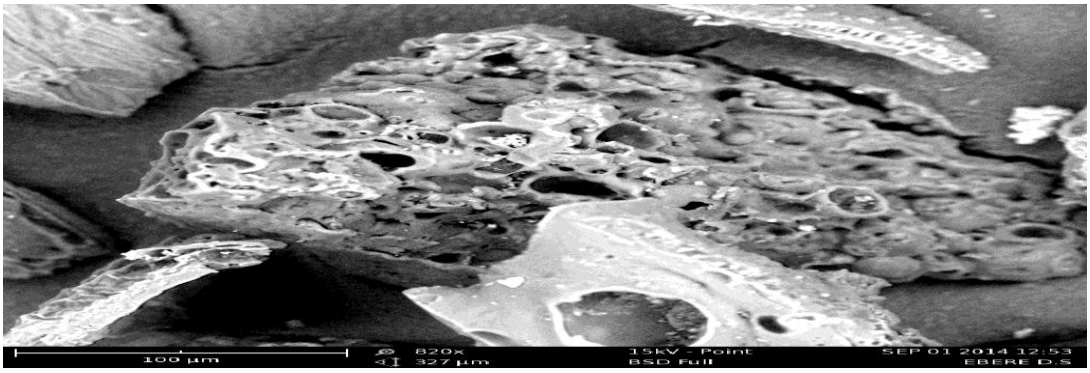

(e)

Fig. 4.1: SEM analysis of MPAHS (a) non activated, (b) activated, (c) microwave regenerated, (d) conventional regenerated, (e) chemical regenerated

4.1.6. Fourier Transform Infrared Spectroscopy (FTIR)

The FTIR analysis of the non activated, activated, Swiss blue dye saturated, and regenerated MPAHS is shown on tables 4.2-4.9, while the spectrum are shown on appendix E. The FTIR spectra of activated carbons indicated presence of fewer functional groups indicating that the surface functional groups of the raw samples experienced chemical changes during carbonization. Many peaks present in the raw samples absolutely disappeared in the activated carbon spectrum while those remaining were weak to a great extent. This is consistent with the breaking of many bonds in the KOH impregnated raw samples leading to the liberation and elimination of volatile species and partial aromatization during carbonization (Salman et. al., 2011; Vagmur et. al., 2008). Spectrum of saturated activated carbon showed many functional groups compared to the unsaturated activated carbon. This can be attributed to the dye adsorbed on the activated carbon. The spectrum of regenerated samples had fewer functional groups compared to saturated activated carbon. This is as a result of desorption of the adsorbed dye which inturn reduced the functional groups present. It can equally be observed that the functional groups on the regenerated carbon where close to the fresh activated carbon.

Table 4.2: FTIR analysis of raw hamburger seed shell

Absorption cm^{-1}	Class of compounds	Assignment	Intensity
672.5205	Alkenes	=C-H bend	m-s, broad
773.2506	Alkyl halides	C-CI Stretch	s
1438.687	Methyl group	C-H bend	m
1008.632-1140.975	Alkyl halides	C-F Stretch	vs
1364.13	Nitro compounds	N-O Symmetric	s
1678.557	Ketones	C=O Stretch	s
1794.615	Acyl chlorides	C=O Stretch	s
2266.137	Alkynes	C ≡ C Stretch	vw- w
2531-974-2743.853	Carboxylic acid	O-H Stretch	s, broad
2977.829	Alkenes and alkyls	C=H stretch	s
3158.33-3385.28	Carboxylic acid	O-H Stretch	s, broad
3549.243-3803.987	Water molecules	O-H Stretch	s
2266.137	Alkyne	C ≡ C Stretch	vw-w

Comparatively, microwave regenerated carbon showed functional groups very close to the fresh carbon, followed by conventionally regenerated carbon and lastely was the chemical regenerated carbon.

The non activated samples (Tables 4.2 and 4.4) show many functional groups. The wide peaks between 3158.033 to 3803.987cm^{-1} indicated O – H stretching vibration of hydroxyl functional groups including hydrogen bonding or adsorbed water. The FTIR spectra of activated carbons (Tables 4.3 and 4.5) indicated presence of fewer functional groups indicating that the surface functional groups of the raw samples experienced chemical changes during carbonization. Many peaks present in the raw samples absolutely disappeared in the activated carbon spectrum while those remaining were weak to a great extent. This is consistent with the breaking of many bonds in the KOH impregnated raw samples leading to the liberation and elimination of volatile species and partial aromatization during carbonization (Salman et. al., 2011; Vagmur et. al., 2008).

Table 4.3: FTIR analysis of microwave prepared activated carbon from hamburger seed shell

Absorption cm^{-1}	Class of compounds	Assignments	Intensity
810.9029	Aromatic Compounds	C-H bend	s
1459.901	Alkanes and alkyls	C-H bend	s
2268.636	Alkynes	C≡ Stretch	vw-w
2597.237-2719.63	Carboxylic acid	O-H Stretch	s, broad
2958.054	Alkanes and alkyls	C-H Stretch	s
3132.707-3333.389	Carboxylic acid	O-H Stretch	s, broad
1301.05	Amines	C-N	m-s

Table 4.4: FTIR analysis of raw spent grain

Absorption cm^{-1}	Class of compounds	Assignments	Intensity
729.4398-925.7625	Alkenes	≡ C-H bend	m-s, bend
1189.447-1320.31	Alkyl halides	C-F Stretch	vs
1541.065	Aromatic Compound	Ring C=C Stretch	m-s
1646.579	Amides	C=O Stretch	s, broad
1792.182	Acyl chloride	C=O Stretch	s

2615.808-3466.766	Carboxylic acid	O-H Stretch	s, broad
854.5732	Aromatic compound	C-H bend	s
2171.686	Akynes	C≡ C Stretch	vw-w
2479.617	Carboxylic acid	O-H Stretch	s, broad
3587.168-3884.425	Water molecules	O-H Stretch	m

Table 4.5: FTIR analysis of microwave prepared activated carbon from spent grain

Absorption cm^{-1}	Class of compounds	Assignments	Intensity
710.9043-778.9919	Aromatic compounds	C-H bend	s
1217.22	Alkyl halides	C-F Stretch	vs
1380.826	Alkanes and alkyls	CH_3 C-H bend	m
1490.494	Aromatic compound	Ring C= C Stretch	m-s
1641.499	Amides	C=O Stretch	s, broad
2566.845-3391.543	Carboxylic acid	O-H Stretch	s, broad
069.0642	Aromatic compound	C- H bend	s
2164.506	Alkynes	C ≡ Stretch	vw – w
3722.289	Water molecule	O-H Stretch	m

Spectrum of saturated activated carbon (Table 4.6) showed many functional groups compared to the unsaturated activated carbon (Tables 4.3 and 4.5). This can be attributed to the adsorbed dye on the activated carbon. The spectrum of regenerated samples had fewer functional groups compared to saturated activated carbon. This is as a result of desorption of the adsorbed dye which inturn reduced the functional groups present.

Table 4.6: FTIR analysis of Swiss blue dye saturated activated carbon

Absorption cm^{-1}	Class of compounds	Assignments	Intensity
547.88-640.52	Alkyl halide	C – Br Stretch	S
733.16-794.92	Aromatic compound	C-H bend	S
887.56-980.2	Alkene	= C-H bend	S
1099.86-1165.45	Alcohols	C-O Stretch	m-s
1227.24	Ethers	= C-O-C Sym.	m-s
1377.78-1443.4	Alkyls and alkanes	C-H bend	S
1566.92	Aromatic compounds	Rings C≡ C Stretch	m-s
1628.68	Amines	N-H bend	w-m
1717.46	Esters	C=O Stretch	S
1813.96	Acyl Chloride	C=O Stretch	S
2153.64-2215.4	Alkyne	C≡ C Stretch	m-w
2153.64-2215.4	Nitriles	C ≡ N Stretch	m-s
2524.2-2863.88	Carboxylic acid	O-H Stretch	s, broad
2987.4	alkanes and alkyls	C=H Stretch	S
3080.04	Aromatic Compounds	Ar-C-H Stretch	M
3168.82-3485.34	Carboxylic acid	O-H Stretch	s, broad
3605-3890.64	Water molecules	O-H Stretch	S

It can equally be observed that the functional groups on the regenerated carbons (Tables 4.7-4.9) where close to the fresh activated carbons (Tables 4.3 and 4.5). Comparatively, microwave regenerated carbon showed functional groups very close to the fresh carbon, followed by conventionally regenerated carbon and lastely was the chemical regenerated carbon.

Table 4.7: FTIR analysis of chemically regenerated carbon

Absorption cm^{-1}	Class of compounds	Assignments	Intensity
520.86-578.76	Alkyl halides	C-Br Stretch	s
671	Alkyne	≡ C-H bend	s, broad
733.16-875.98	Aromatic compound	C-H bend	s
455.24	Alkyl halide	C-I Stretch	s
794.92-949.32	Alkenes	= C-H bend	s
1041.96-1099.86	Alcohols	C-O Stretch	m-s
1227.24-1289	Ethers	= C-O –C Sym. and asym. Stretch	m-s
138.64	Alkanes and alkyls	CH_3C –H bend	m
1505.16-1566.92	Aromatic compound	Ring C= C Stretch	m-s
1624.82	Amines	N-H Bend	w-m
1698.16	Carboxylic acids	C=O Stretch	s
2238.56	Nitriles	C ≡ N Stretch	s
2431.56	Nitriles	C≡ N Stretch	m-s
2524.2-2778.96	Carboxylic acid	O-H Stretch	s, broad
2863.85-2925.64	Alkanes	C-H Stretch	s
3006.70-3199.7	Carboxylic acid	O-H Stretch	s, broad
3450.6	Amide	N-H Symetric and asymmetric stretch	w
3570.26-3971.7	Water molecules	O-H Stretch	s

Table. 4.8: FTIR analysis of microwave regenerated carbon

Absorption cm^{-1}	Class of compounds	Assignments	Intensity
671.4	Alkynes	≡ C-H bend	s, broad
918.44	Alkenes	= C-H bend	m+s
1539.9	Aromatic compound	Ring C=C Stretch	m-s
1624.54	Amides and amines	N-H bend	w-m
1686.58	Amides	C=O Stretch	s, broad
2149.78-2211.54	Alkyne	C≡ C	v w –w
2589.82-2736.5	Carboxylic acid	O-H stretch	s, broad
2813.7-2983.54	Alkanes and alkyls	C=H stretch	s
31418-3454.46	Carboxylic acid	O-H Stretch	s, broad
3574.12-3963.93	Water molecules	O-H Stretch	s

Table 4.9: FTIR analysis of conventionally regenerated carbon

Absorption cm^{-1}	Class of compounds	Assignments	Intensity
640.52	Alkynes	≡ C-H bend	s, broad
435.94-493.84	Alkyl halides	C- I Stretch	s
737.02	Aromatic compound	C-H bend	s
922.3	Alkenes	=C-H bend	mts
1258.12	Ester	=C-O–C Sym. And asym	m=s
1323.74	Alkyl halides	C-F Stretch	vs
1605.52	Amines	N-H bend	w-m
1656.58	Amides	C= O Stretch	S, broads
1752.2	Ketones	C=O Stretch	S
2246.28	Alkynes	C ≡ C Stretch	Vw-w
2585.96-2991.26	Carboxylic acid	O-H Stretch	S, broad
3045.3 -3107.06	Alkene	=C-H Stretch	w-m
3226.72-3419.72	Carboxylic acid	O-H Stretch	S, broads
3512.36-3882.92	Water molecules	O-H Stretch	s

4.2. Effect of activation processes on Swiss Blue dye removal efficiency and carbon yield

Activated carbons were produced from Hamburger seed shell and Brewers' spent grain by chemical activation process using KOH. Chemical activation involved carbonization of the precursors at temperature of 800°C for two hours, and the impregnation of the carbonized sample with 6M KOH solution and subsequent heating conventionally or with microwave. KOH was the choice of activating agent because of maximum carbon yield and removal efficiency recorded on the work done by Foo and Hameed (2012e) on effect of different activating agents on the removal efficiency and yield of activated carbon.

4.2.1 Conventional Activation Process for Swiss blue dye removal

Effective activation of carbon using conventional method involved monitoring different factors that affect the activation which include activation time, activation temperature and concentration of KOH.

a) Effect of Conventional Activation Temperature on Swiss blue dye Removal Efficiency and Carbon Yield

Effect of activation temperature on Swiss blue dye removal efficiency and carbon yield was studied at activation time of the 1 h and KOH concentration of 6M. It can be seen from fig. (4.2), that increase in activation temperature increased the removal efficiency of the Swiss blue dye to 850°C and further increase to 950°C decreased the removal efficiency. Equally, increase in temperature from 550°C to 950°C decreased the carbon yield. New pores were created and existing ones widened as activation temperature was increased. The decrease in removal efficiency at higher activation temperature greater than 850°C might be due to the sintering effect at high temperature, followed by shrinkage of the char, and realignment of the carbon structure which resulted to reduced pore areas with resultant decrease in removal efficiency (Deng et. al., 2010; Asmaa & Muthanna, 2014). It was equally observed that the two precursors used had the same trend for removal efficiency and yield, but brewers' spent grain had high removal efficiency of 99.6% compared to hamburger seed shell that had 95.3%. This can be attributed to the high volatile content of the sample.

Activation temperature played an important role on the yield of activated carbons prepared from the two precursors. It was found that weight loss increased with increase in activation temperature from 550°C to 950^{0}C. The increase in temperature would release increasing volatiles as a result of intensifying dehydration and elimination reaction and also increase the C– KOH reaction rate, thereby resulting in decreasing yield (Lua & Yang 2004; Adinata et. al., 2007). Indeed, the increase in activation temperature quickens the gasification reaction of carbon and therefore, the attack of the amorphous components which obstruct the pores causes a decrease in the carbon yield (Bacaoui et. al., 2007). Activated carbon prepared from the two samples had the same pattern of decrease in yield as activation temperature increased, but the decrease was more with brewers' spent grain activated carbon with yield of 19.1% compared to hamburger seed shell activated carbon that had 25.6%. The high weight loss experienced with brewers' spent grain activated carbon can be attributed to the high volatile matter content of the sample which decreased as activation temperature was increased.

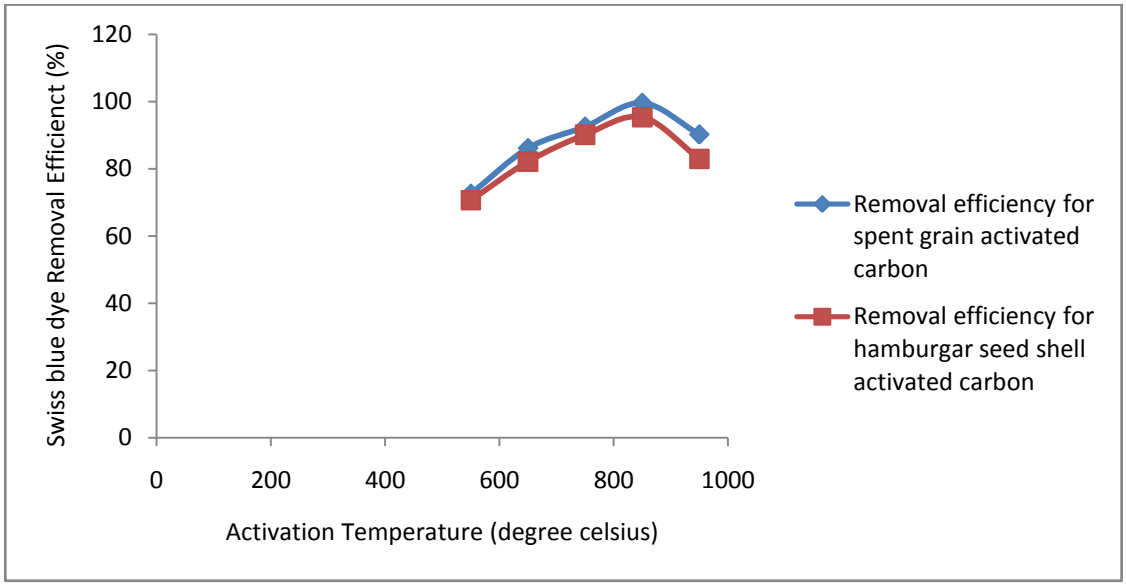

(a)

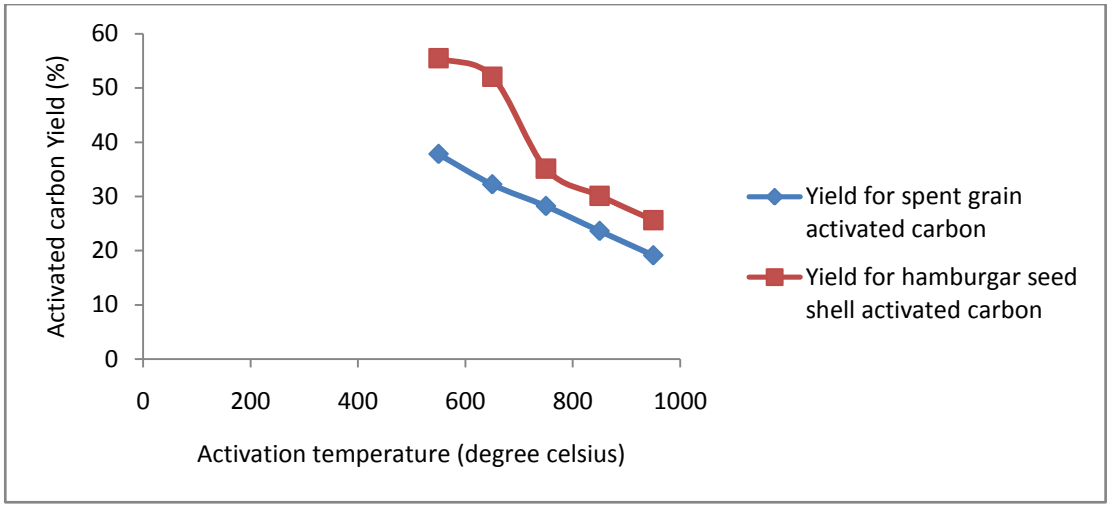

(b)

Fig: 4.2: Effect of conventional activation temperature on Swiss blue dye Removal Efficiency (a) and activated carbon yield (b) for both precursors

b) Effect of Conventional Activation Time on Swiss blue dye Removal Efficiency and Carbon Yield

Effect of activation time on the Swiss blue dye removal efficiency and carbon yield was studied at activation temperature of 850°C and 6M KOH solution at impregnation ratio of (1:1.5) carbon to KOH solution. It can be seen from the result (fig. 4.3) that increase in activation time increased the removal efficiency at 60 mins, beyond 60mins, there was reluctant increase in Swiss blue dye removal efficiency. As activation time was increased beyond 60mins, the surface area was not much affected due to low volatilization of organic matters from the biomass. The non-performance or insignificant activation time variable impact on uptake of basic blue dyes has been observed by a number of researchers. Gratuito et. al. (2008), Sentorum – Shalaby et. al. (2006), and Auta and Hameed (2011) reported that activation time or prolonging time of activation does not necessary lead to yielding of high surface area and enlargement of pores during production of activated carbon. However, Gratuito et. al. (2008) indicated that it is not necessary to prolong activation time so much beyond the basic requirement, as doing so would cause pores enlargement, which may be undesirable depending on the requirement of a specific activated carbon application.

It can be seen that the two precursors used for the production of activated carbon showed the same behaviour of insignificancy at higher activation time. Hamburger

seed shell showed lower removal efficiency of 98.1% compared with activated carbon from spent grain that had 99.6%. Both had insignificant increase in surface area as the activated time was prolonged. This was evidenced from the similar removal efficiencies obtained. Effect of activation time on the carbon yield was equally observed for the activated carbons produced. It was observed that the yield of carbon was almost constant which confirmed the insignificancy of activation time on activated carbon production. Weight loss increases only if there are serious volatilities of the volatile matters. But since prolonging activation time did not appreciably increase volatilization, thus, carbon yield remained almost unchanged. It was equally interesting to know that carbon yield for hamburger activated carbon was higher with a value of 32.6% when compared with spent grain activated carbon that had 25.3%. This can be attributed to high volatile matter content of spent grain which went off during activation resulting to high weight loss.

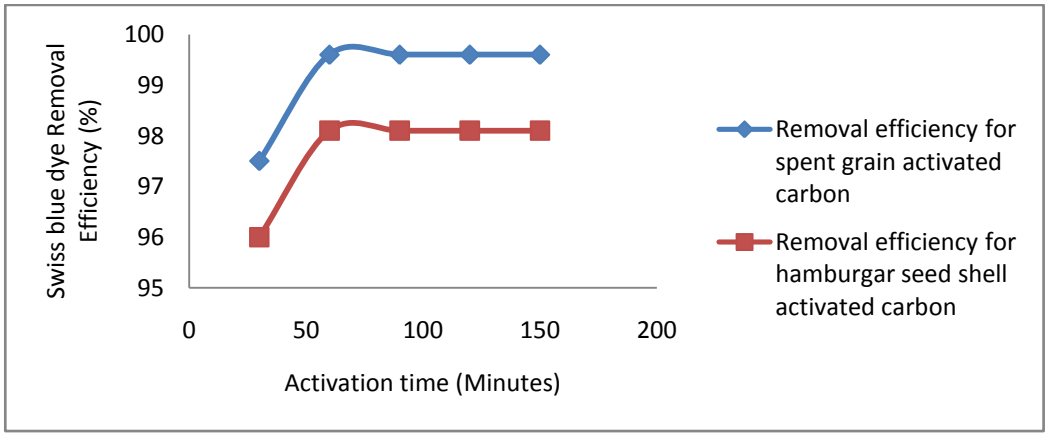

(a)

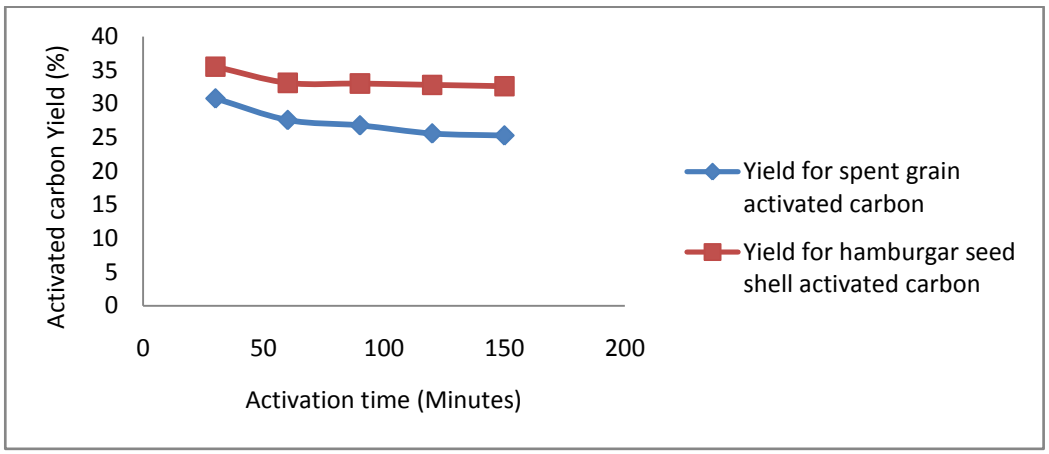

(b)

Fig. 4.3: Effect of Conventional activation time on Swiss blue dye Removal Efficiency (a) and activated carbon yield (b) for both precursors

c) Effect of KOH Concentration on Swiss Blue Dye Removal Efficiency and Carbon Yield for spent grain and hamburger seed shell activated carbons

Effect of concentration of the activating agent KOH was studied at activation temperature of 850°C, activation time of 1hour and 1:1.5 solid / KOH impregnation ratio. Impregnation of the chemical results in the dehydration of the carbon skeleton and widening of the interior canal of the botanic structure followed by the formation of a porous structure (Foo & Hameed, 2012f). It was observed from fig. (4.4) that increase in KOH concentration increased the Swiss blue dye removal efficiency to a point that further increase in KOH concentration led to decrease in Swiss blue dye removal efficiency. This phenomenon is probably due to the fact that upon the impregnation of carbon with KOH, K_2CO_3 was formed with a simultaneous evolution of CO_2 and CO (Diaz-Teran et. al., 2003). As concentration of KOH increased, the catalytic oxidation also caused the widening of micropores to mesopores, therefore increasing the Swiss blue dye removal efficiency. At high KOH impregnation, the microporosity development is mostly due to the intercalation of potassium metal in the carbon structure (Sudaryanto et. al., 2006). Indeed, methylene blue molecules has a minimum molecular cross section of about 0.8nm, and it has been estimated that the minimum pore diameter it can enter is 1.3nm (Barton, 1987). This meant that when mesopores were developed, more swiss blue dye molecules could be absorbed by the activated carbon, therefore, enhancing the adsorption capacity of the activated carbons (Tan et. al., 2008).

However, at high KOH concentration of 7M, Swiss blue dye removal efficiency reduced, this was due to gasification reaction between the excess potassium and the carbon material resulting in the loss of some carbon and also translating to poor development of the pores and its surface area (Auto & Hameed 2011). Equally, El-Hendawy (2009) has observed that too high concentration of KOH might lead to the presence of K_2CO_3 and metallic potassium that was left in the carbon and cannot easily leached even after repeated washing. This may cause blocking of some pores leading to the observed drastic decrease in the accessible area for dye molecules that finally reduced the surface area of the activated carbon prepared.

Equally, effect of KOH concentration on the carbon yield was studied. Increase in KOH concentration decreased the yield and increased the carbon burn off. This was

because when higher concentration was used, the weight loss was due to increasing release of volatile products as a result of intensifying dehydration and elimination reaction (Adinata et. al., 2007). KOH would promote the oxidation process, therefore with high concentration; the gasification of surface carbon atoms was the predominant reaction, leading to increase in the weight loss of carbon (Sudaryanto et. al., 2006). Shevkoplyas and Saranchuk (2000) observed that impregnation of coal with KOH leads to the breaking of C-O-C and C-C bonds, facilitating coal decomposition during pyrolysis and as a result decreasing the carbon yield (Sahu et. al., 2010).

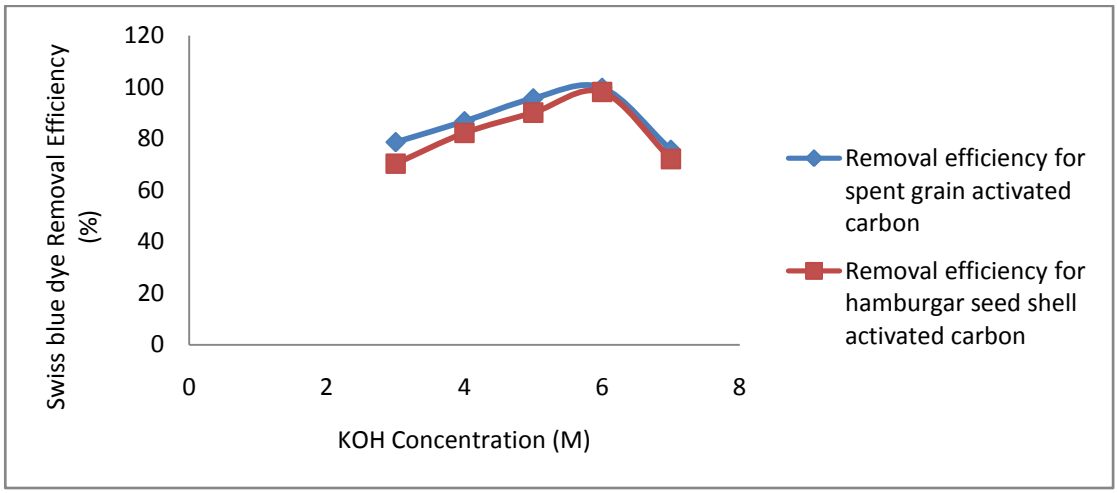

(a)

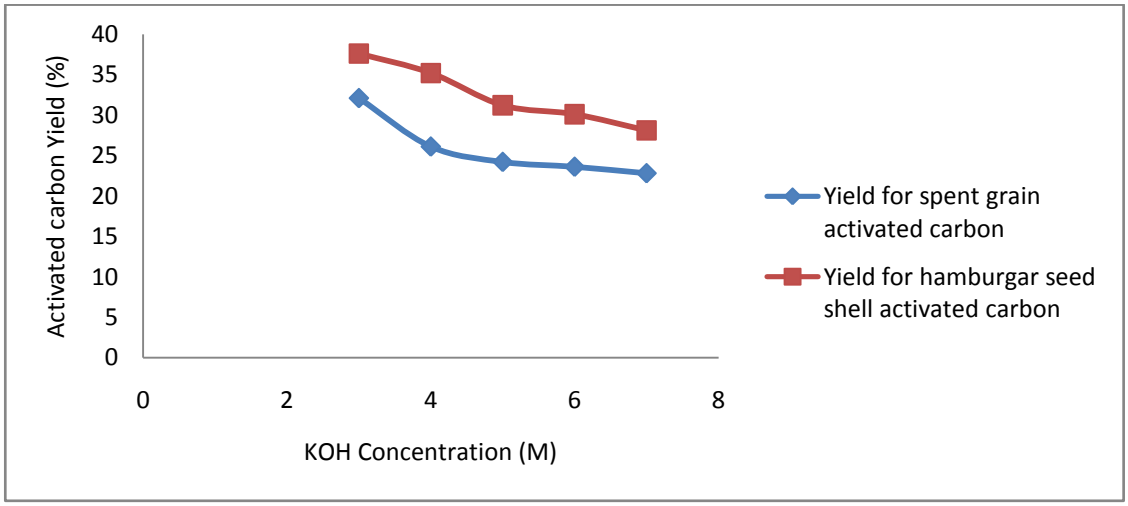

(b)

Fig. 4.4: Effect of KOH concentration on Swiss blue dye Removal Efficiency (a) and activated carbon yield (b) for both precursors

4.2.2 Microwave Activation Process

In this study, microwave activation process was studied using a modified Sonik domestic microwave oven model SMW-90023 with a maximum power output of 900W, delivered at a frequency of 2450MHz. The operational parameters that were studied were power level (%), radiation time (minutes) and the KOH concentration (M).

a) Effect of Microwave power levels on the Swiss Blue Dye Removal Efficiency and Carbon Yield

Effect of microwave power levels were studied at 6M KOH and radiation time of 7minutes.The power level showed the percentage of the total power of the microwave used for a particular study. The effect of power levels was studied at defrost, low, medium high and high corresponding to 18%, 36%, 58%, 81% and 100% power output in watts. From the result (fig. 4.5), it can be seen that Swiss blue dye removal efficiency increased with increase in power level up to a point that further increase in power level resulted to decrease in the removal efficiency.

As suggested by the result, at low power of 18% and 36%, the pore structure was not adequately developed, and their removal efficiency were low indicating no continual reaction between the char and a activating agent. At higher power levels of 58% and 81%, the pore width was successively broadened and new miropores-mesopores were formed in the original pore walls, giving a sustaining increase in removal efficiency. High microwave power improves the development of the pore structures of activated carbon which indicates that microwave power is important in the activation stage. However, the removal efficiency decreased when the power level was increased to 100% due to decrease in the formation rate of new pores and beginning of pore destruction. According to Deng et. al. (2010), the decrease in removal efficiency with further increase in power levels might be due to the sintering effect at high power levels, followed by shrinkage of the char and realignment of the carbon structure which resulted in reduced pore areas as well as volume. Over gasification might occur causing destruction of pore structures, thus decreasing the removal efficiency.

Effect of microwave radiation power on the carbon yield was equally studied. From the resulted, it was ascertained that carbon yield decrease with increase in power levels. At high microwave power levels, absorbed microwave energy exceeded a

certain level which led the plentiful energy to cause excessive destruction of pore structures, and a progressive decrease in carbon yield was observed. The weight loss of carbon increased proportional to the microwave power level, mainly due to the fierce reaction at higher thermal radiation which intensified devolatilization, dehydration and decomposition (Foo & Hameed, 2012e). It was observed that carbon prepared from hamburger seed shell had higher yield than those from spent grain. This can be attributed to the low volatile content of hamburger seed shell.

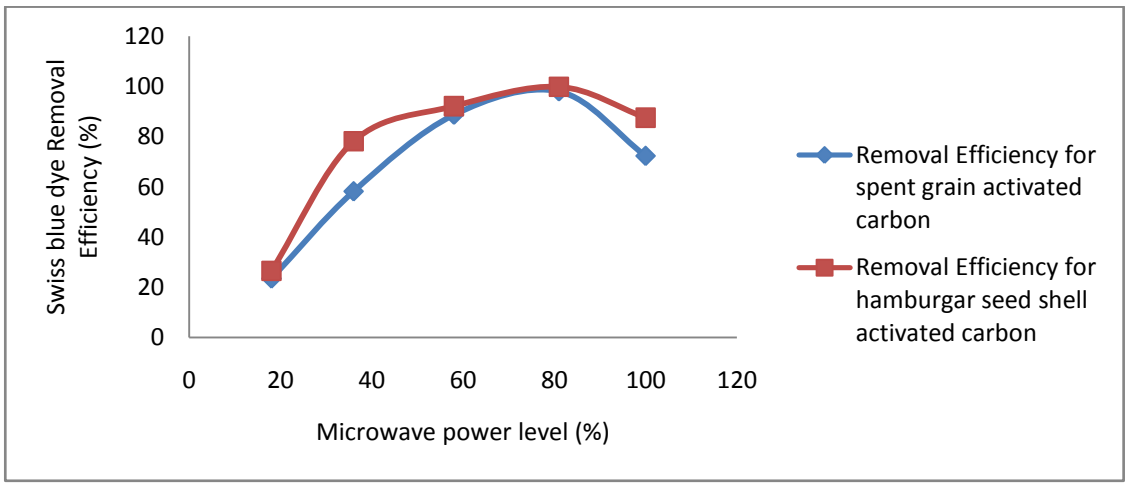

(a)

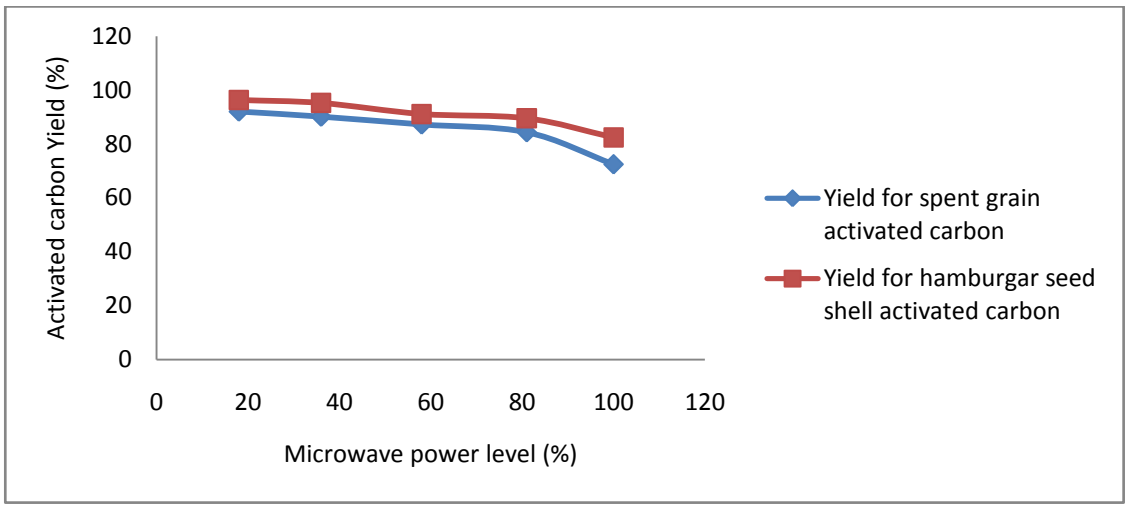

(b)

Fig. 4.5: Effect of Microwave power levels on Swiss blue dye removal Efficiency (a) and activated carbon yield (b) for both precursors.

b) Effect of radiation time on Swiss Blue Dye Removal Efficiency and Carbon Yield

Microwave radiation time is another key parameter affecting the removal efficiency and carbon yield. Result (fig. 4.6) revealed that prolonging the radiation time exhibited an enhancement of removal efficiency. This phenomenon implied that prolonging time exposure promoted an acceleration of temperature, which in turn increased reaction rates thus developing porosity (Foo & Hameed, 2012f). A slight drop was observed at 8mins for activated carbon prepared from both precursors. However as the radiation time arrives at its optimum values (7mins) absorption and reflection of energy tends to balance and the activated carbon achieved their maximum removal efficiency. As activation proceeds, temperature increased dramatically and led to opening of microspores and mesopores which resulted in enlargement of the average diameter. The drop in removal efficiency is probably due to a sintering effect, which largely destroyed the pore walls between adjacent pores. Moreover, high temperature might produce local hotspots, leading to external ablation and collapse of the carbon frame work, resulting in reduced accessibility of carbon actives sites. Higher pyrolytic temperatures could induce C-KOH, C-K_2CO_3, C-K, C-K_2O, C-CO and C-CO_2 reactions, facilitating breaking of the C-O-C and C-C bonds thus decreasing removal efficiency and carbon yield. That was why there were decreases in carbon yield as the radiation time increased. The decrease in carbon yield as radiation time was increased can equally be attributed to rapid evolution of volatile material to form stable compound. This is the reason why the carbon yield of spent grain activated carbon that has high volatile matter was lower than the activated carbon produced from hamburger seed shell.

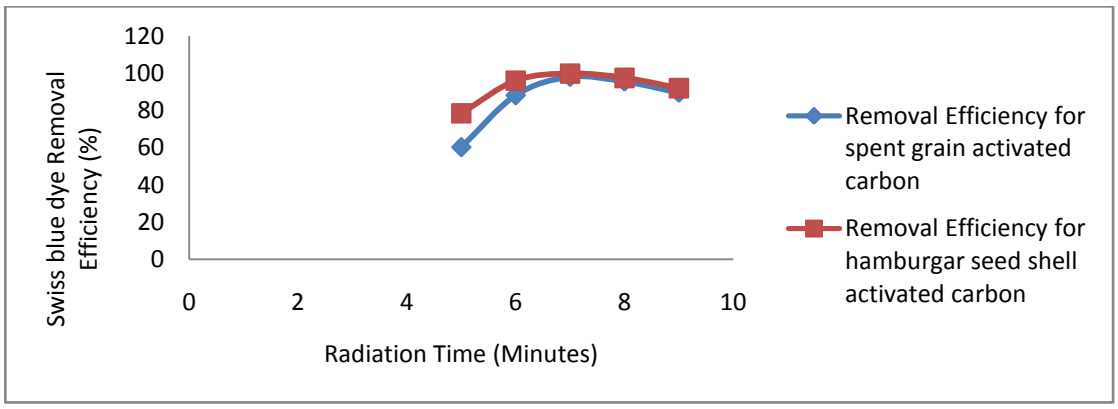

(a)

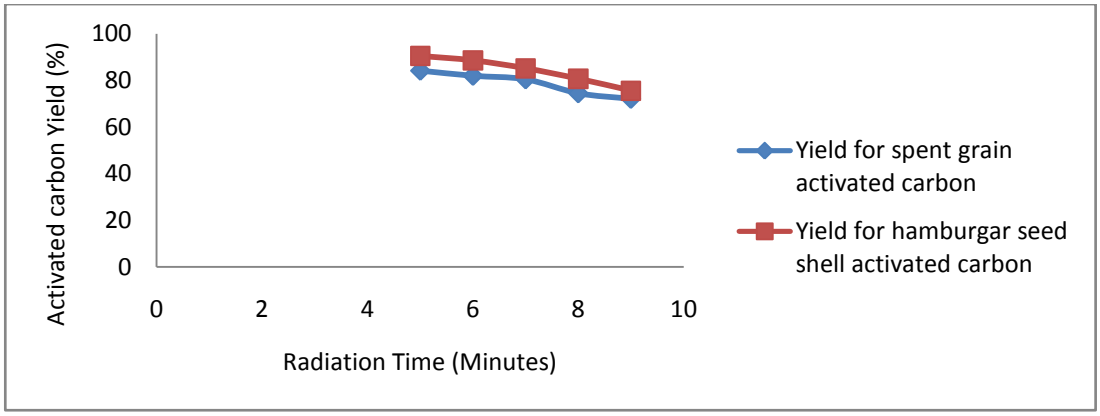

(b)

Fig. 4.6: Effect of Radiation time on Swiss blue dye Removal Efficiency (a) and Activated Carbon yield for both precursors.

c) Effect of KOH concentrationon on Swiss Blue Dye Removal Efficiency and Carbon Yield for Microwave Activation Process

Effect of KOH concentration on the Swiss Blue dye removal efficiency and carbon yield was studied at the microwave power output of 81% and irradiation time of 7mins at 1:1.5 carbon to KOH ratio. Fig. (4.7) shows that augmenting KOH concentration from 2M to 6M showed an increase in Swiss blue dye removal efficiency and carbon yield. Beyond 6M, further increase in KOH concentration illustrated a gradual decrease in Swiss blue dye removal efficiency and carbon yield. KOH activation involves the redox reduction and carbon oxidation to generate porosity. It can be deduced that the pore enlargement related to KOH activation is associated to the redox reduction and oxidative modification responsible for the development of micro and mesoporosity. During which the reaction of CO, CO_2 and H_2 constituents, and additional reactions between the active Intermediates with the carbon surfaces are possible (eqns. 4.1 to 4:3) (Pinero et. al., 2005).

$$6KOH + 2C \rightarrow 2K + 3H_2 + 2K_2CO_3 \quad (4.1)$$

$$K_2CO_3 + C \rightarrow K_2O + 2CO_2 \quad (4.2)$$

$$2K + CO_2 \rightarrow K_2O + CO \quad (4.3)$$

Concurrently, the alkaline and carbonate metal formed during the activation stage are Intercalated to the carbon matrix responsible for both stabilization and widening of pores between the carbon atomic layers. Therefore, by increasing the KOH concentration, the activation process was accelerated and correspondingly, the removal

efficiency was further enhanced (Foo & Hameed, 2011). Beyond the optimum value, the excessive KOH would promote vigorous gasification reaction, which destroys the carbon frame work leading to a drastic decrease of accessible areas besides, excessive KOH molecules might decompose following the reaction (Cao et. al., 2006)

$$2KOH \rightarrow K_2O + H_2O \quad (4.4)$$

$$H_2O + C \rightarrow CO + H_2 \quad (4.5)$$

Therefore, the catalytic oxidation entailed widening of mesopores structures and carbon burn off. Effect of KOH concentration on carbon yield was equally studied. It was observed that carbon yield increased with initial increase in KOH concentration and decreased with further increase in KOH concentration beyond the optimal value. The increase in yield at low KOH concentration was as a result of intercalation of potassium metals on the carbon matrix which resulted to increase in weight. Additionally, a further increase in KOH Concentration beyond the optimal value would intensity a vigorous activation reaction, which leads to carbon burn off and transition of microspores- mesopores into macrospores lowering the carbon yield.

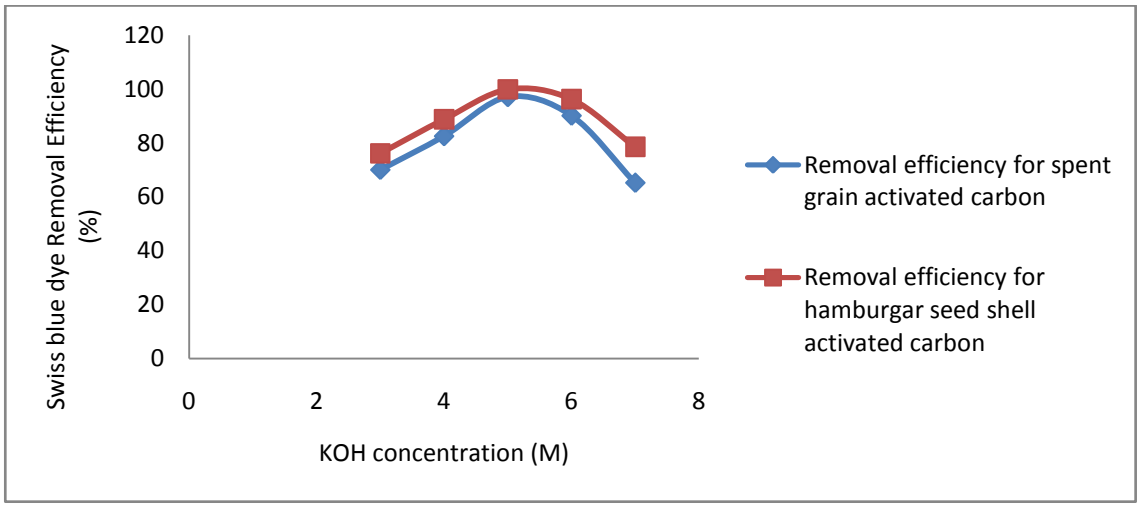

(a)

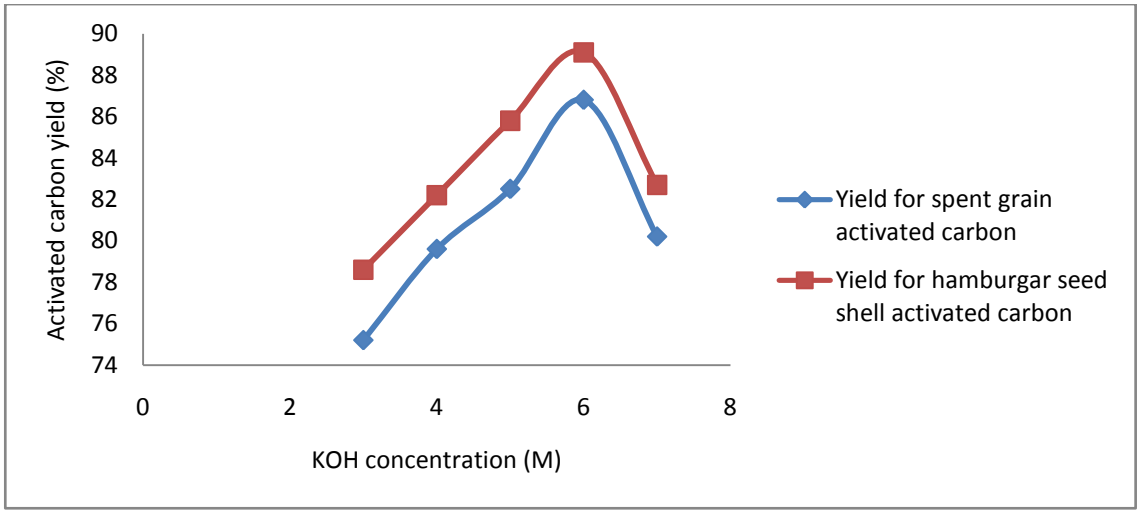

(b)

Fig. 4.7: Effect of KOH Concentration on Swiss blue dye Removal Efficiency (a) and Activated carbon yield (b) for microwave activation.

4.3. Optimization of Activation Conditions for Maximum Removal Efficiency of Swiss Blue Dye

Optimization of activation conditions for both microwave and conventional methods were achieved using three factors full central composite design (CCD). The design involved a two level full factorial design with six star points and six center points. In this work, optimization of the activation conditions were done differently for the two methods because of different operational conditions involved. Each method has three numeric factors and one categoric factor. The categoric factor is the precursor types and had two levels of hamburger seed shell and spent grain. In each design, the two levels of the categoric factor multiplied the total numbers of the experiments resulted from numeric factors to give forty (40) experiments each. The numeric factors for conventional heating are activation time (mins), activation temperature (^{o}C) and KOH concentration (M). The numeric factors for microwave heating are radiation time (mins), power levels (%) and KOH concentration (M).

4.3.1. Selection of a good predictive model for activation processes

A good predictive model is the prerequisite for optimization process. Sequential model sum of squares was used to select the best model based on the highest order model that was significant (small p-value) and not aliased, no lack of fit (p-value > 0.1) and reasonable agreement between adjusted R-Squared and predicted R-squared (within

0.2 of each other). Lack of fit which is the measure of risk was included because some points were replicated (center points) to produce estimate of pure error. Quadratic models were suggested based on the above stated conditions for the two heating methods. The suggested model had significant p-value, non-significant lack of fit value, and good agreement between the adjusted and predicted R-squared (within 0.2 each other).

4.3.2. Analysis of variance (ANOVA) for activation processes

The suggested models were inspected for adequacy for predicting the response using Analysis of variance (ANOVA). ANOVA tested the suggested model, the linear terms, interaction terms and the quadratic terms included in the model. A term was removed from the model only when it had insignificant p-value (> 0.05) or was retained in model to support model hierarchy. For microwave heating (Table 4.10), the model F-value of 85.39 implied that the model was significant. There was only a 0.01% chance that a "Model F-Value" this large could occur due to noise. Values of "prob > F" less than 0.05 indicated model terms were significant. In this case, the linear effect of power level (A), activation time (B), KOH concentration (C), and type of precursor (D) were significant. Equally, the quadratic effects of power levels (A^2) and KOH concentration (C^2) were significant. Values greater than 0.1 indicated the model terms were not significant. The "lack of fit F-value" of 1.32 implied the lack of fit was not significant relative to pure error. There was a 31.16% chance that a "lack of fit F-value" this large could occur due to noise. Adjusted R-squared of 0.9285 was in good agreement with predicted R-squared of 0.9051. R-squared of 0.9395 showed that 93.95% variation on the response can be explained by the model.

For conventional heating (Table 4.11), the model F-value of 126.18 implied the model was significant. There was only 0.01% chance that a model F-value this large could occur due to noise. In this case, the single effect of temperature (A), KOH, activation time (B), KOH concentration (C) and precursor types (D) were significant. Interaction effect of activation temperature and KOH concentration (AC) and quadratic effect of activation temperature (A^2), activation time (B^2) and KOH concentration (C^2) were significant. The lack of fit F-value of 0.99 implied that lack of fit was not significant relative to pure error. There was only a 53.47% chance that a "lack of fit F-value" this large could occur due to noise.

R-squared of 0.9702 showed that 97.02% variation on the response can be explained by the model. Adj. R-squared of 0.9625 was in good agreement with the predicted R-squared of 0.9502. Adequate precision of 38.316 indicated adequate signal.

Table 4.10: ANOVA table for Microwave activation process

Source	Sum of Squares	df	Mean Square	F Value	p-value Prob>F
Model	10642.35	6	1773.72	85.39	< 0.0001
A-Power levels	7803.13	1	7803.13	375.67	< 0.0001
B-Activation time	670.70	1	670.70	32.29	< 0.0001
C-KOH Concentration	656.13	1	656.13	31.59	< 0.0001
D-Type of precursor	337.56	1	337.56	16.25	0.0003
A^2	905.97	1	905.97	43.62	< 0.0001
C^2	117.25	1	117.25	5.64	0.0235
Residual	685.45	33	20.77		
Lack of Fit	520.09	23	22.61	1.37	0.3116
Pure Error	165.36	10	16.54		
Cor Total	11327.80	39			

Table 4.11: ANOVA table for Conventional activation process

Source	Sum of Squares	df	Mean Square	F Value	p-value Prob > F
Model	2413.49	8	301.69	126.18	< 0.0001
A-Activation temperature	727.43	1	727.43	304.24	< 0.0001
B-Activation time	12.07	1	12.07	5.05	0.0319
C-KOH Concentration	973.84	1	973.84	407.30	< 0.0001
D-Type of precursor	26.07	1	26.07	10.90	0.0024
AC	20.09	1	20.09	8.4	0.0068
A^2	336.80	1	336.80	140.87	< 0.0001
B^2	25.30	1	25.30	10.58	0.0028
C^2	450.09	1	450.09	188.25	< 0.0001
Residual	74.12	31	2.39		
Lack of Fit	50.01	21	2.38	0.99	0.5347
Pure Error	24.11	10	2.41		
Cor Total	2487.61	39			

The final equation in coded form after removing the insignificant factors for microwave activation can be represented as follows:

Removal efficiency (%) = +74.13 15.62A – 4.58B + 4.53C – 2.91D – $4.15A^2$ + $1.49C^2$. (4.6)

Final equation in actual form is represented in terms of levels of the categorical factor (D) in equation 4.7 and 4.8.

Microwave prepared activated carbon from hamburger seed shell (MPAHS);

Removal efficiency (%) = +29.41831 + 1.65221 power level – 1.52604 activation time– 7.40402 KOH concentration – 8.18959E – 003 power $level^2$ + 1.49152 KOH $concentration^2$. (4.7)

For microwave prepared activated carbon from Spent grain (MPASG);

Removal efficiency (%) = +123.60831 + 1.65221 power level -1.52604 activation time– 7.40402 KOH concentration – 8.1895E – 003 power $level^2$ + 1.49152 KOH $concentration^2$. (4.8)

The final equation in terms of coded factors after removing the insignificant factors for the conventional activation process can be represented thus:

Removal efficiency (%) = +94.51 + 4.77A + 0.61B + 5.52C – 0.81D – 1.12AC +2.59A^2 – 0.71B^2 – 2.99C^2. (4.9)

In actual form, it can be represented for the two levels of categorical factor (D) as follows;

Conventionally prepared activated Hamburger seed shell (CPAHS);

Removal efficiency (%) = -224.68847+ 0.50658 temperature +0.16232time + 38.41565KOH concentration -0.011206temperature x KOH concentration – 2.58801E -004 $temperature^2$ – 7.88068E – 004$time^2$ -2.99176 KOH $concentration^2$. (4.10)

Conventionally prepared activated spent grain (CPASG);

Removal Efficiency (%) = -222.47397 + 0.50658temperature + 0.16232time + 38.41565KOH concentration – 0.011206temperature x KOH concentration – 0.04$temperature^2$ – 7.88068E-004$time^2$ -2.99176KOH $concentration^2$ (4.11)

4.3.3. 3D Surface plots of interaction effect for conventional activation process

From ANOVA, it was observed that no interaction effect was significant using microwave activation process. Figure 4.8 shows the interaction effect of KOH concentration with activation temperature, while Fig. 4.9 shows the interaction effect of KOH concentration with activation time. It was seen from the plot (fig. 4.8) that increased in both KOH concentration and activation temperature increased the removal efficiency of Swiss blue dye to a point that further increase in both factors decreased the removal efficiency. The result is in agreement with the study carried out by Bello et. al. (2012) that used banana stalk to prepare activated carbon. It was found that activation temperature and impregnation ratio (IR) has significant effects on removal of malachite green dye. This is equally in agreement with Mohd et. al. (2015) that used lime peel to produce activated carbon for malachite green dye removal. An increase in temperature promotes devolatilization rate resulting in significant effect to the pore structure of activated carbon produced (Sudaryanto et. al., 2006). Increase in temperature increased the volatiles released as a result of intensification in dehydrating and elimination reaction which increased the C-KOH reaction rate. In fact, at higher temperature, the activation time should just be enough to eliminate all the moisture and

volatile components for pores to develop (Molid et. al., 2015). Intercalation of potassium metal ions on the carbon sample at high temperatures enhanced the pore development of the activated carbon. KOH been a dehydrating agent, penetrated deep into the structure of the carbon sample, further gasified the carbon, and led to widening of micropore to mesopore (Wu & Tseng 2006). However, excess KOH concentration causes undesirable effect that leads to low removal efficiency. Excess KOH leads to the presence of excess K_2CO_3 and the metallic K blocks the pore of the activated carbon. This was in accordance with the finding of El-Hendawy (2005). This effect can be seen from the plot, that at very high activation temperature and high KOH concentration that the removal efficiency of the Swiss blue dye dropped. The pore size instead of getting widened becomes blocked resulting in a decrease in removal efficiency. Figure 4.8 shows that increase of KOH concentration and activation time increased the removal efficiency that further increase on the factors decreased the removal efficiency. The same shape of the graph was obtained for both precursors used in production of action carbon.

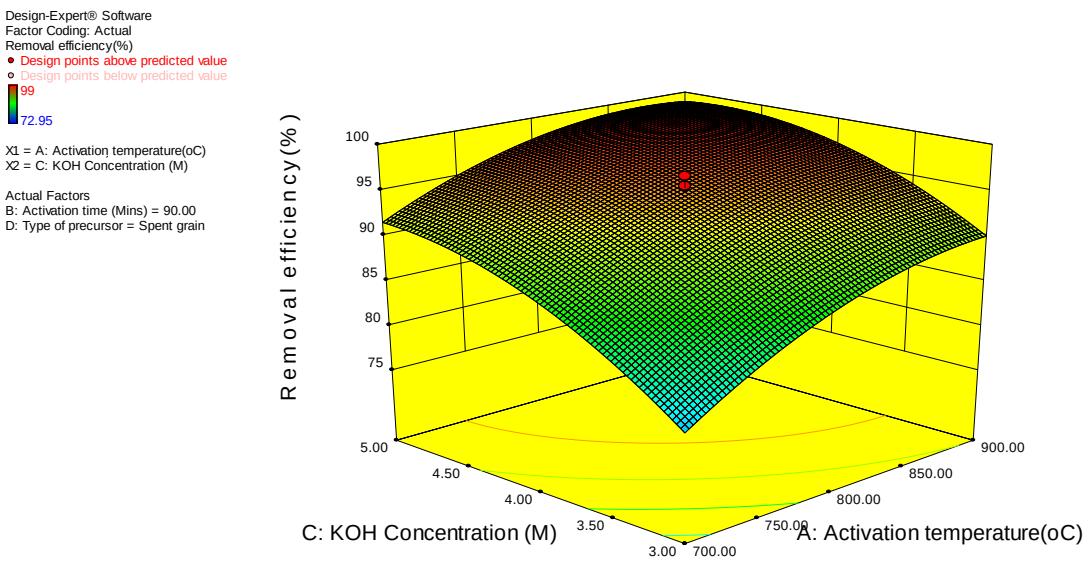

(a)

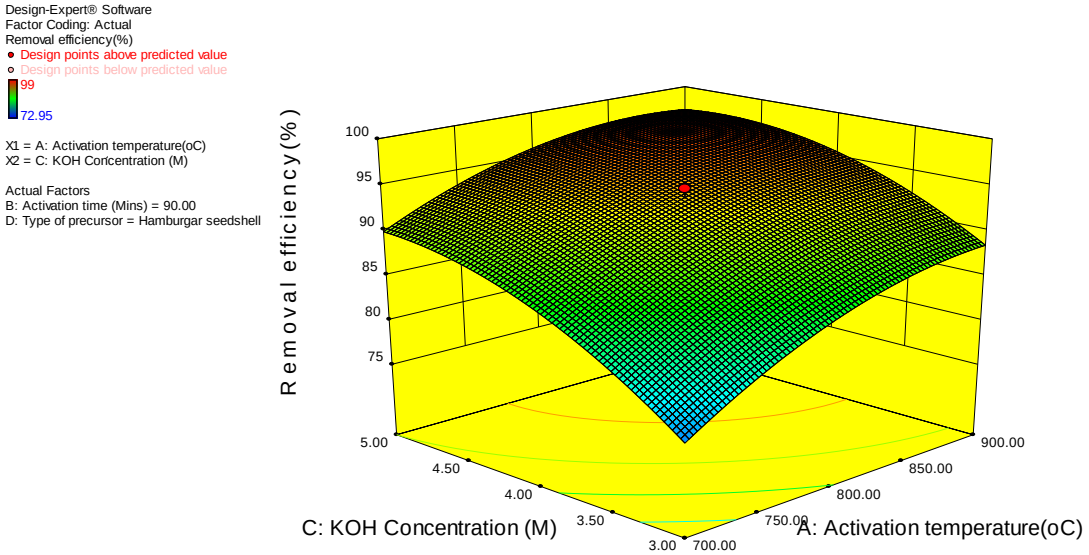

(b)

Fig. 4.8: 3D surface plot for interaction effect of activation temperature with KOH concentration for conventional activation process (a) Spent grain (b) Hamburgar seed shell

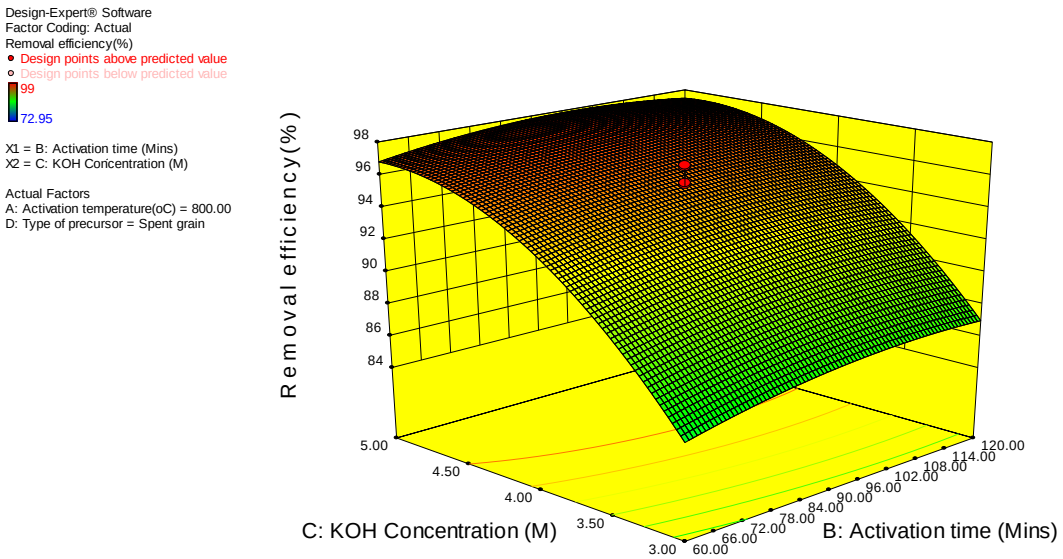

(a)

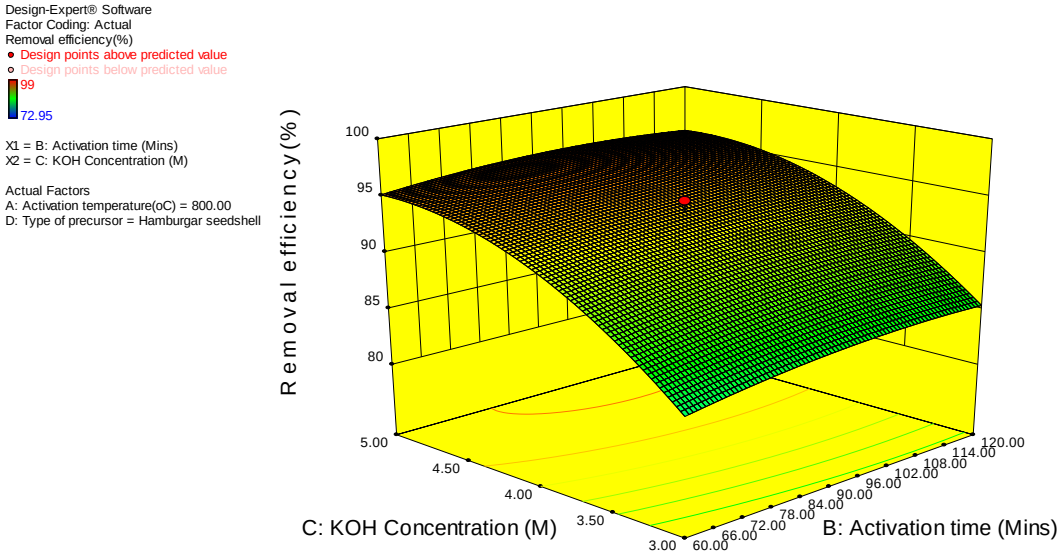

(b)

Fig: 4.9. 3D surface plot for interaction effect of activation time with KOH concentration for conventional activation process (a) Spent grain (b) Hamburgar seed shell

4.3.4. Optimal conditions for activation processes

The negative effect experienced at extreme activated condition necessitated the need for optimization. Numerical optimization was done with the target of maximizing the removal efficiency of the Swiss blue dye. Tables 4.12 and 4.13 show the optimum conditions for conventional activation and microwave activation processes respectively.

Table.4.12: Optimal Conditions for the Conventional Activation Process

Desirability	Precursor Types	Activation Temp.(^{o}C)	Activation Time (mins)	KOH Concentration (M)	Removal Efficiency (%)
1.0	Spent Grain	857.15	83.62	4.77	99.0193
0.935	Hamburgar seed shell	875.40	102.98	4.78	97.7869

Table. 4.13: Optimal Conditions for the Microwave Activation Process

Desirability	Power Level (%)	Radiation Time (Mins)	KOH Conc. (M)	Precursor Types	Removal Efficiency (%)
0.990	81.00	7.0	5.0	Hamburgar Seed Shell	99.70
0.982	81.00	7.0	5.0	Spent Grain	99.51

The optimum conditions obtained were validated with little errors of less than 0.4% (Tables 4.14 and 4.15). This confirmed the adequacy of the model equation in predicting the removal efficiency of swiss blue dye.

Table 4.14: Model validation for Conventional Activation Process

Precursor Type	Activation Temp (^oC)	Activation Time (mins)	KOH Conc. (M)	Removal Efficiency (%)		Error (%)
				Experimental values	Predicted values	
Spent Grain	857.15	83.62	4.77	99.10	99.0193	0.08
Hamburgar seed shell	875.40	102.98	4.78	97.9	97.7869	0.12

Table 4.15: Model validation for Microwave Activation Process

Precursor Type	Power level (%)	Radiation Time (mins)	KOH Conc. (M)	Removal Efficiency (%)		Error (%)
				Experimental values	Predicted values	
Hamburgar seed shell	81.0	7.0	5.0	99.8	99.70	0.1
Spent Grain	81.0	7.0	5.0	98.50	99.51	0.01

4.3.5. Effect of activation methods on the removal efficiency of Swiss blue dye

In order to analyze the effect of different method of activation used in this study (conventional and microwave) on the removal efficiency of swiss blue dye solution, the adsorption was done using 0.02g of each activated carbons prepared using the optimal conditions obtained. The adsorption process was done for 2hrs in a mechanical shaker using 25ml of 30mg/l of Swiss blue dye solution. As can be seen from the results in Fig. 4.10 that all the activated carbons prepared from the two precursors had removal efficiency above 90$^{o}/_{o.}$ Microwave prepared activated carbon from hamburger seed shell (MPAHS) showed highest removal efficiency, followed by microwave prepared activated carbon from spent grain (MPASG), followed by conventionally prepared activated carbon from spent grain (CPASG) and lastly conventional prepared activated carbon from hamburger seed shell (CPAHS).

High removal efficiency experienced by microwave activated carbons was as a result of mode of heating using microwave. The mechanism of microwave heating is different from conventional heating methods. Microwave heating is achieved throughout the volume of the material by direct conversion of electromagnetic waves energy to heat as waves penetrate the substance (Volumetric heating). As a result, the rate of heating is not limited by the thermal diffusivity of material and therefore more uniform heating is assumed to be achieved (Meredith, 1998). Also microwave heating is referred to as selective heating as electromagnetic wave energy is only dissipated as heat in material with suitable dielectric properly and not necessary everything in contact with them.

Conventionally, once heat is received by a material, it is transferred from its surface towards the body center, mainly by conduction. During the course of conventional heating, a large heat gradient is formed from the surface to the core of material. Due to the thermal inertia of the system, the temperature of the materials is always lower than the furnace, to the point that in many cases deep inside the work wall cannot reach the desired temperature (Fernandez et. al., 2011). Moreover, assuming that the surface temperature is controlled precisely, the heat transfer rate from the surface into the body is highly limited by the physical properties of the material such as specific heat, thermal conductivity and density. Furthermore, larger workspace implies longer time to heat the workspace by conventional method and is also much more difficult as well as non-uniform when the material is thick (Meredith, 1998).

In order words, when materials are heated by conventional method, a heat gradient will form with the hottest layer being nearest to the external surface. Primary volatile matter produced near the center of material needs to pass through the higher temperature region towards the external surface, this hotter zone is actually where secondary reactions occur. These secondary reactions results in decomposition of the volatiles and larger amount of amorphours carbon being deposited in the porous structure of activated carbon (Miura et. al., 2004). In contrast, due to the volumetric heating facilitated by microwave heating mechanism, the exterior surface of a material heated in this manner is cooler than its core. This enables volatiles to quickly exit the material before thermal cracking occur inside the material.

Consequently, the porous structure in microwave activated carbon appears to be clear and exhibit a more open structure than activated carbon from conventional method.

The volumetric heating and deep energy penetration reported for microwave heating is believed to produce more uniform heating inside the material. However, a successful treatment with microwave is strongly dependent not only on the operational parameters such as power level, radiation time and cavity design, but equally dependent in the intrinsic dielectric properties of the materials (Clark & Sutton, 1996). This may explain the reason while microwave prepared activated carbon from hamburger seed shell (MPAHS) had more removal efficiency compared to microwave prepared activated carbon from spent grain (MPASG). From the result, it can be deduced that hamburger seed shell had more dielectric property than spent grain. A dielectric material is a substance that is a poor conductor of electricity but an efficient supporter of electrostatic fields. This is the reason while it was able to support more of electrostatic field than spent grain while dispatching minimal energy in form of heat. This resulted to more efficient activation with consequent high Swiss blue dye removal efficiency. Conventional prepared activated carbon from spent grain (CPASG) had more removal efficiency when compared to conventional prepared activated carbon from hamburger seed shell. This can be attributed to the high volatile content on spent grain which escaped during activation with subsequent development of more pores compared to hamburger seed shell.

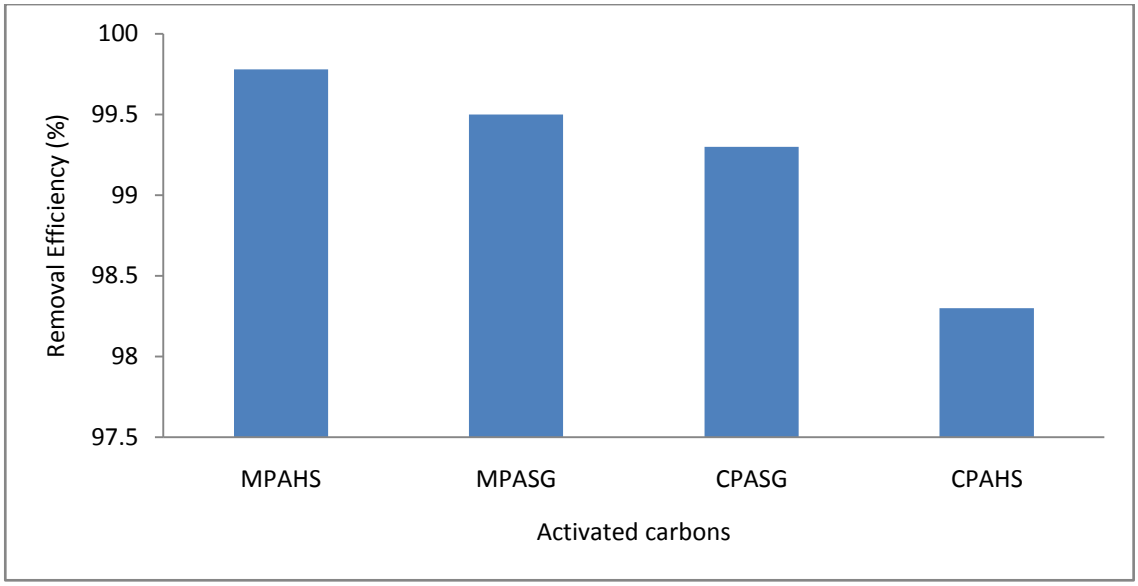

Fig. 4.10: Effect of activation method on the Removal Efficiency of Swiss blue dye

4.4. Effect of process factors on the adsorptive capacity of the carbons

Batch adsorption process was done with the use of isothermal shaker. Effect of some process factors was studied and the performances were determined by calculating the adsorptive capacity at the end of the process.

4.4.1. Effect of contact time on the adsorptive capacity of the carbons

The effect of contact time on the adsorptive capacity of the four activated carbons is shown in Fig. 4.11, it was seen from the result that adsorption capacity increased quickly at the beginning, after about 200mins for microwave prepared activated carbon from spent grain (MPASG), 240mins for conventional prepared activated carbon from hamburger seed shell (CPAHS) and 240mins for other activated carbons (MPAHS, CPASG), adsorption of Swiss blue dye nearly reached equilibrium. From the result, it can be said that kinetics of removal efficiency of the dye were formed in two phases. First an initial rapid phase where the adsorption of dye molecules was fast and instantaneous, and the second phase was a slow stage in which the contribution to the total dyes removal efficiency was relatively small, and finally the removal of the dye reached equilibrium (Han et. al., 2009). The initial rapid uptake can be attributed to large number of vacant sites on the surface of the adsorbent available during the initial stage of adsorption and afterward, it became difficult to occupy the remaining vacant sites due to the repulsive force between the adsorbed molecules on the solid and bulk

phases. The figure equally showed the effect of initial dye concentration on the adsorption of dye onto the adsorbents. All the concentration represented a shape characterized by an initial increase on adsorption capacity which gradually tailed off thereafter. This indicated that equilibrium time was independent of concentration. The result also showed that increase in initial concentration increased the adsorptive capacity of the adsorbents which shows that the adsorption process is highly dependent on the initial concentration. Increase in initial concentration increased the driving force to overcome the mass transfer resistance for Swiss blue dye transfer between the solution and the surface of the activated carbon (Qadeer, 2007). The Swiss blue molecules countered the boundary layer effect and then diffused from the boundary layer film onto adsorbent surface and finally diffuse into the porous structure of the adsorbent (Kumar & Sivenesan, 2006).

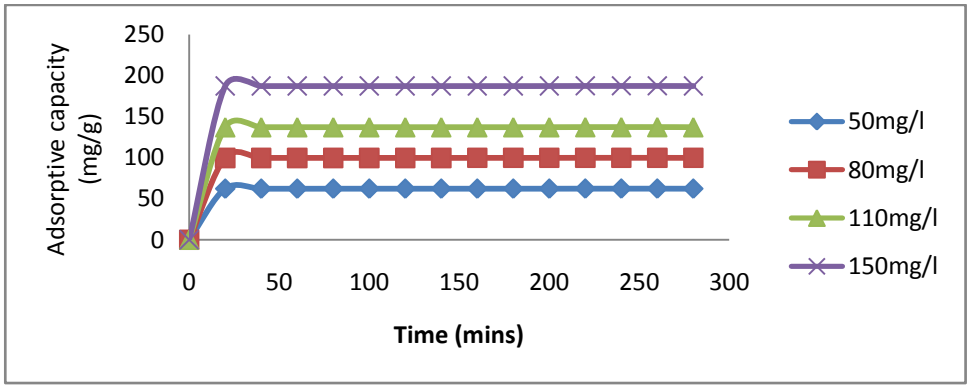

(a)

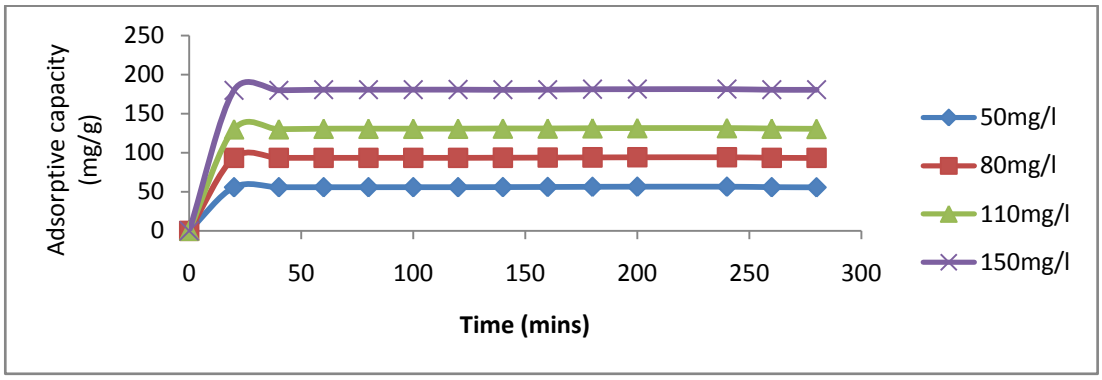

(b)

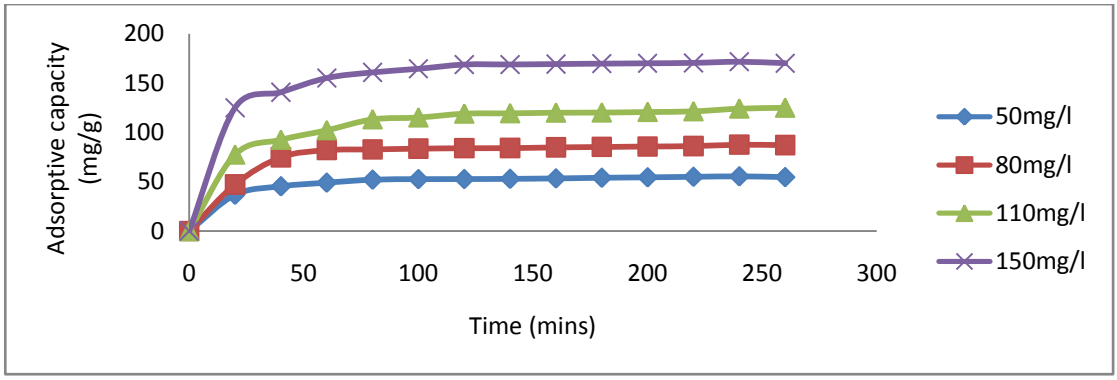

(c)

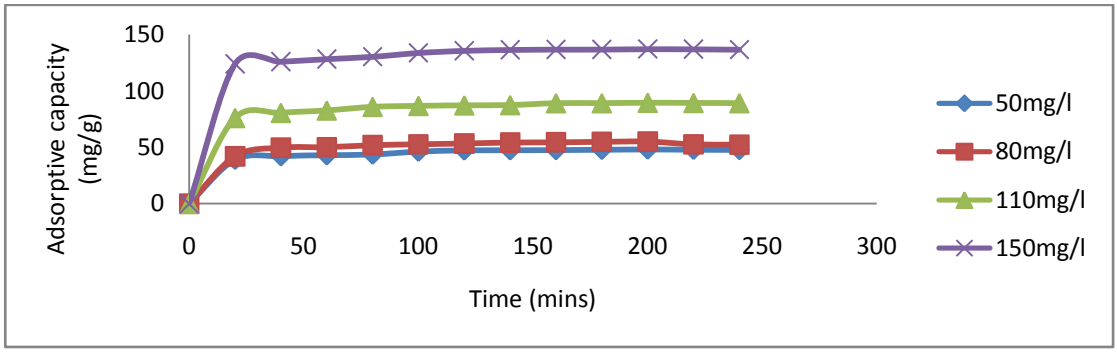

(d)

Fig. 4.11: Effect of contact time on the removal Efficiency of Swiss blue dye (a) MPAHS, (b) MPASG, (c) CPASG, (d) CPAHS.

4.4.2. Effect of adsorbent dosage on the adsorptive capacity of Swiss blue dye

Effect of adsorbent dosage was studied at different initial dye concentration. It is a well-known fact that adsorbent dosage increases the removal efficiency of adsorbents due to increase in adsorption surface area of micropores and the availability of adsorption sites (Emad et. al., 2006; Demirbas, 2009). On the other hand, adsorptive capacity which is the adsorbed amount of dye per unit mass of the adsorbent decreased with the increase in the adsorbent dosage as was observed from this study (Fig. 4.12). This can be attributed to the splitting effect of flux (concentration gradient) between adsorbents with increasing adsorbent concentration causing a decrease in amount of dye adsorbed onto unit weight of adsorbent (Dalia et. al., 2012; Unuabonah et. al., 2009). Equally, the high adsorbent dosage may influence the physical characteristics of the solid-liquid suspension such as by increasing the viscosity and inhibiting the diffusion of dye molecules to the surface of the adsorbents (Sulak et. al., 2007). Since the concentrations of the Swiss blue dye was fixed, the adsorptive capacity decreased with increase in adsorbent dosage. It was equally observed from fig.4.12 that

adsorptive capacity increased as the initial Swiss blue dye concentration was increased. This can be attributed to increase in mass gradient between solution and adsorbent and thus act as driving force for the transfer of dye molecules from bulk solution to the particle surface. The higher adsorptive capacity recorded for microwave hamburger seed shell activated carbon is corresponded to its higher specific surface area when compared to other absorbents used in this study.

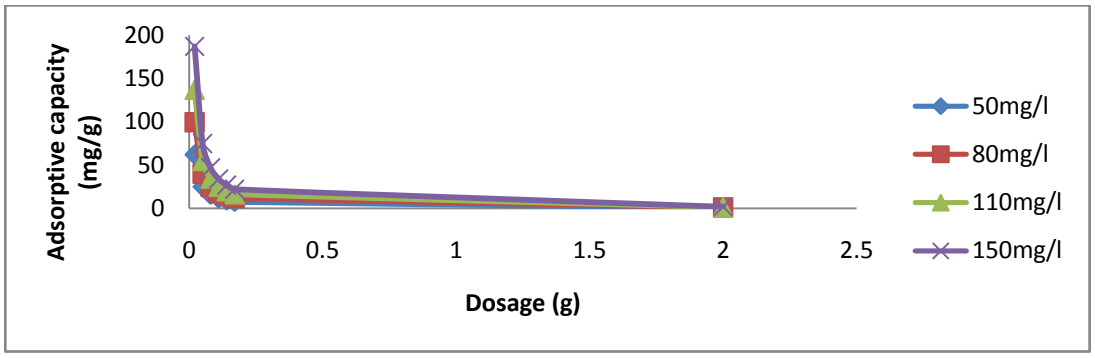

(a)

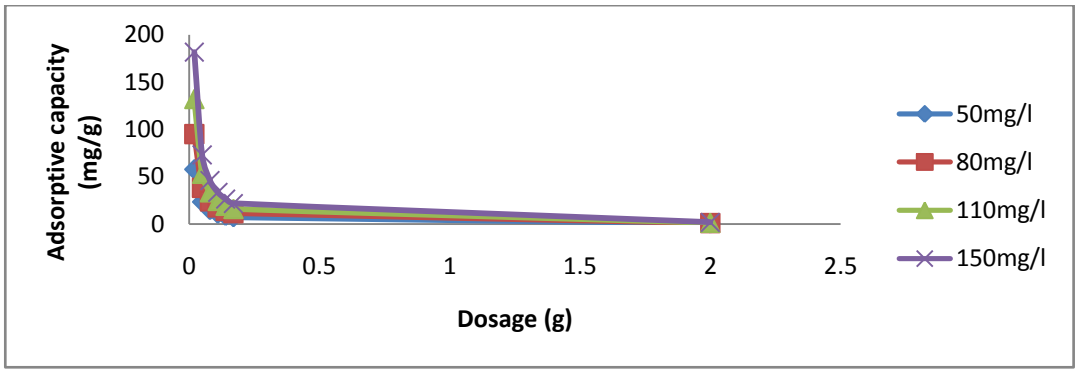

(b)

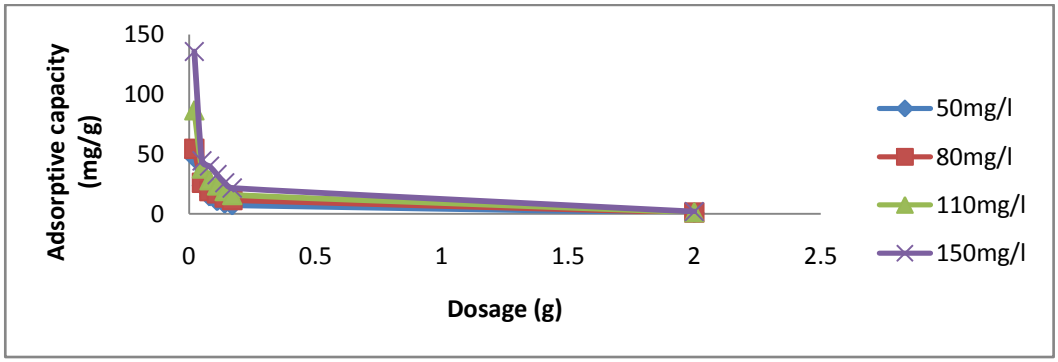

(c)

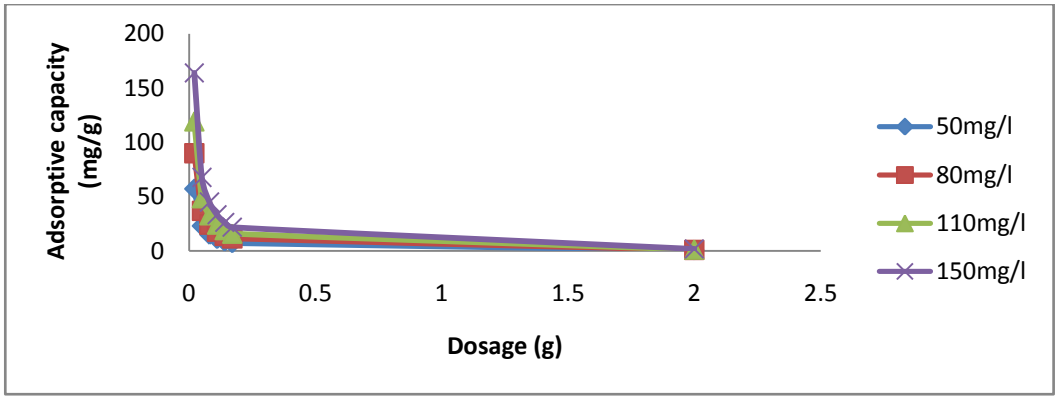

(d)

Fig. 4.12 Effect of dosage on the adsorptive capacity of Swiss blue dye (a) MPAHS, (b) MPASG, (c) CPASG, (d) CPAHS

4.4.3. Effect of pH on the adsorptive capacity of Swiss blue dye

pH plays a major role in the adsorptive removal of dyes from aqueous solution. Dyes exist in the ionic form in the aqueous systems (Safa & Bhatti, 2011), therefore, Swiss blue dye been a cationic dye exist as positive ions in aqueous solution. As charged species, the degree of their adsorption onto the activated carbon surface is primarily influenced by the surface charge on the adsorbent which in turn is affected by the solution pH. The pH of the solution influences the properties of biomass materials, affects the adsorption mechanisms and dissociation of the dye molecules.

Activated carbons are species with amphoteric character, thus depends on the pH of the solution (Al-Othman et. al., 2012). Their surface might be positively charged or negatively charged. The pore walls of activated carbon contained a large number of surface functional groups (Al-Othman et. al., 2012). From the result of P^{H}_{PZC}, it was understood that the active sites of the activated carbons were acidic sites, dominated by acidic functional groups; carboxylic (-COOH), phenolic (ph-OH), etc. The pH dependence of Swiss blue dye adsorption can largely be related to the type and ionic state of these functional groups and also on the adsorbate chemistry in the solution. The pH studies results revealed that electrostatic and ion exchange activities between the Swiss blue dye and the adsorbents increased at elevated pH (fig. 4.13). According to Al-Degs et. al. (1999), pH_{PZC} can be used as an index of the ability of the surface to become either positively or negatively charged. The ability is controlled by the pH of the surrounding solution. When the pH of the solution < pH_{PZC}, the activated carbon

will react as a positive surface and as a negative surface when pH of solution > pH_{PZC}. Thus, as pH was increased, the surface functional groups on the carbons were deprotoned, which resulted in a decrease in surface charge density (Emad et al., 2006). This implies that adsorption of cationic dye could be enhanced at higher pH (Chen & Lin 2001). The experimental determination of the pH_{PZC} of the activated carbons revealed that their pH_{PZC} were in the range of 6.3-6.5 (fig. 4.14). This showed that at higher pH, pHof the solution > pH_{PZC}. In this study, the increase in adsorptive capacity at higher pH can be attributed to the fact that at high pH (basic), the active sites became anionic in nature, the functional groups turns to $–COO^-$, ph-O^- and the negatively charged species started dominating (Purkait et al., 2007). Swiss blue dye been cationic, gets attached to the surface of the activated carbons by electrostatic attraction. The increase in electrostatic attraction between negative charged adsorbents particles and positive charged adsorbate species (cations) led to increase in adsorptive capacity of Swiss blue dye. Also, low pH (acidic pH) retarded the Swiss blue dye adsorption on all the activated carbons. This may be attributed to the repulsion activities by similar ionic charges present, that is, the prevalence of H^+ in the acidic medium and cations of Swiss blue dye. At low pH (acidic), the sites remain cationic (-COOH), (ph-OH) and positively charged species started dominating. Because of inter ionic repulsion between the similar charges, adsorptive capacity decreased. This was in conformity with Auta and Hameed (2012), that studied the clay adsorption of methylene blue dye. It was equally observed from this work that similar trend was observed using different initial Swiss blue dye concentration using all the adsorbents.

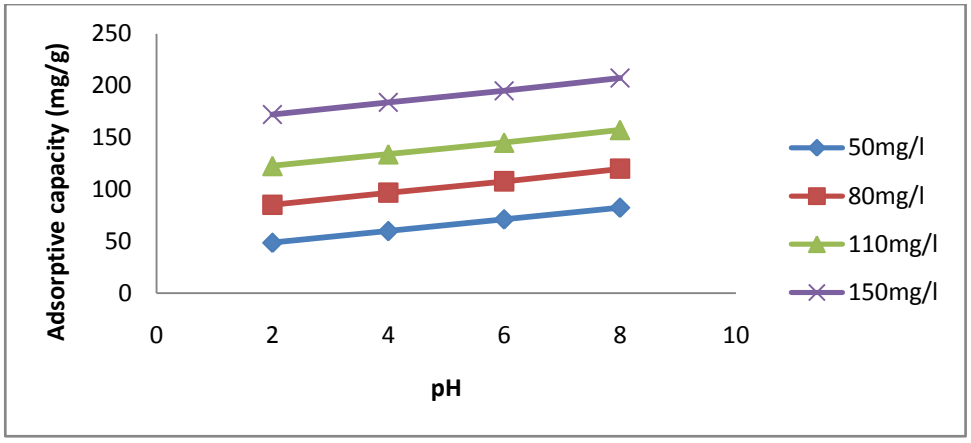
Adsorptive capacity (mg/g)
250
200
150
100
50
0
0
2
4
6
8
10
pH
50mg/l
80mg/l
110mg/l
150mg/l

(a)

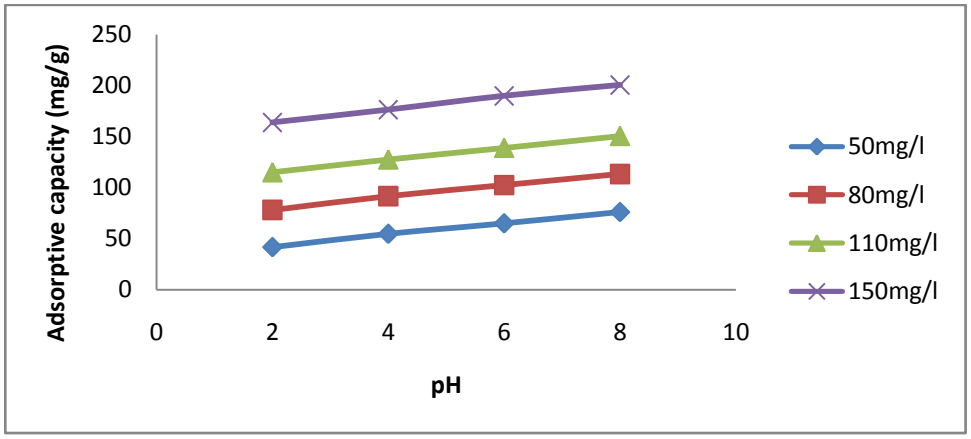
Adsorptive capacity (mg/g)
250
200
150
100
50
0
0
2
4
6
8
10
pH
50mg/l
80mg/l
110mg/l
150mg/l

(b)

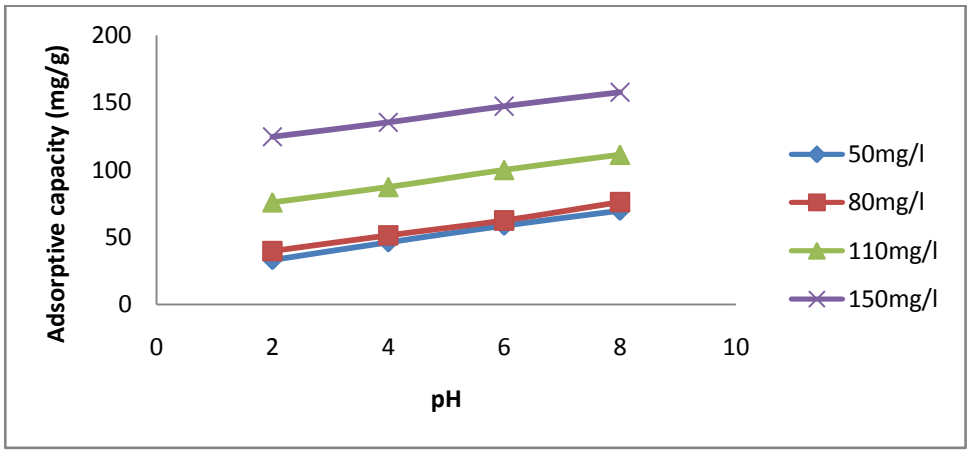
Adsorptive capacity (mg/g)
200
150
100
50
0
0
2
4
6
8
10
pH
50mg/l
80mg/l
110mg/l
150mg/l

(c)

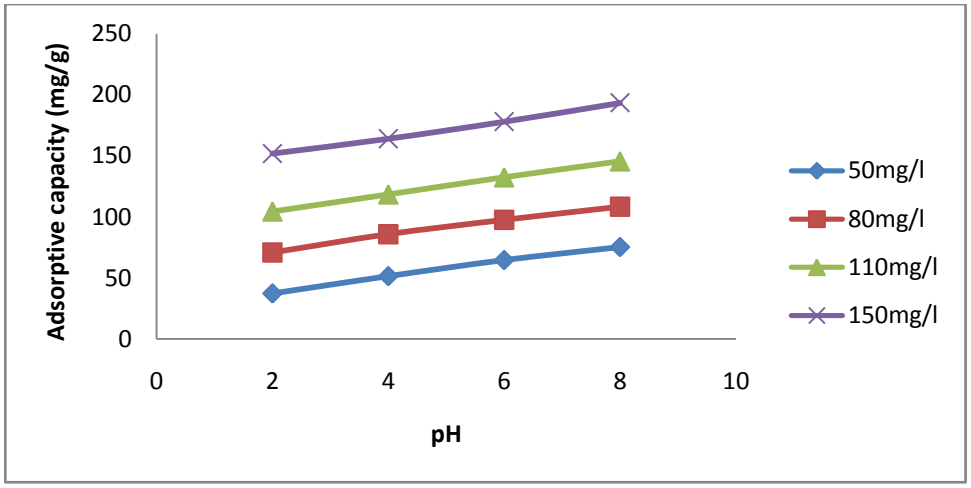

(d)

Fig. 4.13: Effect of pH on the adsorptive capacity of Swiss blue dye (a) MPAHS, (b) MPASG, (c) CPASG, (d) CPAHS

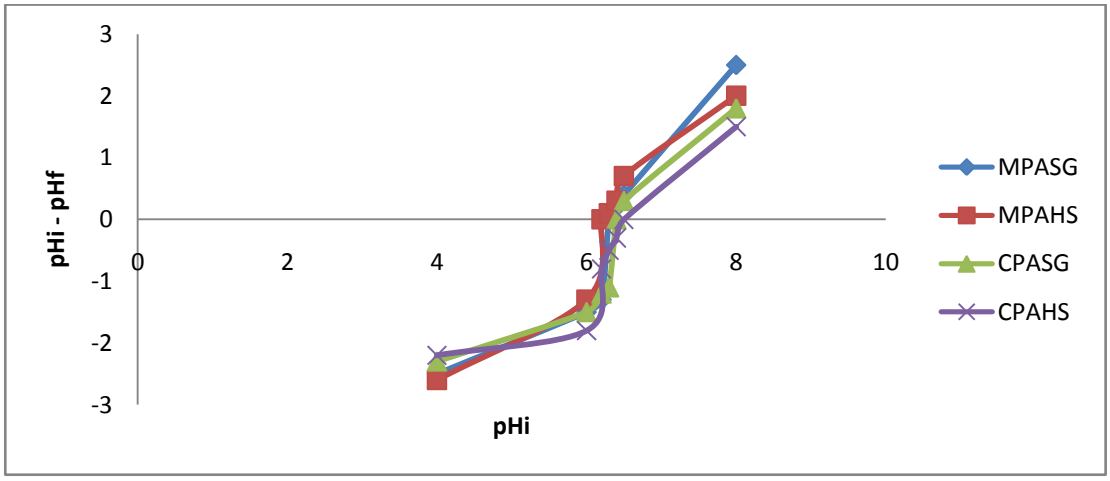

Fig. 4.14: pH of point of zero charge of the activated carbons

4.4.4. Effect of Temperature on the adsorptive capacity of Swiss blue dye

The effect of temperature on the adsorptive capacity of Swiss blue dye is shown on fig.4.15. Results indicated that the extent of adsorption of Swiss blue dye deceased with the increase in temperature. This indicated that the adsorption of Swiss blue dye was controlled by an exothermic process. This may be due to the dissociation of adsorbed dye molecules with increasing temperature. The decrease of adsorption capacity with increasing temperature may be equally due to a decrease in the chemical potential of the adsorbate at higher temperature (Sener, 2008). It may be due to an increase in the tendency of the dye molecules to escape from the solid phase at higher temperature (Sener, 2008). This was in agreement with work done by Sener (2008) on

the use of solid wastes of soda ash plant as an adsorbent for the removal of anionic dye. It was equally observed that adsorption capacities increased with increase in initial dye concentration. This can be attributed to the fact that increase in initial Swiss blue dye concentration increased the mass transfer gradient between the adsorbate and adsorbent thereby acting as driving force for the transfer of dye from the bulk solution to the surface of adsorbent.

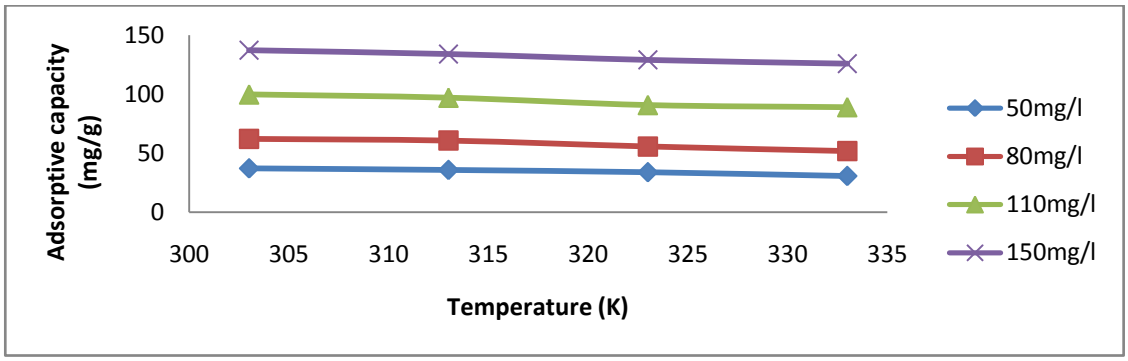

(a)

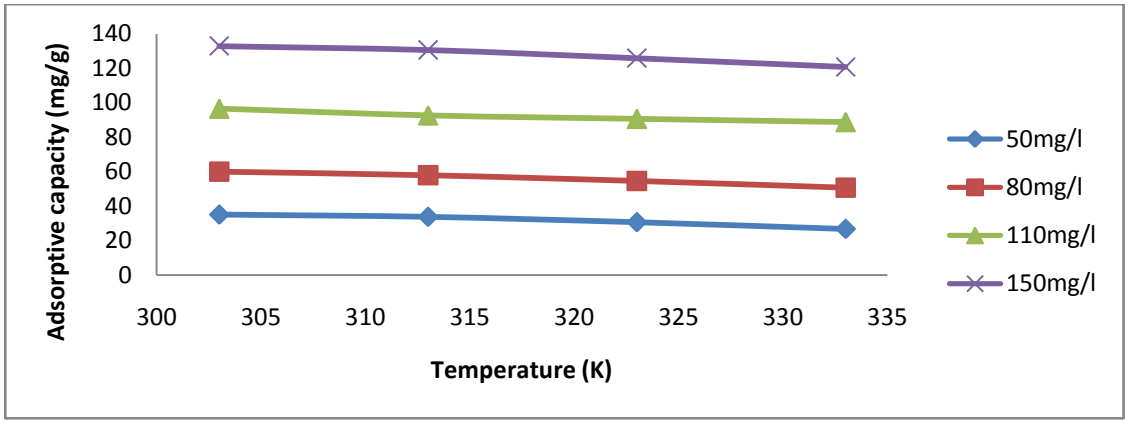

(b)

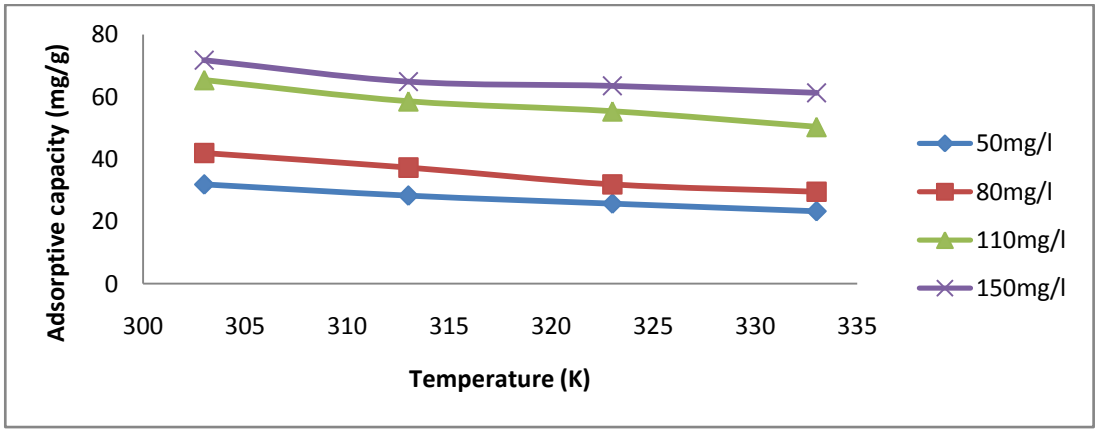

(c)

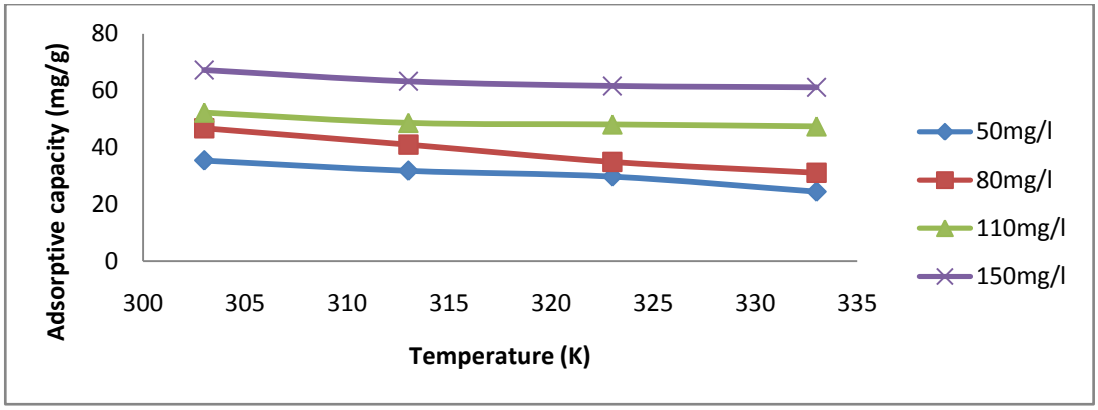

(d)

Fig. 4.15: Effect of Temperature on the adsorptive capacity of Swiss blue dye (a) MPAHS, (b) MPASG, (c) CPASG, (d) CPAHS

4.5. Optimization of adsorption conditions for Maximal Swiss blue dye removal using Box Benhken Design (BBD)

Box-Benhken design (BBD) provides three levels (-1, 0, +1) for each variable, which are equally spaced. The number of experiment required (N) is given by N = 2k(k-1) + Co, where k is the number of variables (numeric) and Co is the number of centre points.

This design is more economical and efficient in terms of the number of required runs than other RSM design. Therefore this design is useful in avoiding experiments that would be performed under extreme conditions, for which unsatisfactory results might occur.

In this study, we have four numeric variables, one categoric variable, and five center points. Four numeric variables with 5 center points gave the total number of experiments to be twenty nine (29). But categoric factor (type of adsorbent) involved had four levels (CPAHS, CPASG, MPASG, MPAHS). These levels multiplied the total number of experiments to get one hundred and sixteen experiments (116).

4.5.1. Analysis of variance for the adsorption process

From ANOVA table (table 4.16), the model F-value of 292.39 implied the model was significant. There was only a 0.01% chance that a model F-value this large could occur due to noise. Values of “Prob > F” less than 0.0500 indicated model terms were significant. In this case, the linear effect of pH, temperature, initial dye concentration, dosage and adsorbent types were significant. The interaction effect of pH and

temperature (AB), interaction effect of pH and initial dye concentration (AC), interaction effect of pH and dosage (AD), interaction effect of temperature and initial dye concentration (BC) and interaction effect of initial concentration and dosage (CD) were significant. Quadratic effect of temperature (B^2) and quadratic effect of dosage (D^2) were significant. Values greater than 0.100 indicated the model terms were not significant. The "lack of fit F-value" of 0.70 implied the lack of fit was not significant relative to the pure error. There was 84.87% chance that a lack of fit "F-value" this large could occur due to noise.

The predicted R-squared of 0.9684 was in reasonable agreement with the "Adj R-squared of 0.9726. R-squared of 0.9759 showed that 97.95% of the variation on the response can be explained by the model.

Table 4.16: ANOVA table for the adsorption process

Source	Sum of Squares	df	Mean Square	F Value	p-value Prob>F
Model	21190.77	14	1513.63	292.39	<0.0001
A-pH	2674.56	1	2674.56	516.66	<0.0001
B-Temp	1346.20	1	1346.20	260.05	<0.0001
C-Initial conc.	5963.24	1	5963.24	1151.94	<0.0001
D-Dosage	2832.23	1	2832.23	547.11	<0.0001
E-Type of adsorbent	5664.54	3	1888.18	364.75	<0.0001
AB	105.06	1	105.06	20.30	<0.0001
AC	40.01	1	40.01	7.73	0.0065
AD	89.30	1	89.30	17.25	<0.0001
BC	46.24	1	46.24	8.93	0.0035
CD	312.32	1	312.32	60.33	<0.0001
B2	1861.73	1	1861.73	359.64	<0.0001
D2	98.13	1	98.13	18.96	<0.0001
Residual	522.84	101	5.18		
Lack of fit	412.47	85	4.85	0.7	0.8487
Pure Error	110.37	16	6.90		
Cor Total	21713.62	115			

4.5.2. Model equation involving categoric factors

Model equation involving a categoric factor with more than two levels is always complex to analyze. Categoric factor levels are represented by indicator "dummy" variables in regression, the values of the dummy variables are "0" if that type is not

present in that treatment/run, and "1" it is present, therefore the four adsorbent type levels by 100, 010, 001 and -1-1-1 respectively as shown on Table 4.17 below.

Table. 4.17: Factors and levels for the categoric factors' levels

S/N	Names	E[1]	E[2]	E[3]
1	CPASG	1	0	0
2	MPASG	0	1	0
3	MPAHS	0	0	1
4	CPAHS	-1	-1	-1

Alphabet "E" means categoric factor with three runs [1], [2] and [3]. Treatment [1] involves only CPASG (100), treatment [2] involves only MPASG (010), treatment [3] involves only MPAHS (0010). Adsorbent type CPAHS (-1-1-1) served as the reference level in which all the adsorbent types were excluded. The model equation involving categoric factors can be seen as four model equations. One comprising of E [1] with all its interactions, two, comprising of E [2] with all its interactions, three, comprising of E[3] with all its interactions. The fourth equation was a reference equation. The fourth equation is equation with all the E terms and their interactions eliminated. The model equation in coded form is shown in as follows;

Removal efficiency (%) = +68.64 + 7.46A + 5.30B – 11.15C + 7.68D + 1.15E[1] – 6.75E[2] + 10.95E[3] – 2.56AB + 1.58AC + 2.36AD – 1.70BC – 4.42CD + 8.21B^2 – 1.89D^2 (4.12)

The model equation can be split into four equations as follows;

Conventional prepared activated carbon from spent grain (CPASG);

Removal efficiency (%) = +68.64 + 7.46A + 5.30B – 11.15C + 7.68D + 1.15E[1] – 2.56AB + 1.58AC+2.36AD–1.70BC–4.42CD +8.21B^2–1.89D^2. (4.13)

Microwave prepared activated carbon fron spent grain (MPASG);

Removal efficiency (%) = 68.48 + 7.46A + 5.30B – 11.15C + 7.68D – 6.75E[2] – 2.56AB + 1.58AC + 2.36AD – 1.70BC – 4.42CD + 8.21B^2 – 1.89D^2. (4.14)

Microwave prepared activated carbon from hamburger seed shell (MPAHS);

Removal efficiency (%) = 68.48 + 7.46A + 5.30B – 11.15C + 7.68D + 10.95E [3] – 2.56AB + 1.58AC + 2.36AD – 1.70BC – 4.42CD + 8.21B^2 – 1.89D^2. (4.15)

Conventional prepared activated carbon from hamburger seed shell (CPAHS);
Removal Efficiency (%) = 68.48 + 7.46A + 5.30B – 11.15C + 7.68D – 2.56AB + 1.58AC + 2.36AD – 1.70BC – 4.42CD + 8.21B^2 – 1.89D^2. (4.16)

4.5.3. Optimal Conditions for the adsorption process

The optimum conditions were generated with the aim of maximixing the Swiss blue dye removal efficiency. Tables (4.18 and 19) show the optimum conditions and the validated conditions respectively for the Swiss blue dye adsorption process.

Table 4.18: Optimal conditions for adsorption of Swiss blue dye

pH	Temp. (^oC)	Initial dye conc. (mg/l)	Dosage (g)	Adsorbent Types	Predicted Values (%)	Desirability
7.47	30.0	50.15	0.09	MPAHS	99.90	1.0
8.57	29.96	52.00	0.1	MPASG	99.79	1.0
8.16	30.00	50.05	0.1	CPASG	99.68	1.0
7.98	30.90	51.40	0.1	CPAHS	99.61	1.0

Table. 4.19: Model validation for the Adsorption of Swiss Blue Dye

pH	Temp. (^oC)	Initial dye conc. (mg/l)	Dosage (g)	Adsorbent types	Removal Efficiency (%)		Error (%)
					Experimental values	Predicted values	
7.47	30.0	50.15	0.09	MPAHS	99.90	99.87	0.03
8.57	29.96	52.00	0.1	MPASG	99.79	99.8	0.01
8.16	30.00	50.05	0.1	CPASG	99.68	99.7	0.02
7.98	30.90	51.40	0.1	CPAHS	99.61	99.66	0.05

As seen from the validation table, the errors obtained were less than 0.1%. This shows the experimental values were very close to the predicted values, thus, the model

equation generated was effective in predicting the removal efficiency of Swiss blue dye.

4.5.4. Adsorption Kinetics of Swiss blue dye

In order to analyze the adsorption kinetics of Swiss blue dye onto the prepared activated carbons, the first order, second order, pseudo first order, pseudo second order, Elovich and intra-particle models were applied to the experimental data. The kinetic data obtained from the models are shown on tables 4.20 -4.23, while the plots are shown on appendix F. The values of rate constant (ki) and the initial dye concentration (C_Ao) for the first order model were obtained from the slope and intercept respectively of plots of Log CAt against t. It is obvious from tables (4.13-4.16) that the model did not fit the experimental data due to the low correlation coefficients (R^2) and poor agreement between the calculated initial concentration (C_Ao) and the experimental initial concentration. This applied to all the adsorption process using the four prepared adsorbents.

Table. 4.20: Kinetic data of Swiss blue dye adsorption on microwave prepared activated carbon from spent grain

First order model				
Initial concentration(mg/l)	50.0	80.0	110.0	150.0
K_1(1/min)	-0.002	-0.002	-0.000	-0.000
C_{AO}(mg/l)	18.323	48.194	47.643	51.050
R^2	0.894	0.742	0.862	0.906
Second order				
Initial concentration(mg/l)	50.0	80.0	110.0	150.0
K_2(1/min)	0.00	8E-05	3E-05	-0.000
C_{AO}(mg/l)	19.230	52.631	50.000	12.658
R^2	0.910	0.716	0.826	0.144
Pseudo first order				
Initial concentration(mg/l)	50.0	80.0	110.0	150.0
Kp_1(1/min)	0.016	0.013	0.018	0.020
q_e(calc)(mg/g)	12.022	42.461	19.010	19.010
q_e(mg/g)exp	47.963	66.761	89.351	136.967
R^2	0.830	0.533	0.842	0.842
Pseudo second order				
Initial	50.0	80.0	110.0	150.0

concentration(mg/l)				
Kp_2(1/min)	0.002	8.5E-04	0.001	0.001
q_e(calc.)(mg/g)	50.00	66.667	100.00	142.857
q_e exp.(mg/g)	47.963	66.761	89.351	136.967
R^2	0.999	0.998	0.999	0.999
		Intra particle diffusion		
Initial concentration(mg/l)	50.0	80.0	110.0	150.0
K_{id}(mg/gmol)	0.941	2.162	1.33	1.527
C(mg/g)	35.62	32.91	71.92	117
R^2	0.937	0.964	0.924	0.949
		Elovich		
Initial concentration(mg/l)	50.0	80.0	110.0	150.0
β(mg/g)	0.242	0.118	0.168	0.151
R^2	0.965	0.925	0.981	0.949

The kinetic data were fitted to second order model. Rate constant and initial concentrations were obtained from the slope and intercepts respectively of the plot of $1/C_At$ Vs. t. From the data, it was observed that the data did not fit the model appropriately due to low correlation coefficients obtained and poor agreements between the calculated initial concentration (C_Ao) and the experimental initial concentration. The poor agreements were recorded for all the adsorbents used.

The pseudo first order rate constant (Kpi) and the adsorptive capacity (qe) were obtained from the slopes and intercepts respectively of the straight line of log (qe – qt) against time (t). The obtained correlation coefficients (R^2) were low for all the concentration and all the adsorbents. It was equally observed that the calculated adsorptive capacities (qe_{calc}) were not in agreement with the experimental adsorptive capacities (qe_{exp}).

The kinetic data were fitted to pseudo second order model and the rate constant (Kp_2) and the calculated adsorptive capacity (qe_{calc}) were obtained from the intercept and slope respectively of linear plot of t/qt versus time (t).

Table 4.21: Kinetic data of Swiss blue dye adsorption on conventional prepared activated carbon from spent grain

First order model				
Initial concentration(mg/l)	50.0	80.0	110.0	150.0
$-K_1$(1/min)	0.000	0.000	0.000	0.000
C_{AO}(mg/l)	5.571	5.610	6.639	6.095
R^2	0.843	0.839	0.903	0.771
Second order				
Initial concentration(mg/l)	50.0	80.0	110.0	150.0
K_2(1/min)	0.000	0.000	0.000	0.000
C_{AO}(mg/l)	5.617	5.649	6.097	1.273
R^2	0.839	0.835	0.912	0.785
Pseudo first order				
Initial concentration(mg/l)	50.0	80.0	110.0	150.0
$-Kp_1$(1/min)	0.004	0.004	0.011	0.006
q_e(calc)(mg/g)	0.966	0.981	2.009	1.468
$q_e$exp.(mg/g)	56.47	93.96	131.48	181.29
R^2	0.195	0.204	0.272	0.283
Pseudo second order				
Initial concentration(mg/l)	50.0	80.0	110.0	150.0
Kp_2(1/min)	0.018	0.016	0.012	0.012
q_e(calc)(mg/g)	58.823	100.00	142.857	200.00
$q_e$exp.(mg/g)	56.4663	93.9646	131.4787	181.2998
R^2	1.00	1.00	1.00	1.00
Intra particle diffussion				
Initial concentration(mg/l)	50.0	80.0	110.0	150.0
K_{id}(mg/gmol)	0.07	0.072	0.138	0.127
C(mg/g)	55.25	92.70	129.3	129.3
R^2	0.743	0.736	0.917	0.795
Elovich				
Initial concentration(mg/l)	50.0	80.0	110.0	150.0
β(mg/g)	3.508	3.401	1.615	1.736
R^2	0.5	0.328	0.414	0.350

It can be seen that the correlation coefficients of the model were 1.0 for all the absorbents used except microwave prepared activated carbon from spent grain (MPASG) and conventional prepared activated carbon from hamburger seed shell (CPAHS) that had correlation coefficients between 0.994-0.999. These high correlation coefficients were recorded for all the initial Swiss blue dye concentration used.

Equally, there were good agreements between calculated (qe_{calc}) and experimental adsorptive capacities (qe_{exp}). These indicated that the adsorption kinetics was better represented by the pseudo second order model. This was in agreement with the work done by Dalia et. al. (2012) in basic dye adsorption using Kenaf fiber char, Unuabonah et. al. (2009) on MB adsorption on defatted carica papaya seed, Dural et. al. (2011) on MB adsorption on activated carbon from posindonia oceanica dead leaves and so many others

Table 4.22: Kinetic data of Swiss blue dye adsorption on microwave prepared activated carbon from hamburger seed shell

First order model				
Initial concentration(mg/l)	50.0	80.0	110.0	150.0
$-K_1$(1/min)	0.000	0.000	0.000	0.000
C_{AO}(mg/l)	0.280	0.285	0.330	0.336
R^2	0.675	0.514	0.631	0.538
Second order				
Initial concentration(mg/l)	50.0	80.0	110.0	150.0
K_2(1/min)	0.005	0.005	0.008	0.006
C_{AO}(mg/l)	0.286	0.291	0.351	0.351
R^2	0.644	0.500	0.613	0.516
Pseudo first order				
Initial concentration	50.0	80.0	110.0	150.0
$-Kp_1$(1/min)	0.00	0.00	0.00	0.00
q_e(calc)(mg/g)	0.085	0.092	0.123	0.129
$q_e$exp.(mg/g)	55.2411	99.7667	137.2885	187.2641
R^2	0.003	0.003	0.014	0.000
Pseudo second order				
Initial concentration	50.0	80.0	110.0	150.0
Kp_2(1/min)	0.001	0.000	0.000	0.000
q_e(calc)(mg/g)	62.500	100.00	142.857	200.00
$q_e$exp.(mg/g)	55.24	99.76	137.29	187.26
R^2	1.000	1.000	1.000	1.000
Intra particle diffussion				
Initial concentration	50.0	80.0	110.0	150.0
K_{id}(mg/gmol)	0.007	0.006	0.009	0.007
C(mg/g)	62.12	99.62	187.0	99.61
R^2	0.616	0.432	0.462	0.518
Elovich				
Initial concentration	50.0	80.0	110.0	150.0
β(mg/g)	34.48	40.0	22.727	30.303
R^2	0.500	0.328	0.414	0.350

Elovich model was equally used to test the kinetic data. The Elovich constant was obtained by slope of the plot of qt versus lnt. The correlation coefficient (R^2) was slightly high for both microwave spent grain and conventional hamburger activated carbons.

The intraparticle diffusion model was equally used to identify the adsorption mechanism and to predict the rate controlling step. The intraparticle diffusion rate constant (kid), and the constant (C), that gives an idea of the thickness of the boundary layer were obtained from the slope and intercept respectively of the plot of qt versus t½. . The intraparticle diffusion model usually includes three steps. The first portion is the external surface adsorption or boundary layer diffusion. The second portion is the gradual stage of adsorption which is the intraparticle diffusion. The third portion is the final equilibrium stage in which the intraparticle diffusion starts to slow down due to the extremely low dye concentration left in the solution (Cheung, et. al., 2007). The plots showed that the linear plot did not pass through the origin which indicated that the intraparticle diffusion was not only the rate controlling step, that the boundary layer diffusion controlled the adsorption to some extent (Cheung, et. al., 2007). This was recorded for all the adsorption using the four prepared activated carbons. This observation can be attributed to the difference in mass transfer rate in the initial and final stage of adsorption (Dalia et. al., 2012; Hameed & Hakimi, 2008). This finding was in accordance with the work done by Dalia et. al., (2012) on basic dye adsorption using treated Kenaf fiber char, Hamed and Hakim (2008) on acid dye removal using durian peel, and many others. The value of intercept (C) which gives the idea of thickness of boundary layer increased as the initial Swiss blue dye concentration was increased for all the adsorbents used. This showed that the boundary layer effect increased as the initial Swiss blue dye concentration was increased.

Table 4.23: Kinetic data of Swiss blue dye adsorption on conventional prepared activated carbon from hamburger seed shell

First order model				
Initial concentration(mg/l)	50.0	80.0	110.0	150.0
K_1(1/min)	-0.004	-0.002	-0.004	-0.004
C_{AO}(mg/l)	16.069	23.604	35.974	39.264
R^2	0.763	0.583	0.818	0.766
Second order model				
Initial concentration(mg/l)	50.0	80.0	110.0	150.0
K_2(1/min)	0.000	0.000	0.000	0.000
C_{AO}(mg/l)	17.24	23.255	43.478	45.454
R^2	0.881	0.754	0.921	0.846
Pseudo first order				
Initial concentration	50.0	80.0	110.0	150.0
K_{p1}(1/min)	0.011	0.011	0.011	0.016
q_e(calc)(mg/g)	15.922	18.578	46.131	45.394
$q_e$exp.(mg/g)	55.241	87.372	124.997	171.586
R^2	0.889	0.844	0.922	0.911
Pseudo second order				
Initial concentration	50.0	80.0	110.0	150.0
K_{p2}(1/min)	0.001	0.001	4.9E-04	4.7E-04
q_e(calc)(mg/g)	58.823	90.909	142.857	200.000
$q_e$exp.(mg/g)	55.241	87.372	124.997	171.586
R^2	0.999	0.998	0.994	0.999
Intra particle diffussion				
Initial concentration	50.0	80.0	110.0	150.0
K_{id}(mg/gmol)	1.433	2.263	3.299	3.765
C(mg/g)	34.74	55.61	75.31	118.8
R^2	0.769	0.563	0.807	0.808
Elovich				
Initial concentration	50.0	80.0	110.0	150.0
β(mg/g)	0.137	0.082	0.058	0.052
R^2	0.884	0.721	0.925	0.915

4.5.5. Isotherm studies of Swiss blue dye adsorption on activated carbons

The equilibrium data were fitted to Langmuir, Freundlich, Dubinin-Radushkevich (D-R), Temkin, Flory-Huggins, Redlich-Peterson, Sip and Toth isotherm models. Tables 4.17 -4.20 show the isotherm data for all the activated carbons.

The Langmuir constants were obtained from the slope and intercept of linear plot of Ce/qe versus Ce. From the tables (4.24-4.27), the correlation coefficients obtained for all the adsorbents used were small which indicated the inability of the model to fit the

data. It was observed that the Langmuir constant obtained decreased with the increase in temperature. This observation suggested exothermic nature of the process.

Table 4.24: Isotherm data for Swiss blue dye adsorption on microwave prepared activated carbon from hamburger seed shell

Temperature(K)	303	313	323	333
-b(mg/g)	2.75	2.77	3.2	3.0
$-k_L$(L/mg)	4.0	3.98	3.93	3.91
$-R_L$	0.0084	0.0084	0.0086	0.0086
R^2	0.9506	0.9645	0.9046	0.9555
		Freundlich		
1/n	25.64	25.0	25.0	23.8
KF (10^{17})(L/mg)	3.7	1.7	1.5	0.23
R^2	0.9761	0.9753	0.9929	0.9979
		Dubinin-Radushkevitch (D-R)		
BD	2E-06	1E-06	1E-06	1E-06
E(kJ/mol)	500.0	707.11	707.11	707.11
R^2	0.9762	0.9748	0.9921	0.9982
		Temkin		
A_T(L/mol)	4.348	4.335	4.322	4.311
b_T	1914.3	1870.9	1863.0	1792.4
R^2	0.9472	0.9316	0.9517	0.9773
		Flory-huggins		
n_{FH}	1.0799	1.0794	1.0603	1.0497
K_{FH}(L/mol)	4.65	4.64	5.70	5.36
R^2	0.9999	0.9999	1.0	0.9999
		Redlich-Peterson (R-P)		
K_R	3.7E17	1.7E17	1.5E17	2.3E16
a_R(l/mg)	3.21	1.01	1.14	1.022
-g	23.516	23.86	23.744	22.572
R^2	0.9762	0.9749	0.9927	0.998
		Sip		
Ks	3.7E17	1.7E17	1.5E17	2.3E17
a_S(l/mg)	1.078	1.012	1.116	1.024
-Bs(l/g)	-25.289	-24.859	-24.76	-23.571
R^2	0.9762	0.9749	0.9927	0.998
		Toth		
a_T(L/mg)	4.95	4.99	4.95	4.94
-t	0.041	0.042	0.042	0.044
-kt	4.0	3.98	3.93	3.91
R^2	0.9763	0.9749	0.9927	0.998

The Freundlich isotherm constant was obtained from the intercept of plot of log qe versus log Ce. The value of the slope (1/n) measures the adsorption intensity or surface heterogenousity. It was observed from the high correlation coefficient (R^2) recorded for all the activated carbons (Tables 4.24-4.27) that freundlich isotherm fitted the data well.

Table 4.25: Isotherm data for Swiss blue dye adsorption on microwave prepared activated carbon from spent grain

		Langmuir		
b(mg/g)	86.96	85.47	98.04	111.111
k_L(L/mg)	0.0863	0.051	0.0275	0.018
R_L	0.278	0.395	0.548	0.649
R^2	0.9599	0.9593	0.8232	0.7337
		Freundlich		
1/n	0.3497	0.4186	0.504	0.5463
K_F (10^{17})(L/mg)	18.005	11.72	7.65	5.719
R^2	0.9329	0.9685	0.9189	0.9152
		D-R		
B_D	3E-06	6E-06	1E-05	1E-05
E(kJ/mol)	408.25	912.87	223.61	223.6
R^2	0.6888	0.7298	0.650	0.6772
		Temkin		
A_T(L/mol)	1.189	0.538	0.298	4.850
B_T	147.89	142.14	129.96	123.28
R^2	0.9004	0.938	0.8776	0.881
		Flory-huggins		
$-n_{FH}$	1.471	2.124	2.583	2.908
K_{FH}(L/mol)	0.00192	0.00138	0.00119	0.00113
R^2	0.9217	0.9381	0.8767	0.7327
		Redlich-Peterson		
K_R	18.005	11.72	7.65	5.719
a_R(1/mg)	0.489	1.522	0.751	0.5101
G	0.8221	0.7221	0.4811	0.5622
R^2	0.9724	0.9734	0.8017	0.8588
		Sip		
Ks	18.005	11.72	7.65	5.719
a_S(l/mg)	1.0	1.0	1.0	1.1
Bs(l/g)	0.3002	0.4185	0.5037	0.5857
R^2	0.9329	0.9685	0.9191	0.9279
		Toth		
a_T(L/mg)	52.311	46.2	42.2	7.962
-t	0.741	0.705	0.665	0.5036
-kt	0.0865	0.0151	0.0275	0.018
R^2	0.9330	0.9685	0.9190	0.9844

This suggested multilayer adsorption with non uniform distribution of adsorption heat and affinities over the heterogenous surface. This was confirmed from the value of n obtained for the adsorption using the two adsorbents. The value of n greater than one showed the favourability of the adsorption process (Al-Othman et. al., 2012, Daneshur et. al., 2002, Malik, 2004).

Temkin isotherm constants were obtained from the slope and intercept of linear plot of qe versus ince. The high correlation coefficients recorded for this model except for conventional hamburger suggested applicability of this model to the adsorption process. The equilibrium binding constant (A) which corresponds to the maximum binding energy decreased with increase in temperature except for conventional hamburger seed shell. The constant (b) which is related to the heat of adsorption equally decreased with the increase in temperature. This suggested the exothermic nature of the process that increase in temperature decreased the rate of adsorption.

This model suggested that the heat of adsorption which is a function of temperature decreased linearly with coverage.

Dubinin-Radushkevich model was equally used to test the data. The constants were calculated from the slope and intercept of linear plot of lnqe vs q^2. It can be deduced from the data, based on the high correlation coefficients (R^2) that the model fitted well to the adsorption process using conventional spent grain and microwave hamburger seed shell. Flory-Huggins isotherm which derives the degree of surface coverage characteristics of adsorbate unto adsorbent was evaluated by linear plot of log (θ/Co) versus log (1- θ). From the tables, it can be seen that Flory-Huggins fitted all the adsorption process using all the adsorbents except conventional spent grain. The Flory-Huggins constant (K_{pH}) decreased with increase in temperature, equally, (n_{fH}) which shows the number of dye occupying adsorption sites decreased with increase in temperature. This suggested the exothermic nature of the process where degree of surface coverage decreases with increase in temperature.

Table 4.26: Isotherm data for Swiss blue dye adsorption on conventional prepared activated carbon from spent grain

		Langmuir		
-b(mg/g)	100.0	107.53	86.96	74.63
$-k_L$(L/mg)	0.1645	0.1527	0.1617	0.1626
$-R_L$	0.2541	0.2793	0.2597	0.2579
R^2	0.4786	0.5132	0.3326	0.3291
		Freundlich		
1/n	1.75	1.70	1.84	2.03
K_F (10^{17})(L/mg)	14.942	14.7367	11.7706	8.3811
R^2	0.8859	0.9101	0.9686	0.9373
		D-R		
BD	3E-07	2E-07	3E-07	3E-07
E(kJ/mol)	1291.0	1581.1	1291.0	1291.0
R^2	0.9298	0.9556	0.7858	0.7788
		Temkin		
A_T(L/mol)	0.7419	0.7331	0.6506	0.6755
B_T	0.061	0.064	0.057	0.063
R^2	0.9739	0.9852	0.9026	0.8929
		Flory-huggins		
n_{FH}	1.7751	1.8985	1.46	1.3676
K_{FH}(L/mol)				
R^2	0.872	0.8732	0.8464	0.8731
		Redlich-Peterson		
K_R	6.1098	6.1233	4.8891	5.068
a_R(1/mg)	1.095	1.045	0.911	0.652
G	0.4788	0.5255	0.3101	0.3395
		Sip		
Ks	14.94	14.73	11.77	8.38
a_S(l/mg)	1.0	7.41	1.0	1.02
Bs(l/g)	1.7527	-3.3879	-1.837	2.01
R^2	0.8859	0.9102	0.7686	0.7307
		Toth		
a_T(L/mg)	0.194	0.0015	5.5E-19	0.0193
-t	-0.3632	1.42	8.26	0.995
-kt	-0.1647	-0.1527	0.1617	0.1626
R^2	0.8859	0.9102	0.7686	0.7307

Redlich-Peterson (R-P) model was tested by plotting ln(kR $^{ce}/_{qe}$) versus lnce. It was observed from the high correlation coefficients that R-P model fitted all the adsorption process using all the adsorbents except conventional spent grain. The freundlich constant (K_R) that gave the maximum correlation coefficient for Redlich-Peterson model decreased with increase in temperature. This equally confirmed the exothermic nature of the adsorption.

The Sip isotherm model had high correlation coefficients on all the adsorption except those involving conventional spent grain. It is three parameter model that was tested by plotting ln (ks/qe) vs lnce. The constants were obtained from slope and intercept of the linear plot. It is a combined form of Langmuir and Freundlich expression deduced from predicting the heterogeneous adsorption system circumventing the limitation of the rising adsorbate concentration associated with Freundlich isotherm model.

The data were equally fitted to Toth isotherm. It involves a linear plot of ln(qe/kt) vs. lnce. From the result, it was noticed that Toth isotherm fitted the process using all the adsorbents as evidenced from the high correlation coefficients recorded. Thus isotherm model confirms heterogeneous adsorption system and improved Langmuir isotherm model. The Langmuir isotherm constant (K_T) decreased with increase in temperature. This shows that increase in temperature did not favour the uptake of the dye.

Table 4.27: Isotherm data for Swiss blue dye adsorption on conventional prepared activated carbon from hamburger seed shell

D: Conventional prepared activated carbon from hamburger seed shell (CPAHS)				
		Langmuir		
b(mg/g)	0.083	0.146	0.0138	0.0098
k_L(L/mg)	0.0565	0.1049	0.0673	0.0226
R_L	0.371	0.241	0.331	0.5959
		Freundlich		
1/n	0.44	0.2501	0.3034	0.5736
K_F (10^{17})(L/mg)	16.09	20.95	16.029	5.63
R^2	0.9628	0.9391	0.9306	0.9907
		D-R		
BD	3E-06	2E-06	3E-06	2E-05
E(kJ/mol)	408.33	500.0	408.33	158.1
R^2	0.6923	0.6747	0.5891	0.8017
		Temkin		
A_T(L/mol)	0.6175	3.07	1.13	0.214
B_T	1000.08	234.3	200.84	122.54
R^2	0.898	0.8774	0.8656	0.9576

		Flory-huggins		
$-n_{FH}$	0.7799	1.4134	1.8242	4.833
K_{FH}(L/mol)	0.0036	0.0022	0.0017	0.0002
R^2	0.7694	0.9263	0.9496	0.9282
		Redlich-petersons		
K_R	16.09	20.95	16.029	5.63
a_R(1/mg)	0.442	0.560	0.588	0.455
G	0.756	0.889	0.813	0.575
R^2	0.958	0.9874	0.9726	0.9742
		Sip		
Ks	16.09	20.95	16.029	5.63
a_S(L/mg)	1.0	1.03	1.02	1.10
Bs(L/g)	0.4403	0.2576	0.3141	0.5743
R^2	0.9635	0.947	0.9178	0.9906
		Toth		
a_T(L/mg)	50.65	69.193	63.181	33.28
T	0.6945	0.80	0.761	0.6354
Kt	0.0565	0.1049	0.0673	0.0226
R^2	0.9629	0.9392	0.9178	0.9907

4.5.6. Thermodynamics studies of adsorption of Swiss blue dye

Thermodynamic reactions of the adsorption process were determined via the adsorption parameters such as change in the standard free energy (ΔG^o), the enthalpy (ΔH^o) and entropy (ΔS^o) associated with the adsorption process using the following relation:

$$\Delta G^0 = \Delta H - T\Delta S^0 \quad (4.17)$$

$$\Delta G^0 = -RT \ln K_C \quad (4.18)$$

Taking advantage of the two above equations, the Van't Hoff equation was written as

$$\text{Ln}\, K_C = \frac{\Delta S}{R} - \frac{\Delta H^0}{RT} \quad (4.19)$$

Where K_c is the equilibrium constant which is the ratio of the equilibrium concentration of the dye on the adsorbent to the equilibrium concentration of the dye ions in solution.

The values of the entropy (ΔS) and enthalpy (ΔS) were obtained from intercept and slope respectively of plot LnKc against $^1/_{T.}$ The free energy change ΔG associated with a reaction tells whether or not the reaction will occur under the specified conditions. From the thermodynamic parameters on table 4.28, it was observed from conventional prepared activated carbon from hamburger seed shell (CPAHS) that enthalpy, entropy and Gibb's free energy were all negative. This suggested the process

as exothermic in nature, less disorder at various temperatures, feasible and spontaneous. The magnitude of Gibb's energy confirmed the adsorption process to be physical process. Conventional prepared activated carbon from spent grain (CPASG) has negative entropy at lower concentration of 30mg/l while entropy was positive at other concentrations. This showed that the process was less disorder at lower concentration while at higher concentrations, it had increased disorder. Negative enthalpy and Gibb's free energy of the process confirmed the process as exothermic in nature, feasible and spontaneous. The magnitude of Gibb's free energy suggested physical adsorption. Microwave prepared activated carbon from spent grain had negative values for enthalpy and enthropy. This suggested the process as exothermic in nature, feasible and spontaneous, while the positive value recorded for enthropy confirmed the process to had increase disorder. The magnitude of Gibb's free energy suggested the process to be physical in nature. Microwave prepared activated carbon from hamburger seed shell had negative enthalpy and Gibb's free enery. This shows that the process is exothermic in nature, spontaneous and feasible. Positive entropy showed that the process had increase disorder at various temperatures. The magnitude of Gibb's free energy suggested the process as physical process. The results showed that Gibb's free energy was negative for all the adsorption processes recorded on all the temperature and initial concentration. This shows that the process was spontaneous and feasible. This negative value depended on whether the reaction is exothermic or endothermic and on the value of entropy. From the results, it was equally seen that enthalpy had negative signs for all the process using all the adsorbent. This confirmed the process to be exothermic in nature; increase in temperature decreased the uptake rate. The entropy that measures degree of disorderliness of the process was negative for microwave prepared activated carbon from spent grain (MPASG) and conventional prepared activated carbon from hamburger seed shell (CPAHS). This showed that the processes were less disorder at various initial concentration of the dye studied, and that the spontaneity of the process depended on the temperature studied. This was confirmed by the negative free energy recorded for the less disordered processes at various temperatures. Conventional prepared activated carbon from spent grain (CPASG) and microwave prepared activated carbon from hamburger seed shell (MPAHS) had positive entropy which showed that the processes had increased disorder. The standard free energies changes for the adsorption were in range of -20 to 0KJ/mol for all the adsorbents. The magnitudes of this Gibb's free energy values were

in the range of multilayer adsorption which occurs by physical process (Bekci et. al., 2006; Wang & Somasundaran, 2007; Ozcan & Ozcan, 2005; Sener, 2008; Yu et. al., 2004; Mattson & Mark 1971). The low values of activation energy confirmed the process to be physical in nature. This confirmed the findings of Ruthven (1984); Mattson and Mark (1971) that the physical adsorption process (either from gas or liquid phase) would be exothermic, thus, adsorption quantity should decrease with increase in temperature. For chemical sorption, value of enthalpy change range from 83 to 830KJ/mol, while for physical sorption, they range from 8 to 25KJ/mol (Vijayakumar et. al., 2012). The low values of ΔH gave clear evidence that the interaction between Swiss blue dye and the adsorbents were weak. On this basis, we conclude that dye sorption by adsorbents was a physical adsorption process. Appendix H shows the thermodynamic plots for adsorption process.

Table 4.28: Thermodynamics parameters of Swiss blue dye adsorption on activated carbons

Conventional Prepared activated carbon from hamburger seed shell (CPAHS)						
Initial Conc.(mg/l)	-ΔH (KJ/mol)	-ΔS (J/mol.K)	-ΔG(KJ/mol)			
			303K	313K	323K	333K
30.0	33.186	91.65	5.366	4.449	3.533	2.616
50.0	25.481	73.679	3.156	2.420	1.683	0.946
80.0	25.787	77.79	2.217	1.439	0.661	0.116
110.0	19.914	61.07	1.410	0.799	0.188	0.421
Conventional prepared activated carbon from spent grain (CPASG)						
Initial Conc.(mg/l)	-ΔH (KJ/mol)	-ΔS (J/mol.K)	-ΔG(J/mol)			
			303K	313K	323K	333K
30.0	8.476	3.2166	7.502	7.470	7.437	7.405
50.0	5.541	-10.2021	8.633	8.735	8.837	8.939
80.0	1.604	-24.428	9.006	9.250	9.495	9.739
110.0	3.183	-19.3505	9.046	9.240	9.433	9.627
Microwave prepared activated carbon from hamburger seed shell (MPAHS)						
Initial Conc.(mg/l)	-ΔH (KJ/mol)	ΔS (J/mol.K)	-ΔG(J/mol)			
			303K	313K	323K	333K
30.0	0.360	40.98	12.777	13.187	13.596	14.006
50.0	0.201	45.55	14.002	14.458	14.913	15.369
80.0	0.438	48.62	15.170	15.656	16.142	16.628

110.0	0.360	51.38	15.929	16.442	16.956	17.470
Microwave prepared activated carbon from spent grain (MPASG)						
Initial Conc.(mg/l)	-ΔH (KJ/mol)	-ΔS (J/mol.K)	-ΔG(KJ/mol)			
			303K	313K	323K	333K
30.0	33.830	96.08	4.718	3.757	2.796	1.835
50.0	23.771	70.864	2.299	1.590	0.882	0.173
80.0	8.655	55.894	1.719	1.160	0.602	0.043
110.0	8.022	24.232	0.680	0.438	0.195	0.046

4.6. Desorption studies for Swiss blue dye loaded activated carbons

Desorption characteristics of spent activated carbon was studied. It helped one to elucidate the nature of adsorption and recyclability of the spent activated carbons. Desorption process was studied on a batch mode similar to the batch adsorption study. The saturated activated carbons were subjected to desorption using five different eluants, and it was observed that chloroform had highest desorption capacity. It was equally observed that the rate of desorption decreased with increase in dosage of saturated activated carbon but increased with increase in temperature.

4.6.1. Effect of initial dye concentration on the solid loading concentration of Swiss blue dye.

Fig.4.16 shows the results of initial solid load concentrations of Swiss blue dye at various initial Swiss blue dye concentrations for all the prepared activated carbons. It was observed that initial solid load increased with increase in initial Swiss blue dye concentrations. The same trend was observed on all the four activated carbons. This can be attributed to the fact that increase in Swiss blue dye concentrations increased the mass transfer driving force necessary to favour the uptake of dye, thereby increasing the initial solid load concentrations. Initial solid load concentration increased in the order; MPAHS, MPASG, CPASG, and CPAHS.

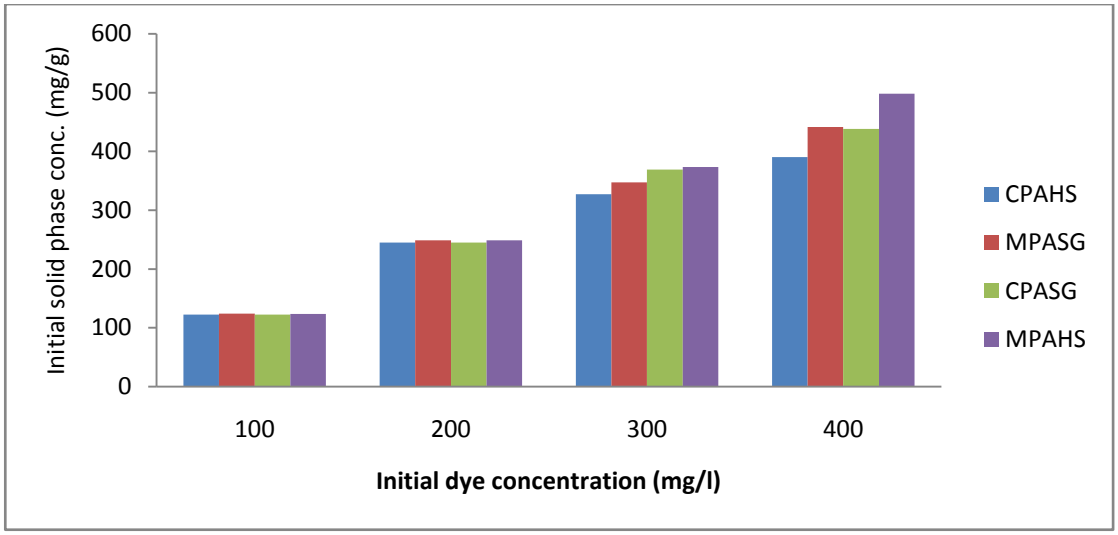

Fig. 4.16. Initial solid phase concentration for desorption process

4.6.2. Effect of Eluants on the desorption efficiency of Spent activated carbon.

Five eluants were tested in batch studies at room temperature and evaluated according to their effectiveness to release Swiss blue dye from the dye loaded activated carbons. The effectiveness was tested by measuring the final concentration of the dye in the eluants after desorption studies. Eluants used were 0.1M NaOH, 0.1M HCL, n-hexane, ethyl acetate and chloroform. The final solid load concentration and the desorption efficiency were calculated. Fig. 4.17 shows the desorption efficiency of spent activated carbons at different initial solid loading concentration. In general, two types of reagents are used for desorption, those with oxidizing ability and those with solubilizing ability (Sufnarski, 1999).

Chloroform was found to be more efficient to recover the dye from the adsorbents compared to other eluants. This is because Swiss blue dye is soluble in chloroform (Boca, 2007). It was observed that desorption efficiencies decreased with increase in initial solid load concentration of dye. This can be attributed to the fact that increase in the concentration of Swiss blue dye increased desorption resistance of Swiss blue dye from the activated carbon to aqueous phase leading to decrease in Swiss blue dye desorption rate (Muhammad et. al., 2011). Chloroform that recorded the highest desorption efficiency was used throughout the work.

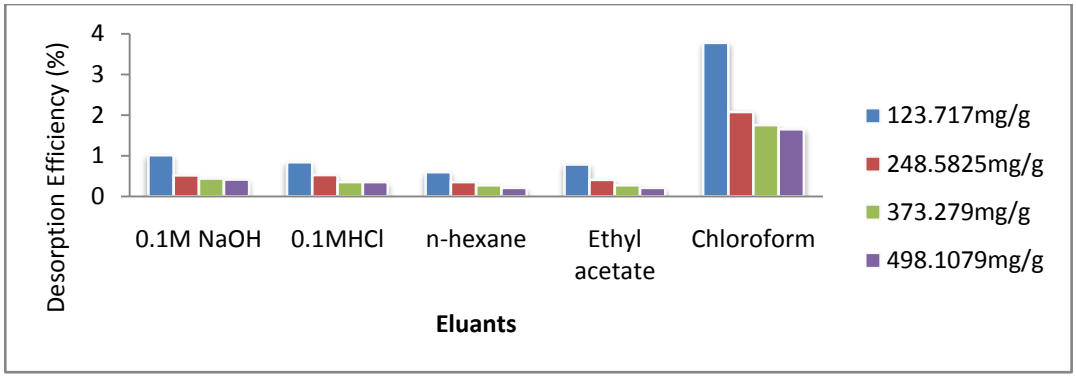

(a)

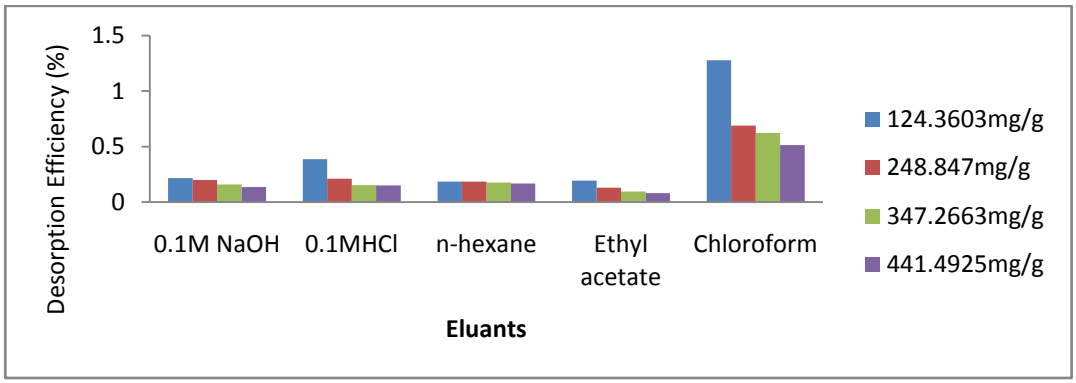

(b)

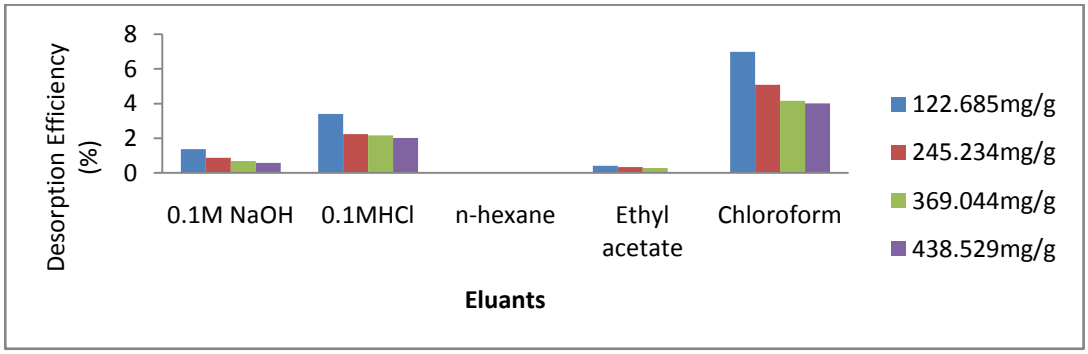

(c)

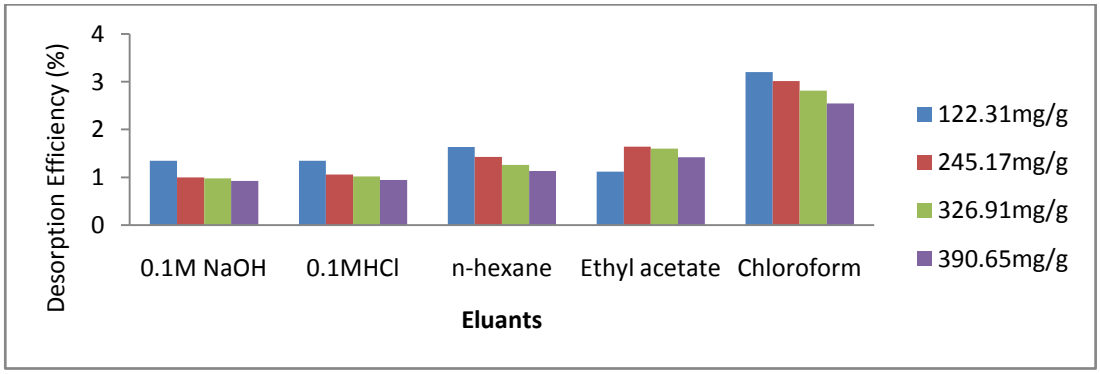

(d)

Fig. 4.17: Effect of eluents on desorption efficiency of Swiss blue dye (a), MPAHS (b), MPASG (c), CPASG (d) CPAHS

4.6.3. Effect of contact time on the desorption capacity of Spent activated carbon.

The extent of Swiss blue dye desorption from the loaded activated carbons was studied as a function of time under different initial solid phase concentrations and temperatures. Figs. 4.18-4.21 show the effect of desorption time on Swiss blue dye desorption capacity from the four prepared activated carbons at various temperatures for different initial loading concentrations. It was observed that the desorption capacity (which is the amount of Swiss blue dye in (mg/g) remaining on the activated carbons after desorption) under different initial solid loading concentration decreased with an increase in time and finally reached equilibrium.

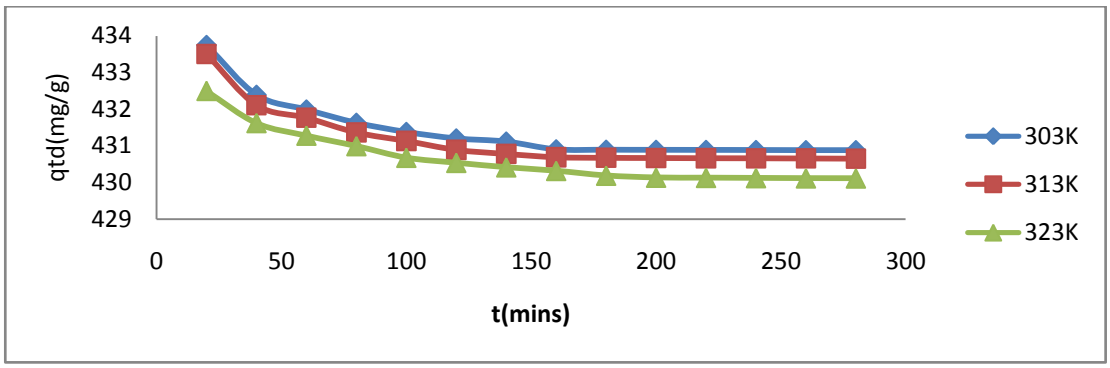

(a)

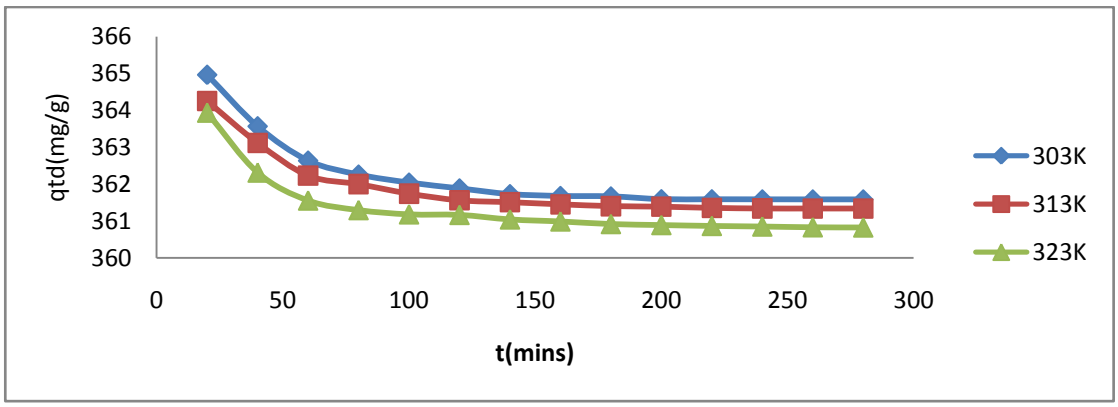

(b)

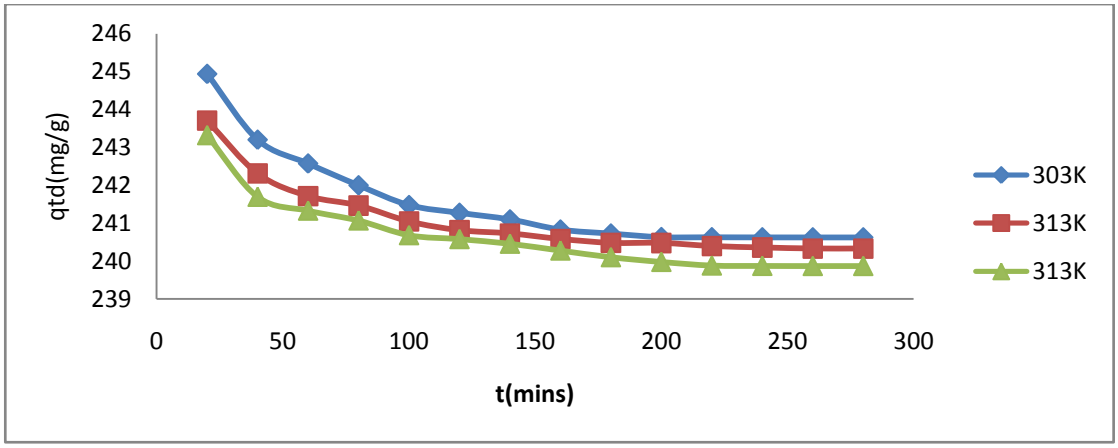

(c)

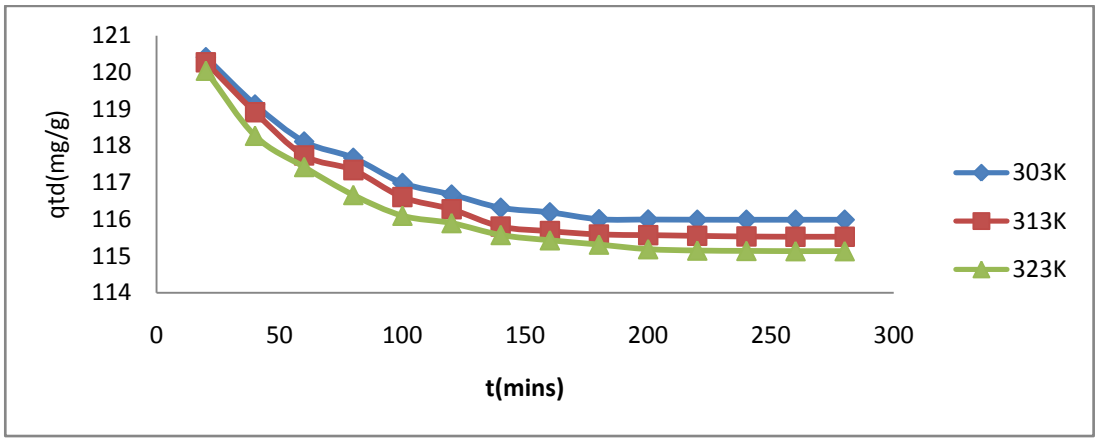

(d)

Fig. 4.18: Effect of time on desorption capacity of MPAHS (a) 498.1079mg/g, (b) 373.279mg/g, (c) 248.58mg/g, (d) 123.72mg/g

The studies showed rapid desorption phase initially becoming slower as it proceeds towards equilibrium. The trend of Swiss blue dye desorption was similar for all the activated carbon, but the quantity desorbed differed. The equilibrium time was almost the same for all the initial solid phase concentration. This implied that equilibrium time was independent of initial solid phase concentration. The equilibrium time was between 220 – 280mins for all the samples, therefore, 300mins was selected as desorption time for the rest of the experimental studies. Desorption capacity decreased with increase in temperature, meaning that increase in temperature favors desorption process. At higher temperatures, the bonds holding the dye to the adsorbents were broken and more dye molecules were freed thereby, reducing the number of dyes remaining on the adsorbents.

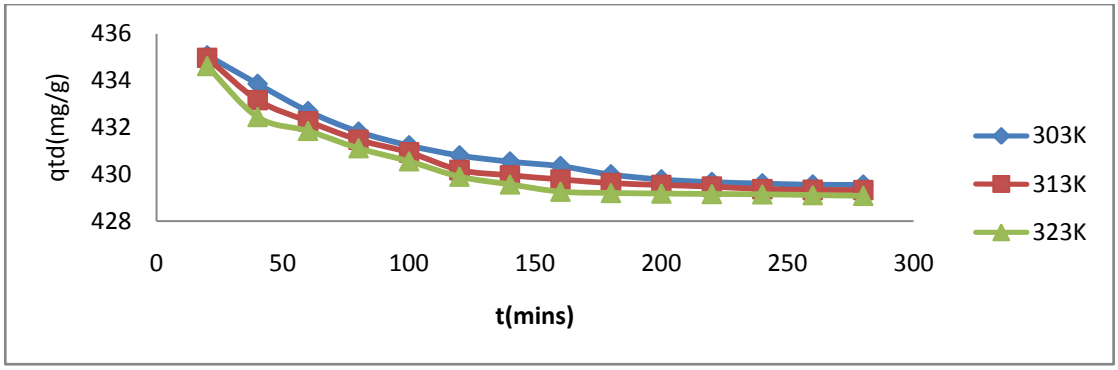

(a)

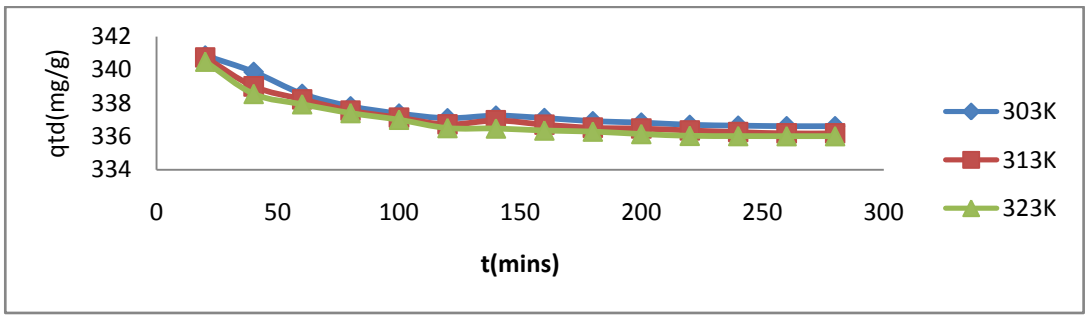

(b)

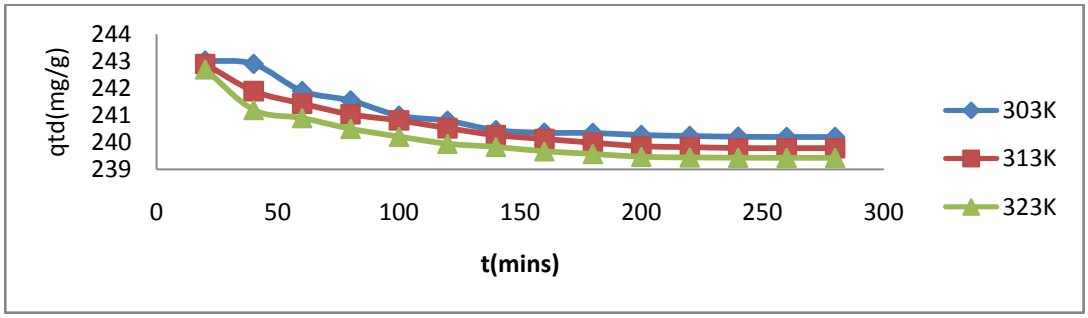

(c)

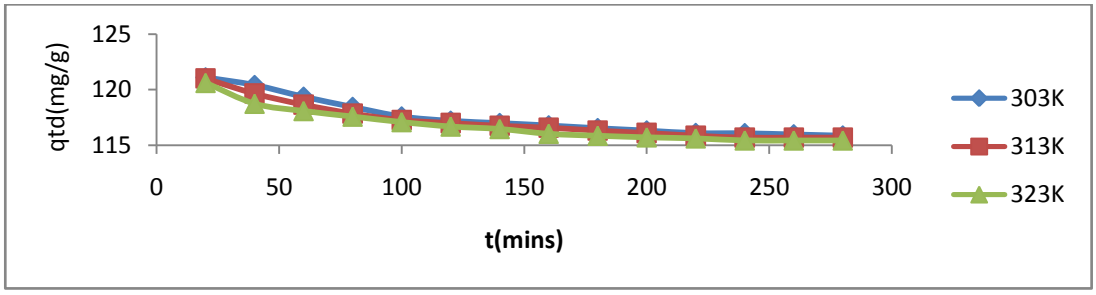

(d)

Fig. 4.19: Effect of time on desorption capacity of MPASG (a) 441.4925mg/g, (b) 347.2663mg/g, (c) 248.847mg/g, (d) 124.3603mg/g

The desorption capacity (mg/g) increased with increase in initial solid phase concentration, implying that the amount desorbed decreased with initial solid phase

concentration. As the concentration of Swiss blue dye gradually increased, it increased desorption resistance of Swiss blue dye from the activated carbons to aqueous phase leading to decrease in Swiss blue dye desorption rate (Muhammad et. al., 2011). This finding can also be attributed to the fact that at lower load of Swiss blue dye, the dye in the activated carbon interacted with the eluent binding sites completely and this facilitated desorption (Qing-Zhu et. al., 2009).

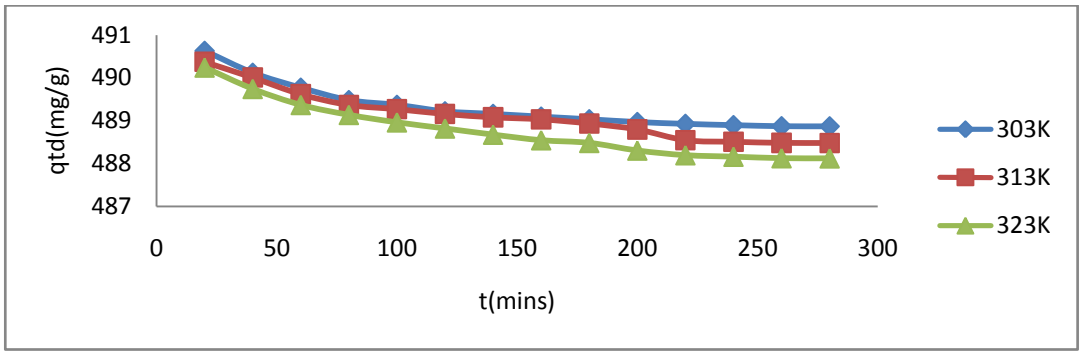

(a)

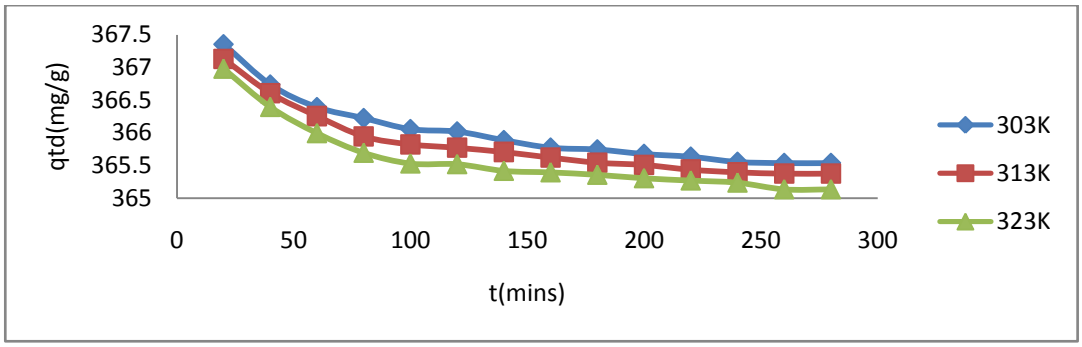

(b)

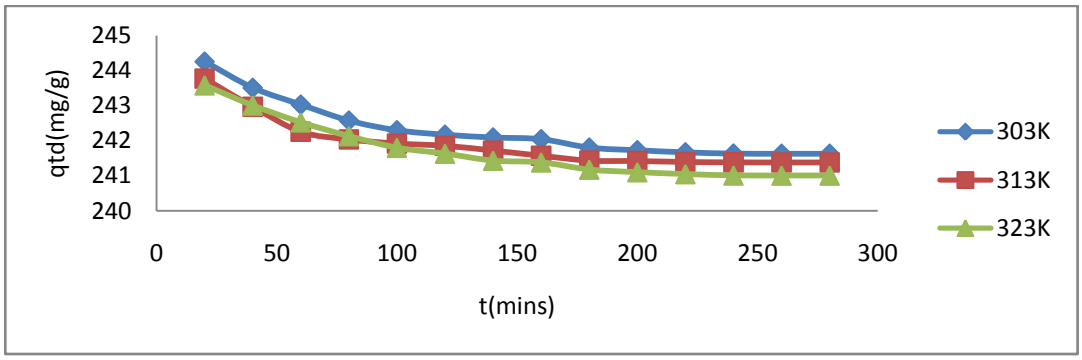

(c)

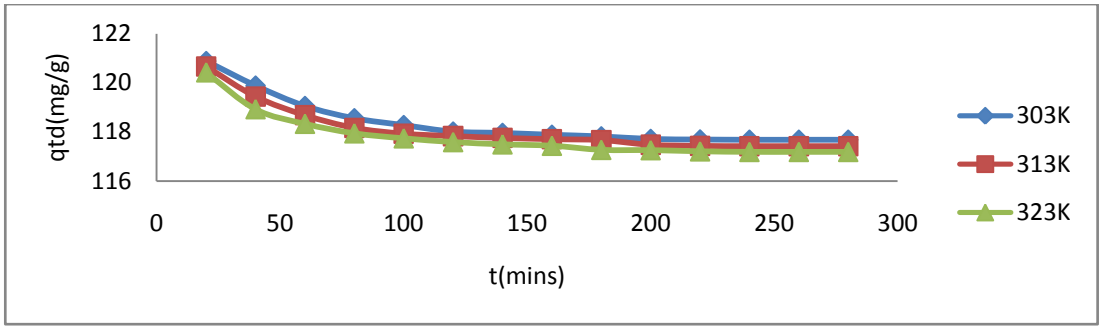

(d)

Fig. 4.20: Effect of time on desorption capacity of CPASG (a) 438.529mg/g, (b) 369.04mg/g, (c) 245.234mg/g, (d) 122.69mg/g

For higher loads of Swiss blue dye, more dye ions without desorption were due to the fact that the eluent binding sites have been saturated (Qing-Zhu et. al., 2009). This finding was in line with the works done by Chefetz et. al. (2004) on the sorption-desorption behavior of triazine and phenylurea herbicides in Kishon river sediments, Muhammad et. al. (2011) on the desorption of β carotene from mesoporous carbon coated monolith, and by Qing-Zhu et. al. (2009) on lead desorption from modified spent grain.

This finding was contrarily to the work done by Gao et. al. (1998) and Gunasekara and Xing (2003). It was found that at high solute concentration, more molecules were taken up by low energy binding sites and therefore can readily be desorbed.

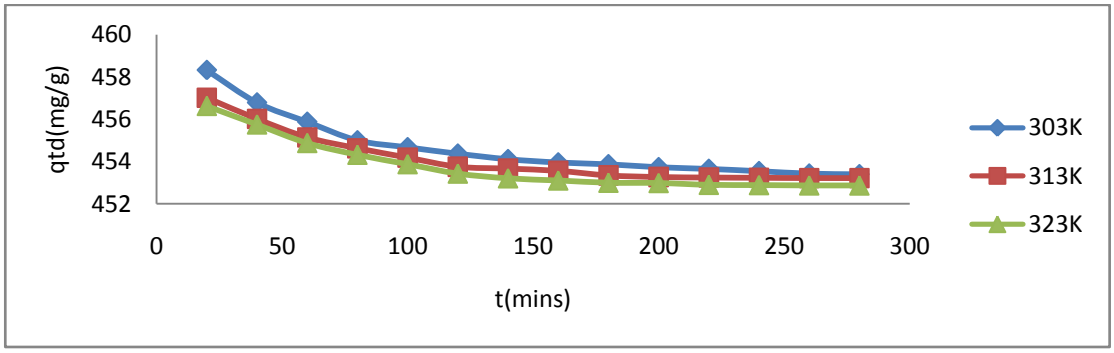

(a)

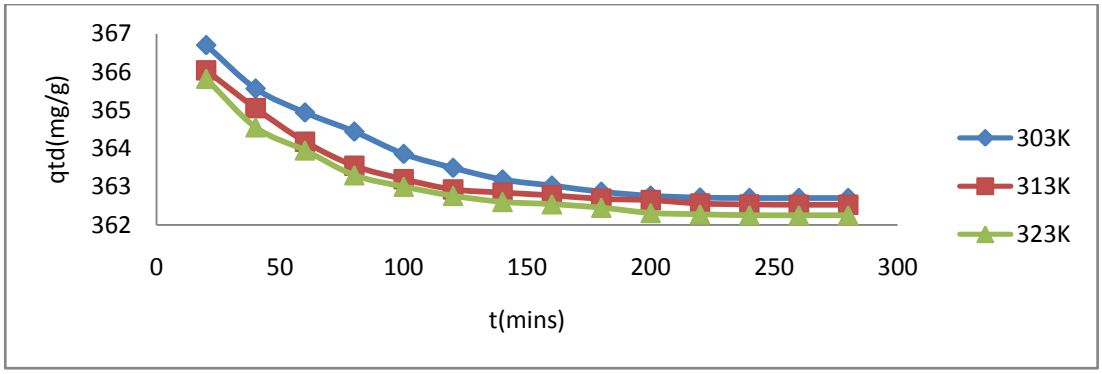

(b)

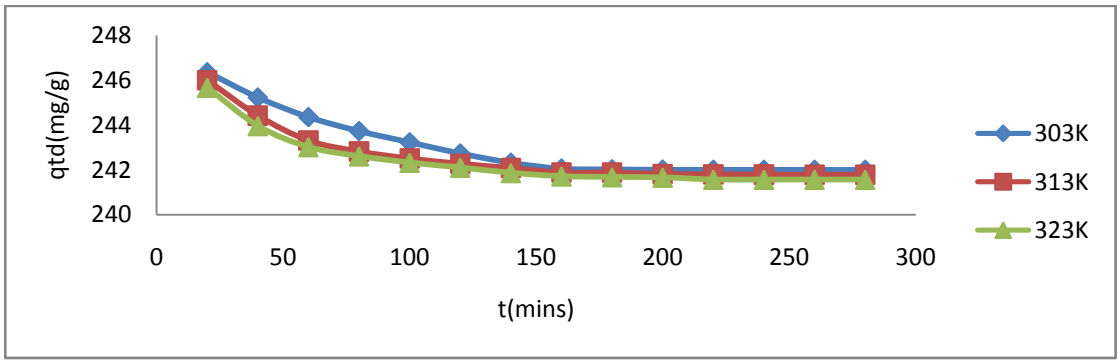

(c)

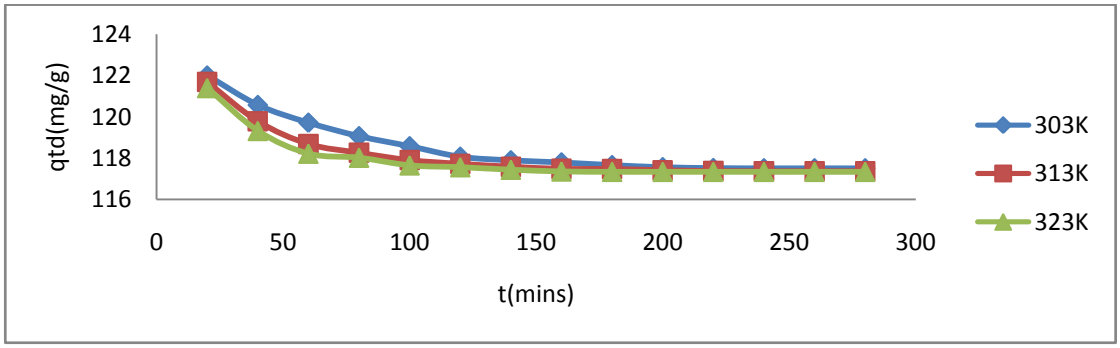

(d)

Fig. 4.21: Effect of time on desorption capacity of CPAHS (a) 390.65mg/g, (b) 326.96mg/g, (c) 245.17mg/g, (d) 122.31mg/g

4.6.4. Effect of dosage of the Swiss blue dye loaded activated carbon on the desorption capacity.

The effect of the dosage of the Swiss blue dye loaded activated carbon on the desorptive capacity was equally studied. Fig. 4.22 shows the effect of dosage on the desorption capacity (mg/g) of Swiss blue dye at different initial solid phase concentration. It was observed from the results that desorption capacity increased with increase in the dosage of the Swiss blue dye loaded activated carbon at different initial

solid phase concentration. The same trend was observed on all the activated carbon used in this study. The increase on desorption capacity recorded as the dosage was increased can be attributed to the effect it had on the physical characteristics of the solid-liquid suspension. The increase in dosage increased the viscosity of the eluent thereby inhibiting the diffusion of the dye molecules to the eluent phase. At low dosage of the loaded activated carbons, the viscosity was low, and the eluent was able to interact effectively with the adsorbed dye molecules thereby facilitating desorption (Qing-Zhu et. al., 2009).

It was equally observed that the desorptive capacity increased as the initial solid phase concentration was increased. The increase inhibited desorption efficiency because the eluent binding sites have been saturated at high initial solid phase concentration (Qing-zhu et. al., 2009). Since the volume of the eluent was fixed, it was unable to interact with high initial dye loading concentration thereby increasing the desorption capacity.

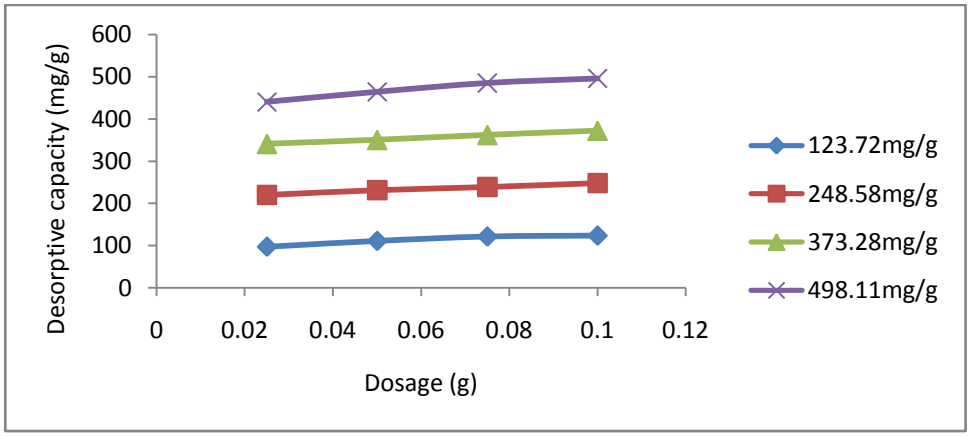

(a)

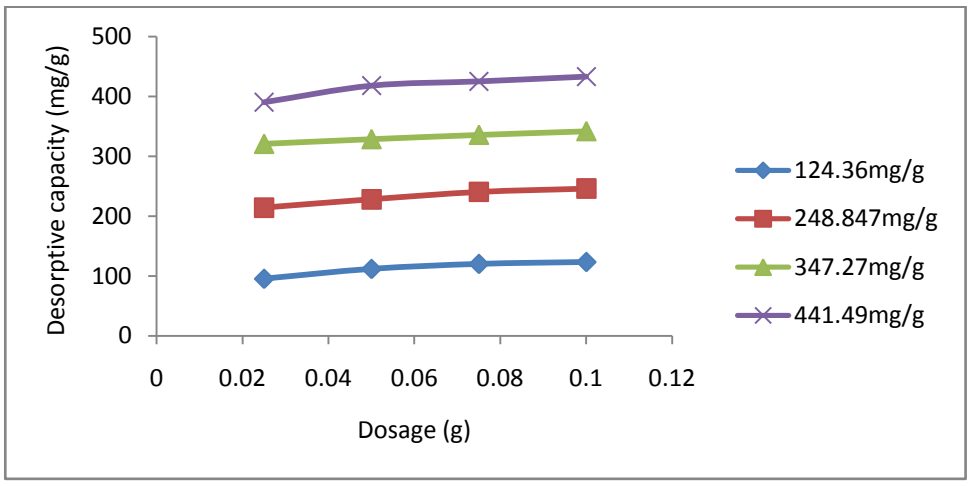

(b)

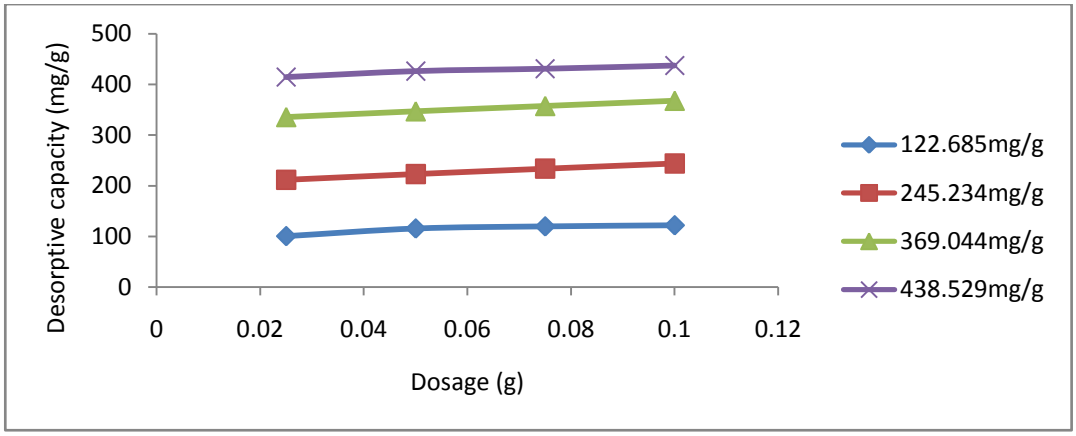

(c)

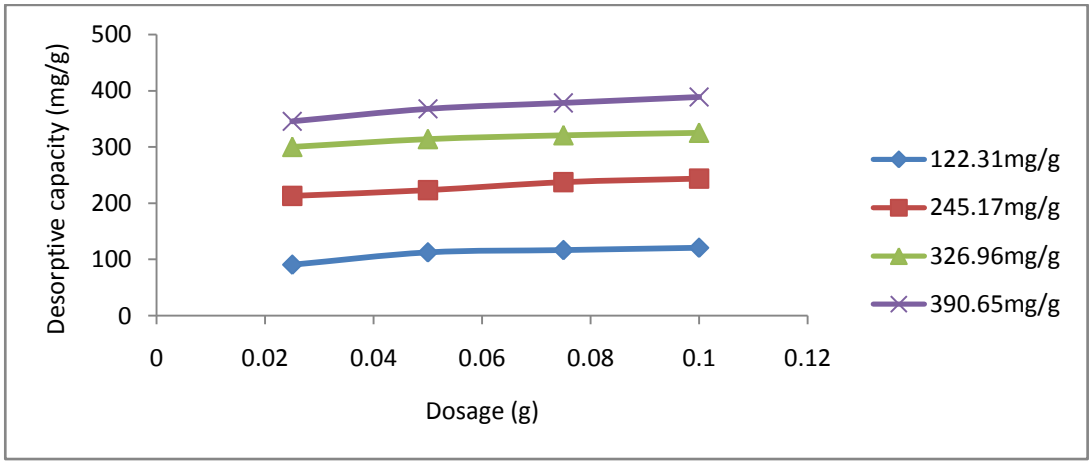

(d)

Fig. 4.22: Effect of dosage on the desorption capacity of Swiss blue dye (a) MPAHS, (b) MPASG, (c) CPASG, (d) CPAHS

4.6.5. Effect of Temperature on the desorptive capacity of Swiss blue dye

The effect of temperatures on desorption of Swiss blue dye from the loaded activated carbons were evaluated at different initial solid phase concentrations. The desorption study was examined at 303K, 313K and 323K only because of the volatility of chloroform used for the desorption. It was observed that at higher temperature, there was tendency of the eluent to vaporize thereby jeopardizing the desorption study. From Fig.4.23, it was observed that the desorptive capacity decreased with increase in temperature from 303K to 323K at various initial solid loading concentrations. This indicated that desorption of Swiss blue dye from the loaded activated carbons was an endothermic process. Because the dye molecules were held to the activated carbons by physical bonds, higher temperature was sufficient to break the bonds and free the adsorbed dye. High temperature shifted the adsorption mechanism in favour of

desorption. It supplied energy greater than the sorptive force to break the bond because sorptive force was achieved at lower temperature. On the other hand, the desorption capacity increased with increase in initial solid loading concentrations. This implied that at higher solid loading, desorption of Swiss blue dye from the activated carbons decreased. As the concentration of the Swiss blue dye increased, it increased the desorption resistance of the dye from the activated carbons to the eluent, leading to decrease in the desorption rate. The high final dye ions without desorption at high initial solid load concentration were due to the saturation of eluent binding sites.

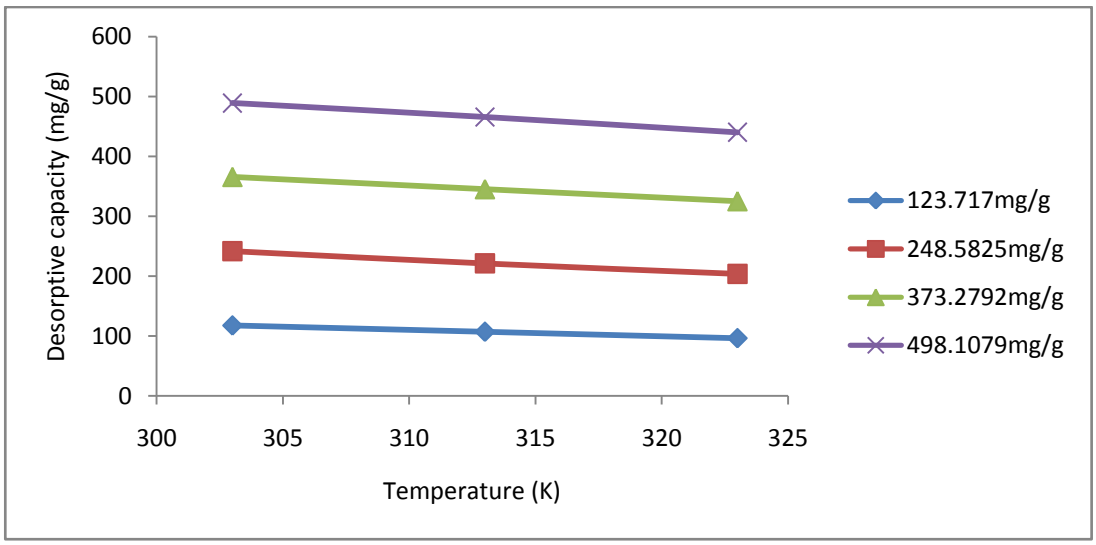

(a)

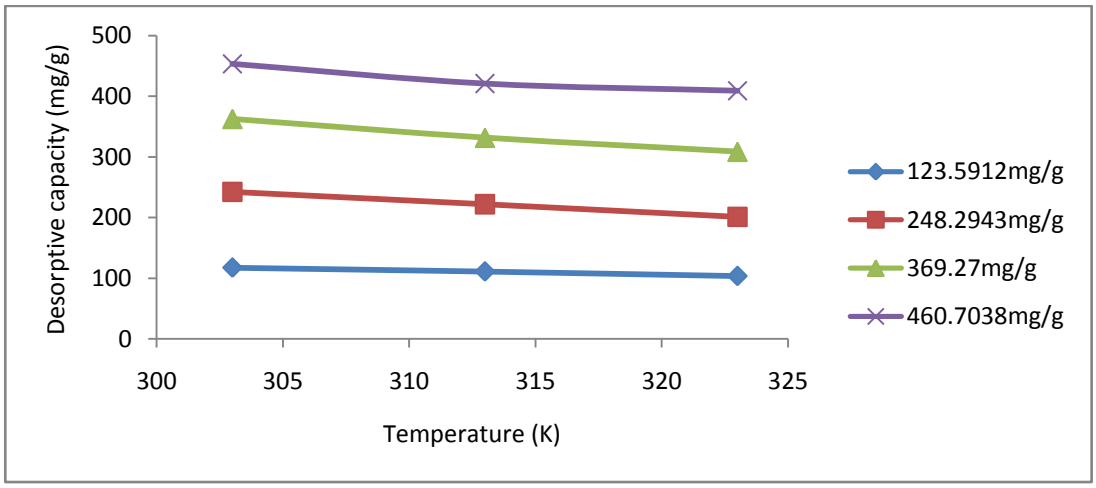

(b)

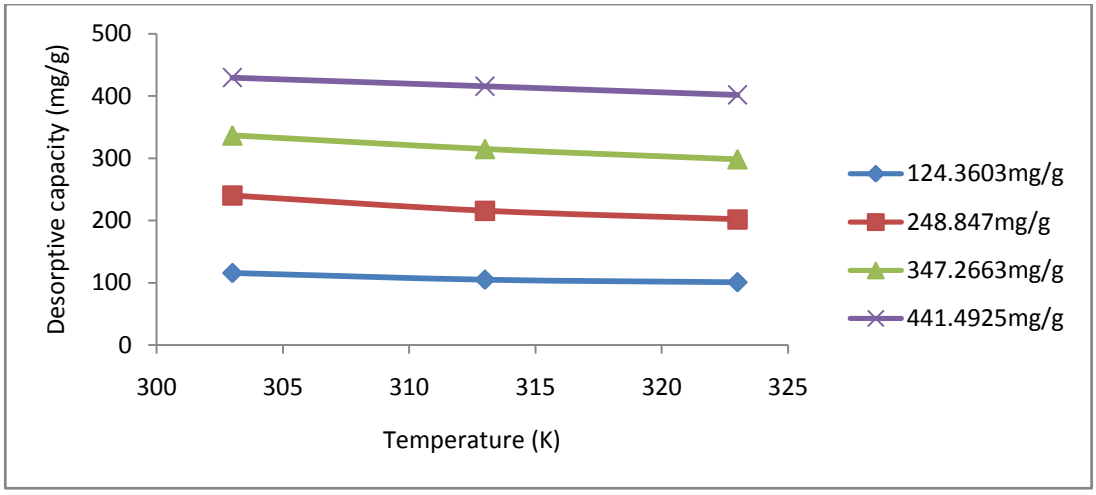

(c)

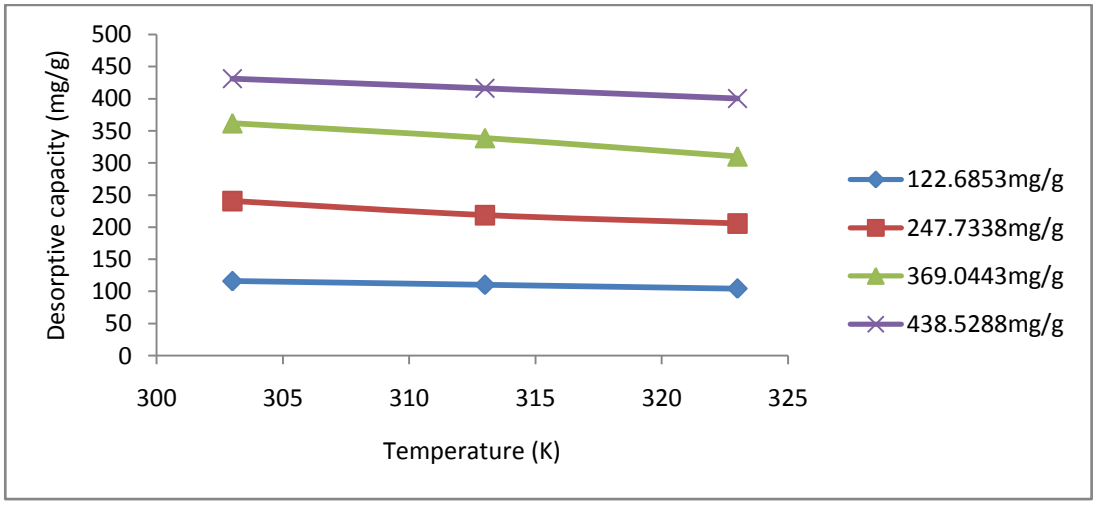

(d)

Fig.4.23: Effect of temperature on the desorption capacity of Swiss blue dye (a) MPAHS, (b) MPASG, (c), CPASG (d) CPAHS

4.6.6. Desorption Kinetics of Swiss blue dye Removal from spent activated carbon

Desorption of Swiss blue dye from the activated carbon was described by mass transfer from the activated carbon to the solvent (Kim & Kim 2004). The kinetic data was obtained at different initial solid phase concentration for all the activated carbons, and was fitted to different kinetic models. The kinetic models verified were first order, pseudo first order, second order, pseudo second order and Elovich model. These models were based on the concentration of Swiss blue dye on the solvent (Ct) and the amount of dye remaining on the activated carbon after desorption (qt).

The kinetic parameters of desorption of Swiss blue dye for the models are shown on Tables 4.29 – 4.32, while the plots are shown on appendix I.

Table 4.29: Kinetics parameters for desorption of Swiss blue dye from spent conventionally prepared activated carbon from hamburger seed shell

Initial dye conc. (mg/l)	100.0	200.0	300.0	400.0
Initial solid phase conc. (qe exp) (mg/g)	122.69	247.73	369.04	441.03
First Order Model				
C_{Ao} (mg/l)	1.995	2.275	2.535	1.2421
K_1(min^{-1})	0.002	0.002	0.002	0.002
R^2	0.788	0.736	0.693	0.758
Pseudo First order Model				
qe calc (mg/g)	0.302	0.275	0.396	0.230
Kp_1(min^{-1})	-0.009	-0.0016	-0.009	-0.013
R^2	0.766	0.450	0.367	0.504
Second Order Model				
C_{Ao} (mg/l)	2.008	2.267	2.50	2.42
K_2(min^{-1})	-0.001	-0.001	-0.001	-0.001
R^2	0.660	0.628	0.567	0.664
Pseudo Second Order Model				
qe calc (mg/g)	125.00	250.00	400.00	500.00
-Kp_2(min^{-1})	0.008	0.006	0.004	0.0038
γ (min)	125	166.67	250	263.16
R^2	1.0	1.0	1.01	1.0
Intra particle Diffusion Model				
C (mg/l)	121.7	246.2	367.0	439.5
Kd(mg/g.min^{-1})	-0.271	-0.271	-0.248	-0.327
R^2	0.961	0.929	0.850	0.925
Elovich Model				
B (g/mg)	-0.700	-0.786	-0.814	-0.691
R^2	0.911	0.987	0.937	0.964

The correlation coefficients (R^2) of different models showed that the data fitted well to pseudo second order model with correlation coefficient almost 1.0 for all the initial solid phase concentration used. The data equally fitted well to the intra particle diffusion model.

This finding was in agreement with the works done by Sarici-Ozdemir (2004) on desorption kinetics behaviour of methylene blue dye on to activated carbon and Kim & Kim (2004) on the apparent adsorption kinetics of phenols in organic solvents from spent activated carbons saturated with phenol. This result was contrary to the work done by Tseng et. al. (2009) on the kinetics and equilibrium of desorption of removal of copper from magnetic polymer adsorbent. They found out that pseudo first order fitted desorption data well.

The validity of pseudo second order was equally ascertained by the values of the predicted solid phase concentration (qed predicted). It was observed that the qed predicted using pseudo second order equation were very close to the initial solid phase concentration used for the experiment (qe experiment) for all the initial solid phase concentrations. On the contrast, the values of the qed predicted using pseudo first order equation were not accurate.

Further examination of the values of desorption rate constants for pseudo second order model (K_{P2}) showed that K_{P2} decreased with increase in initial solid phase concentrations. This might be due to gradual increase in desorption resistance of the dye from activated carbon as the initial solid phase concentration increased (Muhammad et. al., 2011).

The validity of pseudo second order model showed that driving force of desorption might be the difference between the equilibrium concentration in a solvent with the adsorbed amount of dye in activated carbons at a time and the bulk concentration of dye in solvent (Kim & Kim, 2004).

Table 4.30: Kinetic parameters for desorption of Swiss blue dye from spent conventionally prepared activated carbon from spent grain

Initial dye concentration (mg/l)	100.00	200.00	300.00	400.00
Initial solid phase conc. (qe exp) (mg/g)	124.36	248.85	347.27	441.49
First Order Model				
C_{Ao} (mg/l)	2.85	4.246	4.977	5.330
K_1(min^{-1})	0.002	0.000	0.000	0.002
R^2	0.867	0.947	0.900	0.931
Pseudo First Order Model				
qe calc. (mg/g)	0.119	0.237	0.123	0.142
Kp_1(min^{-1})	0.11	0.006	0.013	0.009
R^2	0.757	0.596	0.563	0.914
Second Order Model				
C_{Ao} (mg/l)	2.932	4.374	5.076	5.464
K_2(min^{-1})	0.000	0.000	0.000	0.000
R^2	0.769	0.765	0.867	0.888
Pseudo Second Order Model				
qe calc (mg/g)	125.00	250.00	333.33	500.00
Kp_2(min^{-1})	-0.008	-0.005	-0.004	-0.004
γ(mins)	125	200	250	250
R^2	0.999	1.00	1.00	1.00
Intra particle Diffusion				
C(mg/g)	123.4	244.8	340.21	4437.5
Ki_d(mg/g.min^{-1})	-0.470	-0.264	-0.321	-0.469
R^2	0.981	0.831	0.962	0.983
Elovich Model				
B (g/mg)	-0.440	-0.909	-0.003	-0.447
R^2	0.961	0.708	0.708	0.939

The surface residence (τ) for the Swiss blue dye on the activated carbon was equally calculated using the pseudo second order kinetic rate constant. According to Klavs Christmann, (2011), surface residence time was the inverse of kinetic model rate constant.

$$\tau = {}^{1}/_{Kp2} \qquad (4.20)$$

The residence time is the average time that a molecule will spend on the surface under a given set of conditions. From the results, it was observed that the average time increased with initial solid phase concentrations. This shows that it took lower solid phase concentration shorter time to desorb and longer time for higher solid phase concentration. The shorter equilibrium time is due to less amount of adsorbate to be desorbed. The residence times calculated for all the initial solid phase concentration were very close to the experimental equilibrium time.

It was equally observed that the kinetic data equally fitted well to intra particle diffusion model. The intra particle diffusion was equally used to identify the mechanism of desorption and the rate controlling step. The linear plots at various initial solid phase concentrations do not pass through the origin, which shows that the intra particle diffusion was not the only rate controlling step and the boundary layer diffusion controlled the desorption to some extent.

The value of the intercept (c) which related to the boundary layer resistance increased with increase in initial solid phase concentration. These values were close to the initial solid phase concentration and showed that thickness of the boundary layer increased as the initial solid phase concentration increased. This showed that as the initial solid phase concentration increased, the contribution of the boundary layer in the rate limiting step increased (Sarici-Ozdemir, 2004).

Table 4.31: Kinetics parameters for desorption of Swiss blue dye from spent microwave prepared activated carbon from spent grain

Initial dye conc. (mg/l)	100.00	200.00	300.00	400.00
Initial solid phase conc. qe exp (mg/g)	123.59	248.29	369.28	460.70
First Order Model				
C_{Ao} (mg/l)	0.514	0.792	1.032	1.399
K_1(min^{-1})	0.011	0.006	0.006	0.006
R^2	0.907	0.771	0.830	0.770
Pseudo First Order Model				
qe calc (mg/g)	0.210	0.135	0.071	0.138
Kp_1(min^{-1})	-0.006	-0.02	-0.023	-0.016
R^2	0.310	0.382	0.528	0.645
Second Order Model				
C_{Ao} (mg/l)	0.626	0.807	1.100	1.402
K_2(min^{-1})	-0.009	-0.005	-0.004	-0.002
R^2	0.310	0.651	0.697	0.596
Pseudo Second Order Model				
qe calc (mg/g)	125.0	250.0	333.333	500.00
K_{p2}(min^{-1})	-0.007	-0.005	-0.004	-0.004
γ(mins)	142.86	200	250	250
R^2	0.999	1.000	0.992	1.000
Intra particle Diffusion				
C (mg/g)	124.700	246.60	329.6	39.70
K_d(mg/g.min^{-1})	-0.544	-0.466	-0.649	-0.545
R^2	0.864	0.909	0.954	0.930
Elovich Model				
B (g/mg)	-0.463	-0.472	-0.339	-0.4031
R^2	0.783	0.909	0.951	0.934

Table 4.32: Kinetics parameters for desorption of Swiss blue dye from spent microwave prepared activated carbon from hamburger seed shell

Initial dye conc. (mg/l)	100.00	200.00	300.00	400.00
Initial solid phase conc. qe exp mg/l	123.72	248.58	373.28	498.11
First Order Model				
C_{AO} (mg/l)	2.442	3.196	4.577	5.551
K_1 (min^{-1})	0.002	0.001	0.00	0.00
R^2	0.669	0.642	0.715	0.888
Pseudo First Order Model				
qe calc (mg/g)	0.0645	0.0704	0.1144	0.0425
Kp_1 (min^{-1})	-0.033	-0.037	-0.032	-0.822
R^2	0.808	0.892	0.794	0.822
Second Order Model				
C_{AO} (mg/l)	2.415	3.175	4.762	5.587
K_2 (min^{-1})	0.002	0.001	0.0004	0.0001
R^2	0.669	0.62	0.715	0.888
Pseudo Second Order Model				
qe calc (mg/g)	125.0	250.0	400.0	500.0
$-Kp_2$ (min^{-1})	0.009	0.006	0.004	0.0038
γ(mins)	111.11	166.667	250	263.15
R^2	1.0	1.0	1.0	1.0
Intra particle Diffusion				
C(mg/g)	125.6	249.4	347.7	400.3
K_d ($mg/m.min^{-1}$)	-0.531	-0.342	-0.452	-0.532
R^2	0.918	0.884	0.928	0.952
Elovich Model				
B(g/mg)	-0.835	-0.894	-1.675	-1.370
R^2	0.926	0.897	0.876	0.910

4.6.7. Desorption Kinetics of Swiss blue dye at different temperatures

In order to obtain the activation energy and frequency factor for the desorption process, the kinetic data were obtained at different temperatures of 303K, 313K and 323K. The data were fitted to pseudo second order model that was considered the best kinetic model. The plots of the pseudo second model at different temperature are shown in appendix J. It was observed from the pseudo second order kinetic parameters on tables 4.33-4.36 that the rate constant and correlation coefficients for the model increased with increase in temperature. This suggested that increase in temperature favoured the desorption process

Table 4.33: Pseudo second order kinetics parameters for desorption of Swiss blue dye at various temperatures for conventionally prepared activated carbon from hamburger seed shell

			303K	
Initial Conc. (mg/l)	100.0	200.0	300.0	400.0
qe (exp)(mg/g)	122.69	247.73	369.04	438.53
qe (calc.)(mg/g)	122.36	238.10	357.14	434.78
$-K_d$ x10^{-4}(min^{-1})	80.0	87.0	17.0	163.0
R^2	1.0	1.0	1.0	1.0
			313K	
qe (exp)(mg/g)	122.69	247.73	369.04	438.53
qe (calc.)(mg/g)	114.94	238.1	357.14	434.78
$-K_d$ x10^{-4}(min^{-1})	72.0	85.0	145.0	162.0
R^2	1.0	1.0	1.0	1.0
			323K	
qe (exp)(mg/g)	122.69	247.73	369.04	438.53
qe (calc.)(mg/g)	114.94	238.1	357.14	434.78
$-K_d$ x10^{-4}(min^{-1})	64.0	85.0	127.0	160.0
R^2	1.0	1.0	1.0	1.0

. The correlation coefficients (R^2) were unity for all the adsorbent and initial solid loading concentrations. The rate constants that allowed the best fit to experimental kinetic data (for pseudo second order) of Swiss blue dye concentration in chloroform were applied to Arrhenius equation to determine the activation energy and frequency factor. The relationship between the rate constants and solution temperature was expressed by Arrhenius equation 4.21 (Kim & Kim, 2004; Schroeder & Gottfried 2002; Do & Wang 1998).

$$Kd = Ad \exp\left(\frac{-Edes}{RT}\right) \quad (4.21)$$

Where Ad is the frequency factor or temperature independent factor (min^{-})

E_{des} is the activation energy (J/mol) for desorption process, R is the gas constant (8.314J/mol.K) and T is the solution temperature (K).

Table 4.34: Pseudo second order kinetics parameters for desorption of Swiss blue dye at various temperatures for microwave prepared activated carbon from spent grain

	303K			
qe (exp)(mg/g)	123.59	248.29	369.28	460.70
qe (calc.)(mg/g)	116.28	243.90	357.14	454.55
$-K_d$ x10^{-4}(min^{-1})	525.0	670.0	713.0	807.0
R^2	1.0	1.0	1.0	1.0
	313K			
qe (exp)(mg/g)	123.59	248.29	369.28	460.70
qe (calc.)(mg/g)	117.65	243.90	357.14	454.55
$-K_d$ x10^{-4}(min^{-1})	500.0	610.0	700.0	768.0
R^2	1.0	1.0	1.0	1.0
	323K			
qe (exp)(mg/g)	123.59	248.29	369.28	460.70
qe (calc.)(mg/g)	117.65	243.90	357.14	454.55
$-K_d$ x10^{-4}(min^{-1})	48.0	56.0	63.0	70.0
R^2	1.0	1.0	1.0	1.0

The activation energy measures the magnitude of the forces required to overcome during desorption process (Muhammad et. al., 2011). It determines the chance of the adsorbent dye molecules overcoming the potential barrier to desorption.

Transformation of the equation into linear form gave

$$InKd = InAd - \frac{Eds}{RT} \quad (4.22)$$

Plot of InKd Vs 1/T gave slope of $\frac{-Edes}{R}$ and intercept of InAd. The properness of the Arrhenius equation was checked by a plot of InK_d vs. 1/T on Figure 4.39. The squares of the linear correlation coefficients (R^2) for all the initial solid phase concentration were greater than 0.9. Therefore, the Arrheius relationship could be justifiable for representing the temperature dependency expression of K_d (Kim & Kim, 2004).

Table 4.35: Pseudo second order kinetics parameters for desorption of Swiss blue dye at various temperatures for microwave prepared activated carbon from hamburger seed shell

	303K			
qe (exp)(mg/g)	123.59	248.29	369.28	460.70
qe (calc.)(mg/g)	114.942	238.1	333.33	434.78
$-K_d$ x10^{-4}(min^{-1})	86.0	126.0	143.0	177.0
R^2	1.0	1.0	1.0	1.0
	313K			
qe (exp)(mg/g)	123.59	248.29	369.28	460.70
qe (calc.)(mg/g)	114.942	238.1	333.33	434.78
$-K_d$ x10^{-4}(min^{-1})	757.0	882.0	110.0	128.0
R^2	1.0	1.0	1.0	1.0
	323K			
qe (exp)(mg/g)	123.59	248.29	369.28	460.70
qe (calc.)(mg/g)	114.942	238.1	333.33	434.78
$-K_d$ x10^{-4}(min^{-1})	64.0	78.0	80.0	111.0
R^2	1.0	1.0	1.0	1.0

Furthermore, the excellent temperature dependency expression of K_d might indirectly support the properness of K_d values as well as that of the desorption pseudo second order model. The activation energy, frequency factors and the correlation coefficients of Arrhenius plot is showed in table 4.37.

The variation of results obtained using different initial solid phase concentration and adsorbents suggested that the activation energy values were strongly depended on the adsorbent characteristics (Muhammad et. al., 2011; Johnson & Weber, 2001).

Table 4.36: Pseudo second order kinetics parameters for desorption of Swiss blue dye at various temperatures for conventionally prepared activated carbon from spent grain

	303K			
qe (exp)(mg/g)	124.36	248.85	347.27	441.49
qe (calc.)(mg/g)	117.65	243.90	370.37	500.0
$-K_d$ x10^{-4}(min^{-1})	111.0	116.0	126.0	133.0
R^2	1.0	1.0	1.0	1.0
	313K			
qe (exp)(mg/g)	124.36	248.85	347.27	441.49
qe (calc.)(mg/g)	117.65	243.90	370.37	500.0
$-K_d$ x10^{-4}(min^{-1})	107.0	113.0	118.0	120.0
R^2	1.0	1.0	1.0	1.0
	323K			
qe (exp)(mg/g)	124.36	248.85	347.27	441.49
qe (calc.)(mg/g)	117.65	243.90	370.37	500.0
$-K_d$ x10^{-4}(min^{-1})	103.0	109.0	114.0	118.0
R^2	1.0	1.0	1.0	1.0

When Kd values of Swiss blue dye were expressed as an experimental function of temperature, the equation for each adsorbent at different initial Swiss blue dye concentration used for saturation becomes;

100mg/l;

$$MPASG: Kd(min^{-1}) = 301.69 \exp\left(\frac{366.35}{T}\right) \quad (4.23)$$

$$CPASG: Kd(min^{-1}) = 14355.67 \exp\left(\frac{-1463.5}{T}\right) \quad (4.24)$$

$$CPAHS: Kd(min^{-1}) = 2587.6 \exp\left(\frac{-917.36}{T}\right) \quad (4.25)$$

$$MPAHS: Kd(min^{-1}) = 8112.0 \exp\left(\frac{366.35}{T}\right) \quad (4.26)$$

200mg/l;

$$MPASG: Kd(min^{-1}) = 233.81 \exp\left(\frac{303.02}{T}\right) \quad (4.27)$$

$$CPASG: Kd(min^{-1}) = 185164.52 \exp\left(\frac{-2350.1}{T}\right) \quad (4.28)$$

$$CPAHS: Kd(min^{-1}) = 254.98 \exp\left(\frac{-241.78}{T}\right) \quad (4.29)$$

$$MPAHS: Kd(min^{-1}) = 2833.87 \exp\left(\frac{-893.12}{T}\right) \quad (4.30)$$

300mg/l;

$$MPASG: Kd(min^{-1}) = 404.16 \exp\left(\frac{-492.4}{T}\right) \quad (4.31)$$

$$CPASG: Kd(min^{-1}) = 790167.3 \exp\left(\frac{-2832.5}{T}\right) \quad (4.32)$$

$$CPAHS: Kd(min^{-1}) = 1894.48 \exp\left(\frac{-1031.2}{T}\right) \quad (4.33)$$

$$MPAHS: Kd(min^{-1}) = 989.2 \exp\left(\frac{-596.6}{T}\right) \quad (4.34)$$

400mg/l;

$$MPASG: Kd(min^{-1}) = 530.65 \exp\left(\frac{-590.72}{T}\right) \quad (4.35)$$

$$CPASG: Kd(min^{-1}) = 115844.03 \exp\left(\frac{-2304}{T}\right) \quad (4.36)$$

$$CPAHS: Kd(min^{-1}) = 82.52 \exp\left(\frac{-90.17}{T}\right) \quad (4.37)$$

$$MPAHS: Kd(min^{-1}) = 1198.23 \exp\left(\frac{-690.1}{T}\right) \quad (4.38)$$

As a result of using equations (4.23 - 4.38), the desorption kinetics of Swiss blue dye removal from spent activated carbons using chloroform would be predicted at certain temperatures.

Table 4.37: Arrhenius parameters for desorption of Swiss blue dye from spent activated carbons

A. Microwave prepared activated carbon from Spent Grain (MPASG)

Initial solid phase conc. (mg/g)	123.329	247.797	372.645	497.532
Ad (min^{-1})	301.69	233.81	404.16	530.65
E_{des} (J/mol)	3045.84	2519.31	4094.15	4911.25
R^2	0.9996	0.9816	0.99	0.9786

B. Conventional prepared activated carbon from Spent grain (CPASG**)**

Initial solid phase conc. (mg/g)	124.3603	248.847	347.2663	441.4925
Ad (min^{-1})	14355.67	185164.52	790167.3	115844.03
E_{des} (J/mol)	12167.54	19538.73	23549.41	19155.46
R^2	0.9871	1.0	0.9911	0.9701

C. Conventional prepared activated carbon from Hamburger seed shell (CPAHS)

Initial solid phase conc. (mg/g)	122.69	247.73	369.04	438.53
Ad (min^{-1})	2587.6	254.98	1894.48	82.52
E_{des} (J/mol)	7626.93	2010.16	8573.4	749.68
R^2	0.9959	0.9938	0.9677	0.9429

D. Microwave prepared activated carbon from hamburger seed shell (MPAHS)

Initial solid phase conc. (mg/g)	123.5913	248.2943	369.2791	460.7038
Ad (min^{-1})	8112.0	2833.87	989.20	1198.23
E_{des} (J/mol)	3652.67	7425.4	4959.72	5737.57
R^2	1.0	0.9998	0.929	0.9526

4.6.8. Desorption isotherm of Swiss blue dye from spent activated carbons

When the spent activated carbons were desorbed using chloroform, it was observed that the concentration of Swiss blue dye in the solvent increased with time, whereas the amount of Swiss blue dye on the adsorbents decreased with time. The equilibrium state at which the concentration of Swiss blue dye in the solvent remained constant with time shortly varied at different initial solid phase concentration and temperatures. At equilibrium, the relationship between the concentration of Swiss blue dye in the chloroform (Ce) and the remaining amount on the adsorbents (qe) was expressed like the Lagmuir, Freundlich, Dublin-Radishkevich (D-R), Temkin, Flory-Huggins, Redlich-Peterson (S- P) and Toth-isotherm equations. Desorption data were applied to the linear plots of these isotherm models to describe desorption of Swiss blue dye from the spent adsorbents. The desorption parameters obtained from the model plots (appendix K) are listed in Table 4.38- 4.41.

Table 4.38: Isotherm parameters for Swiss blue dye desorption from spent conventionally prepared activated carbon from spent grain

Temperature (K)	303	313	323
	Langmuir Model		
-b	217.39	169.49	1666.67
$-K_L$(L/mg)	0.163	0.13	
R^2	0.8911	0.8971	0.6221
	Freundlich Model		
N	0.479	0.4472	0.951
K_F(mg/g)(mgL^{-1})-1/n_F	22.36	9.1243	32.164
R^2	0.9913	0.999	0.9993
	Dublin-Radushkevich (D-R) Model		

B_D	2E-06	3E-06	3E-06
E(kJ/mol	353.5534	235.7023	235.7023
R^2	0.9944	0.8658	0.96
		Temkin Model	
A(L/mol)	0.546	0.355	0.476
B	4.98	5.15	10.86
R^2	0.988	0.813	0.9196
		Flory-Huggins Model	
K_{FH}(l/mol)	8.03	7.739	3.72
nF_H	1.7739	1.5294	1.4233
R^2	0.9967	0.9604	0.9864
		Redlich-Peterson Model	
K_R(mg/g)(mg/l)-1/n_F	40.73	33.45	28.2
R^2	0.9311	0.8863	0.3974
		Sip Model	
Ks(mg/g)(mg/l)-1/n_F	40.73	33.45	28.2
B(L/g)	1.0521	2.2357	2.087
αs(L/mg)	1.0	1.0	1.0
R^2	0.9494	0.9291	0.9913
		Toth Model	
K_T(L/mg)	-0.163	-0.131	-0.021
a_T	0.0263	0.2694	0.2029
T	0.489	0.309	0.324
R^2	0.9496	0.9291	0.9913

The regression coefficients (R^2) value for Freundlich model were comparatively higher for all the activated carbons suggesting that desorption of Swiss blue dye from the spent activated carbons were well described by Freundlich model. The applicability of Freundlich model confirmed that heterogeneous sites were actively involved for the adsorption process. This indicates that the adsorption sites on the surface of the adsorbents may possess different potential energies to form surface complex (Tseng et. al., 2009). These results were in agreement with the previous study on adsorption of Swiss blue dye on the adsorbents

Table 4.39: Isotherm parameters for Swiss blue dye desorption from spent conventional prepared activated carbon from hamburger seed shell

Temperature (K)	303	313	323
	Langmuir Model		
-b	200000	25000	1111.11
$-K_L$(l/mg)	0.0	0.45	0.75
R^2	0.7005	0.7631	0.9492
	Freundlich Model		
n	1.005	1.0281	0.832
K_F(mg/g)(mgl^{-1})-1/n_F	120.84	117.41	84.41
R^2	0.9961	0.9901	0.9953
	Dublin-Radushkevich (D-R) Model		
B_D	3E-07	4E-07	6E-07
E(J/mol)	2357.226	1767.77	1178.511
R^2	0.9972	0.9212	0.9459
	Temkin Model		
A(L/mol)	1.58	1.56	1.09
B	10.7	11.3	9.45
R^2	0.9498	0.931	0.9445
	Flory-Huggins Model		
K_{FH}(L/mol)	$3.45x10^7$	$1.93x10^7$	$2.8x10^4$
nF_H	-2.1782	-2.6197	3.5104
R^2	0.539	0.5778	0.8011
	Redlich-Peterson Model		
K_R(mg/g)(mg/l)-1/n_F	120.84	117.41	84.41
R^2	0.8311	0.7313	0.9699

		Sip Model	
Ks(mg/g)(mg/l)-1/n_F	120.84	117.41	84.41
β(L/g)	0.9956	0.9707	1.2022
as(L/mg)	1.002	1.0	1.0
R^2	0.996	0.9902	0.9954
		Toth Model	
K_T(L/mg)	-0.0006	-0.00465	-0.075
a_T	0.0412	0.00585	0.0022
T	0.4541	0.5073	0.5011
R^2	0.9954	0.99	0.9961

These results were in agreement with the work done by Tseng et. al. (2009) on the kinetics and equilibrium desorption for removal of copper from magnetic polymer adsorbent, Kim and Kim (2004) on apparent desorption kinetics of phenol in organic solvents from spent activated carbon saturated with phenol, and Chu et. al. (2004) on desorption of vitamin E from silica based adsorbent. Contrary to these results, Muhammad et. al. (2011) reported the applicability of Lagmuir model for desorption of β-carotene from mesoporus carbon coated monolith. Sip and Redlich-Peterson isotherm models equally recorded high correlation coefficients (R^2). These models were three parameters obtained from Freundlich isotherm constant that recorded high correlation coefficients (R^2). The applicability of Freundlich model for the desorption process showed that at equilibrium, the concentration of Swiss blue dye in the chloroform (Ce) is directly proportional to the remaining Swiss blue dye on the adsorbents (qe). It was equally observed from the results that the equilibrium constants for Freundlich isotherm decreased with increase in temperature. This shows that increase in temperature favoured the desorption process, thus the amount of Swiss blue dye remaining on the adsorbents decreased with increase in temperature.

Table 4.40: Isotherm parameters for Swiss blue dye desorption from spent microwave prepared activated carbon from spent grain

Temperature (K)	303	313	323
		Langmuir Model	
-b	52.08	40.98	34.36
$-K_L$(L/mg)	0.1544	0.1577	0.1582
R^2	0.4446	0.6074	0.8384
		Freundlich Model	
N	0.177	0.148	0.133
K_F(mg/g)(mgl^{-1})-1/n_F	0.02143	0.00308	0.00072
R^2	0.9968	0.9983	0.9977
		Dublin-Radushkevich (D-R) Model	
B_D	2E-05	2E-05	2E-05
E(J/mol)	158.11	158.11	158.11
R^2	0.6907	0.8239	0.9665
		Temkin Model	
A(L/mol)	0.229	0.2193	0.2125
B	1.638	1.472	1.419
R^2	0.8034	0.8963	0.9846
		Flory-Huggins Model	
K_{FH}(L/mol)	0.2625	0.2619	0.2654
nF_H	1.1948	1.1	1.0093
R^2	0.9916	0.9953	0.999
		Redlich-Peterson Model	
K_R(mg/g)(mg/l)-1/n_F	0.0321	0.031	0.0308
R^2	0.3812	0.6893	0.8792

		Sip Model	
Ks(mg/g)(mg/l)-1/n_F	0.0321	0.0331	0.0308
β(L/mg)	9.663	6.7382	7.5645
a_s(L/mg)	1.62	0.992	1.0612
R^2	0.7268	0.7864	0.9422
		Toth Model	
-K_T(L/mg)	0.1544	0.1577	0.1582
a_T	6.444	1.661	1.892
T	0.027	0.1293	0.1171
R^2	0.8235	0.7867	0.9466

It was equally observed that Flory-Huggins fitted the isotherm data well for all adsorbents except conventional prepared activated carbon from hamburger seed shell. It was observed that Flory-Huggins constant decreased with increase in temperature. This shows that the amount of the adsorbed Swiss blue dye decreased with increase in temperature. It equally confirmed the endothermic nature of the desorption process. The number of dye occupying the adsorption site (n_{FH}) on Flory-Huggins model was observed to decrease with increase in temperature. This shows that increase in temperature favoured desorption of Swiss blue dye from the adsorbents.

Table 4.41: Isotherm parameters for Swiss blue dye desorption from spent microwave prepared activated carbon from hamburger seed shell

Temperature (K)	303	313	323
	Langmuir Model		
-b(mg/g)	43.4783	27.0270	12.3450
-K_L(L/mg)	0.23	0.24	0.24
R^2	0.857	0.968	0.914
	Freundlich Model		
N	0.5	0.5618	0.6061
K_f(mg/g) (mgl^{-1})-1/n_F	15.985	20.511	23.471
R^2	0.950	0.998	0.910
	Dublin-Radushkevich (D-R) Model		
B_D	0.987	1.334	2.705
E(J/mol)	0.712	0.612	0.430
R^2	0.992	0.996	0.910
	Temkin Model		
A(L/mol)	0.3320	0.1264	0.2760
B	1.401	1.091	0.573
R^2	0.995	0.953	0.843
	Flory-Huggins Model		
K_{FH}(L/mol)	0.518	0.406	0.287
nF_H	1.153	1.106	1.031
R^2	0.999	1.0	0.999
	Redlich-Peterson Model		
K_R(mg/g)(mg/L)-1/n_F	0.751	0.657	0.582
R^2	0.901	0.975	0.916

		Sip Model	
Ks(mg/g)(mg/l)	0.751	0.657	0.582
B(L/mg)	6.998	9.468	18.820
αs(L/mg)	29.93	10.63	4.85
R^2	0.977	0.977	0.906
		Toth Model	
$-K_T$(l/mg)	0.23	0.24	0.24
a_T	0.665	0.5180	2.7350
T	0.1280	0.0968	0.0510
R^2	0.950	0.998	0.910

4.6.9. Thermodynamics study for Desorption of Swiss blue dye from spent activated carbons

The thermodynamic parameters (ΔHdes, ΔSdes and ΔGdes) were obtained from the combination of Arrhenius equation (Schroeder & Gottfried, 2002; Kim & Kim, 2004; Do & Wang 1998) and Freundlich equilibrium constant (Ke) expressed as an exponential function of temperature (Kim & Kim, 2004; Madras et. al., 1993; Macnaughton & Foster 1995).

When rate constant K_d is described by the Arrhenius equation, we have it that (Kim & Kim 2004; Scroeder & Gottfried 2002; Do & Wang 1998)

$$Kd = Ad \exp\left(\frac{-Edes}{RT}\right) \tag{4.39}$$

Equally, at equilibrium, the relationship between the concentration of the Swiss blue dye in chloroform (Ce) and the adsorbed amount on the activated (qe) might be expressed like the Freundlich isotherm equation.

$$qe = Ke(Ce)^n \tag{4.40}$$

Ke was expressed as an exponential function of temperature as (Kim & Kim, 2004; Madras et. al., 1993; Macnaughton & Foster 1995).

$$Ke(T) = K_O \exp\left(\frac{\gamma}{T}\right) \tag{4.41}$$

Linearization of equation 4.41 gives

$$InKe = InK_O + \gamma\left(\frac{1}{T}\right) \tag{4.42}$$

γ(K) and K_O(mg/g)(mg/l)$^{-n}$ are constants in eqn. (4.42), Ke is Freundlich isotherm constant (mg/g)(mg/l)$^{-n}$ and T is temperature (K).

Plot of InKe against 1/T in equation 4.42 gave InK_o as intercept and γ as slope. Table 4.42 show the parameters obtained from plot of InKe against 1/T while appendix L shows the plot.

It was observed that correlation coefficients (R^2) of all the adsorbents were approximately 1.0. This proved the validity of equation 4.43.

To further understand the nature of the desorption process, Schroeder & Gottfried (2002) stated that differences between activation energy (ΔEdes) and enthalpy change (ΔHdes) are in practice often negligible. Therefore, they assumed that ΔEdes = ΔHdes. They equally stated that the frequency factor (Ad) in the Arrhnius equation (4.39) can be equated to the entropy term as follows (Schroeder & Gottfried 2002);

$$Ad = \frac{K_d T}{\gamma} \exp\left(\frac{\Delta \mathrm{Sdes}}{R}\right) \quad (4.43)$$

Entropy of desorption can be extracted from the frequency factor (Ad) above as;

$$\Delta \mathrm{Sdes} = \mathrm{R}.\left(\frac{InAd.\gamma}{K_d T}\right) \quad (4.44)$$

Where R is the universal gas constant (J/mol.K), γ is constant from equation (4.42) (K), T is the temperature (K), and K_d is the pseudo second order rate constant (1/min).

Change in the standard free energy (ΔG_{des}) can be calculated from the enthalpy (ΔS_{des}) using the following relation (Al-Othman et. al., 2012);

$$\Delta \mathrm{Gdes} = \Delta \mathrm{Hdes} - \mathrm{T}\Delta \mathrm{Sdes} \quad (4.45)$$

The thermodynamic parameters obtained at different initial solid phase concentration and temperatures are shown in table 4.42.

It was observed from the results that the enthalpy change for desorption process using all the activated carbons at different temperatures were positive, indicating endothermic reaction. This means that increase in temperature favoured the desorption process. Desorption process consumed energy from the surrounding in overcoming the activation barrier needed before desorption takes place. Decrease in temperature favoured the adsorption process (exothermic reaction), while increase in temperature the desorption process (endothermic process).

Positive entropy (ΔS) observed on all the adsorbent studied at different initial solid phase concentration suggested that the desorption process had increase disorder at various conditions studied. The entropy values increased as reaction temperature was increased with exception of few. This suggested that the reaction gets more disorder as temperature was increased confirming the endothermic nature of the reaction. The negative Gibbs free energy (ΔG) observed on the entire initial solid phase

concentration at various temperatures confirmed the process to be spontaneous and feasible. Increase in temperature increased the Gibbs free energy (ΔG) with exception of few. This showed that the desorption process becomes more spontaneous as the temperature was increased.

Table 4.42: Parameters of Freundlich equilibrium constant (Ke) expressed as an exponential function of temperature for desorption process

Parameters	MPAHS	MPASG	CPAHS	CPASG
$K_O((mg/g)(mg/l)^{-n})$	0.0103	0.0168	0.4176	0.1077
γ(K)	1911.7	195.68	1716.0	1798.8
R^2	1.0	0.998	1.0	1.0

Table 4.43: Thermodynamic parameters for desorption of Swiss blue dye from spent activated carbon.

Initial solid phase conc. (mg/g)	ΔH_{des} (KJ/mol)	ΔS_{des} (J/mol.K)			- ΔG_{des}(KJ/mol)		
		303K	313K	323K	303K	313K	323K
Microwave prepared activated carbon from spent grain (MPASG)							
123.329	3.045	138.48	138.53	138.58	38.92	38.93	38.94
247.797	2.519	136.044	135.95	135.99	38.69	38.67	38.69
372.645	4.094	139.87	140.14	140.17	38.29	38.37	38.38
497.532	4.911	141.68	142.27	142.14	38.02	38.20	38.26
Conventional prepared activated carbon from spent grain (CPASG)							
124.3603	12.167	153.07	153.86	155.0	34.21	34.45	34.80
248.847	19.538	190.30	173.85	174.61	38.12	33.14	33.36
347.2663	23.549	201.31	203.22	186.47	37.45	38.03	38.95
441.4925	19.155	183.58	186.00	186.93	36.47	37.20	37.48
Conventional prepared activated carbon from hamburger seed shell (CPAHS)							
122.69	7.627	139.04	139.64	140.36	34.50	34.69	34.90
247.73	2.010	119.07	119.00	118.74	34.07	34.05	33.91

369.02	8.673	149.32	150.38	151.22	36.67	37.00	37.25
438.53	0.749	141.97	141.75	141.59	42.27	42.20	42.15
Microwave prepared activated carbon from hamburger seed shell (MPAHS)							
123.5913	3.652	133.99	134.12	134.20	36.95	36.99	37.01
248.2943	7.425	123.22	123.73	124.18	29.91	30.06	30.20
369.2771	4.959	113.95	113.83	114.45	29.57	29.53	29.72
460.7038	5.737	114.51	114.66	115.16	28.96	29.00	29.16

4.7. Optimization of desorption process using Box Behnken design (BBD)

Optimization of desorption process was achieved using BBD. It involved three numeric factors which were temperature, initial dye concentration used for saturation and dosage of the saturated activated carbons and one categoric factor which is type of activated carbon with four levels which were microwave prepared activated carbon from hamburger seed shell (MPAHS), microwave activated carbon from spent grain (MPASG), conventionally prepare activated carbon from hamburger seed shell (CPAHS), and conventionally prepared activated carbon from spent grain (CPASG). Analysis of variance was established and model equation developed was validated.

4.7.1. Analysis of variance for the desorption process

Table 4.44 shows the analysis of variance for the desorption process. The Model F-value of 24.46 implied the model was significant. There was only a 0.01% chance that a "Model F-Value" this large could occur due to noise. Values of "Prob > F" less than 0.0500 indicate model terms were significant. In this case temperature (A), dosage (B), initial dye concentration used for saturation (C), type of adsorbent (D), interaction of temperature and dosage (AB), interaction of temperature and initial dye concentration used for saturation (AC), quadratic effect of initial dye concentration used for saturation (C^2) were significant model terms. Values greater than 0.1000 indicated the model terms were not significant. The "Lack of Fit F-value" of 1.40 implied the Lack of Fit was not significant relative to the pure error. There was a 23.45% chance that a "Lack of Fit F-value" this large could occur due to noise. The "Pred R-Squared" of 0.7016 is in reasonable agreement with the "AdjR-Squared" of 0.7591."Adeq Precision" measures the signal to noise ratio. A ratio greater than 4 is desirable. The ratio of 23.418 indicated an adequate signal.

Table 4.44: ANOVA table for the desorption process

Source	Sum of Squares	Df	Mean Square	F Value	p-value Prob>F
Model	714.95	9	79.44	24.46	<0.0001
A-Temperature	101.41	1	101.41	31.23	<0.0001
B-Dosage	244.28	1	244.28	75.23	<0.0001
C-Initial conc.	33.02	1	33.02	10.17	0.0023
D-Type of adsorbent	254.47	3	84.82	26.12	<0.0001
AB	31.57	1	31.57	9.72	0.0028
AC	18.40	1	18.40	5.67	0.0206
C^2	31.79	1	31.79	9.79	0.0027
Residual	188.34	58	3.25		
Lack of fit	148.13	42	3.53	1.40	0.2345
Pure Error	40.21	16	2.51		
Cor Total	903.29	67			

4.7.2. Model equation for desorption process

Model equation involving a categoric factor was presented both in coded and actual form. Equation 4.46 is the equation in coded form. Because the categoric factor has four levels, the coded equation was split into four (equation 4.47-4.50) each representing each level effects with its interactions. The fourth equation is the reference equation without any level and its interactions.

Final Equation in Terms of Coded Factors:

Equilibrium concentration after desorption (mg/l) = +10.58 +1.78 A -2.76B -1.02C +2.1D[1] +1.23 D[2] -2.94D[3] -1.40AB -1.07AC -1.37C^2 (4.46)

Microwave prepared activated carbon from hamburgar seed shell (MPAHS);

Equilibrium concentration after desorption (mg/l) = +10.58 +1.78 A -2.76B -1.02C +2.1D[1]-1.40AB-1.07AC-1.37C^2 (4.47)

Microwave prepared activated carbon from spent grain (MPASG);

Equilibrium concentration after desorption (mg/l) = +10.58 +1.78 A -2.76B -1.02C +1.23D[2]-1.40AB-1.07AC-1.37C^2 (4.48)

Conventionally prepared activated carbon from hamburgar seed shell (CPAHS);

Equilibrium concentration after desorption (mg/l) = +10.58 +1.78 A -2.76B -1.02C-2.94D[3]-1.40AB-1.07AC-1.37C^2 (4.49)

Conventionally prepared activated carbon from spent grain (CPASG);

Equilibrium concentration after desorption (mg/l) = +10.58 +1.78 A -2.76B -1.02C -1.40AB -1.07AC -1.37C^2 (4.50)

Final Equation in Terms of Actual Factors:

Microwave prepared activated carbon from hamburgar seed shell (MPAHS);

Equilibrium concentration after desorption (mg/l)=-9.37877+0.53830 Temperature +5.38835Dosage+0.087535Initial dye concentration used for saturation (mg/l) -0.26504TemperatureDosage-1.07253E-003 Temperature Initial dye concentration used for saturation(mg/l)-1.36979E-004Initial dye concentration used for saturation$(mg/l)^2$ (4.51)

Microwave prepared activated carbon from spent grain (MPASG);

Equilibrium concentration after desorption (mg/l) =-10.29589+0.53830 Temperature+5.38835Dosage+0.087535Initial dye concentration used for saturation (mg/l)-0.26504TemperatureDosage-1.07253E-003 Temperature Initial dye concentration used for saturation(mg/l)-1.36979E-004 Initial dye concentration used for saturation $(mg/l)^2$ (4.52)

Conventionally prepared activated carbon from hamburgar seed shell (CPAHS);
Equilibrium concentration after desorption (mg/l) =-14.46554+0.53830 Temperature+5.38835Dosage+0.087535Initial dye concentration used for saturation (mg/l)-0.26504Temperature Dosage-1.07253E-003 Temperature Initial dye concentration used for saturation (mg/l)-1.36979E-004 Initial dye concentration used for saturation $(mg/l)^2$ (4.53)

Conventionally prepared activated carbon from spent grain (CPASG);
Equilibrium concentration after desorption (mg/l) =-11.97810+0.53830 Temperature+5.38835Dosage+0.087535Initial dye concentration used for saturation (mg/l)-0.26504TemperatureDosage-1.07253E-003 Temperature Initial dye concentration used for saturation (mg/l)-1.36979E-004 Initial dye concentration used for saturation $(mg/l)^2$ (4.54)

4.7.3. Optimum conditions for the desorption process

The optimum conditions were generated with the aim of maximixing the Swiss blue dye removal efficiency. Tables (4.45 and 46) show the optimum conditions and the validated conditions respectively for the Swiss blue dye adsorption process.

Table 4.45: Optimal conditions for desorption of Swiss blue dye

Temp. (^oC)	Initial dye conc. (mg/l)	Dosage (g)	Adsorbent Types	Predicted Values (mg/l)
50.00	100.00	0.02	MPAHS	19.4773
50.00	100.00	0.02	MPASG	18.5601
50.00	100.05	0.02	CPASG	16.8779
50.00	100.40	0.02	CPAHS	14.3905

Table. 4.46: Model validation for the desorption of Swiss Blue Dye

Temp. (^oC)	Initial dye conc. (mg/l)	Dosage (g)	Adsorbent types	Removal Efficiency (%)		Error (%)
				Experimental values	Predicted values	
50.00	100.00	0.02	MPAHS	19.5001	19.4773	0.12
50.00	100.00	0.02	MPASG	18.621	18.5601	0.33
50.00	100.00	0.02	CPASG	16.949	16.8779	0.42
50.00	100.00	0.02	CPAHS	14.410	14.3905	0.14

As seen from the validation table, the errors obtained were small. This showed that the experimental values were very close to the predicted values, thus, the model equation generated was effective in predicting the desorption equilibrium concentration.

4.8. Regeneration studies on Swiss blue dye loaded activated carbons

The objective of this section is to desorb the accumulated Swiss blue dye and restore the original porous structure and activity of the carbon with as little damage as possible to the carbon itself. Vliet, (1991) pointed out that the economic feasibility of using activated carbon for the recovery of precious metals or the purification of water or waste water is contingent upon the reuse of the carbon in multiple adsorption-regeneration cycles.

Three different techniques namely; chemical regeneration, conventional regeneration and microwave regeneration were used to study the re-utilization potential of the activated carbons. The efficiency of the regenerated activated carbons was evaluated by adsorption on Swiss blue dye which is a standard method to assess the performance of the activated carbons. The regeneration efficiencies were judged on the extent that it recovers the adsorption capacities of the spent activated carbons. Six successive cycles of adsorption-desorption of Swiss blue dye were carried out in the batch system to assess the reusability of the activated carbons for the Swiss blue dye adsorption. Cycle 0 corresponds to the adsorptive capacity of the original activated carbon.

4.8.1. Chemical Regeneration Cycles of Swiss blue dye loaded activated carbons

Chemical regeneration can be carried out by desorption of adsorbents using specific solvents or by decomposition of adsorbed species using oxidizing chemical agents (Purkait et. al., 2007). In this study, chloroform was used as the chemical based on the preliminary work done that confirmed it as the best eluant. 30% H_2O_2 (hydrogen peroxide) was used as an oxidizing chemical agent to aid the decomposition of the adsorbed substances. Sufnarski (1999) reported that two types of reagents are used for chemical regeneration; those with oxidizing ability and those with solubilizing ability.

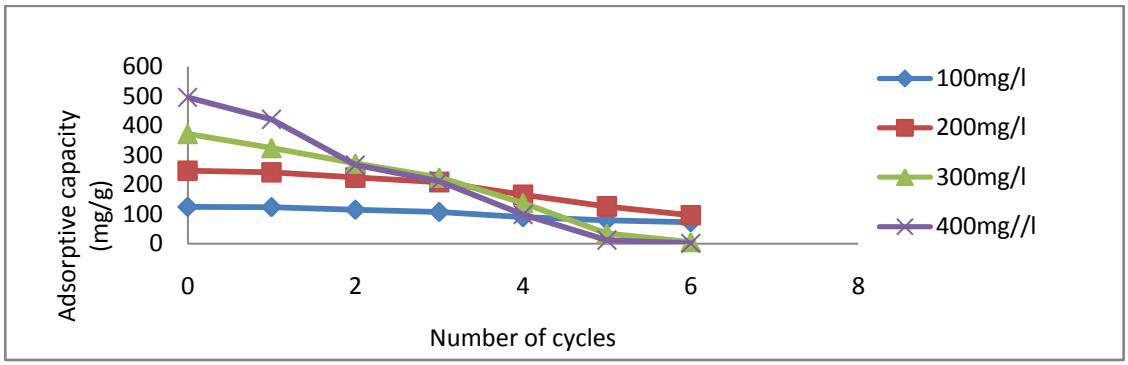

(a)

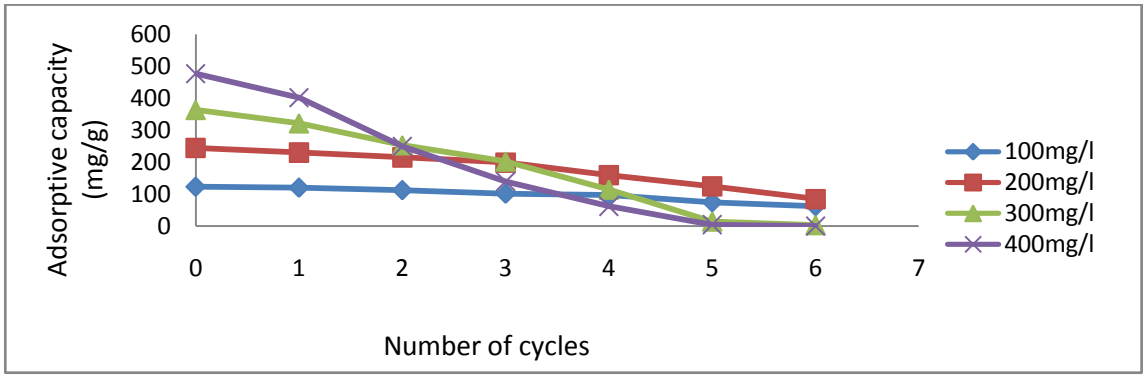

(b)

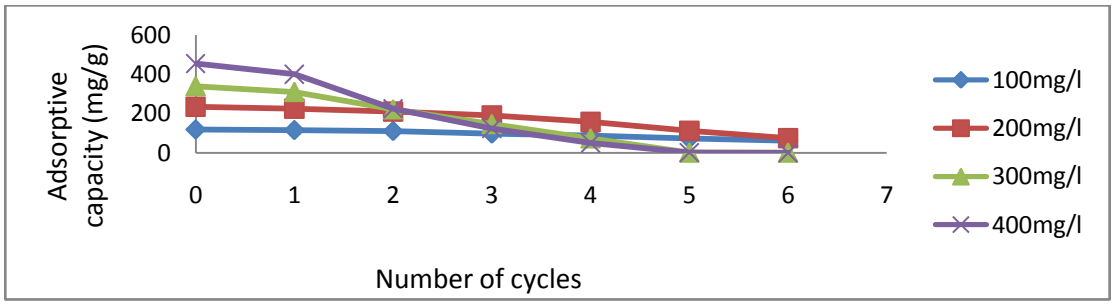

(c)

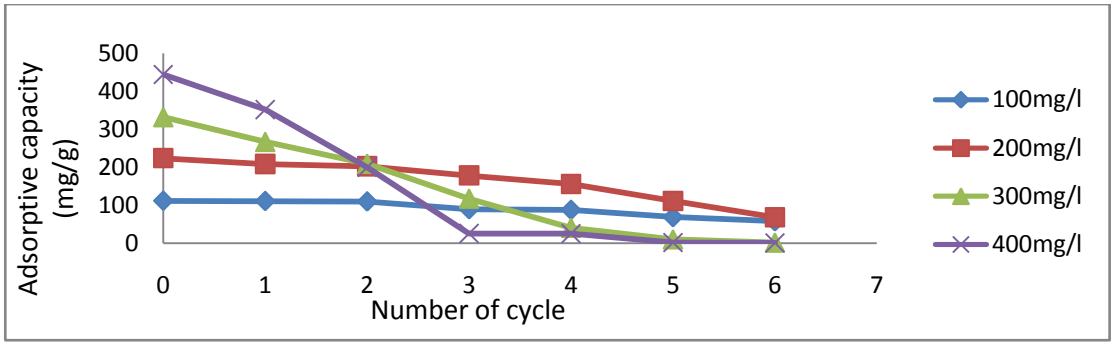

(d)

Fig. 4.24: Effect of Chemical Regeneration cycles on the adsorptive capacity of the spent activated carbons (a) MPAHS, (b) MPASG, (c) CPASG, (d) CPAHS

The regeneration efficiencies recorded in this section compared to the regeneration efficiencies recorded on my previous work on section 4.8.2. on effect of eluant was as a result of oxidizing agent used in this section. Swiss blue dye is soluble in chloroform (Boca, 2007) while hydrogen peroxide helped to oxidize the adsorbed dye. The lower regeneration efficiencies recorded compared to other methods can be attributed to the room temperature used for the regeneration since higher temperature was found to favour desorption process.

To study the chemical regeneration, the activated carbons were saturated with 100mg/l, 200mg/l, 300mgl and 400mg/l initial Swiss blue dye solution for twenty four hours to make sure that the pores were fully saturated. The adsorption-regeneration process was done for six cycles. Cycle 0 corresponds to the adsorption capacity of the original activated carbon. It was observed from fig. 4.24 on the effect of regeneration cycle on the adsorptive capacities of the regenerated activated carbons that increase in initial dye concentration increased the adsorptive capacity. This trend was observed on all the cycles for lower initial dye concentrations (100-200mg/l), but for higher initial dye concentrations, (300-400mg/l), the trend was contradicted on the higher cycles (3-6). The increase in adsorptive cycle as initial dye concentration was increased was attributed to mass transfer gradient recorded at high concentration which tends to favour dye uptake. At lower initial dye concentrations, chemical regeneration was effective in freeing the pores for subsequent adsorption.

The decrease observed on higher cycles for the high initial dye concentration can be attributed to high initial solid phase concentration involved which was inefficiently

removed by chemical regeneration. This blocked the pores thereby reducing the uptake rate. For lower initial solid phase load concentration (100-200mg/l), the dyes on the adsorbents interacted with the eluent binding sites completely and thus facilitate desorption. For higher solid load concentration, more dye ions without desorptions were due to the saturation of eluent binding sites (Qing-Zhu, et. al., 2009). It was observed from fig. 4.25 that the regeneration efficiencies decreased with increase in cycle for all the initial dye concentration. This could be due to a decrease in the number of binding sites over the activated carbon as a result of inefficient desorption (Machado et. al., 2002). The degradation of the activated carbon's surfaces might be the other reason (Zhang et. al., 2011). It was equally observed that the chemical regeneration efficiencies decreased with increase in initial dye concentration. This can be linked to initial solid phase concentration obtained as the initial dye concentration was increased. The high initial dye concentrations were very difficult to be desorbed according to Qing-Zhu (2009). This led to the blockage of the pore with consequential decrease in regeneration efficiencies.

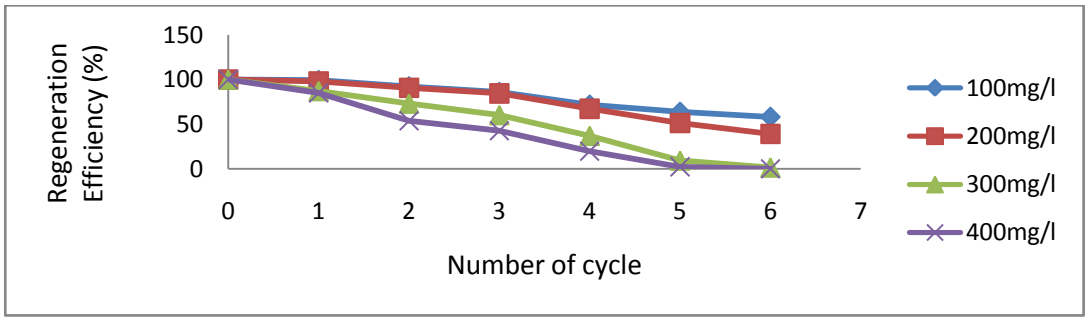

(a)

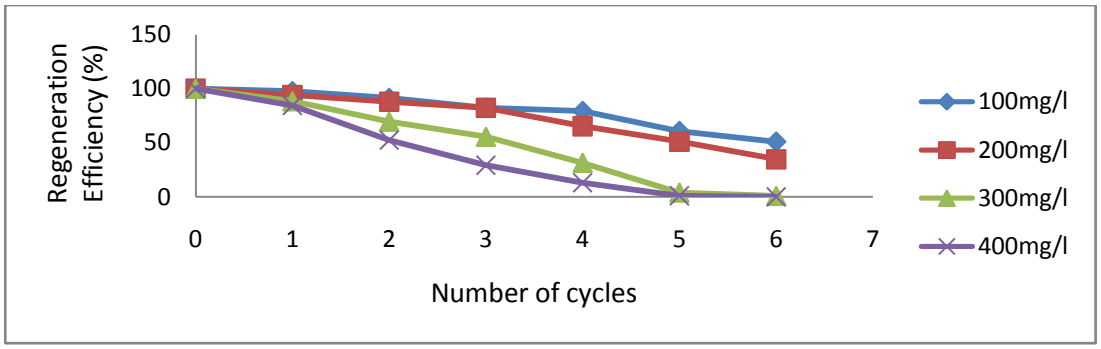

(b)

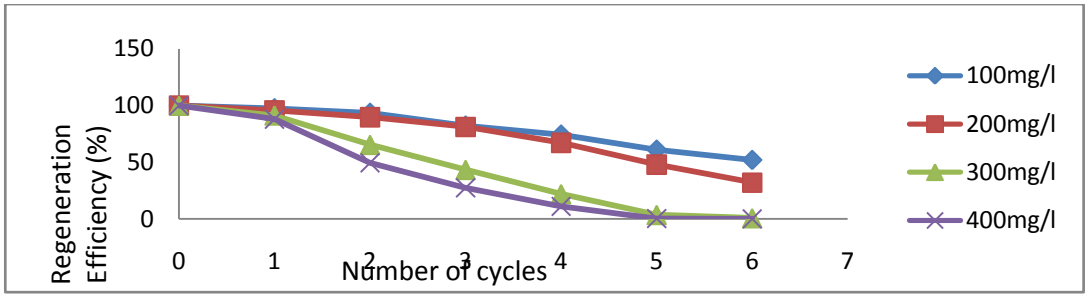

(c)

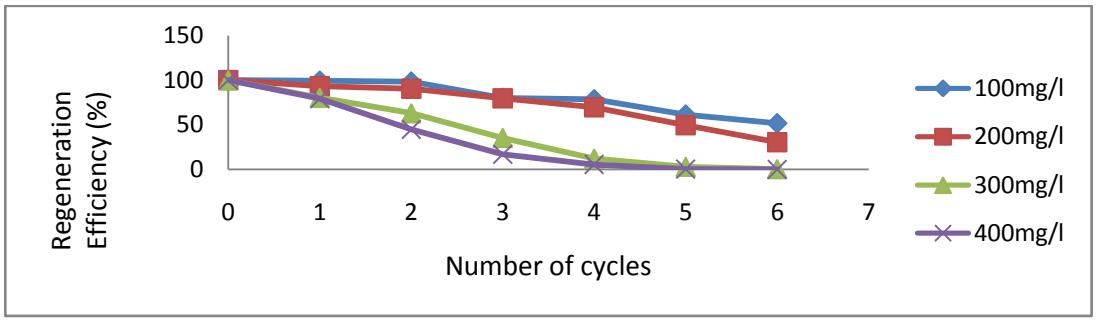

(d)

Fig. 4.25: Effect of Chemical Regeneration cycles on the Regeneration efficiency of the spent activated carbons (a) MPAHS, (b) MPASG, (c) CPASG, (d) CPAHS

4.8.2. Microwave Regeneration Cycles of Swiss blue dye loaded activated carbons

The activated carbons were saturated with 100mg/l, 200mg/l, 300mg/l and 400mg/l initial Swiss blue dye concentration for twenty four hours. After saturation, Swiss blue dye loaded activated carbons were exposed to microwave irradiation at 81% power level corresponding to 719W for 10 minutes. The effectiveness of the radiation on the activated carbons was measured by adsorbing the same concentration of Swiss blue dye. The impact of six cycle of adsorption regeneration was studied and the adsorptive capacity and regeneration efficiencies calculated. The regeneration was studied with 30% H_2O_2 as an oxidant. Fig. 4.26 shows the effect of cycle numbers on the adsorptive capacities of the regenerated adsorbents. It was observed from the plots, contrarily to that of chemical regeneration that the adsorptive capacities of the regenerated activated carbons increased with increase in initial dye concentration for all the cycles. This shows the effectiveness of microwave heating in desorbing the adsorbates. The decrease on the adsorptive capacities as the number of cycles was increased can be attributed to the weakening of the pores as a result of successive heating.

The effect of number of cycles on the regeneration efficiencies (fig. 4.27) shows that the regeneration efficiencies decreased as number of cycles and initial dye concentrations were increased. It was equally observed that the regeneration efficiencies were slightly above hundred at 100mgl initial dye concentration for cycles (1 – 4). Microwave prepared activated carbon from spent grain (MPASG) and conventional prepared activated carbon from spent grain (CPASG) equally recorded regeneration efficiencies above hundred at 200mg/l. Further treatment resulted in slight decrease of regeneration efficiencies. For higher initial dye concentrations, it was observed that the adsorptive capacities were slightly preserved as observed on the regeneration efficiencies which were slightly less than 100. This phenomenon might be attributed to the reorganization of internal structures as a consequence of the adsorbate molecules evolving during the microwave irradiation stage (Foo & Hameed, 2012a).

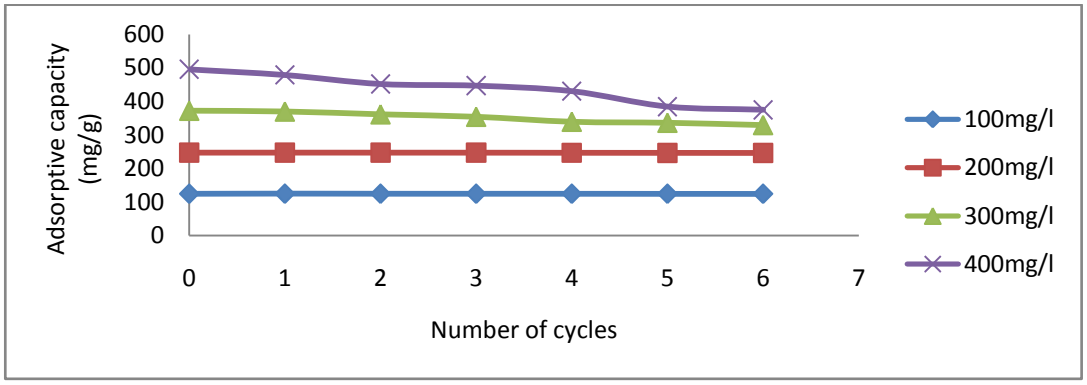

(a)

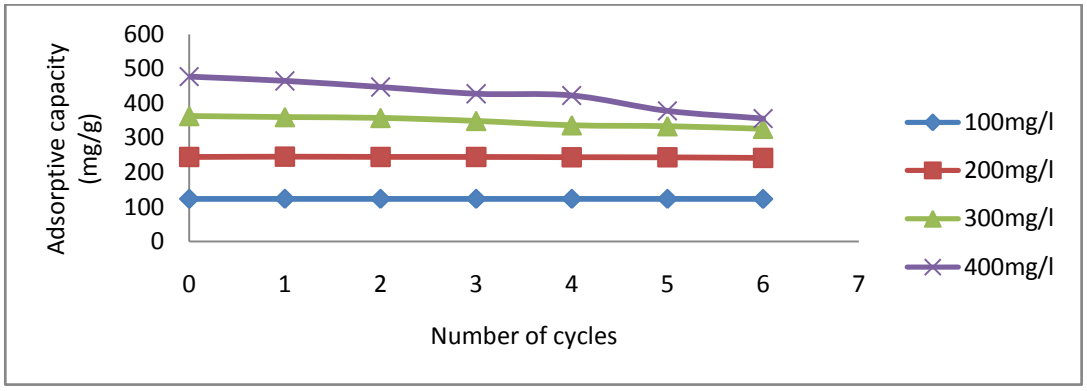

(b)

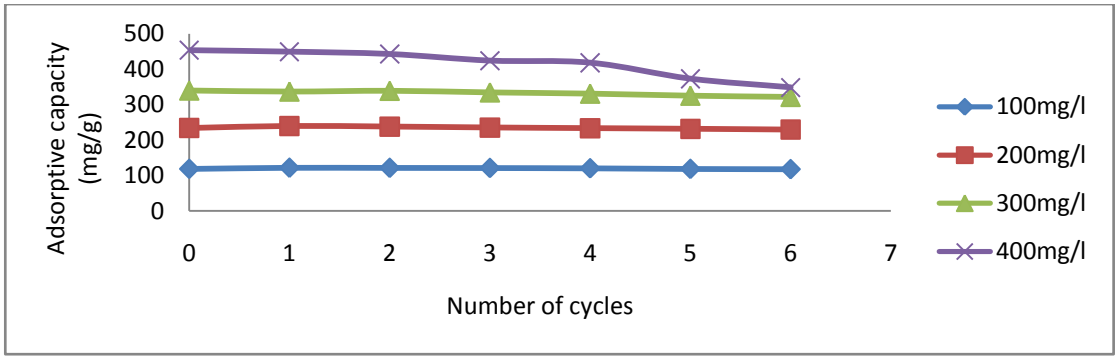

(c)

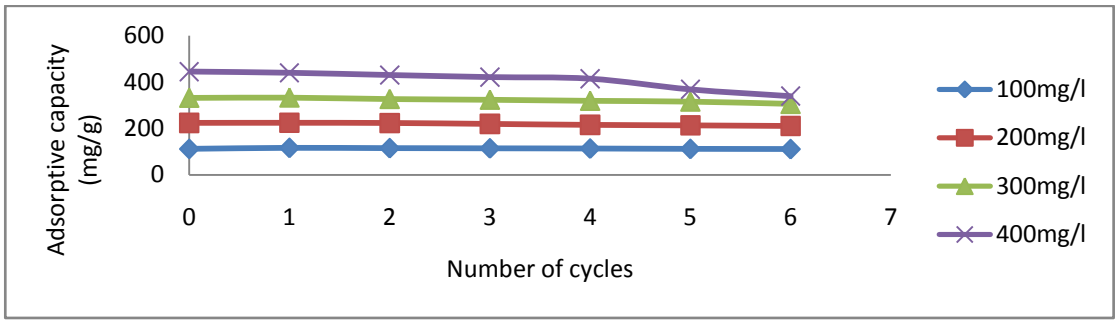

(d)

Fig. 4.26: Effect of Microwave Regeneration cycles on the Adsorptive capacity of the spent activated carbons a) MPAHS, (b) MPASG, (c) CPASG, (d) CPAHS

This finding was in agreement with the work done by Dehdashti et. al. (2010) on the regeneration of granular activated carbon saturated with gaseous toluene by microwave irradiation. Dehdashti et. al. (2010) observed that after five repetitive treatment cycles by microwave energy, the adsorption capacities remained approximately constant at higher power levels, after which slight reduction was observed at subsequent cycles. Preservation of adsorptive capacity by microwave heating implied, improvement in surface and porosity characteristic as a result of the radiation. The surface area, mesopore volume and mesopore volume of activated carbon regenerated with microwave for 15 minutes increased with increase in treatment cycles (Delidashti 2010). His findings confirmed previous literature on the effect of microwave irradiation on the textural properties of carbon (Ania et. al., 2005). It can be recalled that mesopores was responsible for adsorption of Swiss blue dye, thus increase in adsorptive capacity was recorded for microwave radiation on spent activated carbons.

The lower regeneration efficiencies recorded at higher initial dye concentration can be attributed to initial solid phase concentration at higher initial dye concentrations which were not properly desorbed.

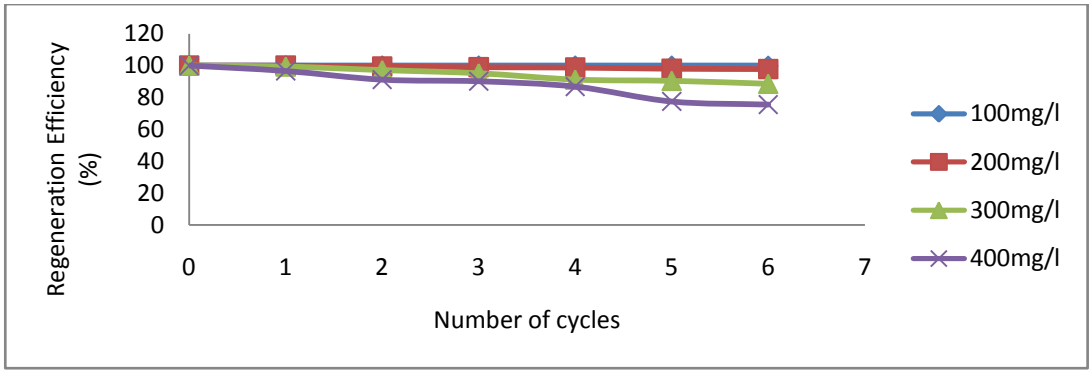

(a)

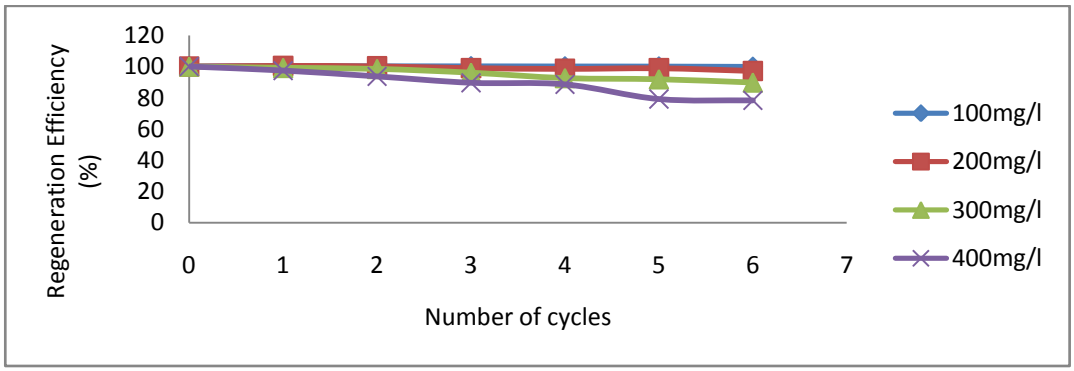

(b)

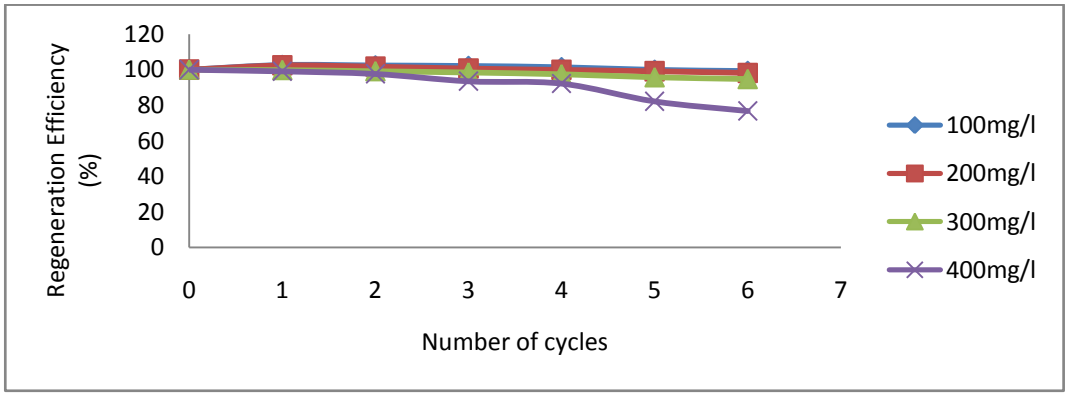

(c)

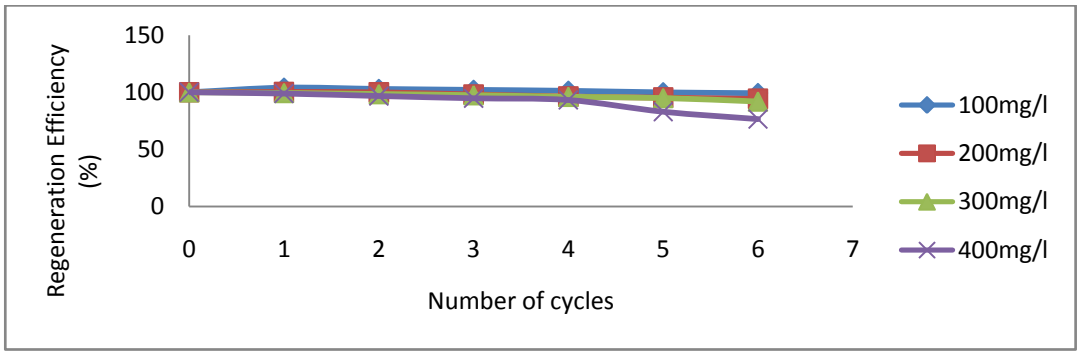

(d)

Fig. 4.27: Effect of Microwave Regeneration cycles on the Regeneration efficiency of the spent activated carbons (a) MPAHS, (b) MPASG (c) CPASG, (d) CPAHS

4.8.3. Conventional Regeneration cycle of Swiss blue dye loaded activated carbons

The conventional regeneration involved subjecting the spent activated carbon to temperature of 500°C in an electric furnace for 30 minutes. The regeneration efficiency and the adsorptive capacities of the regenerated observed carbons were evaluated. It was observed from Fig. 4.28 on the effect of number of cycles on the adsorptive capacity of the regenerated activated carbon that conventional regeneration of activated carbon after successive treatment decreased the adsorptive capacity significantly. This is attributed to the adverse changes in the adsorbent physical structure (Bahen, 2003). One disadvantage of thermal regeneration is a loss of adsorption capacity caused by changes in the pore structure of the carbon (Surfnarsk, 1999). This was in agreement with the work done by Muhammad et. al. (2011) on the adsorption of β-carotene and the regeneration studies. It was equally observed that adsorptive capacities of the regenerated activated carbons increased with increase in initial dye concentration. This shows that conventional regeneration to an extent compared with chemical regeneration desorbed the adsorbate.

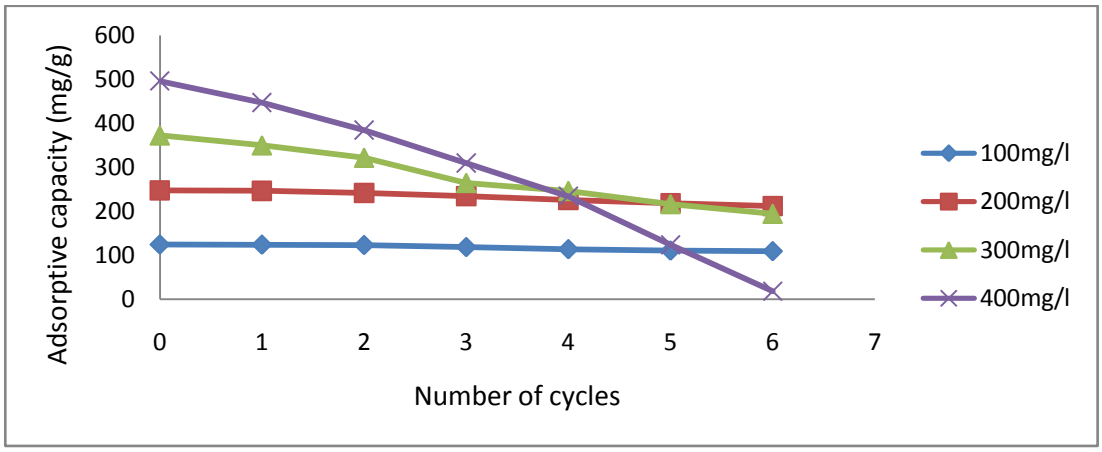

(a)

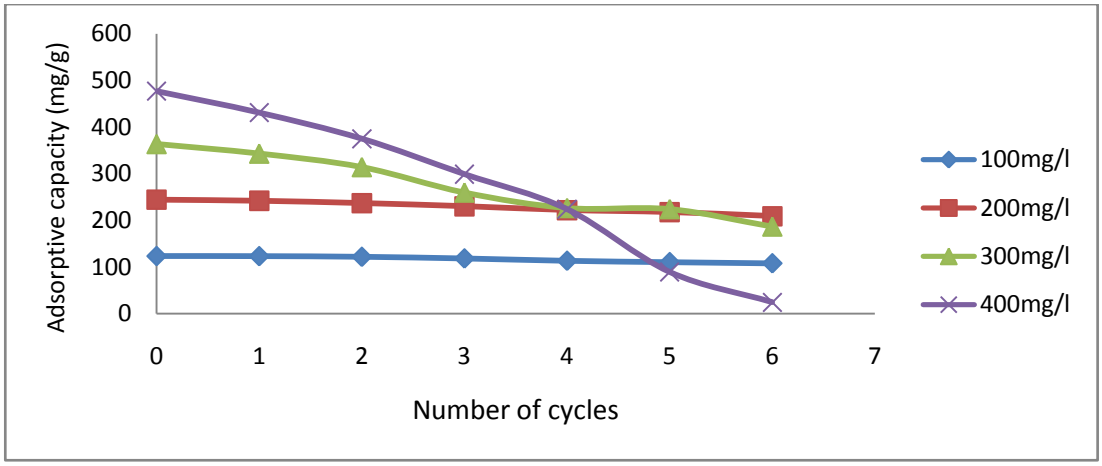

(b)

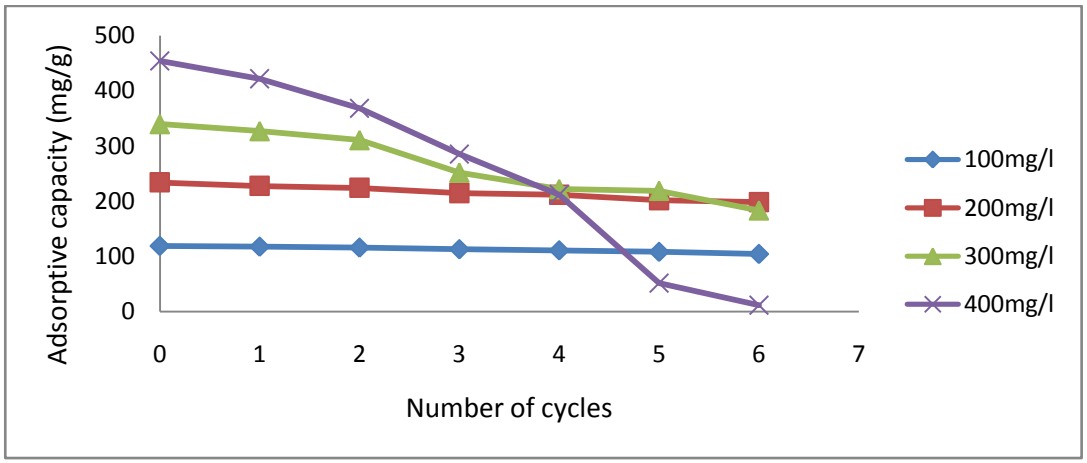

(c)

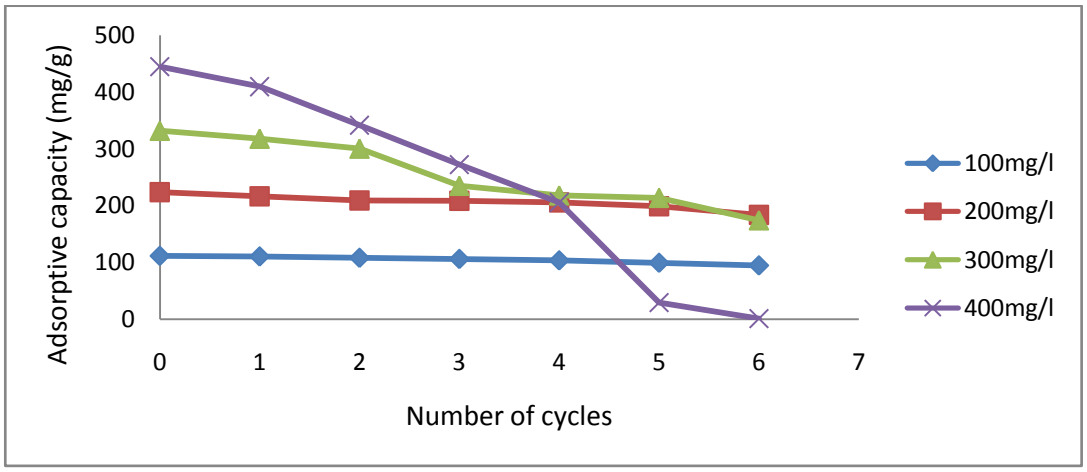

(d)

Fig. 4.28: Effect of Conventional Regeneration cycles on the Adsorptive capacity of the spent activated carbons (a) MPAHS, (b) MPASG, (c) CPASG (d) CPAHS

Regeneration efficiencies (Fig. 4.29) were observed to decrease with successive cycles of adsorption – regeneration. Low regeneration efficiencies recorded can be attributed to the shrinkage of pores on the carbon surface resulting to decrease in total surface area thereby reducing the accessible surface for Swiss blue dye binding (Tsezos, et. al., 1989). Widening of mesopores due to thermal treatment might also be the possible cause for reduction in capacity (Misra, et. al., 2002). It was equally observed that the regeneration efficiencies decreased with increase in initial dye concentrations. This was as a result of inefficient desorption recorded at higher initial solid phase concentration used.

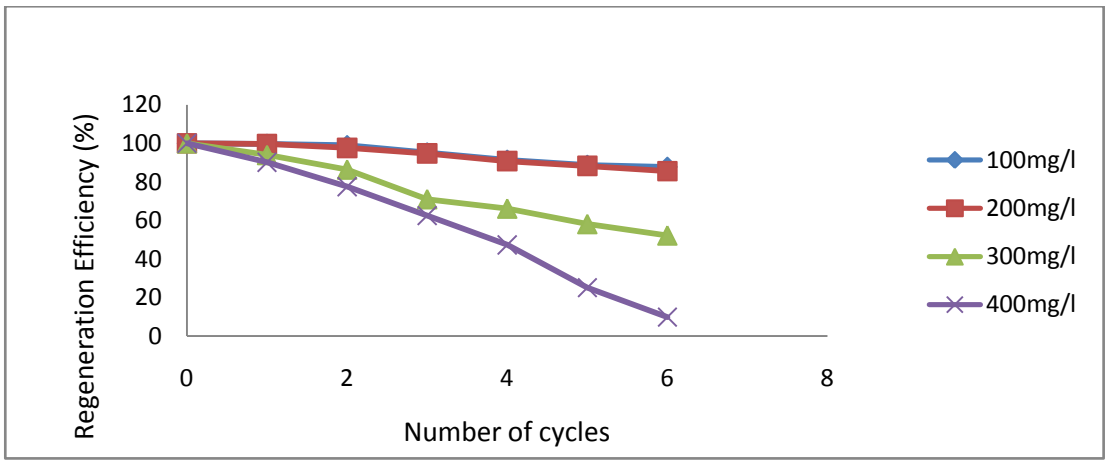

(a)

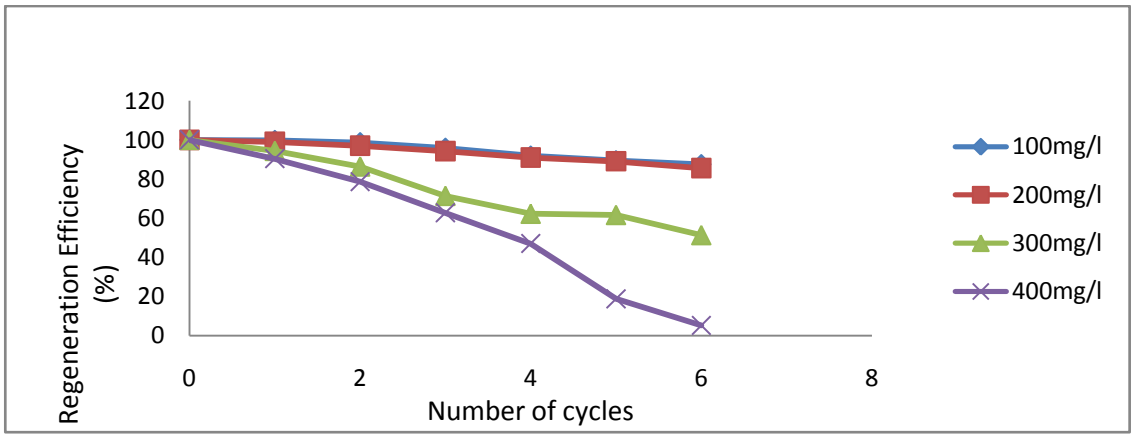

(b)

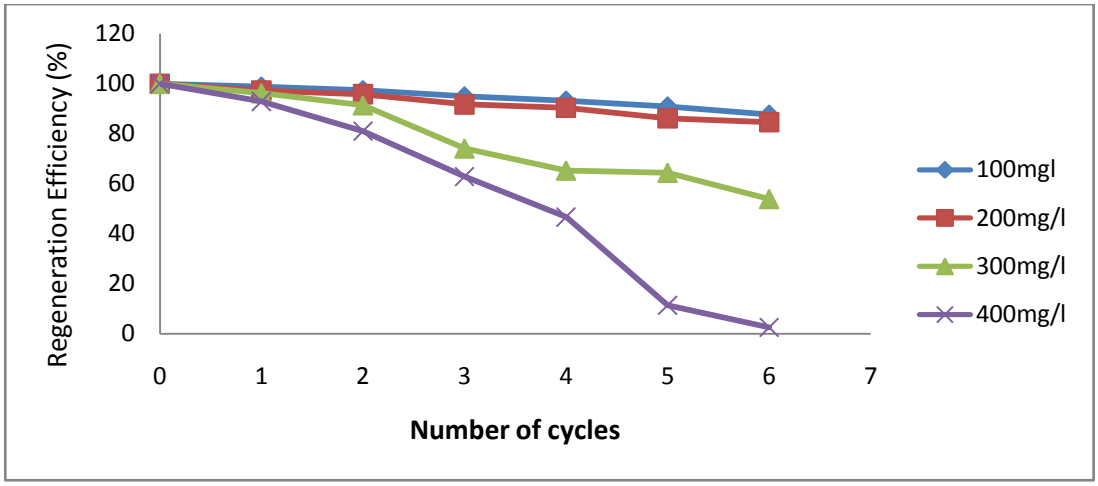

(c)

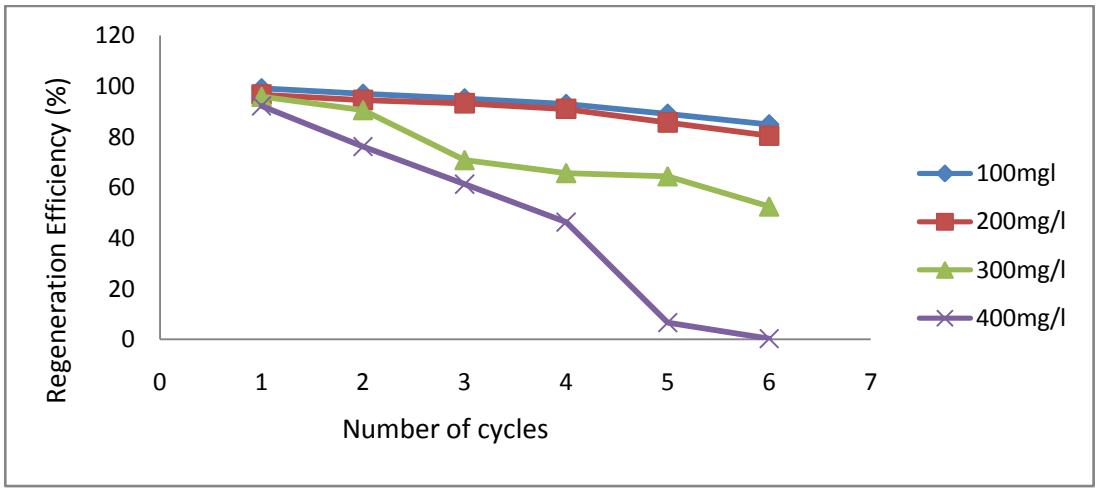

(d)

Fig. 4.29: Effect of Conventional Regeneration cycles on the Regeneration efficiency of the spent activated carbons (a) MPAHS, (b) MPASG (c) CPASG, (d) CPAHS

4.9. Effect of different regeneration Conditions on the Adsorptive Capacity of Regenerated Activated Carbons

Different process factors that affect regeneration efficiency of the spent activated carbon were studied. The desorption-adsorption studies were done for one cycle with zero (0) corresponding to the adsorptive capacity of the fresh activated carbon. The process conditions studied were microwave power levels (18, 36, 81, 100%), irradiation time (5, 10, 15, 20mins), conventional time (10, 20, 30. 40, 50mins) and conventional temperature (200, 300, 400, 500, 600°C). These process conditions were studied with and without an oxidant. Oxidant that was used in this study is 30% H_2O_2. 30% H_2O_2 was selected in this work because it is cheap, effective, relatively harmless and highly stable oxidant (Darren, 2013).

Oxidants have oxidizing power to open the block pores and remove the surface functional groups of the spent activated carbons which may block the adsorption of colour (Sun et. al., 2009). The regenerated activated carbons were soaked in 30% H_2O_2 at room temperature for one hour after which they were centrifuged and washed before the next adsorption process.

4.9.1. Effect of Microwave Power Levels on the Adsorptive Capacity of Regenerated Activated Carbons

Microwave power level was considered a crucial variable in examining the impact of irradiation on activated carbons. To better understand this, the spent activated carbons were exposed to various microwave power levels at 18%, 36%, 81% and 100%. This microwave gives out maximum power of 900W. Therefore, 18%, 36%, 81% and 100% corresponded to 162W, 324W, 729W and 900W respectively. Other conditions were constant at 10mins irradiation time and 100mg/l of initial Swis blue dye used for saturation. Fig. 4.30 shows the plot of power levels (%) against adsorptive capacity of the regenerated activated carbons. It was observed that the adsorptive capacities of the regenerated activated carbons at different power levels were very close to the fresh adsorbents, though less than that, except 81% that had adsorptive capacity slightly more than the fresh adsorbents. It was evident from the results that increase in power levels enhanced the removal of adsorbed dye due to rapid increase in adsorbent bed temperature. At power level of 81%, it was observed that the adsorptive capacity of spent activated carbon was restored and slightly increased. The phenomenon might be attributed to the reorganization of internal structures as a consequence of the large amount of adsorbate molecule evolving during the microwave irradiation stage thereby activating the activated carbon more (Foo & Hameed, 2012f). The adsorptive capacities of the adsorbents regenerated without oxidant were less than those regenerated with oxidant. According to Foo and Hammed (2012f), gradual blockage of porous structure seemed to occur due to the fraction of adsorbed molecules which did not evolve from the carbon surface during regeneration. These molecules may remain inside the pore network of the activated carbons and give rise to carbonaceous residue (Ania et. al., 2005). This carbonaceous residue blocked the pores thereby decreasing the adsorptive capacities without oxidant. The oxidant tends to clear the pores of the regenerated activated carbon. This finding was in agreement of the work done by Ania et. al. (2007) on the effect of microwave assisted regeneration of activated carbons

loaded with pharmaceuticals. They found out that microwave irradiation causes no damage to the carbon but preserve the porous structure and increased the surface area. Equally, Foo and Hameed (2012f) reported that integration of microwave irradiation promoted the preservation of porosity and adsorption performance in a short heating period. It was observed that excessive power levels beyond 81% reduced the adsorptive capacity of adsorbents. This could be caused by some carbon ablation under a high level of radiation which might undermine the pore structures (Guocheng et. al., 2012). A sudden and intense bright sparks was observed at high power levels resulting in hot spots and red carbons. The whole activated carbons turned red within a few minutes and remained in that condition for the entire time interval. This possibly led to carbon attrition that reduced the surface area for adsorption. These results were in agreement with my previous studies on the use of microwave irradiation in producing activated carbons.

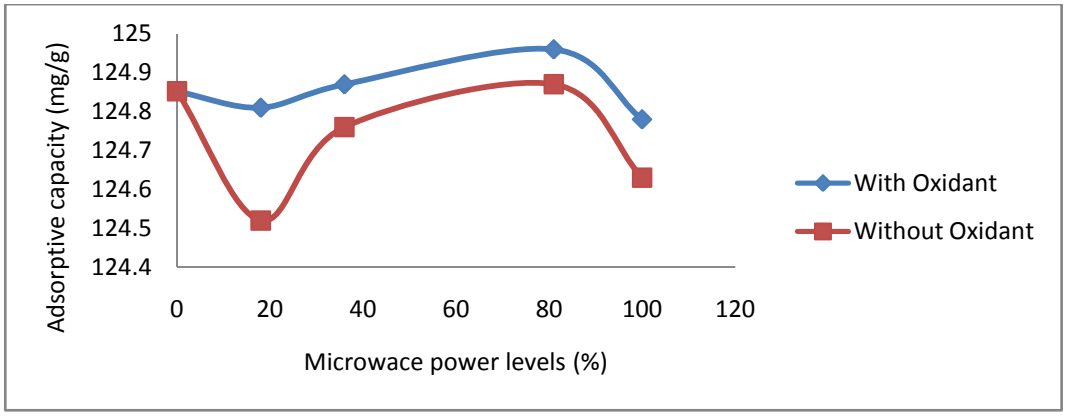

(a)

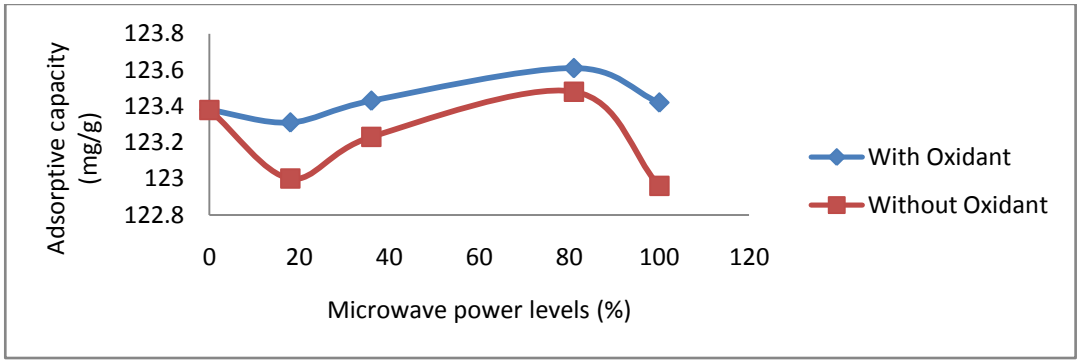

(b)

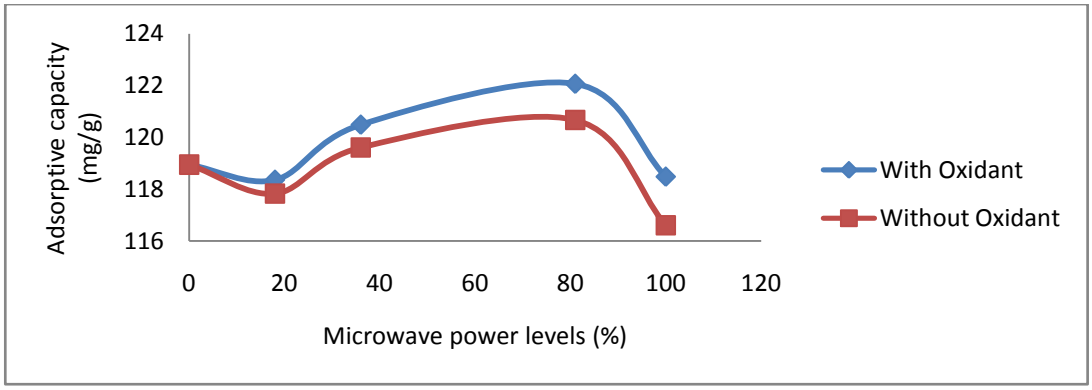

(c)

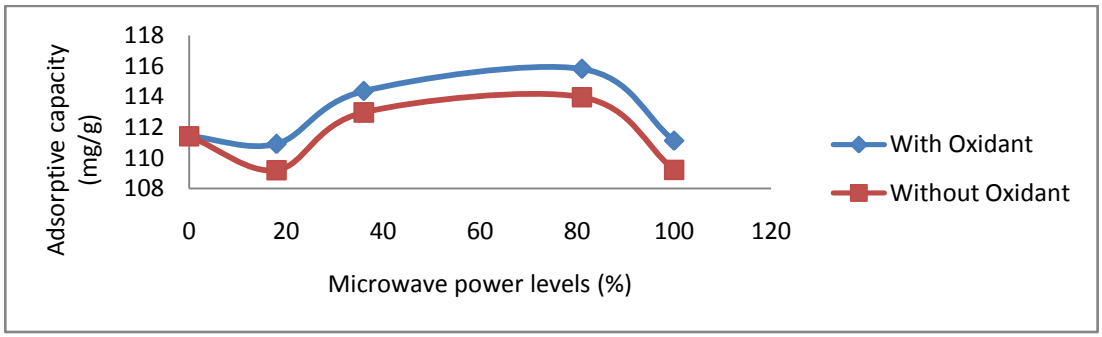

(d)

Fig.4.30: Effect of Microwave power levels on the adsorptive capacity of regenerated activated carbons (a) MPAHS, (b) MPASG (c) CPASG, (d) CPAHS

4.9.2. Effect of Microwave irradiation time on the adsorptive capacity of the regenerated activated carbons

Irradiation time was equally considered as an important factor that affects the regeneration efficiency of an adsorbent. The effect of irradiation time was studied at time intervals of 5mins, 10mins, 15mins and 20mins. The time 0 used showed the adsorptive capacity of the fresh adsorbent. The adsorptive capacity was evaluated for one regeneration cycle only. The irradiation time was studied at 81% power level and initial dye concentration of 100mg/l. Fig. 4.31 shows the graph of irradiation time versus adsorption capacity of the regenerated adsorbent for all the adsorbent samples. It was observed from the plots that adsorptive capacities of the adsorbent slightly decreased as irradiation time was increased to 10mins beyond which there was slight decrease again in adsorptive capacities. It was observed that the adsorptive capacity at 10mins was higher than that of the fresh adsorbent. This trend was observed on all the adsorbents regenerated with and without oxidant. The high adsorptive capacity recorded at higher time of 10mins implied that prolonged exposure time promoted an

acceleration of temperature which in turn increased the adsorbent bed temperature. The high temperature succeeded in breaking the bonds holding the adsorbate to the adsorbent and further reactivates the carbon. The drop observed beyond 10mins was probably due to sintering effect which largely destroyed the pore walls between adjacent pores. The high temperature can equally lead to collapse of carbon active sites which in turn reduces the adsorptive capacity.

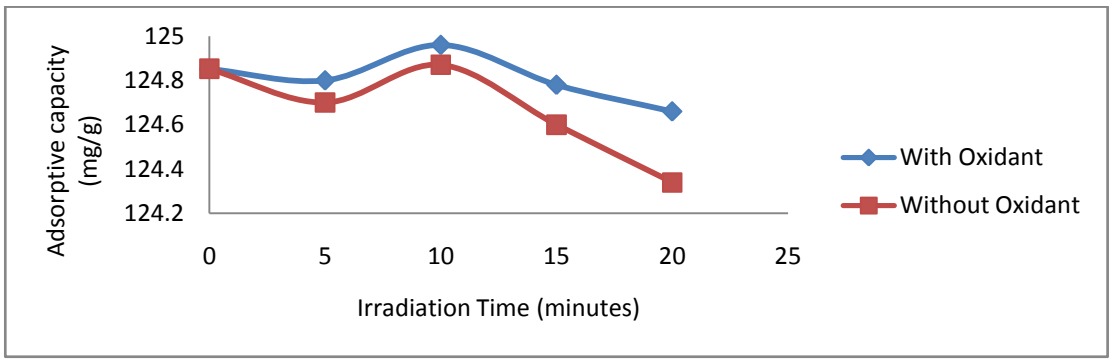

(a)

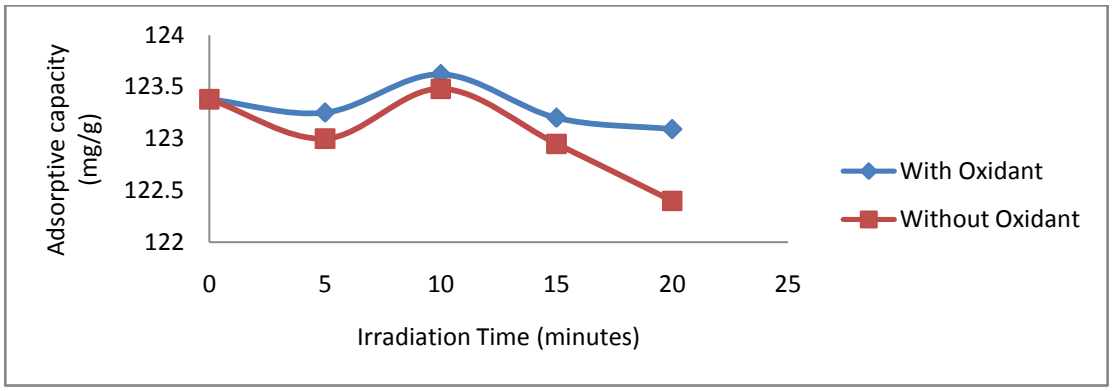

(b)

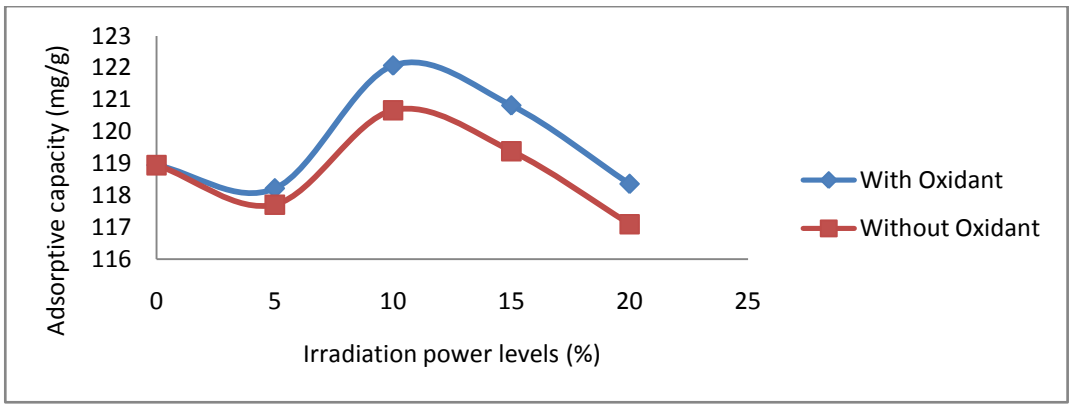

(c)

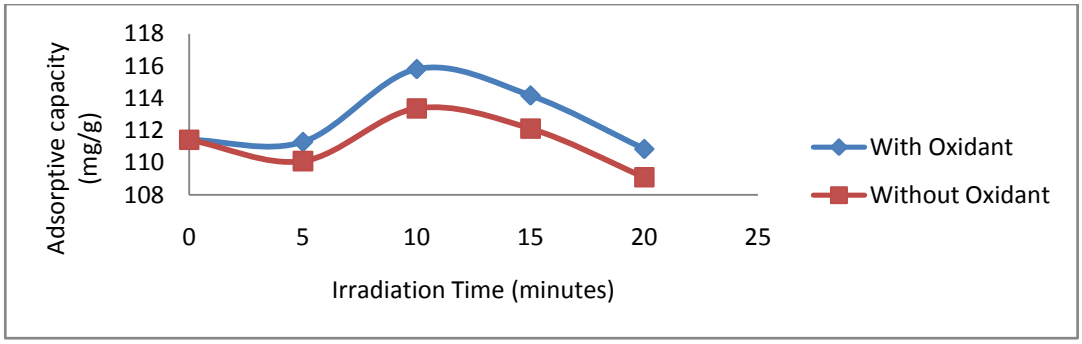

(d)

Fig.4.31: Effect of Microwave irradiation time on the adsorptive capacity of regenerated activated carbons (a) MPAHS (b) MPASG, (c) CPASG, (d) CPAHS

4.9.3. Effect of Conventional Regeneration Temperature on the Adsorptive Capacity of the Regenerated Activated carbons

The effect of conventional temperature was studied at contact time of 30mins and the activated carbons were saturated with initial Swiss blue dye concentration of 100mg/l. Time of 0 was used to represent the adsorptive capacity of the fresh adsorbent. It was observed from Fig. 4.32 that the adsorptive capacities of the regenerated activated carbons were lower than the fresh ones. It was equally observed that the adsorptive capacities increased with an increase in temperature from 200°C to 500°C. Beyond 500°C, there was decrease on the adsorptive capacities. The following steps are usually involved in the thermal regeneration of spent carbon (Vliet, 1991; Sufnarski, 1999);

a. Drying which eliminates the highly volatile adsorbates at temperatures up to about 200°C
b. Vaporization of the volatile adsorbates, and decomposition of the unstable adsorbates to form volatile fragments from about 200-500°C
c. Pyrolysis of the non-volatile adsorbates at about 500-700°C which results in the decomposition of carbonaceous residue on the surface of the activated carbon
d. Selective oxidation of the pyrolysed residue (at about 700°C and higher) by steam, carbon dioxide and any oxidizing agent.

Swiss blue dye adsorption was a physisorption process, thereby was easily desorbed at temperature between 200-500°C. As the temperature was increased, there was volatilization of the adsorbate to temperature of 500°C. Drop on adsorptive capacities recorded at higher temperature can be attributed to the blocking of the pores by decomposed carbonaceous residue at higher temperature. In conventional heating, the

heat source is located outside the carbon bed, and the bed is heated by conduction and convection. A temperature gradient is established from the surface to the core of material and the temperature of the carbons becomes lower than the furnace (Fernandez et. al., 2011). Primary volatile matter produced near the center of material needs to pass through the higher temperature region towards the external surface, this hotter zone is actually where secondary reactions occur. These secondary reactions results in decomposition of the volatiles and larger amount of amorphours carbon being deposited in the porous structure of activated carbon (Miura et. al., 2004). The drop can equally be attributed to carbon attrition and ablation at higher temperature since the regeneration was not done at completely inert environment.

The lower adsorptive capacities obtained for the regenerated activated carbons compared to the fresh activated carbons shows that conventional regeneration studied under the specified conditions cannot restore completely the adsorptive capacity of spent activated carbon. This was on agreement with works done by Magne and Walker (1986) and Ferro-Garcia et. al. (1993). They reported that thermal regeneration of activated carbon previously contaminated with phenol did not restore total adsorption capacity. Contrary to my findings, Vliet (1991) reported in his literature survey on regeneration of activated carbon that thermal regeneration effectively restores the activity of carbon loaded with organic adsorbates.

There was a sharp and distinct difference between the adsorptive capacities of the spent activated carbons regenerated with and without oxidant at lower temperature, but the differences were minimal at higher temperatures. At lower temperatures, the oxidant succeeded in removing any carbonaceous residue blocking the pores with resultant increase in adsorptive capacities. At higher temperatures, the oxidant was unable to remove appreciable amount of the decomposed residue because of the non oxidizing atmosphere used. Vliet (1991) reported that pyrolysis should not be conducted at higher temperatures in a non-oxidizing atmosphere since graphitization of the pyrolysed residue can occur resulting in a structure similar to that of activated carbon and equally refractive. Hence, during subsequent selective oxidation, it would be difficult to remove the residue without extensively damaging the structure of the activated carbon. Pyrolysed residues obtained at lower temperatures were reported to be more reactive, and therefore more readily oxidizable than activated carbon (Jones & Gwinn, 1983). This was the reason why adsorptive capacities of the regenerated

adsorbents were almost the same for regeneration with and without oxidants at higher temperature of 600°C.

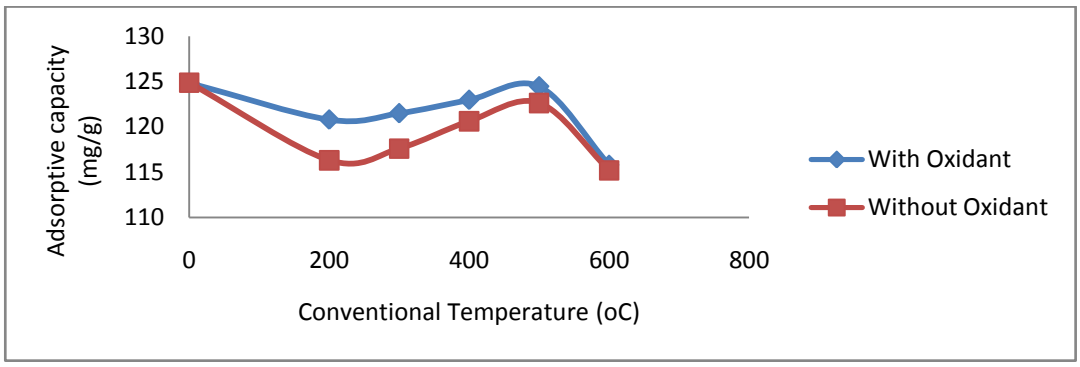

(a)

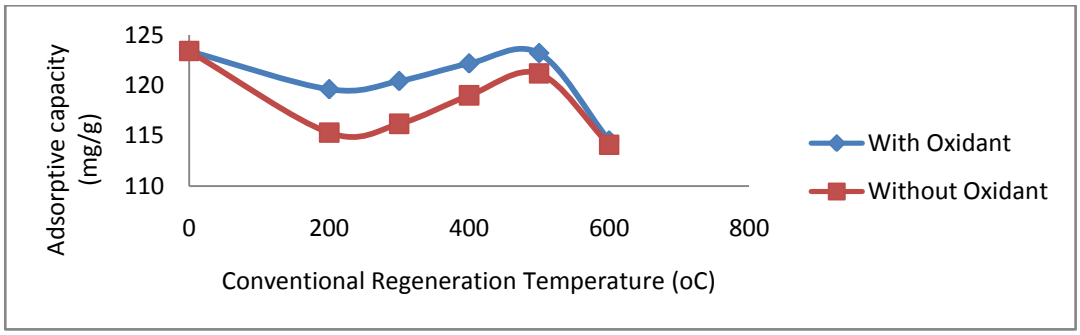

(b)

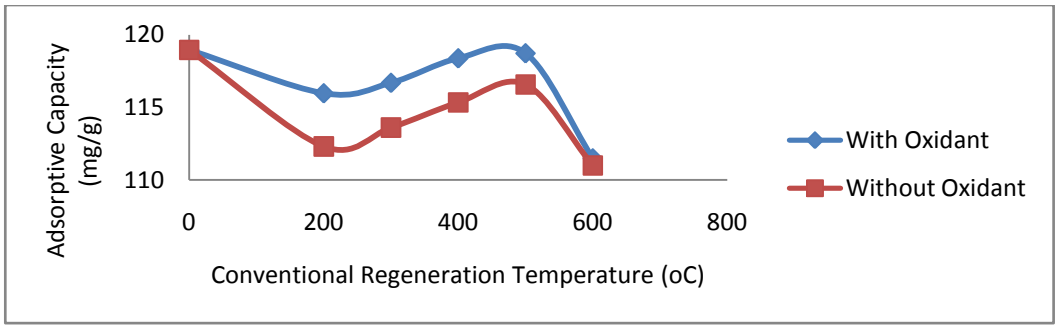

(c)

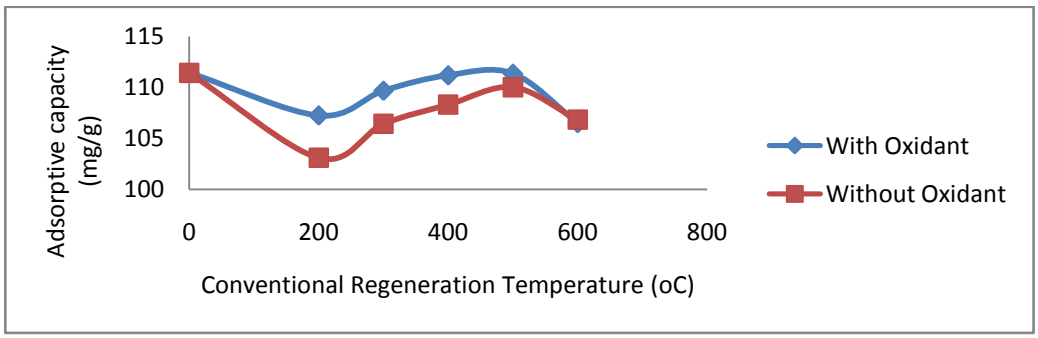

(d)

Fig.4.32: Effect of Conventional Regeneration temperature on the adsorptive capacity of regenerated activated carbons (a) MPAHS, (b) MPASG, (c) CPASG (d) CPAHS

4.9.4. Effect of Conventional Regeneration Time on the Adsorptive Capacity of Regenerated Activated Carbon

The effect of contact time was studied at interval of 10mins, 20mins, 30mins, 40mins and 50mins. This was achieved at temperature of 500°C. It was observed from Fig. 4.33 that the desorptive capacities of regenerated activated carbons were lower than the fresh adsorbents. This can be linked to the inefficient desorption using conventional method. It was equally observed that the adsorptive capacity increased with increase in time from 10mins to 30mins for all the activated carbons beyond which there was decrease in adsorptive capacity. During the residence time interval from 10 to 30mins, an almost stoichiometric conversion of the micropores to mesoporess took place, but the macro pores were largely unaffected (Vliet, 1991). The slight increase in adsorptive capacity during this period was probably due to erosion of the matrix between the micro pores. Meso pores are often expressed as a methylene blue number as it is assumed that large molecules such as methylene blue cannot penetrate the micro pores (Rouquerol et. al., 1994). Therefore, the erosion of micro pores walls to mesopores increased the chances of more Swiss blue dye to be adsorbed. After 30minutes, there was decrerase in adsorptive capacity. This can be attributed to the fact that at higher time intervals, further conversion of micro pores to larger pore types occurred, as well as progressive destruction of the activated carbon matrix to yield additional large pore sizes. The net result was an extensive loss of micropore volume, an increase in mesopore and macro pore volume and a concomitant decrease in mechanical strength (Vliet, 1991). The increase in macro pore volume resulted to decrease in adsorptive capacities as Swiss blue dye cannot be adsorbed on a macro pore. These findings were in accordance with the work done by Vliet and Venter (1985) on infrared thermal regeneration of spent activated carbon from water reclamation. They found out that the micropore volume decreased by 44% during the total 60minute residence time, and the mesopore and macropore volumes increased by 66 and 50% respectively. It was also observed that the regeneration done with oxidant had a higher adsorptive capacity than those ones done without oxidant. There were clear differences because the regeneration temperature was regulated at 500°C to avoid formation of carbonaceous residue that is more reactive and therefore more readily oxidizable than activated carbon (Jones & Gwinn, 1983).

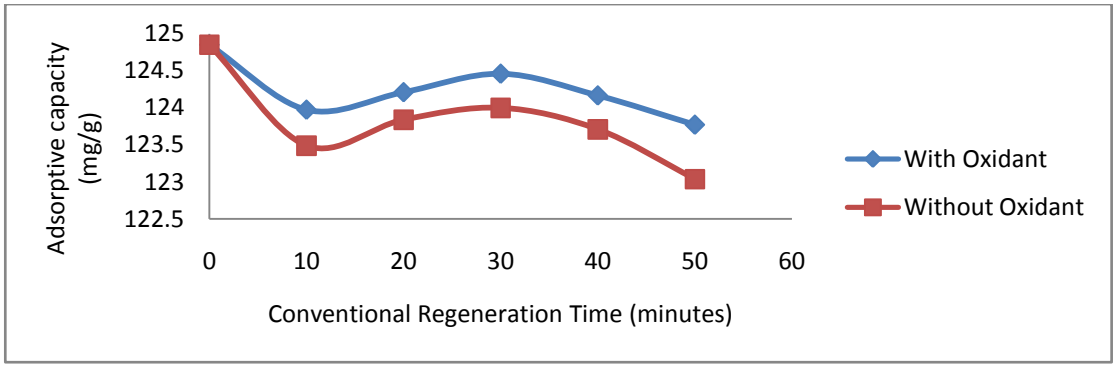

(a)

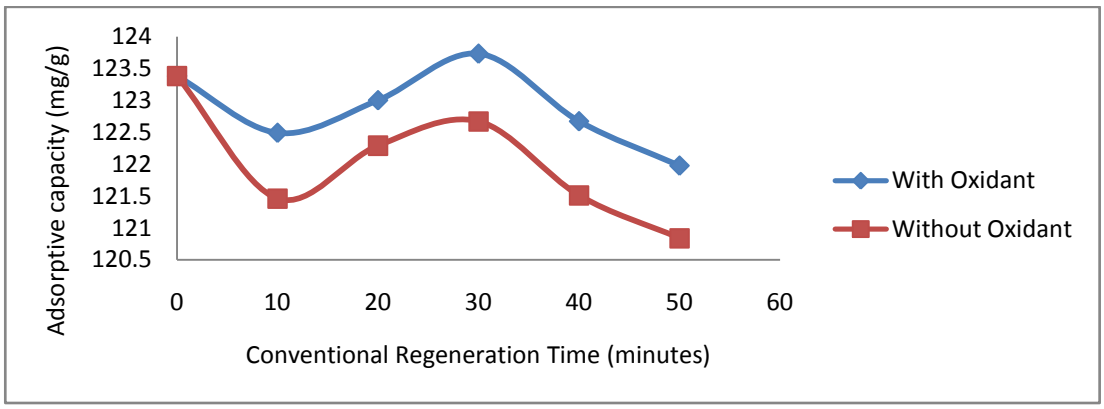

(b)

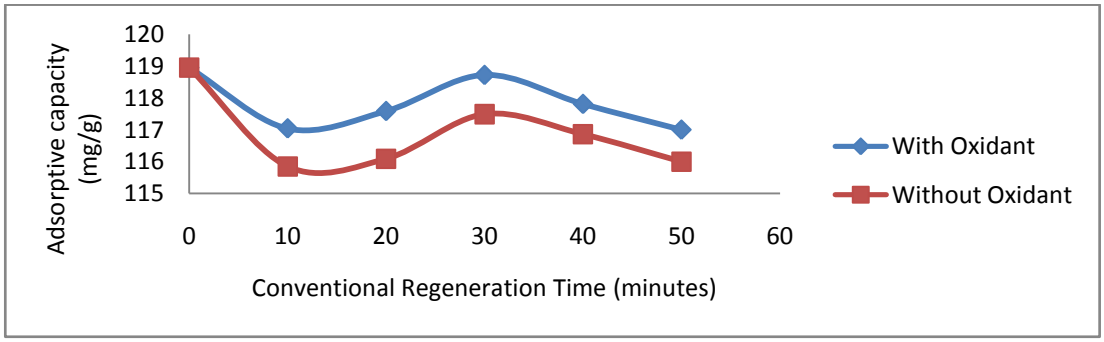

(c)

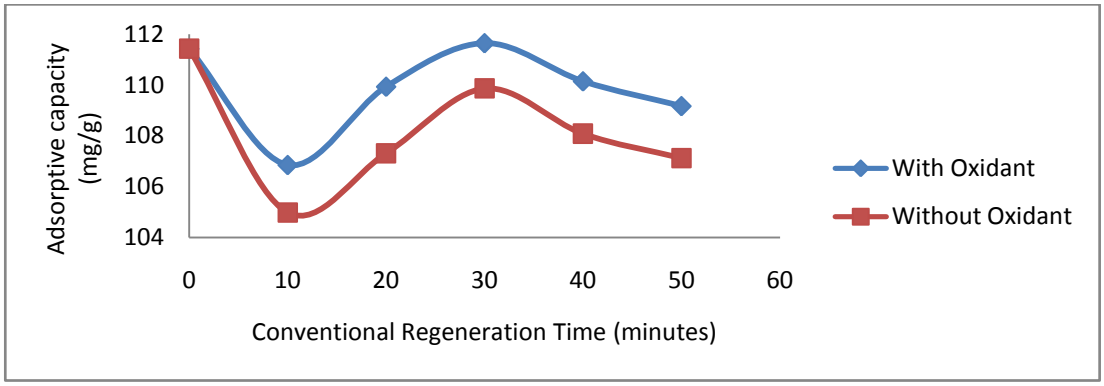

(d)

Fig.4.33: Effect of Conventional Regeneration time on the adsorptive capacity of regenerated activated carbons (a) MPAHS, (b) MPASG, (c) CPASG (d) CPAHS

4.10. Optimization of Microwave regeneration process using CCD

Microwave regeneration process was optrimized using central composite design (CCD). It involved three numeric factors which were power levels (%), radiation time (mins), initial dye concentration used for saturation (mg/l) and one categoric factor which is type of adsorbent. The categoric factor has four levels of microwave prepared activated carbon from hamburger seed shell (MPAHS), microwave prepared activated carbon from spent grain (MPASG), conventionally prepared activated carbon from hamburger seed shell (CPAHS), conventionally prepared activated carbon from spent grain (CPASG). The rgeneration study was done for only one cycle without an oxidant. The extent of the regeneration was evaluated by carrying out adsorption process with the regenerated carbon using 50mg/l of Swiss blue dye solution. The adsorptive capacity after regeneration was calculated as the response.

4.10.1. Analysis of variance for Microwave regeneration process

The analysis of variance for microwave regeneration process is shown on Table 4.47. The Model F-value of 100.74 implied the model was significant. There was only a 0.01% chance that a "Model F-Value" this large could occur due to noise. Values of "Prob > F" less than 0.0500 indicated model terms were significant. In this case power level (A), initial dye concentration used for saturation (B), radiation time (C), type of adsorbent (D), interaction of power level and radiation time (AC), quadratic effect of power level (A^2), quadratic effect of initial dye concentration (B^2), and quadratic effect of radiation time (C^2) were significant model terms. The "Lack of Fit F-value" of 0.59 implied the Lack of Fit wass not significant relative to the pure error. There was a 93.17% chance that a "Lack of Fit F-value" this large could occur due to noise.

The "Pred R-Squared" of 0.9139 was in reasonable agreement with the "Adj R-Squared" of 0.9266. "Adeq Precision" measures the signal to noise ratio. A ratio of 43.065 indicated an adequate signal.

Table 4.47: ANOVA table for the Microwave regeneration process

Source	Sum of Squares	df	Mean Square	F Value	p-value Prob>F
Model	7041.39	10	704.14	100.74	<0.0001
A-Power level	1122.45	1	1122.45	160.58	<0.0001
B-Initial dye Con.	235.82	1	235.82	33.74	<0.0001
C-Radiation time	2152.12	1	2152.12	307.89	<0.0001
D-Type of adsorbent	1602.92	3	534.31	76.44	<0.0001
AC	59.38	1	59.38	8.50	0.0048
A^2	740.12	1	740.12	105.88	<0.0001
B^2	96.44	1	96.44	13.80	0.0004
C^2	989.51	1	989.51	141.56	<0.0001
Residual	482.30	69	6.99		
Lack of fit	285.29	49	5.82	0.59	0.9317
Pure Error	197.01	20	9.85		
Cor Total	7523.69	79			

4.10.2. Model equation for microwave regeneration process

The model equations was represented both in coded and actual form. Because the categoric factor has four levels, the coded equation (4.55) was split into four equations (4.56-4.59) each representing each level. The last equation, which involved no level with its interactions was used as the reference level. It represented the level with least effect on the response

The model equation in coded form is shown as follows;

$$\text{Adsorptive capacity(mg/g)}=+51.62+4.19A-1.92B+5.80C+5.31\,D[1]+3.51D[2]-3.81D[3]-1.36AC-2.71A^2+0.98\,B^2-3.14C^2 \quad (4.55)$$

The coded equation can be split into four equations as follows;

Adsorptive capacity(mg/g)=+51.62+4.19A-1.92B+5.80C+5.31 D[1]-1.36AC-2.71A^2+0.98 B^2-3.14C^2 (4.56)

Adsorptive capacity(mg/g)=+51.62+4.19A-1.92B+5.80C+3.51D[2] -1.36AC-2.71A^2+0.98 B^2-3.14C^2 (4.57)

Adsorptive capacity(mg/g)=+51.62+4.19A-1.92B+5.80C-3.81D[3]-1.36AC-2.71A^2+0.98 B^2-3.14C^2 (4.58)

Adsorptive capacity(mg/g)=+51.62+4.19A-1.92B+5.80C-1.36AC-2.71A^2+0.98 B^2-3.14C^2 (4.59)

Final equation in terms of actual factors:

Microwave prepared activated carbon from hamburgar seed shell (MPAHS);

Adsorptive capacity(mg/g) = -295.86147+1.35798 Power level (%) - 0.15590 Initial dye conc.(mg/l) + 65.80142Radiation time (mins) - 0.060545 Power level (%) Radiation time (mins) - 5.35855E-003Power level $(\%)^2$ + 3.91705E-004 Initial dye conc.$(mg/l)^2$ - 3.13671 Radiation time $(mins)^2$ (4.60)

Microwave prepared activated carbon from spent grain (MPASG);

Adsorptive capacity(mg/g)=-297.65799 +1.35798 Power level (%)-0.15590 Initial dye conc.(mg/l)+65.8014 Radiation time (mins)-0.060545Power level (%)Radiation time (mins)-5.35855E-003Power level $(\%)^2$+3.91705E-004 Initial dye conc.$(mg/l)^2$-3.13671Radiation time $(mins)^2$ (4.61)

Conventionally prepared activated carbon from spent grain (CPASG);

Adsorptive capacity(mg/g) = -304.98213+1.35798Power level (%) -0.15590 Initial dye conc.(mg/l)+65.80142Radiation time (mins) - 0.060545Power level (%) Radiation time (mins) - 5.35855E-003Power level $(\%)^2$ +3.91705E-004 Initial dye conc.$(mg/l)^2$ - 3.13671Radiation time $(mins)^2$ (4.62)

Conventionally prepared activated carbon from hamburgar seed shell (CPAHS);

Adsorptive capacity(mg/g) = -306.17987 +1.35798Power level (%) -0.15590 Initial dye conc.(mg/l) +65.80142 Radiation time (mins) -0.060545 Power level (%) Radiation time (mins) -5.35855E-003 Power level $(\%)^2$ +3.91705E-004

Initial dye conc.(mg/l)^2 -3.13671Radiation time (mins)^2 (4.63)

4.10.3. 3D surface plot for microwave regeneration process

From the analysis of variance table, it was seen that the intearction effects of power levels and radiation time was significant. Figure 4.34 shows the 3D plot for the interaction effect. It can be seen from the plot that increase on power level and radiation time increased the adsorptive capacity of the regenerated carbon to a point that further increase on both factors decreased the adsorptive capacity. The same trend was observed for all the activated carbons though of different magnitude. The increase on both factors increased the adsorbent bed temperature which in turn increased rate of devolatilization. This consequently led to reorganization of carbon structure, reopening of blocked pores and creation of new pores. The decrease recorded at higher process factors can be attributed to sintering effect as a result of high temperature. This led to collapse of carbon frames and destruction of some pores.

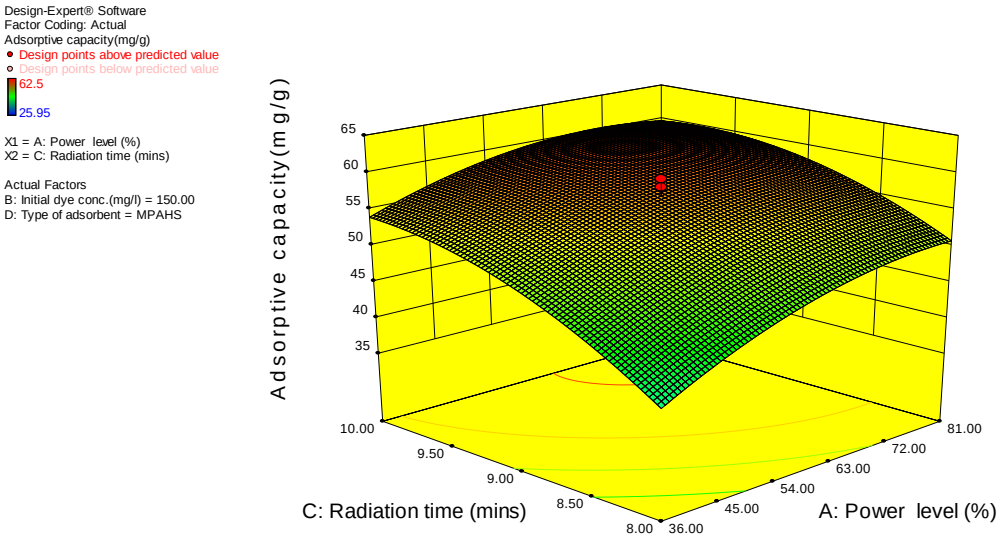

(a)

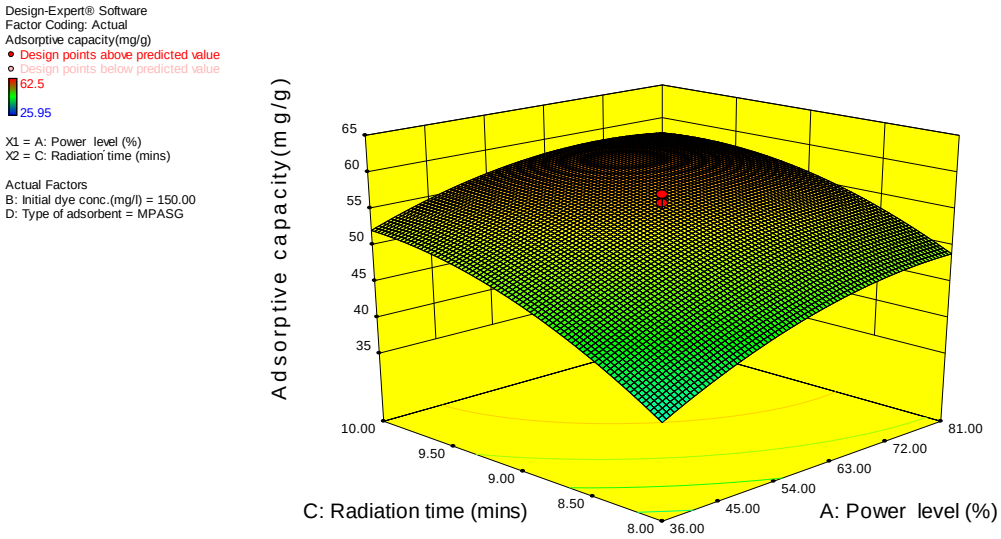
Design-Expert® Software
Factor Coding: Actual
Adsorptive capacity(mg/g)
Design points above predicted value
Design points below predicted value
62.5
25.95
X1 = A: Power level (%)
X2 = C: Radiation time (mins)
Actual Factors
B: Initial dye conc.(mg/l) = 150.00
D: Type of adsorbent = MPASG
Adsorptive capacity(mg/g)
65
60
55
50
45
40
35
10.00
9.50
9.00
8.50
8.00
C: Radiation time (mins)
36.00
45.00
54.00
63.00
72.00
81.00
A: Power level (%)

(b)

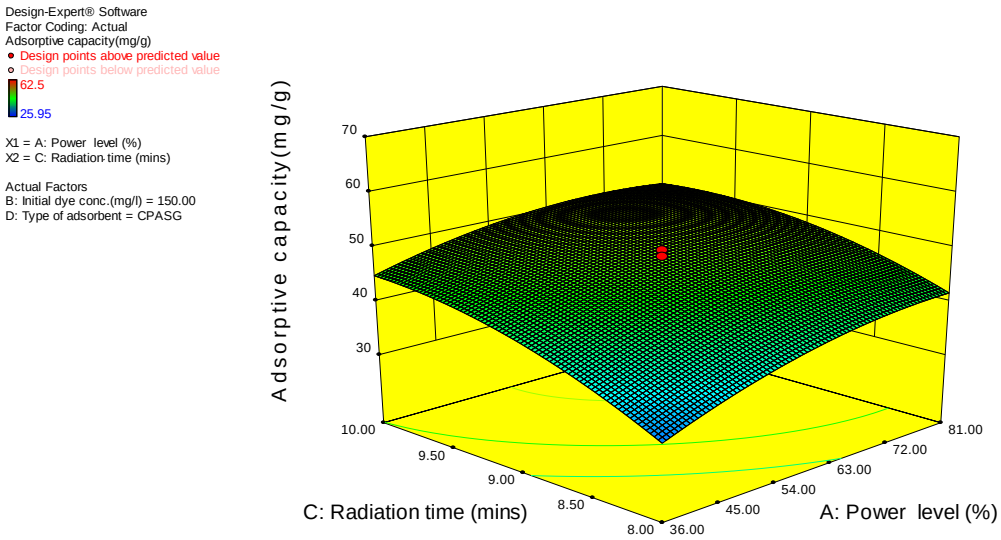
Design-Expert® Software
Factor Coding: Actual
Adsorptive capacity(mg/g)
Design points above predicted value
Design points below predicted value
62.5
25.95
X1 = A: Power level (%)
X2 = C: Radiation time (mins)
Actual Factors
B: Initial dye conc.(mg/l) = 150.00
D: Type of adsorbent = CPASG
Adsorptive capacity(mg/g)
70
60
50
40
30
10.00
9.50
9.00
8.50
8.00
C: Radiation time (mins)
36.00
45.00
54.00
63.00
72.00
81.00
A: Power level (%)

(c)

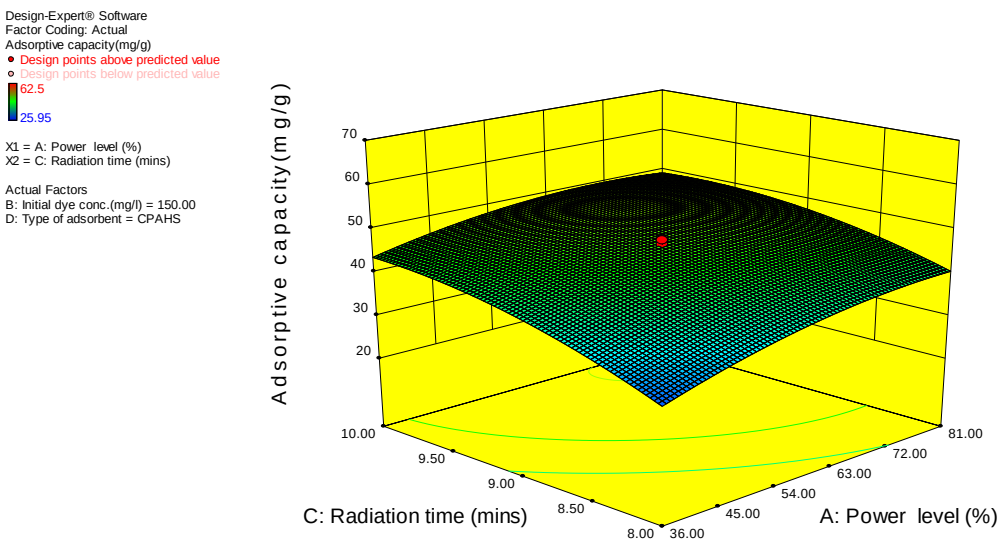

(d)

Figure 4.34: 3D surface plots for the interaction effect of power level and radiation time (a) MPAHS, (b) MPASG, (c) CPASG, (d) CPAHS

4.10.4. Optimal conditions for microwave regeneration process

Numerical optimization was used to obtain the optimum conditions for the regeneration process. The aim is to maximize the adsorptive capacity of the regenerated carbon. Table 4.48 shows the optimim conditions for the regeneration process, while table 4.49 shows the validation of the optimum conditions. It can be seen from table 4.49 that the deviations between the predicted values and experimental values were less as evidenced by the low errors recorded. This actually showed that the generated model equations can predict the adsorptive capacity of the regenerated carbon very well.

Table 4.48: Optimal conditions for Microwave regeneration process

Power levels (%)	Initial dye conc. (mg/l)	Radiation time (mins)	Adsorbent Types	Predicted Values (mg/g)
81.0	100.00	10.0	MPAHS	62.6067
81.0	100.00	9.51	MPASG	60.9577
81.0	100.00	9.51	CPASG	53.6336
81.0	100.00	9.51	CPAHS	52.4359

Table. 4.49: Model validation for microwave regeneration process

Power levels (%)	Initial dye conc. (mg/l)	Radia. time (mins)	Adsorbent types	Adsorptive capacity (mg/g)		Error (%)
				Experimental values	Predicted values	
81.0	100.0	10.0	MPAHS	62.66937	62.6067	0.1
81.0	100.0	9.51	MPASG	60.9638	60.9577	0.01
81.0	100.0	9.51	CPASG	53.6551	53.6336	0.04
81.0	100.0	9.51	CPAHS	52.4516	52.4359	0.03

4.11. Optimization of Conventional regeneration process using CCD

Conventional regeneration process was optrimized using central composite design (CCD). It involved three numeric factors which were temperature (^{o}C), time (mins), initial dye concentration used for saturation (mg/l) and one categoric factor which is type of adsorbent. The categoric factor has four levels of microwave prepared activated carbon from hamburger seed shell (MPAHS), microwave prepared activated carbon from spent grain (MPASG), conventionally prepared activated carbon from hamburger seed shell (CPAHS), conventionally prepared activated carbon from spent grain (CPASG). The rgeneration study was done for only one cycle without an oxidant. The extent of the regeneration was evaluated by carrying out adsorption process with the regenerated carbon using 50mg/l of Swiss blue dye solution. The adsorptive capacity after regeneration was calculated as the response.

4.11.1. Analysis of variance for conventional regeneration process

Analysis of variance table for conventional regeneration process is shown on table 4.50. The Model F-value of 52.17 implied the model was significant. There was only a 0.01% chance that a "Model F-Value" this large could occur due to noise. Values of "Prob > F" less than 0.0500 indicated model terms were significant. In this case conventional temperature (A), initial dye concentration used for saturation (B), conventional tiem (C), type of adsorbent (D), quadratic effect of temperature (A^2), quadratic effect of initial dye concentration (B^2), quadratic effect of time (C^2) were significant model terms. Values greater than 0.1000 indicated the model terms were not significant.

The "Lack of Fit F-value" of 0.45 implied the Lack of Fit was not significant relative to the pure error. There was a 98.78% chance that a "Lack of Fit F-value" this large could occur due to noise. The "Pred R-Squared" of 0.8297 was in reasonable agreement with the "Adj R-Squared" of 0.8536. "Adeq Precision" measured the signal to noise ratio. A ratio of 34.131 indicated an adequate signal.

Table 4.50: ANOVA table for the Conventional regeneration process

Source	Sum of Squares	df	Mean Square	F Value	p-value Prob>F
Model	2274.9	9	252.77	52.17	<0.0001
A-Temp.	334.66	1	334.66	69.07	<0.0001
B-Initial Con.	124.42	1	124.42	25.68	<0.0001
C- time	757.99	1	757.99	156.45	<0.0001
D-Type of adsorbent	383.05	3	127.68	26.35	<0.0001
A^2	170.66	1	170.66	35.22	<0.0001
B^2	90.24	1	90.24	18.64	<0.0001
C^2	342.31	1	342.31	70.65	<0.0001
Residual	339.15	70	4.85		
Lack of fit	180.18	50	3.60	0.45	0.9878
Pure Error	158.97	20	7.95		
Cor Total	2614.05	79			

4.11.2. **Model equation for conventional regeneration process**

The model equations was represented both in coded and actual form. Because the categoric factor has four levels, the coded equation (4.64) was split into four equations (4.65-4.68) each representing each level. The last equation, which involved no level with its interactions was used as the reference level. It represented the level with least effect on the response

The model equation in coded form is shown as follows;

$$\text{Adsorptive capacity (mg/g)} = +50.69+2.29A-1.39B+3.44C+3.08D[1]+0.92D[2]-1.36D[3]-1.30A^2+0.95B^2-1.84C^2 \quad (4.64)$$

Coded equation was split into four equations as follows;

Adsorptive capacity (mg/g)= +50.69+2.29A-1.39 B+3.44C+3.08 D[1]-1.30A^2 +0.95B^2-1.84 C^2 (4.65)

Adsorptive capacity (mg/g)= +50.69+2.29A-1.39 B+3.44C+ D[2]-1.30A^2+0.95B^2-1.84 C^2 (4.66)

Adsorptive capacity (mg/g)= +50.69+2.29A-1.39 B+3.44C-1.36D[3]-1.30A^2 +0.95B^2-1.84 C^2 (4.67)

Adsorptive capacity (mg/g)= +50.69+2.29A-1.39 B+3.44C-1.30A^2+0.95B^2 -1.84 C^2 (4.68)

Model equations in actual form;

Microwave prepared activated carbon from hamburgar seed shell (MPAHS);

Adsorptive capacity (mg/g) =+15.5476 +0.14011 Conventional temperature(oC) -0.14156 Initial dye conc. (mg/l)+1.08211 Conventional time (mins) – 1.30266E-004 Conventional temperature(oC)^2 +3.78906E-004 Initial dye conc. (mg/l)^2-0.018449 Conventional time(mins)^2 (4.69)

Microwave prepared activated carbon from spent grain (MPASG);

Adsorptive capacity (mg/g)= +13.38676+0.14011 Conventional temperature(oC)-0.14156 Initial dye conc. (mg/l)+1.08211Conventional time (mins)-1.30266E-004 Conventionaltemperature(oC)^2+3.78906E-004 Initial dye conc. (mg/l)^2 -0.018449 Conventional time(mins)^2 (4.70)

Conventionally prepared activated carbon from spent grain (CPASG);

Adsorptive capacity (mg/g) =+11.10941+0.14011Conventional temperature(oC) -0.14156 Initial dye conc. (mg/l)+1.08211 Conventional time (mins)-1.30266E-004 Conventionaltemperature(oC)^2+3.78906E-004 Initial dye conc. (mg/l)^2-0.018449 Conventional time (mins)^2 (4.71)

Conventionally prepared activated carbon from hamburgar seed shell (CPAHS);

Adsorptive capacity(mg/g)=+9.82635+0.14011 Conventional temperature(oC) -0.14156Initial dye conc. (mg/l)+1.08211 Conventional time (mins)-1.30266E-004 Conventional temperature(oC)^2+3.78906E-004 Initial dye conc. (mg/l)^2-0.018449 Conventional time (mins)^2 (4.72)

4.11.3. Optimal conditions for conventional regeneration process

Numerical optimization was used to obtain the optimum conditions for the regeneration process. The aim is to maximize the adsorptive capacity of the regenerated carbon. Table 4.51 shows the optimim conditions for the regeneration process, while table 4.52 shows the validation of the optimum conditions. It can be seen from table 4.52 that the deviations between the predicted values and experimental values were small as evidenced by the low errors recorded. This actually showed that the generated model equations can predict the adsorptive capacity of the regenerated carbon very well.

Table 4.51: Optimal conditions for conventional regeneration process

Time (^oC)	Initial dye conc. (mg/l)	Time (mins)	Adsorbent Types	Predicted Values (mg/g)
537.75	100.00	29.33	MPAHS	58.7209
537.76	100.00	29.34	MPASG	56.56
537.76	100.00	29.34	CPASG	54.2827
537.76	100.00	29.34	CPAHS	52.9996

Table. 4.52: Model validation for conventional regeneration process

Temp (^oC)	Initial dye conc. (mg/l)	Time (mins)	Adsorbent types	Adsorptive capacity (mg/g)		Error (%)
				Experimental values	Predicted values	
537.75	100.0	29.33	MPAHS	58.7503	58.7209	0.05
537.76	100.0	29.34	MPASG	56.5883	56.56	0.05
537.76	100.0	29.34	CPASG	54.2881	54.2827	0.01
537.76	100.0	29.34	CPAHS	53.0155	52.9996	0.03

4.12. Comparisons of the three methods of regeneration

The effectiveness of the three methods of regeneration used in this study was compared at the best operating conditions established for each method. The comparison was based on regeneration efficiency (%), carbon loss (%) and carbon yield (%). The objective of the regeneration of spent activated carbons was to desorb accumulated adsorbates and restore the original porous structure with little or no damage to the

carbon itself. The carbon yield is defined as the weight of regenerated activated carbon per weight of Swiss blue dye loaded activated carbon utilized for regeneration. The carbon loss (%) was evaluated by deducting the final weight of the regenerated sample from the initial weight of the carbon used for saturation assuming complete desorption. The activated carbons were saturated with 100mg/l of the dye solution for 24 hours. The regenerated sample was soaked in an oxidant for one hour after which they were centrifuged, washed and dried. The adsorption – regeneration cycle was done for six cycles. After adsorption at the sixth cycle; the carbons were regenerated again using different methods. The regenerated carbons were weighed to evaluate the carbon yield and carbon loss. The weight of carbon used for saturated was constant at 15.0g while the weight of the carbon loaded with Swiss blue dye varied with different activated carbons used but remained constant for each regeneration methods. The saturated samples were divided into three, each part for each type of regeneration method.

Fig. 4.35 shows the comparative values of the three methods of regeneration used.

Comparatively, the regeneration efficiencies of microwave regenerated carbons were highest, followed by conventional regeneration and finally chemical regeneration. It was observed that regeneration efficiencies of the microwave regenerated carbons were higher than 97% after seventh cycle. This shows that microwave regeneration had proved itself as the best method that can preserve the adsorptive capacity of the spent activated carbon. The textural properties of the microwave regenerated carbons, with the shorter irradiation period compared with conventional heating were better preserved (Foo & Hameed 2012). Foo and Hameed (2012a) compared the key parameters of the regenerated carbons after five regeneration cycle. They observed that the BET surface area, micropore volume and micropore surface area of the microwave treated samples were decreased, while the mesopore volume and external surface area, which is more accessible for the adsorbate molecules, do not differ noticeably from the parent carbons (Foo & Hameed 2012b, c). The decomposition of the adsorbed adsorbates inside the carbon matrix was not favoured under microwave heating, which contributed to the preservation of the porous structure (Ania et. al., 2005). In conventional heating, the heat source is located outside the carbon bed, and the bed is heated by conduction and convention. A temperature gradient is established until steady state conditions are reached. As a result, the desorbed adsorbates have to transverse through a high temperature region before they can migrate to the surface. This causes decomposition of the desorbed molecules, formation of coke deposits and

physical rupture of the carbon pore walls leading to a greater decrease in the apparent surface areas and micropore volumes (Matsumoto et. al., 2011). Conversely, the tremendous thermal gradient of internal and volumetric heating of microwave heating system allow microwave - induced regeneration to occur more effectively at lower bulk temperature and shorter processing time (Foo & Hameed, 2009).

It is noteworthy that considerable changes in the surface properties were achieved within a short time, which facilitate desorption of adsorbate retained on the carbon surface.

Chemical regeneration recorded lowest regeneration because the regeneration efficiency depended on the solubility of the sorbed substance and the type of bond involved in the reaction. The regeneration efficiencies were low because desorption was done at lower temperature. The carbon yield for chemical regeneration was the highest and no carbon loss was observed compared to other methods. This can be attributed to the weight of undesorbed adsorbate on the pores of the carbon as a result of incomplete desorption. No carbon loss was recorded because the mass of carbon yield were more than the mass of the activated carbon used for saturation. Assuming complete desorption, microwave regeneration had high carbon yield compared to conventional regeneration. This showed that conventional regeneration resulted in loss of carbon as evidenced in the result of carbon loss. The high carbon loss observed for conventional regeneration can be attributed to attrition and oxidation of carbon surface (Robers et. al., 2005). According to Vliet (1991) at high conventional temperature, there is invariably some oxidation and the excessive oxidation of selected carbons. Foo and Hameed (2012a) reported that thermal regeneration is expensive in terms of energy consumption, time consuming and suffers from 5 to 15% carbon loss due to oxidation and attrition. Mguel et. al., (2001) reported that conventional regeneration results to considerable amount of carbon (5 – 15%) is usually lost by attrition, burn-off and washout. Sufnarski (1999) reported a 5 – 10% loss of carbon due to surface oxidation. Dehdashti et. al. (2010) reported 4.2% carbon loss after 10 successive adsorption and regeneration cycles under microwave irradiation at 900W for period of 10 minutes. In this study, the carbon losses recorded using microwave regeneration were less than 3.0%. The result was as a result of microwave power of 719W used in this study for ten minutes.

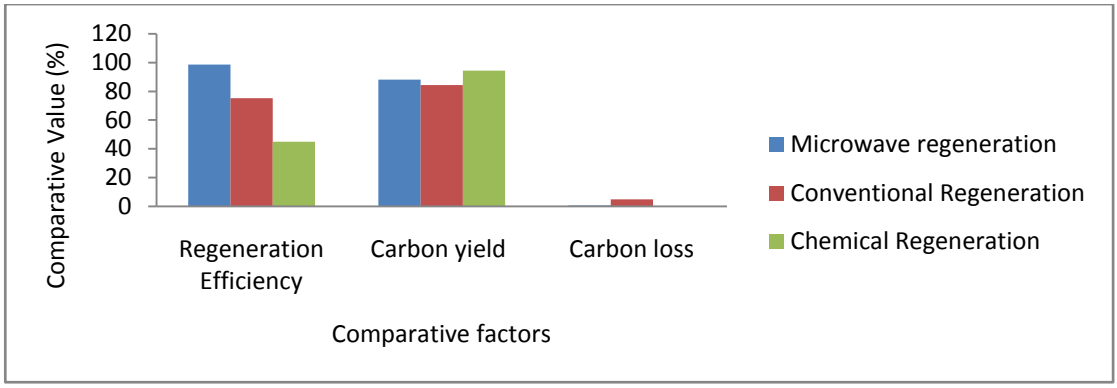

(a)

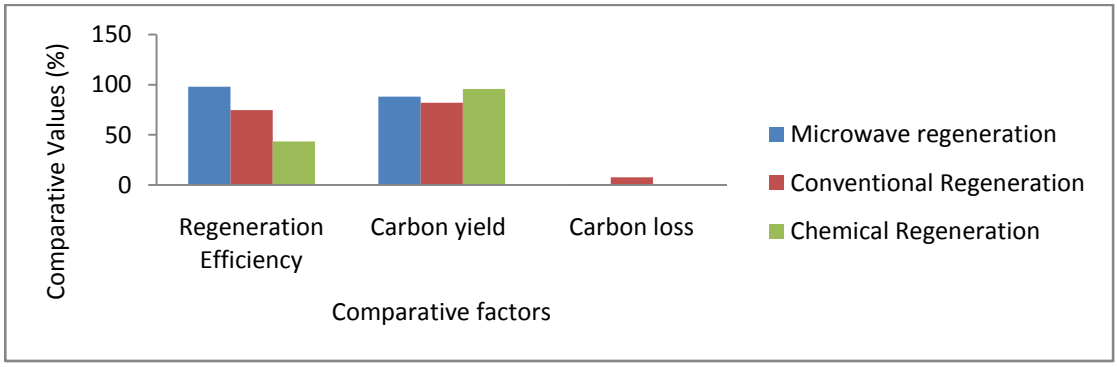

(b)

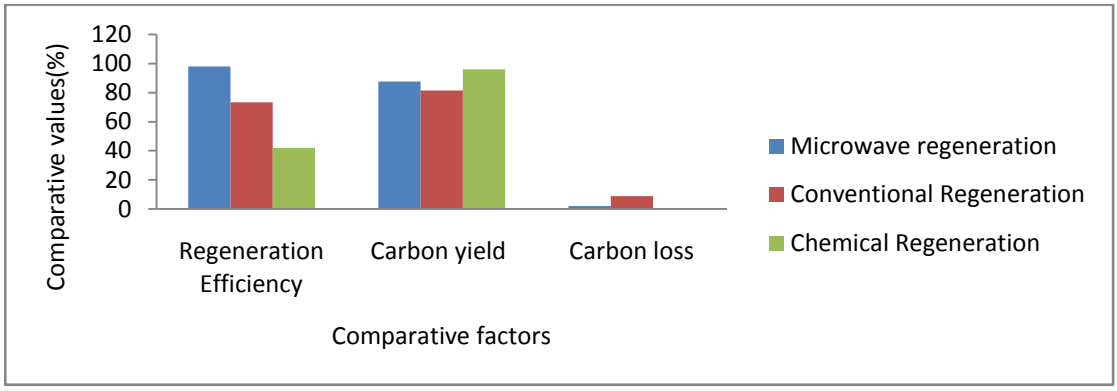

(c)

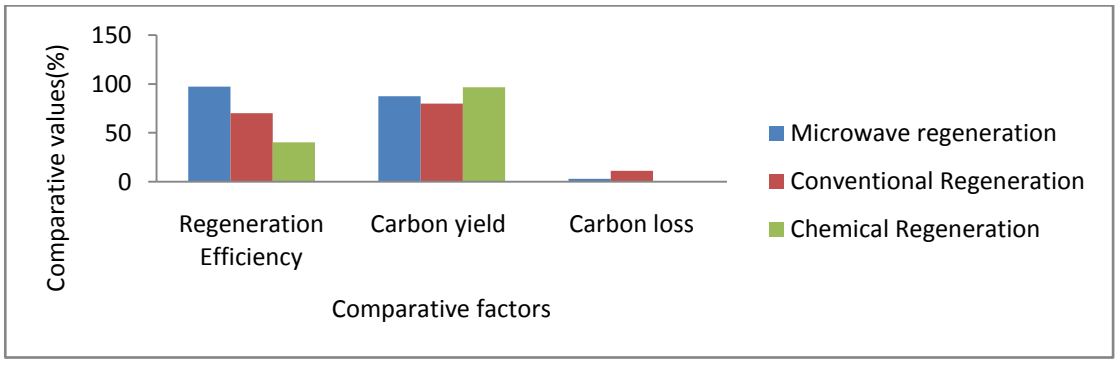

(d)

Fig. 4.35: Comparative values of the three methods of regeneration used (a) MPAHS, (b) MPASG, (c) CPASG, (d) CPAHS

CHAPTER FIVE
CONCLUSION AND RECOMMENDATIONS

5.1. Conclusion

This study has demonstrated the effectiveness of conventional and microwave activation for production of activated carbon from hamburger seed shell and brewers' spent grain and the regeneration of spent activated carbons using chemical regeneration, microwave regeneration and conventional regeneration.

The conclusions drawn from the results of this study are listed as follows:

1. Microwave and conventional methods can effectively be used to prepare activated carbons and for the adsorption of Swiss blue dye using the prepared activated carbons, microwave prepared activated carbon from hamburger seed shell (MPAHS) gave the best result of 99.71% Swiss blue dye removal efficiency followed by microwave prepared activated carbon from spent grain (MPASG) that had 99.51%, conventional prepared activated carbon from spent grain (CPASG) had 99.02%, and lastly conventional prepared activated carbon from hamburger seed shell (CPAHS) that had 97.79%.
2. For adsorption process, Pseudo second order fitted the kinetic data, Freundlich model fitted the isotherm data, while the thermodynamic parameters indicated the process as exothermic, feasible and spontaneous in nature.
3. For desorption process, Pseudo second order fitted the kinetic data, Freundlich model fitted the isotherm data, while the thermodynamic parameters indicated the process as endothermic, feasible and spontaneous in nature.
4. Reuse study showed that the use of 30% H_2O_2 as an oxidant increased the adsorptive capacity of the regenerated carbons.
5. Comparative studies done on all the three methods showed that microwave regeneration recorded highest regeneration efficiency of 98.71% followed by conventional regeneration that had 75.31% and lastly chemical regeneration that had 45.08%. Chemical regeneration recorded no loss on carbon while loss on carbon for microwave regeneration was lower (0.038% - 0.144%) than conventional regeneration samples (0.25% - 0.554%). Chemical regeneration had highest carbon yield between 5.306% - 5.385%, followed by microwave regeneration (4.856% - 4.962%) and lastly, conventional regeneration (4.446% - 4.75%).

5.2. Recommendations

Consequent upon the findings, the following recommendations are made;

1. Conventional and microwave activation should be used in regenerating spent activated carbons.
2. Chemical regeneration of activated carbons is achievable and can be used in solving environmental problems.
3. Microwave power level should be quantified in degrees as against the conventional percentage system while modifying the microwave for proper comparism with thermal system.
4. Regeneration of adsorbents contaminated with multiple adsorbates is recommended since most industrial waste water contains heterogenous mixtures of organic compounds.
5. Improvement in the modification of microwave is recommended so as to reduce devitrification of the glassware reactor.
6. CO_2 and steam should be used as oxidants at higher temperature to reduce carbon loss during regeneration.

5.3. Contribution to Knowledge

This work has added information on the the microwave activation of spent grain and Hamburger seed shell. It has also considered the effect of oxidants on the microwave and conventional methods of regeneration.

i. This work has established optimal conditions for conventional activation (857°C, 83.62mins and 4.77M KOH) and microwave activation (81%, 5M KOH, and 7mins) of hamburger seed shell and spent grain, adsorption of Swiss blue dye from aqueous solution (pH of 8, 30°C, and 50mg/l), microwave (81%, 100mg/l and 10mins) and conventional regeneration (537.75^{o}C, 100mg/l, and 29.33mins) of spent hamburger seed shell and spent grain carbons.
ii. The result is useful in understanding the influence of hydrogen peroxide as oxidants in regeneration.
iii. Large data bank has also been established for desorption kinetics (first order, pseudo first order, second order, pseudo second order and Elovich model.) and

isotherm studies (Lagmuir, Freundlich, Dublin-Radishkevich (D-R), Temkin, Flory-Huggins, Redlich-Peterson (S- P) and Toth-isotherm).

iv. This work has also established desorption rate constant equations for Swiss blue dye at different initial Swiss blue concentrations.

v. Desorption thermodynamic parameters (ΔH, ΔS, ΔG) were established.

REFERENCES

Adams, V. (1990). *Water and wastewater examination manual*. Lewis publishers, Boca Raton London New York Washington, D.C.

Adewale, K.O. & Mozie, O.S. (2010) Names of Different Soup Thickness in some Tribes in Nigeria (Discussion) Personal Communication, 20th March 2010.

Adinata, D. Daud, W.M.A.W. & Aroua, M.K. (2007). Preparation and characterization of activated carbon from palm shell by chemical activation with K_2CO_3. *Bioresource Technology*, 98: 145-149.

Ahmad, M. A. & Alrozi, R. (2010). Optimization of preparation conditions for mangosteen peel-based activated carbons for the removal of Remazol Brilliant Blue R using response surface methodology. *Chemical Engineering Journal*, 165: 883-890.

Ahmadpour, A. & Do, D.D. (1996). The preparation of active carbon from coal by chemical and physical activation. *Carbon*, 34: 471-479.

Ajemba, R. O. Igbokwe, P. K. & Onukwuli, O. D. (2012). Kinetics, equilibrium, and thermodynamics studies of colour pigments removal from palm oil using activated ukpor clay. *Archives of Applied Science Research*, 4 (5):1958-1966

Al – Degs, Y.S. Khraishen, M.A. Allen, S. & Ahmad, M.N. (1999). Adsorption of Remdzol Reactive Black B on Different Types of Activated carbon: Adsorption H. and L. *Carbon, Advance Research*. 3(2) :132 – 138.

Aliyu, S. & Bala, M. (2011). Brewer's spent grain: A review of its potentials and applications. *African Journal of Biotechnology*, 10(3): 324-331.

Alley, R. E. (2007). *Water quality control handbook*, 2nd Edition, New York, Norway. McGraw-Hill, Inc.

Al-Othman, Z.A. Ali, R. & Naushad, M.U. (2012). Hexavalent chromium removal from aqueous medium by activated carbon prepared from peanut shell. Adsorption kinetics, equilibrium and thermodynamic studies. *Chemical Engineering Journal*, 184: 234-247.

Alvarez, P.M. Beltran, F.J. Gomez-Serrano, V. Jaramillo, J. & Rodriguez. E.M. (2004). Comparison between thermal and ozone regenerations of spent activated carbon exhausted with phenol. *Water Research* 38: 2155-2165.

Ania, C. O. Menéndez, J. A. Parra, J. B. & Pis, J.J. (2004). Microwave-induced regeneration of activated carbons polluted with phenol. A comparison with conventional thermal regeneration. *Carbon*, 42: 1377-81.

Ania, C.O. Parra, J.B. & Menendez, J.A. (2005). Effect of microwave and conventional Regeneration on the microporous and Mesoporous Network and on the Adsorptive capacity of Activated carbons. *Micropore Mesopore Material*, 87: 7-15.

Ania, C.O. Menendez, J.A. Parra, J.B. & Pis, J.J (2007). Microwave assisted regeneration of activated carbons loaded with pharmaceuticals. *Water Resources*, 41: 3299-3306

Appleton, T. J. Colder, R. J. Kingman, S. W. Lowndes, J. S. & Read, A. G. (2005). Microwave technology for energy-efficient processing of waste. *Applied Energy*, 81:85-113.

Asmaa, A.F. & Muthanna, A. J. (2014). Optimization of activated carbon preparation from date stones by microwave assisted K_2CO_3 activation. *Iraqi Journal of chemical and petroleum Engineering*, 15(1): 33-42

Atwater, J. E. & Wheeler, R. R. (2004). Temperature dependent complex permittivities of graphitized carbon blacks at microwave frequencies between 0.2 and 26 GHz. *Journal of Material Science*, 39: 151-7.

Augugliaro, V. Litter, M. Palmisano, L. & Soria, J. (2006) The combination of heterogeneous photocatalysis with chemical and physical operations: A tool for improving the photoprocess performance, Journal of Photochemistry and Photobiology C: *Photochemistry Reviews*, 7(4):127–144.

Auta, M. & Hameed, B.H. (2012). Modified Mesoporous Clay Adsorbent for Adsorption, Isotherm and Kinetics of Methylene Blue. *Chemical Engineering Journal*, 198: 219 – 227.

Auta, M. & Hameed, B. H. (2011). Optimization of waste tea activated carbon for adsorption of MB and Acid Blue 29 dyes using Response surface methodology . *Chemical Engineering journal* 175: 233-243.

Azubike, C. P. Rodriguez, H. Okhamafe, A. O. & Rogers, R. D. (2012). Physicochemical properties of maize cob cellulose powder reconstituted from ionic liquid solution, *Cellulose*, 19(8): 425-433.

Babel, S. & Kurniawan, T.A. (2004). Cr(VI) removal from synthetic wastewater using coconut shell charcoal and commercial activated carbon modified with oxidizing agents and/or chitosan. *Chemosphere*, 54 (7): 951-967.

Baçaoui, A. Yaacoubi, A. Dahbi, A. Bennouna, C. Phan, T. L. R. Maldonado-Hodar, F. J. Rivera-Utrilla, J. & Moreno- Castilla, C. (2001). Optimization of conditions for the preparation of activated carbons from olive-waste cakes. *Carbon*, 39: 425-432.

Bagreev, A. Rahman, H. & Bandosz, T.J. (2001). Thermal regeneration of a spent activated carbon previously used as Hydrogen sulfide adsorbent. *Carbon* 39: 1319-1326.

Baker, D. (2008). Thermodynamic limits to thermal regeneration in adsorption cooling cycle. *International Journal of Refrigeration* 31: 55-64.

Ballari, M. D. L. M. Brandi, R. Alfano, O. & Cassano, A. (2008) Mass transfer limitations in photocatalytic reactors employing titanium dioxide suspensions, *Chemical Engineering Journal*, 136(1): 50–65.

Bandosz, T. J. (2006) *Activated Carbon Surfaces in Environmental Remediation*. Academic Press. New York.

Bansal, R.C. Donnet, J.B. & Stoeckli, H.F. (1988). *Active carbon.* Marcel Dekker, New York.

Bansal, R. C. & Goyal, M. (2005). *Activated carbon adsorption*, Boca Raton, Florida CRC Press.

Barton, S.S. (1987). The adsorption of MB by active carbon, *carbon* 25: 343-350

Basava, R. V.V. & Ram, M. R. S. (2006). Adsorption studies on treatment of textile dyeing industrial effluent by flyash. *Chemical Engineering Journal* 116: 77–84.

Bathen, D. (2003). Physical waves in adsorption technology: An overview. *Separation and purification technology*, 33: 163-177.

Beguin, F. & Frackowiak, E. (2010). *Carbons for Electrochemical Energy Storage and Conversion Systems.* CRC Press

Bekci, Z. Seki, Y. & Yurdakoc, M.K. (2006). Equilibrium Studies for trimethoprim Adsorption on Montmorillonite KSF, *Journal of Hazardous Material*, 133: 233 – 242.

Bello, O. S. Ahmad, M. A. & Ahmad, N. (2012). Adsorption features of banana (Musa Paradisiaca) stalk activated carbon for malachite green dye removal. *Chemical Ecology* 28: 153-167.

Benadjemia, M. Millière, L. Reinert, L. Benderdouche, N. & Duclaux, L. (2011) Preparation, characterization and Methylene Blue adsorption of phosphoric acid activated carbons from globe artichoke leaves, *Fuel Processing Technology*. Elsevier B.V., 92(6): 1203–1212.

Berteli, M. N. & Marsaioli J.R.A. (2005). Evaluation of short cut pasta air dehydration assisted by microwaves as compared to the conventional drying process. *Journal of Food Engineering*, 68: 175-183.

Boca, R. (2007). *Handbook of chemistry and physics* 88th Edition , CRS press, Taylor and Francis pp 3-350.

Boehm, H.P. (1994). Some aspects of the surface chemistry of carbon blacks and other carbons. *Carbon*, 32 (5): 759-769.

Bottani, E. J. & Tascon, J. M. D. (2008). *Adsorption by carbon*. Elsevier Science. ISBN: 978-0-08-044464-2.

Bradshaw, S.M. Van-Wyk, E. J. & Swardt, J.B. (1998). Microwave heating principles and the application to the regeneration of granular activated carbon. *The Journal of South African Institute of Mining and Metallurgy* 98: 201-210.

Brady, R. D, (2005). *Activated carbon processes, In Water treatment Plant Design,* New York, NY, AWWA, ASCE, McGraw Hill, pp. 14.1-14.38.

Brewers' Guardian (2011). Brewers' Grains. Opportunities Abound. Advantage Publishing Ltd, New York.

Cabal, B. Tsyntsarski, B. Budinova, T. Petrov, N. Parra, J. B. & Ania, C. O. (2009) *Journal of Hazardous Material*, 166(23): 1289-1295.

.

Caliskan, G. Bermudez, J.M. Parra, J.B. Menendez, J.A. Mahramanlioglu, M. & Ania, C.O. (2012). Low Temperature Regeneration of Activated carbon Using Microwaves: Revising Conventional Wisdom. *Journal of Environmental management*, 102: 134 – 140.

Cao, Q. Xie, K.C. Lv, Y.K. & Bao, W.R. (2006). Process effects of activated carbon with large surface area from corn cob, *Bioresource Technology* 97: 110-115.

Carp, O. (2004) Photoinduced reactivity of titanium dioxide, *Progress in Solid State Chemistry*, 32(1- 2): 33–177.

Cazetta, A. L. Alexandro, V. M. Eurca, N. M. Marcos, K. H. Marcos, G. R. Alessandro, M. C. Tais, S. L. Juliana, M. C.G. & Vitor, A. C. (2011). NaOH – Activated carbon of High Surface Area Produced from Coconut Shell: Kinetics and Equilibrium Studies from the methylene Blue Adsorption. *Chemical Engineering Journal*. 174: 117 – 125.

Cha, C.Y. & Carlisle, C.T. (2001). Microwave process for volatile organic compound abatement. *Journal of Air and Waste Management Association* 51: 628-1641.

Challa, S. Little, W. E. & Cha, C. Y. (1994). Measurement of the dielectric properties of char at 2.45 GHz. *Journal of Microwave Power and Electromagnetic Energy*, 29: 131-7.

Chefetz, B. Bilki, Y. I. & Polubesova, T. (2004). Sorption-desorption behaviour of triazine and phenylurea herbicides in kishon river sediments. *Water Resource*, 38: 4383-4394.

Chen, J.P. & Lin, M. (2001). Equilibrium and Kinetics of Metal on Adsorption Onto a Commercial H – Types Granular Activated carbon: Experimental and Modelling Studies. *Water. Resourse*. 35(10): 2385 – 2394.

Cheremisinoff, P. N. & Ellerbusch, F. (1978). *Carbon Adsorption Handbook.* Ann Arbor, MI, Ann Arbor Science Publishers, Inc.

Chern, J. & Wu, C. (2001). Desorption of Dye from Activated carbon Beds: Effects of Temperature, pH and Alcohol. *Water. Resource*. 35(17): 4159 – 4165.

Cheung, W. H. Szeto, Y.S. & Mckay, G. (2007). Intraparticle Diffusion Processes during Acid Dye Adsorption onto Chitosan, *Bioresource Technology*, 98: 2897 – 2904.

Chong, M. N. Jin, B. Chow, C. W. K. & Saint, C. (2010) Recent developments in photocatalytic water treatment technology: a review., *Water research.* Elsevier Ltd, 44(10): 2997–3027.

Chu, B.S. Baharin, B.S. Cheman, Y.B. & Quek, S.Y. (2004). Separation of vitamine E from palm fatty acid distillate using silica III.Batch desorption study. *Journal food Engineering*. 64: 1-7.

Clark, D.E. & Sutton, W.H. (1996). Microwave processing of materials. *Annual reviews of material science*, 26: 299-331.

Cook, D. Newcombe, G. & Sztajnbok, P. (2001). The application of powdered activated carbon for mib and geosmin removal: predicting pac doses in four raw waters. *Water Research*, 35 (5): 1325-1333.

Coss, P.M. & Cha, C.Y. (2000). Microwave regeneration of Activated carbon used for removal of solvents from vented air. *Journal of Air and Waste Management Association* 50: 529-535.

Dıaz-Teran, J. Nevskaia, D. M. Fierro, J. L. Lopez-Peinado, G. A. J. & Jerez, A. (2003). Study of chemical activation process of a lignocellulosic material with KOH by XPS and XRD, *Microporous Mesoporous Material* 60: 173–181.

Dalia, K. M. Mohamad, A. S. Wan, A. Wan, A. K. Azni, I. A. & Zurina, Z. A. (2012). Batch adsorption of basic dye using acid treated kenaf fibre char: Equilibrium, kinetic and thermodynamic studies. *Chemical Engineering Journal* 181: 449–457

Daneshur, N. Salari, D. & Aber, S. (2002). Chromium Adsorption and Cr(V) Reduction to Tribalent Chromium in Aqueous Solutions by Soya Cake. *Journal of Hazardous Materials*, 94: 49 – 61.

Darren, G. (2013). *Use of oxidants.* North Island College, UK.

Dehdashti, A. Khavanin, A. Rezaee, A. & Asilian, H. (2010). Regeneration of granular activated carbon saturated with gaseous toluene by microwave irradiation. Turkish, *Journal Engineering Environmental Science* 34: 49-58.

Demirbas, A. (2009). Agricultural Based Activated carbons for the Removal of Dye from Aqueous Solutions. A Review *Journal Hazardous Matter* 167: 1-9.

Deng, H. L. I. G. Yang, H. & Jang J. (2010). Preparation of activated carbon from cotton stack by microwave assited KOH and K_2CO_3 activation. *Chemical. Engineering Journal* 163: 373- 381

Derbyshire, F. Andrews, R. Jaques, D. Jagtoyen, M. Kimber, G. & Rantell, T. (2001). Synthesis of isotropic carbon fibers and activated carbon fibers from pitch precursors. *Fuel*, 80 (3): 345-356.

Dhodapkar, R. Rao, N. N. Pande, S. P. Nandy, T. & Devotta, S. (2007) Adsorption of cationic dyes on Jalshakti, super absorbent polymer and photocatalytic regeneration of the adsorbent', *Reactive and Functional Polymers*. Elsevier, 67(6), pp. 540–548.

Do, D.D. & Wang, K. (1998). A New Model for the Desorption of Adsorption Kinetics in Heterogenous Activated carbon. *Carbon* 36 (10): 1539 – 1554.

Dural, M. U. Levent, C. Sergios, K. P. & Fotis, K. K. (2001). Methylene Blue Adsorption on Activated Carbon Prepared from Posidonia Oceanica (L) Dead Leaves: Kinetics and Equilibrium Studies. *Chemical Engineering Journal* 168: 77 – 85.

Ekpette, O.A. & Horsfall, M. J. N. R. (2011) Preparation and characterization of Activated carbon derived from fluted pumpkin stem waste (Telfairia occidentalis Hook f) *Research journal of Chemical Science*, 1(3): 10-17

El-Hendawy, A. N. A. Samra, S. E. & Girgis, B. S. (2001). Adsorption characteristics of activated carbons obtained from corncobs. *Colloids and Surfaces A: Physicochemical and Engineering Aspects*, 180(3): 209-221.

EL-Hendawy, A. N. A. (2009) An insight into the KOH activation mechanism through the production of microporous activated carbon for the removal of Pb2+ cations, *Application of surface Science* 25(5): 3723- 3730

Elijah, O. C. & Nwabanne, J. T. (2014a). Adsorption Studies on the Removal of Eriochrome Black-T from Aqueous Solution using Nteje Clay. *Sop transactions on Applied Chemistry*, 1(2): 2373-2450

Elijah, O.C. & Nwabanne, J T. (2014b). Adsorption Kinetics for Malachite Green Removal from Aqueous Solution Using Nteje Clay. *Journal of Environment and Human*. 1(2): 2373-2495.

El-Sayed, Y.M. & Bandosz, T. J. (2004). Adsorption of Valeric Acid from Aqueous Solution Unto Activated carbon: Role of Surface Basic Sites, *Journal of Colloid Interface Science* 273: 64 -72.

Emad, N. E. Stephen, J. A. & Gavin, M. W. (2006).Adsorption of Methylene Blue onto activated carbon produced from steam activated bituminous coal: A study of equilibrium adsorption isotherm. *Chemical Engineering Journal* 124: 103–110

Emmanuel, U. I. Gilbert, U. A. Lora, O. O. & Olalere, G. A. (2009). Multistage optimization of the adsorption of methylene blue dye onto defatted Carica papaya seeds. *Chemical Engineering Journal*, 155: 567–579.

Ezueh, M. I. (1997). Cultivation and Utilization at Minor Food Legumes in Nigeria. *Tropical Grain Legume Bulleting*. International Institute of Tropical Agriculture, Ibadan, Nigeria.

Fan, M. Marshall, W. Daugaard, D. & Brown, R. C. (2004). Steam activation of chars produced from oat hulls and corn stover. *Bioresource Technology*. 93(1): 103-107.

Fang, C. & Lai, P. (1996). Microwave Regeneration of Spent Activated Carbon. *Chemical Engineering Communications* 147: 17-27.

Fang Z. Li, C. Sun, J. Zhang, H. & Zhang, J. (2007). The electromagnetic characteristics of carbon foams. *Carbon*, 45: 2873-9.

Fernandez, Y. Arenillas, A. & Menendez, J. A. (2011). Microwave heating applied to pyrolysis. In Grundas, S. (Ed.), *Advances in induction and microwave heating of mineral and organic materials*, ISBN: 978-953-307-522-8.

Ferro, M. A. Utrera, E. Rivera, J. & Moreno, C. (1993). Thermal regeneration of spent activated carbon. *Carbon* 31: 857.

Ferro-Garcia, M.A. Utrera-Hidalgo, E. Rivera-Utrilla, J. Moreno-Castilla, C. & Joly, J.P. (1993). Regeneration of activated carbons exhausted with chlorophenols, *carbon*, 31: 857-863.

Foo, K.Y. & Hameed, B.H. (2009). Recent developments in the preparation and regeneration of activated carbons by microwaves. *Advance Colloid Interface Science* 149: 19–27.

Foo, K.Y. & Hameed, B.H. (2010). Recent developments in the preparation and regeneration of activated carbons by microwaves, *Advances of Colloid interface Science* 149: 19-27

Foo K.Y. and Hameed B.H. (2012a). Microwave- assisted regeneration of activated carbon. *Bioresource Technology* 119: 234-240

Foo K.Y. & Hameed B.H. (2012b). Textural porosity, surface chemistry and adsorptive properties of durain shell derived activated carbon prepared by microwave assisted NAOH activation *Chemical Engineering Journal* 189: 53-62.

Foo, K.Y. & Hameed, B.H. (2012c). Preparation, Characterization and Evaluation of Adsorptive Properties of Orange Pell Based Activated Carbon Via Microwave Induced K_2CO_3 Activation. *Bioresource Technology* 104: 679 -686.

Foo, K.Y. & Hameed, B.H. (2012d). Microwave- assisted preparation and adsorption performance of activated carbon from biodiesel industry solid residue : influence of operational parameters . *Bioresource Technology* 103: 398-404.

Foo, K.Y. & Hameed, B.H. (2012e). Coconut husk derived activated carbon via microwave induced activation: Effects of activation agents, preparation parameters and adsorption performance by adsorption onto chitosan. *Chemical Engineering Journal* 184: 571–586

Foo, K.Y. & Hameed, B.H., (2012f). Microwave-assisted preparation of oil palm fiber activated carbon for methylene blue adsorption. *Chemical Engineering Journal* 166: 792–795

Fukuda, M. Kanaauchi, O. Araki, Y. Andoh, A. Mitsuyama, K. Takaagi, K. Toynaga, A. Sata, M. Fujiyama, Y. Fukuoka, M. Matsumoto, Y. & Bamba, T., (2002). Prebiotic Treatment of Experimental Colitis with Germinated Barley Foodstuff: A Comparison with probiotic or Antibiotic Treatment. *International of Molecular Medicine* 9: 65 – 70.

Gao, J.P. Maguhn.J. Spitzauer, P. & Kettrup, A. (1998) Sorption of pesticides in the sediment of the Teufelweiher pond (southern Germany).II: competitive adsorption, desorption of aged residues and effect of dissolved organic carbon, *water Resource* 32: 2089-2094

Gimba, C. & Musa. I. (2007). Preparation of activated carbon from agricultural waste cyanide binding with activated carbon matrix from coconut shell. *Journal of Chemistry Nigeria* .32: 167-170

Girgis, B.S. Yunis, S.S. & Soliman, A. M. (2002). Characteristics of activated carbon from peanut hulls in relation to conditions of preparation. *Materials Letters*. 57(1): 164-172.

Gitchel, W. Meidl, J. & Berndt, C. (1980). Characteristics of active carbon regenerated by wet oxidation. *AlchE symposium series*, 76(192): 51-59.

Gogate, P. R. & Pandit, A. B. (2004) A review of imperative technologies for wastewater treatment I: oxidation technologies at ambient conditions, *Advances in Environmental Research*, 8: 3-4.

Gottipati, R. (2012). Preparation and Characterisation of microporus activated carbon from biomass and its application on the removal of chromium (VI) from aqueous phase. *Unpublished PhD thesis*, Department of Chemical Engineering Natural Institute of Technology Rourkela Odisha.

Gratuito, M. K. B. Panyathonmaporan, T. Chumnan, K. R, A. Sirimuntawittaya, N. & Dutta, A. (2008). Production of Activated carbon from coconut shell: optimization using response surface methodology .*Bioresource Technology* 99: 4887-4895

Gregori, A. Svagelj, M. Pahor, B. Berovic, M. & Pohleven, F. (2008). The use of spent brewery grains for Pleurotus ostreatus cultivation and enzyme production. *New Biotechnology* 25(2-3): 157-161.

Gu, J. Faquir, N. M. & Bart, H-J. (1999). Drying of an activated carbon column after steam regeneration. *Chemical Engineering and Technology*, 22(10): 859-864.

Gunassekara, A.S. & Xing, B. (2003). Sorption and desorption of naphthalene by soil organic matter importance of aromatic aliphatic components. *Journal of Environmental Quality*. 32: 240-246.

Guocheng, L.V. Lime, WU. Xiaoyu, W. L. L. Zhauhui, L. I. & Wenhui, H. (2012). Regeneration of Carmel Saturated Activated carbon Jointly by Microwave and Extractive Method. *International Journal of Chemical Reactor Engineering*. 10(1): 1515-1528.

Gurses, A. Karaca, S. Dogar, C. & Yalcin, M. (2004). Determination of adsorptive properties of clay/water system: methylene blue sorption. *Journal of Colloid and interface Science*, 269(2): 310-4.

Hamdaoui, O. & Naffrechoux, E. (2007) Modeling of adsorption isotherms of phenol and chlorophenols onto granular activated carbon. Part I. Two-parameter models and equations allowing determination of thermodynamic parameters. *Journal of hazardous materials*, 147(1-2): 381–394.

Hameed, B.H. & Hakimi, H. (2008). Utilization of Clurian (Durio Zibethinus Murray) Peel as Low Cost Sorbent for the Removal of Acid Dye from Aqueous Solutions. *Biochemical Engineering Journal* 39: 338 – 343.

Hameed, B.H. Mahound, B.K. & Ahmad, A.L. (2008). Equilibrium modeling and kinetic Studies on the Adsorption of Basic Dye bya Low-Coast Adsorbent: Coconut (Cocos nulifera) Bunch Waster, *Journal of Hazardous Materials*, 158: 65 – 72.

Hameed, B.H. Salman, J.M. & Ahmad, A.L. (2010). Adsorption isotherm and kinetic modeling of 2,4-α pesticide on activated carbon derived from date stones. *Journal of Hazardous Materials*, 163(1): 121-126.

Han, R. Zhang, J. Han, P. Wing, V. Zhao, Z. & Tan, M. (2009). Study of equilibrium, kinetic and thermodynamic parameters about methylene blue adsorption onto nature zeolite. *Chemical Engineering .Journal*. 145: 496-504

Haque, K. E. (1999). Microwave energy for mineral treatment processes - A brief review. *International Journal of Mineral Process*, 57:1-24.

Harriott, P. & Cheng, A.T. (1988). Kinetics of spent activated carbon regeneration. *AIChE Journal*., 34(10): 1656-1662.

Hashisho, Z. Rood, M. & Botich, L. (2005). Microwave-swing adsorption to capture and recover vapors from air streams with activated carbon fiber cloth. *Environmental Science and Technology* 39: 6851-6859.

Herrmann, J. (1999). Heterogeneous photocatalysis: fundamentals and applications to the removal of various types of aqueous pollutants, *Catalysis Today*, 53(1): 115–129.

Hosseini, S. Moonis, A. K. Mohamed, R. M. Willie, C. & Thomas, C. S. Y. (2011). Carbon Coated Mmolith, a Mesoporous material for the Removal of methyl orange from Aqueous Phase: Adsorption and Desorption Studies. *Chemical Engineering Journal*, 17: 1124 – 1231.

Huling, S. G. Jones, P. K. Ela, W. P. & Arnold, R. G. (2005) Fenton-driven chemical regeneration of MTBE-spent GAC., *Water research*, 39(10): 2145–53.

Huling, S. G. Jones, P. K. & Lee, T. R. (2007). Iron optimization for Fenton-driven oxidation of MTBE-spent granular activated carbon., *Environmental science & technology*, 41(11): 4090–6.

Huling, S. G. Kan, E. & Wingo, C. (2009). Fenton-driven regeneration of MTBE-spent granular activated carbon—Effects of particle size and iron amendment procedures', *Applied Catalysis B: Environmental*, 89(3-4): 651–658.

Huling, S.G. Ko, S. Park, S. & Kan, E. (2011). Persulfate oxidation of MTBE-and chloroform-spent granular activated carbon, *Journal of Hazardous Materials*. 192: 1484–1490.

Huling, S. G. Kan, E. Caldwell, C. & Park, S. (2012) Fenton-driven chemical regeneration of MTBEspent granular activated carbon--a pilot study. *Journal of hazardous materials*. Elsevier B.V., 205: 55–62.

Igwegbe, C. A. Onyechi, P. C. & Onukwuli, O. D. (2015). Kinetic, Isotherm and Thermodynamic Modelling on the Adsorptive Removal of Malachite Green on *Dacryodes edulis* Seeds. *Journal of Scientific and Engineering Research*, 2(2): 23-39

Irfan, K. S. Pascaline, P. & Babu, J. A. (2013). Steam Regeneration of Adsorbents: An Experimental and Technical Review. *Chemical Science Transactions*. 2(4): 1078-1088.

Jankowska, H. Swiatkowski, A. & Choma, J. (1991). *Active Carbon*. Market Cross House, Cooper Street, Chichester, West Sussex, PO19 1EB, England: Ellis Horwood Limited.

Jeon, J.K. Kim, H. Park, Y.K. Pedenc, C.H.F. & Kim, D.H. (2011). Regeneration of field-spent activated carbon catalysts for low-temperature selective catalytic reduction of NOx with NH_3, *Chemical Engineering Journal* 174: 242–248.

Johnson, M.D. & Weber, W.J. (2001) Rapid prediction of long term rates of contaminant desorption from soils and sediments. *Environmetal Science Technology* 35: 427-433.

Jones, J.L. & Gwinn, J.E. (1983). Activated carbon regeneration apparatus *Environmental Progress*, 2(4): 226-235

Jou, G. (1998). Application of Activated Carbon in a microwave radiation field to treat trichloroethylene. *Carbon* 36: 1643-1648.

Kanauchi, O. Mitsuyama, K. & Araki, Y. (2001). Development of a Functional Germinated barley Foodstuff from Brewers' Spent Grain for the Treatment of Ulcerative Colitis. *Journal of the American Society of Brewing Chemist* 59: 59 – 62.

Kennedy, L.J. Vijaya, J.J. Kayalvizhi, K. & Sekaran, G. (2007). Adsorption of phenol fromaqueous solutions using mesoporous carbon prepared by two-stage process. *Chemical Engineering Journal*, 132: 279-287.

Kim, S. & Kim, Y. (2004). Apparent desorption kinetics of phenol In organic solvents from spent activated carbon saturated with phenol. *Chemical Engineering Journal* 98: 237-243.

Klaus, C. (2011). Energetic of Asorption and Desorption. *Introductory Block Course Chemistry and Physics of Surfaces.* Institute for Chie Freren Universtat Berlin.

Knopp, P. Gitchel, J. Meidl, J. & Berndl, C. (1978). *Wet oxidation regeneration. Carbon adsorption handbook,* Cheremisinoff, P; Ellerbusch, F; Eds. Ann Arbor Science: Ann Arbor; MI: 539-625.

Ko, Y.N. Choi, U.S. Kim, J.S. & Park, Y.S. (2002). Novel synthesis and characterization of activated carbon fiber and dye adsorption modeling. *Carbon*, 40 (14): 2661-2672.

Kumar, V. K. & Sivenesan, S. (2006). Isotherm parameters for basic dye onto activated carbon comparison of linear and non linear method. *Journal of hazardous materials* 13 (129): 147-150.

Kuntzel, J. Ham, R. & Melin, T. (1999). Regeneration of hydrophobic zeolites with steam. *Chemical Engineering and Technology*, 22(12): 991-994.

Lee, H.Y. Lee, C.L. & Jou, C., (2010). Comparison of degradation of pentachlorophenol using microwave induced nanoscale Feo and activated carbon. *Water Air and Soil Pollution* 211: 17-24.

Leng, C. & Pinto, N. (1996). An Investigation of the Mechanisms of Chemical Regeneration of Activated Carbon. *Industrial Engineering Chemistry Research* 35(6): 2024-2031.

Liu, S.X. Wang, Y. & Zhang, W.C. (2001). Progress in Activated Carbon Regeneration, *Carbon Techniques*, 29: 61.

Liu, X. Quan, X. Bo, L. Chen, S. & Zhao, Y., (2004a). Simultaneous pentachlorophenol decomposition and granular activated carbon regeneration assisted by microwave irradiation. *Carbon* , 42 (2): 415-422.

Liu, X. Quan, X. Bo, L. Chen, S. Zhao, Y. & Chang, M. (2004b). Temperature measurement of GAC and decomposition of PCP loaded on GAC and GACsupported copper catalyst in microwave irradiation. *Applied Catalysis A: General* 264: 53-58.

Lyman, W. (1978). Applicability of carbon adsorption to the treatment of hazardous Industrial wastes. *Carbon adsorption handbook.* Cheremisinoff, P., Ellerbush, F., eds. Ann Arbor Science: Ann Arbor, MI: 131-165.

Lua A. C. & Yang, T. (2004). Effect of activation temperature on the textural and chemical properties of potassium hydroxide activated carbon prepared from pistachio-nut shell, *Journal of Colloid and Interface Science* 274 pp. 594-601.

Ma, J. Fang, M. Li, P. Zhu, B. Lu, X. Lau, N.T. (1997). Microwave-assisted catalytic combustion of diesel soot. *Applied Catalyst*, 159: 211-28.

Machado, R. Carvalho, J. R. Joana, N. Correia, M. (2002). Removal of trivalat chromium(111) from solution by biosorption in cork powder . *Journal of Chemical Technology Biotechnology* 77: 1340-1348.

Macnaughton, S.I. & Foster, N. R. (1995). Supercritical Adsorption and Desorption Behaviour of DDT on Activated carbon Using Carbon Dioxide. *Industrial and Engineering Chemistry Research* 34: 275.

Madras, G. Erkey, C. & Akgerman, A. (1993). Supercritical Fluid Regeneration of Activated carbon Loaded with Heavy Molecular Weight organics. *Industrial and Engineering Chemistry Research*. 32: 1163

Magne, P. & Walker, Jr. P. L. (1986). Phenol adsorption on activated carbons., application to the regeneration of activated carbons; application to the regeneration of actvated carbons polluted with phenol . *carbon* 24: 101-107.

Mahmound, D. K. Salleh, M. A. M. Karim, W. A. W.A. Idris, A. & Abidin, Z. Z. (2012). Batch adsorption of basic dye using treated kenaf fiber char: Equilibrium, Kinetics and thermodynamics studies. *Chemical Engineering Journal*, 181-182: 449-457.

Malik, P. K (2004). Dye Removal from Wastewater Using Activated Carbon Developed from Sawdust: Adsorption Equilibrium and Kinetics. *Journal of Hazardous materials*, 113: 81 – 88.

Mall, I. D. Srivastava, V. C. & Agarwal, N. K. (2006). Removal of orange- G and methyl violet dyes by adsorption onto bagasse fly ash, Kinetics study and equilibrium isotherm analyses. *Dyes pigments*, 69 : 210-223.

María, A. C. M. (2015) Regeneration of Activated Carbon by Photocatalysis using Titanium Dioxide. *Unpublished Doctoral Thesis* Chemical Engineering, Loughborough University.

Marland, S. Merchant, A. & Rowson, N. (2001). Dielectric properties of coal. *Fuel*, 80: 1839-49.

Marsh, H. & Rodríguez-Reinoso, F. (2006). Activation Processes (Thermal or Physical), in *Activated Carbon*, Elsevier Science Ltd: Oxford: 243-321.

Mata, Y.N. Blazguez, M.L. Balleste, A. Gorizale, F. & Munoz, J.A. (2010). Studies on Sorption, Desorption, Regeneration and Reuse of Sugar – Beet Pectin Gels for heavy metal Removal. *Journal of Hazardous Materials*, 178: 243 – 248.

Matsumoto, A. Tsubaki, S. Sakamoto, M. & Azuma, J.I. (2011). A novavel saccharification method of starch using microwave irradiation with addition of activated carbon. *Bioresource Technology* 102: 3985-3988.

Mattson, J. & Mark, H. (1971). Activated carbon: *Surface Chemistry and Adsorption from Solution*. Marcel Dekka Inc. New York.

McKay, G. (1996a). Adsorbent regeneration, in: G. McKay (Ed.), Use of Adsorbents for the Removal of Pollutants from Wastewaters, CRC Press, Tokyo: 175– 179.

McKay, G. (1996b). Regeneration of adsorbents In use of adsorbents for the removal of pollutants from wastewaters, Boca Raton, FL, CRC Press.

McKee, D. W. (1981). The catalyzed gasification reaction of carbon. *Chemistry and Physics of carbon*. 16:183-199.

Menard, D. Py, X. & Mazet, N. (2007). Activated carbon Mmolith of High Thermal Conductivity for Adsorption Processes Improvement: Part B. Thermal Regeneration. *Chemical Engineering Process*, 46: 565 – 572.

Menéndez, J.A. Arenillas, A. Fidalgo, B. Fernández, Y. Zubizarreta, L. Calvo, E.G. & Bermúdez, J.M. (2010) Microwave heating processes involving carbon materials. *Fuel Processing Technology*, 91 (1): 1-8

Menendez-Diaz, J.A. & Martin-Gullon, I. (2006). Types of carbon adsorbents and their production. *Interface Science and Technology*, 7: 1-47.

Meredith R. (1998). *Engineers' Handbook of Industrial Microwave Heating*. The Institution of Electrical Engineers, London, UK.

Mezey, E. & Dinovo, S. (1982). Adsorbent Regeneration and gas Seperation by Microwave Heating. US Patent no. 4322394.

Mguel, G. G. lambert, S.D. & Graham, N.J.D. (2001). The Regeneration of Field Spent Activated carbons *Water Resourse* 35(11): 740 – 748.

Minkova, V. Razvigorova, M. Bjornbom, E. Zanzi, R. Budinova, T. & Petrov, N. (2001). Effect of water vapour and biomass nature on the yield and quality of the pyrolysis products from biomass. *Fuel Processing Technology*, 70(1): 53-61.

Misra, K. Kapoor, S.K. & Bansal, R.C. (2002). Regeneration of granular activated carbon loaded with explosive. *Journal of Environmental Monitoring*.4: 462-464.

Miura, M. Kaga, H. Sakurai, A. Kakuchi, T. I. & Takahashi, K. I. (2004). Rapid pyrolysis of wood block by microwave heating. *Journal of Analytical and Applied Pyrolysis*, 71: 187-199.

Modell, M. Defillipi, R. & Krukonis, V. (1980). Regeneration of activated carbon with supercritical carbondioxide. *Active carbon adsorption of organics from the aqueous phase*, Suffet, I. H; Mchuire, M.J., eds. Ann Arbor Science; Ann Arbor, M.I. 1: 447-461.

Mohd, A. A. Nur, S. A. & Olugbenga, S. B. (2005). Optimization of process variables by Response Surface Methodology for malachite green dye removal using lime peel activated carbon. *Application water Science*. DOI. 10.1007/513201-015-0284-0.

Moreno-Castilla, C. Rivera-Utrilla, J. Joly, J.P. Lopez-Raman, M.V. Ferro- Garcia, M.A. & Carrasco- Marin, F., (1995). Thermal regeneration of an activated carbon exhausted with different substituted phenols. *Carbon*, 33: 1417-1423.

Moseley, J. D. & Woodman, E. K. (2009). Energy efficiency of microwave- and conventionally heated reactors compared at meso scale for organic reactions. *Energy and Fuels*, 23: 5438-5447.

Mourand, J. T. Crittenden, J. C. Hand, D. W. Perram, D. L. & Notthakun, S. (1995) Regeneration of spent adsorbents using homogeneous advanced oxidation, *Water Environment Research*, 67(3): 355–363.

Mozia, S. (2010) Photocatalytic membrane reactors (PMRs) in water and wastewater treatment. A review, *Separation and Purification Technology*. Elsevier B.V., 73(2): 71–91.

Muhammad, Moonis, A. K. Thomas, S.Y. C. Chuah, T.G. Robiah, Y. Taufig, Y. Y.H. (2011). Desorption of β-Carotene from mesoporous carbon monolith. Isotherm, Kinetics and regeneration studies .*Chemical Engineering Journal*, 173: 474-479.

Mundale, V. Joglekar, A. & Joshi, J. (1991). Regeneration of Spent Activated carbon by Wet Air Oxidation. *Journal of Canadian Chemical Engineering* 69: 1149 – 1159.

Muranaka, C. & Julcour, C. (2009) Regeneration of activated carbon by (photo)-Fenton oxidation, *Industrial and Engineering Chemistry Research*, 49(3): 989–995.

Mussatto S.T. Dragone, G. & Roberto, J. C. (2006). Brewers' Spent Grain: Generation, Characteristics and Potential Application. *Journal of Cereal Science* 43: 1-14.

Mussato, S. I. & Roberto, I. C. (2006). Chemical characterisation and liberation of pentose sugars from brewer's spent grain. *Journal of Chemical Technology Biotechnology*, 81: 268-274

Nahil, M.A. & Williams, P.T. (2011). Recycling of carbon fiber reinforced polymeric waste for the production of activated carbon fibers. *Journal of Analytical and Applied Pyrolysis*, 91 (1): 67-75.

Nahm, S. W. Wang, G. S. Young – Kwon, P. & Sanng, C. K. (2012). Thermal and Chemical Regeneration of Spent Activate carbon and Its Adsorption Property for toluene. *Chemical Engineering Journal*, 210: 500 – 509.

Nkpa, U. I. (2004). The Effect of Length of Freezing on the Thickening Property of Ukpo (*Mucuna Sloanei*). *Unpublished B.Sc. Tech. Thesis*. Federal University of Technology, Owerri., Imo State.

Nora, M. H. Emam, A.A. El-Bayaa, A.A. & Zidan, A.E. (2013). Adsorption of barium and iron from aqueous solution by activated carbon produced from mazoo ash. *Life science Journal*, 10 (3): 2011-2020

Notthakun, S. Hand, D. W. Perram, D. L. & Mullins, M. E. (1993) Regeneration of adsorbents using heterogeneous advanced oxidation, *Journal of Environmental Engineering*, 119(4): 695.

Nwabanne, J.T. & Igbokwe, P.K. (2008). Kinetics and equilibrium modelling of Nickel adsorption by cassava peel. *Journal of Engineering and applied science*. 3(11): 829-834.

Nwabanne, J.T. Asomugha, V.N. & Onyemelukwe, N. (2010). Equilibrium and kinetic modelling of adsorption of methyl orange dye on palmyra palm nut. *Journal of Engineering and Applied Sciences* 6: 11-16

Nwabanne, J.T. & Igbokwe, P.K. (2011). Copper (II) Uptake by Adsorption Using Palmyra Palm Nut. *Advances in Applied Science Research*, 2 (6):166-175

Nwabanne, J.T. & Igbokwe, P. K. (2012a). Thermodynamic and Kinetic Behaviors of Lead (II) Adsorption on Activated Carbon Derived from Palmyra Palm Nut. *International Journal of Applied Science and Technology*, 2(3): 245-254.

Nwabanne, J.T. & Igbokwe, P. K. (2012b). Comparative Study of Lead (II) Removal from Aqueous Solution Using Different Adsorbents. *International Journal of Engineering Research and Applications* (IJERA), 2(4): 1830-1838

Nwabanne, J.T. & Igbokwe, P.K. (2012c). Mechanism of Copper (II) Removal from Aqueous Solution Using Activated Carbon Prepared from Different Agricultural Materials. *International Journal of Multidisciplinary Sciences and Engineering,* 3(7): 46-52.

Oh, W.C. & Jang, W.C. (2003). Physical properties and biological effects of activated carbon fibers treated with the herbs. *Carbon*, 41 (9): 1737-1742.

Oin, Y.C. Wang, H.T. & Zhu, H.Z. (2001). Regeneration Methods of Activated carbon, *Carbon Techniques.* 117: 29.

Onwu. D. O. (1999). *Coal fundamentals and conversion technology*. Immaculate publications, Ogui New Layout, Enugu.

Oya, A. Wakahara, T. & Yoshida, S. (1993). Preparation of pitch-based antibacterial activated carbon fiber. *Carbon*, 31 (8): 1243-1247.

Ozcan, A. & Ozcan A. S (2005). Adsorption of Acid Red 576 from Aqueous Solution onto Surfactant Modified Sepiolite, *Journal of Hazardous Materials* 125: 252 – 259.

Paraskeva, P. Kalderis, D. & Diamadopoulos, E. (2008). Production of activated carbon from agricultural by-products. *Journal of Chemical Technology and Biotechnology*, 83(5): 581-592.

Parmele C S. O'Connell, W. L. & Basdekis, H. S. (1979). Vapor-phase Adsorption Cuts Pollution, Recovers Solvents, *Chemical Engineering*: 58-70.

Pelech R, Milchert, E & Wróblewska, A. (2005) Desorption of chloroorganic compounds from a bed of activated carbon. *Journal of Colloid Interface Science*, 285(2): 518-524.

Pelekani, C. & Snoeyink, V. L. (1999) Competitive adsorption in natural water: role of activated carbon pore size, *Water Research*, 33(5): 1209–1219.

Pelekani, C. & Snoeyink, V. (2000) Competitive adsorption between atrazine and methylene blue on activated carbon: the importance of pore size distribution, *Carbon*. Elsevier, 38(10): 1423– 1436.

Peng, X. Luan, Z. & Zhang, H. (2006). Montmorillonite–Cu(II)/Fe(III) oxides magnetic material as adsorbent for removal of humic acid and its thermal regeneration. *Chemosphere* 63: 300-306.

Pérez-cid, B. Lavilla, I. & Bendicho, C. (1999). Application of microwave extraction for partitioning of heavy metals in sewage sludge. *Analytica Chimica Acta*, 378: 201-210.

Pinchukova, N. A. Chebanov, V. A. Gorobets, N. Y. Gudzenko, l. V. Ostras, K. S. Shishkin, O. V. Hulshof, l. A. & Voloshko, A. Y. (2011). Beneficial energy-efficiencies in the microwave-assisted vacuum preparation of polyphosphoric acid. *Chemical Engineering and Processing: Process Intensification*, 50: 1193-1197.

Pinero, E. R. Azais, P. Cacciaguerra, T. Amoros, D.S. Solano, A. L. & Beguin, F. (2005). KOH and NaOH activation mechanisms of multiwalled carbon nanotubes with different structural organization, *Carbon*, 43: 786-795.

Price, D.W. & Schmidt, P.S. (1998). VOC recovery through microwave regeneration of adsorbents:comparative economic feasibility studies. *Journal of Air and waste Management Association* 48: 1146-1155.

Purkait , M. K. Macti, A. & Dasgupta, S. D. (2007). Removal of Congo red using activated carbon and its regeneration. *Journal of Hazardous materials* 145: 287-295

Qadeer, R. (2007) Adsorption behavior of ruthenium ims on activated charcoal from nitric acid medium, *Colloids surface* 293: 217-223.

Qing-Zhu, L. Chai, L. Zhao, J. Yang, Z. & Wang, Q. (2009). Lead desorption from modified spent grain. *Transaction of nonferrous metals society of chain* 19: 1371-1376.

Radovic, L.R. Silva, I.F. Ume, J.I. Menendozi, J.A. Leon, C.A. Leon, Y.A. & Scaroni, A.W. (1997). An Experimental and Theoretical Study of the Adsorption of Aromatics Possessing Electron - Withdrawing and Electron – Donating. *Carbon* 35: 1339- 1349.

Rege, S. U. & Yang, R. T. (1998). Desorption by ultrasound: phenol on activated carbon and polymeric Resin. *Alche journal*, 44(7): 1519-1528.

Rengaraj, S. Seung –Hyeon, M. & Sivabalm, S. (2012). Agricultural solid waste for the removal of organic adsorption of phenol from waste and waste water by palm seed coat activated carbon. *Waste management*, 22: 543-548.

Robers, A. Figura, M. Thiesen, P.H. & Niemeye, B. (2005). Desorption of Ador-active Compounds by Microwave, Ultrasound and Water. *Alche, Journal*, 51: 502-510.

Rouquerol, J. Avnir, D. Fairbridge, C. W. Everett, D. H. Haynes, J. M. Pernicone, N. Ramsay, J. D. F. Sing, K. S. W. & Unger, K. K. (1994). Recommendations for the characterisation of porus solids (Technical reports). *Pure and applied chemistry*, 66(8): 1739-1758.

Ruthven, D.M. (1984). *Principles of Adsorption and Adsorption Process*. A Wiley-Interscience Publication, John Wily and Sons, New York.

Sabio, E. Gonzalez, E. Gonzalez, J.F. Gonzalez-Garcia, C.M. Ramiro, A. & Ganan, J., (2004). Thermal regeneration of Activated carbon Saturated with pnitrophenol. *Carbon* 42: 2285-2293.

Saeed, A. Akhter, M.W. & Igbal, M. (2005). Removal and recovery of heavy metal from aqueous solution using papaya wood as a new biosorbent. *Separation and Purification technology*. 45: 25-31.

Safa, Y. & Haq, N. B. (2011). Adsorptive removal of direct textile dye by low cost agricultural waste: Application of factorial design analysis. *Chemical Engineering Journal*, 167: 35-41.

Sag, Y.A. & Kutsal, T. (1996). Fully Competitive Biosorption of Chromium (VI) and Iron (II) Ions from Binary Metal Mixtures by R. Arrhizus: Use of the Competitive Langmuir Model, *process Biochemical*, 31: 561-579.

Sahu, J.N. Achanga, J. & Meikap B.C. (2010). Optimization of production conditions for activated carbon from terminal wood by zinc chloride using response surface methodology, *bioresource technology* 10: 1974-1982

Salema, A.A. & Ani, F.N. (2011). Microwave Induced Pyrolysisof Oil Palm Biomas. *Bioresource Technology* 10: 3388 – 3395.

Salihu, A. & Muntari, B. (2011). Brewer's spent grain: A review of its potentials and applications. *African Journal of Biotechnology*, 10(3): 324-331.

Salman, J.M. Njoku, V.O. & Hameed, B.H. (2011). Batch and Fixed Bed Adsorption of 2, 4 – Dichloro Phenoxy Acetic Acid onto Oil palm Frond Activated carbon. *Chemical Engineering Journal*, 174: 33 – 40.

Salvador, F. & Jimenez, S. C. (1996). A new method for regenerating activated carbon by thermal desorption with liquid water under supercritical conditions. *Carbon*, 34 (4): 511-516.

Sarici- Ozdemir, C. D. (2004) Adsorption and desorption kinetics behaviour of methylene blue onto activated carbon. *Physicochemical problems of mineral processing*, 48(2): 441-454.

Schroeder, S. L. M. & Gottfried, M. (2002). Temperature- programmed Desorption (TPD) Thermal Desorption spectroscopy (TDS) *Advanced physical chemistry laboratory* Fu- Berlin: 1-22.

Schulz, H. & Wei, M., (1999). Deactivation and thermal regeneration of zeolite HZSM 5 for methanol conversion at low temperature (260-290°C). *Microporous and Mesoporous Materials* 29: 205-218.

Schweiger, T. A. J. (1989). Experimental and Theoretical studies of steam regeneration of a solvent adsorber, Charlottesville, VA (USA), University of Virginia.

Sears, G.W. (1976). Determination of specific surface area of colloidal silica by titration with sodium hydroxide. *Analytical chemistry*, 28: 1981-1983

Sener, S. (2008). Use of Solid Waste of the Soda Ash Plant as an Adsorbent for the removal of Anionic Dye: Equilirium and Kinetic Studies. *Chemical Engineering Journal* 138: 207 – 214.

Sentorum-Shalaby, C. Ucak- Astarhog, M. G. Artok, C, L. & Sarici, C. (2006) preparation and characterization of Activated carbons by one- step steam pyrolysis/activation from apricot stones, *Microporous and Mesoporous materials* 88: 126- 134

Shevkophlyas, V, N. & Saranchuk ,V.I. (2000), The Impregnation effect on low and middle rank coals structure effect on low and middle rank coals structure reorganization and their behavior during pyrolysis, *fuel* 79: 557-565.

Smithson, G. (1978). Regeneration of activated carbon: Thermal, chemical, solvent, vacuum and miscellaneous regeneration techniques. *Carbon adsorption*

handbook; Cheremisinoff, P., Ellerbusch, F., eds. Ann Arbor Science: Ann Arbor, M. I: 879-903.

Stuerga, D. & Delmotte, M. (2002). Wave-Material Interactions, Microwave Technology and Equipment. In: Loupy A., editor, *Microwaves in Organic Synthesis,* Wiley- VCH, ISBN 3-527-30514-9

Su, C.H. Wu, S.H. Shen, S.J. Shiue, G.Y. Wang, Y.W. & Shu, C.M., (2009). Thermal characterstics and regeneration analyses of adsorbents by differential scanning calorimetry and scanning electron microscope. *Journal of Thermal Analysis and Calorimetry* 96: 765-769.

Sudaryanto, Y. Hartono, S.B. Irawaty, W. Hindarso, H. & Ismadji, S. (2006). High surface area activated carbon prepared from cassava peel by chemical activation, *Bioresource Technology*, 97: 734-739.

Sufnarski, M. D. B. S. (1999). The regeneration of granular activated carbon using Hydrothermal Technology. *Unpublished Doctoral thesis*, faculty of the graduate school of the University of Texas at Austin.

Sulak, M.T. Demirbas, E. & Kobya, M. (2007). Removal of Astrazon Yellow 7GL from aqueous solutions by adsorption onto wheat bran, *Bioresource Technology* 98: 2590–2598.

Sun, K. Jiang, J. & Jun-ming, X. (2009). Chemical regeneration of Exhausted Granular activated carbon used in citric acid fermented solution Decoloration. *Iran Chemical Engineering*, 28(4): 79-83.

Suzuki, M. Misic, D. M. Koyama, O. & Kawazoe, K. (1975). Study of thermal regeneration of spent activated carbons: Thermogravimetric measurement of 50 various single component organics loaded on activated carbons. *Chemical Engineering Science*, 33: 271-279.

Tai, H.S. & Jou, C. J. G. (1999). Application of granular activated carbon packed-bed reactor in microwave radiation field to treat phenol. *Chemosphere* 25: 2667-2680.

Tai, H.S. & Lee, C.L. (2007). Desorption of methy-ethyl-ketone from granular activated carbon with microwave radiation. *Environmental Progress* 26: 299-303.

Tamanna, C. (2012). Microwave Assisted Regeneration of Na-ETS-10. *Unpublished thesis* submitted to the Faculty of Graduate Studies and Research for the degree of Master of Science in Environmental Engineering Civil and Environmental Engineering, University of Alberta.

Tan, I.A.W. Hameed, B.H. & Ahmad, A.L. (2007). Equilibrium and kinetic studies on basic dye adsorption by oil palm fibre activated carbon. Chemical *Engineering Journal* 127: 111–119

Tan, I. A. W. Ahmed, A.L. & Hameed, B. H. (2008). Optimization of preparation conditions for activated carbons from coconut husk using response surface methodology. *Chemical Engineering Journal* 137: 462- 470.

Tseng, J. Ching – Yuan, C. Chiung-Chsng, Yi-Hung, C. Chia-Chi, C. Dar- Ren, J. Chun-Yu, C. & Pen – Chi, C. (2009). Kinetics and equilibrium of desorption removal of copper from magnetic polymer adsorbate. *Journal of Hazardous materials*, 171: 370-377.

Tsezos, M. Mecready, R.G.L. & Bell, J.P. (1989). The continuous recovery of uranium from spent activated carbon. *Biotechnology Bioengineering* 34: 10-17.

Udo, K. & Christof, H. (2010). Electromagnetic techniques for moisture content determination of materials. *Measurement Science and Technology*, 21(8): 26-38.

Ugonabo, V. I. Onukwuli, O. D. & Igbokwe, P.K. (2008). Treatment of wastewater from vegetable oil industry using modified laterite adsorbent. *Journal of Engineering and Applied*, 4: 46 – 51.

Umehara, T. Harriot, P. & Smith, J.M. (1983). Regeneration of activated carbon. Part 2. Gasification kinetics with steam. *AIChE J.*, 29(4): 737-741.

Vagmur, E. Ozmak, M. & Aktas, Z. (2008). A Novel method for production of Activated carbon from Wastte by Chemical Activation with Microwave Energy *Fuel*. 87: 3278 – 3285.

Vargas, A. M. M. Cazetta, A.L. Kunita, M. H. Silva, T. L. & Almeida, V.C. (2011). Adsorption of Methlene Blue on Activated carbon produced from Flamboyant Pods (Delonix regia). Study of Adsorption Isotherms and Kinetic Models. *Chemical Engineering Journal* 168: 722 – 730.

Vijaykumar, G. Tamilarasan, R. & Dharmendirakumar, M. (2012). Adsorption, Kinetic, Equilibrium and Thermodynamic Studies on the Removal of Basic Dye Rhodamine – B from Aqueous Solution by the Use of Natural Adsorbent Perlite *Journal of Material and Environmental Science* 3(1): 157 – 170.

Vitolo, S. Bresci, B. Seggiani, M. & Gallo, M.G. (2001). Catalytic upgrading of pyrolytic oils over HZSM-5 zeolite: behaviour of the catalyst when used in repeated upgrading- regenerating cycles. *Fuel*, 80: 17-26.

Vliet, V. B. M. (1982). Comparactive efficacy of extractive and thermal regeneration of activated carbon. Proceedings of the 14th IWSA International Congress, Zurich, 6-10 September.

Vliet, V. B. M. (1991). The regeneration of activated carbon Journal of the southern *African institute of mining and metallurgy*. 91(5): 159-167.

Vliet, H. M. & Venter, L (1985). Infrared thermal regeneration of spent activated carbon from water reclamation. *Water Science and Technology*, 17: 1029-1042.

Wang, Y. Wu, J. & Wei, F. (2003). A treatment method to give separated multi-walled carbon nano tubes with high purity, high crystallization and a large aspect ratio. *Carbon*,41: 2939–2948.

Wang, J. & Somasundaran, P. (2007). Study of Galactomannose Interaction with Solid using AFM, IR and Allied techniques. *Journal of Colloid and Interface Science*. 309, (2): 373 – 383.

Wang, Z. M. Yamashita, N. Wang, Z. X. Hoshinoo, K. & Kanoh, H. (2004). Air oxidation effects on microporosity, surface property, and CH_4 adsorptivity of pitch-based activated carbon fibers. *Journal of Colloid and Interface Science*, 276 (1): 143-150.

Wang, S. Zhu, Z. H. Coomes, A. Haghseresht, F. & Lu, G. Q. (2005). The physical and surface chemical characteristics of activated carbons and the adsorption of methylene blue from wastewater, *Journal of colloid and interface science*, 284(2): 440–446.

Weber, W. J. (1972). Physicochemical Processes for Water Quality Control, pp 199-259, John Wiley and Sons, Inc., USA.

Woodmansee, D. E. & Carroll, J.J. (1993). In place regeneration of adsorbents using Microwaves. US Patent no. 5227598.

Wu, F. & Tseng, R. (2006). Preparation of highly porus carbon from fir wood by KOH etching and CO_2 gasification for adsorption of dyes and phenols from water. *Journal of Colloid and Interface Science*, 294(1): 21-30.

Wu, K. H. Ting, T. H. Wang, G. P. Yang, C. C. & Tsai, C. W. (2008). Synthesis and microwave electromagnetic characteristics of bamboo charcoal/polyaniline composites in 2-40GHz. *Synthetic Matrial*.158: 688-94.

Xing, Y. Liu, D. & Zhang, L. P. (2010) Enhanced adsorption of Methylene Blue by EDTAD-modified sugarcane bagasse and photocatalytic regeneration of the adsorbent, *Desalination. Elsevier* B.V., 259(1-3): 187–191.

Yang, J-K. & Wu, Y-M. (1987). Relation between dielectric property and desulphurization of coal by microwaves. *Fuel,* 66: 1745-7.

Yang, J. & Qju, K. (2010). Preparation of Activated carbon from Walnut Shell Via Application for Methylene Blue Removal. *Chemical Engineering Journal* 162: 209 – 219.

Yao, Y. Jänis, A. & Klement, U. (2008). Characterization and dielectric properties of β-SiC nanofibres. *Journal of Material Science*, 43: 1094-101.

Yu, J. Li, B. Sun, X. Jun, Y. & Chi, R. (2009). Adsorption of methylene blue and rhodamine B on baker's yeast and photocatalytic regeneration of the biosorbent, *Biochemical Engineering Journal*, 45(2): 145–151.

Zhang, L. Su, M. & Guo, X. (2008). Studies on the treatment of brilliant green solution by combination microwave induced oxidation with CoFe2O4, *Seperation Purification Technology* 62: 458–463.

Zhang L. & Zhu, H. (2009). Dielectric, magnetic, and microwave absorbing properties of multi-walled carbon nanotubes filled with S_2O_3 nanoparticles. *Material Letter* 63: 272-4.

Zlotorzynski, A. (1995). The application of microwave radiation to analytical and environmental chemistry. Critical Review *Analytical Chemistry*, 25: 43-76.

APPENDIX A

FACTORS AND LEVELS FOR OPTIMIZATION PROCESSES

a) Factors and levels for Conventional activation using CCD

	Factors	Units	Levels				
			-α	-1	0	+1	+α
1	Activation Temp.	^{o}C	450.0	550.0	650.0	750.0	850.0
2	Activation time	Mins	30.0	60.0	90.0	120.0	150.0
3	KOH Concentration	M	2.0	3.0	4.0	5.0	6.0
4	Type of precursor						
A	Hamb. Seed shell						
b	Brewers' spent grain						

b) Factors and levels for the adsorption conditions using BBD

	Factors	Units	Levels		
			-1	0	+1
1	Temperature	^{O}C	30	35	40
2	pH	-	3.0	6.0	9.0
3	Dosage	grams	0.05	0.075	0.10

4	Initial Concentration	mg/l	50.0	100.0	150.0
5	Adsorbents types				
A	CPASG				
B	CPAHS				
C	MPAHS				
D	MPASG				

c) Factors and levels for the desorption process using BBD

	Factors	Units	Levels		
			-1	0	+1
1	Temperature	oC	30	40	50
2	Dosage	grams	0.02	0.55	1.08
3	Initial dye conc.	mg/l	100.0	200.0	300.0
5	Adsorbents types				
A	CPASG				
B	CPAHS				
C	MPAHS				
D	MPASG				

d) Factors and levels for Microwave regeneration process using CCD

	Factors	Units	Levels				
			-α	-1	0	+1	+α
1	Power levels	%	13.5	36.0	58.5	81.0	103.5

2	Radiation time	Mins	7.0	8.0	9.0	10.0	11.0
3	Initial dye Conc.	mg/l	50.0	100.0	150.0	200.0	250.0
4	Type of precursor						
A	MPAHS						
B	MPASG						
C	CPAHS						
D	CPASG						

e) Factors and levels for Conventional regeneration process using CCD

	Factors	Units	Levels				
			-α	-1	0	+1	+α
1	Temp.	^{o}C	200.0	300.0	400.0	500.0	600.0
2	Time	Mins	20.0	30.0	40.0	50.0	60.0
3	Initial dye Conc.	mg/l	50.0	100.0	150.0	200.0	250.0
4	Type of precursor						
A	MPAHS						

B	MPASG
C	CPAHS
D	CPASG

APPENDIX B

Design matrix for optimization of conventional activation process using CCD

Std Order	Run order	Temp (oC)	Time (mins)	KOH Conc. (M)	Types of Precursors	RE (%)
33	1	800.00	90.00	2.00	Hamburgar seedshell	72.95
6	2	900.00	60.00	5.00	Spent grain	99
28	3	900.00	120.00	5.00	Hamburgar seedshell	97.2
4	4	900.00	120.00	3.00	Spent grain	87.14
38	5	800.00	90.00	4.00	Hamburgar seedshell	94.67
31	6	800.00	30.00	4.00	Hamburgar seedshell	89.73
25	7	700.00	60.00	5.00	Hamburgar seedshell	88.81
9	8	600.00	90.00	4.00	Spent grain	75.81
35	9	800.00	90.00	4.00	Hamburgar seedshell	90.71
21	10	700.00	60.00	3.00	Hamburgar seedshell	73.87
3	11	700.00	120.00	3.00	Spent grain	77.18
8	12	900.00	120.00	5.00	Spent grain	98.18
20	13	800.00	90.00	4.00	Spent grain	96.62
11	14	800.00	30.00	4.00	Spent grain	91.52
7	15	700.00	120.00	5.00	Spent grain	92.58
34	16	800.00	90.00	6.00	Hamburgar seedshell	91.05
14	17	800.00	90.00	6.00	Spent grain	92.87
27	18	700.00	120.00	5.00	Hamburgar seedshell	90.76
26	19	900.00	60.00	5.00	Hamburgar seedshell	98.2
30	20	1000.00	90.00	4.00	Hamburgar seedshell	92.86
23	21	700.00	120.00	3.00	Hamburgar seedshell	75.67
13	22	800.00	90.00	2.00	Spent grain	74.41
17	23	800.00	90.00	4.00	Spent grain	96.52
22	24	900.00	60.00	3.00	Hamburgar seedshell	84.29
16	25	800.00	90.00	4.00	Spent grain	95.46
36	26	800.00	90.00	4.00	Hamburgar seedshell	94.63
2	27	900.00	60.00	3.00	Spent grain	88.98
37	28	800.00	90.00	4.00	Hamburgar seedshell	94.73
24	29	900.00	120.00	3.00	Hamburgar seedshell	89.43
29	30	600.00	90.00	4.00	Hamburgar seedshell	74.32
1	31	700.00	60.00	3.00	Spent grain	75.35
19	32	800.00	90.00	4.00	Spent grain	95.56
5	33	700.00	60.00	5.00	Spent grain	90.59
40	34	800.00	90.00	4.00	Hamburgar seedshell	93.59
10	35	1000.00	90.00	4.00	Spent grain	94.75
39	36	800.00	90.00	4.00	Hamburgar seedshell	93.69
15	37	800.00	90.00	4.00	Spent grain	96.56
18	38	800.00	90.00	4.00	Spent grain	92.52
32	39	800.00	150.00	4.00	Hamburgar seedshell	92.35
12	40	800.00	150.00	4.00	Spent grain	94.2

APPENDIX C

Design matrix for optimization of adsorption process using BBD

Std Order	Run Order	pH (-)	Temp. (^oC)	Initial Conc.(mg/l)	Dosage (g)	Adsorbent Type	Removal Eff. (%)
64	1	6.00	35.00	150.00	0.05	MPAHS	64.4
92	2	6.00	35.00	50.00	0.05	CPAHS	62
36	3	6.00	35.00	50.00	0.10	CPASG	83.3
47	4	9.00	35.00	50.00	0.08	CPASG	75.5
107	5	9.00	35.00	150.00	0.08	CPAHS	61
18	6	9.00	35.00	50.00	0.08	MPASG	85.5
6	7	6.00	35.00	150.00	0.05	MPASG	54.39
73	8	6.00	30.00	150.00	0.08	MPAHS	71.1
35	9	6.00	35.00	150.00	0.05	CPASG	48
102	10	6.00	30.00	150.00	0.08	CPAHS	55
94	11	6.00	35.00	50.00	0.10	CPAHS	85
25	12	6.00	35.00	100.00	0.08	MPASG	71
5	13	6.00	35.00	50.00	0.05	MPASG	68.8
34	14	6.00	35.00	50.00	0.05	CPASG	60.8
4	15	9.00	40.00	100.00	0.08	MPASG	92.1
24	16	6.00	40.00	100.00	0.10	MPASG	88.8
43	17	6.00	40.00	50.00	0.08	CPASG	95.1
16	18	6.00	40.00	150.00	0.08	MPASG	71
78	19	9.00	35.00	150.00	0.08	MPAHS	77.7
66	20	6.00	35.00	150.00	0.10	MPAHS	69.9
104	21	3.00	35.00	50.00	0.08	CPAHS	66
26	22	6.00	35.00	100.00	0.08	MPASG	60
1	23	3.00	30.00	100.00	0.08	MPASG	61.1
62	24	9.00	40.00	100.00	0.08	MPAHS	99
48	25	3.00	35.00	150.00	0.08	CPASG	43.1
41	26	9.00	35.00	100.00	0.10	CPASG	74.5
19	27	3.00	35.00	150.00	0.08	MPASG	48.8
97	28	9.00	35.00	100.00	0.05	CPAHS	57

29	29	6.00	35.00	100.00	0.08	MPASG	71
90	30	3.00	40.00	100.00	0.08	CPAHS	70
14	31	6.00	40.00	50.00	0.08	MPASG	98.2
101	32	6.00	40.00	50.00	0.08	CPAHS	97
32	33	3.00	40.00	100.00	0.08	CPASG	68.6
31	34	9.00	30.00	100.00	0.08	CPASG	75.5
99	35	9.00	35.00	100.00	0.10	CPAHS	76
15	36	6.00	30.00	150.00	0.08	MPASG	61.1
81	37	6.00	30.00	100.00	0.10	MPAHS	89.9
17	38	3.00	35.00	50.00	0.08	MPASG	73.3
79	39	6.00	30.00	100.00	0.05	MPAHS	72.2
54	40	6.00	35.00	100.00	0.08	CPASG	62.7
95	41	6.00	35.00	150.00	0.10	CPAHS	54
13	42	6.00	30.00	50.00	0.08	MPASG	83.3
39	43	9.00	35.00	100.00	0.05	CPASG	55.9
87	44	6.00	35.00	100.00	0.08	MPAHS	81.04
8	45	6.00	35.00	150.00	0.10	MPASG	59.9
115	46	6.00	35.00	100.00	0.08	CPAHS	64
70	47	9.00	35.00	100.00	0.10	MPAHS	94.4
76	48	9.00	35.00	50.00	0.08	MPAHS	95.5
77	49	3.00	35.00	150.00	0.08	MPAHS	58.8
109	50	6.00	40.00	100.00	0.05	CPAHS	64
27	51	6.00	35.00	100.00	0.08	MPASG	71
57	52	6.00	35.00	100.00	0.08	CPASG	60.8
84	53	6.00	35.00	100.00	0.08	MPAHS	81
67	54	3.00	35.00	100.00	0.05	MPAHS	65.5
44	55	6.00	30.00	150.00	0.08	CPASG	53.9
59	56	3.00	30.00	100.00	0.08	MPAHS	71.1
96	57	3.00	35.00	100.00	0.05	CPAHS	50
38	58	3.00	35.00	100.00	0.05	CPASG	49
69	59	3.00	35.00	100.00	0.10	MPAHS	76.6
2	60	9.00	30.00	100.00	0.08	MPASG	85.5
100	61	6.00	30.00	50.00	0.08	CPAHS	75
33	62	9.00	40.00	100.00	0.08	CPASG	81.3

21	63	6.00	30.00	100.00	0.05	MPASG	62.2
45	64	6.00	40.00	150.00	0.08	CPASG	62.7
86	65	6.00	35.00	100.00	0.08	MPAHS	81
111	66	6.00	40.00	100.00	0.10	CPAHS	80
83	67	6.00	35.00	100.00	0.08	MPAHS	81
82	68	6.00	40.00	100.00	0.10	MPAHS	98.8
113	69	6.00	35.00	100.00	0.08	CPAHS	62
106	70	3.00	35.00	150.00	0.08	CPAHS	44
89	71	9.00	30.00	100.00	0.08	CPAHS	77
110	72	6.00	30.00	100.00	0.10	CPAHS	72
63	73	6.00	35.00	50.00	0.05	MPAHS	78.8
116	74	6.00	35.00	100.00	0.08	CPAHS	64
53	75	6.00	40.00	100.00	0.10	CPASG	78.4
103	76	6.00	40.00	150.00	0.08	CPAHS	64
51	77	6.00	40.00	100.00	0.05	CPASG	62.7
108	78	6.00	30.00	100.00	0.05	CPAHS	56
50	79	6.00	30.00	100.00	0.05	CPASG	54.9
91	80	9.00	40.00	100.00	0.08	CPAHS	83
22	81	6.00	40.00	100.00	0.05	MPASG	71
80	82	6.00	40.00	100.00	0.05	MPAHS	81
10	83	9.00	35.00	100.00	0.05	MPASG	63.3
12	84	9.00	35.00	100.00	0.10	MPASG	84.4
9	85	3.00	35.00	100.00	0.05	MPASG	55.5
105	86	9.00	35.00	50.00	0.08	CPAHS	77
20	87	9.00	35.00	150.00	0.08	MPASG	67.7
58	88	6.00	35.00	100.00	0.08	CPASG	62.7
114	89	6.00	35.00	100.00	0.08	CPAHS	64
30	90	3.00	30.00	100.00	0.08	CPASG	53.9
3	91	3.00	40.00	100.00	0.08	MPASG	77.7
28	92	6.00	35.00	100.00	0.08	MPASG	67.7
40	93	3.00	35.00	100.00	0.10	CPASG	58.8
56	94	6.00	35.00	100.00	0.08	CPASG	59.8
11	95	3.00	35.00	100.00	0.10	MPASG	66.6
88	96	3.00	30.00	100.00	0.08	CPAHS	55

55	97	6.00	35.00	100.00	0.08	CPASG	62.7
23	98	6.00	30.00	100.00	0.10	MPASG	79.9
93	99	6.00	35.00	150.00	0.05	CPAHS	49
98	100	3.00	35.00	100.00	0.10	CPAHS	60
72	101	6.00	40.00	50.00	0.08	MPAHS	99.6
49	102	9.00	35.00	150.00	0.08	CPASG	59.8
85	103	6.00	35.00	100.00	0.08	MPAHS	77.7
65	104	6.00	35.00	50.00	0.10	MPAHS	99.3
68	105	9.00	35.00	100.00	0.05	MPAHS	73.3
112	106	6.00	35.00	100.00	0.08	CPAHS	64
7	107	6.00	35.00	50.00	0.10	MPASG	94.4
52	108	6.00	30.00	100.00	0.10	CPASG	70.6
46	109	3.00	35.00	50.00	0.08	CPASG	64.7
61	110	3.00	40.00	100.00	0.08	MPAHS	87.7
75	111	3.00	35.00	50.00	0.08	MPAHS	83.3
37	112	6.00	35.00	150.00	0.10	CPASG	52.9
60	113	9.00	30.00	100.00	0.08	MPAHS	95.5
74	114	6.00	40.00	150.00	0.08	MPAHS	81
42	115	6.00	30.00	50.00	0.08	CPASG	73.5
71	116	6.00	30.00	50.00	0.08	MPAHS	93.3

APPENDIX D

DESIGN MATRIX FOR THE OPTIMIZATION OF REGENERATION STUDIES

A. DESIGN MATRIX FOR OPTIMIZATION OF DESORPTION PROCESS

Std Order	Run order	Temp (oC)	dosage (g)	initial dye conc. (mg/l)	Type of adsorbent	Equilibrium conc. (mg/l)
46	1	40.00	1.08	300.00	CPAHS	4.576
15	2	40.00	0.55	200.00	MPAHS	15.1032
4	3	50.00	1.08	200.00	MPAHS	8.7885
57	4	50.00	0.55	100.00	CPASG	12.8033
24	5	30.00	0.55	300.00	MPASG	8.7102
68	6	40.00	0.55	200.00	CPASG	9.5368
26	7	40.00	0.02	100.00	MPASG	13.2966
63	8	40.00	1.08	300.00	CPASG	6.24
33	9	40.00	0.55	200.00	MPASG	6.6441
52	10	30.00	0.02	200.00	CPASG	9.9304
19	11	50.00	0.02	200.00	MPASG	19.35
36	12	50.00	0.02	200.00	CPAHS	11.825
47	13	40.00	0.55	200.00	CPAHS	7.727
54	14	30.00	1.08	200.00	CPASG	5.6644
61	15	40.00	1.08	100.00	CPASG	6.7965
9	16	40.00	0.02	100.00	MPAHS	14.774
6	17	50.00	0.55	100.00	MPAHS	17.071
17	18	40.00	0.55	200.00	MPAHS	14.049
48	19	40.00	0.55	200.00	CPAHS	7.2413
11	20	40.00	0.02	300.00	MPAHS	11.838
60	21	40.00	0.02	100.00	CPASG	11.0805
16	22	40.00	0.55	200.00	MPAHS	13.166
38	23	50.00	1.08	200.00	CPAHS	4.8337
14	24	40.00	0.55	200.00	MPAHS	12.7895
13	25	40.00	0.55	200.00	MPAHS	14.7
1	26	30.00	0.02	200.00	MPAHS	13.2405
41	27	30.00	0.55	300.00	CPAHS	5.3229
53	28	50.00	0.02	200.00	CPASG	16.125
18	29	30.00	0.02	200.00	MPASG	11.9165
29	30	40.00	1.08	300.00	MPASG	7.488
35	31	30.00	0.02	200.00	CPAHS	7.28231
30	32	40.00	0.55	200.00	MPASG	13.5923
51	33	40.00	0.55	200.00	CPAHS	8.3067
20	34	30.00	1.08	200.00	MPASG	6.7973
5	35	30.00	0.55	100.00	MPAHS	2.7297
55	36	50.00	1.08	200.00	CPASG	6.5914
44	37	40.00	1.08	100.00	CPAHS	4.9841
34	38	40.00	0.55	200.00	MPASG	13.23
8	39	50.00	0.55	300.00	MPAHS	11.15
3	40	30.00	1.08	200.00	MPAHS	7.5525
23	41	50.00	0.55	100.00	MPASG	15.3639
59	42	50.00	0.55	300.00	CPASG	8.3625
40	43	50.00	0.55	100.00	CPAHS	9.3891

2	44	50.00	0.02	200.00	MPAHS	21.5
28	45	40.00	0.02	300.00	MPASG	10.6542
31	46	40.00	0.55	200.00	MPASG	12.6441
67	47	40.00	0.55	200.00	CPASG	9.8745
49	48	40.00	0.55	200.00	CPAHS	7.034
56	49	30.00	0.55	100.00	CPASG	10.2364
22	50	30.00	0.55	100.00	MPASG	12.2837
39	51	30.00	0.55	100.00	CPAHS	7.5067
50	52	40.00	0.55	200.00	CPAHS	8.085
45	53	40.00	0.02	300.00	CPAHS	6.5109
10	54	40.00	1.08	100.00	MPAHS	9.062
64	55	40.00	0.55	200.00	CPASG	11.3274
66	56	40.00	0.55	200.00	CPASG	11.025
7	57	30.00	0.55	300.00	MPAHS	9.678
21	58	50.00	1.08	200.00	MPASG	7.9097
37	59	30.00	1.08	200.00	CPAHS	4.1539
65	60	40.00	0.55	200.00	CPASG	9.5921
12	61	40.00	1.08	300.00	MPAHS	8.32
43	62	40.00	0.02	100.00	CPAHS	8.1257
25	63	50.00	0.55	300.00	MPASG	10.035
32	64	40.00	0.55	200.00	MPASG	11.8494
62	65	40.00	0.02	300.00	CPASG	8.8785
42	66	50.00	0.55	300.00	CPAHS	6.1325
58	67	30.00	0.55	300.00	CPASG	7.2585
27	68	40.00	1.08	100.00	MPASG	8.1558

B. DESIGN MATRIX FOR OPTIMIZATION OF MICROWAVE REGENERATION PROCESS USING CCD

Std Order	Run order	Power level (%)	initial dye conc. (mg/l)	radiation time (mins)	Type of adsorbent	Adsorptive capacity (mg/g)
13	1	58.50	150.00	7.00	MPAHS	34.851
24	2	81.00	200.00	8.00	MPASG	46.973
10	3	103.50	150.00	9.00	MPAHS	57.225
34	4	58.50	150.00	11.00	MPASG	53.155
69	5	13.50	150.00	9.00	CPAHS	27.32
5	6	36.00	100.00	10.00	MPAHS	57.641
38	7	58.50	150.00	9.00	MPASG	55.949
79	8	58.50	150.00	9.00	CPAHS	47.67
53	9	58.50	150.00	7.00	CPASG	27.41
46	10	81.00	100.00	10.00	CPASG	52
40	11	58.50	150.00	9.00	MPASG	57.137
26	12	81.00	100.00	10.00	MPASG	61.02
30	13	103.50	150.00	9.00	MPASG	55.146
14	14	58.50	150.00	11.00	MPAHS	55.157
11	15	58.50	50.00	9.00	MPAHS	62.5
15	16	58.50	150.00	9.00	MPAHS	59.172
28	17	81.00	200.00	10.00	MPASG	56.719
7	18	36.00	200.00	10.00	MPAHS	54.836

32	19	58.50	250.00	9.00	MPASG	54.585
70	20	103.50	150.00	9.00	CPAHS	45.86
66	21	81.00	100.00	10.00	CPAHS	51.2
72	22	58.50	250.00	9.00	CPAHS	45.35
45	23	36.00	100.00	10.00	CPASG	48.1195
37	24	58.50	150.00	9.00	MPASG	56.059
22	25	81.00	100.00	8.00	MPASG	47.5734
58	26	58.50	150.00	9.00	CPASG	49.62
2	27	81.00	100.00	8.00	MPAHS	49.4696
73	28	58.50	150.00	7.00	CPAHS	25.95
49	29	13.50	150.00	9.00	CPASG	28.81
21	30	36.00	100.00	8.00	MPASG	38.32
67	31	36.00	200.00	10.00	CPAHS	43.76
77	32	58.50	150.00	9.00	CPAHS	43.71
75	33	58.50	150.00	9.00	CPAHS	47.63
44	34	81.00	200.00	8.00	CPASG	40.14
50	35	103.50	150.00	9.00	CPASG	47.75
54	36	58.50	150.00	11.00	CPASG	45.87
61	37	36.00	100.00	8.00	CPAHS	30.5635
63	38	36.00	200.00	8.00	CPAHS	28.67
56	39	58.50	150.00	9.00	CPASG	49.52
23	40	36.00	200.00	8.00	MPASG	36.237
16	41	58.50	150.00	9.00	MPAHS	58.006
76	42	58.50	150.00	9.00	CPAHS	47.73
35	43	58.50	150.00	9.00	MPASG	52.781
19	44	58.50	150.00	9.00	MPAHS	58.116
18	45	58.50	150.00	9.00	MPAHS	59.282
59	46	58.50	150.00	9.00	CPASG	35.52
33	47	58.50	150.00	7.00	MPASG	33.245
20	48	58.50	150.00	9.00	MPAHS	59.216
12	49	58.50	250.00	9.00	MPAHS	56.62
39	50	58.50	150.00	9.00	MPASG	57.093
68	51	81.00	200.00	10.00	CPAHS	47.29
17	52	58.50	150.00	9.00	MPAHS	54.772
42	53	81.00	100.00	8.00	CPASG	40.6996
9	54	13.50	150.00	9.00	MPAHS	36.391
41	55	36.00	100.00	8.00	CPASG	32.1175
52	56	58.50	250.00	9.00	CPASG	47.2
65	57	36.00	100.00	10.00	CPAHS	46.2505
51	58	58.50	50.00	9.00	CPASG	62.024
64	59	81.00	200.00	8.00	CPAHS	38.43
31	60	58.50	50.00	9.00	MPASG	62.444
27	61	36.00	200.00	10.00	MPASG	52.836
55	62	58.50	150.00	9.00	CPASG	49.56
1	63	36.00	100.00	8.00	MPAHS	40.0293
43	64	36.00	200.00	8.00	CPASG	30.18
4	65	81.00	200.00	8.00	MPAHS	48.854
62	66	81.00	100.00	8.00	CPAHS	38.9758
78	67	58.50	150.00	9.00	CPAHS	46.69
25	68	36.00	100.00	10.00	MPASG	55.576

48	69	81.00	200.00	10.00	CPASG	49.18
57	70	58.50	150.00	9.00	CPASG	48.56
8	71	81.00	200.00	10.00	MPAHS	58.798
3	72	36.00	200.00	8.00	MPAHS	37.898
29	73	13.50	150.00	9.00	MPASG	34.752
6	74	81.00	100.00	10.00	MPAHS	61.9
80	75	58.50	150.00	9.00	CPAHS	46.59
36	76	58.50	150.00	9.00	MPASG	57.203
71	77	58.50	50.00	9.00	CPAHS	60.676
47	78	36.00	200.00	10.00	CPASG	45.58
60	79	58.50	150.00	9.00	CPASG	48.46
74	80	58.50	150.00	11.00	CPAHS	44.05

C. DESIGN MATRIX FOR THE OPTIMIZATION OF CONVENTIONAL REGENERATION PROCESS USING CCD

Std Order	Run order	Temp (oC)	initial dye conc. (mg/l)	Time (mins)	Type of adsorbent	Adsorptive capacity (mg/g)
43	1	350.00	200.00	10.00	CPASG	39.9
27	2	350.00	200.00	30.00	MPASG	51.615
9	3	250.00	150.00	20.00	MPAHS	43.113
13	4	450.00	150.00	0.00	MPAHS	42.317
1	5	350.00	100.00	10.00	MPAHS	44.9941
56	6	450.00	150.00	20.00	CPASG	49.35
22	7	550.00	100.00	10.00	MPASG	48.8944
25	8	350.00	100.00	30.00	MPASG	53.032
52	9	450.00	250.00	20.00	CPASG	48.7
28	10	550.00	200.00	30.00	MPASG	53.623
36	11	450.00	150.00	20.00	MPASG	53.839
15	12	450.00	150.00	20.00	MPAHS	54.891
62	13	550.00	100.00	10.00	CPAHS	44.4494
49	14	250.00	150.00	20.00	CPASG	39.19
23	15	350.00	200.00	10.00	MPASG	43.034
65	16	350.00	100.00	30.00	CPAHS	48.2105
20	17	450.00	150.00	20.00	MPAHS	54.288
7	18	350.00	200.00	30.00	MPAHS	52.65
73	19	450.00	150.00	0.00	CPAHS	37.72
77	20	450.00	150.00	20.00	CPAHS	48.94
63	21	350.00	200.00	10.00	CPAHS	39.12
47	22	350.00	200.00	30.00	CPASG	47.86
72	23	450.00	250.00	20.00	CPAHS	47.75
50	24	650.00	150.00	20.00	CPASG	48.989
78	25	450.00	150.00	20.00	CPAHS	46.9
64	26	550.00	200.00	10.00	CPAHS	44.17
74	27	450.00	150.00	40.00	CPAHS	47.07
71	28	450.00	50.00	20.00	CPAHS	55.668
29	29	250.00	150.00	20.00	MPASG	42.266
68	30	550.00	200.00	30.00	CPAHS	48.75
26	31	550.00	100.00	30.00	MPASG	55.85

55	32	450.00	150.00	20.00	CPASG	47.83
2	33	550.00	100.00	10.00	MPAHS	49.8748
16	34	450.00	150.00	20.00	MPAHS	54.345
30	35	650.00	150.00	20.00	MPASG	52.809
6	36	550.00	100.00	30.00	MPAHS	56.3
33	37	450.00	150.00	0.00	MPASG	31.147
37	38	450.00	150.00	20.00	MPASG	53.282
40	39	450.00	150.00	20.00	MPASG	51.587
70	40	650.00	150.00	20.00	CPAHS	48.01
80	41	450.00	150.00	20.00	CPAHS	48.92
75	42	450.00	150.00	20.00	CPAHS	48.44
21	43	350.00	100.00	10.00	MPASG	44.11
39	44	450.00	150.00	20.00	MPASG	53.816
69	45	250.00	150.00	20.00	CPAHS	38.42
58	46	450.00	150.00	20.00	CPASG	49.92
38	47	450.00	150.00	20.00	MPASG	53.873
54	48	450.00	150.00	40.00	CPASG	48.01
31	49	450.00	50.00	20.00	MPASG	61.2355
3	50	350.00	200.00	10.00	MPAHS	43.892
60	51	450.00	150.00	20.00	CPASG	49.4
48	52	550.00	200.00	30.00	CPASG	49.73
67	53	350.00	200.00	30.00	CPAHS	46.92
44	54	550.00	200.00	10.00	CPASG	45.05
17	55	450.00	150.00	20.00	MPAHS	54.914
5	56	350.00	100.00	30.00	MPAHS	54.09
46	57	550.00	100.00	30.00	CPASG	57
57	58	450.00	150.00	20.00	CPASG	49.9
34	59	450.00	150.00	40.00	MPASG	51.78
61	60	350.00	100.00	10.00	CPAHS	38.19
35	61	450.00	150.00	20.00	MPASG	40.1003
76	62	450.00	150.00	20.00	CPAHS	48.39
8	63	550.00	200.00	30.00	MPAHS	54.698
53	64	450.00	150.00	0.00	CPASG	38.47
24	65	550.00	200.00	10.00	MPASG	48.584
14	66	450.00	150.00	40.00	MPAHS	52.815
32	67	450.00	250.00	20.00	MPASG	52.519
12	68	450.00	250.00	20.00	MPAHS	53.57
11	69	450.00	50.00	20.00	MPAHS	62.457
45	70	350.00	100.00	30.00	CPASG	49.1768
59	71	450.00	150.00	20.00	CPASG	49.95
4	72	550.00	200.00	10.00	MPAHS	49.557
10	73	650.00	150.00	20.00	MPAHS	53.884
19	74	450.00	150.00	20.00	MPAHS	52.616
41	75	350.00	100.00	10.00	CPASG	40.9037
79	76	450.00	150.00	20.00	CPAHS	48.98
42	77	550.00	100.00	10.00	CPASG	45.3407
18	78	450.00	150.00	20.00	MPAHS	54.948
51	79	450.00	50.00	20.00	CPASG	56.779
66	80	550.00	100.00	30.00	CPAHS	50.77

APPENDIX E
FTIR SPECTRA OF ACTIVATED CARBONS

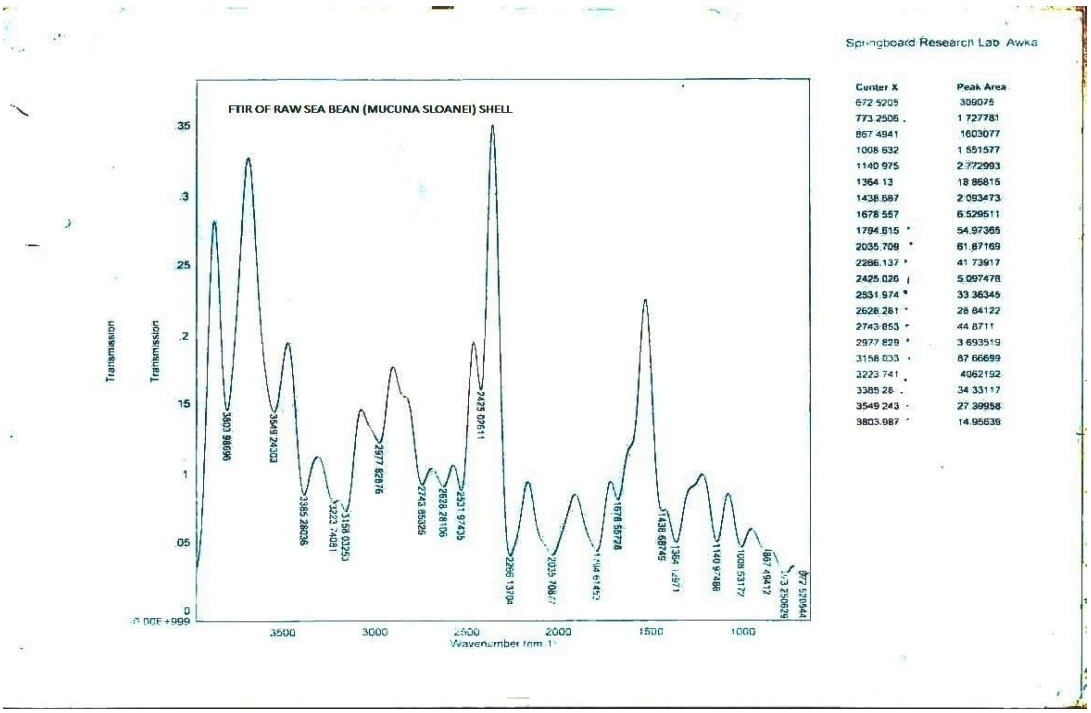

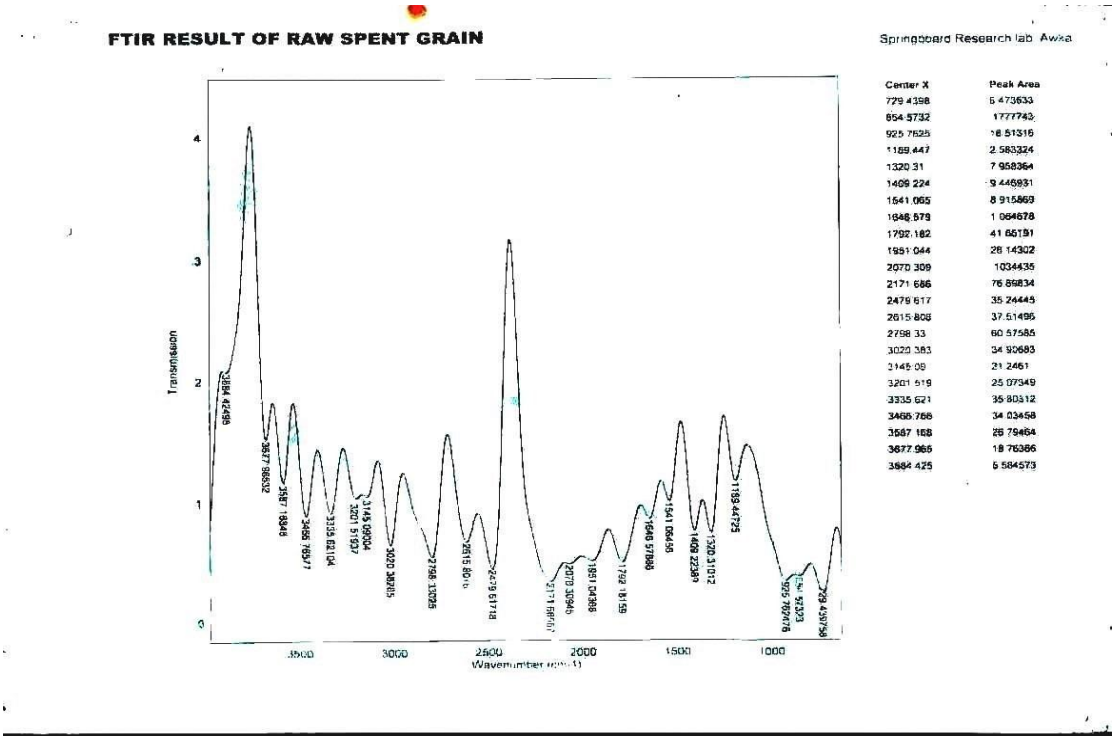

FTIR RESULT OF ACTIVATED HAMBURGAR

Springboard Research Lab Awka

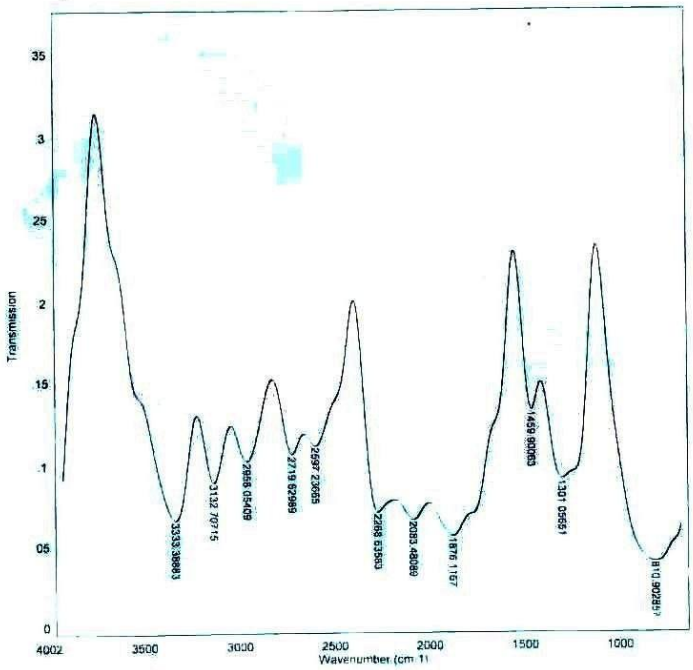

Center X	Peak Area
810.9029	28.13256
1301.057	43.79635
1459.901	3.298042
1876.117	71.39521
2083.481	34.7377
2268.636	33.78009
2597.237	35.8323
2719.63	26.47724
2958.054	37.27331
3132.707	33.11498
3333.389	82.70182

FTIR RESULT OF SPENT GRAIN ACTIVATED CARBON

Springboard research Lab Awka

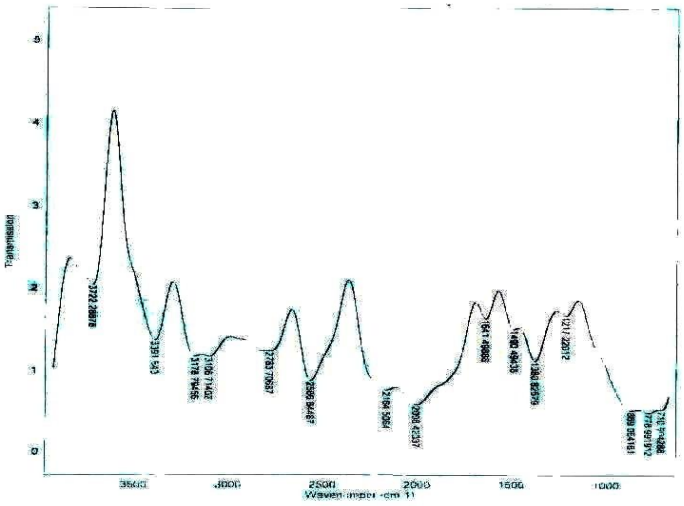

Center X	Peak Area
710.9043	2561125
778.8919	14.29834
860.0542	5.481755
1217.22	6801101
1380.826	14.28696
1490.494	1631684
1841.469	1.585474
2006.423	91.29973
2164.505	8.133114
2566.845	48.32967
2783.707	53.48586
3105.714	34.13762
3178.795	34.20368
3391.543	67.63837
3722.289	15.5333

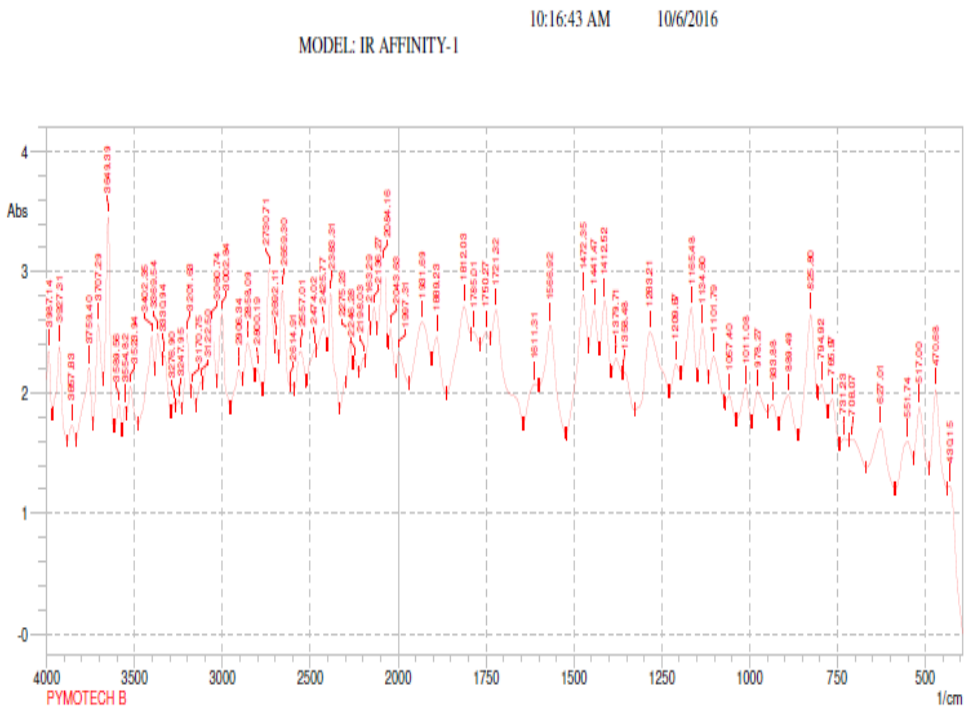

Saturated MPAHS

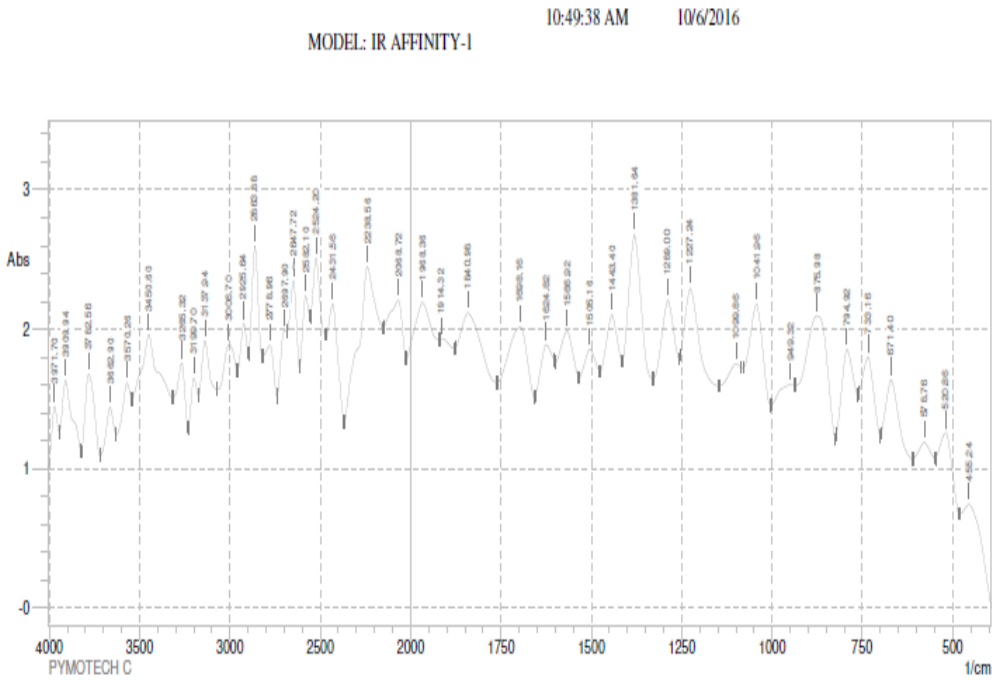

Chemical regenerated MPAHS

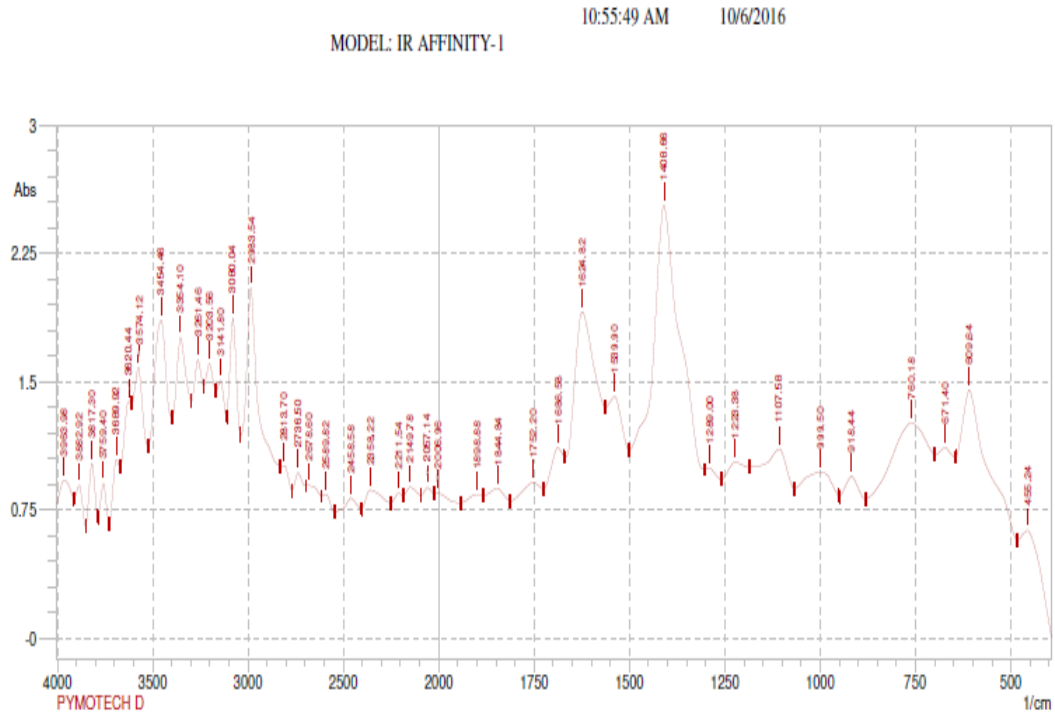

Microwave regenerated MPAHS

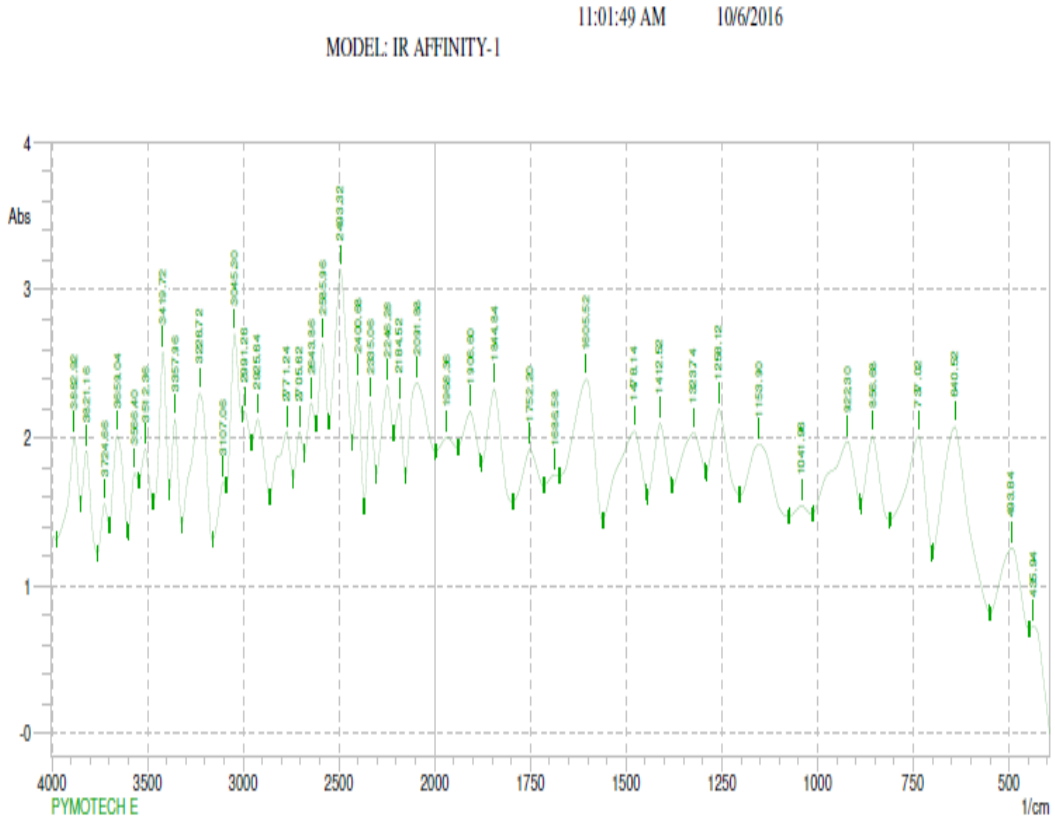

Conventional regenerated MPAHS

APPENDIX F
KINETICS PLOTS FOR SWISS BLUE DYE ADSORPTION PROCESS

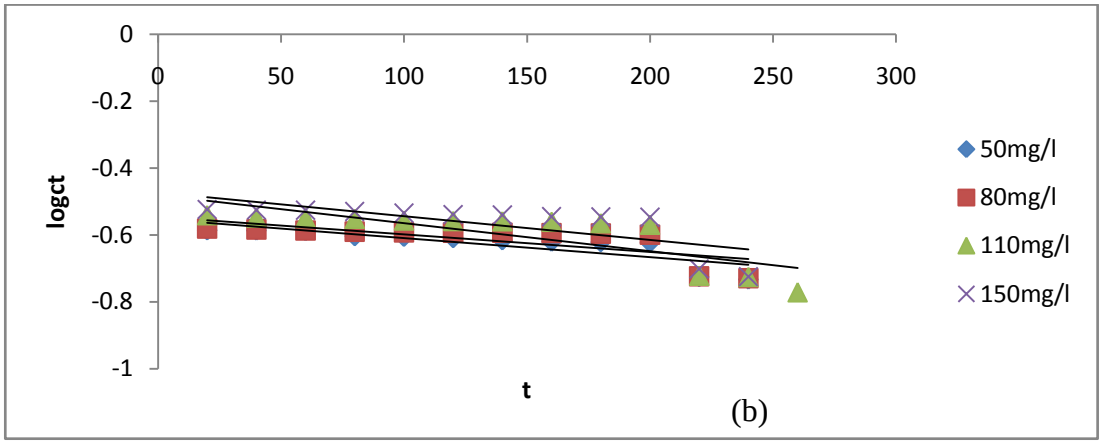

(a)

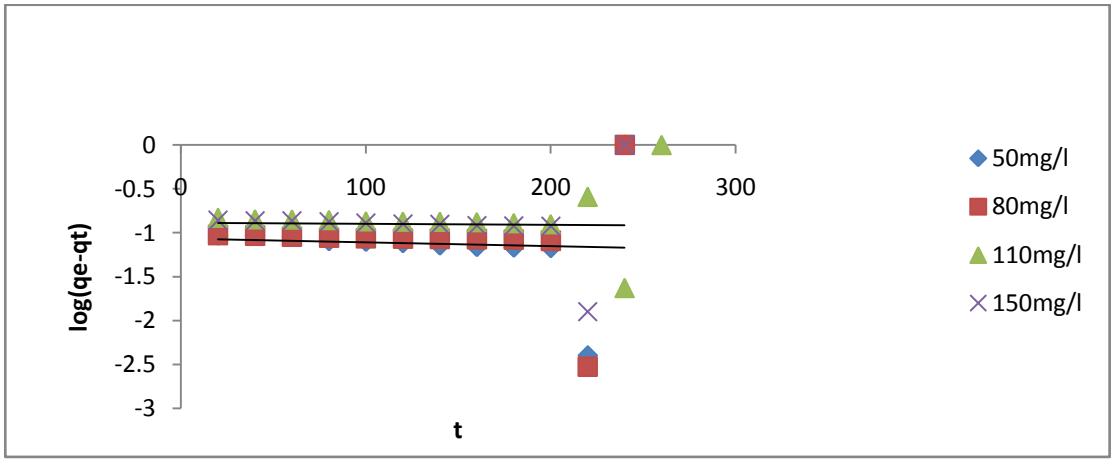

(b)

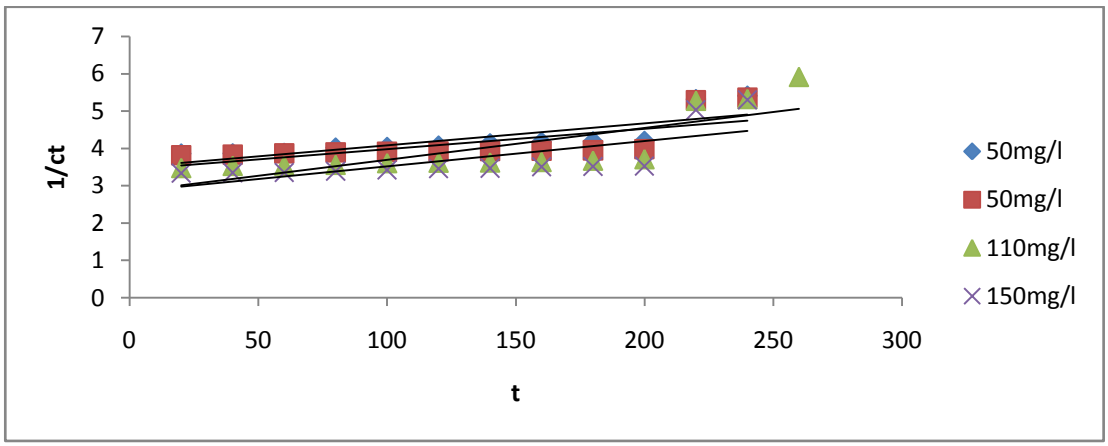

(c)

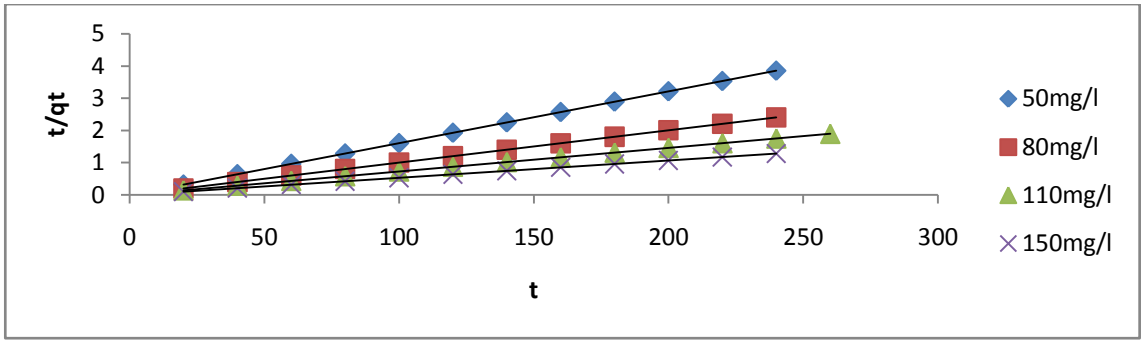

(d)

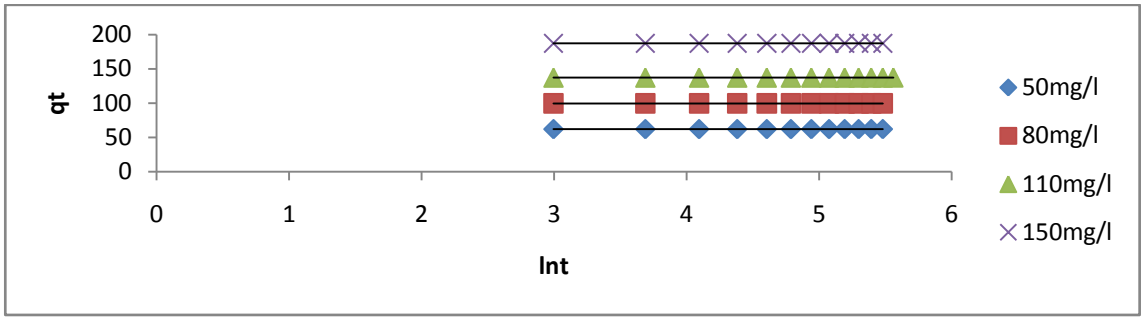

(e)

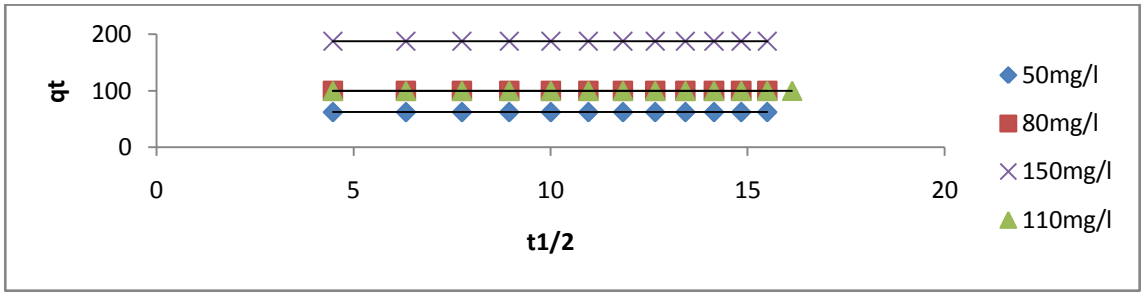

(f)

Kinetic plots of Swiss blue dye adsorption on MPAHS (a) First order, (b) Pseudo first order, (c) Second order, (d) Pseudo second order, (e) Elovich, (f) Intra particle diffusion models

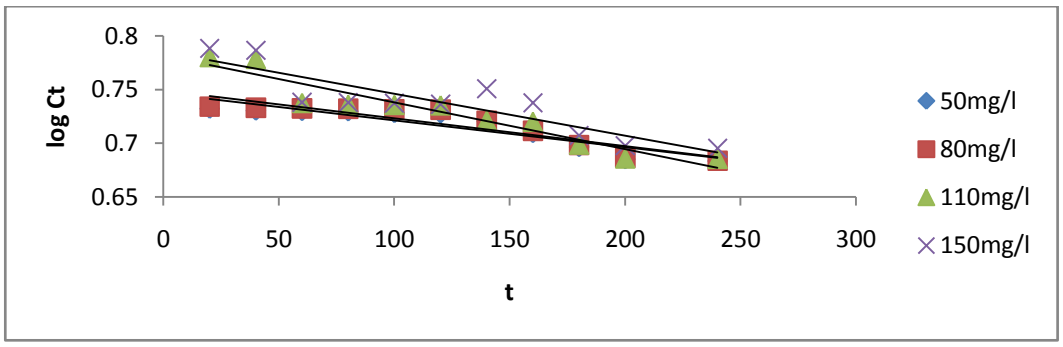

(a)

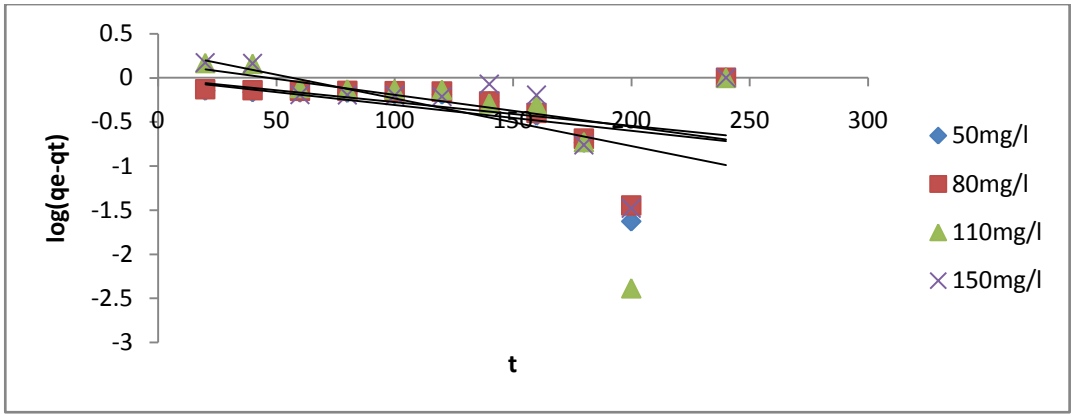
0.5
0
-0.5
-1
-1.5
-2
-2.5
-3
0
50
100
150
200
250
300
log(qe-qt)
t
50mg/l
80mg/l
110mg/l
150mg/l

(b)

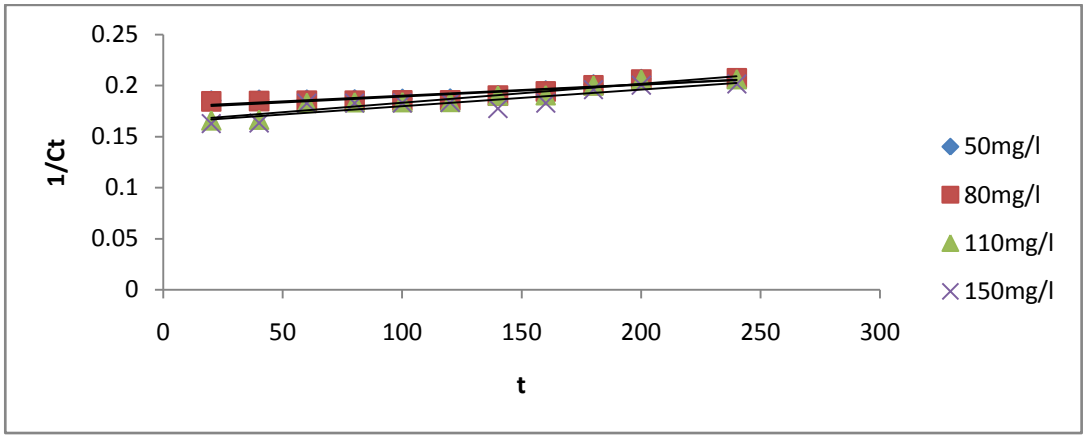
0.25
0.2
0.15
0.1
0.05
0
0
50
100
150
200
250
300
1/Ct
t
50mg/l
80mg/l
110mg/l
150mg/l

(c)

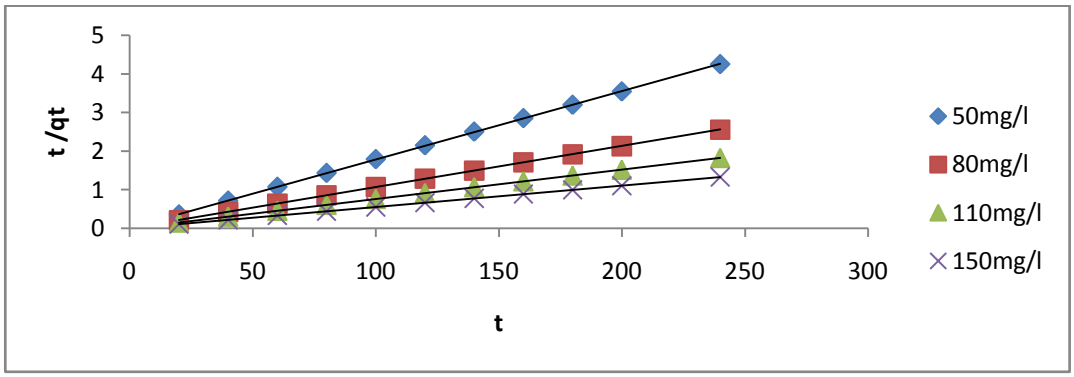
5
4
3
2
1
0
0
50
100
150
200
250
300
t /qt
t
50mg/l
80mg/l
110mg/l
150mg/l

(d)

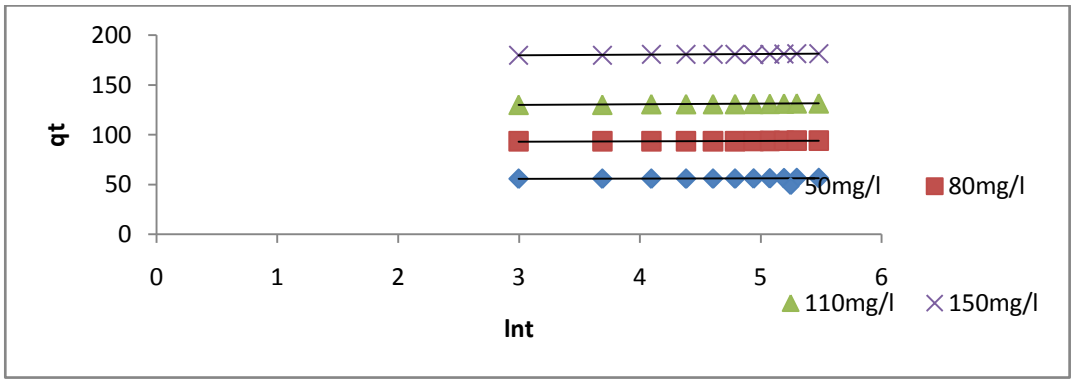
200
150
100
50
0
0
1
2
3
4
5
6
qt
lnt
50mg/l
80mg/l
110mg/l
150mg/l

(e)

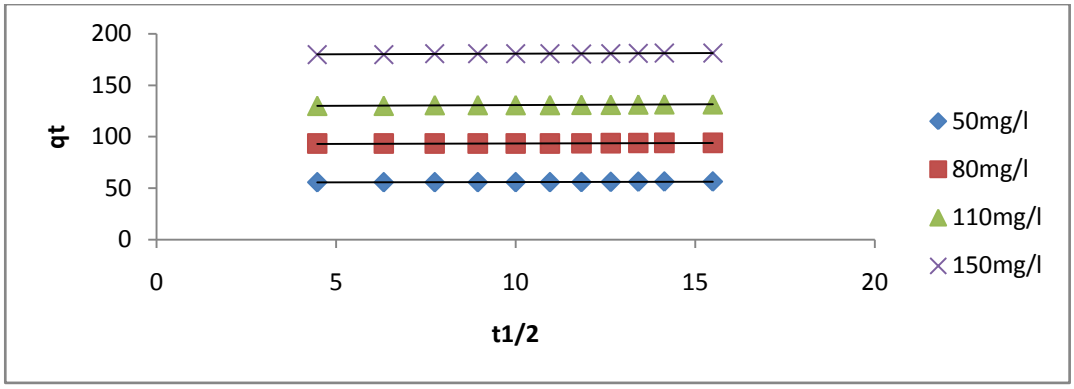

(f)

Kinetic plots of Swiss blue dye adsorption on MPASG (a) First order, (b) Pseudo first order, (c) Second order, (d) Pseudo second order, (e) Elovich, (f) Intra particle diffusion models

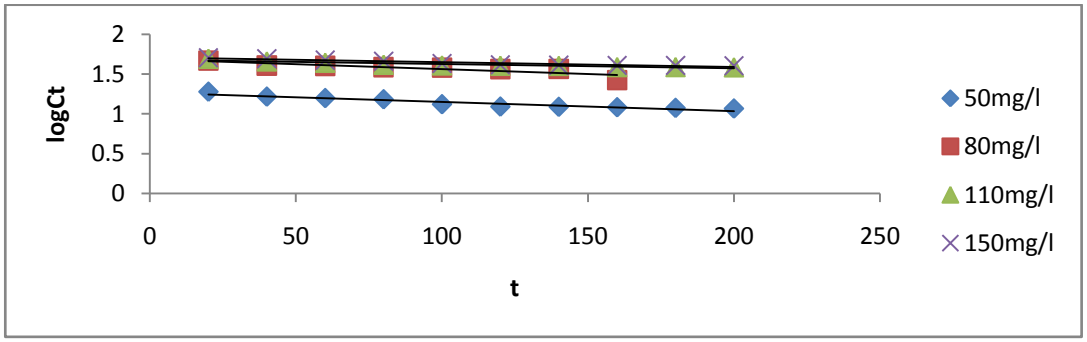

(a)

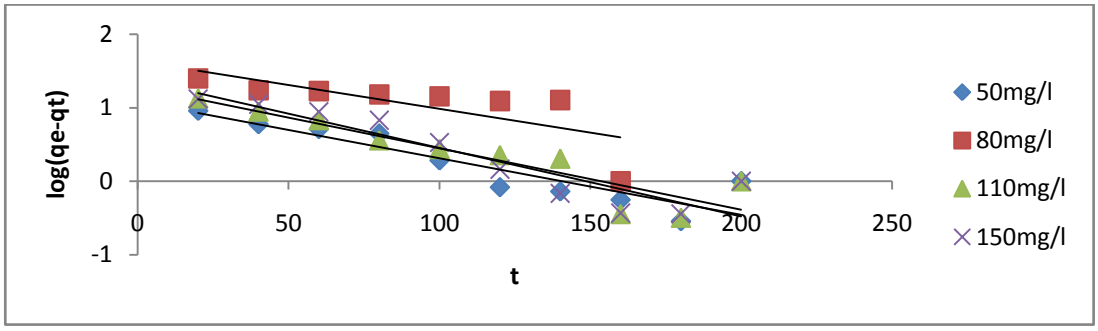

(b)

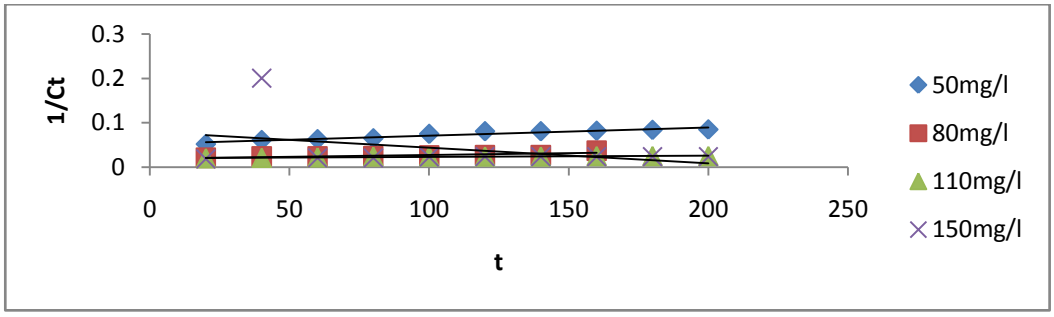

(c)

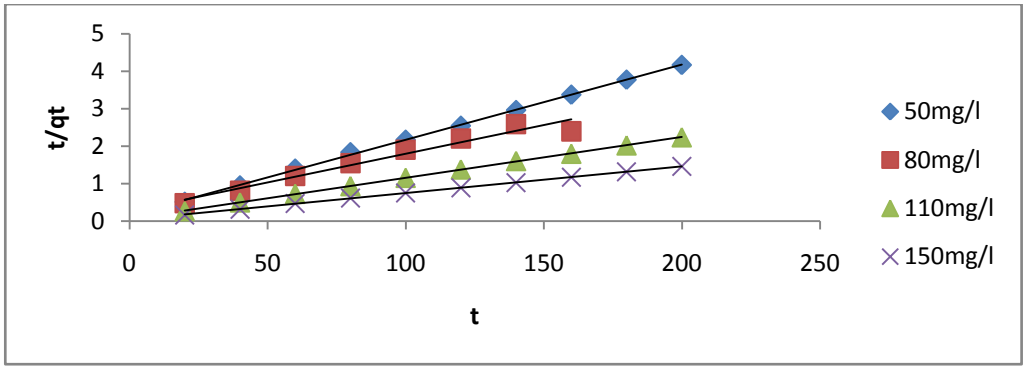

(d)

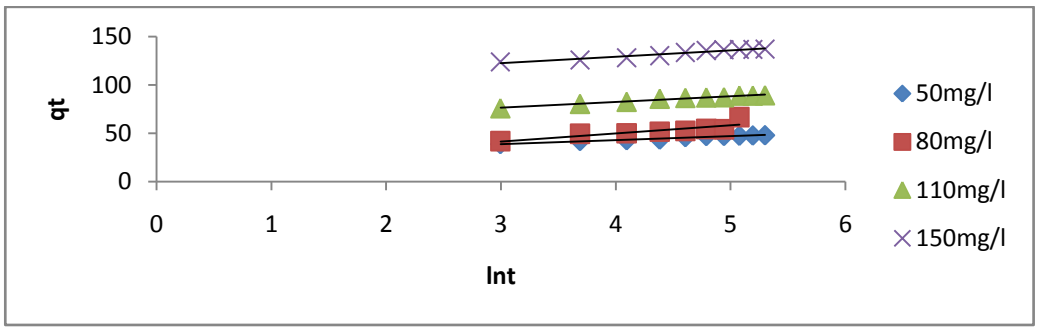

(e)

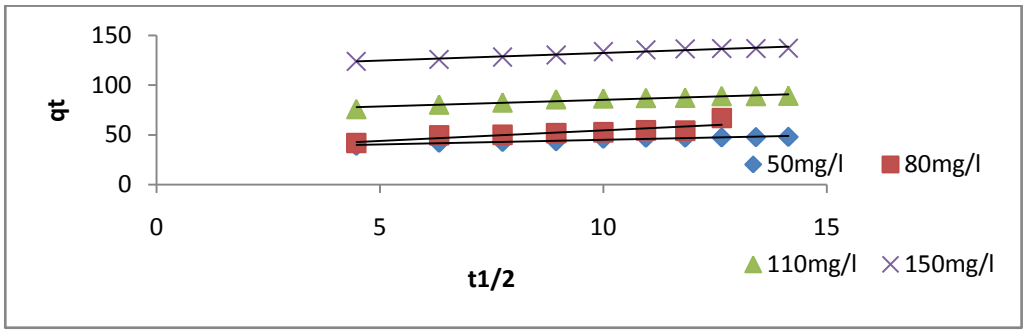

(f)

Kinetic plots of Swiss blue dye adsorption on CPASG (a) First order, (b) Pseudo first order, (c) Second order, (d) Pseudo second order, (e) Elovich, (f) Intra particle diffusion models

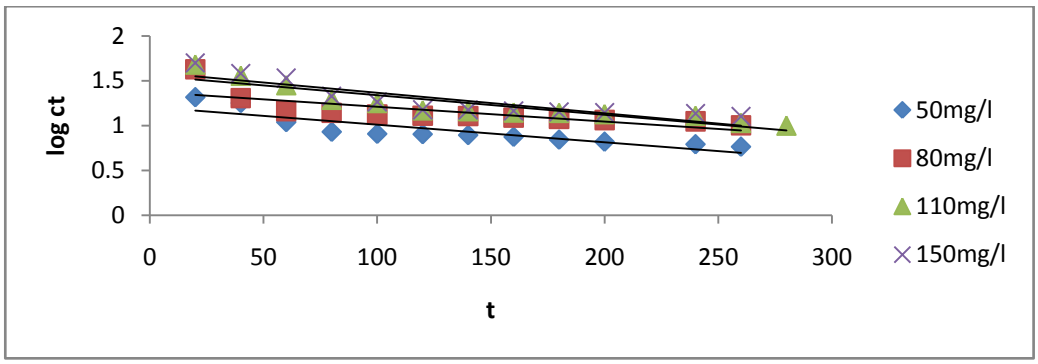

(a)

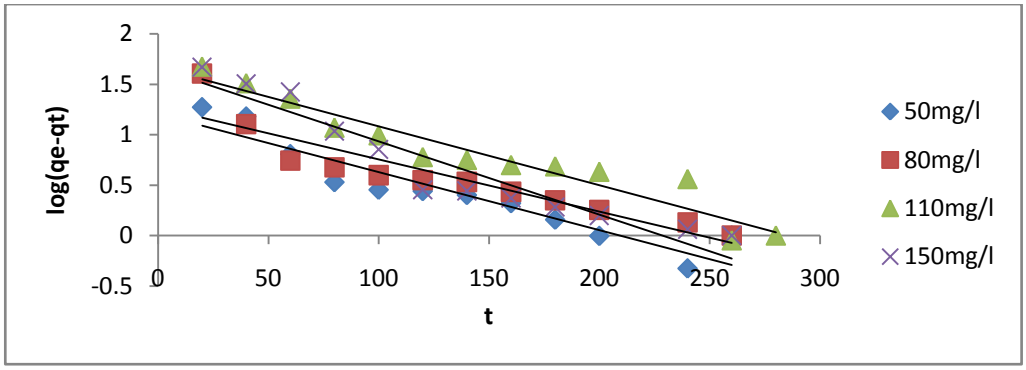
log(qe-qt)
2
1.5
1
0.5
0
-0.5
0
50
100
150
200
250
300
t
50mg/l
80mg/l
110mg/l
150mg/l

(b)

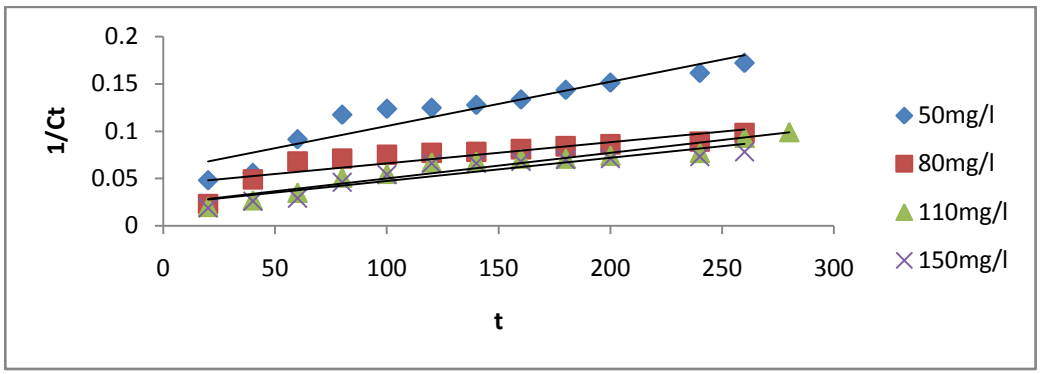
1/Ct
0.2
0.15
0.1
0.05
0
0
50
100
150
200
250
300
t
50mg/l
80mg/l
110mg/l
150mg/l

(c)

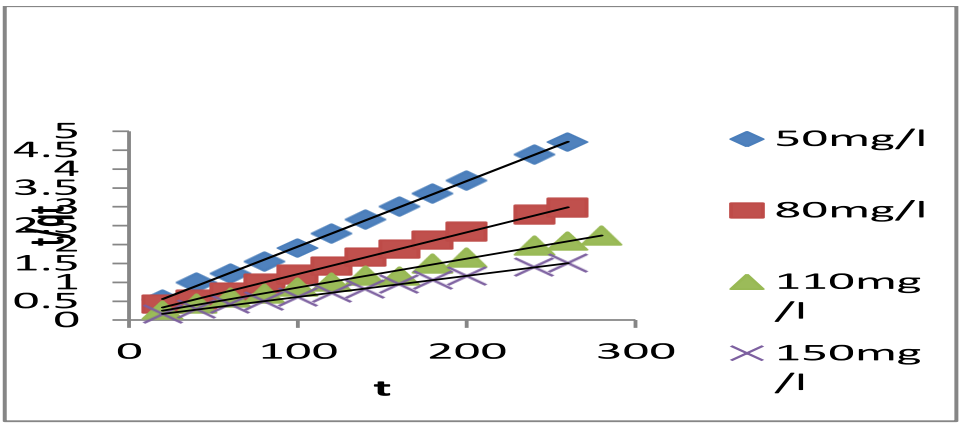
t/qt
4.5
3.5
2.5
1.5
0.5
0
0
100
200
300
t
50mg/l
80mg/l
110mg/l
150mg/l

(d)

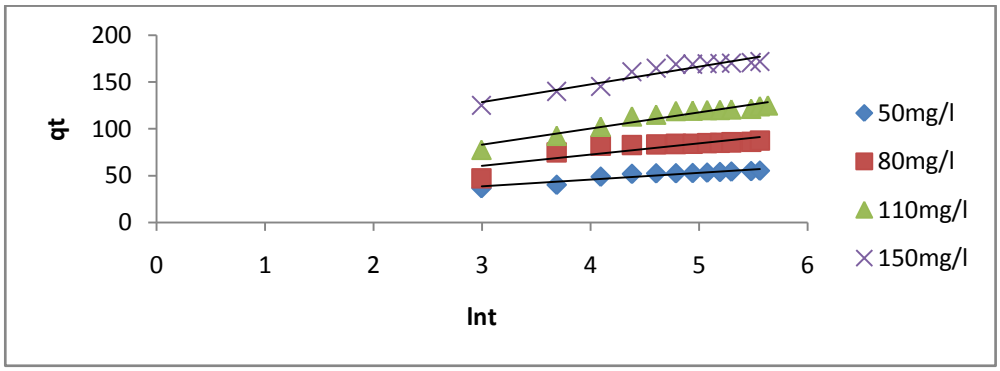
qt
200
150
100
50
0
0
1
2
3
4
5
6
lnt
50mg/l
80mg/l
110mg/l
150mg/l

(e)

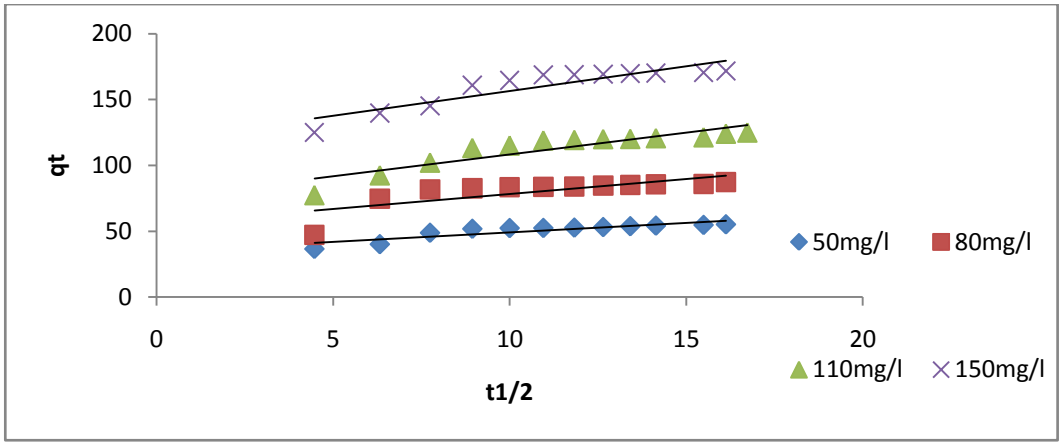

(f)

Kinetic plots of Swiss blue dye adsorption on CPAHS (a) First order, (b) Pseudo first order, (c) Second order, (d) Pseudo second order, (e) Elovich, (f) Intra particle diffusion models

APPENDIX G
ISOTHERM PLOTS FOR SWISS BLUE DYE ADSORPTION PROCESS

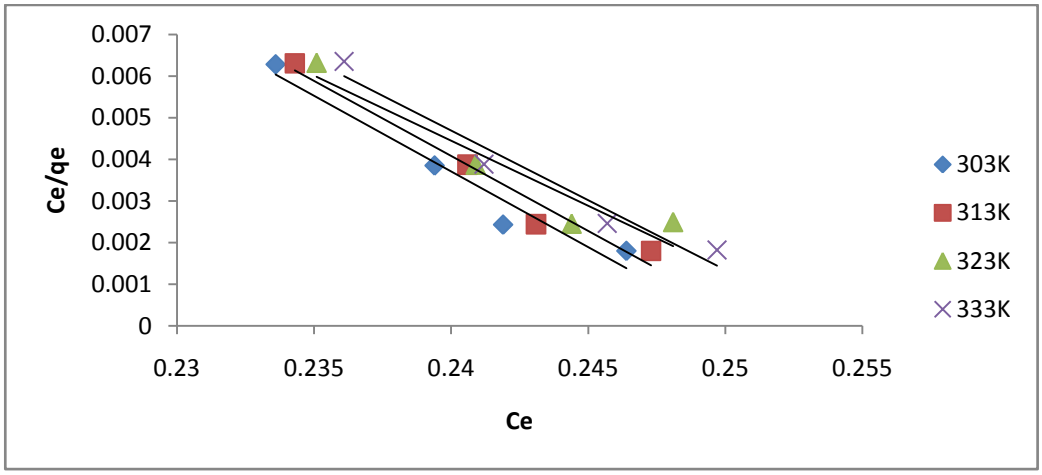

(a)

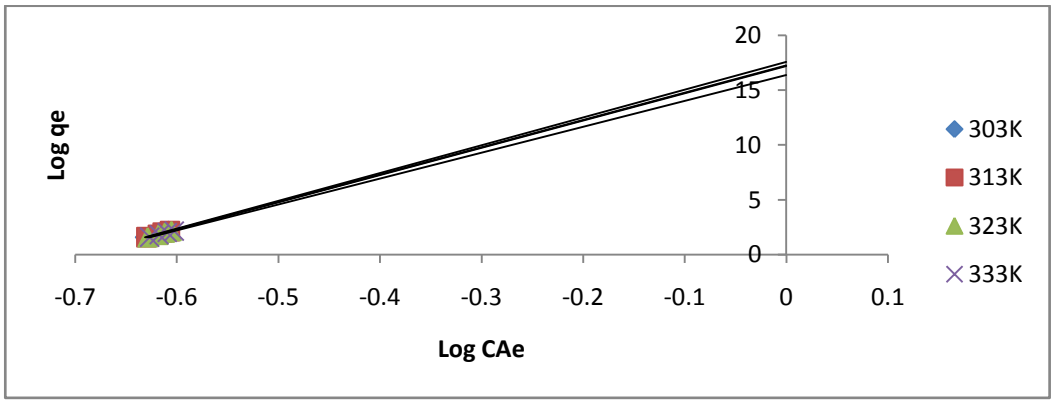

(b)

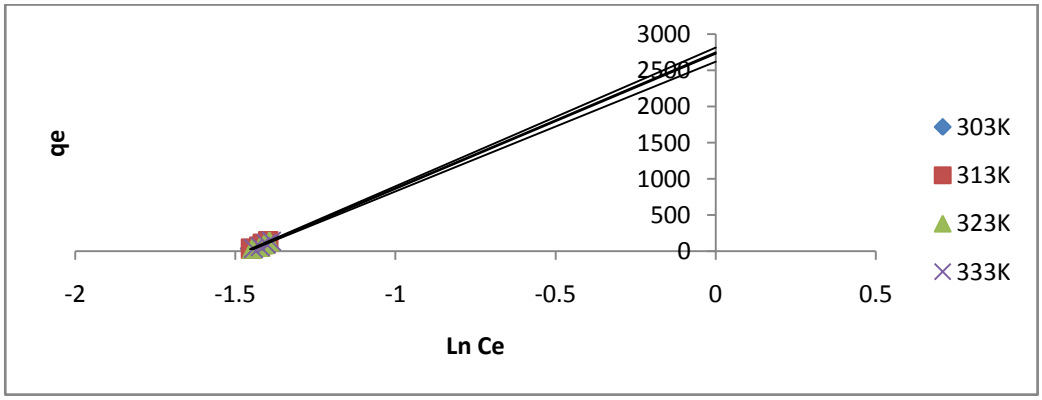

(c)

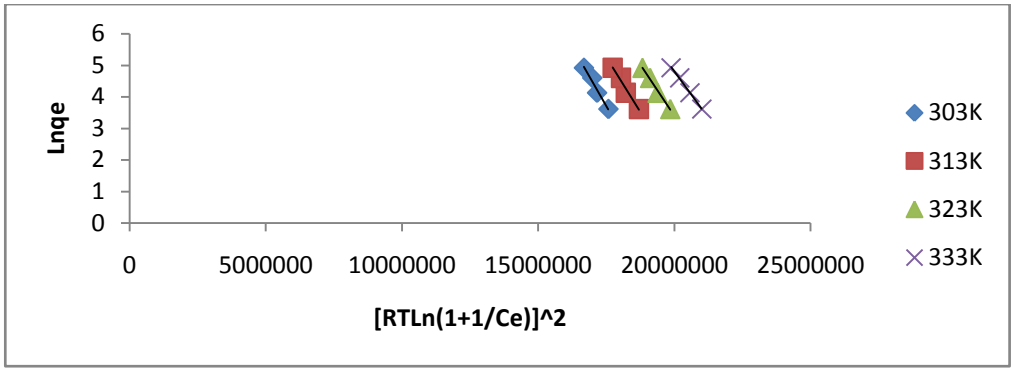

(d)

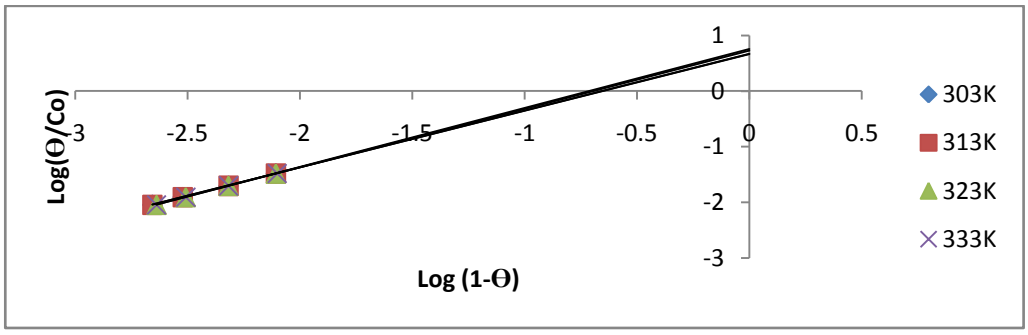

(e)

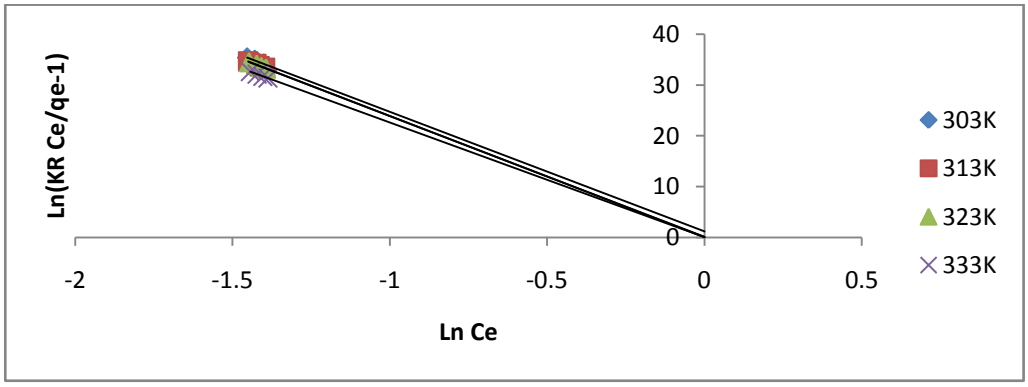

(f)

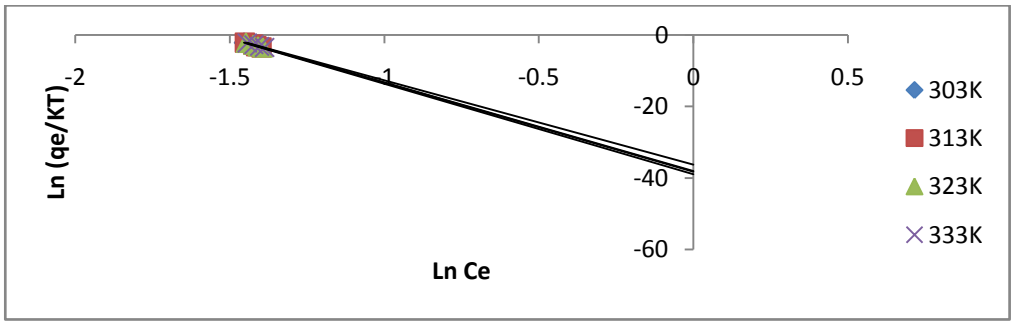

(g)

Isotherm model plots of Swiss blue dye adsorption on MPAHS (a) Langmuir (b) Freundlich, (c) Temkin, (d) D-R (e) Flory-huggins, (f) Redlich Peterson, (g) Toth, (h) Sip

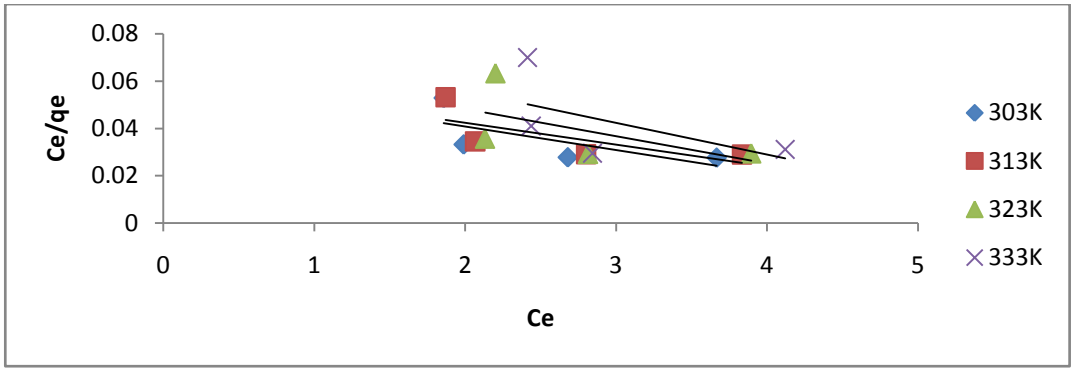
0.08
0.06
0.04
0.02
0
Ce/qe
0
1
2
3
4
5
Ce
303K
313K
323K
333K

(a)

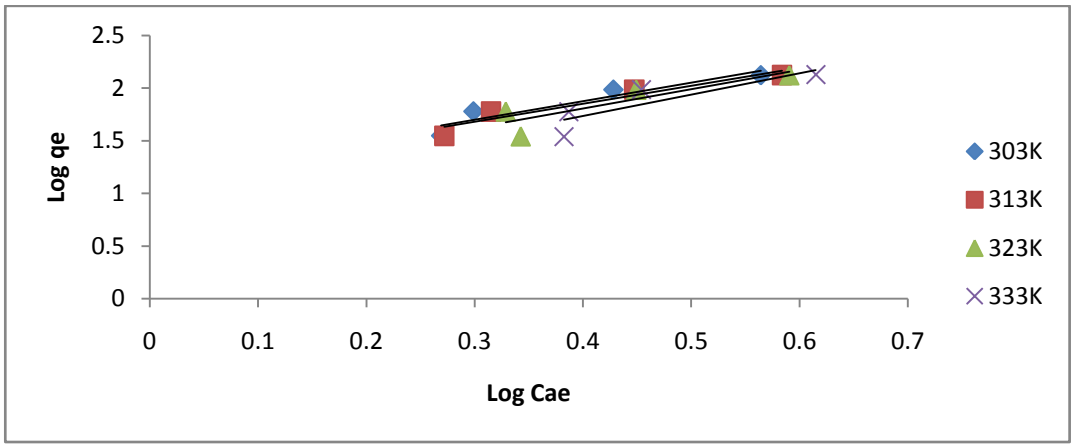
2.5
2
1.5
1
0.5
0
Log qe
0
0.1
0.2
0.3
0.4
0.5
0.6
0.7
Log Cae
303K
313K
323K
333K

(b)

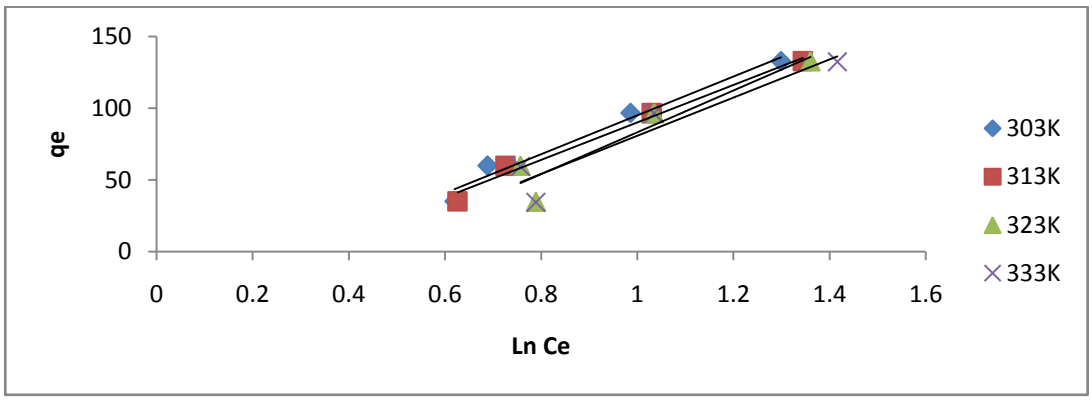
150
100
50
0
qe
0
0.2
0.4
0.6
0.8
1
1.2
1.4
1.6
Ln Ce
303K
313K
323K
333K

(c)

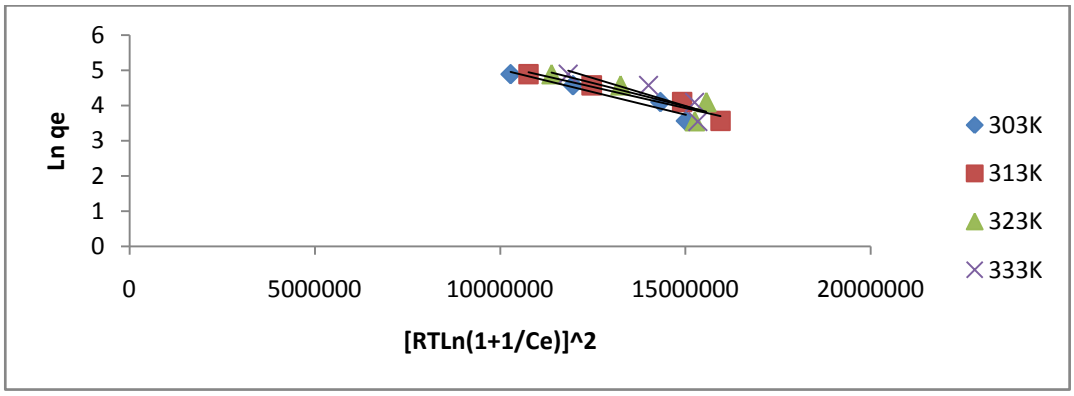
6
5
4
3
2
1
0
Ln qe
0
5000000
10000000
15000000
20000000
[RTLn(1+1/Ce)]^2
303K
313K
323K
333K

(d)

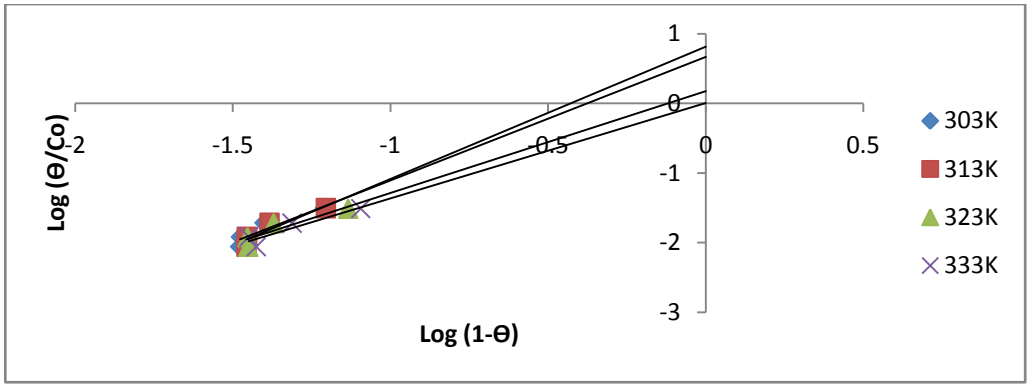

(e)

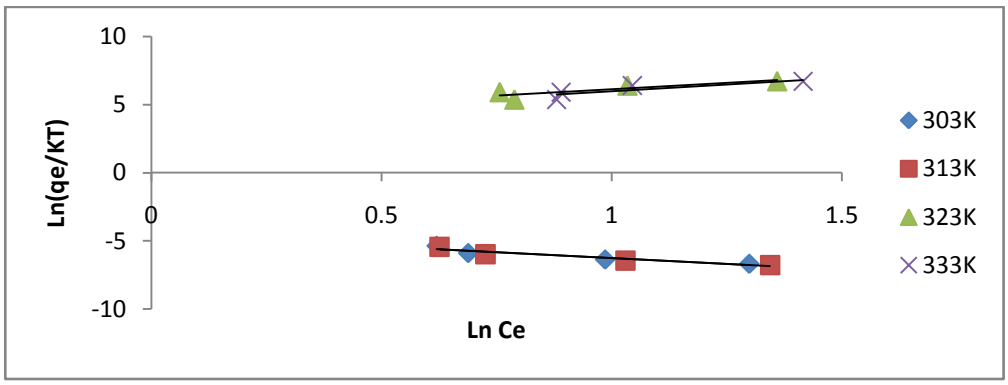

(f)

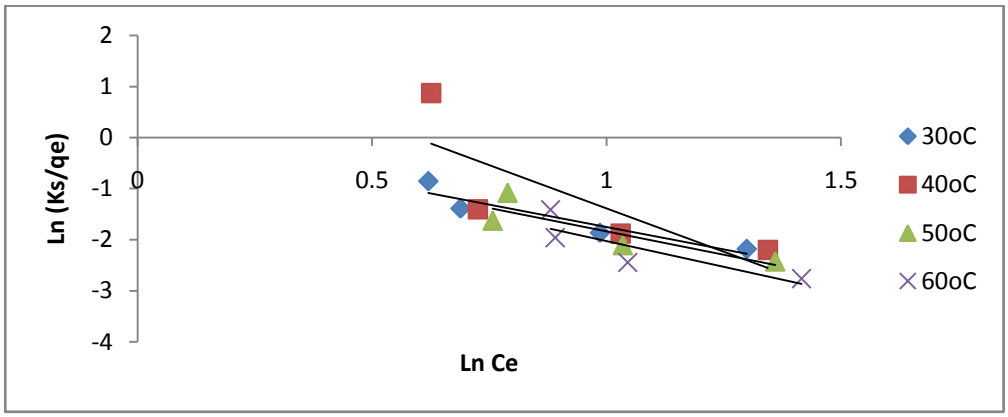

(g)

Isotherm plots of Swiss blue dye adsorption on MPASG (a) Langmuir (b) Freundlich, (c) Temkin, (d) D-R (g) Toth, (h) Sip

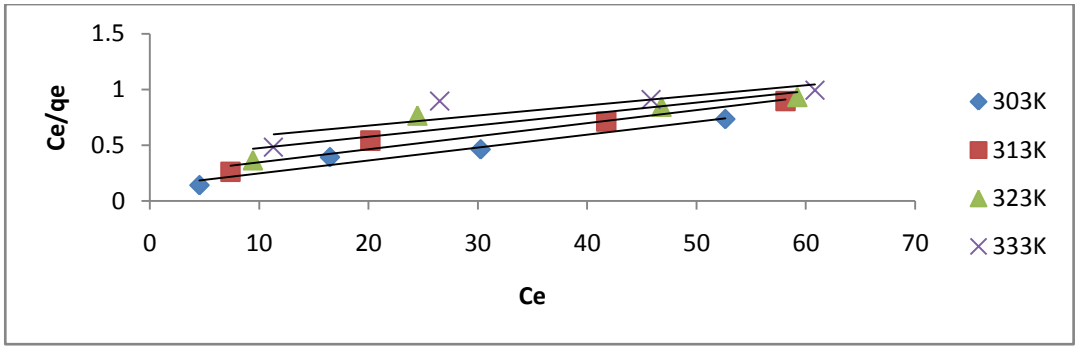
1.5
1
0.5
0
Ce/qe
0
10
20
30
40
50
60
70
Ce
303K
313K
323K
333K

(a)

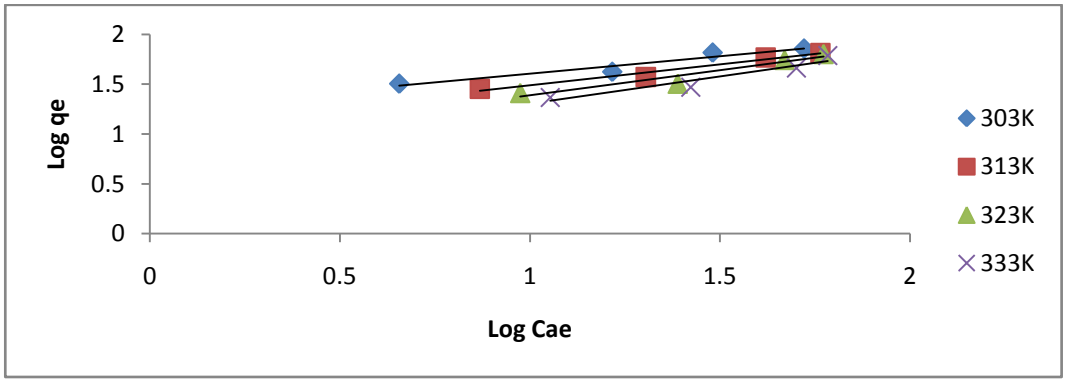
2
1.5
1
0.5
0
Log qe
0
0.5
1
1.5
2
Log Cae
303K
313K
323K
333K

(b)

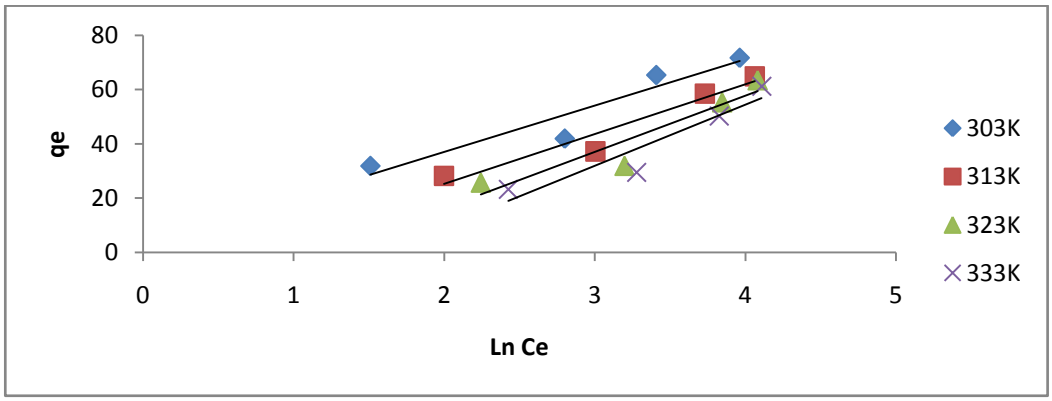
80
60
40
20
0
qe
0
1
2
3
4
5
Ln Ce
303K
313K
323K
333K

(c)

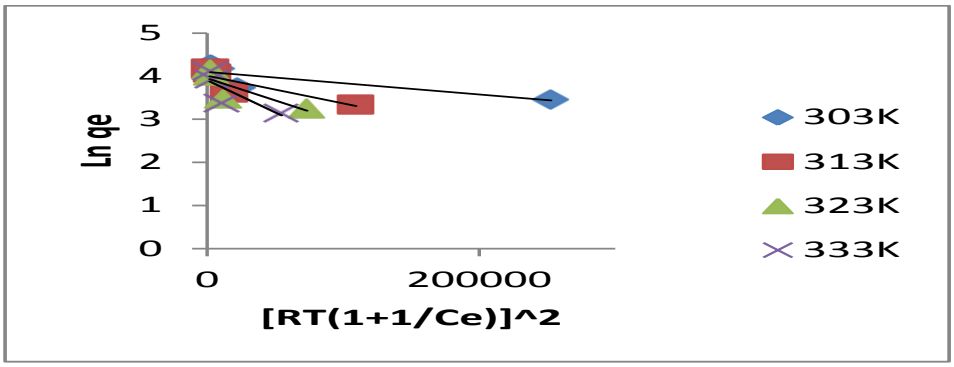
Ln qe
5
4
3
2
1
0
0
200000
[RT(1+1/Ce)]^2
303K
313K
323K
333K

(d)

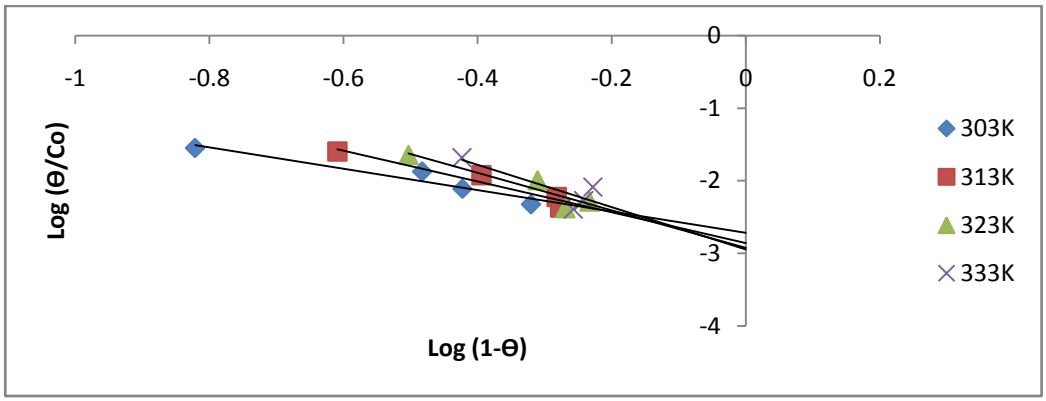
Log (Θ/Co)
-1
-0.8
-0.6
-0.4
-0.2
0
0.2
0
-1
-2
-3
-4
Log (1-Θ)
303K
313K
323K
333K

(e)

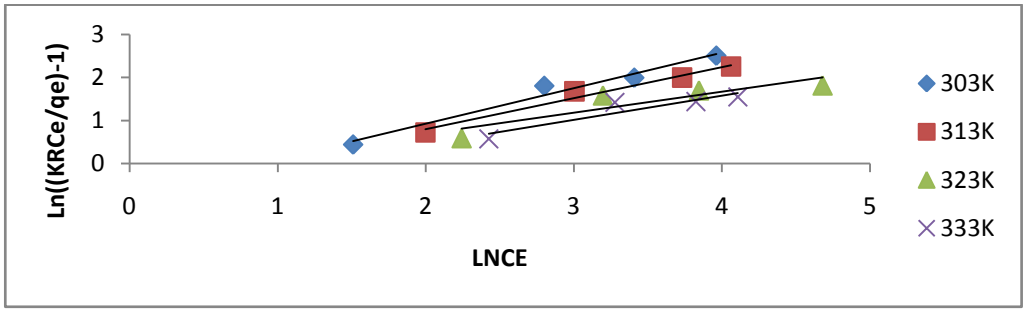
Ln((KRCe/qe)-1)
3
2
1
0
0
1
2
3
4
5
LNCE
303K
313K
323K
333K

(f)

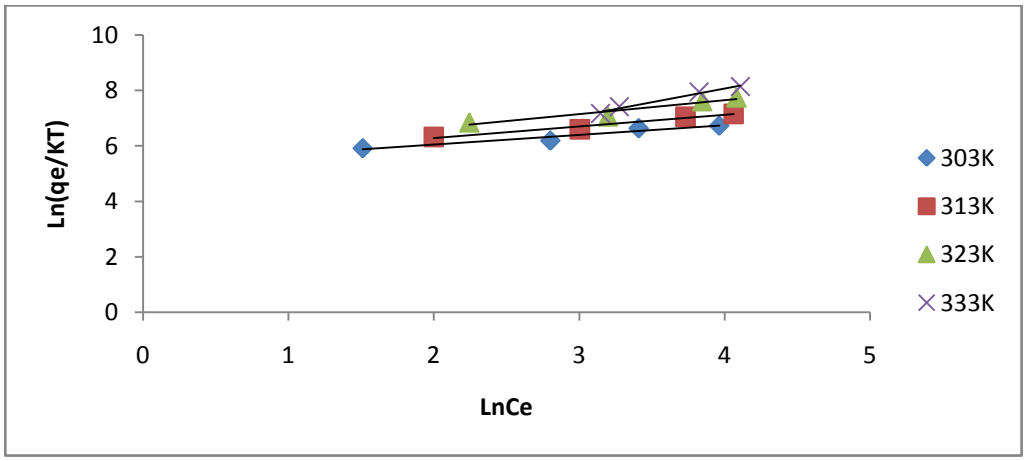
Ln(qe/KT)
10
8
6
4
2
0
0
1
2
3
4
5
LnCe
303K
313K
323K
333K

(g)

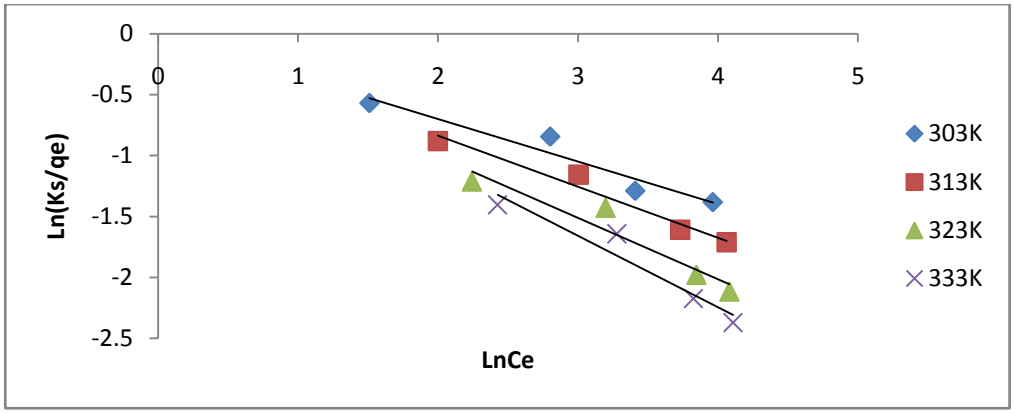

(h)

Isotherm plots of Swiss blue dye adsorption on CPASG (a) Langmuir (b) Freundlich, (c) Temkin, (d) D-R (e) Flory-huggins, (f) Redlich Peterson, (g) Toth, (h) Sip

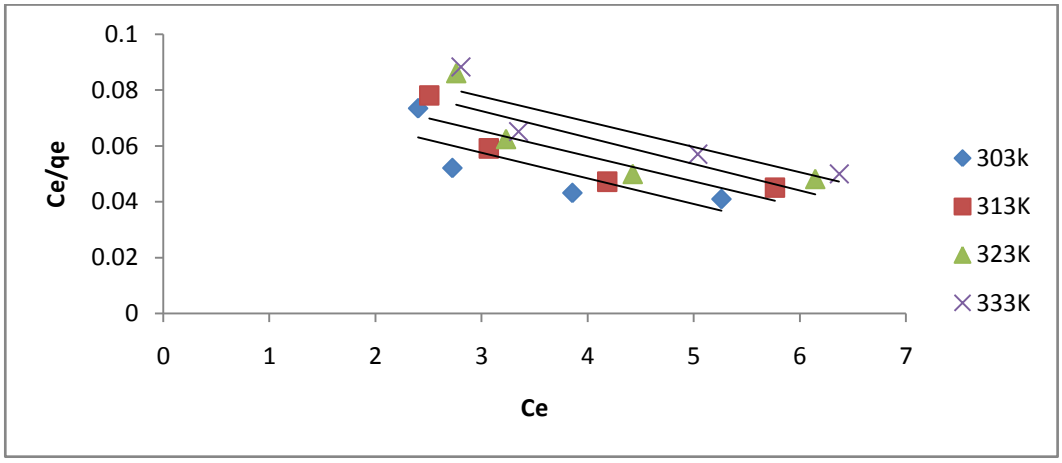

(a)

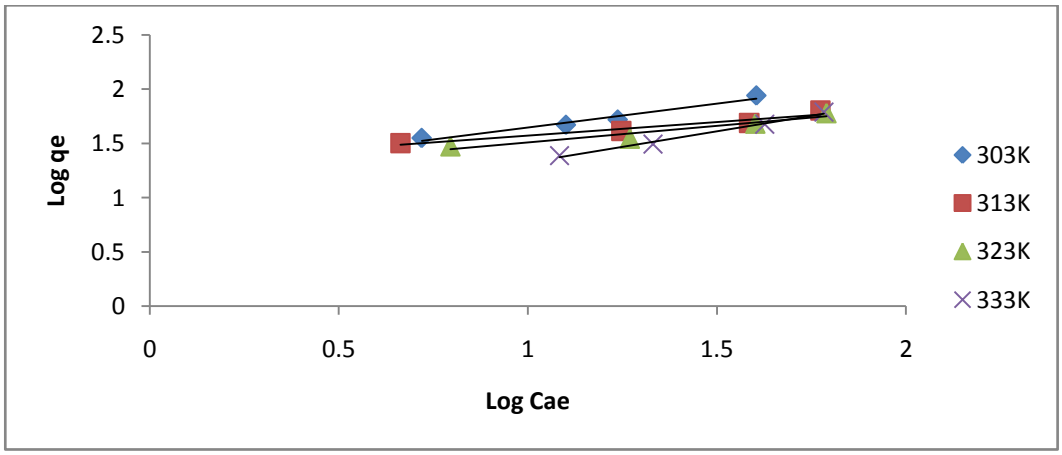

(b)

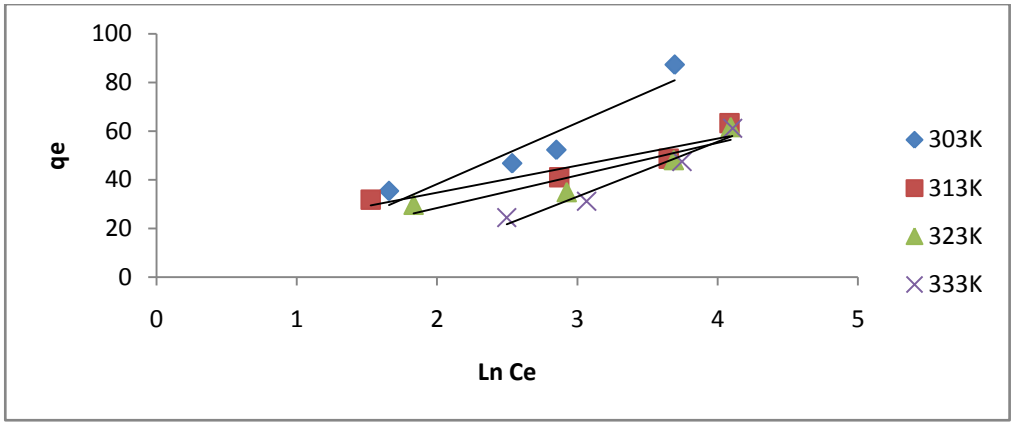
100
80
60
40
20
0
qe
0
1
2
3
4
5
Ln Ce
303K
313K
323K
333K

(c)

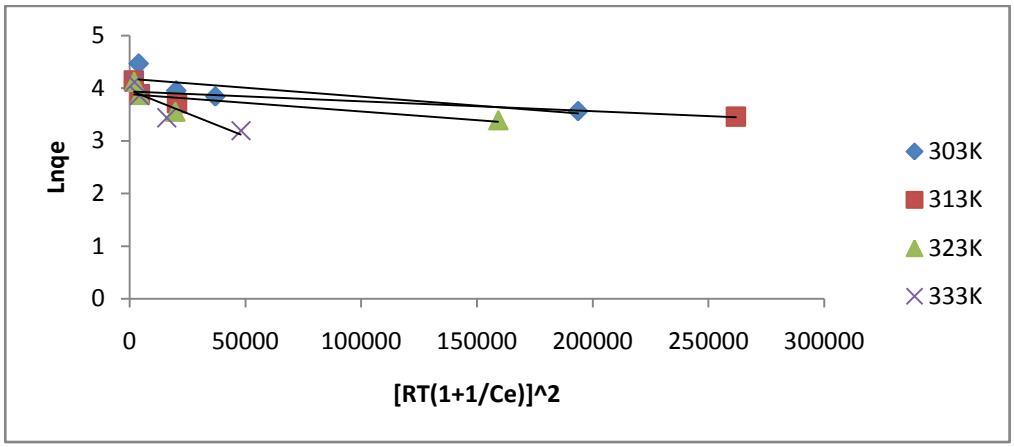
5
4
3
2
1
0
Lnqe
0
50000
100000
150000
200000
250000
300000
[RT(1+1/Ce)]^2
303K
313K
323K
333K

(d)

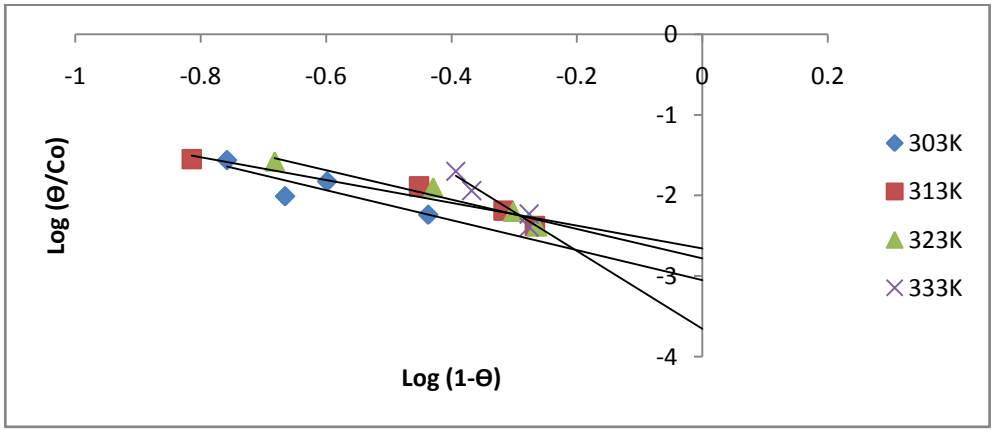
-1
-0.8
-0.6
-0.4
-0.2
0
0.2
0
-1
-2
-3
-4
Log (Θ/Co)
Log (1-Θ)
303K
313K
323K
333K

(e)

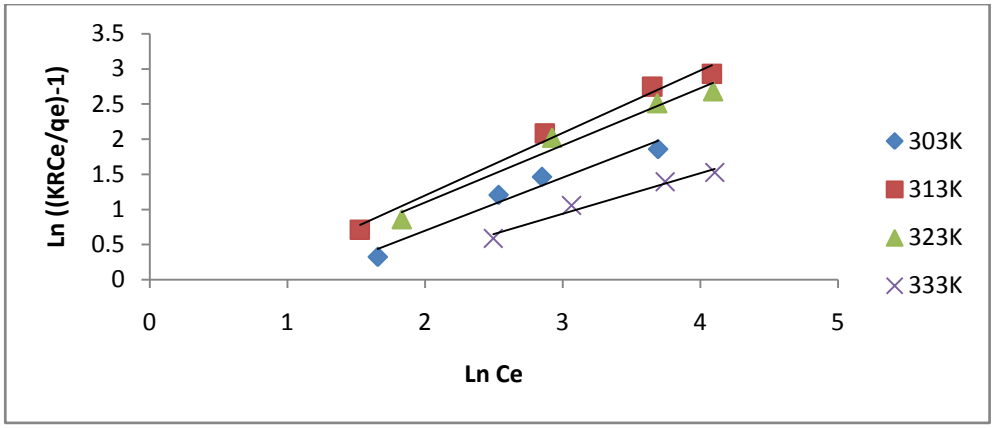

(f)

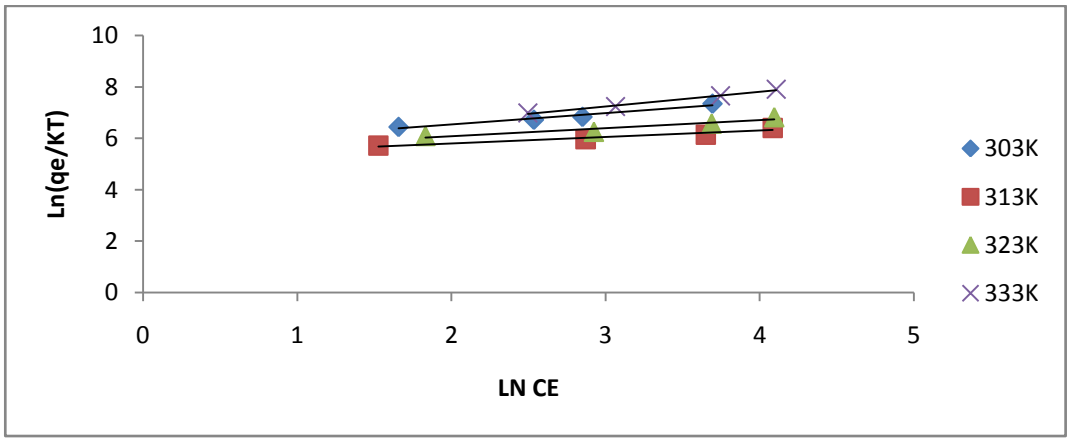

(g)

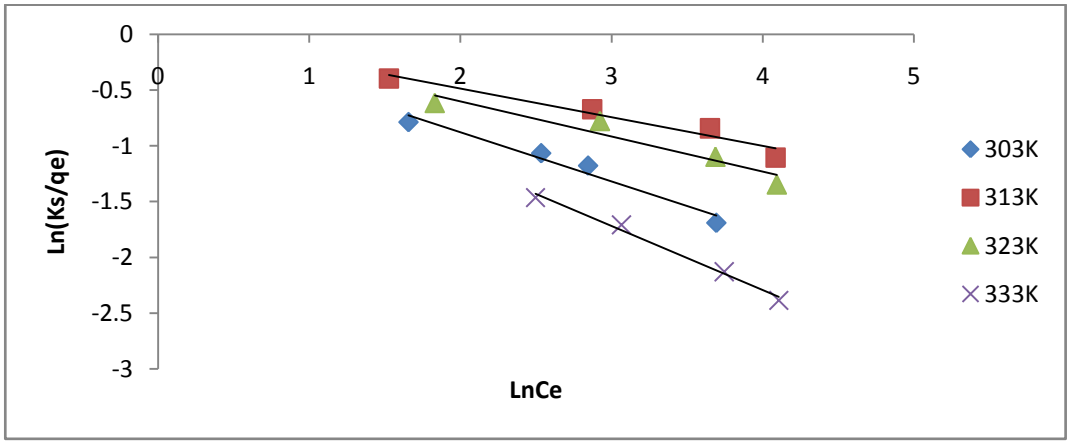

Isotherm plots of Swiss blue dye adsorption on CPAHS (a) Langmuir (b) Freundlich, (c) Temkin, (d) D-R, (e) Flory-huggins, (f) Redlich Peterson (g) Toth, (h) Sip

APPENDIX H.
THERMODYNAMIC PLOTS FOR ADSORPTION PROCESS

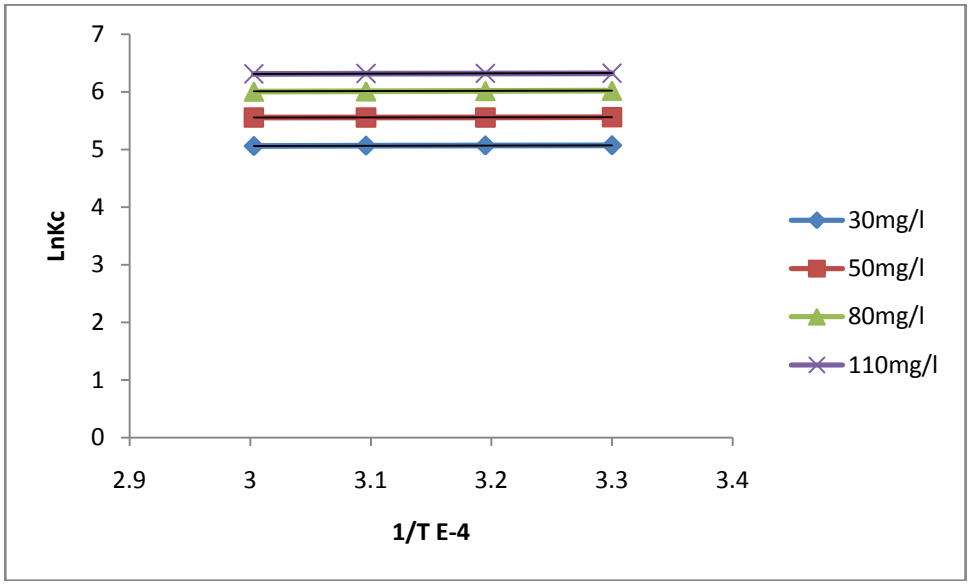

(a) MPAHS

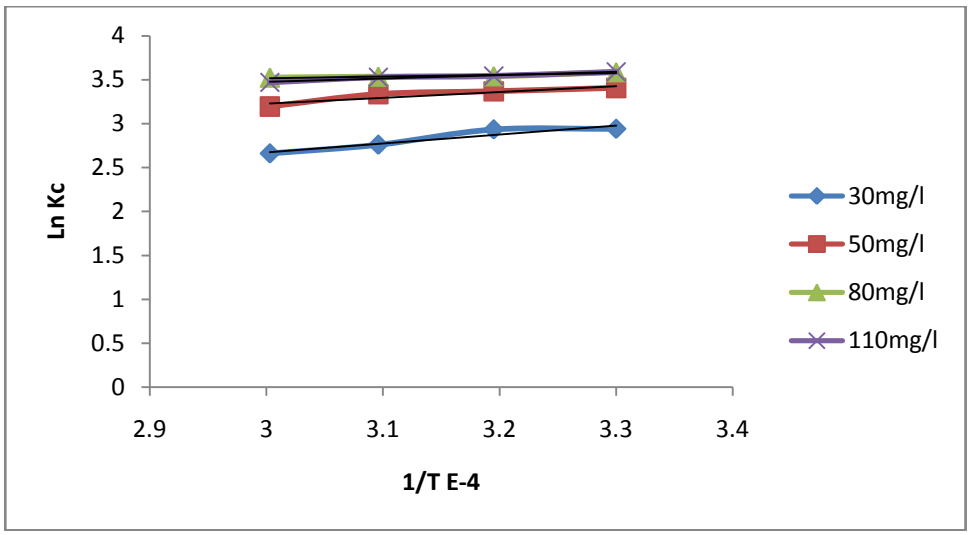

(b) MPASG

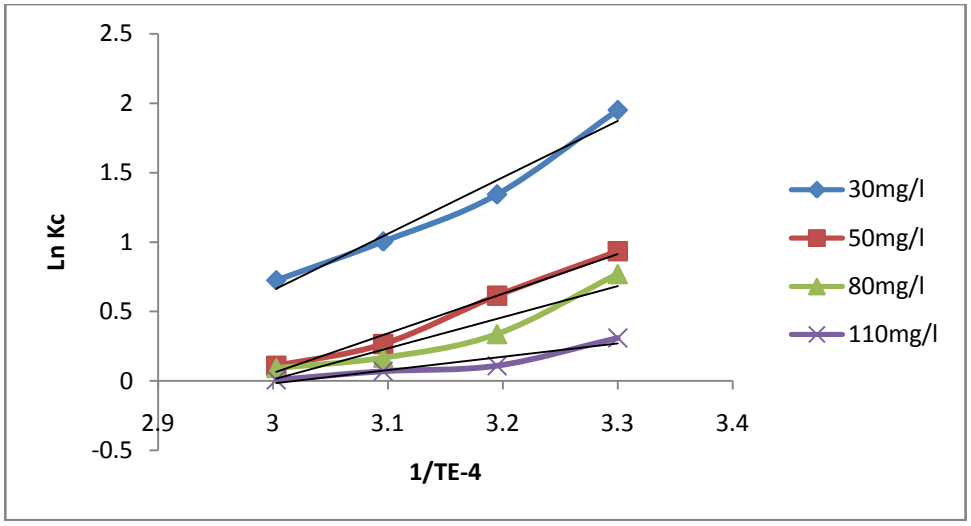

(c) CPASG

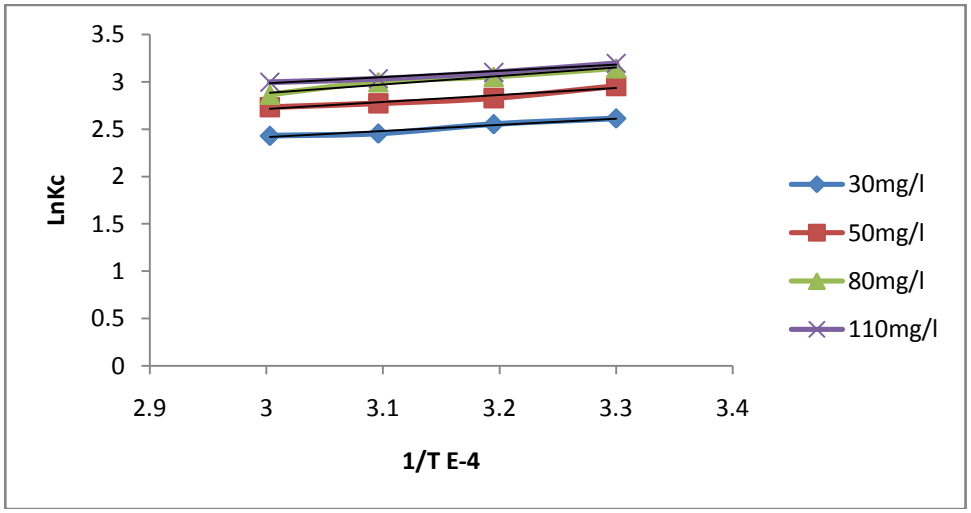

(d) CPAHS

APPENDIX I

KINETICS PLOTS FOR DESORPTION STUDIES

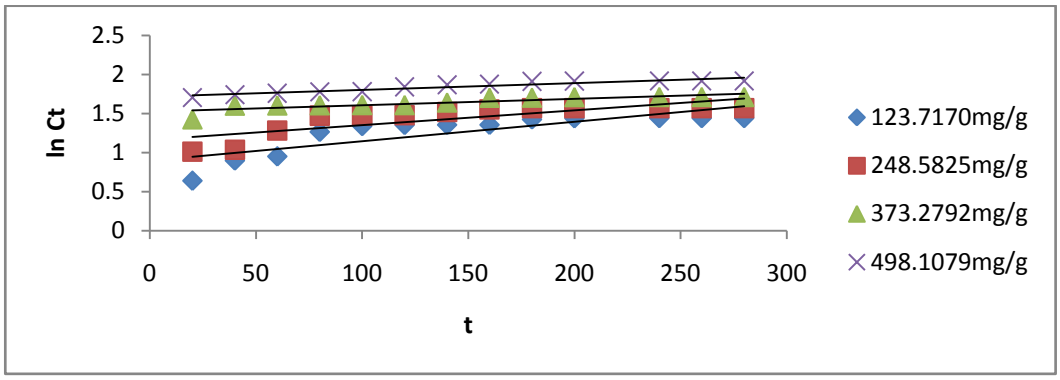

(a)

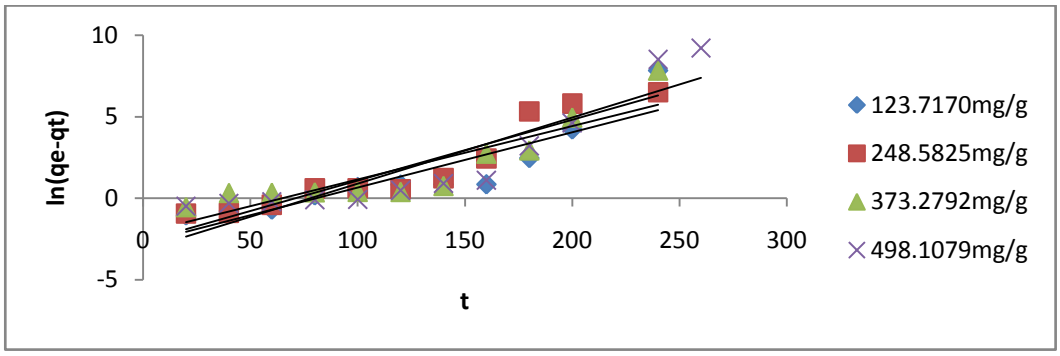

(b)

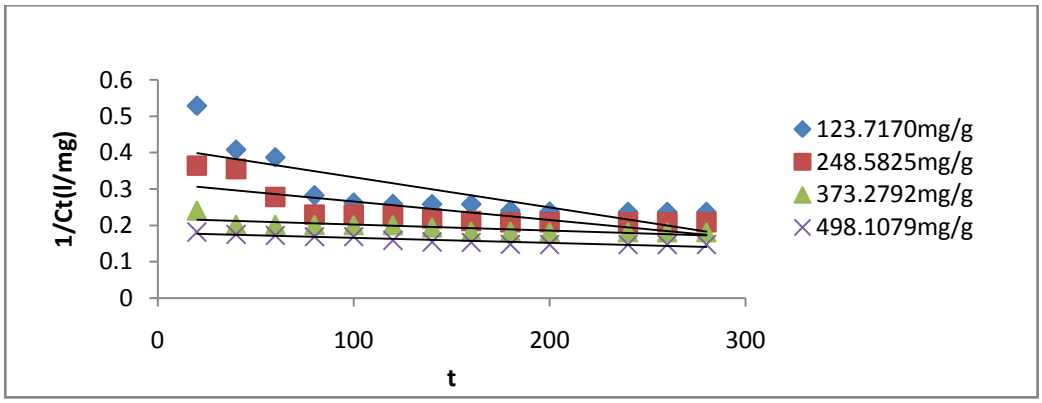

(c)

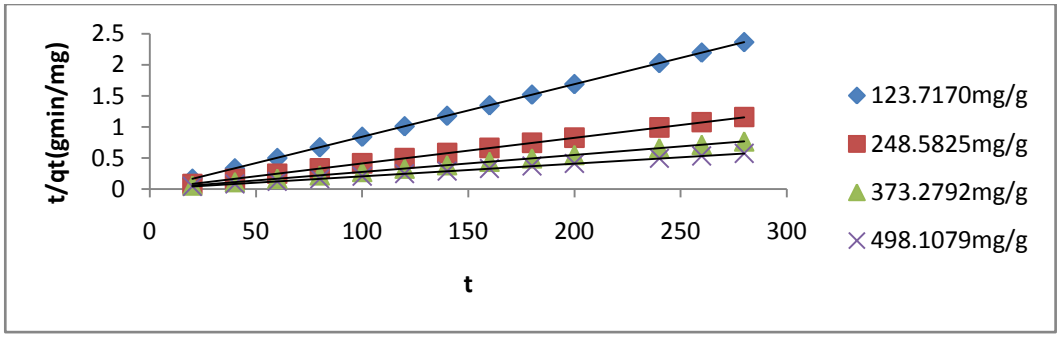

(d) Fig. 4.31. Kinetic plots of Swiss blue dye desorption from spent MPAHS (a) First order, (b) Pseudo first order, (c) Second order, (d) Pseudo second order

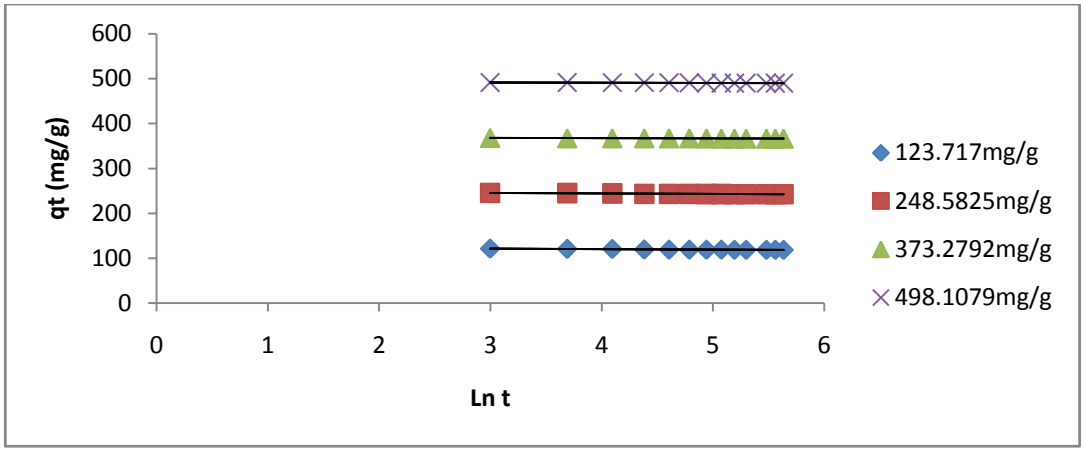

(e)

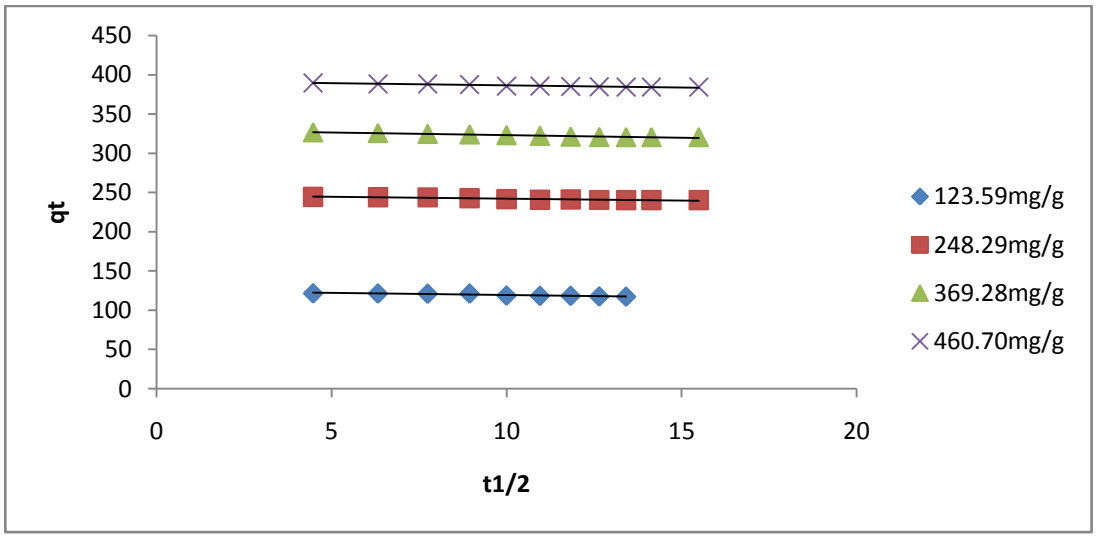

(f)

Kinetic plots of Swiss blue dye desorption from spent MPAHS (e) Elovich, (f) Intra particle diffusion

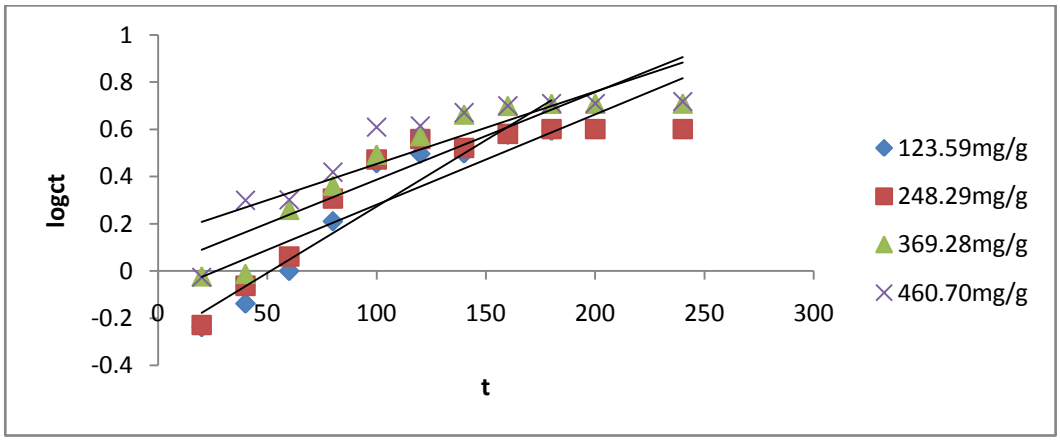

(a)

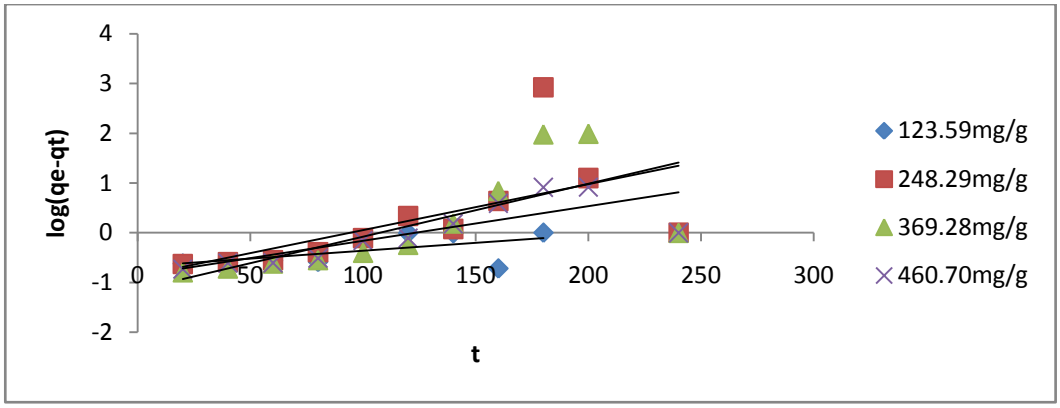

(b)

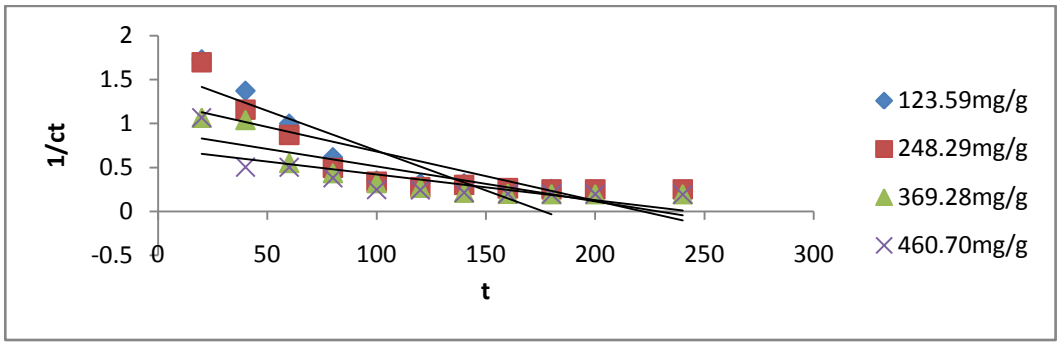

(c)

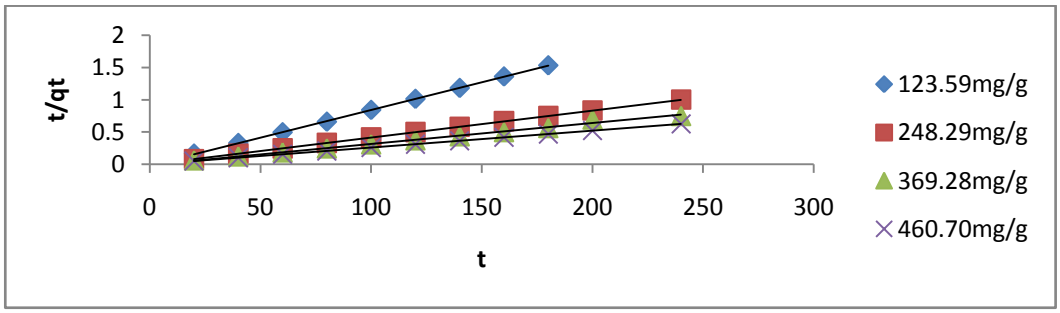

(d)

Kinetic plots of Swiss blue dye desorption from spent MPASG (a) First order, (b) Pseudo first order, (c) Second order, (d) Pseudo second order

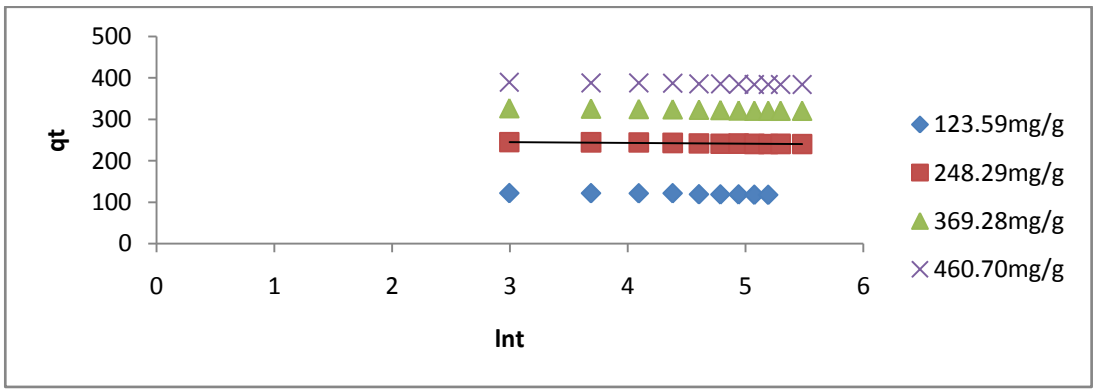

(e)

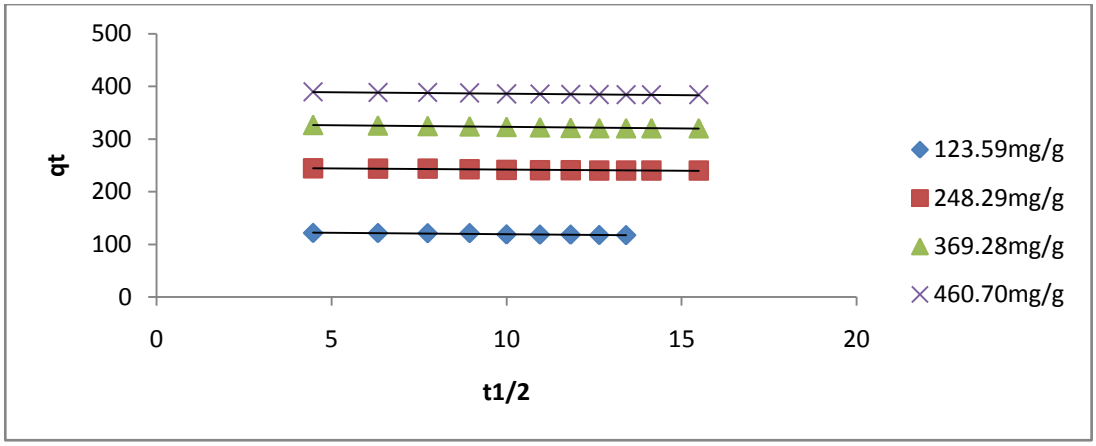

(f)

Kinetic plots of Swiss blue dye desorption from spent MPASG (e) Elovich, (f) Intra particle diffusion

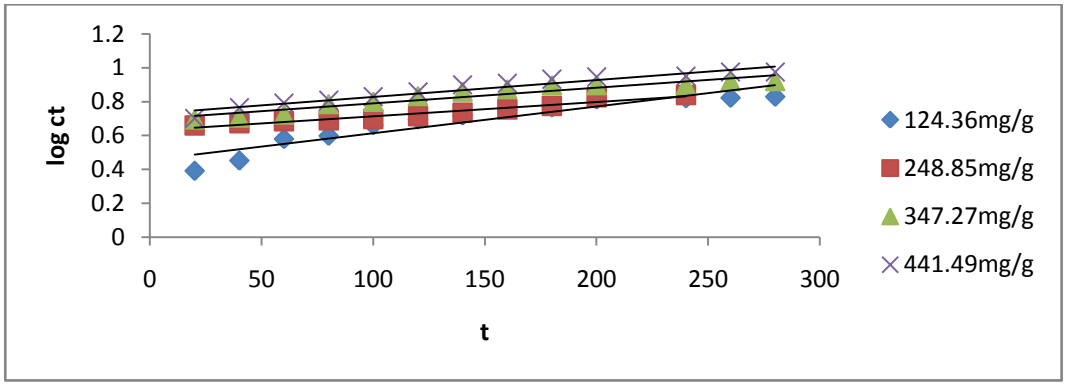

(a)

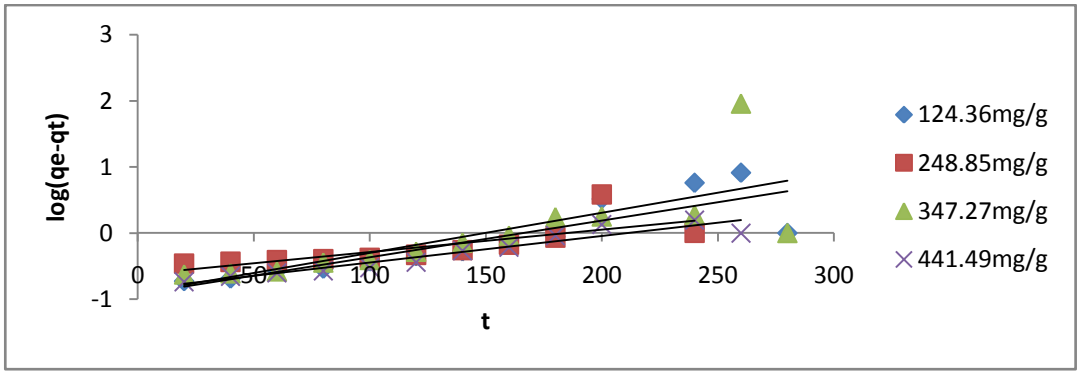

(b)

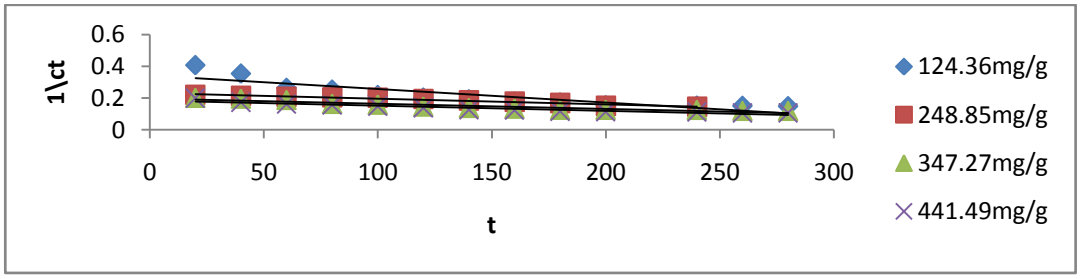

(c)

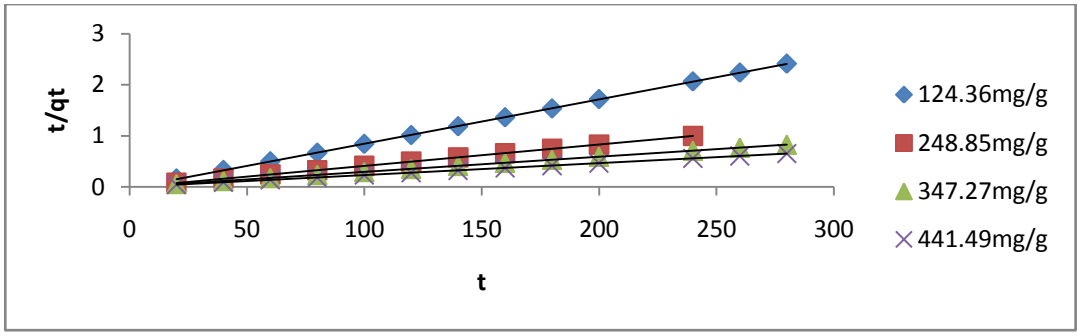

(d) Kinetic plots of Swiss blue dye desorption from spent CPASG (a) First order, (b) Pseudo first order, (c) Second order, (d) Pseudo second order

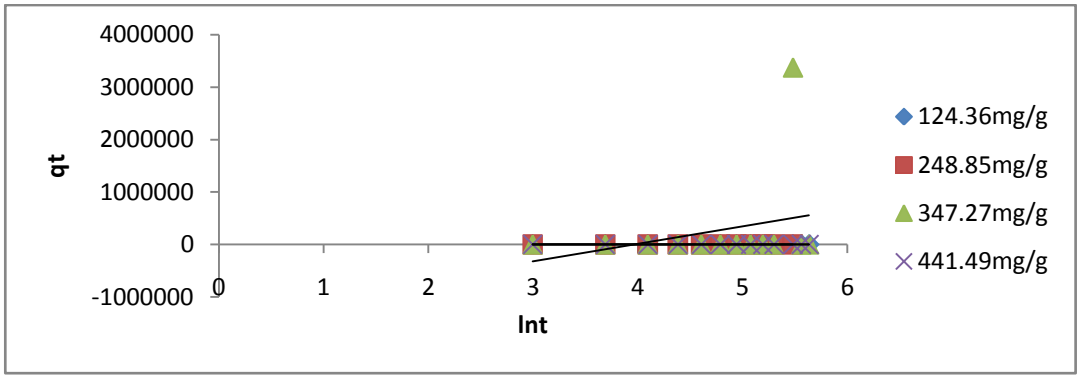

(e)

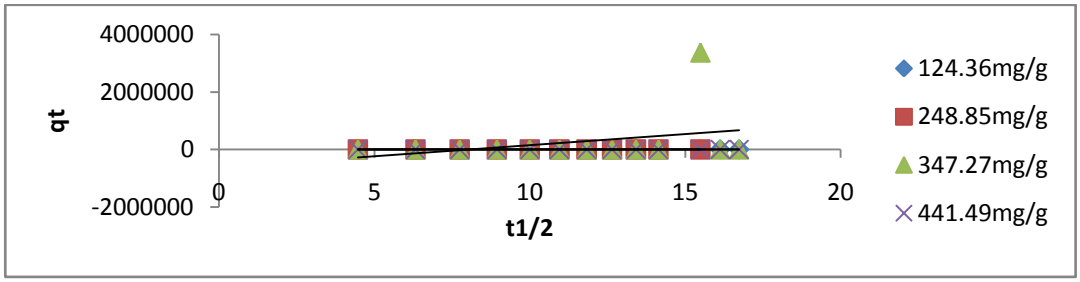

(f)

Kinetic plots of Swiss blue dye desorption from spent CPASG (e) Elovich, (f) Intra particle diffusion

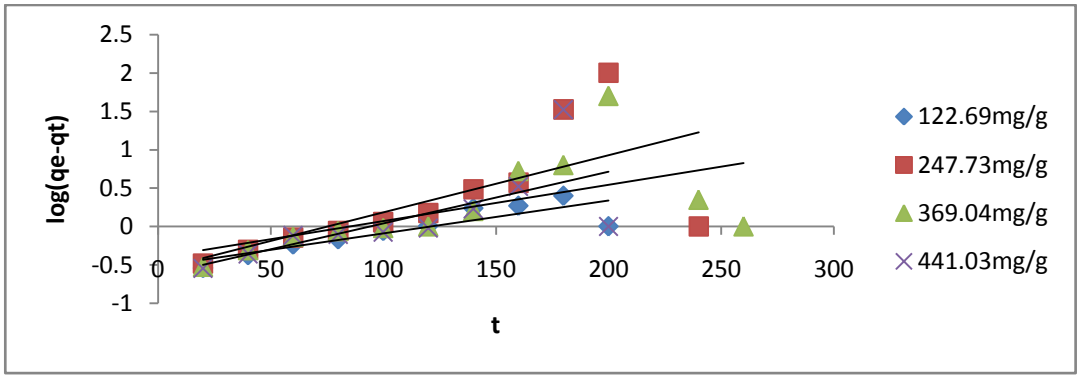

(a)

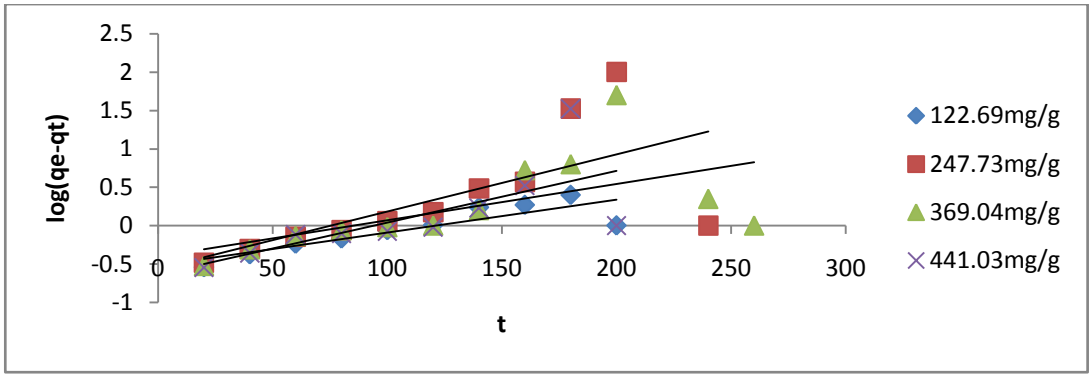

(b)

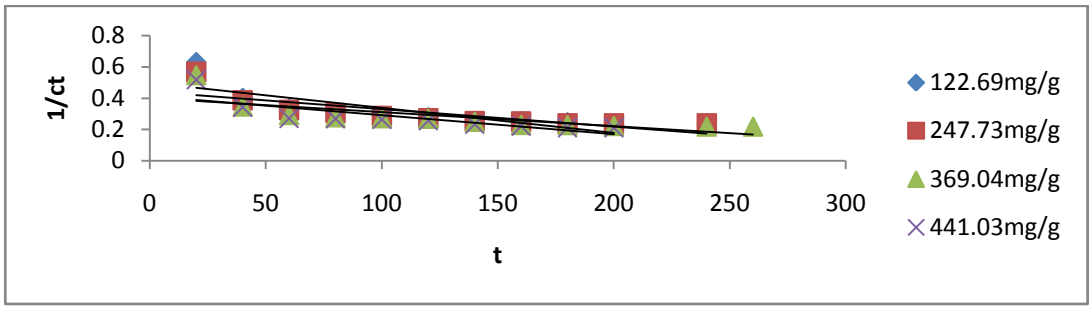

(c)

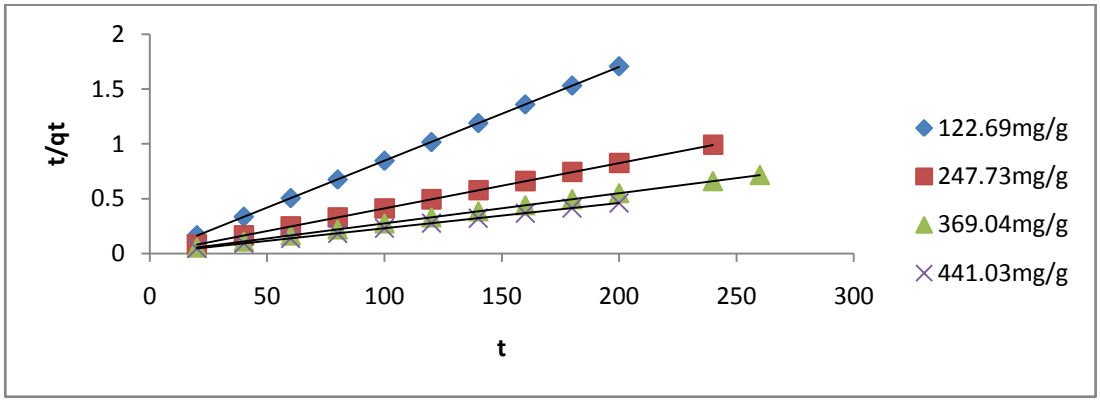

(d) Kinetic plots of Swiss blue dye desorption from spent CPAHS (a) First order, (b) Pseudo first order, (c) Second order, (d) Pseudo second order

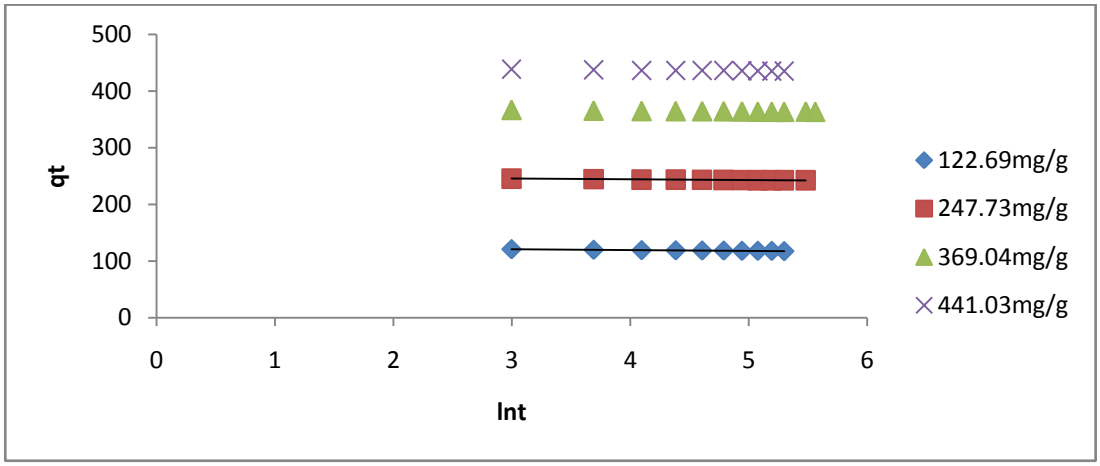

(e)

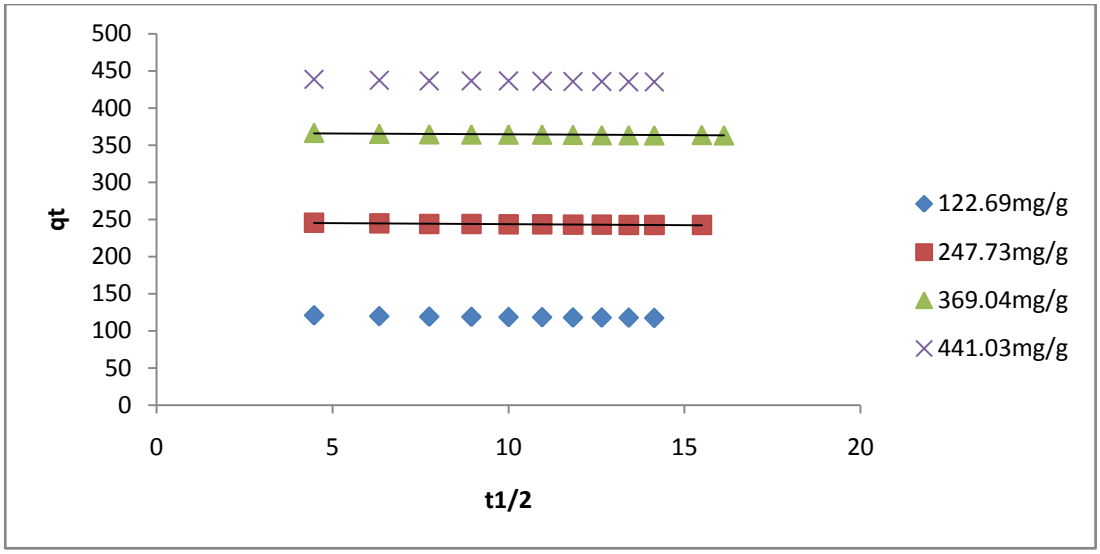

(f)

Kinetic plots of Swiss blue dye desorption from spent CPAHS (e) Elovich, (f) Intra particle diffusion

PSEUDO SECOND ORDER PLOTS AT DIFFERENT TEMPERATURES

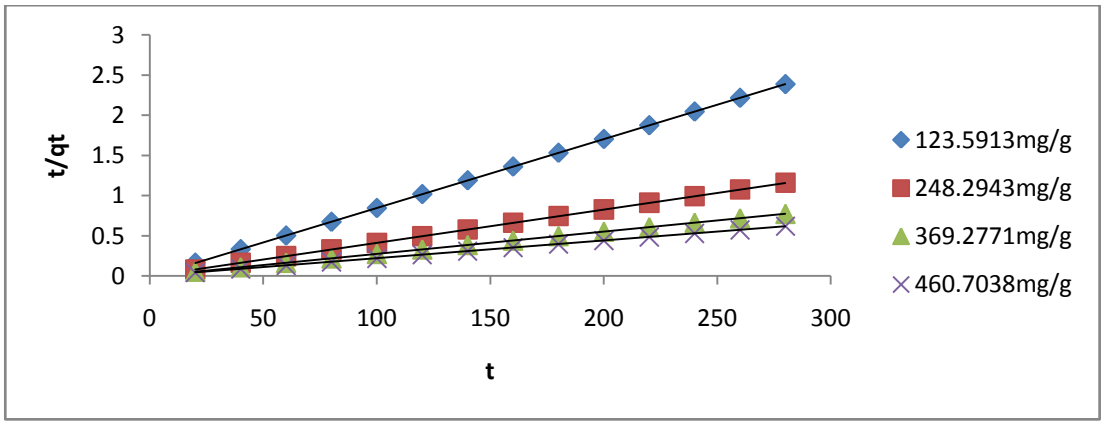

(a)

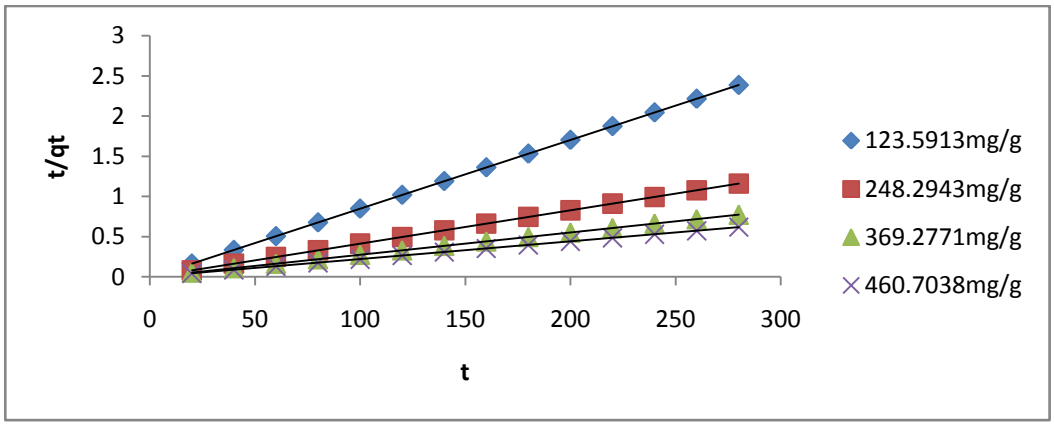

(b)

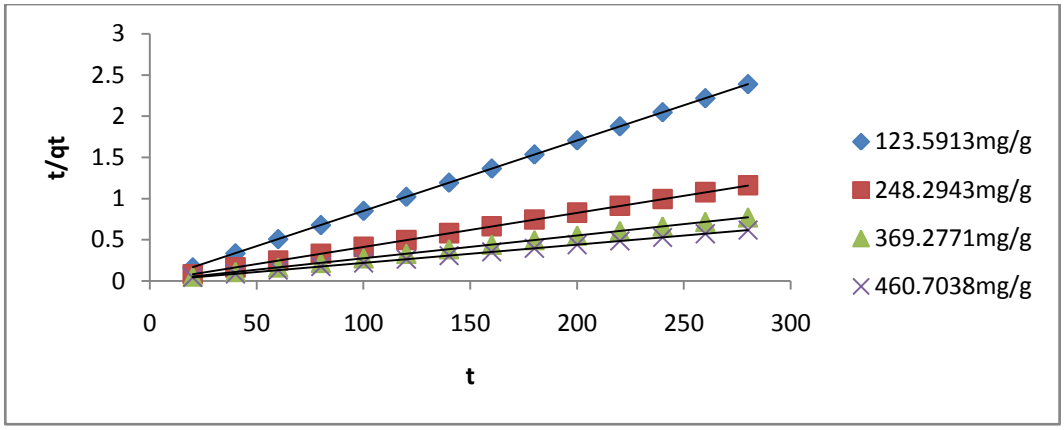

(c)

MPAHS (a) 303K, (b) 313K, (c) 323K.

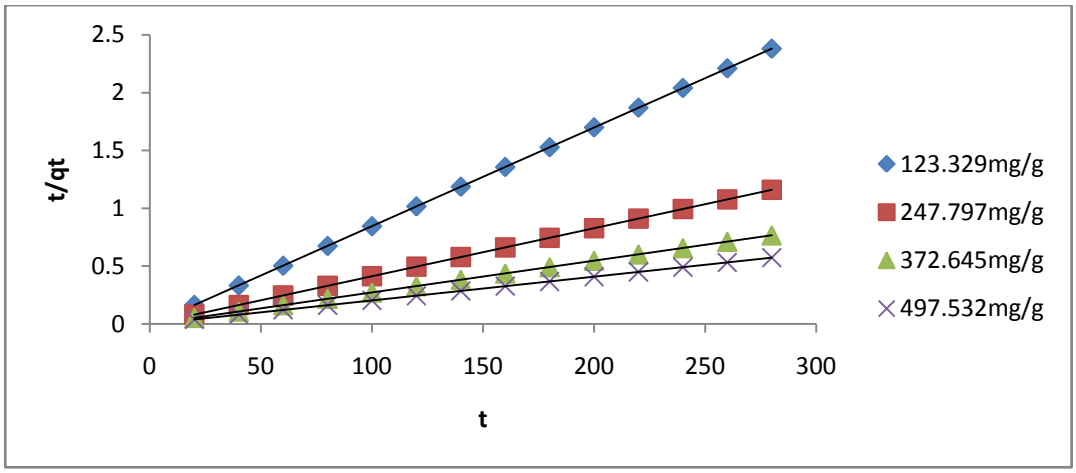

(a)

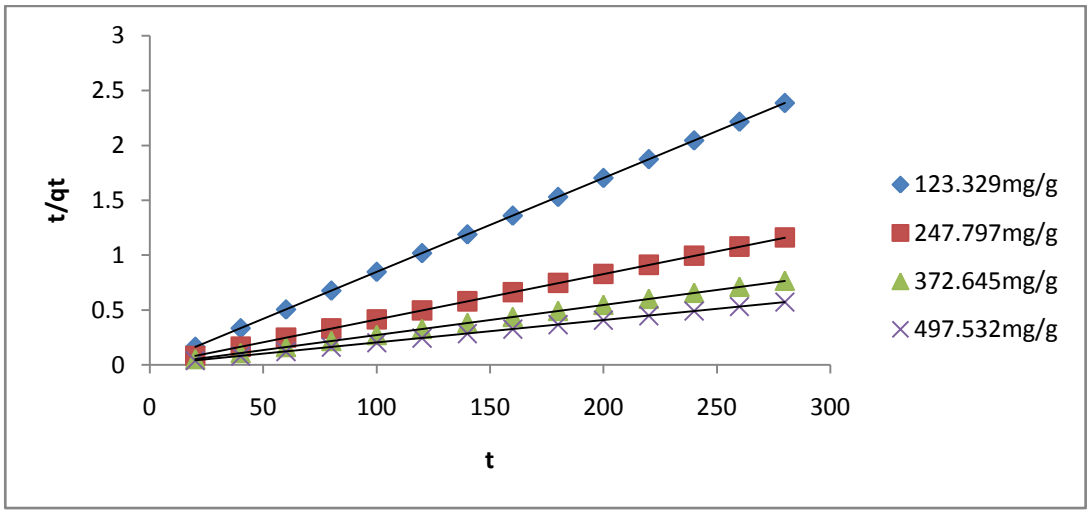

(b)

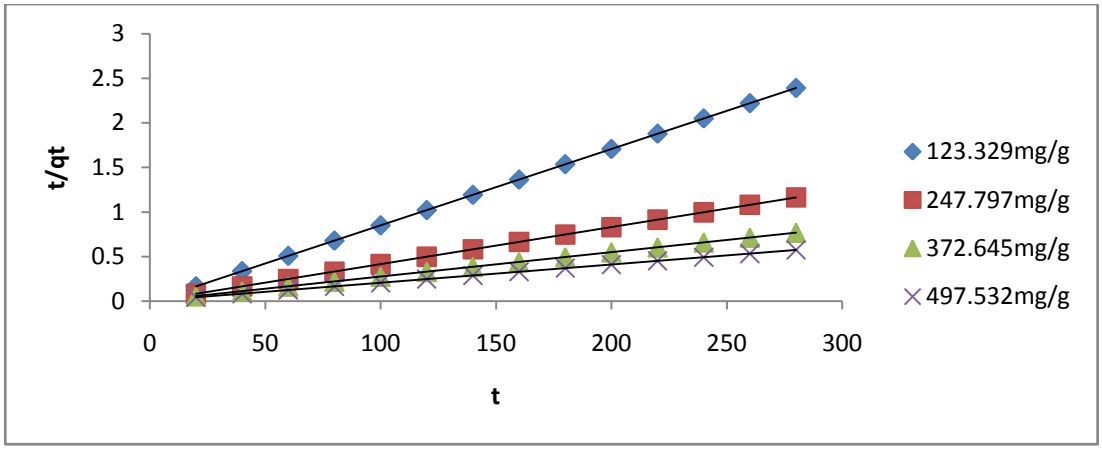

(c)

MPASG (a) 303K, (b) 313K, (c) 323K.

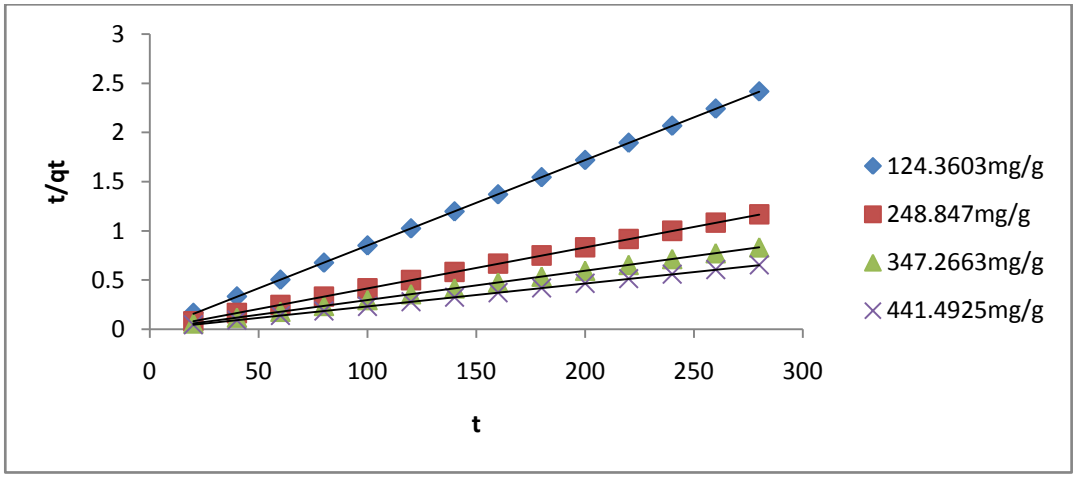

(a)

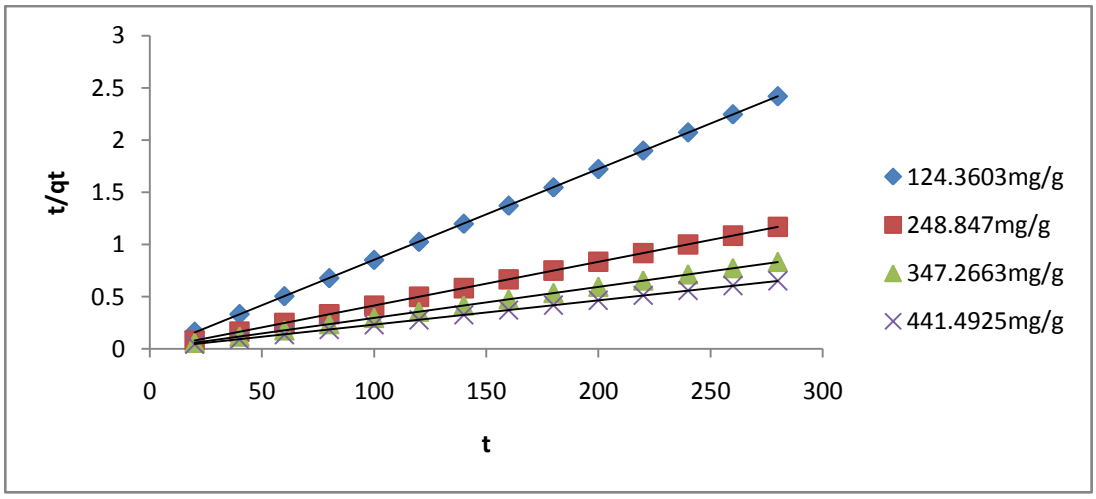

(b)

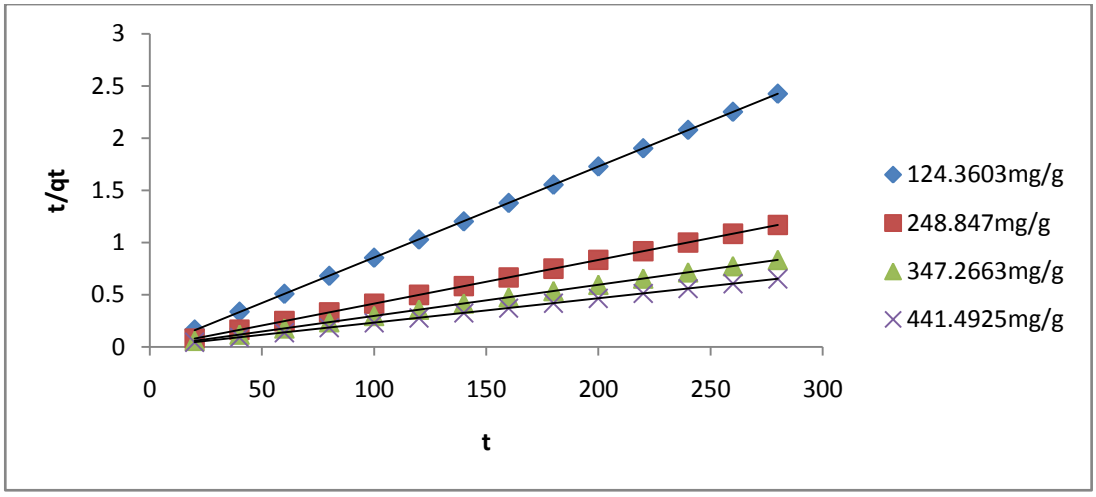

(c)

CPASG (a) 303K, (b) 313K, (c) 323K.

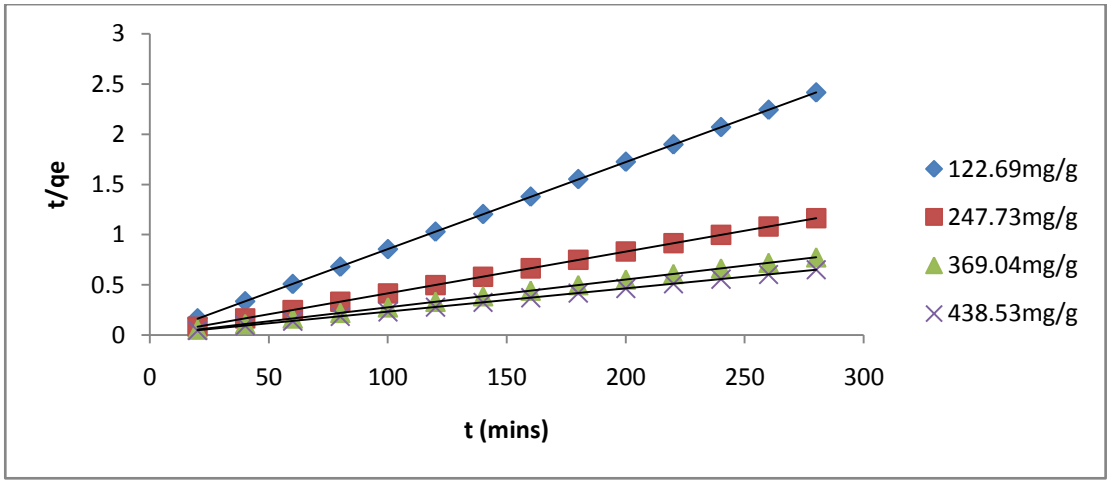

(a)

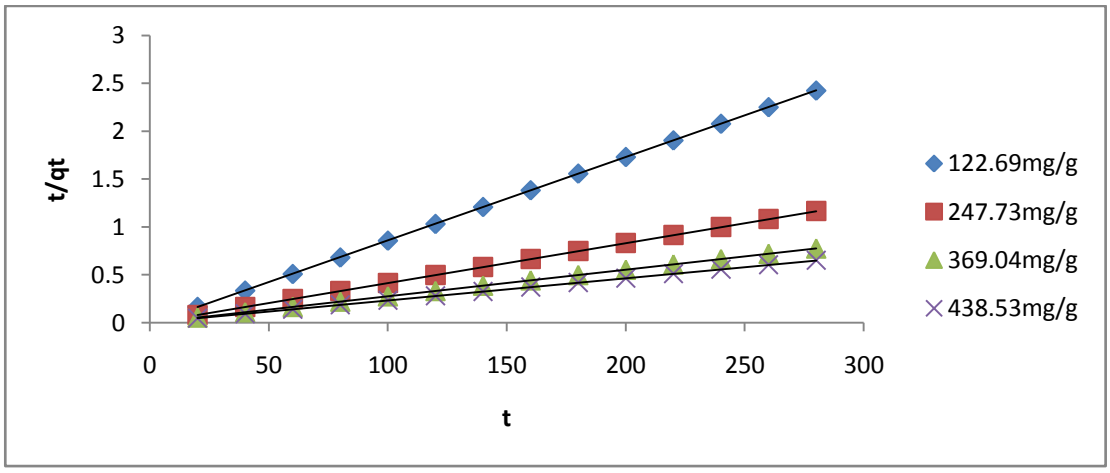

(b)

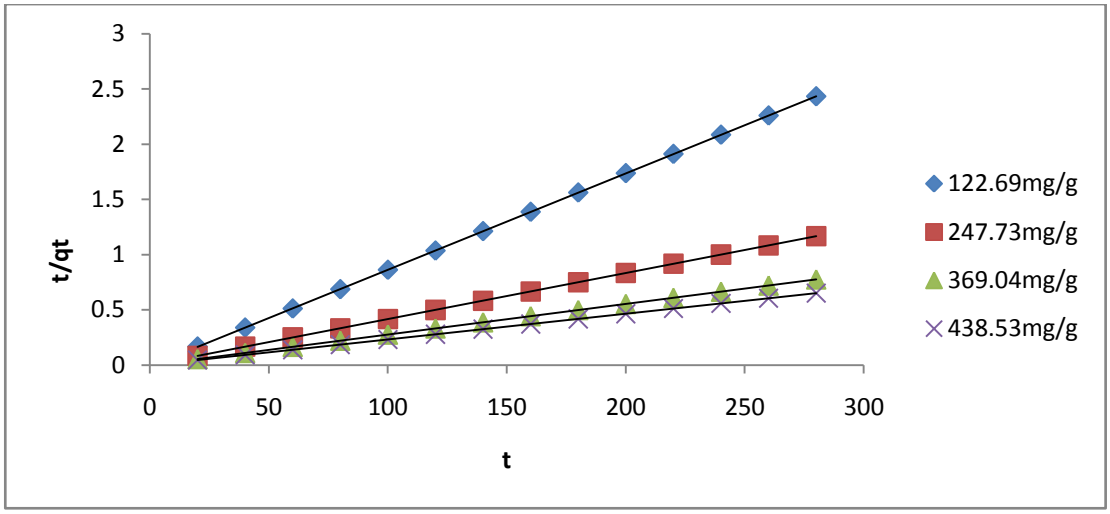

(c)

CPAHS (a) 303K, (b) 313K, (c) 323K.

APPENDIX J
ARRHENIUS PLOTS FOR DESORPTION PROCESS

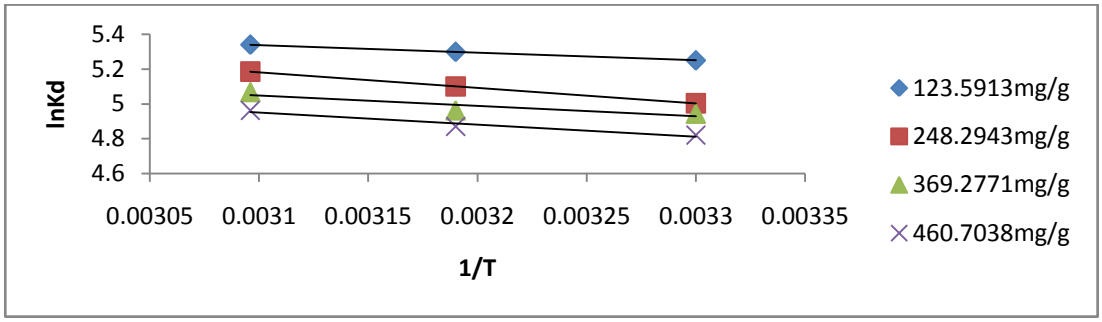

(a)

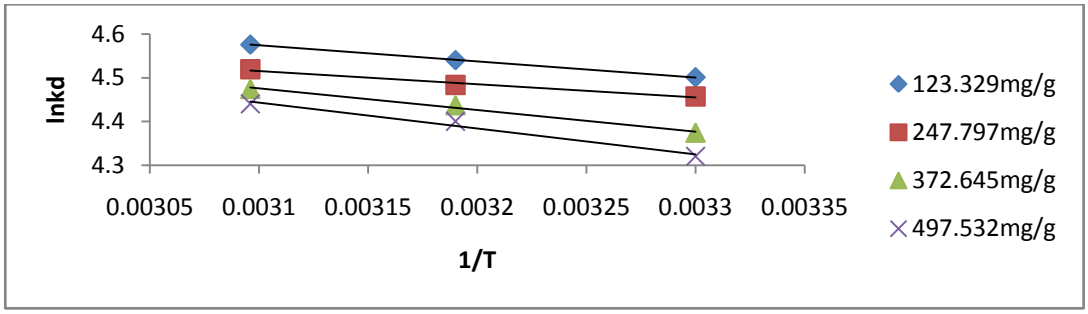

(b)

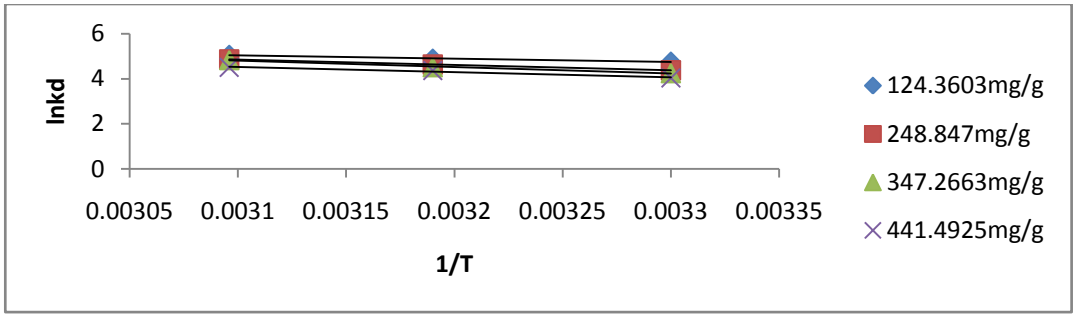

(c)

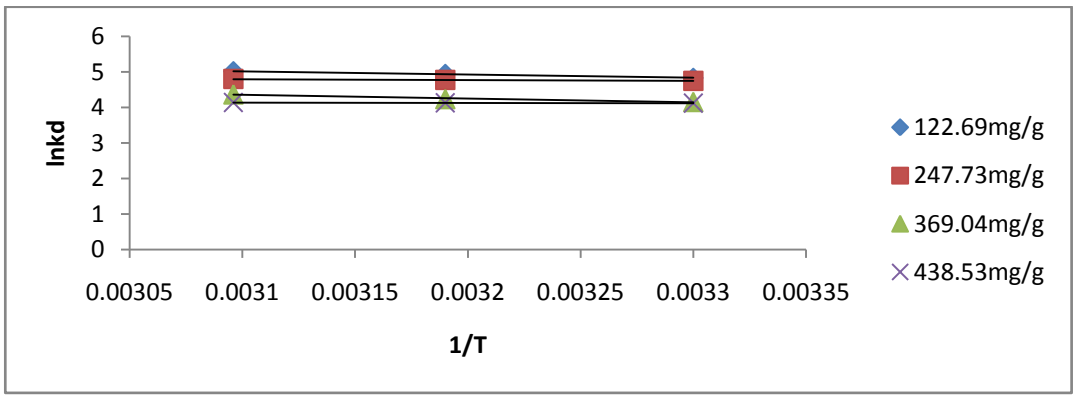

(d)

(a) MPAHS, (b) MPASG, (c) CPASG, (d) CPAHS

APPENDIX K

DESORPTION ISOTHERM PLOTS

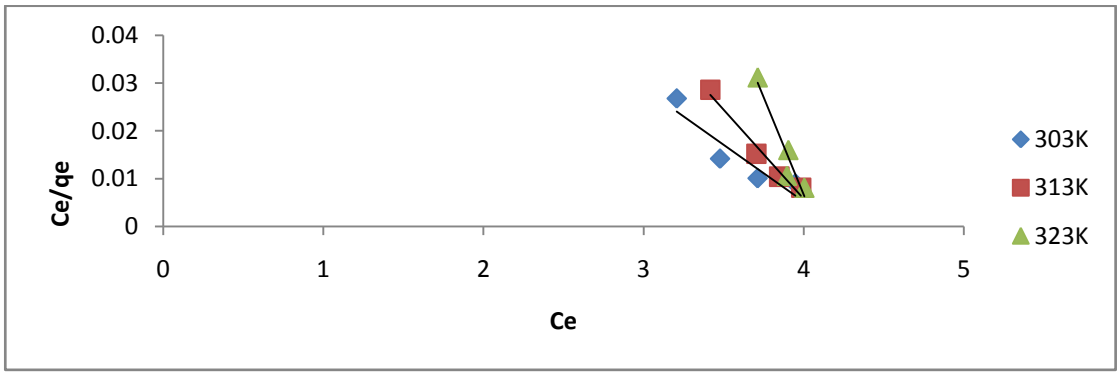

(a)

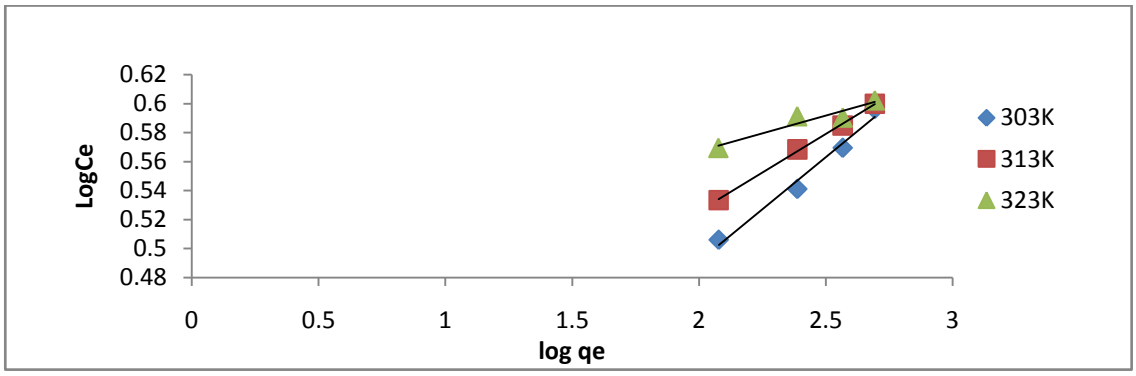

(b)

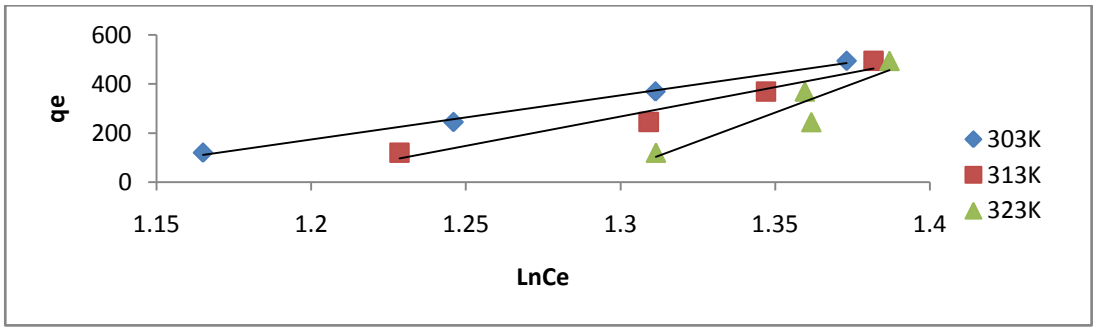

(c)

MPAHS (a) Langmuir, (b) Freundlich, (c) Temkin

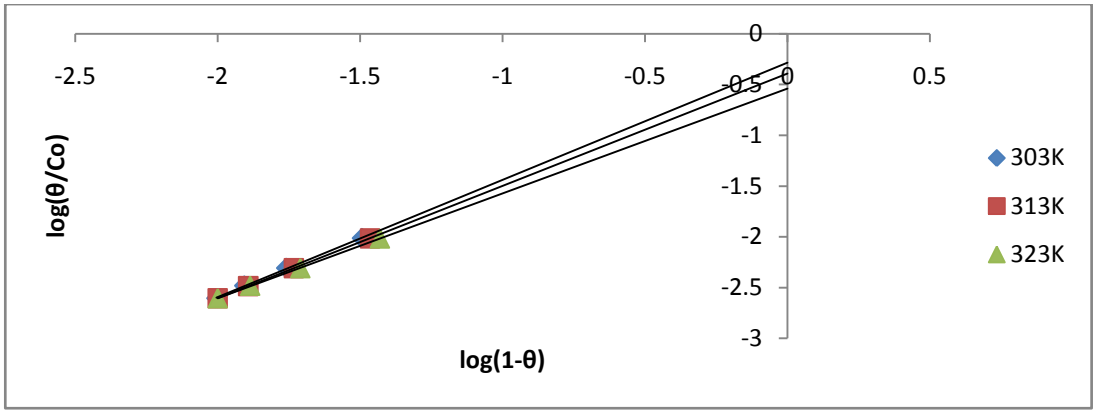

(d)

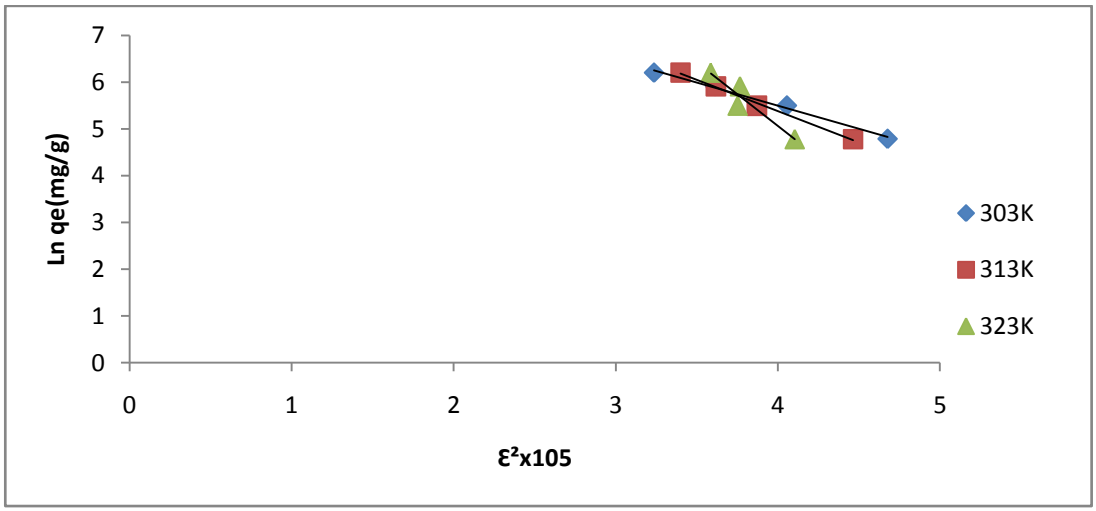

(e)

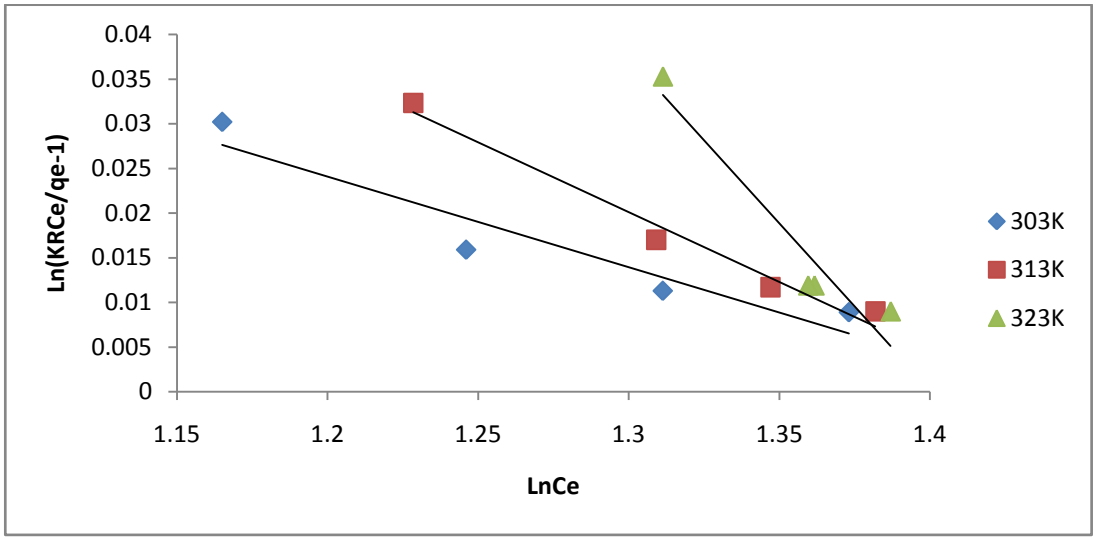

(f)

MPAHS (d) Flory-Huggins, (e) D-R, (f) Redlich – Peterson, (g) Sip, (h) Toth

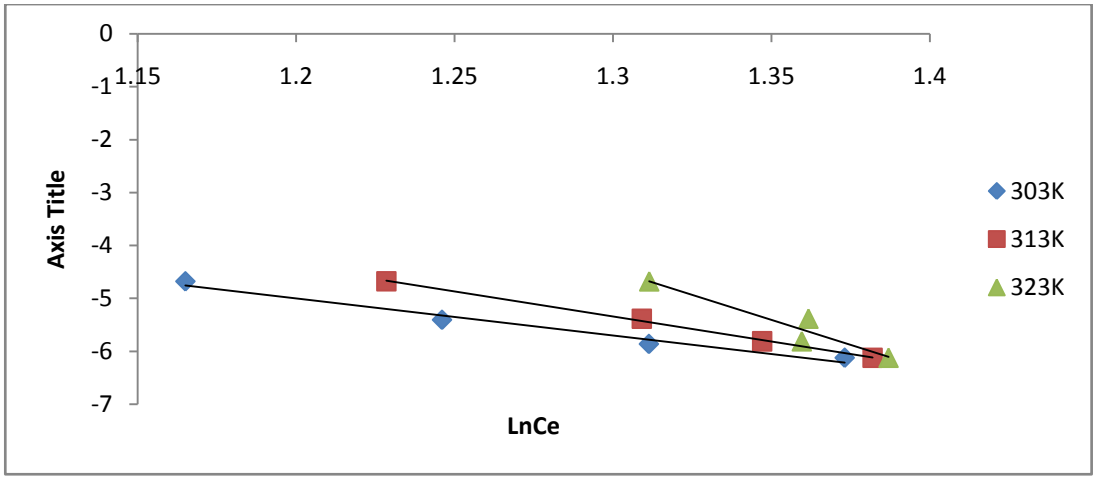

(g)

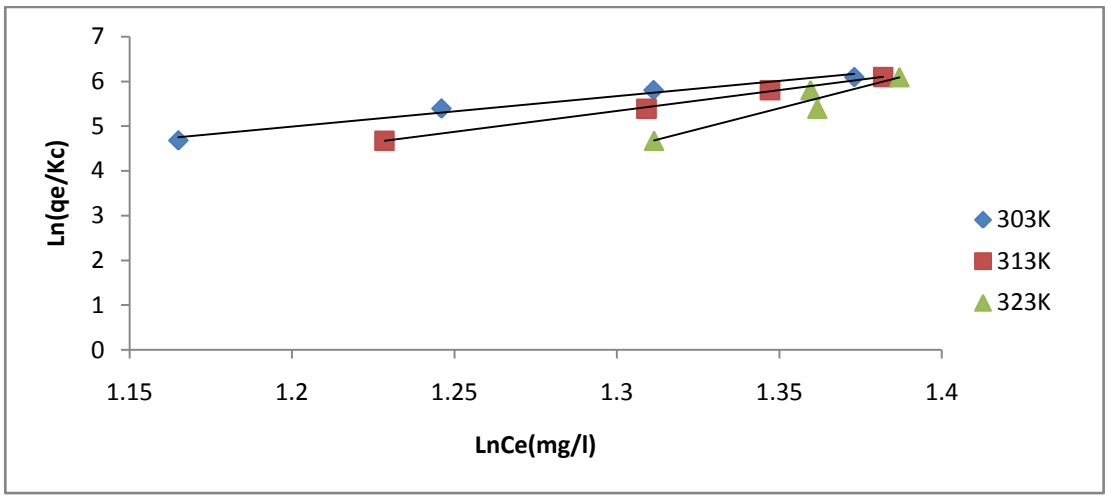

(h)

MPAHS (g) Sip, (h) Toth

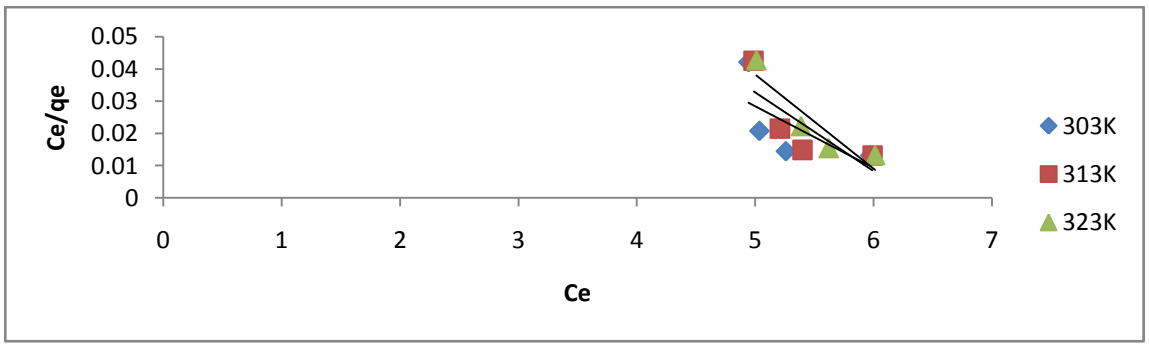

(a)

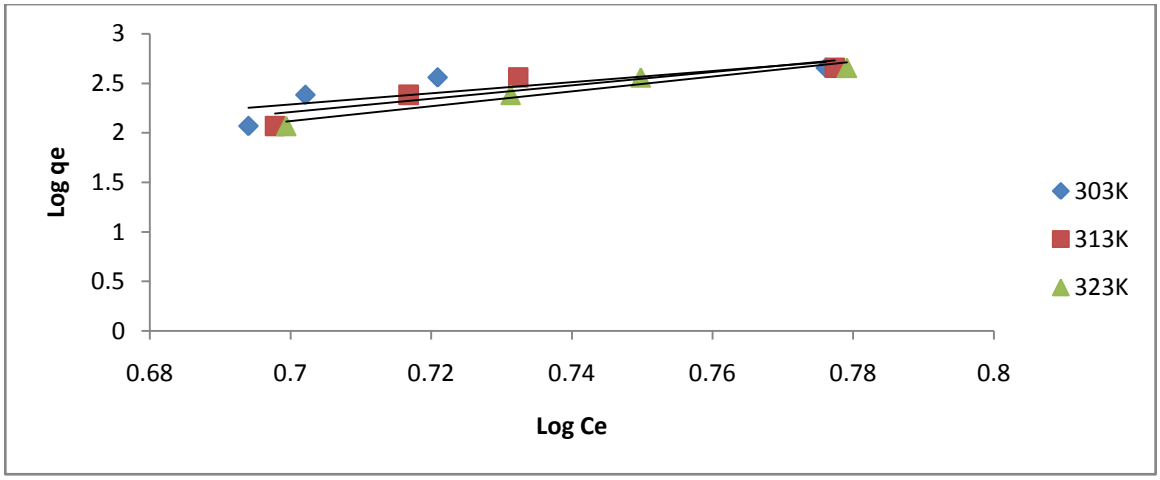

(b)

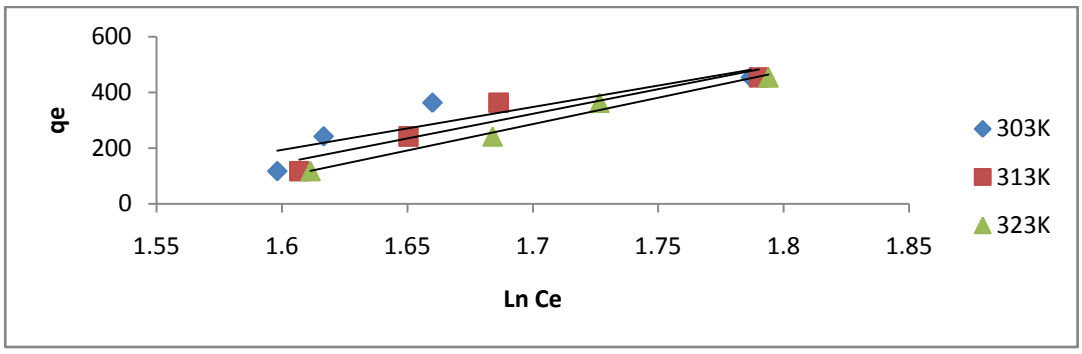

(c)

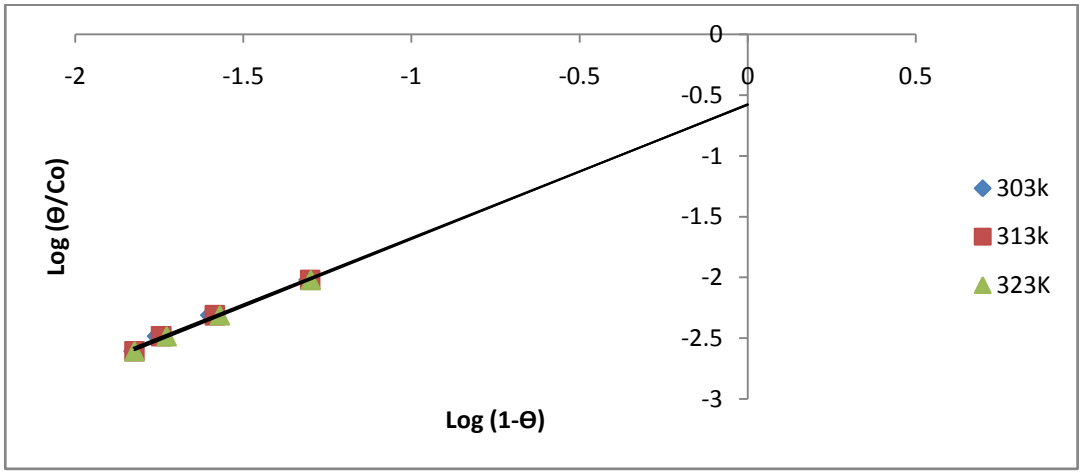

(d)

MPASG (a) Langmuir, (b) Freundlich, (c) Temkin, (d) Flory-Huggins

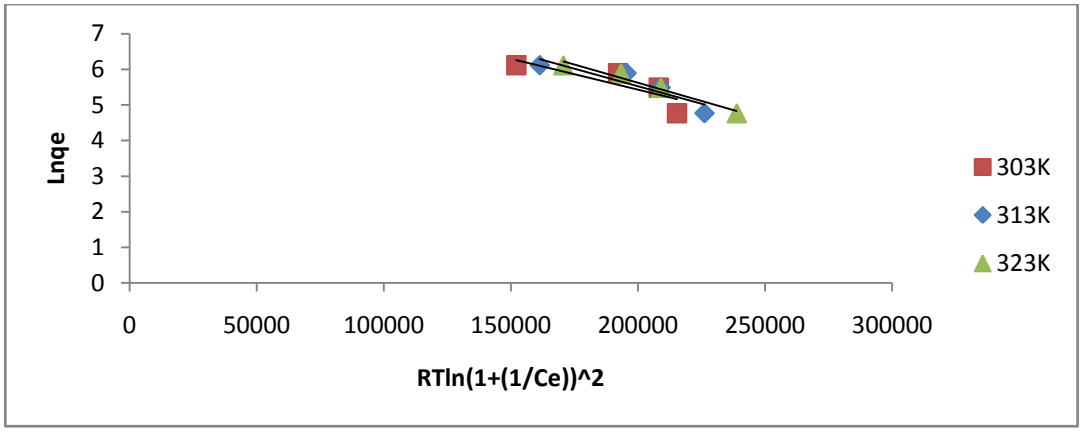

(e)

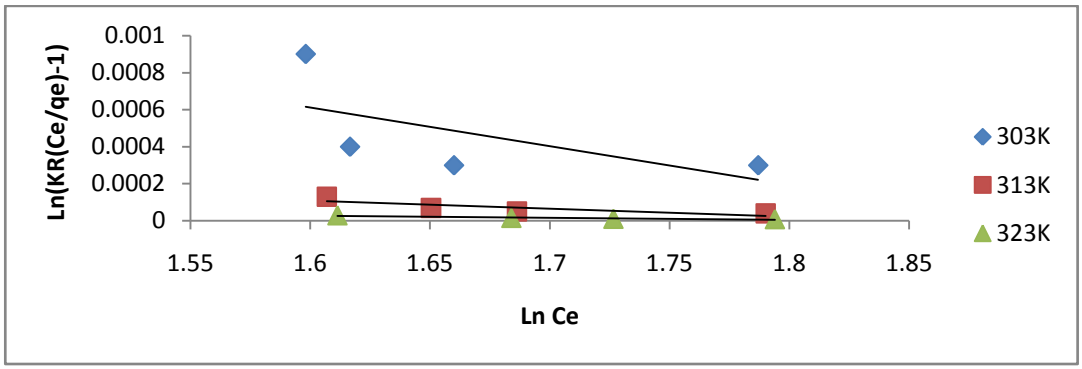

(f)

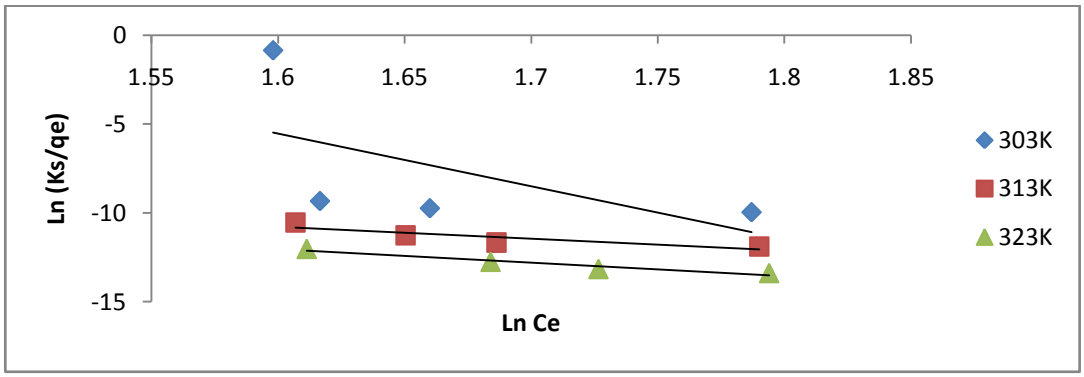

(g)

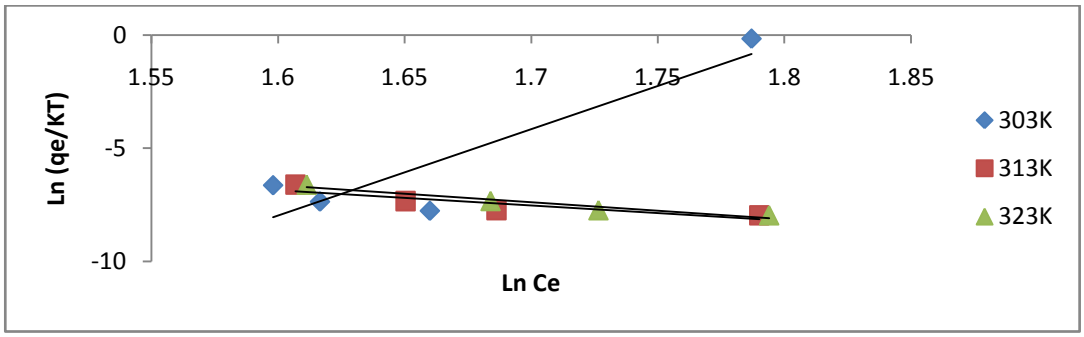

(h)

MPASG (e) D-R, (f) Redlich – Peterson, (g) Sip, (h) Toth

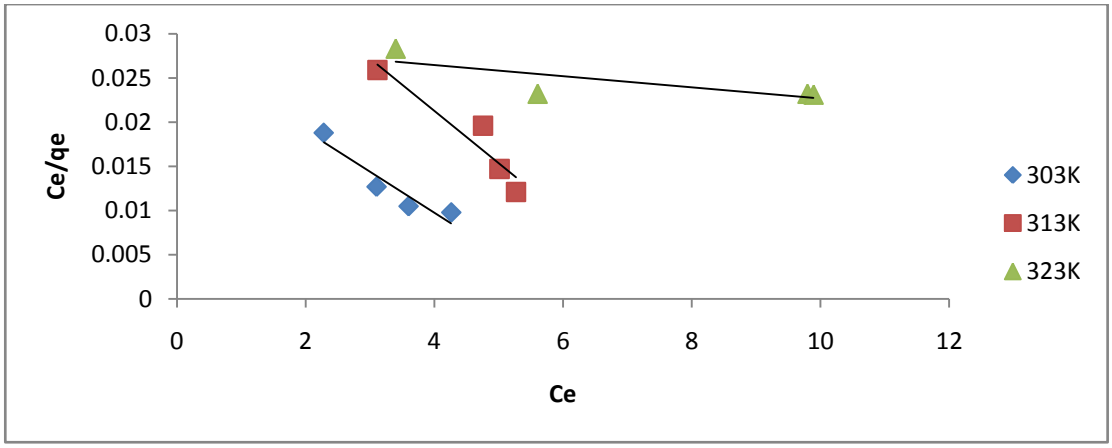

(a)

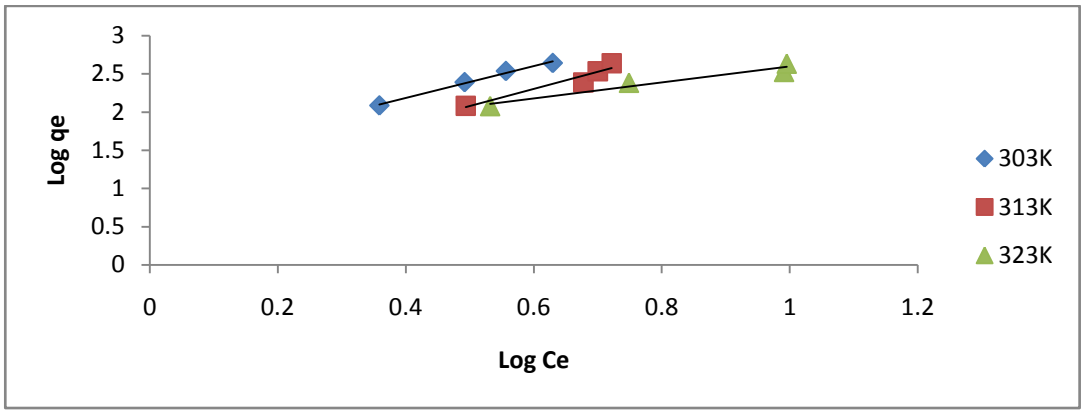

(b)

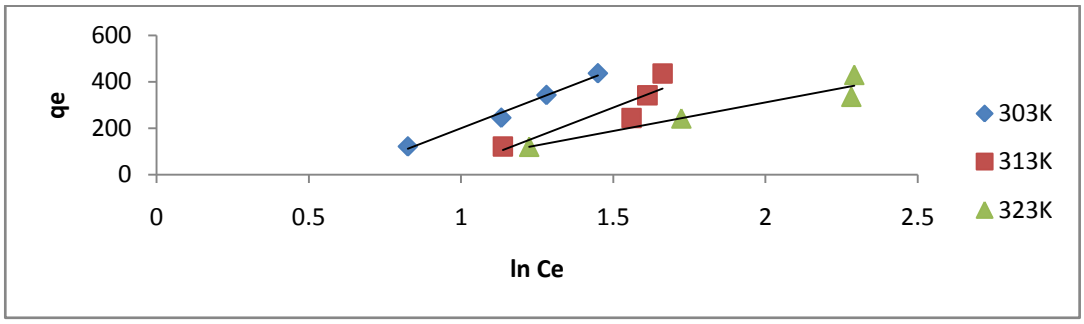

(c)

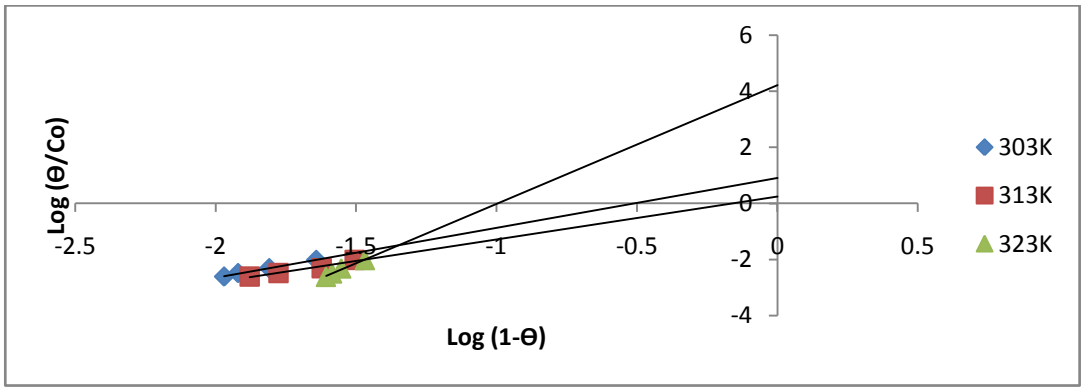

(d)

CPASG (a) Langmuir, (b) Freundlich, (c) Temkin, (d) Flory-Huggins

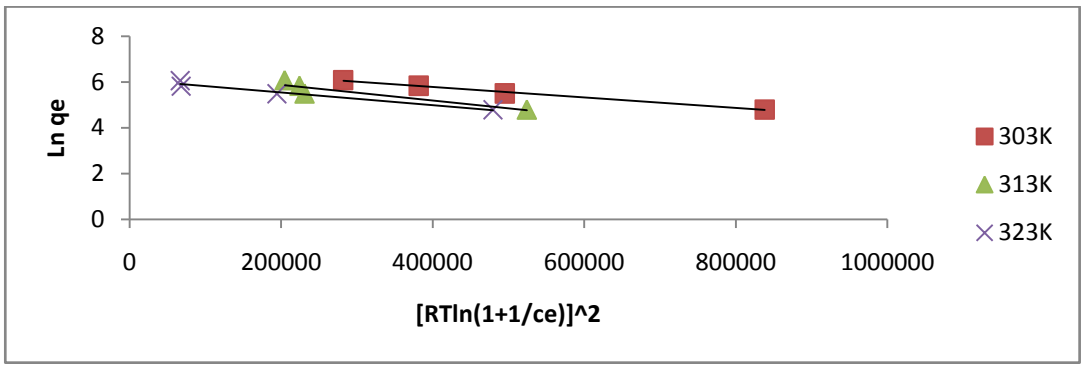

(e)

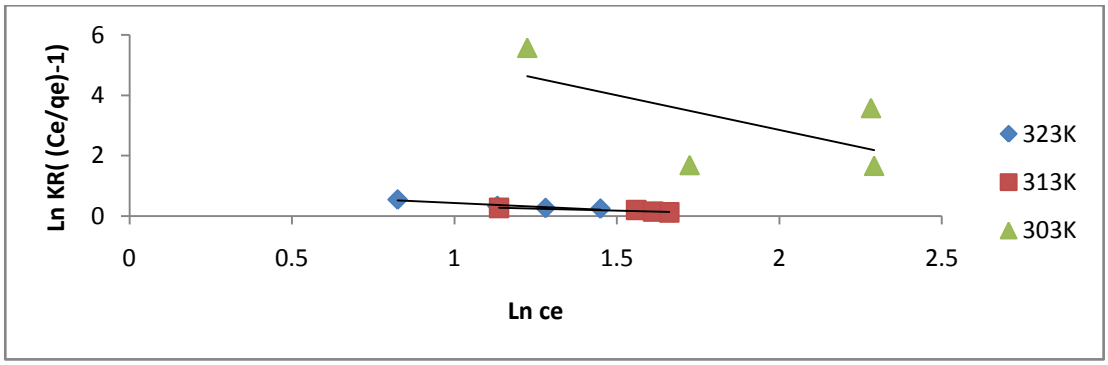

(f)

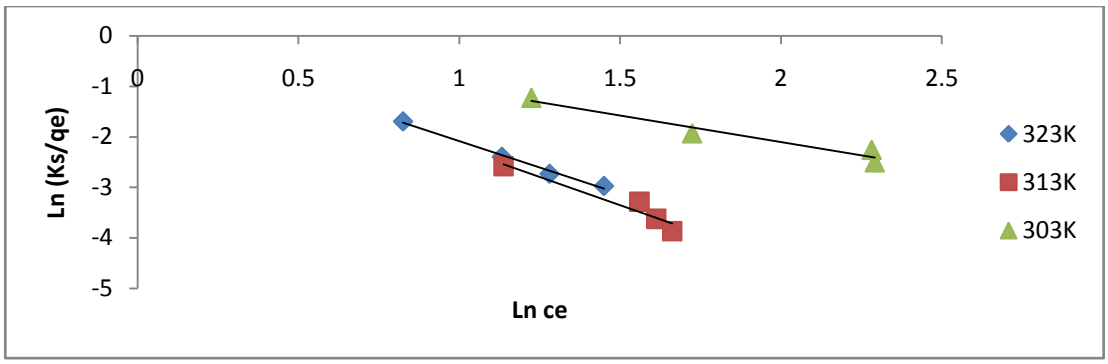

(g)

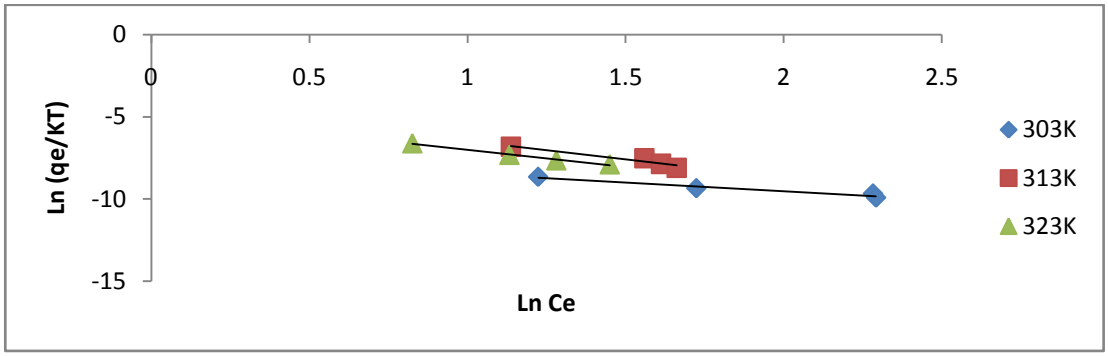

(h)

CPASG (e) D-R, (f) Redlich – Peterson, (g) Sip, (h) Toth

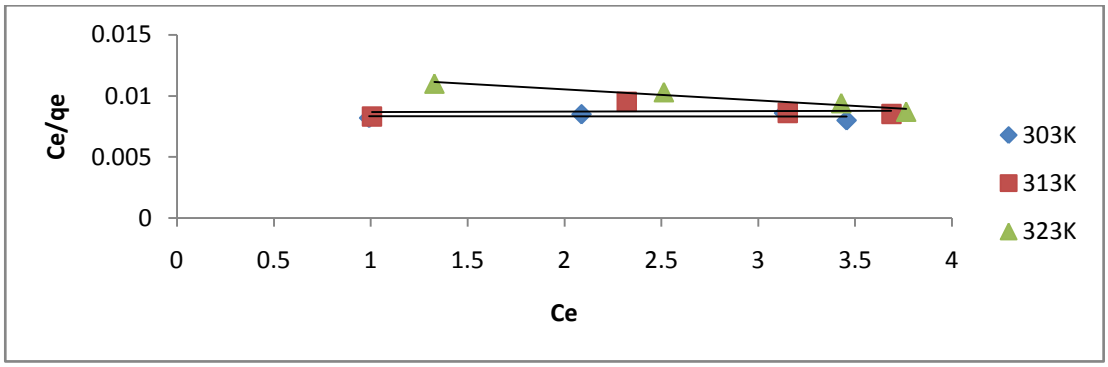

(a)

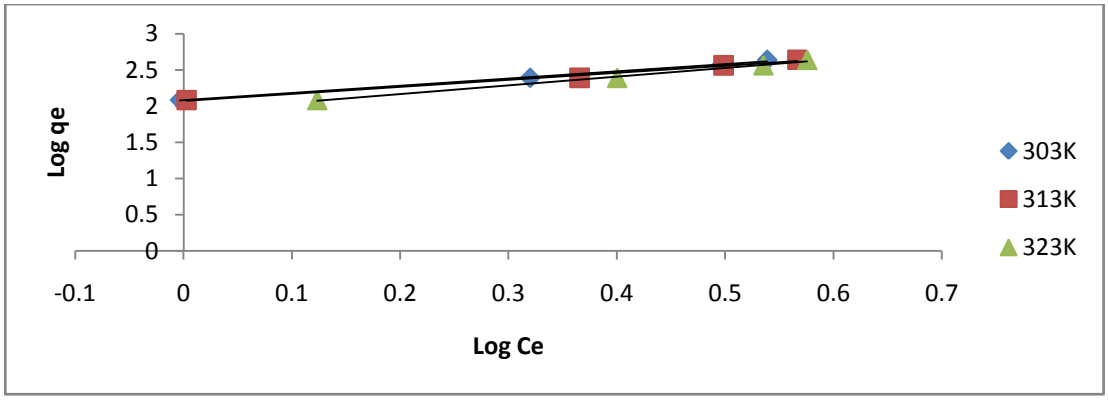

(b)

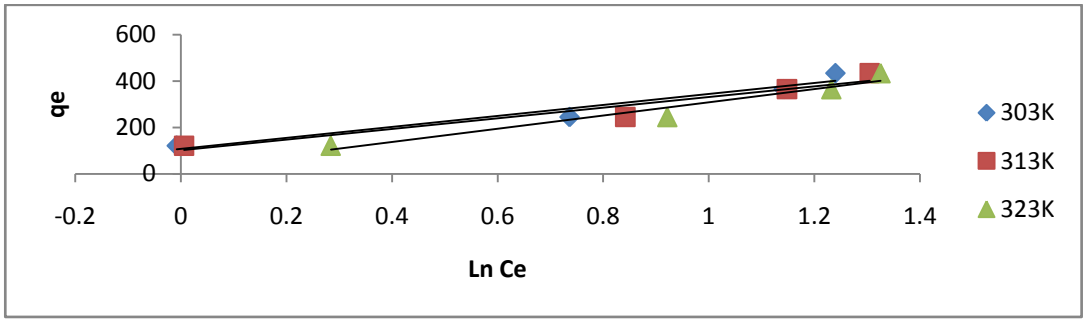

(c)

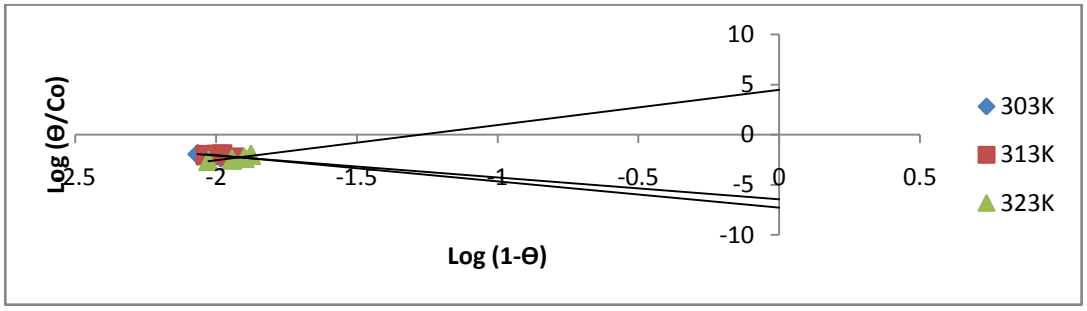

(d)

CPAHS (a) Langmuir, (b) Freundlich, (c) Temkin, (d) Flory-Huggins

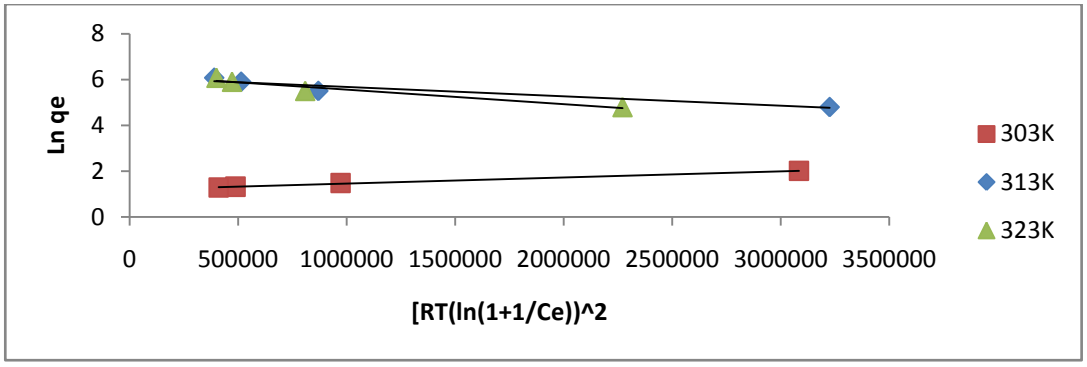

(e)

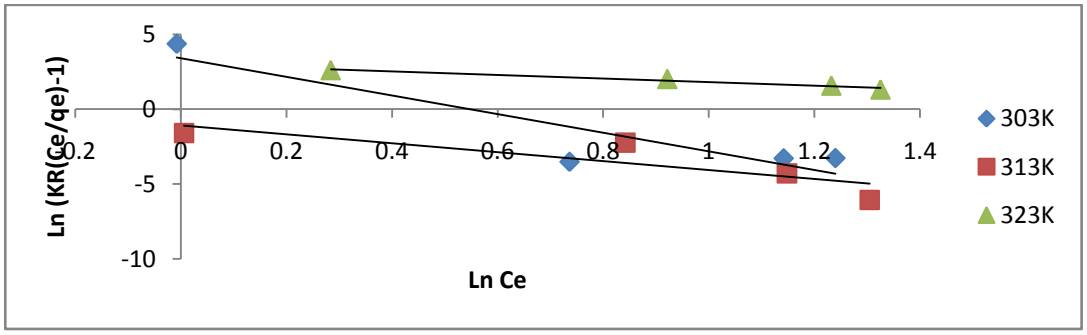

(f)

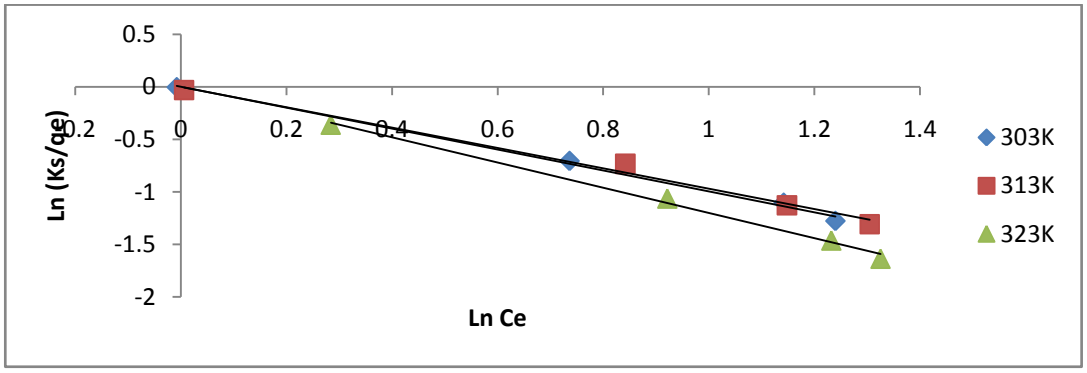

(g)

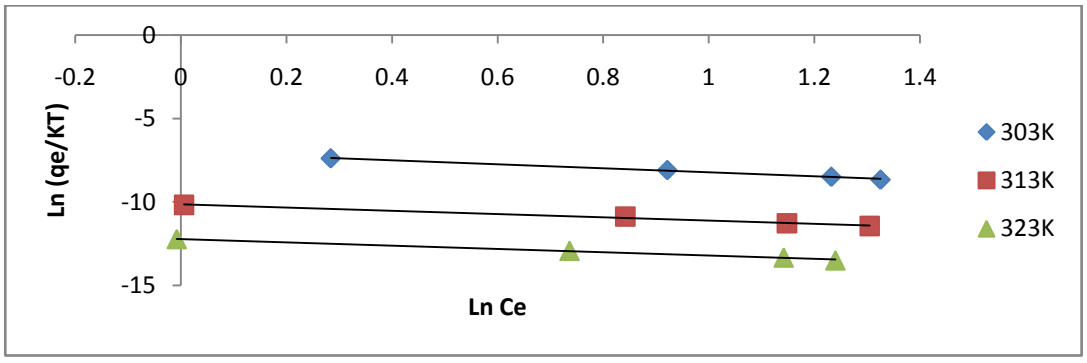

(h)

CPAHS (e) D-R, (f) Redlich – Peterson, (g) Sip, (h) Toth

APPENDIX L

PLOTS OF FREUNDLICH CONSTANTS AGAINST RECIPROCAL OF TEMPERATURE.

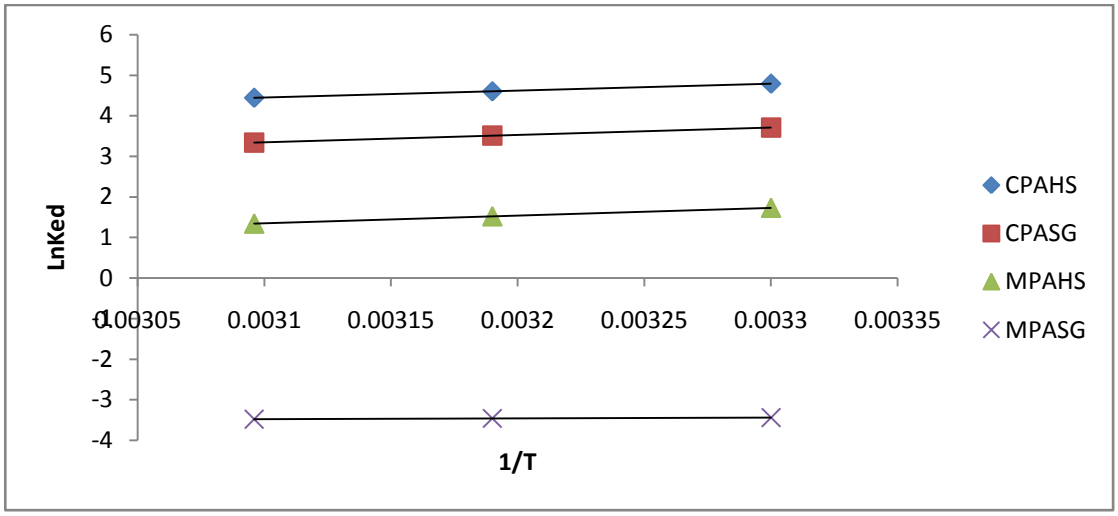

APPENDIX M

COMPARATIVE STUDIES ON THE THREE METHODS OF REGENERATIONS

Samples	Carbon Yield (g)	Carbon Loss (g)	Initial Carbon Weight(g)
		Chemical Regeneration	
MPAHS	5.306	-	5.624
MPASG	5.385	-	5.617
CPASG	5.3712	-	5.595
CPAHS	5.363	-	5.557
		Microwave Regeneration	
MPAHS	4.962	0.038	5.624
MPASG	4.949	0.051	5.617
CPASG	4.901	0.099	5.595
CPAHS	4.856	0.144	5.557
		Conventional Regeneration	
MPAHS	4.75	0.25	5.624
MPASG	4.615	0.385	5.617
CPASG	4.562	0.438	5.595
CPAHS	4.446	0.554	5.557

APPENDIX N

Effect of time on adsorptive capacity of the activated carbons

A. MPASG

Time	50mg/l	80mg/l	110mg/l	150mg/l
0	0	0	0	0
20	55.7525	93.2253	129.9633	179.8221
40	55.7807	93.2418	129.9927	179.8517
60	55.7865	93.251	130.6697	180.6592
80	55.791	93.2555	130.6952	180.6633
100	55.8143	93.2638	130.6981	180.6715
120	55.8203	93.2696	130.7036	180.6886
140	55.929	93.4261	130.9246	180.4565
160	56.0948	93.5663	130.9386	180.6672
180	56.283	93.761	131.2515	181.1277
200	56.4428	93.929	131.4346	181.2668
240	56.4463	93.9646	131.4387	181.2998
260	55.836	93.331	130.8165	180.5085
280	55.6378	93.1292	130.505	180.4987

B. MPAHS

TIME	50mg/l	80mg/	110mg/l	150mg/l
0	0	0	0	0
20	62.1758	99.6725	137.1402	187.1257
40	62.1761	99.674	137.1461	187.1271
60	62.1771	99.6767	137.1468	187.1276
80	62.1886	99.6791	137.1488	187.131
100	62.19	99.6803	137.1532	187.1348
120	62.1928	99.681	137.1545	187.1387
140	62.1973	99.6815	137.155	187.1397

160	62.2	99.6823	137.1562	187.1437
180	62.201	99.6833	137.1596	187.1445
200	62.202	99.6857	137.1631	187.1453
220	62.2648	99.7637	137.2628	187.2515
240	62.2688	99.7667	137.265	187.2641
260	62.2595	99.756	137.2885	187.2508
280	62.21	99.6917	137.1547	187.1525

C. CPAHS

TIME	50mg/l	80mg/l	110mg/l	150mg/l
0	0	0	0	0
20	36.5975	47.146	77.493	124.985
40	45.17	74.666	92.51	140.686
60	48.8425	81.848	102.161	155.09
80	51.8621	82.637	113.225	160.788
100	52.3981	83.415	115.118	164.456
120	52.4846	83.83	118.996	168.741
140	52.7198	83.975	119.373	168.817
160	53.1487	84.667	119.996	169.24
180	53.8035	85.136	120.137	169.67
200	54.2488	85.578	120.705	170.008
220	54.7678	86.021	121.365	170.435
240	55.2411	87.372	124.103	171.586
260	54.4552	86.968	124.997	170.125
280	54.4552	86.968	124.997	170.06

D. CPASG

TIME	50mg/l	80mg/l	110mg/l	150mg/l
0	0	0	0	0
20	38.9	41.9	75.915	123.835
40	42.02	49.51	80.423	125.805

60	42.85	49.99	82.55	128.128
80	43.509	51.715	85.738	130.211
100	46.048	52.546	86.598	133.591
120	47.138	53.2325	87.08	135.505
140	47.24	54.094	87.316	136.283
160	47.406	54.261	88.993	136.598
180	47.679	54.733	89.032	136.606
200	47.964	54.965	89.351	136.967
220	47.718	52.498	89.218	136.84
240	47.519	52.249	89.056	136.511
260	47.414	52.201	88.87	136.239
280	47.414	52.2	88.87	136.218

APPENDIX O

Effect of activated carbon dosage on the adsorptive capacity of activated carbons

A. MPAHS

Dosage(g)	50mg/l	80mg/l	110mg	150mg
0.02	61.87	99.37	136.83	186.77
0.05	24.75	39.75	54.73	74.71
0.08	15.471	24.84	34.21	46.71
0.11	11.27	18.08	24.9	33.99
0.14	8.869	14.22	19.57	26.71
0.17	7.33	11.74	16.15	22.03
2	0.623	0.999	1.375	1.874

B. MPASG

Dosage (g)	50mg	80mg/l	110mg/l	150mg/l
0.02	57.571	95.0098	132.0472	181.6546
0.05	23.2805	38.162	53.0878	73.0739
0.08	14.7886	24.117	33.5032	46.0299
0.11	10.8796	17.6438	24.4326	33.5166
0.14	8.608	13.941	19.2941	26.4342
0.17	7.1416	11.5511	15.9624	21.8445
2	0.62194	0.9966	1.3717	1.8713

C. CPASG

Dosage (g)	50mg	80mg	110mg	150mg/l
0.02	46.915	54.29	86.5887	135.71
0.05	23.4512	25.8395	37.87	44.3088
0.08	14.4272	18.9071	28.1162	39.8553
0.11	10.5292	17.0536	23.7701	32.7811

0.14	8.4173	13.6179	19.0608	25.9061
0.17	7.001	11.3889	15.7445	21.5272
2	0.6219	0.9921	1.3648	1.8506

D. CPAHS

Dosage (g)	50mg/l	80mg/	110mg/l	150mg/l
0.02	57.3462	89.9753	119.2412	163.8112
0.05	23.0904	37.0314	48.5935	67.6995
0.08	15.0085	24.3816	32.9287	44.9585
0.11	11.0802	17.8084	24.3635	33.3854
0.14	8.7566	14.1053	19.2959	26.3351
0.17	7.26	11.6286	16.0286	21.8096
2	0.6224	0.997	1.3632	1.8624

APPENDIX P

Kinetics of adsorption process

A. CPAHS at 50mg/l

Time	Ct	LogCt	**Q**t	(qe – qt)	Log(qe–qt)	1/Ct	t/qt	t1/2	Lnt
20	20.7220	1.3164	36.5975	18.6436	1.2705	0.0482	0.5464	4.4721	2.9957
40	17.8640	1.2519	40.1700	15.0711	1.1781	0.0559	0.9957	6.3245	3.6888
60	10.9260	1.0384	48.8425	6.3986	0.8060	0.0915	1.2284	7.7459	4.0943
80	8.5103	0.9299	51.8621	3.3790	0.5287	0.1175	1.5425	8.9442	4.3820
100	8.0815	0.9074	52.3981	2.8430	0.4537	0.1237	1.9084	10.0000	4.6051
120	8.0123	0.9037	52.4846	2.7565	0.4403	0.1248	2.2863	10.9544	4.7874
140	7.8241	0.8934	52.7198	2.5213	0.4016	0.1278	2.6555	11.8321	4.9416
160	7.4810	0.8739	53.1487	2.0924	0.3206	0.1336	3.0104	12.6491	5.0751
180	6.9572	0.8424	53.8035	1.4376	0.1576	0.1437	3.3455	13.4164	5.1929
200	6.6009	0.8196	54.2488	0.9923	-0.0035	0.1514	3.6867	14.1421	5.2983
240	6.1857	0.7913	54.7678	0.4733	-0.3248	0.1616	4.3821	15.4919	5.4806
260	5.8071	0.7639	55.2411	0.0000	0.0000	0.1722	4.7066	16.1245	5.5606
280	6.4358	0.8086	54.4552	0.7859	-0.1046	0.1553	5.1418	16.7332	5.6347

B. CPASG at (50mg/l)

Time	Ct	LogCt	Qt	(qe – qt)	Log(qe–qt)	1/Ct	t/qt	t1/2	Lnt
20	18.881	1.276	38.898	9.065	0.957	0.052	0.514	4.472	2.995
40	16.386	1.214	42.017	5.946	0.774	0.061	0.951	6.324	3.688
60	15.720	1.196	42.850	5.113	0.708	0.063	1.400	7.745	4.094
80	15.193	1.181	43.508	4.455	0.648	0.065	1.838	8.944	4.382
100	13.162	1.119	46.047	1.916	0.82	0.075	2.171	10.000	4.605
120	12.290	1.089	47.137	0.826	0.083	0.081	2.545	10.954	4.787
140	12.208	1.086	47.240	0.723	0.140	0.08	2.963	11.832	4.941
160	12.075	1.081	47.406	0.557	0.254	0.082	3.375	12.649	5.075
180	11.857	1.073	47.678	0.285	0.545	0.084	3.775	13.416	5.192
200	11.629	1.065	47.963	0.000	0.000	0.085	4.169	14.142	5.298

260	11.826	1.072	47.717	0.246	0.609	0.084	5.448	16.124	5.560
280	11.985	1.078	47.518	0.445	0.351	0.083	5.892	16.733	5.634

C. MPASG at (50mg/l)

Time	Ct	LogCt	Qt	(qe- qt)	Log(qe–qt)	1/Ct	t/qt	t1/2	Lnt
20	5.3980	0.7322	55.7525	0.7138	-0.1464	0.1852	0.3587	4.4721	2.9957
40	5.3754	0.7304	55.7807	0.6856	-0.1639	0.1860	0.7170	6.3245	3.6888
60	5.3708	0.7300	55.7865	0.6798	-0.1676	0.1861	1.0755	7.7459	4.0943
80	5.3672	0.7297	55.7910	0.6753	-0.1705	0.1863	1.4339	8.9442	4.3820
100	5.3485	0.7282	55.8143	0.6520	-0.1857	0.1869	1.7916	10.0000	4.6051
120	5.3437	0.7278	55.8203	0.6460	-0.1897	0.1871	2.1497	10.9544	4.7874
140	5.2568	0.7207	55.9290	0.5373	-0.2697	0.1902	2.5031	11.8321	4.9416
160	5.1241	0.7096	56.0948	0.3715	-0.4300	0.1951	2.8523	12.6591	5.0751
180	4.9736	0.6966	56.2830	0.1833	-0.7368	0.2010	3.1981	13.4164	5.1929
200	4.8457	0.6853	56.4428	0.0235	-1.6289	0.2063	3.5434	14.1421	5.2983
240	4.8269	0.6836	56.4663	0.0000	0.0000	0.2071	4.2503	15.4919	5.4806
260	5.3312	0.7268	55.8360	0.6303	-0.2004	0.1875	4.6564	16.1245	5.5606
280	5.4897	0.7395	55.6378	0.8285	-0.0817	0.1821	5.0325	16.7332	5.6347

D. CPASG at (80mg/l)

Time	Ct	LogCt	Qt	(qe – qt)	Log(qe – qt)	1/Ct	t/qt	t1/2	Lnt
20	46.479	1.667	41.901	24.860	1.395	0.021	0.477	4.472	2.995
40	40.392	1.606	49.510	17.251	1.236	0.024	0.807	6.324	3.688
60	40.007	1.602	49.991	16.770	1.227	0.024	1.200	7.745	4.094
80	38.628	1.586	51.715	15.046	1.177	0.025	1.546	8.944	4.382
100	37.963	1.579	52.546	14.215	1.152	0.026	1.903	10.000	4.605
120	36.414	1.561	54.482	12.279	1.089	0.027	2.202	10.954	4.787
140	36.725	1.564	54.093	12.668	1.102	0.027	2.588	11.832	4.941
160	26.591	1.424	66.761	0.000	0.000	0.027	2.396	12.649	5.075
180	36.214	1.558	54.732	12.029	1.080	0.027	3.288	13.416	5.192
200	37.928	1.578	52.590	14.171	1.151	0.026	3.803	14.142	5.298

260	38.002	1.579	52.497	14.264	1.154	0.026	4.952	16.124	5.560
280	38.201	1.582	52.248	14.513	1.161	0.026	5.359	16.733	5.634

E. MPASG at (80mg/l)

Time	Ct	LogCt	Qt	(qe – qt)	Log(qe–qt)	1/Ct	t/qt	t1/2	Lnt
20	5.4198	0.7339	93.2252	0.7394	-0.1311	0.1845	0.2145	4.4721	2.9957
40	5.4005	0.7329	93.2418	0.7228	-0.1409	0.1849	0.4289	6.3245	3.6888
60	5.3992	0.7323	93.2510	0.7136	-0.1465	0.1852	0.6434	7.7459	4.0943
80	5.3889	0.7320	93.2555	0.7091	-0.1492	0.1853	0.8578	8.9442	4.3820
100	5.3889	0.7315	93.2638	0.7008	-0.1544	0.1855	1.0722	10.0000	4.6051
120	5.3843	0.7311	93.2696	0.6950	-0.1580	0.1857	.2865	10.9544	4.
140	5.2591	0.7209	93.4261	0.5385	-0.2688	0.1901	1.4985	11.8321	4.
160	5.1469	0.7115	93.5663	0.3983	-0.3997	0.1942	1.7100	12.6491	5.0751
180	4.4912	0.6982	93.7010	0.2036	-0.6912	0.2003	1.9197	13.4164	5.1929
200	4.8568	0.6863	93.9290	0.0356	-1.4485	0.2058	2.1292	14.1421	5.29883
240	4.8283	0.6837	93.9646	0.0000	0.0000	0.2071	2.5541	15.4919	5.4806
260	5.3352	0.7271	93.3310	0.6336	-0.1981	0.1874	2.7857	16.1245	5.5606
280	5.4966	0.7400	93.1291	0.8354	-0.0781	0.1819	3.0065	16.7332	5.6347

F. MPAHS at (80mg/l)

Time	Ct	LogCt	Qt	(qe – qt)	Log(qe–qt)	1/Ct	t/qt	t1/2	Lnt
20	0.2620	-0.5816	99.6725	0.0942	-1.0259	3.8167	0.2006	4.4721	2.9957
40	0.2608	-05836	99.6740	0.0927	-1.0329	3.8343	0.4013	6.3245	3.6888
60	0.2586	-0.5873	99.6767	0.0900	-1.0457	3.8669	0.6019	7.7459	4.0943
80	0.2567	-0.5905	99.6791	0.0876	-1.0574	3.8955	0.8025	8.9442	4.3820
100	0.2557	-0.5922	99.6803	0.0864	-1.0534	3.9108	1.0032	10.0000	4.6051
120	0.2552	-0.5931	99.6810	0.0857	-1.0670	3.9184	1.2038	10.9544	4.7874
140	0.2548	-0.5938	99.6815	0.0852	-1.0695	3.9246	1.4044	11.8321	4.9416
160	0.2541	-0.5948	99.6823	0.0844	-1.0736	3.9354	1.6050	12.6491	5.0751
180	0.2533	-0.5963	99.6833	0.0834	-1.0788	3.9478	1.8057	3.4164	5.1929
200	0.2514	-0.5996	99.6857	0.0810	-1.0915	3.9777	2.0063	14.1421	5.2983

220	0.1890	-0.7235	99.7637	0.0030	-2.5228	5.2910	2.2052	4.8323	5.3936
240	0.1866	-0.7290	99.7667	0.0000	0.0000	5.3590	2.4056	15.4919	5.4806
260	0.1952	-0.7095	99.7560	0.0077	-2.1135	5.1229	2.6063	16.1245	5.5606
280	0.2466	-0.6080	99.6917	0.0720	-1.1426	4.0551	2.8086	16.7332	5.6347

G. CPAHS at (80mg/l)

Time	Ct	LogCt	Qt	(qe – qt)	Log(qe – qt)	1/Ct	t/qt	t1/2	Lnt
20	42.283	1.626	47.146	40.226	1.604	0.023	0.424	4.472	2.995
40	20.267	1.306	74.666	12.706	1.104	0.049	0.535	6.324	3.688
60	14.521	1.161	8.848	5.524	0.742	0.068	0.733	7.745	4.094
80	13.890	1.142	82.637	4.735	0675	0.071	0.968	8.44	4.382
100	13.268	1.122	83.415	3.957	0.597	0.075	1.198	10.000	4.605
120	12.936	1.111	83.830	3.542	0.549	0.077	1.431	10.954	4.787
140	12.820	1.107	83.975	3.397	0.531	0.078	1.667	11.832	4.941
160	12.266	1.088	84.667	2.705	0.432	0.081	1.889	12.649	5.075
180	11.891	1.075	85.136	2.236	0.349	0.084	2.114	13.416	5.192
200	11.537	1.062	85.578	1.794	0.253	0.086	2.337	14.142	5.298
240	11.183	1.048	86.021	1.351	0.130	0.089	2.790	15.491	5.480
260	10.102	1.004	87.372	0.000	0.000	0.098	2.975	16.124	5.560
280	12.825	1.108	83.963	3.404	0.531	0.077	2.334	16.733	5.634

H. CPASG at (110mg/l)

Time	Ct	LogCt	Qt	(qe – qt)	Log(qe– qt)	1/Ct	t/qt	t1/2	Lnt
20	49.268	1.692	75.915	13.436	1.128	0.020	0.263	4.472	2.995
40	45.661	1.659	80.423	8.928	0.950	0.021	0.497	6.324	3.688
60	43.963	1.643	82.546	6.805	0.832	0.022	0.726	7.745	4.094
80	41.409	1.617	85.738	3.613	0.557	0.024	0.933	8.944	4.382
100	40.721	1.609	86.598	2.753	0.439	0.024	1.154	10.000	4.605
120	40.336	1.605	87.080	2.271	0.356	0.024	1.378	10.954	4.787
140	40.147	1.603	87.316	2.035	0.308	0.024	1.603	11.832	4.941
160	38.805	1.588	88.993	0.358	-0.446	0.025	1.797	12.649	5.075

180	38.774	1.588	89.032	0.319	-0.496	0.025	2.021	13.416	5.192
200	38.519	1.585	89.351	0.000	0.000	0.025	2.238	14.142	5.298
260	38.625	1.586	89.218	0.133	-0.876	0.025	2.914	16.124	5.560
280	38.755	1.588	89.056	0.295	-0.530	0.025	3.144	6.733	5.634

G. MPASG at (110mg/l)

Time	Ct	LogCt	Qt	(qe – qt)	Log(qe – qt)	1/Ct	t/qt	t1/2	Lnt
20	6.0293	0.7802	129.9633	1.4754	0.1689	0.1658	0.1538	4.4721	12.9957
40	6.0058	0.7785	129.9927	1.4460	0.1601	0.1665	0.3077	6.33245	3.6888
60	5.4642	0.7375	130.6697	0.7690	-0.1140	0.1830	0.4591	7.7459	4.0943
80	5.4438	0.7359	130.6952	0.7435	-0.1287	0.1836	0.6121	8.9442	4.3820
100	5.4415	0.7357	130.6981	0.7406	-0.1304	0.1837	0.7651	10.0000	4.6051
120	5.4371	0.7353	130.7036	0.7351	-0.1336	0.1839	0.9181	10.9544	4.7874
140	5.2603	0.7210	130.9246	0.5141	-0.2889	0.1901	1.0693	11.8321	4.9416
160	5.2491	0.7200	130.9386	0.5001	-0.3009	0.1905	1.229	12.6491	5.0751
180	4.9988	0.6988	131.2515	0.1872	-0.7276	0.2000	1.3714	13.4164	5.1929
200	4.8523	0.6859	131.4346	0.0041	-2.3872	0.2060	1.5216	14.1421	5.2983
240	4.8490	0.6856	131.4387	0.0000	0.0000	0.2062	1.8259	15.4919	5.4806
260	5.3468	0.7280	130.8165	0.6222	-0.2060	0.1870	1.9875	16.1245	5.5606
280	5.5960	0.7478	130.5050	0.9337	-0.0297	0.1876	2.1455	16.7332	5.6347

I. MPAHS at (110mg/l)

Time	Ct	LogCt	Qt	(qe – qt)	Log(qe– qt)	1/Ct	t/qt	t1/2	Lnt
20	0.2878	-0.5409	137.1402	0.1483	-0.8288	3.4746	0.1458	4.4721	2.9957
40	0.2831	-0.5480	137.1461	0.1424	-0.8464	3.5323	0.2916	6.3245	3.6888
60	0.2825	-0.5489	137.1468	0.1417	-0.8486	3.5398	0.4374	7.7459	4.0943
80	0.2809	-0.5514	137.1488	0.1397	-0.8548	3.5599	0.5833	8.9442	4.3820
100	0.2774	-0.5568	137.1532	0.1353	-0.8687	3.6049	0.7291	10.000	4.6051
120	0.2764	-0.5584	137.1545	0.1340	-0.8728	3.6179	0.8749	10.9544	47874
140	0.2760	-0.5590	137.1550	0.1335	-0.8745	3.6231	1.0207	11.8321	4.9416

160	0.2750	-0.5606	137.1562	0.1323	-0.8784	3.6363	1.1665	12.6491	5.0751
180	0.2723	-0.5649	137.1596	0.1289	-0.8897	3.6724	1.3123	13.4164	5.1929
200	0.2695	-0.5694	137.1631	0.1254	-0.9017	3.7105	1.4581	14.1421	5.2983
220	0.1897	-0.7219	137.2628	0.1257	-0.5900	5.2714	1.6027	14.8323	5.3936
240	0.1880	-0.7258	137.2650	0.0235	-1.6289	5.3191	1.7484	15.4919	5.4806
260	0.1692	-0.7715	137.2885	0.000	0.0000	5.9101	1.8938	16.1245	5.5606
280	0.2762	-0.5587	137.1547	0.1338	-0.8735	3.6205	2.0414	16.7332	5.6347

J. CPAHS at (110mg/l)

Time	Ct	LogCt	Qt	(qe – qt)	Log(qe–qt)	$^{1}/Ct$	$^{t}/qt$	$^{t1}/2$	Lnt
20	48.005	1.681	77.493	47.504	1.676	0.020	0.258	4.472	2.995
40	35.992	1.556	92.510	32.487	1.511	0.027	0.432	6.324	3.688
60	28.271	1.451	102.161	22.836	1.358	0.035	0.587	7.745	4.094
80	19.420	1.288	113.225	11.772	1.070	0.051	0.706	8.944	4.382
100	17.905	1.252	115.118	9.879	0.994	0.055	0.868	10.000	4.605
120	14.803	1.170	118.996	6.001	0.778	0.067	1.008	10.954	4.787
140	14.501	1.161	119.373	5.624	0.750	0.068	1.172	11.832	4.941
160	14.003	1.146	119.996	5.001	0.699	0.071	1.166	12.649	5.075
180	13.890	1.142	120.137	4.800	0.686	0.071	1.498	13.416	5.192
200	13.436	1.128	120.705	4.292	0.632	0.074	1.656	14.142	5.298
240	12.908	1.110	121.365	3.632	0.560	0.077	1.977	15.491	5.480
260	10.717	1.030	124.103	0.894	-0.048	0.093	2.095	16.124	5.560
280	10.002	1.000	124.997	0.000	0.000	0.099	2.240	16.733	5.634

K. CPASG at (150mg/l)

Time	Ct	LogCt	Qt	(qe – qt)	Log(qe – qt)	$^{1}/Ct$	$^{t}/qt$	T ½	Lnt
20	50.932	1.706	123.835	13.132	1.118	0.019	0.161	4.472	2.995
40	49.356	1.693	125.805	11.162	1.047	0.020	0.317	6.324	3.688
60	47.498	1.676	128.127	8.840	0.946	0.021	0.468	7.745	4.094
80	45.831	1.661	130.211	6.756	0.829	0.021	0.614	8.944	4.382
100	43.127	1.634	133.591	3.376	0.528	0.023	0.748	10.000	4.605

120	41.596	1.619	135.505	1.462	0.164	0.024	0.885	10.954	4.787
140	40.973	1.612	136.283	0.684	-0.164	0.024	1.027	11.832	4.941
160	40.721	1.609	136.598	0.369	-0.432	0.024	1.171	12.649	5.075
180	40.715	1.609	136.606	0.361	-0.442	0.024	1.317	13.416	5.192
200	40.426	1.606	136.967	0.000	0.000	0.024	1.460	14.142	5.298
260	40.528	1.607	136.840	0.127	-0.986	0.024	1.900	16.124	5.560
280	40.791	1.610	136.511	0.456	-0.341	0.024	2.051	16.733	5.634

L. CPAHS at (110mg/l)

Time	Ct	LogCt	Qt	(qe – qt)	Log(qe – qt)	$^{1}/Ct$	$^{t}/qt$	$t^{1}/2$	Lnt
20	6.1423	0.7883	179.8221	1.4777	0.1695	0.1628	0.1112	4.4721	2.9957
40	6.1186	0.7866	179.8517	1.4481	0.1607	0.1634	0.2224	6.3245	3.6888
60	5.4726	0.7381	180.6592	0.6406	-0.1934	0.1827	0.3321	7.7459	4.0943
80	5.4693	0.7379	180.6633	0.6365	-0.1962	0.1828	0.4428	8.9442	4.3820
100	5.4628	0.7374	180.6715	0.6283	-0.2018	0.1830	0.5534	0.0000	4.6051
120	5.4491	0.7363	180.6886	0.6112	-0.2138	0.1835	0.6641	10.9544	4.7874
140	5.6348	0.7508	180.4565	0.8433	-0.-740	0.1774	0.7758	11.8321	4.0416
160	5.4662	0.7376	180.6672	0.6326	-0.1988	0.1829	0.8856	12.6491	5.0751
180	5.0978	0.7073	181.1277	0.1721	-0.7642	0.1961	0.9937	13.4164	5.1929
200	4.9865	0.6977	181.2668	0.0330	-1.4814	0.2005	1.1033	14.1421	5.2983
240	4.9601	0.6954	181.2998	0.0000	0.0000	0.2016	1.3237	15.4919	5.4806
260	5.5932	0.7476	180.5085	0.7913	-0.1016	0.1787	1.4403	16.1245	5.5606
280	5.6010	0.7482	180.4987	0.8011	-0.-963	0.1785	1.5512	16.7332	5.6347

M. CPASG at (150mg/l)

Time	Ct	LogCt	Qt	(qe- qt)	Log(qe– qt)	$^{1}/Ct$	$^{t}/qt$	t ½	Lnt
20	0.2994	-0.5237	187.1257	0.1384	-0.8588	3.3400	0.1068	4.4721	2.9957
40	0.2983	-0.5253	187.1271	0.1370	-0.8632	3.3532	0.2137	6.3245	3.6888
60	0.2979	-0.5259	187.1276	0.1365	-0.8648	3.3568	0.3206	7.7459	4.0943
80	0.2952	-0.5298	187.1310	0.1331	-0.8758	3.3815	0.4275	8.9442	4.3820
100	0.292	-0.5344	187.1348	0.1293	-0.8884	3.4234	0.5343	10.0000	4.6051

120	0.2890	-0.5391	187.1387	0.1254	-0.9017	3.4602	0.6412	10.9544	4.7874
140	0.2882	-0.5403	187.1397	0.1244	-0.9051	3.4698	0.7481	11.8321	4.9416
160	0.2850	-0.5451	187.1437	0.1204	-0.9193	3.5087	0.8549	12.6491	5.0751
180	0.2844	-0.5460	187.1445	0.1196	-0.9222	3.5161	0.9618	13.4164	5.1929
200	0.2837	-0.5471	187.1453	0.1188	-0.9251	3.5248	1.0686	14.1421	5.2983
220	0.1988	-0.7015	187.2515	0.0126	-1.8996	5.0301	1.1748	14.8323	5.3936
240	0.1887	-0.7242	187.2641	0.0000	0.0000	5.2994	1.2816	15.4919	5.4806
260	0.1993	-0.7004	187.2508	0.0133	-1.8761	5.0175	1.3885	16.1245	5.5606

N. CPAHS at (150mg/l)

Time	Ct	LogCt	Qt	(qe-qt)	Log(qe – qt)	$^{1}/Ct$	$^{t}/qt$	$t^{1}/2$	Lnt
20	50.012	1.699	124.985	46.601	1.668	0.019	0.160	4.472	2.995
40	38.251	1.582	139.686	31.900	1.503	0.026	0.286	6.324	3.688
60	33.928	1.530	145.090	26.496	1.423	0.029	0.413	7.745	4.094
80	21.369	1.329	160.788	10.798	1.033	0.046	0.497	8.944	4.382
100	18.435	1.265	164.456	7.130	0.853	0.054	0.608	0.000	4.605
120	15.007	1.176	168.741	2.845	0.454	0.066	0.711	10.954	4.787
140	14.946	1.174	168.817	2.769	0.442	0.066	0.829	11.832	4.941
160	14.608	1.164	169.240	2.346	0.370	0.068	0.945	12.649	5.075
180	14.264	1.154	169.670	1.916	0.282	0.070	1.060	13.416	5.192
200	13.993	1.145	170.008	1.578	0.198	0.071	1.176	14.142	5.298
240	13.652	1.135	170.435	1.151	0.061	0.073	1.408	15.491	5.480
260	12.731	1.104	171.586	0.000	0.000	0.078	1.515	16.124	5.560
280	13.900	1.143	170.125	1.461	0.164	0.071	1.645	16.733	5.634

O. MPAHS at 150mg/L

Time	Ct	LogCt	Qt	(qe-qt)	Log(qe–qt)	$^{1}/Ct$	$^{t}/qt$	t ½
20	0.2594	-0.5860	62.1758	0.093	-1.0315	3.8551	0.3217	4.4721
40	0.2591	-0.5865	62.1761	0.0927	-1.0329	3.8595	0.6433	6.3246
60	0.2583	-0.5879	62.1771	0.0917	-1.0376	3.8715	0.9650	7.7460
80	0.2491	-0.6036	62.1886	0.0802	-1.0958	4.0145	1.2864	8.9443

100	0.2480	-0.6055	62.190	0.0788	-1.1034	4.0323	1.6080	10.000
120	0.2458	-0.6094	62.1928	0.076	-1.1191	4.0683	1.9295	10.9545
140	0.2422	-0.6158	62.1973	0.0715	-1.1456	4.1288	2.2509	11.8321
160	0.2400	-0.6198	62.20	0.0688	-1.1624	4.1667	2.5723	12.6491
180	0.2391	-0.6214	62.2011	0.0677	-1.1694	4.1824	2.8938	13.4164
200	0.2384	-0.6227	62.202	0.0668	-1.1752	4.1946	3.2153	14.1421
220	0.1882	-0.7254	62.2648	0.004	-2.3979	5.3135	3.5333	14.8324
240	0.1850	-0.7328	62.2688	0	0	5.4054	3.8543	15.4919
260	0.1924	-0.7157	62.2595	0.0093	-2.0315	5.1975	4.1760	16.1245
280	0.2392	-0.6212	62.2010	0.0678	-1.1687	4.1806	4.5015	16.7332

APPENDIX Q

Desorption Kinetic study

1. CPASG

A. First order model

Time (mins)	124.36mg/g	248.85mg/g	347.27mg/g	441.49mg/g
20	0.3906	0.6595	0.6943	0.7015
40	0.4513	0.6721	0.7057	0.7639
60	0.5787	0.6835	0.7237	0.7919
80	0.5974	0.6906	0.7853	0.808
100	0.6604	0.6973	0.7987	0.8289
120	0.6937	0.714	0.8327	0.8566
140	0.7172	0.7346	0.8586	0.8995
160	0.7538	0.7544	0.873	0.9087
180	0.765	0.7747	0.8964	0.9319
200	0.8117	0.8249	0.8971	0.9457
240	0.8187	0.8383	0.8984	0.95
260	0.8214	0.8279	0.9207	0.9741
280	0.8277	0.8279	0.9211	0.9741

B. Pseudo first order

Time (mins)	124.36mg/g	248.85mg/g	347.27mg/g	441.49mg/g
20	-0.7271	-0.4635	-0.6274	-0.7396
40	-0.6879	-0.4376	-0.6103	-0.655
60	-0.5646	-0.412	-0.5806	-0.6059
80	-0.5392	-0.395	-0.4469	-0.5733
100	-0.4295	-0.378	-0.4083	-0.5248
120	-0.3488	-0.3311	-0.2834	-0.4458
140	-0.2764	-0.2622	-0.1453	-0.2692
160	-0.119	-0.1797	-0.0391	-0.2167

180	-0.0531	-0.0691	0.2395	-0.0381
200	0.5161	0.5831	0.2504	0.1272
240	0.7604	0	0.2744	0.1967
260	0.9129	0.6907	1.9586	0
280	0	0.6907	0	0

C. Second order

Time (mins)	124.36mg/g	248.85mg/g	347.27mg/g	441.49mg/g
20	0.4067	0.219	0.2021	0.1988
40	0.3537	0.2127	0.1969	0.1721
60	0.2637	0.2072	0.1888	0.1614
80	0.2526	0.2038	0.1639	0.1555
100	0.2185	0.2007	0.1589	0.1482
120	0.2024	0.1931	0.1469	0.139
140	0.1917	0.1842	0.1384	0.126
160	0.1762	0.176	0.1339	0.1233
180	0.1717	0.1679	0.1269	0.1169
200	0.1542	0.1496	0.1267	0.1133
240	0.1518	0.145	0.1263	0.1121
260	0.1508	0.1486	0.12	0.1061
280	0.1486	0.1486	0.1199	0.1061

D. Pseudo second order

Time (mins)	124.36mg/g	248.85mg/g	347.27mg/g	441.49mg/g
20	0.1648	0.0822	0.0586	0.0459
40	0.331	0.1646	0.1173	0.0921
60	0.5015	0.247	0.1761	0.1383
80	0.6699	0.3295	0.2355	0.1845
100	0.8428	0.4121	0.2946	0.2309
120	1.0153	0.495	0.3542	0.2774

140	1.188	0.5783	0.4139	0.3243
160	1.3644	0.6618	0.4734	0.3709
180	1.5373	0.7456	0.5334	0.4178
200	1.7203	0.8316	0.5927	0.4646
240	2.0667	0.999	0.7113	0.5576
260	2.2399	1.0813	0.7718	0.605
280	2.4147	1.1645	0.8312	0.6515

E. Intra particle diffusion

t1/2	124.36mg/g	248.85mg/g	347.27mg/g	441.49mg/g
4.4721	121.2868	243.1428	341.0862	435.2032
6.3245	120.8262	242.9743	340.9221	434.2308
7.7459	119.6215	242.8175	340.6525	433.7481
8.9442	119.4132	242.7185	339.6438	433.4563
10	118.6408	242.6233	339.4057	433.0602
10.9544	118.1847	242.3788	338.7656	432.5031
11.8321	117.8418	242.0642	338.2425	431.5705
12.6491	117.2673	241.748	337.9393	431.359
13.4164	117.0823	241.4077	337.4211	430.8037
14.1421	116.2567	240.4963	337.4068	430.4578
15.4919	116.1256	240.2352	3373765	430.3475
16.1245	116.0742	240.439	336.856	429.7118
16.7332	115.952	240.439	336.845	429.7118

F. Elovich model

lnt	124.36mg/g	248.85mg/g	347.27mg/g	441.49mg/g
2.9957	121.2868	243.1428	341.0862	435.2032
3.6888	120.8262	242.9743	340.9221	434.2308
4.0943	119.6215	242.8175	340.6525	433.7481
4.382	119.4132	242.7185	339.6438	433.4563

4.6051	118.6408	242.6233	339.4057	433.0602
4.7874	118.1847	242.3788	338.7656	432.5031
4.9416	117.8418	242.0642	338.2425	431.5705
5.0751	117.2673	241.748	337.9393	431.359
5.1929	117.0823	241.4077	337.4211	430.8037
5.2983	116.2567	240.4963	337.4068	430.4578
5.4806	116.1256	240.2352	3373765	430.3475
5.5606	116.0742	240.439	336.856	429.7118
5.6347	115.952	240.439	336.845	429.7118

2. MPAHS

A. First order

Time(mins)	123.7170mg/g	248.5825mg/g	373.2792mg/g	498.1079mg/g
20	0.638	1.0106	1.4235	1.7044
40	0.8969	1.0362	1.5992	1.741
60	0.9495	1.281	1.6012	1.7583
80	1.2633	1.4729	1.6039	1.7772
100	1.3374	1.4734	1.6065	1.7789
120	1.3522	1.4783	1.6061	1.8398
140	1.3535	1.5187	1.639	1.8668
160	1.354	1.5541	1.7	1.8753
180	1.4231	1.5681	1.7017	1.9105
200	1.4367	1.5684	1.7084	1.9141
240	1.4394	1.5687	1.7094	1.9152
260	1.4395	1.5689	1.7094	1.9152
280	1.4395	1.5689	1.7094	1.9152

B. Pseudo first order

Time(min)	123.7170mg/g	248.5825mg/g	373.2792mg/g	498.1079mg/g
20	-1.0671	-0.943	-0.541	-0.4822

40	-0.7922	-0.9078	0.3275	-0.3054
60	-0.7143	-0.4065	0.3443	-0.2088
80	0.1602	0.5989	0.3683	-0.09
100	0.67	0.6042	0.3924	-0.0786
120	0.8189	0.5451	0.3886	0.4835
140	0.8331	1.2245	0.7559	0.913
160	0.8393	2.4304	2.735	1.1032
180	2.4534	5.3185	2.9356	3.2164
200	4.2064	5.8091	4.9477	4.6253
240	7.824	6.5023	7.824	8.5172
260	0	0	0	9.2103

C. Second order

Time(mins)	123.7170mg/g	248.5825mg/g	373.2792mg/g	498.1079mg/g
20	0.5283	0.364	0.2409	0.1819
40	0.4078	0.3548	0.202	0.1753
60	0.3869	0.2777	0.2017	0.1723
80	0.2827	0.2292	0.2011	0.1691
100	0.2625	0.2291	0.2006	0.1688
120	0.2587	0.228	0.2007	0.1588
140	0.2583	0.219	0.1942	0.1546
160	0.2582	0.2114	0.1827	0.1533
180	0.241	0.2084	0.1824	0.148
200	0.2377	0.2084	0.1812	0.1475
240	0.2371	0.2083	0.181	0.1473
260	0.237	0.2083	0.181	0.1473
280	0.237	0.2083	0.181	0.1473

D. Pseudo second order

Time(mins)	123.7170mg/g	248.5825mg/g	373.2792mg/g	498.1079mg/g

20	0.1648	0.0816	0.0543	0.0407
40	0.3315	0.1632	0.109	0.0815
60	0.498	0.2458	0.1634	0.1222
80	0.6706	0.329	0.2179	0.163
100	0.8406	0.4113	0.2724	0.2038
120	1.0094	0.4936	0.3264	0.2448
140	1.1777	0.5764	0.3816	0.2857
160	1.3459	0.6593	0.4366	0.3266
180	1.5186	0.742	0.4912	0.3676
200	1.6883	0.8244	0.5459	0.4085
240	2.0263	0.9893	0.6551	0.4902
260	2.1951	1.0718	0.7097	0.531
280	2.364	1.1542	0.7643	0.5719

G. Elovich model

lnt(min)	123.7170(mg/g)	248.5825(mg/g)	373.2792mg/g	498.1079mg/g
2.9957	121.351	245.1484	368.0897	491.2419
3.6889	120.6519	245.0595	367.0927	490.9794
4.0943	120.4864	244.0821	367.0807	490.8544
4.382	119.2957	243.13	367.0639	490.7164
4.6052	118.9554	243.1271	367.0474	490.704
4.7875	118.8846	243.1004	367.0499	490.2388
4.9416	118.8784	242.8745	366.8416	490.0235
5.0752	118.8757	242.6686	366.4369	489.954
5.193	118.5297	242.5855	366.4251	489.6623
5.2983	118.4586	242.5836	366.3791	489.632
5.4806	118.4441	242.5821	366.3722	489.6224
5.5607	118.4437	242.5806	366.372	489.6223
5.6348	118.4437	242.5806	366.372	489.6222

APPENDIX R

Initial solid phase concentration (mg/g) for desorption studies

A. Isotherm

	100mg/l	200mg/l	300mg/l	400mg/l
CPAHS	122.6853	247.7338	369.0443	438.5288
MPASG	123.5913	248.2943	369.2771	460.7038
CPASG	124.3603	248.847	347.2603	441.4925
MPAHS	124.717	248.5825	373.279	498.1079

B. Other studies

	100mg/l	200mg/l	300mg/l	400mg/l
CPAHS	122.31	245.17	326.96	390.65
MPASG	124.36	248.847	347.27	441.49
CPASG	122.69	245.23	369.04	438.52
MPAHS	123.717	248.5825	373.279	498.108

APPENDIX S

EFFECT OF TEMPERATURE ON THE DESORPTION CAPACITY OF ACTIVATED CARBONS

A. MPASG

Initial solid phase conc (mg/g)	303K	313K	323K
123.5912	117.4118	111.1	103.64
248.2943	241.9996	221.732	201.006
369.27	362.7032	331.72	308.53
460.7038	453.2397	420.743	408.942

B. CPASG

Initial solid phase conc (mg/g)	303K	313K	323K
124.3603	115.7841	105.04	100.94
248.847	240.1995	215.643	201.921
347.2663	336.6088	314.92	298.463
441.4925	429.5525	415.731	401.67

C. CPAHS

Initial solid phase conc. (mg/g)	303K	313K	323K
122.6853	115.9888	110.32	104.53
247.7338	240.6288	218.631	205.663
369.0443	361.5838	338.62	310.167
438.5288	430.8825	415.831	400.051

D. MPAHS

Initial solid phase conc.(mg/g)	303K	313K	323K
123.717	117.6815	107.2	96.5
248.5825	241.632	221	203.53
373.2792	365.5375	345.02	324.88
498.1079	488.867	465.64	440.113

APPENDIX T

EFFECT OF ELUANTS ON THE DESORPTION CAPACITY OF LOADED ACTIVATED CARBONS

A. MPASG

Initial solid phase conc. (mg/g)	0.1M NaOH	0.1MHCl	n-hexane	Ethyl acetate	Chloroform
124.3603	122.991	121.947	123.209	123.139	116.41
248.847	246.37	246.231	246.539	247.343	239.362
347.2663	344.496	344.628	344.22	345.609	336.48
441.4925	438.48	438.168	437.803	439.67	430.132

B. MPAHS

Initial solid phase conc. (mg/g)	0.1M NaOH	0.1MHCl	n-hexane	Chloroform	Ethylacetate
123.717	122.467	122.678	122.985	119.051	122.747
248.5825	247.298	247.28	247.699	243.407	247.57
373.279	371.636	371.966	372.244	366.737	372.263
498.1079	496.053	496.348	497.043	489.87	497.068

C. CPASG

Initial solid phase conc. (mg/g)	0.1M NaOH	0.1MHCl	n-hexane	Ethyl acetate	Chloroform
122.685	121.013	118.514	122.646	122.178	114.127
245.234	243.125	239.765	245.168	244.423	232.765
369.044	366.518	361.047	368.97	367.99	353.672
438.529	436.007	429.706	438.406	436.931	420.953

D. CPAHS

Initial solid phase conc. (mg/g)	0.1M NaOH	0.1MHCl	n-hexane	Ethyl acetate	Chloroform
122.31	120.66	120.66	120.31	120.211	118.4
245.17	242.72	242.57	241.67	241.14	237.77
326.91	323.71	323.575	322.79	321.67	317.71
390.65	387.046	386.95	386.2	385.105	321.67

APPENDIX U

DESORPTION RATE CONSTANTS

A. MPAHS

1/T	123.5913mg/g	248.2943mg/g	369.2771mg/g	460.7038mg/g
0.0033	5.2495	5.0027	4.943	4.8196
0.00319	5.2983	5.099	4.962	4.8691
0.003096	5.3391	5.185	5.0672	4.9618

B. MPASG

1/T	123.329mg/g	247.797mg/g	372.645mg/g	497.532mg/g
0.0033	4.5008	4.4568	4.3741	4.32
0.00319	4.5399	4.483	4.4368	4.4
0.003096	4.5756	4.519	4.4741	4.4397

C. CPASG

1/T	124.3603mg/g	248.847mg/g	347.2663mg/g	441.4925mg/g
0.0033	4.7514	4.3741	4.2477	4.0345
0.00319	4.8836	4.631	4.5132	4.3575
0.003096	5.0515	4.8536	4.828	4.5008

D. CPAHS

1/T	122.69mg/g	247.73mg/g	369.04mg/g	438.53mg/g
0.0033	4.828	4.7444	4.1541	4.1166
0.00319	4.939	4.7677	4.2351	4.1227
0.003096	5.0146	4.7939	4.3662	4.1352

APPENDIX V

REGENERATION CYCLES

A. CHEMICAL REGENERATION CYCLES

1. ADSORPTIVE CAPACITY (mg/l) for 100mg/l

	MPAHS	MPASG	CPASG	CPAHS
Ist Adsorption	124.852	123.383	118.947	111.424
2nd Adsorption	123.988	120.435	116.04	110.694
3rd Adsorption	115.194	112.72	111.3	109.574
4th Adsorption	107.316	101.644	97.85	89.173
5th Adsorption	89.61	97.85	88.349	87.5
6th Adsorption	79.588	75.00	72.5	68.368
7th Adsorption	72.5	62.875	61.674	57.494

2. Regeneration Efficiency (%) for 100mg/l

	MPAHS	MPASG	CPASG	CPAHS
0 Cycle	100.00	100.00	100.00	100.00
1st Cycle	99.31	97.61	97.56	99.34
2nd Cycle	92.264	91.36	93.588	98.34
3rd Cycle	85.955	82.38	82.27	80.03
4th Cycle	71.77	79.31	74.28	78.53
5th Cycle	63.75	60.786	60.95	61.36
6th cycle	58.07	50.96	51.85	51.6

3. Adsorptive capacity (mg/l) for 200mg/l

	MPAHS	MPASG	CPASG	CPAHS
Ist Adsorption	247.66	244.45	233.89	223.78
2nd Adsorption	242.30	229.98	223.92	208.36
3rd Adsorption	224.40	214.48	210.00	202.36
4th Adsorption	209.14	198.83	190.01	178.4
5th Adsorption	166.54	159.61	157.11	155.84

6th Adsorption	126.68	124.61	112.11	111.05
7th Adsorption	97.11	85.00	75.00	68.38

4. Regeneration Efficiency (%) for 200mg/l

	MPAHS	MPASG	CPASG	CPAHS
0 Cycle	100.00	100.00	100.00	100.00
1st Cycle	97.84	94.08	95.74	93.11
2nd Cycle	90.61	87.94	89.79	90.43
3rd Cycle	84.45	81.34	81.23	79.72
4th Cycle	67.25	65.29	67.17	69.64
5th Cycle	51.15	50.98	47.93	49.62
6th cycle	39.11	34.77	32.07	30.56

5. Adsorptive capacity (mg/l) for 300mg/l

	MPAHS	MPASG	CPASG	CPAHS
Ist Adsorption	372.36	363.49	339.61	331.93
2nd Adsorption	324.51	321.52	310.23	266.80
3rd Adsorption	272.11	253.02	222.11	208.99
4th Adsorption	224.38	202.18	147.15	117.11
5th Adsorption	137.98	114.42	74.61	40.31
6th Adsorption	341.86	14.6	2.3	9.86
7th Adsorption	5.85	3.35	2.5	1.25

6. Regeneration Efficiency (%) for 300mg/l

	MPAHS	MPASG	CPASG	CPAHS
0 Cycle				
1st Cycle	87.15	88.45	91.35	80.38
2nd Cycle	73.08	69.61	65.40	62.97
3rd Cycle	60.26	55.62	43.33	35.28
4th Cycle	37.06	31.48	21.97	12.14
5th Cycle	9.36	4.02	3.62	2.97

6th cycle	1.571	0.92	0.74	0.38

7. Adsorptive capacity (mg/l) for 400mg/l

	MPAHS	MPASG	CPASG	CPAHS
Ist Adsorption	495.93	476.81	453.78	444.41
2nd Adsorption	421.56	402.11	399.34	352.11
3rd Adsorption	267.11	249.87	224.6	199.45
4th Adsorption	212.11	139.17	124.22	75.0
5th Adsorption	989.4	61.73	49.88	24.61
6th Adsorption	12.4	4.61	1.13	1.25
7th Adsorption	1.93	0.125	0.125	0.25

8. Regeneration Efficiency (%) for 400mg/l

	MPAHS	MPASG	CPASG	CPAHS
0 Cycle				
1st Cycle	85.00	84.33	88.00	79.23
2nd Cycle	53.86	52.40	49.50	44.88
3rd Cycle	42.77	29.19	27.37	16.88
4th Cycle	19.95	12.95	10.99	5.54
5th Cycle	2.5	0.97	0.25	0.28
6th cycle	0.23	0.026	0.03	0.06

B. CONVENTIONAL REGENERATION CYCLES

1. Adsorptive capacity (mg/l) for 100mg/l

	MPAHS	MPASG	CPASG	CPAHS
Ist Adsorption	124.852	123.383	118.947	111.424
2nd Adsorption	124.460	123.173	117.548	110.39
3rd Adsorption	123.585	121.791	115.849	107.986
4th Adsorption	118.916	118.298	112.910	105.974
5th Adsorption	114.166	113.349	110.853	103.488
6th Adsorption	110.849	110.416	108.1	99.225

7th Adsorption	109.598	107.975	104.224	94.581

2. Regeneration Efficiency (%) for 100mg/l

	MPAHS	MPASG	CPASG	CPAHS
0 Cycle	100.00	100.00	100.00	100.00
1st Cycle	99.69	99.83	98.82	99.07
2nd Cycle	98.99	98.71	97.39	96.91
3rd Cycle	95.25	95.88	94.92	95.11
4th Cycle	91.441	91.87	93.20	92.88
5th Cycle	88.78	89.49	90.88	89.05
6th cycle	87.78	87.51	87.62	84.88

3. Adsorptive capacity (mg/l) for 200mg/l

	MPAHS	MPASG	CPASG	CPAHS
Ist Adsorption	247.66	244.45	233.89	223.78
2nd Adsorption	246.66	242.11	227.586	216.243
3rd Adsorption	241.924	237.11	224.16	209.178
4th Adsorption	234.774	230.415	214.585	208.523
5th Adsorption	225.0	222.148	211.424	205.581
6th Adsorption	218.79	217.791	201.559	198.798
7th Adsorption	212.113	209.174	198.055	193.736

4. Regeneration Efficiency (%) for 200mg/l

	MPAHS	MPASG	CPASG	CPAHS
0 Cycle	100.00	100.00	100.00	100.00
1st Cycle	99.60	99.04	97.30	96.63
2nd Cycle	97.68	97.00	95.84	93.47
3rd Cycle	94.80	94.26	91.75	93.18
4th Cycle	90.85	90.88	90.39	91.87
5th Cycle	88.35	89.09	86.18	88.84
6th cycle	85.65	85.57	84.68	83.00

5. Adsorptive Capacity (mg/l) for 300mg/l

	MPAHS	MPASG	CPASG	CPAHS
Ist Adsorption	372.36	363.49	339.61	331.91
2nd Adsorption	349.863	342.98	326.798	317.911
3rd Adsorption	321.799	314.061	310.488	300.425
4th Adsorption	264.6	259.605	251.673	234.99
5th Adsorption	246.260	226.468	221.68	217.965
6th Adsorption	216.60	224.168	218.615	213.749
7th Adsorption	194.613	186.843	182.974	174.173

6. Regeneration Efficiency (%) for 300mg/l

	MPAHS	MPASG	CPASG	CPAHS
0 Cycle	100.00	100.00	100.00	100.00
1st Cycle	93.96	94.36	96.23	95.78
2nd Cycle	86.42	86.40	91.42	90.51
3rd Cycle	71.06	71.42	74.11	70.8
4th Cycle	69.82	62.30	65.27	65.67
5th Cycle	58.17	61.67	64.37	64.40
6th cycle	52.26	51.40	53.88	52.48

7. Adsorptive capacity (mg/l) for 400mg/l

	MPAHS	MPASG	CPASG	CPAHS
Ist Adsorption	495.93	476.81	453.78	444.41
2nd Adsorption	447.113	430.855	421.611	409.238
3rd Adsorption	384.413	375.025	367.899	341.349
4th Adsorption	309.75	299.1	285.354	272.099
5th Adsorption	234.363	224.149	211.849	205.563
6th Adsorption	124.225	89.5	51.725	29.291
7th Adsorption	48.813	24.688	11.65	1.338

8. Regeneration Efficiency (%) for 400mg/l

	MPAHS	MPASG	CPASG	CPAHS
0 Cycle	100.00	100.00	100.00	100.00
1st Cycle	90.16	90.36	92.91	92.09
2nd Cycle	77.51	78.65	81.07	76.81
3rd Cycle	62.46	62.73	62.88	61.23
4th Cycle	47.26	47.01	46.69	46.26
5th Cycle	25.05	18.77	11.40	6.59
6th cycle	9.8	5.18	2.57	0.30

C. MICROWAVE REGENERATION CYCLES

1. Adsorptive capacity (mg/l) for 100mg/l

	MPAHS	MPASG	CPASG	CPAHS
Ist Adsorption	124.852	123.383	118.947	111.424
2nd Adsorption	124.960	123.586	122.074	115.81
3rd Adsorption	124.880	123.516	121.773	114.599
4th Adsorption	124.870	123.489	121.773	114.599
5th Adsorption	124.856	123.397	120.59	112.835
6th Adsorption	124.81	123.305	118.835	111.359
7th Adsorption	124.770	123.095	118.081	110.6

2. Regeneration Efficiency (%) for 100mg/l

	MPAHS	MPASG	CPASG	CPAHS
0 Cycle	100.00	100.00	100.00	100.00
1st Cycle	100.09	100.16	102.63	103.94
2nd Cycle	100.02	100.11	102.38	102.85
3rd Cycle	100.01	100.09	102.09	102.07
4th Cycle	100.0	100.01	101.38	101.27
5th Cycle	99.97	99.94	99.91	99.94
6th cycle	99.93	99.77	99.27	99.26

3. Adsorptive capacity (mg/l) for 200mg/l

	MPAHS	MPASG	CPASG	CPAHS
Ist Adsorption	247.66	244.45	233.89	223.78
2nd Adsorption	247.75	245.42	239.54	224.13
3rd Adsorption	247.68	244.698	237.92	223.35
4th Adsorption	247.59	244.62	235.42	219.39
5th Adsorption	247.10	243.83	233.60	215.42
6th Adsorption	246.80	243.36	231.80	213.31
7th Adsorption	246.45	241.65	229.61	210.85

4. Regeneration Efficiency (%) for 200mg/l

	MPAHS	MPASG	CPASG	CPAHS
0 Cycle	100.00	100.00	100.00	100.00
1st Cycle	100.04	100.40	102.42	100.16
2nd Cycle	100.00	100.10	101.72	99.81
3rd Cycle	99.97	100.07	100.65	98.04
4th Cycle	99.77	99.75	99.88	96.26
5th Cycle	99.65	99.55	99.11	95.32
6th cycle	99.51	98.85	98.17	94.22

5. Adsorptive capacity (mg/l) for 300mg/l

	MPAHS	MPASG	CPASG	CPAHS
Ist Adsorption	372.36	363.49	339.61	331.91
2nd Adsorption	370.00	360.42	336.67	332.92
3rd Adsorption	361.66	357.98	338.87	326.67
4th Adsorption	354.35	349.24	334.30	318.80
5th Adsorption	339.57	336.67	330.84	315.18
6th Adsorption	336.60	333.97	325.05	305.17
7th Adsorption	329.73	326.42	321.60	

6. Regeneration Efficiency (%) for 300mg/l

	MPAHS	MPASG	CPASG	CPAHS
0 Cycle	100.00	100.00	100.00	100.00
1st Cycle	99.37	99.16	99.78	99.39
2nd Cycle	97.13	98.48	99.13	98.42
3rd Cycle	95.16	96.08	98.44	97.46
4th Cycle	91.19	92.62	97.42	96.05
5th Cycle	90.40	91.88	95.71	94.96
6th cycle	88.55	89.80	94.70	91.94

7. Adsorptive capacity (mg/l) for 400mg/l

	MPAHS	MPASG	CPASG	CPAHS
Ist Adsorption	495.93	476.81	453.78	444.41
2nd Adsorption	479.04	464.54	449.61	439.22
3rd Adsorption	452.09	446.74	442.97	429.60
4th Adsorption	447.11	427.33	424.24	420.76
5th Adsorption	430.59	422.26	418.36	413.92
6th Adsorption	384.36	377.8	372.98	368.12
7th Adsorption	374.87	355.60	348.36	339.22

8. Regeneration Efficiency (%) for 400mg/l

	MPAHS	MPASG	CPASG	CPAHS
0 Cycle	100.00	100.00	100.00	100.00
1st Cycle	96.59	97.43	99.08	98.83
2nd Cycle	91.16	93.69	97.62	96.67
3rd Cycle	90.16	89.62	93.49	94.68
4th Cycle	86.82	88.59	92.19	93.14
5th Cycle	77.50	79.23	82.19	82.83
6th cycle	75.59	78.36	76.77	76.33

APPENDIX W

EFFECT OF MICROWAVE REGENERATION CONDITIONS

1. Adsorptive capacity (mg/l) with oxidant (30% H_2O_2)

Time (mins)	MPAHS	MPASG	CPASG	CPAHS
0	124.852	123.38	118.95	111.42
5	124.8	122.27	118.22	111.29
10	124.96	123.59	122.07	115.81
15	124.88	123.48	120.82	114.17
20	124.68	123.09	118.36	110.85

2. Adsorptive capacity (mg/l) without oxidant

Time (mins)	MPAHS	MPASG	CPASG	CPAHS
0	124.852	123.38	118.95	111.42
5	124.84	123.34	118.71	110.10
10	124.87	123.58	120.67	113.36
15	124.86	123.35	119.39	112.11
20	124.34	122.81	117.10	109.10

3. Adsorptive capacity (mg/l) with oxidant (30% H_2O_2)

Power level (%)	MPAHS	MPASG	CPASG	CPAHS
0	124.852	123.38	118.95	111.42
18	124.8	123.25	119.36	112.91
36	124.87	123.53	120.49	114.36
81	124.96	123.59	122.07	115.81
100	124.78	123.22	118.48	111.12

4. Adsorptive capacity (mg/l) without oxidant

Power level (%)	MPAHS	MPASG	CPASG	CPAHS
0	124.852	123.38	118.95	111.42

18	124.68	123.22	118.83	112.21
36	124.72	123.43	119.61	112.97
81	124.87	123.58	120.67	113.36
100	124.73	122.96	116.61	109.23

APPENDIX X

EFFECT OF CONVENTIONAL REGENERATION CONDITIONS

1. Adsorptive capacity (mg/l) with oxidant (30% H_2O_2)

Time (mins)	MPAHS	MPASG	CPASG	CPAHS
0	124.852	123.38	118.95	111.42
10	123.97	122.489	117.041	106.849
20	124.21	122.835	117.586	109.328
30	124.46	123.73	118.72	111.64
40	124.166	122.674	117.809	110.14
50	123.766	121.974	117.00	109.166

2. Adsorptive capacity (mg/l) without oxidant

Time (mins)	MPAHS	MPASG	CPASG	CPAHS
0	124.852	123.38	118.95	111.42
10	123.49	121.46	115.85	104.98
20	123.84	122.49	117.09	107.61
30	124.00	122.67	117.49	109.02
40	123.91	122.51	118.36	108.86
50	123.04	121.84	116.54	107.12

3. Adsorptive capacity (mg/l) with oxidant (30% H_2O_2)

Temp (^oC)	MPAHS	MPASG	CPASG	CPAHS
0	124.852	123.38	118.95	111.42
200	120.798	119.599	115.964	107.25
300	121.5	120.41	116.684	109.669
400	122.973	122.154	118.374	111.179
500	124.460	123.173	118.72	111.34
600	115.8	114.51	111.48	106.50

4. Adsorptive capacity (mg/l) without oxidant (30% H_2O_2)

Temp (^oC)	MPAHS	MPASG	CPASG	CPAHS

0	124.852	123.38	118.95	111.42
200	116.31	115.30	111.31	103.11
300	117.6	116.17	113.61	106.43
400	120.61	118.99	115.31	108.31
500	122.62	121.06	116.57	110.018
600	115.71	114.505	111.49	106.834

APPENDIX Y

EFFECT OF DOSAGE ON DESORPTION CAPACITY

A. MPASG

Initial solid phase conc. (mg/g)	0.025g	0.05g	0.075g	0.1g
124.36	95.31	111.74	120.12	123.337
248.847	213.96	228	240.348	245.94
347.27	320.47	328.35	335.564	341.655
441.49	390.199	417.83	425.021	432.983

B. MPAHS

Initial solid phase conc. (mg/g)	0.025g	0.05g	0.075g	0.1g
123.72	97.095	100.864	121.145	123.28
248.58	220.058	231.175	238.639	247.86
373.28	340.793	350.318	361.962	372.075
498.11	440.11	463.989	484.932	495.702

C. CPASG

Initial solid phase conc. (mg/g)	0.025g	0.05g	0.075g	0.1g
122.685	100.396	115.53	119.69	121.911
245.234	211.857	223.184	233.709	243.986
369.044	335.453	346.893	357.411	367.764
438.529	414.622	426.24	430.859	437.125

D. CPAHS

Initial solid phase conc. (mg/g)	0.025g	0.05g	0.075g	0.1g
122.31	90.7	112.65	116.736	120.88
245.17	212.97	223.17	237.29	243.58
326.96	300.3	314.11	320.9	325.28
390.65	345.45	367.62	378.206	388.76